Identification of Wastewater Primary Sludge Composition using Augmented Batch Tests and Mathematical Models

by

Christopher Gaszynski

GSZCHR001

Degree of

Doctor of Philosophy (PhD)

Water Research Group (WRG)

Department of Civil Engineering

University of Cape Town

December 2020

Supervisors: Professor George A. Ekama and Dr David S. Ikumi

Declaration

I, Christopher Gaszynski, hereby declare that the work on which this thesis is based is my original work (except where acknowledgements indicate otherwise). This thesis/dissertation has been submitted to the Turnitin module (or equivalent similarity and originality checking software) and I confirm that my supervisor has seen my report and any concerns revealed by such have been resolved with my supervisor.

Signature: Signed by candidate

Date: 2020/12/02

Acknowledgements

Professor George Ekama – Thank you for all of the support, guidance and assistance through my undergraduate and postgraduate projects. You are one of the most inspiring people that I have ever met, and I am so thankful for the opportunity to have worked with you. I really wish that we could have finished this together.

Dr David Ikumi – Thank you for everything David, I cannot express how much you helped me throughout this project and in my academic career in general. I really appreciate that your door was always open, and that you were always happy to jump in and help out where you could.

Professor Eveline Volcke and Dr Kimberly Solon – Thank you Eveline and Kimberly for my time spent at UGent. You made me feel so welcomed and I really enjoyed our time working together.

Chris Brouckaert – Thank you Chris for all the long discussions regarding the modelling and analytical procedures. You were an integral part of my understanding for many aspects of this project.

My Parents and Family – Thank you Angelina, Andrzej, Alicja and Dorota for all the support over the years, it's been a long road and you have all been there every step of the way.

My Friends – To my friends in Cape Town, thank you Shane, Brad, Niel, Caitlin, Rory and Josh for all of the support, you all helped to provide the perfect balance between work and down time. To my friends in Belgium, thank you Farhang, Janis, Laurence, Quan Le, Mingsheng, Stijn, Thiago, Xinyu, David and Tine for making my UGent experience an experience I will always remember fondly.

My UCT Colleagues – Thank you Dyllon, Njabulo, Hector, Theo, Tasneem and Paul for everything over my years as a postgraduate. Thank you for the long hours spent in the lab and the hours spent teaching students.

Avril – Thank you Avril for everything this year, it was definitely an interesting one and I couldn't have done it without you.

Abstract

The composition (chemical formula - $C_XH_YO_ZN_AP_B$) of organic substrates contained in wastewater have a profound effect on the performance of wastewater treatment unit operations such as anaerobic digestion. The identification of the biodegradable organic composition, as well as accurately characterising the influent fed to the anaerobic digester, allows for better system control, prediction of operating conditions and unit design. The physical and chemical characteristics of the organic substrate directly influence factors such as biogas production and process stability, such as alkalinity generation and anaerobic digester performance (including potential failure).

The popularity of modelling the anaerobic digestion process has been increasing over the years with the development of mathematical bioprocess models that can accurately predict the operating conditions within the anaerobic digester, the biogas production and nutrient recovery potential. However, these models require a detailed characterisation of the influent to ensure that the results obtained are reliable and accurate. Therefore, this thesis aims to improve current analytical biodegradability test methods (The biochemical methane potential (BMP) test by augmenting it – Augmented (Aug)BMP test), as well as develop a novel analytical biodegradability test (The Augmented Biochemical Sulphide Potential Test - AugBSP test). The methodology was developed such that the accuracy relating to the required input parameters for mathematical modelling could be improved.

Identifying the influent substrate's biodegradable organics can be challenging, as the most accurate methods for identifying the input parameters are expensive, complicated, and time-consuming. Alternative methods available for identifying the composition include elemental analysis; however, the equipment required may not be readily available and is expensive to purchase. Therefore, this thesis introduces two improved biodegradability tests, the AugBMP and AugBSP tests, which are relatively straight forward to operate. The equipment required is inexpensive to purchase, and the test can be performed in a laboratory without the need for sending samples away for further testing. Furthermore, large samples can be taken, and a wide array of measurements can be performed, giving an accurate characterisation of the substrate in question. Both tests make use of a control reactor (into which only the inoculum is placed) and a test reactor (into which both the inoculum and substrate is placed). The control reactor is

used to determine the baseline for the material released due to the breakdown of biodegradable organics and biomass present in the inoculum. The test reactor is used to quantify the material released due to the chosen biodegradable substrate. Both of the augmented batch reactors (control and test) are run for an extended period of time (>20 days) to ensure that all the utilisable organic substrate is degraded.

The sulphidogenic biodegradability test (AugBSP) makes use of sulphate reducing bacteria instead of methanogenic organisms, which subsequently allows for the batch test to be conducted in a completely sealed reactor with no headspace. The advantage of this configuration is that all the bioprocesses and their associated measurements are conducted in the aqueous phase, which alleviates the gas measurement error associated with the biochemical methane potential tests, allowing for higher accuracy and precision regarding the composition identification and influent characterisation.

The composition of the biodegradable organics was identified using two approaches:

1. A stoichiometric approach, which used mass balanced bioprocess stoichiometry together with the measured starting and ending concentrations conducted on both the augmented batch control and test reactors.
2. A parameter estimation and data reconciliation approach, which made use of the PWM_SA_AD model and the parameter estimation function.

The identification of the biodegradable organics present in the influent organic substrate were determined using three different types of anaerobic digesters for both the methanogenic and sulphidogenic systems - (i) a steady state parent anaerobic digester (SSPAD), (ii) an augmented batch control reactor and (iii) an augmented batch test reactor. The SSPAD was used to grow the inoculum required for the augmented batch control and test reactors.

Two different biodegradable substrates were used for this investigation, one with a known composition and one with an unknown composition.

1. Casein Hydrolysate: A protein found in bovine milk which was used to directly compare and validate the results obtained by both the AugBMP and AugBSP tests as the composition of casein has been well documented by Hoover and Porges (1952), as $C_1H_{1.47}O_{0.35}N_{0.25}$, and Schrieke and Winter (2011) as $C_1H_{1.59}O_{0.31}N_{0.25}P_{0.005}$.

2. Primary Sewage Sludge (PSS): A substrate consisting of majority (>95%) particulate COD collected from the bottom of the primary settling tank at Potsdam. The primary objective of this thesis was to identify the unknown composition of the biodegradable particulate organics.

Casein hydrolysate was chosen as a substrate for both the AugBMP and AugBSP experiments such that the compositions determined by each respective test could be compared.

Source	**Casein Composition**
Hoover and Porges (1952)	$C_1H_{1.47}O_{0.35}N_{0.25}$
Schrieke and Winter (2011)	$C_1H_{1.59}O_{0.31}N_{0.25}P_{0.005}$
Methanogenic (AugBMP)	$C_1H_{1.588}O_{0.596}N_{0.249}P_{0.004}$
Sulphidogenic (AugBSP)	$C_1H_{1.406}O_{0.577}N_{0.22}P_{0.001}$

It was observed that the AugBMP test had a high level of error associated with the gas measurements taken, as the modelled AugBMP test reactor predicted a significantly higher methane gas production. However, the volume of methane gas produced was not used as a variable for the parameter estimation (PE) conducted on the AugBMP test experiment; nonetheless, the PE was still able to identify the composition of the casein accurately. The AugBSP test was proposed to alleviate the gas measurement error associated with the BMP test. The AugBMP and AugBSP test experiments were used to identify the composition of the biodegradable organics present in PSS, taken from Potsdam, Western Cape. The compositions determined for the biodegradable organics in PSS were:

Type of experiment	**Composition**
Methanogenic PSS-1	$C_1H_{2.964}O_{0.829}N_{0.071}P_0$
Methanogenic PSS-2	$C_1H_{2.654}O_{0.236}N_{0.18}P_{0.002}$
Methanogenic PSS-3	$C_1H_{1.056}O_{0.048}N_{0.093}P_{0.001}$
Sulphidogenic PSS-1	$C_1H_{1.856}O_{0.555}N_{0.0707}P_{0.004}$
Sulphidogenic PSS-2	$C_1H_{2.365}O_{0.323}N_{0.0723}P_{0.004}$
Sulphidogenic PSS-3	$C_1H_{1.004}O_{0.431}N_{0.032}P_0$

It was observed that the compositions identified by each of the methanogenic (AugBMP) and sulphidogenic (AugBSP) test experiments differed, which was expected as the biodegradable particulates fluctuate based on the treatment plant and the collection time. The results obtained for both the AugBMP and AugBSP test reactors showed that the composition, as well as the dynamics regarding the breakdown of the PSS, could be accurately represented by the PWM_SA_AD model. Therefore, the augmented batch test coupled with mass balanced mathematical models could improve current analytical methods for substrate characterisation, and composition identification, with a specific focus on biodegradability. The primary objective of the thesis was the identification of the composition of these biodegradable organics such that AD failure can be predicted and prevented, as the performance of the AD system is directly dependent on the composition (CHONP) of the biodegradable organics fed to it.

Table of Contents

Table of Contents

Declaration ..... *i*

Acknowledgements ..... *ii*

Abstract ..... *iii*

Table of Contents ..... *vii*

List of Tables ..... *xiii*

List of Figures ..... *xvii*

List of Abbreviations Used ..... *xxiv*

Chapter 1: Introduction *1*

1.1 Background to problem **1**

1.2 Research questions and hypothesis **4**

1.3 Project objectives **4**

1.4 Specific objectives **6**

1.5 Scope and Limitations **7**

1.6 New knowledge contribution **9**

1.6.1 Development of augmented analytical testing equipment 10

1.6.2 Identification of wastewater organics 11

1.6.3 Calibration of the mathematical model 11

1.7 Thesis Structure **12**

Chapter 2: Literature Review *15*

2.1 Introduction **15**

2.2 Introduction to anaerobic digestion **15**

2.3 Anaerobic digestion processes and microbiology **17**

2.3.1 Hydrolysis 19

2.3.2 Acidogenesis 21

2.3.3 Acetogenesis 23

2.3.4 Acetoclastic methanogenesis 23
2.3.5 Hydrogenotrophic methanogenesis 24
2.3.6 Sulphate Reduction: A Competitor to Methane Production 25
2.3.7 Sulphidogenesis 26
2.3.8 PWM_SA_AD Validation 28

2.4 Biochemical Methane Potential Test 28

2.4.1 Introduction 28
2.4.2 Batch test configuration 29
2.4.3 Good BMP practice 29
2.4.4 Inoculum 30
2.4.5 Substrate 31
2.4.6 Experimental setup 32
2.4.7 Gas measurements 33

2.5 Primary Sewage Sludge 35

2.5.1 Overview 35
2.5.2 PSS hydrolysis rate in methanogenic and sulphidogenic systems 36
2.5.3 Stoichiometry of PSS degradation by methanogenic anaerobic digestion 37
2.5.4 Stoichiometry of PSS degradation by sulphidogenic anaerobic digestion 39

2.6 Casein 40

2.7 Mathematical bioprocess modelling 42

2.7.1 Overview 42
2.7.2 Parameter Estimation 42

Chapter 3: Materials and Methods 48

3.1 Introduction 48

3.2 Steady-state reactor design and operation 49

3.2.1 Methanogenic Parent Digester 49
3.2.2 Sulphidogenic Parent Digester 52

3.3 Feed 54

3.3.1 Methanogenic system feed preparation 55
3.3.2 Sulphidogenic system feed preparation 55

3.4 Augmented BMP Experiment 57

3.4.1 Overview 57
3.4.2 Experimental set-up 57
3.4.3 Seeding Procedure 59

3.4.4 Sampling Procedure 61
3.4.5 Gas Measurement 62
3.5 Augmented BSP Experiment 63
3.5.1 Overview 63
3.5.2 Experimental set-up 63
3.5.3 Seeding Procedure 65
3.5.4 Sampling Procedure 67
3.6 Analytical Procedures 68
3.6.1 Overview 68
3.6.2 Measurements performed 68
3.6.3 COD 69
3.6.4 TKN and FSA 71
3.6.5 TP and OP 71
3.6.6 Solids 71
3.6.7 Alkalinity 72
3.6.8 pH 74
3.6.9 Sulphate 75
3.6.10 Gas Chromatography 75
3.6.11 Summary 75
3.7 Evaluation of Experimental Results 76
3.7.1 Overview 76
3.7.2 Mass Balances 77
3.7.3 Methanogenic COD mass balance 78
3.7.4 Sulphidogenic COD mass balance 83
3.7.5 TKN and TP Balance 84
3.7.6 Experimental error and uncertainty 84
3.8 Influent fractionation 86
3.8.1 Overview 86
3.8.2 Methanogenic SSPAD 88
3.8.3 Sulphidogenic SSPAD 94
3.8.4 Augmented batch tests 97
3.9 Calculating the organic composition 101
3.9.1 Overview 101
3.9.2 Composition determination using stoichiometry 102
3.9.3 Composition determination using mathematical models 104

3.10 Modelling the Steady-State digesters 106
3.10.1 Overview 106
3.10.2 Influent fractionation 107
3.10.3 Hydrolysis kinetics 109
3.10.4 Composition Determination 111
3.10.5 Modelled SSPAD evaluation 113
3.10.6 Modelled methanogenic SSPAD 114
3.10.7 Modelled Sulphidogenic SSPAD 114
3.11 Modelling the augmented batch experiments 116
3.11.1 Overview 116
3.11.2 Control reactors 117
3.11.3 Test reactors 121
Chapter 4: Steady-state parent anaerobic digester results and modelling 128
4.1 Introduction 128
4.2 Methanogenic SSPAD 130
4.2.1 Gas Chromatography 133
4.2.2 Mass Balances 134
4.2.3 Modelling the Methanogenic SSPAD 138
4.3 Sulphidogenic SSPAD 151
4.3.1 Mass Balances 154
4.3.2 Modelling the Sulphidogenic SSPAD 157
4.4 Conclusions 167
Chapter 5: Augmented batch control reactor results and modelling 169
5.1 Introduction 169
5.2 AugBMP Control Reactors 170
5.2.1 Gas Measurement 173
5.2.2 Mass Balances 174
5.2.3 Stoichiometric Composition Identification 179
5.2.4 Modelling the AugBMP control experiment 183
5.2.5 Modelled Composition Identification 185
5.2.6 Modelled AugBMP Results 185
5.3 AugBSP Control Reactors 205
5.3.1 Mass Balances 208

5.3.2 Stoichiometric Composition Identification 209
5.3.3 Modelling the AugBSP control experiment 212
5.3.4 Modelled AugBSP Results 213

5.4 Conclusions 231

Chapter 6: Augmented batch test reactor results and modelling 234

6.1 Introduction 234

6.2 Casein Experiment 236

6.2.1 AugBMP test casein mixture 237
6.2.2 AugBSP test casein mixture 238
6.2.3 Results for augmented batch test experiments using casein 239
6.2.4 Gas Measurement 241
6.2.5 Mass Balances 241
6.2.6 Stoichiometric Composition Identification 244
6.2.7 Modelling the casein experiment 248
6.2.8 Modelled Composition Identification 251
6.2.9 Casein hydrolysate analysis 252
6.2.10 Modelled casein experiment results 255
6.2.11 Conclusions from the casein experiment 267

6.3 PSS Experiments 269

6.3.1 Starting mixture 270
6.3.2 Results for augmented batch test experiments on PSS 270
6.3.3 AugBMP test gas measurement 275
6.3.4 AugBMP test mass balances 276
6.3.5 AugBSP test mass balances 279
6.3.6 Stoichiometric Composition Identification 280
6.3.7 Modelling the PSS experiment 284
6.3.8 Modelled Composition Identification 286
6.3.9 Modelled AugBMP test PSS experiment results 288
6.3.10 Modelled AugBSP test PSS experiment results 305
6.3.11 Conclusions from the PSS experiment 320

Chapter 7: Conclusions and Recommendations 322

7.1 Conclusions 322
7.2 Recommendations 328

Chapter 8: References 332

Appendix A: Weak Acid/Base Chemistry *342*

Appendix B: Gas Chromatography Data *343*

Appendix C: Methanogenic Steady State Reactor Data *346*

Appendix D: Sulphidogenic Steady State Reactor Data *347*

Appendix E: Methanogenic Batch Test (AugBMP) Data *348*

Appendix F: Sulphidogenic Batch Test (AugBSP) Data *352*

Appendix G: Casein Analysis *356*

List of Tables

Table 2. 1:Casein Compositions 41
Table 3. 1: AugBMP experiment starting mixture 61
Table 3. 2: AugBSP starting mixture 67
Table 3. 3: Standard measurements performed 69
Table 3. 4: Additional sulphidogenic system measurements 69
Table 3. 5: Required measurements 76
Table 3. 6: Conversion for WEST influent generator 108
Table 3. 7: Observed hydrolysis rate adapted from Sötemann *et al*. (2005) 110
Table 3. 8: KM and KS values adaped from Ikumi *et al*. (2015) 111
Table 3. 9: Mass fractions for UPO 112
Table 3. 10: AugBMP PE parameters 120
Table 3. 11: AugBMP/AugBSP test PE parameters for casein 124
Table 3. 12: AugBMP test PE parameters for PSS 126
Table 3. 13: AugBSP test PE parameters for PSS 127
Table 4. 1: Experiment Periods 129
Table 4. 2: Methanogenic SSPAD results 131
Table 4. 3: Gas chromatography results 134
Table 4. 4: Methanogenic SSPAD COD balance 136
Table 4. 5: Methanogenic SSPAD TKN/TP balance 137
Table 4. 6: Calculated methanogenic SSPAD biomass COD concentration 139
Table 4. 7: Total COD change in AugBMP control reactors 140
Table 4. 8: Methanogenic SSPAD residual biodegradable organics 141
Table 4. 9: Methanogenic SSPAD influent fractionation 142
Table 4. 10: Adjusted methanogenic SSPAD influent fractionation 143
Table 4. 11: Methanogenic SSPAD influent COD/VSS fractions 144
Table 4. 12: Methanogenic SSPAD hydrolysis rate constants 144
Table 4. 13: Methanogenic SSPAD organic compositions 146
Table 4. 14: Modelled methanogenic SSPAD results 148
Table 4. 15: Methanogenic SSPAD active biomass concentrations 150
Table 4. 16: Sulphidogenic SSPAD results 152
Table 4. 17: Sulphidogenic SSPAD Sulphur Balance 155
Table 4. 18: Sulphidogenic SSPAD TKN/TP Balance 156
Table 4. 19: Sulphidogenic SSPAD sulphide concentrations 159

Table 4. 20: Calculated sulphidogenic SSPAD biomass COD concentration..... 160
Table 4. 21: Sulphidogenic SSPAD influent fractionation 160
Table 4. 22: Adjusted sulphidogenic SSPAD influent fractionation..... 161
Table 4. 23: Sulphidogenic SSPAD influent COD/VSS fractions 161
Table 4. 24: Sulphidogenic SSPAD influent organic compositions..... 163
Table 4. 25: Modelled sulphidogenic SSPAD results 164
Table 4. 26: Sulphidogenic SSPAD active biomass concentrations 166
Table 5. 1: Experiment Periods 170
Table 5. 2: AugBMP control results..... 171
Table 5. 3: Gas chromatography results..... 175
Table 5. 4: MC1 AugBMP control COD balance 176
Table 5. 5: Adjusted MC1 AugBMP control COD balance..... 176
Table 5. 6: MP1 AugBMP control COD balance..... 177
Table 5. 7: Adjusted MP1 AugBMP control COD balance 177
Table 5. 8: MP2 AugBMP control COD balance..... 178
Table 5. 9: MP3 AugBMP control COD balance..... 178
Table 5. 10: AugBMP control TKN/TP balance 179
Table 5. 11: AugBMP control stoichiometric composition determination 181
Table 5. 12: Modelled AugBMP control variables 184
Table 5. 13: Modelled AugBMP control composition identification..... 185
Table 5. 14: Modelled MC1 and MP1 AugBMP control results..... 187
Table 5. 15: Modelled MP2 and MP3 AugBMP control results 188
Table 5. 16: Measurement error associated with data set and manner in which error was handled for modelling 189
Table 5. 17: Modelled AugBMP control COD balance 204
Table 5. 18: AugBSP control results 206
Table 5. 19: AugBSP control mass balance 208
Table 5. 20: AugBSP control stoichiometric composition determination..... 210
Table 5. 21: Modelled SC1 and SP1 AugBSP control results..... 214
Table 5. 22: Modelled SP2 and SP3 AugBSP control results 215
Table 6. 1: Experiment Periods 235
Table 6. 2: AugBMP/AugBSP test results for casein..... 239
Table 6. 3: Gas chromatography results..... 242
Table 6. 4: MC1 AugBMP test COD balance 242

Table 6. 5: Adjusted MC1 AugBMP test COD balance 243
Table 6. 6: SC1 AugBSP test sulphur balance 244
Table 6. 7: MC1/SP1 AugBMP/AugBSP test TKN/TP balance 244
Table 6. 8: AugBMP and AugBSP test stoichiometric composition identification for casein 245
Table 6. 9: Modelled AugBMP test variables for casein 250
Table 6. 10: Modelled AugBSP test variables for casein 250
Table 6. 11: Modelled AugBMP and AugBSP test composition identification for casein 251
Table 6. 12: Casein composition comparison to the literature stated values 251
Table 6. 13: Casein hydrolysate powder analysis 253
Table 6. 14: Casein hydrolysate powder COD, OrgN and OrgP content 254
Table 6. 15: Casein hydrolysate powder comparison with AugBMP/AugBSP PE Casein (1g/l) 254
Table 6. 16: Modelled MC1 AugBMP test results for casein 255
Table 6. 17: Modelled SC1 AugBSP test results for casein 256
Table 6. 18: Modelled MC1 AugBMP test COD balance 266
Table 6. 19: AugBMP test results for PSS 271
Table 6. 20: AugBSP test results for PSS 272
Table 6. 21: Gas chromatography results 276
Table 6. 22: MP1 AugBMP test COD balance 277
Table 6. 23: MP2 AugBMP test COD balance 277
Table 6. 24: MP3 AugBMP test COD balance 277
Table 6. 25: AugBMP test TKN/TP balance for PSS 278
Table 6. 26: AugBSP test mass balance for PSS 279
Table 6. 27: AugBMP test stoichiometric composition identification for PSS 282
Table 6. 28: AugBSP test stoichiometric composition identification for PSS 283
Table 6. 29: Modelled AugBMP test variables for PSS 285
Table 6. 30: Modelled AugBSP test variables for PSS 286
Table 6. 31: Modelled AugBMP test composition identification for PSS 287
Table 6. 32: Modelled AugBSP test composition identification for PSS 288
Table 6. 33: Modelled MP1 and MP2 AugBMP test results for PSS 290
Table 6. 34: Modelled MP3 AugBMP test results for PSS 291
Table 6. 35: Modelled AugBMP test COD balance for PSS 304
Table 6. 36: Modelled SP1 and SP2 AugBSP test results for PSS 306

Table 6. 37 :Modelled SP3 AugBSP test results for PSS 307
Table B. 1: GC Data 04.05.2018 343
Table B. 2: GC Data 03.12.2018 343
Table B. 3: GC Data 22.05.2018 344
Table B. 4: GC Data 11.12.2018 345
Table C. 1: Methanogenic Steady State Digester Data 346
Table D. 1: Sulphidogenic Steady State Digester Data 347
Table E. 1: MC1 Data 348
Table E. 2: MP1 Data 349
Table E. 3: MP2 Data 350
Table E. 4: MP3 Data 351
Table F. 1: SC1 Data 352
Table F. 2: SP1 Data 353
Table F. 3: SP2 Data 354
Table F. 4: SP3 Data 355
Table G. 1: Data for Casein Wet Chemistry Analysis for 1g/l 356
Table G. 2: Summary Casein Wet Chemistry Analysis for 1g/l 356

List of Figures

Figure 1. 1: Mind map of the thesis structure 14
Figure 2. 1: ADM1 anaerobic digestion pathways 18
Figure 2. 2: PWM_SA_AD methanogenic pathway 19
Figure 2. 3: PWM_SA_AD sulphidogenic pathway 27
Figure 2. 4: Variable criteria in WEST PE 46
Figure 2. 5: Parameter estimation function in WEST 47
Figure 3. 1: Chapter 3 layout 48
Figure 3. 2: Methanogenic Steady-State Parent Anaerobic Digester (SSPAD) 50
Figure 3. 3: Methanogenic SSPAD Photograph 51
Figure 3. 4: Wet-tip gas meter 51
Figure 3. 5: Sulphidogenic Steady-State Parent Anaerobic Digester (SSPAD) 53
Figure 3. 6: Sulphidogenic SSPAD Photograph 54
Figure 3. 7: Sulphidogenic SSPAD feed mixture 56
Figure 3. 8: AugBMP experiment set-up 58
Figure 3. 9: AugBMP experiment photograph 59
Figure 3. 10: AugBSP experiment design 64
Figure 3. 11: AugBSP experiment photograph 65
Figure 3. 12: AugBMP COD distribution 80
Figure 3. 13: Water mass in AugBMP M2 experiment (x-axis = hours; y-axis = grams) 81
Figure 3. 14: COD mass in AugBMP M2 Experiment (x-axis = hours; y-axis = grams) 82
Figure 3. 15: COD concentration in AugBMP M2 Experiment (x-axis = hours; y-axis = mgCOD/l) 82
Figure 3. 16: COD fractionation 87
Figure 3. 17: Methanogenic SSPAD COD groups 90
Figure 3. 18: Sulphidogenic SSPAD COD groups 96
Figure 3. 19: Augmented batch test COD fractionation 100
Figure 3. 20: SSPAD layout 107
Figure 3. 21: WEST influent file 109
Figure 3. 22: Augmented batch test layout 117
Figure 4. 1: Methanogenic SSPAD mass flux MC1 SSPAD 135

Figure 5. 1: MC1 AugBMP control CH_4 COD 174
Figure 5. 2: MP1 AugBMP control CH_4 COD 174
Figure 5. 3: MP2 AugBMP control CH_4 COD 174
Figure 5. 4: MP3 AugBMP control CH_4 COD 174
Figure 5. 5: MC1 AugBMP control total COD 190
Figure 5. 6: MP1 AugBMP control total COD 190
Figure 5. 7: MP2 AugBMP control total COD 191
Figure 5. 8: MP3 AugBMP control total COD 191
Figure 5. 9: MC1 AugBMP control soluble COD 192
Figure 5. 10: MP1 AugBMP control soluble COD 192
Figure 5. 11: MP2 AugBMP control soluble COD 192
Figure 5. 12: MP3 AugBMP control soluble COD 192
Figure 5. 13: MC1 AugBMP control FSA 193
Figure 5. 14: MP1 AugBMP control FSA 193
Figure 5. 15: MP2 AugBMP control FSA 194
Figure 5. 16: MP3 AugBMP control FSA 194
Figure 5. 17: MC1 AugBMP control OP 194
Figure 5. 18: MP1 AugBMP control OP 194
Figure 5. 19: MP2 AugBMP control OP 195
Figure 5. 20: MP3 AugBMP control OP 195
Figure 5. 21: MC1 AugBMP control carbonate alkalinty 196
Figure 5. 22: MP1 AugBMP control carbonate alkalinty 196
Figure 5. 23: MP2 AugBMP control carbonate alkalinty 196
Figure 5. 24: MP3 AugBMP control carbonate alkalinty 196
Figure 5. 25: MC1 AugBMP control total alkalinty 197
Figure 5. 26: MP1 AugBMP control total alkalinty 197
Figure 5. 27: MP2 AugBMP control total alkalinty 198
Figure 5. 28: MP3 AugBMP control total alkalinty 198
Figure 5. 29: MC1 AugBMP control VSS 199
Figure 5. 30: MP1 AugBMP control VSS 199
Figure 5. 31: MP2 AugBMP control VSS 199
Figure 5. 32: MP3 AugBMP control VSS 199
Figure 5. 33: MC1 AugBMP control VFA 200
Figure 5. 34: MP1 AugBMP control VFA 200

Figure 5. 35: MP2 AugBMP control VFA 200
Figure 5. 36: MP3 AugBMP control VFA 200
Figure 5. 37: MC1 AugBMP control pH 201
Figure 5. 38: MP1 AugBMP control pH 201
Figure 5. 39: MP2 AugBMP control pH 201
Figure 5. 40: MP3 AugBMP control pH 201
Figure 5. 41: MC1 AugBMP control methane 203
Figure 5. 42: MP1 AugBMP control methane 203
Figure 5. 43: MP2 AugBMP control methane 203
Figure 5. 44: MP3 AugBMP control methane 203
Figure 5. 45: SC1 AugBSP control total COD 218
Figure 5. 46: SP1 AugBSP control total COD 218
Figure 5. 47: SP2 AugBSP control total COD 218
Figure 5. 48: SP3 AugBSP control total COD 218
Figure 5. 49: SC1 AugBSP control soluble COD 219
Figure 5. 50: SP1 AugBSP control soluble COD 219
Figure 5. 51: SP2 AugBSP control soluble COD 219
Figure 5. 52: SP3 AugBSP control soluble COD 219
Figure 5. 53: SC1 AugBSP control soluble sulphide COD 220
Figure 5. 54: SP1 AugBSP control soluble sulphide COD 220
Figure 5. 55: SP2 AugBSP control soluble sulphide COD 220
Figure 5. 56: SP3 AugBSP control soluble sulphide COD 220
Figure 5. 57: SC1 AugBSP control sulphate 221
Figure 5. 58: SP1 AugBSP control sulphate 221
Figure 5. 59: SP2 AugBSP control sulphate 222
Figure 5. 60: SP3 AugBSP control sulphate 222
Figure 5. 61: SC1 AugBSP control FSA 222
Figure 5. 62: SP1 AugBSP control FSA 222
Figure 5. 63: SP2 AugBSP control FSA 223
Figure 5. 64: SP3 AugBSP control FSA 223
Figure 5. 65: SC1 AugBSP control OP 223
Figure 5. 66: SP1 AugBSP control OP 223
Figure 5. 67: SP2 AugBSP control OP 224
Figure 5. 68: SP3 AugBSP control OP 224

Figure 5. 69: SC1 AugBSP control carbonate alkalinity 225
Figure 5. 70: SP1 AugBSP control carbonate alkalinity 225
Figure 5. 71: SP2 AugBSP control carbonate alkalinity 225
Figure 5. 72: SP3 AugBSP control carbonate alkalinity 225
Figure 5. 73: SC1 AugBSP control total alkalinity 227
Figure 5. 74: SP2 AugBSP control total alkalinity 227
Figure 5. 75: SP2 AugBSP control total alkalinity 227
Figure 5. 76: SP3 AugBSP control total alkalinity 227
Figure 5. 77: SC1 AugBSP control VSS 228
Figure 5. 78: SP1 AugBSP control VSS 228
Figure 5. 79: SP2 AugBSP control VSS 228
Figure 5. 80: SP3 AugBSP control VSS 228
Figure 5. 81: SC1 AugBSP control VFA 229
Figure 5. 82: SP1 AugBSP control VFA 229
Figure 5. 83: SP2 AugBSP control VFA 230
Figure 5. 84: SP3 AugBSP control VFA 230
Figure 5. 85: SC1 AugBSP control pH 231
Figure 5. 86: SP1 AugBSP control pH 231
Figure 5. 87: SP2 AugBSP control pH 231
Figure 5. 88: SP3 AugBSP control pH 231
Figure 6. 1: MC1 AugBMP test CH_4 COD 241
Figure 6. 2: MC1 AugBMP test total COD 257
Figure 6. 3: SC1 AugBSP test total COD 257
Figure 6. 4: MC1 AugBMP test soluble COD 258
Figure 6. 5: SC1 AugBSP test soluble COD 258
Figure 6. 6: SC1 AugBSP test soluble sulphide COD 258
Figure 6. 7: SC1 AugBSP test sulphate 258
Figure 6. 8: MC1 AugBMP test FSA 259
Figure 6. 9: SC1 AugBSP test FSA 259
Figure 6. 10: MC1 AugBMP test OP 260
Figure 6. 11: SC1 AugBSP test OP 260
Figure 6. 12: MC1 AugBMP test carbonate alkalinity 261
Figure 6. 13: SC1 AugBSP test carbonate alkalinity 261
Figure 6. 14: MC1 AugBMP test total alkalinity 262

Figure 6. 15: SC1 AugBSP test total alkalinity 262
Figure 6. 16: MC1 AugBMP test VSS 263
Figure 6. 17: SC1 AugBSP test VSS 263
Figure 6. 18 : MC1 AugBMP test VFA 264
Figure 6. 19: SC1 AugBSP test VFA 264
Figure 6. 20: MC1 AugBMP test pH 265
Figure 6. 21: SC1 AugBSP test pH 265
Figure 6. 22: MC1 AugBMP test methane 266
Figure 6. 23: MP1 AugBMP test CH_4 COD 275
Figure 6. 24: MP2 AugBMP test CH_4 COD 275
Figure 6. 25: MP3 AugBMP test CH_4 COD 275
Figure 6. 26: MP1 AugBMP test total COD 292
Figure 6. 27: MP2 AugBMP test total COD 292
Figure 6. 28: MP3 AugBMP test total COD 292
Figure 6. 29: MP1 AugBMP test soluble COD 293
Figure 6. 30: MP2 AugBMP test soluble COD 293
Figure 6. 31: MP3 AugBMP test soluble COD 293
Figure 6. 32: MP1 AugBMP test FSA 294
Figure 6. 33: MP2 AugBMP test FSA 294
Figure 6. 34: MP3 AugBMP test FSA 294
Figure 6. 35: MP1 AugBMP test OP 295
Figure 6. 36: MP2 AugBMP test OP 295
Figure 6. 37: MP3 AugBMP test OP 296
Figure 6. 38: MP1 AugBMP test carbonate alkalinity 296
Figure 6. 39: MP2 AugBMP test carbonate alkalinity 296
Figure 6. 40: MP3 AugBMP test carbonate alkalinity 297
Figure 6. 41: MP1 AugBMP test total alkalinity 298
Figure 6. 42: MP2 AugBMP test total alkalinity 298
Figure 6. 43: MP3 AugBMP test total alkalinity 298
Figure 6. 44: MP1 AugBMP test VSS 299
Figure 6. 45: MP2 AugBMP test VSS 299
Figure 6. 46: MP3 AugBMP test VSS 299
Figure 6. 47: MP1 AugBMP test VFA 300
Figure 6. 48: MP2 AugBMP test VFA 300

Figure 6. 49: MP3 AugBMP test VFA 301
Figure 6. 50: MP1 AugBMP test pH 301
Figure 6. 51: MP2 AugBMP test pH 301
Figure 6. 52: MP3 AugBMP test pH 302
Figure 6. 53: MP1 AugBMP test methane 303
Figure 6. 54: MP2 AugBMP test methane 303
Figure 6. 55: MP3 AugBMP test methane 303
Figure 6. 56: SP1 AugBSP test total COD 308
Figure 6. 57: SP2 AugBSP test total COD 308
Figure 6. 58: SP3 AugBSP test total COD 309
Figure 6. 59: SP1 AugBSP test soluble COD 310
Figure 6. 60: SP2 AugBSP test soluble COD 310
Figure 6. 61: SP3 AugBSP test soluble COD 310
Figure 6. 62: SP1 AugBSP test soluble sulphide COD 311
Figure 6. 63: SP2 AugBSP test soluble sulphide COD 311
Figure 6. 64: SP3 AugBSP test soluble sulphide COD 311
Figure 6. 65: SP1 AugBSP test sulphate 312
Figure 6. 66: SP2 AugBSP test sulphate 312
Figure 6. 67: SP3 AugBSP test sulphate 312
Figure 6. 68: SP1 AugBSP test FSA 313
Figure 6. 69: SP2 AugBSP test FSA 313
Figure 6. 70: SP3 AugBSP test FSA 313
Figure 6. 71: SP1 AugBSP test OP 314
Figure 6. 72: SP2 AugBSP test OP 314
Figure 6. 73: SP3 AugBSP test OP 314
Figure 6. 74: SP1 AugBSP test carbonate alkalinty 315
Figure 6. 75: SP2 AugBSP test carbonate alkalinty 315
Figure 6. 76: SP3 AugBSP test carbonate alkalinty 316
Figure 6. 77: SP1 AugBSP test total alkalinty 316
Figure 6. 78: SP2 AugBSP test total alkalinty 316
Figure 6. 79: SP3 AugBSP test total alkalinty 317
Figure 6. 80: SP1 AugBSP test VSS 317
Figure 6. 81: SP2 AugBSP test VSS 317
Figure 6. 82: SP3 AugBSP test VSS 318

Figure 6. 83: SP1 AugBSP test VFA.....319
Figure 6. 84: SP2 AugBSP test VFA.....319
Figure 6. 85: SP3 AugBSP test VFA.....319
Figure 6. 86: SP1 AugBSP test pH.....320
Figure 6. 87: SP2 AugBSP test pH.....320
Figure 6. 88: SP3 AugBSP test pH.....320

List of Abbreviations Used

AD	Anaerobic Digester
ADM1	Anaerobic Digestion Model Number 1
ATA	Anaerobic Toxicity Assay
AugBMP Test	Augmented Biochemical Methane Potential Test
AugBSP Test	Augmented Biochemical Sulphide Potential Test
BPO	Biodegradable Particulate Organic
BSR	Biological Sulphate Reduction
BMP	Biochemical Methane Potential
COD	Chemical Oxygen Demand
CHP	Combined Heat and Power
CSTR	Continuously Stirred Tank Reactor
EDC	Electron Donating Capacity
FBSO	Fermentable Biodegradable Soluble Organic
FSA	Free and Saline Ammonia
GC	Gas Chromatograph
IWA	International Water Association
MD	Mean Difference
MSL	Model Specific Language
OFMSW	Organic Fraction of Municipal Solid Waste
OP	Orthophosphate
PSSAD	Parent Steady-State Anaerobic Digester
PE	Parameter Estimation
PST	Primary Settling Tank
PSS	Primary Sewage Sludge
PWM_SA_AD	Plant-Wide-Model South Africa for Anaerobic Digestion
SS	Sewage Sludge
SRB	Sulphate Reducing Bacteria
TKN	Total Kjeldahl Nitrogen
TP	Total Phosphate
UPO	Unbiodegradable Particulate Organic
USO	Unbiodegradable Soluble Organic

UCT	University of Cape Town
UCTADM1	University of Cape Town Anaerobic Digestion model 1
VFA	Volatile Fatty Acid
VS	Volatile Solids
VSS	Volatile Suspended Solids
WAS	Waste Activated Sludge
WRRF	Water Resource Recovery Facilities

Chapter 1: Introduction

The composition (chemical formula - $C_XH_YO_ZN_AP_B$) of organic substrates contained in wastewater have a profound effect on the performance of wastewater treatment unit operations such as anaerobic digestion. Anaerobic digestion has become an essential process for the treatment of organic matter, allowing energy to be recovered as a by-product. However, precise control over the anaerobic digester (AD) is required to operate the system at maximum efficiency. This precision can be achieved with the aid of mathematical bioprocess modelling; however, the input parameters to the system need to be known and well defined. This project proposes an analytical methodology for characterising and identifying the composition of the biodegradable organic substrates present in wastewater, focusing on primary sewage sludge (PSS).

1.1 Background to problem

Currently, the measurements performed at most wastewater treatment plants are not sufficient to allow for comprehensive characterisation of the sewage organics (which includes the required organic elemental composition). This can be problematic as many models and simulations depend on the composition of the various significant organic groups to be known and entered as an input. Municipal wastewater contains an array of organics which can include the organic fraction of municipal solid waste (OFMSW) and even food waste. This makes the composition and charge of the influent organics fed to the anaerobic digester challenging to establish, as the particulate biodegradable organics have high variability (Ekama and Brouckaert, 2020 in preparation).

Anaerobic digestion has become widely used as a critical process for the treatment of organic matter and energy recovery. However, in order to achieve the benefits associated with anaerobic digestion, precise system control is required (Jimenez *et al.*, 2014). Some factors directly influence the design and performance of ADs, of which many are related to the substrate characteristics and operating conditions. The physical and chemical characteristics of the organic substrate are the most influential, as they directly affect biogas production and process stability during anaerobic digestion (Zhang, 2007).

Currently, the most accurate methods for determining the AD input parameters are expensive, complicated and time-consuming. Therefore, a simple, affordable and effective characterisation method for identifying the input parameters, such as the biodegradable organic composition, is required (Botha, 2015). It is theoretically possible to determine the composition of the biodegradable organics in wastewater using bio-process stoichiometry and the conservation of mass. The bioprocesses transform the material entering the system from one chemical compound to another without a change in total material content flux exiting the system. Therefore, if the material content of the products produced by the reaction can be measured accurately, the material composition of the reactants entering the system can be determined using the relevant bio-process stoichiometry (Ekama and Brouckaert, 2020 in preparation).

The Biochemical Methane Potential (BMP) test (a test commonly used in industry to measure the biodegradability of an unknown substrate), provided the basis for developing a methodology to characterise the influent substrate adequately. Previous studies have shown that the biodegradability of the substrate stays the same whether digested aerobically or anaerobically (Ekama and Wentzel, 2006; Ikumi *et al*., 2014), and subsequently, the literature suggests that the batch tests can be performed in any environment. The BMP test makes use of both a control reactor (into which only the inoculum is placed) which sets the baseline for the products released, and a test reactor (into which both the inoculum and substrate is placed) which determines the influence of the biodegradable organics in the substrate. The BMP test was extended by developing two additional testing procedures, which took an array of additional measurements and aimed to increase the accuracy of the influent characterisation:

1. The Augmented BMP (AugBMP) Test: A test run identically to the BMP test but extended to include the methane and carbon dioxide production, the Chemical Oxygen Demand (COD), the aqueous phase volatile fatty acids (VFAs), the H_2CO_3 and total alkalinity, the ammonia and the orthophosphate concentrations, and the reactor pH. The additional variables are intentionally included to get specific parameters that are not routinely measured, allowing for a multi-dimensional approach to the influent characterisation.

2. The Augmented Biochemical Sulphide Potential (AugBSP) Test: A test aimed at improving the accuracy of the AugBMP test, as methanogenesis is replaced by Biological Sulphate Reduction (BSR). Furthermore, all measurements are conducted in the aqueous phase, minimising the gas measurement error commonly experienced during the BMP test.

The International Water Association (IWA) Anaerobic Digestion Model Number 1 (ADM1) (Batstone *et al.*, 2002) was designed to reach a common basis for AD model development and validation studies. However, due to a large number of model components, as well as the detailed substrate characterisation required, the model is susceptible to errors. The characterisation of the substrate is the most influential model input for correctly predicting the methane flow. There have been numerous studies aimed at defining default values of the kinetic and stoichiometric parameters. In order for the model to achieve realistic simulations, an adequate inflow characterisation is required (Astals *et al*., 2013). The identification of individual substrate compositions from ADM1 requires specific and not readily available analytical techniques. Many authors have proposed experimental procedures and methods that aim to characterise ADM1 variables. (Jimenez *et al*., 2014)

The PWM_SA_AD model (Ikumi *et al*., 2015) is a three-phase plant-wide model that extends the UCTADM1 model of Sötemann *et al*. (2005). The PWM_SA_AD model requires that the composition and mass of each group of influent organics be known. The substrate uptake, growth and death rates of each group of organisms are also adjustable. With the composition and mass of each organic correctly identified, the model determines the AD bioprocess products. Currently, the PWM_SA_AD model is coded inside DHI WEST® wastewater treatment software, which allows the user to perform an input parameter estimation (PE). This PE adjusts the input parameters, i.e. the composition of the organics, the organism growth rates, or both, such that the desired output concentrations are achieved (in this case the laboratory measurements performed on the AugBMP and AugBSP tests).

If successful, the procedure proposed for identifying the composition of the biodegradable organics in a chosen substrate, could be used to prevent AD failure caused by biological and biochemical reactions. Consequently, the operation efficiency of an AD can be maximised, as factors that are directly influenced by the influent organic composition, such as digester pH, can be foreseen and the necessary corrections made before digester failure.

1.2 Research questions and hypothesis

The characterisation of the biodegradable organics entering an AD are challenging to identify accurately. In municipal wastewater, the organics entering the WWTP comprise of an array of organic material from multiple sources. Consequently, it is not possible to isolate each individual organic present in the influent stream. Instead, the organics present in the influent wastewater are fractionated into groups based on their physical and biological properties.

The overarching aim of this thesis is how accurately the biodegradable portion of the influent organics can be isolated and characterised, with the primary focus on the composition that best represents the biodegradable organic group. In order to identify the composition of the biodegradable group in the organics, two new testing procedures are proposed: The Augmented BMP test and the Augmented BSP test. Each test tracks the organics and inorganics released into the reactor's aqueous and gas phases throughout the duration of the reaction.

Subsequently, it is this release of organic and inorganic material, due to the degradation of the influent biodegradable material, that allows for the composition of the organics to be identified, as mass is conserved in each of the proposed augmented batch tests. Therefore, it is hypothesised that the augmented batch tests are a reliable and accurate analytical method that can be performed, alongside mathematical modelling (used for data reconciliation), for identifying the composition of the biodegradable organics present in a chosen substrate. It is further hypothesised that, the AugBSP test will be favoured over the AugBMP test, as the gas measurement error associated with the BMP test is alleviated by measuring all products in the aqueous phase of the AugBSP test.

1.3 Project objectives

The main objective is to accurately identify the composition of the biodegradable organic group present in a chosen substrate. The composition will be identified using stoichiometric calculations, as well as the PWM_SA_AD model, making use of the PE function in WEST®. In order to identify and characterise the biodegradable organics present in a chosen substrate as accurately as possible, both experimental work, as well as mathematical modelling is required. The experimental work involves the design and setup of the required reactors, and

the modelling work requires that all of the collected data is correctly entered and analysed withing the PWM_SA_AD model. Therefore, to complete the main objective of developing an improved analytical methodology for identifying the composition of the influent biodegradable organics, the following seven tasks need to be accomplished.

1. Start and maintain two separate laboratory-scale ADs, one methanogenic and one sulphidogenic. Each of these respective ADs will be fed PSS continuously throughout the project and serve as the parent steady-state anaerobic digester (PSSAD). A PSSAD for each bioprocess is required to provide a seed inoculum for both the AugBMP and AugBSP experiments, respectively. The dimensions and operating specifications of each PSSAD are given in Chapter 3, Section 3.2.

2. Design and fabricate the AugBMP and AugBSP experimental reactors. The equipment required for the AugBMP experiment can be readily purchased, except for the water bath and support rig for the water columns, which need to be fabricated. The AugBSP experiment will be conducted in a completely sealed reactor with zero headspace. This type of reactor is not commercially available and subsequently needs to be fabricated. The specifications of both the AugBMP and AugBSP experimental reactors is given in Chapter 3, Sections 3.4 and 3.5.

3. Conduct extensive data collection for each respective system. This includes collecting data from each of the PSSADs, the AugBMP control and test reactors, and the AugBSP control and test reactors. The extensive data collection will include multiple measurements of each required constituent, which will be collected routinely throughout the experiments. The extensive data set aims to provide an adequate amount of data, such that the PE can identify the composition of the biodegradable organics, even with an elevated level of experimental error.

4. Accurately replicate the experimental conditions in WEST® using the PWM_SA_AD model. Therefore, in order for each of the respective PSSADs to be virtually replicated in the models, extensive testing on both the feed PSS to the ADs, as well as the PSSAD effluent is required. Furthermore, the effluent from the methanogenic and sulphidogenic PSSADs will then be used to seed the AugBMP and AugBSP experiments, respectively. Therefore, correctly characterising and modelling the

SSPADs will improve the accuracy of the modelled AugBMP and AugBSP experiments, as the degradation of residual biodegradable organics and active biomass affect the concentration of products released into the liquid and gas phases of the AugBMP and AugBSP reactors.

5. Using the extensive data sets obtained from the AugBMP and AugBSP experiments, a PE will be conducted in WEST® to identify the required input parameters, which allow for the best fit in the modelled experiments by minimising the error across the observed experiments. The required input parameters, such as the composition of the biodegradable organics in the chosen substrate or the hydrolysis rate, affect the concentration and the rate at which organics and inorganics are released into the reactor aqueous and gas phases. This portion of the project is crucial as data reconciliation will be required to accurately identify the composition of the biodegradable organics, as the PE minimises the error across the observed measurements by taking the mean.

6. The accuracy of the proposed augmented batch tests will be evaluated by identifying the composition for a relatively well-known substrate, casein. Casein will be used in both the AugBMP and AugBSP tests to compare the composition identified. The comparison is imperative as it is currently believed that sulphidogenesis and methanogenesis are closely linked and differ mainly with the electron acceptor utilised. If a significant discrepancy is observed, the core principles of each proposed augmented batch test may need to be revised, or the stoichiometry and kinetics in the PWM_SA_AD model may need to be adjusted.

7. Finally, the AugBMP and AugBSP tests will be used to identify the composition of the biodegradable particulate organics present in PSS.

1.4 Specific objectives

1. Start and maintain a parent steady-state anaerobic digester for both the methanogenic and sulphidogenic systems, such that a stable inoculum is readily available.

2. Conduct both the AugBMP and AugBSP tests on a known substrate, casein, such that the compositions identified from each test can be compared to the literature stated compositions.

3. Conduct both the AugBMP and AugBSP tests on an unknown substrate, PSS, such that the composition of the biodegradable particulate material is identified.

4. Using the stoichiometric approach, identify the composition of the biodegradable substrate (both casein and PSS) using the measured starting and ending concentrations of the constituents present in each of the control and test reactors.

5. Using the dynamic mathematical anaerobic digestion model (PWM_SA_AD) of Ikumi *et al*. (2015), as well as data reconciliation in the form of parameter estimation, identify the composition of the biodegradable substrate (both casein and PSS) and the kinetic parameters using the entire data set for the measured concentrations of the constituents present in each of the control and test reactors.

1.5 Scope and Limitations

The primary focus of this project will be to identify the composition of the biodegradable organics present in a chosen substrate (either casein or PSS). Furthermore, the project will experimentally calibrate current mathematical models and bioprocess stoichiometry that can theoretically predict the composition of these organics.

Due to the extensive work required for this thesis, specific details were not possible to investigate further, and subsequently literature-based assumptions needed to be made. For instance, the composition of the unbiodegradable particulate organics (UPO) was determined using mass ratio values from the literature. These mass ratios for UPO have been around for decades in activated sludge models since the steady-state model of Marais and Ekama (1976). However, the scope of this thesis did not aim to improve or adjust the UPO composition, and subsequently the literature values were used throughout the thesis. In addition, specific input parameters, such as growth and death rates, were taken as defined in the literature. More details on these specific assumptions are given where necessary.

The experimental testing procedures include a full analysis of two steady-state anaerobic digesters, one methanogenic and one sulphidogenic, as well as the proposed augmented batch experiments. The accuracy of the expected results will be directly influenced by the proposed testing procedures, which have been modified from existing methods for this investigation. If the project is unsuccessful in characterising the composition of the biodegradable organics, either the testing procedures or their associated models will be adjusted accordingly to obtain the best possible outcome in the given timeframe.

The stoichiometry of each bioprocess is based on the conservation of strict elemental mass balances. Therefore, each element, present as input reactants, should be equal to the output element products, which may take on a different form or speciation. Experimentally this can be problematic, as measuring various compounds associated with the elements can be challenging. For example, the AugBMP test converts the influent biodegradable COD into various products, of which some have a measurable COD component, such as the biomass and the CH_4. The gas produced by this reaction contains both CO_2 and CH_4, of which CO_2 has no COD. The problems and errors associated with gas measurement significantly increase the difficulty of achieving an elemental C balance, as gas measurements are prone to error and difficult to conduct accurately. Therefore, in cases where a mass balance is not achieved, the PWM_SA_AD model (which is mass balanced) will be used to reconcile the data to identify the composition using the PE function, which minimises the error across all of the observed measurements.

The AugBSP experiment aims to obviate the gas production, as it is done inside a sealed batch reactor with no headspace, thus allowing all measurements to be taken in the aqueous phase using wet chemistry testing procedures. However, one of the most considerable limitations of the project is the accuracy of the testing procedures, the assumptions made, and the equipment and funding available to validate the experimental and modelling work conducted.

The substrate in this thesis was limited to casein and PSS. However, the analytical testing methods proposed can be used on any substrate, either soluble or particulate. However, at its current development, the PWM_SA_AD model is unable to solve for both biodegradable soluble and particulate organics simultaneously, as the number of unknown parameters is too high. However, future work is proposed to address a simultaneous identification of both soluble and particulate substrates.

Furthermore, the scope is also limited by the PWM_SA_AD model and the defined bioprocesses. The most current version of the PWM_SA_AD model was used for this project. However, small changes were made to specific components within the model to achieve the desired outcomes. However, it was not in the scope of this thesis to change the kinetic equations or stoichiometry of the bioprocesses, or to perform a sensitivity analysis. Also, the PWM_SA_AD model, and therefore the identification of the composition, is limited based on the available components and reactions present within the model (e.g., as heavy metals are not currently components of the PWM_SA model, it was not possible to include them in the elemental composition of the PSS).

1.6 New knowledge contribution

This project contains several components that will contribute to gaining a better understanding of how methanogenic and sulphidogenic systems operate under batch conditions when fed PSS, with the overarching aim of using each respective system to identify the composition of the biodegradable organics fed to it.

Currently, there exists no definitive method, which is easily accessible and does not require expensive elemental analysis, for identifying the composition of the biodegradable organics present in wastewater. The general approach is to assign a single composition to each group. This can be achieved by assigning a COD, C, N and P value, such that the $C_XH_YO_ZN_AP_B$ matches the proportion and composition of fats, carbohydrates and lipids in each of the fermentable biodegradable soluble organics (FBSO), non-settleable biodegradable particulate organics (BPO) and settleable BPO. However, assigning a composition to each of these groups is time consuming as trial and error is required, and the composition may not represent the release of material into the aqueous and gas phases accurately.

Therefore, the project proposes two augmented analytical methods (the AugBMP and AugBSP tests) for identifying the biodegradability and the composition of the organic material present in an unknown substrate. Additionally, the project will make use of the PWM_SA_AD model to identify the unknown input parameters using experimentally measured data. The use of the PWM_SA_AD model will not only calibrate the model but will identify the key parameters required for fitting the model to the observed data. The use of the dynamic PWM_SA_AD

model allows for the AD process kinetic parameters to be identified. However, the overarching aim of the thesis is to develop a method that can be used to characterise the influent biodegradable organics for use in either a simple steady-state spreadsheet model or a more complex dynamic model. The contribution of new knowledge is broken down as follows:

1.6.1 Development of augmented analytical testing equipment

The AugBMP test was developed in an attempt to improve the accuracy of the BMP test. The AugBMP test introduces a broader spectrum of measurements that include: COD, VFA, Free and Saline Ammonia (FSA), Orthophosphate (OP), Volatile Suspended Solids (VSS), Alkalinity via the 5-point titration method, methane potential and pH. The addition of these measurements allows for a more holistic understanding of the biological interactions within the system. For instance:

- The release of inorganics such as FSA and OP indicates the hydrolysis degradation rate of the organics
- The build-up of VFAs indicates the uptake rate of the acetoclastic organisms and can identify possible inhibition
- The measurement of COD aims to track material through the system by performing a mass balance.

Additionally, the AugBSP test was developed to alleviate the gas measurement problems associated with biogas production, as found in methanogenic systems. The experiment is conducted in a completely sealed purpose-built reactor with zero headspace. This lack of headspace allows for all constituents to remain in the aqueous phase, which can subsequently be measured using routine wet chemistry analysis. The AugBSP test includes many of the same measurements as the AugBMP test, such as COD, FSA, OP, VSS, VFA, Alkalinity and pH, with additional measurements such as the sulphide and sulphate concentrations. The development of these tests will allow future work to be conducted on sulphidogenic systems in which all measurements are performed in the aqueous solution.

1.6.2 Identification of wastewater organics

The project will conduct both AugBMP and AugBSP experiments using PSS and casein as a substrate. The primary objective will be to investigate if the composition (chemical formula) of the organic substrate can be identified using each respective testing procedure. If the composition can be determined with high accuracy, modelling the anaerobic digestion process can be significantly improved as it relies heavily on identifying the composition of the biodegradable organics fed to it. The identification of the substrate composition will allow current models to be calibrated on certain parameters such as biogas and methane production, substrate biodegradability and potential pH and alkalinity changes. Therefore, the identification of the organic substrate aims to improve the efficiency and predictability of anaerobic digestion systems and their associated models.

Identifying the composition of the influent wastewater organics will allow designers and plant operators to track the various elements and materials through the entire system. The composition of the influent organics determines the concentrations of the products that the system will produce. This is important for several reasons, the two most important being effluent quality and cost. The composition of the organics will also affect the pH, nutrient recovery and removal, as well as various system operating procedures. From a cost perspective, knowing the composition of organics is extremely useful. For example, it is possible to predict the quantity of methane and carbon dioxide produced through anaerobic digestion, by determining the amount of elemental carbon present, or the amount of struvite produced by determining the elemental phosphorus and nitrogen present. The recovery of material through wastewater treatment not only ensures the preservation of clean water but allows for economic benefits as well, which directly relate to sustainable practices.

1.6.3 Calibration of the mathematical model

The anaerobic digestion model used was the PWM_SA_AD model (Ikumi *et al*., 2015). This three-phase plant-wide model that extends the UCTADM1 model of Sötemann *et al*. (2005) to include the hydrolysis of multiple organic types (PS, ND WAS, NDEBPR WAS and PS-WAS blends), the Ekama and Wentzel (2004) ISS model and the Brouckaert *et al*. (2010) speciation model which facilitates ionic speciation and multiple mineral precipitation and calculation of

pH. The model has recently been extended further by Ghoor *et al*. (2020) to include biological sulphate reduction (BSR). The mechanisms and pathways of the PWM_SA_AD model differ to that of ADM1. The PWM_SA_AD model has been tailored towards identifying and isolating the separate groups of organics present in wastewater. The PWM_SA_AD model achieves this by assigning each specific group of organics a composition and mass, from which all other constituents (COD, Total Kjeldahl Nitrogen (TKN), Total Phosphorus (TP)) can be determined. This framework allows for the composition of the BPOs to be isolated and identified using PE.

Therefore, the experimental data collected will be used as the objective values for the PWM_SA_AD model. The experimental data will be collected daily such that the model can be examined under both steady-state and dynamic conditions. If the results differ significantly, the root of the discrepancy will be investigated, and the appropriate changes made. It is unlikely that the models will need to be reconstructed, but they may require a change in stoichiometry and kinetic rates. Therefore, evaluating the model's accuracy to determine and predict the bioprocess products also forms part of the proposed project. This aims to give a holistic investigation into the parameters affecting the two systems in question, including the development of the testing equipment, the experimental observations, and finally leading into the system modelling. The outcome of the model calibration will help to identify the strengths and weaknesses of the model and propose recommendations for future work.

1.7 Thesis Structure

The content of the thesis was divided into seven chapters. The background for the investigation and the research questions are introduced in Chapter 1, which also discusses the project objectives, limitations and new knowledge contributions. The literature regarding the biological processes and how they are represented in the models, the guidelines for conducting BMP tests, the substrates used for the investigation, the mass balanced stoichiometry, and the parameter estimation function are discussed in the literature review of Chapter 2. The materials and methods for operating the required reactors, the analytical procedures used, the characterisation and identification of the biodegradable organics, as well as the modelling, are discussed in Chapter 3. The inoculum required for the augmented batch control and test reactors was grown using steady-state parent anaerobic digesters, which were thoroughly

tested, and included steady-state modelling to quantify the active biomass present, which is explained in Chapter 4.

The inoculum from the steady-state parent anaerobic digesters was then taken and placed in both the augmented batch control and test reactors. The augmented batch control reactors were used to set the baseline to quantify the material released into the system due to the residual biodegradable material present in the inoculum, which is explained in Chapter 5. Chapter 5 includes the seeding, the results obtained, the stoichiometric composition identification, and the modelling and parameter estimation for the augmented batch control reactors. Chapter 6 describes how the compositions of the biodegradable organics in the casein and PSS were determined stoichiometrically, as well as using the parameter estimation function and the PWM_SA_AD model. The results from the parameter estimation on the residual organics in the inoculum from Chapter 5 were used for the augmented batch test reactors in Chapter 6. The casein used was a stable laboratory grade casein, which allowed for the composition identified by both the AugBMP and AugBSP tests to be compared. This comparison evaluated the accuracy of the AugBMP and AugBSP test to determine the composition of a known substrate, as well as evaluating whether the AugBSP test could potentially replace the BMP test. The PSS was used as the unknown substrate, for which identifying the composition is important for improving the efficiency of anaerobic digesters. Finally, the report is concluded, and recommendations are made for improving the accuracy of the proposed methodology in Chapter 7. The structure of the thesis is shown visually in Figure 1.1.

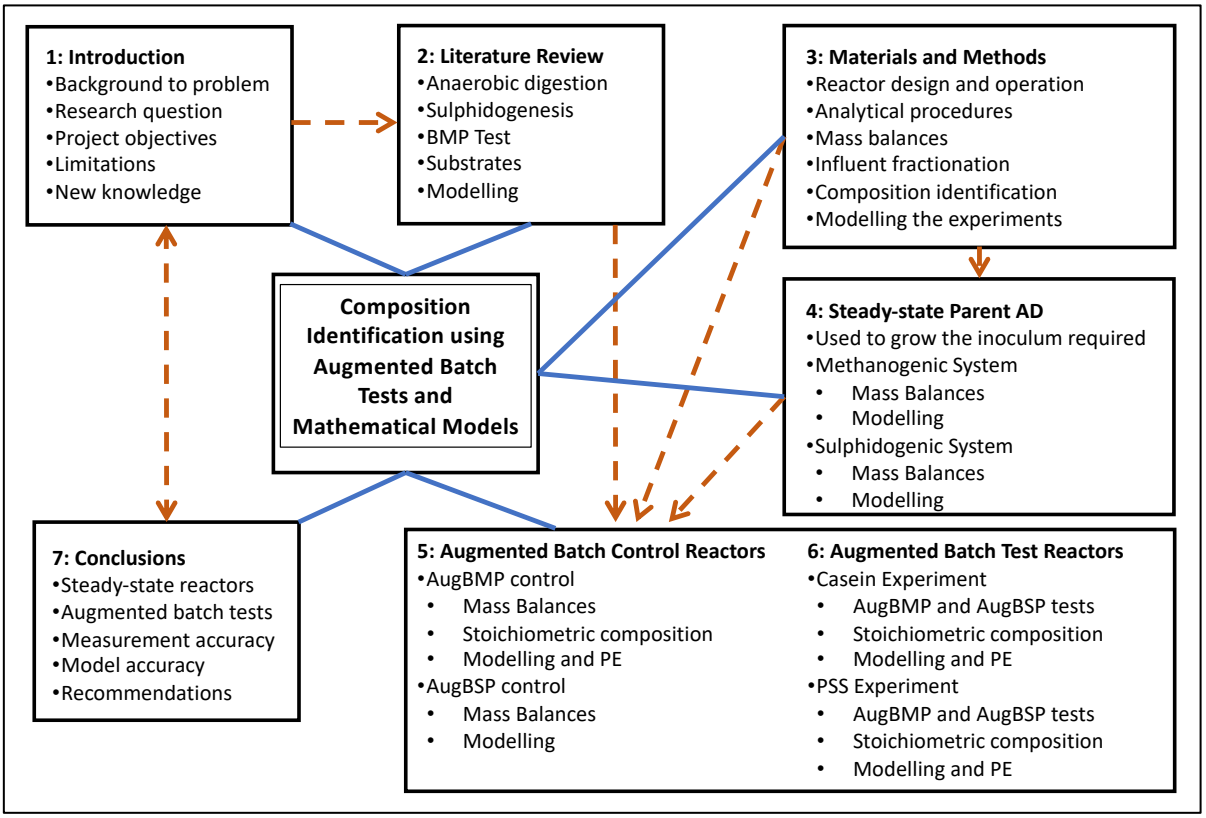

Figure 1. 1: Mind map of the thesis structure

Chapter 2: Literature Review

2.1 Introduction

The main research objectives were described in Chapter 1. In this chapter, the relevant literature concerning the various components of the thesis is reviewed and discussed. The review will focus on topics such as anaerobic digestion, Biological Sulphate Reduction (BSR), analytical testing procedures (such as the BMP test), and mathematical bioprocess modelling.

2.2 Introduction to anaerobic digestion

For more than a century, anaerobic digestion has been used as an effective process for stabilising sewage sludge (SS) at wastewater treatment plants (Astals *et al.*, 2012). Anaerobic digestion can be referred to as the process in which organic carbon is degraded by fermentation through subsequent oxidations and reductions to its most oxidised form (CO_2), and its most reduced form (CH_4) (Angelidaki *et al.*, 2003). Anaerobic digestion (also referred to as biological gasification) produces methane from biomass, which utilise organic substrates for energy, via the mechanism of biological methanogenesis (Chynoweth *et al.*, 2001). The process is facilitated by a consortium of different organisms which inhabit numerous environments, including animals' intestines, landfills and sediments. The process requires a low redox potential, occurring in systems in which no oxygen is present. Under the right conditions, anaerobic digestion is a very efficient way for removing biodegradable organic compounds, producing various mineralised compounds such as methane (CH_4), phosphate (PO_4^{3-}) and sulphide (S^{2-}) as by-products (Henze *et al.*, 2008). The gas produced as a result of the methanogenic anaerobic digestion process is referred to as biogas. Biogas is composed primarily of methane and carbon dioxide with traces of hydrogen sulphide (H_2S) and water vapour (Chynoweth *et al.*, 2001).

The most significant advantages of anaerobic digestion are that it can be conducted in technically simple systems; it can be applied at any scale; it produces far less sludge than aerobic systems; the sludge that is produced is relatively stable; and the process produces useful methane gas as a by-product (Henze *et al.*, 2008). When methane is produced under controlled conditions, it is seen as an ideal fuel compared to fossil fuels, as it produces few atmospheric pollutants and emits lower quantities of carbon dioxide per unit energy. Anaerobic digestion is

a beneficial biofuel production process, as 2-3 times more Gibbs Free Energy can be recovered, compared to other biofuel production processes such as bioethanol or biodiesel (Kleerebezem *et al*., 2015). Furthermore, the production of methane via anaerobic digestion would benefit humanity as it could potentially lower the dependence on energy generated by fossil fuels and reduce the associated environmental impacts. (Chynoweth *et al.*, 2001).

Wastewater treatment plants have used anaerobic digestion for years in both energy production and waste treatment. Specifically, the anaerobic process is used in four sectors of waste treatment (Angelidaki *et al.*, 2003):

1. For the treatment of PSS, collected and concentrated in the Primary Settling Tank (PST), and for the treatment of Waste Activated Sludge (WAS), produced during the aerobic treatment of municipal sewage (Gu Shin *et al.*, 2010). Either the PSS, the WAS or both are treated in an Anaerobic Digester (AD) in order to stabilise the final sludge. This treatment process produces biogas, which can be used to recover the energy required by the treatment plant for heating or aeration.
2. For the treatment of industrial wastewaters containing high concentrations of organic material.
3. For the treatment of livestock waste in order to recover energy or improve the fertilising qualities of manure.
4. For the treatment of OFMSW, lowering the quantity of organic material sent to landfills and incineration plants.

The anaerobic digestion process is not limited to biological methanogenesis and can occur in systems containing an array of electron acceptors. When sulphate (SO_4^{2-}), sulphite (SO_3^{2-}), or thiosulphate ($S_2O_3^{2-}$) are present in the wastewater, Sulphate Reducing Bacteria (SRB) can use several of the intermediates of the anaerobic process, such as acetate, propionate and hydrogen, as a source of energy. The SRB convert sulphate, the electron acceptor, into hydrogen sulphide, and in the presence of sulphate, compete for the available organic substrate with the methanogens (Ristow *et al.*, 2005; Henze *et al.,* 2008). Furthermore, the presence of Fe^{3+} has a significant effect on the anaerobic digestion process. Bodegom and Stams (1999) found that Fe^{3+} reduction suppressed CH_4 almost completely as ferric-iron reducers can utilise acetate and H_2 at concentrations far below that of methanogens or sulfate reducers (Lovely and Phillips, 1987).

2.3 Anaerobic digestion processes and microbiology

This particular section aims to highlight critical aspects of the microbial processes that occur during anaerobic digestion. Furthermore, this section highlights how these processes are represented in current mathematical bioprocess models. The models chosen for comparison are the Anaerobic Digestion Model No.1 (ADM1) (Batstone *et al.*, 2002) and the University of Cape Town Anaerobic Digestion Model No 1 (UCTADM1) (Sötemann *et al*., 2005), which forms part of the Plant Wide Model South Africa (PWM_SA) (Ikumi *et al.,* 2015). The PWM_SA_AD model is a sub-model contained inside the PWM_SA model, which is currently used by the Water Research Group (WRG) at UCT for simulating anaerobic digestion. Subsequently, the PWM_SA_AD model is regularly updated following ongoing research within the group. Therefore, the PWM_SA_AD model was selected for the modelling component of this project as it contained the required structure for determining the composition of the influent organics. However, ADM1 is a popular choice amongst bioprocess modellers when simulating anaerobic digestion. Therefore, for readers who are unfamiliar with PWM_SA_AD but have prior knowledge on ADM1, the differences between each model's representation of the anaerobic digestion bioprocesses are briefly outlined and explained in this section. Additionally, alternative kinetic models are available such as Benneouala *et al.* (2017) and Jimenez *et al.* (2020).

Four main groups of organisms mediate the anaerobic digestion process. These groups are categorised as acidogens (acid-forming), acetogens, acetoclastic methanogens and hydrogenotrophic methanogens (Mosey, 1983). Gujer and Zehnder (1983) identified six distinct processes performed by these organisms inside an AD:

1. Hydrolysis of biopolymers
    i. Hydrolysis of proteins
    ii. Hydrolysis of carbohydrates
    iii. Hydrolysis of lipids
2. Fermentation of amino acids and sugars
3. Anaerobic oxidation of long-chain fatty acids and alcohols
4. Anaerobic oxidation of intermediate products such as volatile acids (except for acetate)
5. Conversion of acetate to methane
6. Conversion of hydrogen to methane.

The processes mentioned above can be arranged into three overall biochemical steps: acidogenesis, acetogenesis and methanogenesis, and include an extracellular disintegration step and an extracellular hydrolysis step. Of the processes mentioned above, three of them, hydrolysis, acidogenesis and acetogenesis, have parallel reactions (Batstone *et al.*, 2002). The reaction scheme for anaerobic digestion, as represented by ADM1, is summarised in Figure 2.1.

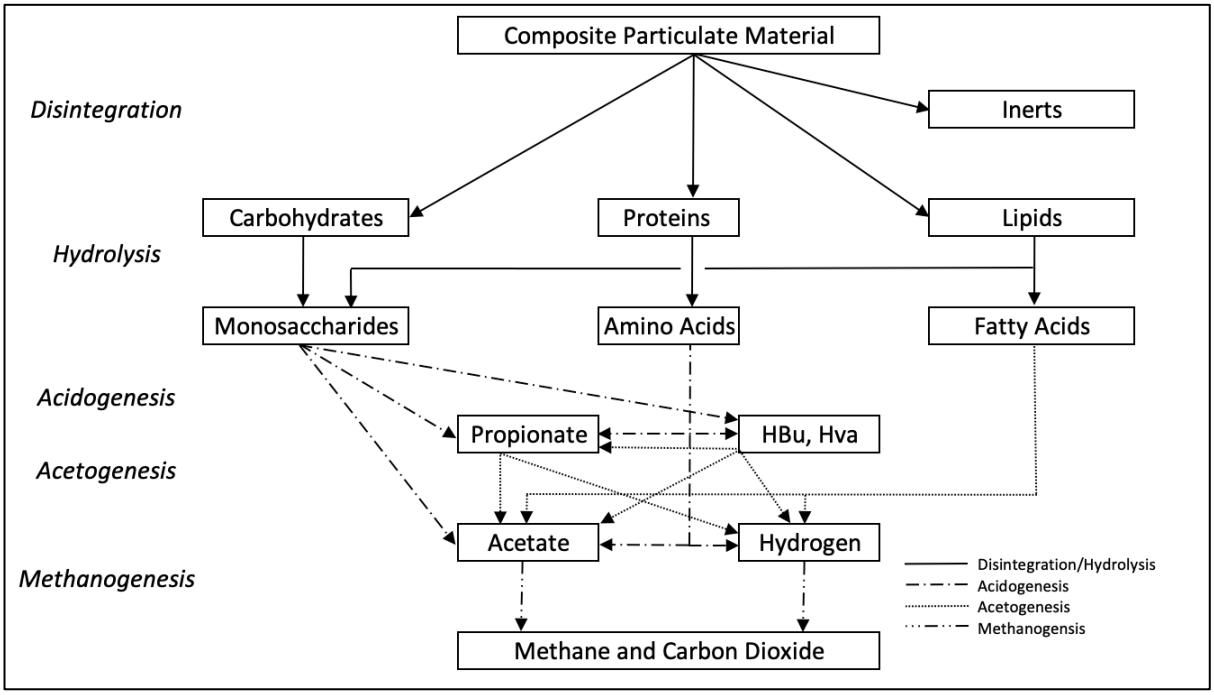

Figure 2. 1: ADM1 anaerobic digestion pathways

With these processes in mind, Sötemann *et al.* (2005) proposed the UCTADM1, the reaction scheme for which is shown in Figure 2.2. The UCTADM1 modified the Gujer and Zehnder (1983) reaction scheme such that:

1. The hydrolysis of carbohydrates, proteins and lipids were condensed into a single hydrolysis step acting on a generic organic material, which is represented by $C_XH_YO_ZN_AP_B$ (McCarty, 1974). This approach requires the determination of the C, H, O, N and P content, so that the X, Y, Z, A and B values can be identified.
2. Following the single hydrolysis step, a single end product was required. The end product chosen was glucose.
3. With a single hydrolysis step, the separate anaerobic oxidation of fatty acids was no longer required.

4. Instead of a fixed proportion of hydrolysis end products being converted to propionate and butyrate, and the remaining portion converted directly to acetate, the influence of the hydrogen partial pressure on acidogenesis of glucose to propionate, as proposed by Sam – Soon *et al.* (1991), was included.

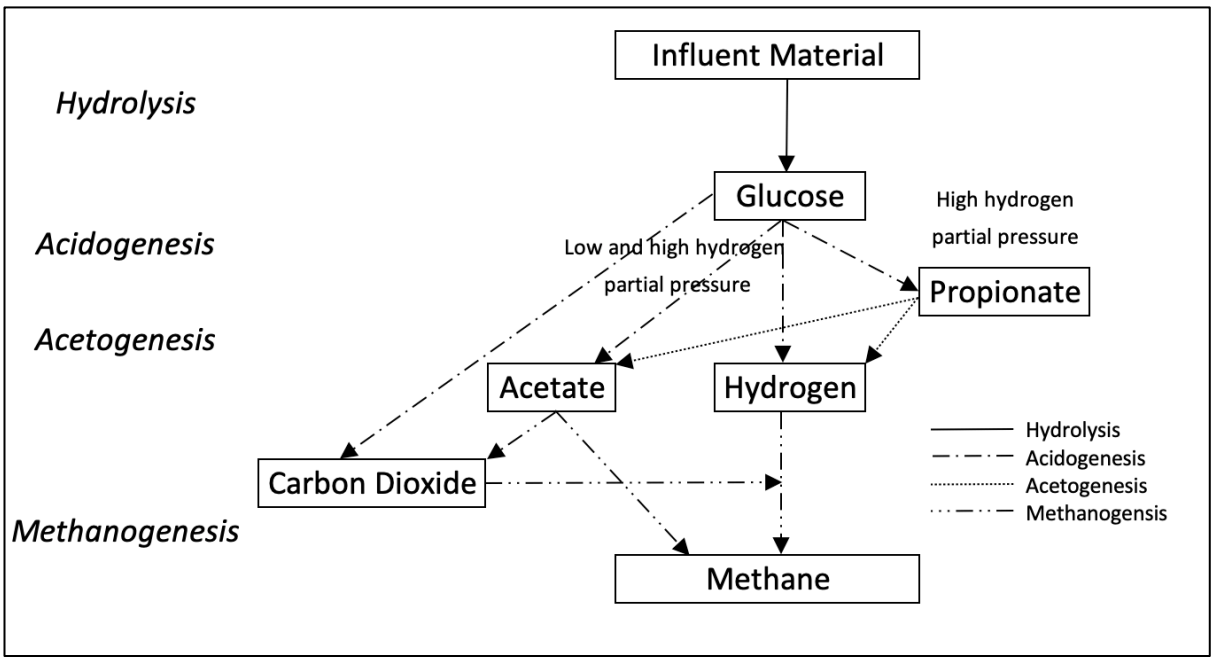

Figure 2. 2: PWM_SA_AD methanogenic pathway

2.3.1 Hydrolysis

Hydrolysis is the process by which polymers and complex organic material are broken down via extracellular enzymatic action into monomers and soluble substrates (Batstone *et al.*, 2002; Ristow *et al.*, 2005). The hydrolysis step is necessary as particulate material cannot be transported across the cell membrane and subsequently needs to be broken down into smaller units that can be utilised (Ristow *et al.*, 2005). The hydrolysis process is mediated by the acidogens so that the products (relatively simple compounds) can be further fermented or anaerobically oxidised (Sötemann *et al*., 2005). This process is especially important when using a particulate substrate such as PSS.

There is much debate among authors on the exact products formed by the hydrolysis process. When constructing ADM1, Batstone *et al.* (2002) defined the most significant products formed from the degradation of carbohydrates, proteins and lipids to be monosaccharides, amino acids

and long-chain fatty acids, respectively. This follows the approach defined by Gujer and Zehnder (1983), which supported the work of Kaspar and Wuhrmann (1978). Furthermore, Batstone *et al.* (2002) identified the process of disintegration and hydrolysis to be extracellular and non-biological.

The disintegration step is fundamental for the breakdown and solubilisation of complex organics to utilisable soluble substrates. The step also results in the production of a low portion of inert particulate and soluble material. The disintegration step is crucial when modelling WAS or PSS, as it represents lysis of whole cells and the separation of composites. The disintegration step is thought to precede more complex hydrolytic steps and is generally used when the primary substrate can be described and modelled using lumped kinetics and biodegradable parameters. Disintegration combines an array of steps such as lysis, non-enzymatic decay, phase separation and physical breakdown. (Batstone *et al.*, 2002)

Batstone *et al.* (2002) defined hydrolysis as "the degradation of a defined particulate or macromolecular substrate to its soluble monomers", of which the most crucial particulate substrates were identified to be carbohydrates, proteins and lipids. For ADM1, this results in the formation of monosaccharides, amino acids and long-chain fatty acids, which subsequently become the substrates for the acidogenesis process. It is believed that the hydrolysis process is catalysed by the organism directly benefiting from the compounds produced through two distinct mechanisms (Batstone *et al.*, 2002):

1. The organism releases an enzyme into the bulk liquid which interacts with the soluble or particulate substrate, resulting in simple soluble substrates that can be directly utilised by the organism.
2. The organism attaches itself to a particle and produces enzymes in the particle's proximity, absorbing the simple soluble products released.

The hydrolysis mechanism present in PWM_SA_AD follows the approach developed in the UCTADM1 (Sötemann *et al*., 2005). This includes the simplification of the products formed during the hydrolysis step from the three defined above to just one, glucose. The simplification recognises that measuring the concentrations of carbohydrates, proteins and lipids present in sewage sludges are challenging to perform routinely and accurately. Therefore, the process of hydrolysis acts on a single generic influent organic material representing the sewage sludge

which is defined as $C_XH_YO_ZN_AP_B$ (McCarty, 1974). The simplification is reasonable as the end products of hydrolysis and acidogenesis of the three organic groups (monosaccharides, amino acids and long-chain fatty acids) generally result in the same compound, namely short-chain fatty acids.

Therefore, following the simplification of the hydrolysis process in UCTADM1, the formation of three separate hydrolysis products (monosaccharides, amino acids and long-chain fatty acids) are no longer required. Glucose was chosen as the end product, as Mosey (1983) adequately established the pathways for its metabolism. Furthermore, the acidogenic/fermentation processes that convert glucose to SCFA are unlikely ever to be rate-limiting. Subsequently, the accumulation of glucose, even under digester failure, will not occur (Sötemann *et al*., 2005). Furthermore, the COD, C, H, O and N balances are maintained as water and carbon dioxide are taken up from the bulk liquid of the digester to generate glucose from the sewage sludge.

The approach of the PWM_SA_AD model, which contains UCTADM1, is advantageous when characterising the organic constituents present in wastewater. Currently, eight groups of organics present in wastewater can be identified: volatile fatty acids (VFA), readily fermentable soluble organics (FBSO), unbiodegradable soluble organics (USO), biomass, biodegradable particulate organics (BPO), unbiodegradable particulate organics (UPO), of which BPO and UPO can be separated into settleable and non-settleable (Ekama, 2011). The structure of PWM_SA_AD allows for each group of organics to have their unique composition (chemical formula). Subsequently, the compositions of each of these groups can be determined using routinely available wet chemistry analysis, such as COD, TKN, FSA, TP, OP, VSS, Alkalinity and pH.

2.3.2 Acidogenesis

Acidogenesis is mediated by acidogens, acid-forming organisms, which are fast-growing and have a minimum doubling time of around thirty minutes. The organisms ferment glucose and produce a mixture of biomass, intermediates such as propionate and butyrate, as well as acetate and hydrogen (Mosey, 1983; Gujer and Zehnder, 1983). The fermentation of monosaccharides and amino acids is defined as a microbial process in which organic compounds serve as both

the electron donors, as well as the electron acceptors (Gujer and Zehnder, 1983). This implies that no additional electron acceptors or donors are required (Batstone *et al*., 2002).

The preferred product of acidogenesis is the conversion of glucose to acetate, as it provides the organisms with the most significant energy yield for growth, as well as supplying the acetoclastic methanogens with their primary substrate for methane production. (Mosey, 1983). However, the organisms can also produce propionic and butyric acids as a response to increased concentrations of hydrogen during surge loads. The formation of propionic acid causes the process of hydrogen production to become reversed such that the organisms can control the redox potential during heavy surge loads.

Batstone *et al.* (2002) chose to use glucose as ADM1's main monomer. There are many possible end-products when using glucose as a substrate; however, acetate, propionate and butyrate were selected as the most significant for monosaccharide acidogenesis. Additionally, simultaneous acidogenesis of amino acids occurs in two possible pathways: Stickland oxidation-reduction paired fermentation or the oxidation of a single amino acid.

The anaerobic oxidation of fatty acids occurs separately to that of acidogenesis of monosaccharides and amino acids. The anaerobic oxidation of fatty acids is the microbial process in which molecular hydrogen is the main sink for electrons (Gujer and Zehnder, 1983). Therefore, an external electron acceptor is required, and the process subsequently falls under acetogenesis (Batstone *et al.*, 2002).

The PWM_SA_AD model includes the influence of the hydrogen partial pressure on the acidogenesis of glucose to acetate and propionate, which was previously proposed by Sam-Soon *et al.* (1991). It is believed that this inclusion of the hydrogen partial pressure allows for a better description of AD failure. Furthermore, the acidogenesis process was separated into two sub-processes: The generation of acetic and propionic acids with H_2 and CO_2 under high hydrogen partial pressure conditions, and the generation of only acetic acid together with H_2 and CO_2 under low hydrogen partial pressures. The generation of butyrate and higher SCFAs were not considered, as these are usually found in low concentrations in sewage sludges. The PWM_SA_AD model does not consider the anaerobic oxidation of fatty acids, as a single hydrolysis step occurs, converting all biodegradable organics to glucose, and therefore, producing no long chain fatty acids.

2.3.3 Acetogenesis

The acetogenesis process is mediated by acetogenic bacteria, which as their name implies, synthesise acetate from the reduction of CO_2 and organic acids such as propionic and butyric acids (Mosey, 1983; Angelidaki *et al.*, 2011). As previously mentioned, an external electron acceptor is required for acetogenesis as there is no internal electron acceptor for the oxidation of higher organic acids to acetate. Therefore, this oxidation step requires the organisms to utilise an additional electron acceptor such as hydrogen ions or carbon dioxide for the formation of hydrogen gas or formate (Batstone *et al.*, 2002).

The acetogens are crucial in the anaerobic digestion process as methane-producing bacteria are unable to metabolise propionate and butyrate directly. However, these organisms grow relatively slowly even under optimum conditions, as the reactions that they perform are energetically difficult and are easily inhibited by the accumulation of dissolved hydrogen gas (Mosey, 1983).

Included in the acetogenesis process is the degradation of long chain fatty acids, which above propionate occurs by β-oxidation (Gujer and Zehnder, 1983; Batstone *et al.*, 2002), as shown by Jeris and McCarty (1965). In ADM1, three primary fatty acid substrates of importance are identified: butyrate, valerate and LCFA. Subsequently, three acetogenic bacterial groups were proposed: one for propionate, one for butyrate and valerate, and one for LCFA.

For the PWM_SA_AD model, acetogenesis occurs as the primary mechanism for removing propionate from the bulk liquid. When the hydrogen partial pressure is sufficiently low, acetogens convert propionic acid, which was generated under high hydrogen partial pressure, to acetic acid (Sötemann *et al*., 2005). The acetic acid is then utilised by the acetoclastic methanogens for the production of CH_4 and CO_2.

2.3.4 Acetoclastic methanogenesis

The process of acetoclastic methanogenesis is mediated by acetoclastic methanogens, classified as obligate Archaea anaerobes, which convert acetic acid into a mixture of CH_4 and CO_2 (Mosey, 1983; Demirel and Scherer, 2008). The majority of methane (70%) produced in

anaerobic digestion is produced by the decarboxylation of acetic acid, subsequently making acetate the primary precursor for CH_4 production (Gujer and Zehnder, 1983; Ristow *et al.*, 2005).

Two organisms responsible for the fermentation of acetic acid to carbon dioxide and methane are *Methanothrix spp*. and *Methanosarcina spp*. The species differ in both morphology and growth kinetics. *Methanothrix spp.* are good scavengers with a high affinity for acetate, but are slow-growing, with minimum doubling times around 4 days. *Methanosarcina spp*. are less effective scavengers but grow faster, with a minimum doubling time of around 1.5 days (Gujer and Zehnder, 1983; McCarty and Mosey, 1991). Batstone *et al.* (2002) include *Methanosaeta* amongst acetoclastic methanogens as a genera that dominate below 10^{-3}M acetate, having lower yields, higher k_m values, lower K_S values and higher sensitivity to pH than *Methanosarcina.* Furthermore, Batstone *et al.* (2002) advise that a single group of acetoclastic methanogens be used, adjusting the kinetics and inhibitory parameters based on the model's intended application and experimental observations.

Acetoclastic methanogens are slow-growing, as previously indicated by their large doubling times, and are generally the most susceptive to inhibitory compounds. Inhibition of methane production can occur due to high concentration of anaerobic digestion products such as acetic acid, ammonia and undissociated hydrogen sulphide (Ristow *et al.*, 2005). In order for optimal digester operation, acetogens and acetoclastic methanogens need to utilise propionate and acetate respectively as soon as they are produced, such that a neutral digester pH can be maintained (Sötemann *et al*., 2005). Both the ADM1 and the PWM_SA_AD models recognise acetoclastic methanogenesis as a single process, in which acetate (and inorganics such as NH_3) are taken up to form CO_2, CH_4 and biomass (Batstone *et al.,* 2002; Sötemann *et al*., 2005).

2.3.5 Hydrogenotrophic methanogenesis

Hydrogenotrophic methanogenesis is mediated by hydrogen-utilising organisms that convert hydrogen and carbon dioxide to methane and water. The organisms are effective scavengers and have a high growth rate, with a minimum doubling time around 6 hours and remove the majority of hydrogen present in the digester (Mosey, 1983). The partial pressure of hydrogen present in the digester during the anaerobic digestion process is crucial. A syntrophic

relationship between acetogens and hydrogenotrophic methanogenesis exists to maintain an extremely low hydrogen partial pressure to ensure favourable thermodynamic conditions for the conversion of volatile acids and alcohols to acetate (Speece, 1983). Subsequently, hydrogenotrophic methanogens are essential for stable and efficient anaerobic digester performance and regulate the formation of volatile acids, as hydrogen controls the rates at which propionic and butyric acids are converted back to acetic acid (Mosey, 1983; Demirel and Scherer, 2008).

Additionally, as with the acetoclastic methanogens, the hydrogenotrophic methanogens are also sensitive to pH. However, decreasing reactor pH would cause significant inhibition to the acetoclastic methanogens before affecting the hydrogenotrophic methanogens. As shown above for acetoclastic methanogenesis, both the ADM1 and the PWM_SA_AD models recognise hydrogenotrophic methanogenesis as a single process, in which hydrogen, CO_2 (and inorganics such as NH_3) are taken up to form CH_4 and biomass (Batstone *et al.,* 2002; Sötemann *et al*., 2005).

2.3.6 Sulphate Reduction: A Competitor to Methane Production

When sulphate, sulphite, thiosulphate or elemental sulphur are present in the wastewater, SRB can use several of the intermediates of the anaerobic process, such as acetate, propionate and hydrogen, as a source of energy (Henze *et al*., 2008, Hao *et al*., 2014). In fact, biological sulphate reduction is more favourable kinetically and thermodynamically than methanogenesis for common substrates. Furthermore, SRB can tolerate the toxic sulphide produced by the bioprocess better than methanogens (Ristow *et al.*, 2005). The SRB convert sulphate, the electron acceptor, into hydrogen sulphide, and in the presence of sulphate, compete for the available substrate with the methanogens. A diverse range of carbon sources and electron donors are involved in the SRB metabolism depending on the type of growth, either autotrophic or heterotrophic. Hydrogen serves as an efficient energy source for many species of SRB to grow on using sulphate as the electron donor (Hao *et al*., 2014).

The production of hydrogen sulphide poses a series of problems regarding methane production as some of the organic materials will be used by the SRB rather than the methanogenic bacteria resulting in lower methane yields. Not only does the methane yield decrease, but hydrogen

sulphide is now present within the biogas, and further treatment is necessary to remove it, in order to avoid problems associated with rapid corrosion of any metals present. A portion of the sulphide will also be present within the effluent, as dissolved H_2S, and will require additional post-treatment to remove (Henze *et al*., 2008). Ristow *et al.* (2005) showed that hydrogen sulphide at concentrations higher than 500mgH_2S-S/*l* affects the hydrolysis rate of organics under methanogenic and sulphidogenic conditions. However, for this project, provided the biodegradability of the organics does not change between methanogenesis and sulphidogenesis (Ristow *et al.*, 2005), SRB will be used as a beneficial alternative because hydrogen sulphide gas can be retained in solution, where it can be measured with a higher level of accuracy.

2.3.7 Sulphidogenesis

Sulphur is a crucial component of the biosphere, making up approximately 1% of all living organisms' dry mass. A diverse range of oxidation states of sulphur is possible; however, the three most abundant forms found in nature are sulphide (-2), elemental sulphur (0) and sulphate (+6) (Hao *et al*., 1996). In the presence of oxygen (aerobic conditions), the thermodynamically stable form of sulphur is sulphate. When oxygen is removed (anaerobic conditions), the sulphur is found as hydrogen sulphide. When reviewing reduction potentials, it is seen that sulphate is not favoured as an electron acceptor in the presence of oxygen and nitrate. Therefore, in order for efficient sulphate reduction in wastewater to occur, the reduction potential of the system should always be negative. (Liamleam, 2007).

The biological sulphate reduction process is mediated by SRB, and although morphologically diverse, are considered to be a physiologically unified group, alongside phototrophic or methanogenic organisms. SRB are obligatory anaerobes that use sulphate as an electron acceptor and obtain energy from the oxidation of organic substrates by removing hydrogen atoms from their molecules (Hao *et al*., 1996).

SRB can be divided into two groups, heterotrophic SRB and autotrophic SRB. The heterotrophic group prefers organic compounds such as organic acids, volatile acids and alcohols as the electron donors, and sulphate as the electron acceptor. The formation of these products occurs from the fermentation of carbohydrates, proteins and lipids during the anaerobic digestion process. Therefore, SRB are comparable to that of methanogenic

organisms (Hao *et al*., 1996; Liamleam, 2007). Few species contribute to the autotrophic group, which utilise CO_2 as the carbon source for biomass formation (anabolism) and obtain the required electrons from the oxidation of electron donors such as H_2. (Liamleam, 2007).

Ghoor *et al.* (2020) added the biochemical processes of biological sulphate reduction to the PWM_SA_AD model. The biological sulphate reduction process was added such that the initial hydrolysis steps were identical to that of methanogenesis, which follows the approach of Sötemann *et al*. (2005) and uses a generic organic compound (McCarty, 1974). Following the hydrolysis step, the same subdivision of acidogenesis for both low and high hydrogen partial pressures was utilised. Thus, the initial two degradation steps, hydrolysis and acidogenesis used identical stoichiometry for both methanogenesis and sulphidogenesis. This is a critical realisation, as the determination of the organic composition depends on the end products measured in each respective system, i.e methanogenic or sulphidogenic, but follows the identical degradation procedure for both preliminary steps of hydrolysis and acidogenesis.

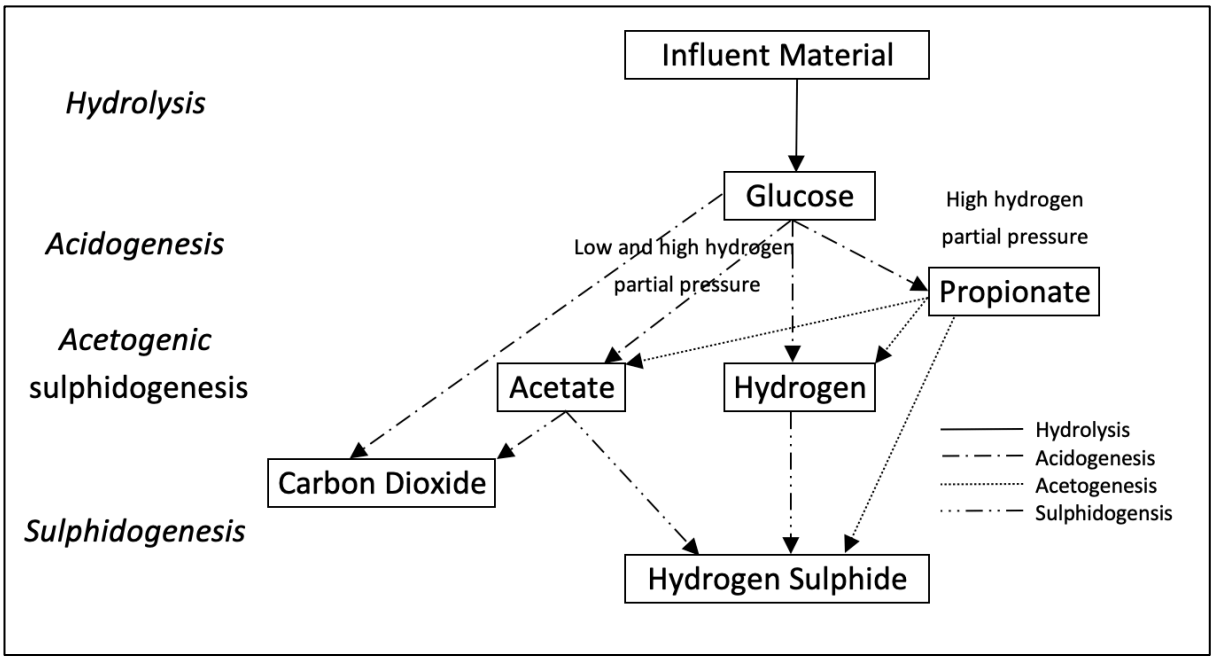

Figure 2. 3: PWM_SA_AD sulphidogenic pathway

Following the two initial degradation processes, Ghoor *et al.* (2020) separated the biochemical processes of methanogenesis and sulphidogenesis by including a series of separate sulphate reducing steps to the PWM_SA_AD model. Following hydrolysis and acidogenesis for the sulphidogenic pathway of the PWM_SA_AD model is acetogenic sulphidogenesis, in which

propionate is taken up to form an array of products including acetate, hydrogen and hydrogen sulphide. Finally, the sulphidogenesis process is mediated by acetoclastic SRB and hydrogenotrophic SRB, from which H_2S is produced utilising acetate and sulphate, as well as H_2 and sulphate, respectively.

2.3.8 PWM_SA_AD Validation

The model of Ghoor *et al.* (2020) was validated by using a calibrated version of the PWM_SA_AD model to simulate digester failure. The digester failure was compared to that of an identical digester run using the Anaerobic Digestion Model No.1 (ADM1). The outcome showed that PWM_SA_AD did predict failure in the same way as ADM1, but the failure occurred at lower influent alkalinity concentrations. Nevertheless, the verification of the model allowed for it to be used as is (without any additions) for the purpose of this thesis.

2.4 Biochemical Methane Potential Test

This section will discuss the BMP test as a commonly used analytical testing procedure for determining the biodegradability and methane potential of various substrates.

2.4.1 Introduction

The popularity of anaerobic digestion as a renewable energy resource has rapidly increased over the years. With this increase in popularity, the importance of obtaining a reliable biogas potential for various influent substrates has become critical (De Vrieze *et al.*, 2015). The biogas potential plays a crucial role in assessing design, as well as economic and management issues for anaerobic digestion for full-scale implementation (Angelidaki *et al.*, 2009). Depending on the quality of the influent waste stream, the biogas potential can vary substantially. Consequently, the BMP test could become a crucial analysis tool for determining the biogas potential for an array of substrates (Strömberg *et al.*, 2014).

The BMP assay was first proposed and established by Owen *et al.* (1979) as a simple and inexpensive procedure for determining the biochemical methane potential of substrates or as a way to provide an Anaerobic Toxicity Assay (ATA). The BMP test can be performed using

both continuous and batch fed techniques. Using a continuously fed reactor allows for a reasonable estimate of how the anaerobic digester will operate at full-scale but tends to increase the cost of the required facilities, equipment, time and personnel. Alternatively, batch-fed reactors do not have these constraints and allow for a wide range of variables to be evaluated (Owen *et al.*, 1979). That being said, many authors stress that in order for the results to be reliable, the testing procedure needs to be standardised (Angelidaki *et al.*, 2009; Raposo *et al.*, 2011; Esposito *et al.*, 2012; Strömberg *et al.*, 2014; De Vrieze *et al.*, 2015; Holliger *et al.*, 2016).

2.4.2 Batch test configuration

As previously mentioned, the BMP test can be performed in either a batch or continuous set-up. Conducting the BMP as a batch test allows for the determination of factors such as biodegradability, inoculum activity or inhibition (Raposo *et al.*, 2011). Furthermore, batch tests are effective for assessing the methane potential and performance of full-scale anaerobic digestion processes (Jensen *et al.*, 2011). Raposo *et al.* (2011) describe the general principle of all batch tests as the incubation of an inoculum populated with a diverse range of microorganisms at a neutral pH and a chosen temperature (either mesophilic or thermophilic). The inoculum is mixed with a chosen substrate that acts as the carbon source and provides energy for the microorganisms. Once mixed, the degree of degradation and the conversion rate of the substrate is assessed by taking measurements at regular time intervals. Furthermore, the inclusion of blank controls (endogenous test in which only the inoculum is added) allows for the gas produced by the degradation of the organic material present in the inoculum to be accounted for.

2.4.3 Good BMP practice

In order to validate the data collected during a BMP test, it is good practice to ensure that a range of parameters are considered. Angelidaki *et al.* (2009) aimed to define a standard protocol for conducting batch tests by considering a diverse range of parameters affecting the BMP outcome. Holliger *et al.* (2016) built on this work for further standardising the BMP test protocol and recommends that the following elements must be fulfilled in order for the results from a BMP test to be valid:

1. In addition to a reactor containing the substrate and inoculum, the experiment needs to have blank assays, into which only the inoculum is placed such that the background methane produced can be determined.
2. The test must be conducted in triplicate, i.e. at least three blank assays and three substrate assays (positive controls).
3. The duration of the experiment should not be determined in advance. Instead, the test should only be terminated when the daily methane production during three consecutive days is less than 1% of the accumulated volume of methane.
4. The BMP should be expressed as the volume of dry methane gas under standard conditions (273.15K and 101.33kPa) per mass of volatile solids (VS) added.
5. The gas produced by the substrate and the positive control is calculated by subtracting the methane production of the blanks from the gross methane production of the substrate assay.
6. The standard deviation of the blanks must be taken into account.
7. The test must be rejected following the violation of the relative standard deviation (RSD) for specific circumstances involving the blank and positive control.

2.4.4 Inoculum

The inoculum used in the BMP test contains a consortium of microorganisms that vary depending on the substrate fed to the parent (source) reactor. Therefore, it is challenging to standardise the source from which the inoculum is taken (Raposo *et al.*, 2011). Subsequently, inoculum taken from a range of different sources will show variations in its ability to convert substrate to methane (De Vrieze *et al.*, 2015).

Angelidaki *et al.* (2009) recommend using an inoculum taken from an active anaerobic digester which has been fed a complex substrate such that a diverse range of microbes is present. Furthermore, the inoculum should be degassed. Degassing is a pre-incubation step that removes any residual biodegradable material present in the inoculum. Degassing is achieved by allowing the anaerobic digestion process to continue after the inoculum has been removed from the parent reactor by placing it in an oxygen-free environment at the same temperature for 2 to 5 days. The inoculum should not be washed to remove the residual substrate and should represent the reactor from which it was taken as best as possible. An alternative to using a

single inoculum is to mix inoculum from a range of different sources to increase microbial diversity (Holliger *et al.*, 2016).

2.4.5 Substrate

The primary purpose of the BMP test is to identify the methane potential of unknown substrates. However, where possible, the substrate should be characterised as thoroughly as possible (Angelidaki *et al.,* 2009). The characterisation of potential samples should be well documented before the start of the experiment (Holliger *et al.*, 2016). Characterisation of the substrate is essential as the anaerobic biodegradability of the organic material is proportional to its elemental composition (Raposo *et al.*, 2011).

Angelidaki *et al.* (2009), Raposo *et al.* (2011) and Holliger *et al.* (2016) all state that one of the most crucial and compulsory measurements needed for the characterisation of the substrate is total solids (TS) and volatile solids (VS). However, the concentration of VS can be underestimated as volatile compounds may be lost during the drying process. Subsequently, to avoid the loss associated with drying, the TS determination should be performed at a maximum temperature of 90°C, instead of 105°C (Angelidaki *et al.,* 2009). It is also beneficial to include additional measurements such as FSA, TKN, pH, VFA and alkalinity as knowing the concentrations of these compounds can help to identify potential inhibition problems experienced during the BMP test (Holliger *et al.*, 2016).

The substrate samples used in the BMP test should be as fresh as possible. However, if this is not possible, the substrate can also be stored. Storing the substrate correctly is crucial for maintaining freshness. The substrate can be stored at 4°C for a period of two to five days. For extended periods, the substrate should be frozen and stored at -20°C and then thawed at 4°C, before slowly increasing to ambient temperatures for the start of the BMP test. Furthermore, the drying of substrates for storage should be avoided (Holliger *et al.*, 2016).

The particle size of the substrate can also influence the biodegradability results, as particle size and surface area affect the ratio between surface and volume for each organic particle (Esposito *et al.*, 2012), which subsequently influences the initial degradation rate (Raposo *et al.*, 2011). For substrates containing large particles, the following is advised (Holliger *et al.*, 2016):

1. All course inert particles such as gravel, sand or plastics should be removed.
2. If the organic particles are too large, shredding or grinding may be necessary to allow for a more homogeneous substrate.
3. Care should be taken during shredding as this may cause heat, leading to the loss of volatile compounds.
4. All particulate material should not exceed 10mm in any dimension (length, diameter).
5. The test report should provide adequate detail on the preparation of the substrate.

The proposed augmented batch tests (AugBMP and AugBSP) can be applied to any substrate. In this thesis, the method was applied to PSS, most of which is BPO (Sotemann *et al.,* 2005). The same type of experiment can be applied to soluble organics. The method is not generic, as it is a method to test the substrate. The composition outcome will change based on the source of pollutants contributing to the substrate in the wastewater stream.

2.4.6 Experimental setup

The BMP test needs to be conducted in a sealed vessel void of oxygen in order to maintain an anaerobic environment. The vessel should be flushed with inert gas, such as nitrogen, or other gases such as carbon dioxide or biogas before the experiment is started to ensure anaerobic conditions (Angelidaki *et al.,* 2009). Holliger *et al.* (2016) recommend using a vessel with a total volume of 500-1000m*l*. The vessels must be sealed with a gastight butyl septa, thick enough to be pierced by a needle repeatably, or the vessel must be connected to the gas measurement apparatus through gastight connectors and tubing that ensure that no gas is lost.

The BMP test should be conducted in at least triplicate (Angelidaki *et al.,* 2009). Therefore, a minimum of six test vessels (three test and three controls) is required to ensure repeatability. The transfer of inoculum should be done with a 100ml syringe with a large orifice. The syringe should have tubing attached to the orifice to ensure that the bottom of the inoculum storage bottle can be reached. If using granular inoculum, the granules should be collected and drained using a sieve. Once drained, the granules are then distributed evenly to each respective reactor using a spoon (Angelidaki *et al.,* 2009).

The BMP test should be conducted under either mesophilic or thermophilic conditions, as the temperature does not have a significant effect on the BMP. However, biogas production rates are affected by temperature. Subsequently, the BMP test should be conducted in a temperature-controlled environment with maximum temperature fluctuations of 2°C. Typical incubations and operating temperatures for mesophilic and thermophilic reactors are 37°C and 55°C, respectively (Holliger *et al.*, 2016).

Angelidaki *et al.* (2009), Moody *et al.* (2009) and Raposo *et al.* (2011) state that the inoculum to substrate ratio (ISR) is one of the crucial factors that affect the outcome of anaerobic assays. However, many research papers do not make mention of the ISR used. The ISR should be stated using either TS, VS or COD. The inoculum concentration should always exceed that of the substrate concentration. (Angelidaki *et al.,* 2009). Theoretically, the ISR should only affect the kinetics of the reactions, as the total methane yield depends on the composition of the organic material; however, inhibition has been reported in cases with a low ISR, where the concentration of substrates is far higher than the concentration of inoculum. Furthermore, if the ISR is too high, and the inoculum concentration is far greater than the substrate concentration, the induction of the enzyme necessary for biodegradation may be inhibited (Elbeshbishy *et al.*, 2012).

2.4.7 Gas measurements

Angelidaki *et al.* (2009) stated: "The result of a BMP test is the definition of the methane (or biogas) produced from a given weight of a certain substrate". Therefore, for the BMP test, substrate biodegradability is defined by the total amount of methane (or biogas) produced. Subsequently, it is crucial to measure the methane produced during the BMP test as accurately as possible. Two different gasometric methods are most frequently used to quantify the biogas produced. The first is a manometric gas measurement in which volume is kept constant, and the increase in pressure is measured. The second is a volumetric gas measurement in which the pressure is kept constant, and the increase in gas volume is measured (Raposo *et al.,* 2011).

The manometric method keeps volume and temperature constant and measures the overpressure generated by the production of biogas using a common differential manometer, or a more complex pressure transducer (Esposito *et al.*, 2012). Additionally, when calculating

methane production, complementary biogas analysis is required. Manometric gas measurements are prone to error. The most considerable difficulty for accurately measuring gas production emerge from the solubility of carbon dioxide in the bulk liquid of the digester, which is affected by pressure, pH, the headspace volume, temperature and thermodynamic equilibrium of dissolved carbonate species (Raposo *et al.,* 2011). Furthermore, the pressure in the assay must not exceed 300kPa to avoid excessive dilution of CO_2 or explosions (Holliger *et al.*, 2016).

The volumetric method measures gas production via displacement. Displacement can be measured using a piston in a cylinder, or liquid displacement. In the case of liquid displacement, the reactor is connected via a gas tube to an external measurement apparatus. The biogas produced by the reactor is then directed through the barrier solution, and the equivalent volume of liquid is displaced (Raposo *et al.,* 2011). A common way to measure the displacement of liquid is using an inverted column, which is placed inside a bath containing the barrier solution. Volumetric gas measurement is also prone to error, and precaution must be taken with the barrier solution to ensure that specific biogas components are not lost.

The accuracy of the BMP is influenced by the choice of barrier solution as specific gas components are soluble. This influence is especially apparent for CO_2 as its solubility in water at 25°C is around 25 times higher when compared to methane (Strömberg *et al.*, 2014). Parajuli (2011) explored the most important and commonly used biogas measurement techniques and identified the source of measurement error associated with each of them. Most importantly, the effect of biogas diffusion in different barrier solutions was investigated. The experiment tested carbonated distilled water, tap water, acidified water with varying pH, NaCl with varying pH and Orsat as potential barrier solutions. The results from the study are summarised as follows (Parajuli, 2011):

1. Carbonated distilled water had a high resistance to CO_2 diffusion at the beginning of the experiment. However, by the end of the experiment, carbonated distilled water lost more CO_2 than other solutions, with 89% of CO_2 lost during the experimental period.
2. Acidified water at varying pH readings (pH 0.5 – pH 2) did not prevent CO_2 solubility. Subsequently, the loss of CO_2 throughout the experiment exceeded 70%.

3. For the NaCl solutions, it was observed that an increase in salt concentration showed a decrease in gas solubility. Subsequently, the higher the salt concentration, the lower the CO_2 gas loss. However, over time, crystallisation of salt appeared at the bottom of the gasometers containing high salt concentrations.
4. Overall the loss of methane compared to CO_2 was quite low as methane is only slightly soluble when compared to CO_2. However, for pure tap water, the loss of methane throughout the experiment was 14%.

Therefore, the accuracy of the BMP test is influenced by numerous parameters. One of which is the chosen barrier solution. For this thesis, tap water was used as the barrier solution, and gas measurements were taken twice daily. This outcome may affect the cumulative gas collected during the AugBMP based on the amount of CO_2 that diffused into solution.

2.5 Primary Sewage Sludge

2.5.1 Overview

The particulate constituents present in wastewater comprise of both settleable and nonsettleable material. The term settleable refers to a physical property of the material, which under the influent of gravity, will collect at the bottom of an Imhoff cone after a minimum period of 2 hours. The Primary Settling Tank (PST) is a common addition to wastewater treatment plants and facilitates the settling process. The settled material removed from the PST is referred to as Primary Sewage Sludge (PSS) (Ekama, 2011).

The removal of settleable material to produce PSS in wastewater treatment plants is becoming popular due to the potential for nutrient and resource recovery when fed to an AD (Biller *et al.*, 2017). PSS makes up approximately two-thirds of the total solids contained in sewage sludges. The treatment of PSS is crucial to remove organics before disposal. One of the most common treatment methods of PSS is anaerobic digestion, which results in a stabilised sludge with a low residual sludge volume (Ristow *et al.*, 2005).

Ristow *et al.* (2005) state that under three possible operating conditions (methanogenesis, acidogenesis and sulphate-reducing), hydrolysis of the particulate PSS is the rate-limiting

process. Sötemann *et al*. (2005) further acknowledge that the process of hydrolysis and acidogenesis were the rate-limiting step in a sewage sludge AD. To account for this, Sötemann *et al*. (2005) considered four kinetic equations for the hydrolysis of PSS:

1. First-order with respect to the residual biodegradable particulate organic COD concentration
2. First-order with respect to the residual biodegradable particulate organic COD concentration and the acidogen biomass concentration that mediate the process.
3. Monod kinetics
4. Saturation (Contois) kinetics.

However, Sötemann *et al*. (2005) were unable to determine which of the equations mentioned above were superior for modelling hydrolysis and acidogenesis. However, they accepted saturation kinetics for the UCTADM1 model because the fraction of unbiodegradable organics in the PSS ($f_{PS,up}$) of 0.36 matched closely to that of O'Rouke's (1967) value of 0.34.

2.5.2 PSS hydrolysis rate in methanogenic and sulphidogenic systems

This thesis supports the idea of using an Augmented Biochemical Sulphide Potential (AugBSP) test to determine the composition of an unknown substrate. The AugBSP is crucial in obviating the gas measurement error experienced during the BMP test. The foundation for running the AugBSP test in parallel to the AugBMP test was established by Ristow *et al.* (2005). They concluded that the hydrolysis rate of PSS under methanogenic and sulphidogenic conditions does not change significantly, provided the sulphide concentration does not increase above 500 mgH_2S-S/*l*.

This conclusion was achieved by conducting a series of experiments in completely mixed ADs under sulphate-reducing conditions, which were run in parallel to methanogenic systems. The models developed for methanogenesis were applied to the sulphate reducing systems, and the methanogenic biomass was replaced with aceticlastic sulphate-reducing biomass, which had different growth constants to that of the methanogens. A series of four different experiments were conducted to determine the hydrolysis rate of the sulphate-reducing systems (Ristow *et al.*, 2005).

In summary, the outcome of the experiment conducted by Ristow et al. (2005) concluded that:

1. The hydrolysis rate under limited sulphate reducing conditions compared to purely methanogenic conditions was strictly similar.
2. The experiment showed that the hydrolysis rate was the same for both systems under stable sulphate reducing conditions.
3. Sulphate-reducing conditions had no significant influence on PSS hydrolysis rate compared to the equivalent methanogenic systems.
4. The hydrolysis rate for both systems was the same for the pH range 6.5-7.5.

From the findings listed above, it should be possible to conduct the AugBMP and AugBSP tests in parallel. Furthermore, the sulphate-reduction bioprocess can be modelled using principles from methanogenic anaerobic conditions because the rate of hydrolysis does not differ significantly. As a result, the hydrolysis kinetics for methanogenic anaerobic digestion can be used in systems containing sulphate. The hydrolysis kinetics play a crucial role in the overall process as hydrolysis is assumed to be the slowest process.

2.5.3 Stoichiometry of PSS degradation by methanogenic anaerobic digestion

The mass balanced bio-process stoichiometry maintains equilibrium between the flux of elements entering the biological system with the flux of elements exiting it. For example, in an AD, the flow of CH_4 and CO_2, as well as the aqueous phase pH are solely defined and dependent on the CHONPS and charge of the biodegradable organics fed to it (Ekama and Brouckaert, 2020 in preparation). This stoichiometry applies to all organics, which include PSS.

However, when modelling biological processes such as anaerobic digestion, additional factors such as speciation, affect the concentration of specific products. The concentration of these products is directly influenced by the system pH, which drives chemical equilibrium. Therefore, the stoichiometry is a useful equation when defining the reactants and products for biological reactions but may be limited when speciating the products correctly. Nevertheless, in some steady-state models, specific aqueous phase speciation reactions can be included in the bio-process stoichiometry, but the emphasis should be put on external speciation routines for correctly modelling dynamic situations (Ekama and Brouckaert, 2020 in preparation).

The general stoichiometric reaction for methanogenic anaerobic digestion, when the system is fed a biodegradable organic with a chemical composition of $C_xH_yO_zN_aP_bS_c^{ch}$, broken down into biomass, phosphate, ammonia, sulphate, carbonate, methane and carbon dioxide, at an operating pH around 7 is described in Equation 2.1 (Ekama and Brouckaert, 2020 in preparation):

$$C_xH_yO_zN_aP_bS_c^{ch} + \left(2_x - z + a + b(2 + f_{op}) + 2_c - ch - \frac{2\gamma_S}{8}(1-E) - E\frac{\gamma_S}{\gamma_B}\left[2k - m + n + p(2 + f_{op}) + 2s\right]\right)H_2O$$
$$\rightarrow E\frac{\gamma_S}{\gamma_B}C_kH_lO_mN_nP_pS_s + f_{op}\left(b - pE\frac{\gamma_S}{\gamma_B}\right)H_2PO_4^- + (1-f_{op})\left(b - pE\frac{\gamma_S}{\gamma_B}\right)HPO_3^{2-} + \left(a - nE\frac{\gamma_S}{\gamma_B}\right)NH_4^+$$
$$+\left(c - sE\frac{\gamma_S}{\gamma_B}\right)SO_4^{2-} + \left(a - b(2 - f_{op}) - 2c - ch - E\frac{\gamma_S}{\gamma_B}\left[n - p(2 - f_{op}) - 2s\right]\right)HCO_3^- + \left(\frac{\gamma_S}{8}(1-E)\right)CH_4$$
$$+\left(x - a + b(2 - f_{op}) + 2c + ch - \frac{\gamma_S}{8}(1-E) - E\frac{\gamma_S}{\gamma_B}\left[k - n + p(2 - f_{op}) + 2s\right]\right)CO_2 \qquad (2.1)$$

where:

γ_S = 4x+y-2z 3a +5b+6c-ch = EDC per mole biodegradable organics $C_xH_yO_zN_aP_bS_c$

ch = charge on electron donor(sign must be retained)

γ_B = 4k+l-2m-3n+5p = EDC per mole biomass $C_kH_lO_mN_nP_p$

EDC = electron donating capacity (COD)

M_S = molar mass of organics 12x+y+16z+14a+31b (g/mol)

M_B = molar mass of biomass 12k+l+16m+14n+31p (g/mol)

f_{op} = fraction $H_2PO_4^-$ of the OP species formed (OP = $H_2PO_4^-$ + HPO_4^{2-})

E = the mass of COD exiting the digester as active (Z_{BAD}) and endogenous (Z_{EAD}) sludge mass per day as a fraction of the mass of biodegradable organics (COD) utilised in the digester per day at steady state (note the unbiodegradable sludge mass is not included because it does not originate from the influent biodegradable organics), i.e. from the COD-based kinetic model:

E = V_d (Z_{BAD} + Z_{EAD})/[R_s (Q_i S_{bpi} -Q_w S_{bp})]

=$Y_{AD}(1+f_{AD}b_{AD}R_s)/[1+ b_{AD}R_s(1- Y_{AD}\{1-f_{AD}\})]$(sludge COD produced/COD utilised)

where

Z_{BAD}, Z_{EAD} = COD concentration of the anaerobic biomass and endogenous residue respectively (gCOD/*l*).

V_d = volume of the digester (l)

R_S = sludge age (d)

S_{bpi} = biodegradable particulates concentration in the influent (gCOD/*l*)

S_{bp} = biodegradable particulate concentration (gCOD/*l*)

Q_i = influent flow to digester (l/d)

Q_W = bed waste flow from the digester (l/d)

For the stoichiometry given in Equation 2.1 above, some important observations can be made (Ekama and Brouckaert, 2020 in preparation):

1. The COD of the CH_4 equates to the COD of the biodegradable organics that are degraded minus a small fraction used for biomass growth. Subsequently, CH_4 and biomass are the main two products formed from the available COD.
2. The C content of the organics defines the amount of C present in the CO_2 and CH_4, minus the small fraction used for biomass growth.
3. The C not taken up as CH_4 becomes CO_2 (either gaseous or dissolved HCO_3^-).
4. The N content of the organics forms NH_4^+ and a small fraction of biomass. In the pH range of 6.8-8.6, the NH_3 is present as NH_4^+. This re-speciation requires an additional H^+ from the aqueous solution, which subsequently influences the alkalinity of the system.
5. The organically bound P is released as H_3PO_4, but re-speciates to form either $H_2PO_4^-$ or HPO_4^{2-}. The formation of H_3PO_4 does not occur at the operating pH of 6.8-8.6. Subsequently, either one H^+ ion or two H^+ ions are released into the aqueous solution, which subsequently influences the alkalinity of the subspecies, but does not affect the total alkalinity of the system as H_3PO_4 is the reference species.
6. For this project, the S content of the PSS was not considered. However, the stoichiometry takes S into consideration.

2.5.4 Stoichiometry of PSS degradation by sulphidogenic anaerobic digestion

The stoichiometry in Equation 2.1 has also been applied to BSR using organics as an e^- donor (Poinapen *et al*, 2009). However, Poinapen and Ekama (2010) found that most organics present in wastewater are 'carbon deficient'. Carbon deficiency occurs in organics when they can donate more electrons for BSR than supply carbon for the HCO_3^- alkalinity to increase. In order for this to occur, the COD/TOC must be higher than 2.67. Subsequently, for most organics in wastewater, the stoichiometry results in the gaseous CO_2 term being negative. This means that another system needs to provide the shortfall for the alkalinity to increase. For BSR, the sulphide system provides the required alkalinity in the form of HS^-. Therefore, for BSR there

is no CO_2 gas production, provided the CO_2 headspace partial pressure is not sufficiently low to allow for CO_2 to be expelled from the liquid phase. The revised stoichiometry for BSR using wastewater organics is given in Equation 2.2 (Ekama and Brouckaert, 2020 in preparation):

$$C_xH_yO_zN_aP_bS_c^{ch} + \left(3_x - z + 4b + 4c - \frac{4\gamma_S}{8}(1-E) - E\frac{\gamma_S}{\gamma_B}[3k - m + 4p + 4s]\right)H_2O$$
$$+\left(\frac{\gamma_S}{8}(1-E) - \left[c - sE\frac{\gamma_S}{\gamma_B}\right]\right)SO_4^{2-} \rightarrow E\frac{\gamma_S}{\gamma_B}C_kH_lO_mN_nP_pS_s + f_{op}\left(b - pE\frac{\gamma_S}{\gamma_B}\right)H_2PO_4^- + (1-f_{op})\left(b - pE\frac{\gamma_S}{\gamma_B}\right)HPO_3^{2-}$$
$$+\left(a - nE\frac{\gamma_S}{\gamma_B}\right)NH_4^+ + \left(-x + a - b(2-f_{op}) - 2c - ch + \frac{2\gamma_S}{8}(1-E) + E\frac{\gamma_S}{\gamma_B}\left[k - n + p(2-f_{op}) + 2s\right]\right)HS^-$$
$$+\left(x - a + b(2-f_{op}) + 2c + ch - \frac{\gamma_S}{8}(1-E) - E\frac{\gamma_S}{\gamma_B}\left[k - n + p(2-f_{op}) + 2s\right]\right)H_2S + \left(x - kE\frac{\gamma_S}{\gamma_B}\right)HCO_3^- \quad (2.2)$$

However, the assumption of zero CO_2 production is not entirely realistic as CO_2 gas can diffuse out of solution. In situations where the HCO_3^- concentration is high, a high H_2CO_3 concentration in the aqueous phase is established, and at low ρ_{CO2} (~0.0005 atm), CO_2 can diffuse out of solution. This diffusion has a negligible effect on the C mass balance; however, the pH of the system is significantly affected. Subsequently, while the concept of carbon deficiency validates that the HS^- system contributes towards the total alkalinity, absolute zero CO_2 production is not realistic and will affect the digester pH (Ekama and Brouckaert, 2020 in preparation).

2.6 Casein

Casein is one of the two primary protein sources present in milk, making up approximately 3% of cow's milk. Casein was chosen for this experiment as it contains organically bound nitrogen and phosphorus, similar to the nitrogen and phosphorus contained in the biodegradable organics present in PSS (Schrieke and Winter, 2011).

Casein micelles are protein-based particles present in mammalian milk. The particles are composed primarily of phosphoproteins (known as caseins) and inorganic calcium phosphate and are highly hydrated, stable, polydisperse colloidal particles (Dalgleish, 2011). Furthermore, casein particles can be described as supramolecular, containing multiple molecular entities that are held together by means of non-covalent intermolecular binding

interactions (McMahon and Oommen, 2012). Bovine milk can be separated into four different casein fractions (α_{S1-}, α_{S2-}, β-, κ - caseins) (Dalgleish, 2011).
The casein used in this project was casein hydrolysate. Hydrolysates are commonly produced by incubating with proteolytic enzymes at elevated temperatures, in the range of 37 - 40°C. An essential characteristic of this process is the degree of hydrolysis and is defined as the percentage of peptide bonds cleaved (Boland, 2011).

Understanding these properties is of importance to this project as casein micelles are considered to be colloidal particles (Dalgleish, 1998). Furthermore, all caseins contain substantial amounts of hydrophobic amino acids. Micelles are constructed by self-assembly of amphiphilic molecules (Joseph *et al.*, 2017). Micelles contain a long hydrophobic carbon chain and a small hydrophilic head group (Margineanu, 2019), and are formed in aqueous solution, consisting of a polar region that faces the outside surface, with a nonpolar region forming the core (Joseph *et al.*, 2017). These properties affect the interaction and solubility of casein with water. The casein used in this experiment was supplied by Sigma-Aldrich, a German company owned by Merck KGaA. The solubility of casein hydrolysate as specified by Merck was 310 g*/l* (Sigmaaldrich.com).

Additionally, the chemical formula of casein is of particular interest for this project, as casein was used to validate the accuracy of the AugBMP and AugBSP tests' ability to identify the composition of a 'known' influent substrate. The composition of casein was taken from Hoover and Porges (1952), and Schrieke and Winter (2011). The elemental composition of casein is presented in Table 2.1

Table 2. 1:Casein Compositions

	Hoover and Porges (1952)		Schrieke and Winter (2011)	
Constituent	Weight (%)	Composition	Weight (%)	Composition
C	52.85	1	53.9	1
H	6.48	1.47	7.13	1.59
O	24.76	0.35	22.14	0.31
N	15.12	0.25	15.8	0.25
P	-	-	0.71	0.005

Therefore, the literature stated values of casein by Hoover and Porges (1952) and Schrieke and Winter (2011) are $C_1H_{1.47}O_{0.35}N_{0.25}$ and $C_1H_{1.59}O_{0.31}N_{0.25}P_{0.005}$, respectively.

2.7 Mathematical bioprocess modelling

2.7.1 Overview

Computer-based modelling is considered to be an inherent part of the design and operation of wastewater treatment processes. The use of mathematical models is possible during all stages of design, operation and optimisation of wastewater treatment systems. The chosen software tool for modelling the biological AD for this project was WEST®. The simulation platform present in WEST® is written in MSL (Model Specific Language), which is a high-level object-orientated language, in which the dynamics of specific systems can be accurately represented (Vanhooren *et al*., 2003).

Modelling and simulating wastewater treatment plants and the treatment process is an essential result of growing environmental awareness. Models vary in complexity, and at the fundamental level, a design model may be purely conceptual. The virtual design space may include empirical models, which incorporate a statistical approach to mimicking the end-results published in studies on the physical model. Ultimately, models may be developed based on mechanistic knowledge. Mechanistic models are powerful because they allow for extrapolation of the design space to conditions beyond that experienced in the physical model. This means that a large variety of feasible solutions may be evaluated quickly and inexpensively, highlighting the most accessible solutions based on physical constraints (Vanhooren et al., 2003).

2.7.2 Parameter Estimation

The PWM_SA model has been coded into WEST® wastewater treatment software. The software includes a PE function that allows the user to search for desired parameters by inputting a set of variables. The PE process compares the model predicted variables with the corresponding experimentally measured variables. The PE process seeks to minimise the error between the simulated results and the collected experimental data by adjusting selected

parameters, such as organic composition or growth and death rates. The PE process involves a large number of model simulations and interactions which calibrate a set of user-selected model parameters (Ekama and Brouckaert, 2020 in preparation).

PE is an essential part of this thesis for identifying the desired parameters from the experimental data. Therefore, the fundamentals of the process, as executed in WEST®, will be briefly explained. Claeys (2008) laid the foundation for the solver by defining the Object Evaluation Experiment (ExpObjEval) environment. "The ExpObjEval experiment type is capable of computing a large variety of objective values on the basis of the results of a dynamic simulation experiment." (Claeys, 2008).

To achieve a result from the PE, the environment first runs the simulation experiment and stores the trajectories of several selected quantities to an internal buffer. This buffer is then used to compute the individually selected objective values. Lastly, the environment sums up the individual objective values (each of which has the option of being individually weighted) to achieve a final overall objective value. This final objective value is used to minimise the error across each of the measured variables by adjusting the simulation parameters. Fundamentally, this environment contains several complex interactions and solvers, which are not mentioned in this thesis.

For simplicity, the object ExpObjEval environment can be broken down into three essential levels (excluding the solver and call-back environment):

1. Overall objective value
2. Quantity objective value
3. Sub-objective value

1. The concept of the overall objective value is essential. The overall objective value is the weighted mean of the quantity objective values. Both the quantities that are used in the evaluation process, as well as their associated weighting, can be specified by the user. The quantities and weighting are combined and used in the computation of the overall objective value. This is represented as (Claeys, 2008):

$$J = \frac{\sum_{i=1}^{n_q} \omega_{q_i} \times J_{q_i}}{\sum_{i=1}^{n_q} \omega_{q_i}} \tag{2.3}$$

2. Each of the quantity objective values is a weighted mean of sub-objective differences. The sub-objective differences are achieved by computing sub-objective values and then comparing them with the desired value. There are four possible error criteria in which to find the quantity objective value (Claeys, 2008):

   a. Absolute error:

$$J_{qi} = \frac{\sum_{j=1}^{n_o} \omega_{o_{i,j}} \times \left| J_{o_{i,j}} - \hat{J}_{o_{i,j}} \right|}{\sum_{i=1}^{n_q} \omega_{o_{i,j}}} \tag{2.4}$$

   b. Relative error:

$$J_{qi} = \frac{\sum_{j=1}^{n_o} \omega_{o_{i,j}} \times \left| \frac{J_{o_{i,j}} - \hat{J}_{o_{i,j}}}{J_{o_{i,j}}} \right|}{\sum_{i=1}^{n_q} \omega_{o_{i,j}}} \tag{2.5}$$

   c. Squared error:

$$J_{qi} = \sqrt{\frac{\sum_{j=1}^{n_o} \omega_{o_{i,j}} \times (J_{o_{i,j}} - \hat{J}_{o_{i,j}})^2}{\sum_{i=1}^{n_q} \omega_{o_{i,j}}}} \tag{2.6}$$

d. Squared relative error:

$$J_{qi} = \sqrt{\frac{\sum_{j=1}^{n_o} \omega_{o_{i,j}} \times \left(\frac{J_{o_{i,j}} - \hat{J}_{o_{i,j}}}{J_{o_{i,j}}} \right)^2}{\sum_{i=1}^{n_q} \omega_{o_{i,j}}}} \tag{2.7}$$

3. Finally, the sub-objective value of quantity can be defined. Equations 2.4 to 2.7 above show that multiple sub-objective values can be used for each quantity. The only sub-objective value used in this thesis was the Mean Difference (MD). MD allows for the simulated trajectories to be compared with a reference time series. This means that the value of the MD sub-objective is defined as "a weighted mean of the mean differences between the simulated trajectory and each of the reference series" (Claeys, 2008). This was crucial as the lab data was recorded daily. Therefore, the error associated with the mean differences of the daily measured values was minimised, allowing for the composition and kinetics of the AugBMP and AugBSP tests to be identified. MD is defined as:

$$J_{o_i}^{MeanDiff} = \frac{\sum_{l=1}^{n_s} \omega_{s_{i,l}} \times J_{s_{i,l}}^{MeanDiff}}{\sum_{i=1}^{n_q} \omega_{s_{i,l}}} \tag{2.8}$$

where:

J	= Overall objective value
J_{qi}	= Objective value of quantity i
$J_{o_{i,j}}$	= Value of sub-objective j of quantity i
$\hat{J}_{o_{i,j}}$	= Desired value of sub-objective j of quantity i
ω_{q_i}	= Weight of quantity i
$\omega_{o_{i,j}}$	= Weight of sub-objective j of quantity i
$\omega_{s_{i,l}}$	= Weight of reference time series l of quantity i

Figure 2.4 and Figure 2.5 show the PE environment in WEST®. In Figure 2.4, the measured variables can be chosen, and the desired value, weighting and difference criterion can be selected. Figure 2.5 shows a PE run in which the overall objective value is minimised over multiple iterations to find the best solution, highlighted in orange.

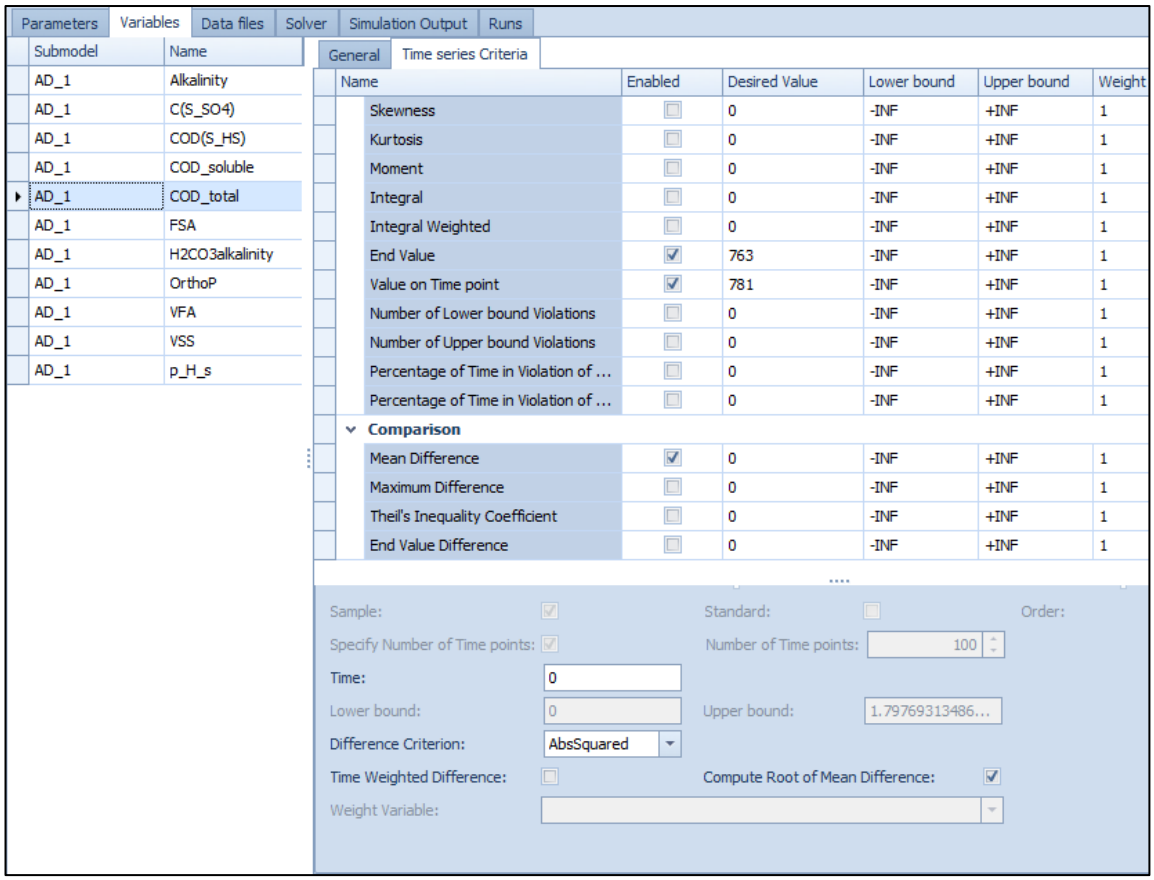

Figure 2. 4: Variable criteria in WEST PE

The overall objective value incorporated into the PE function is crucial as it allows the parameters in question, namely the composition of the organics, to be determined using specific criteria. This criteria are imperative as laboratory measurements are prone to error, which can affect the outcome of determining the organic composition or kinetic rates. The overall objective value allows for the laboratory measurements to be weighted appropriately. This weighting ensures that error is distributed throughout the PE based on the confidence of the experimental measurements.

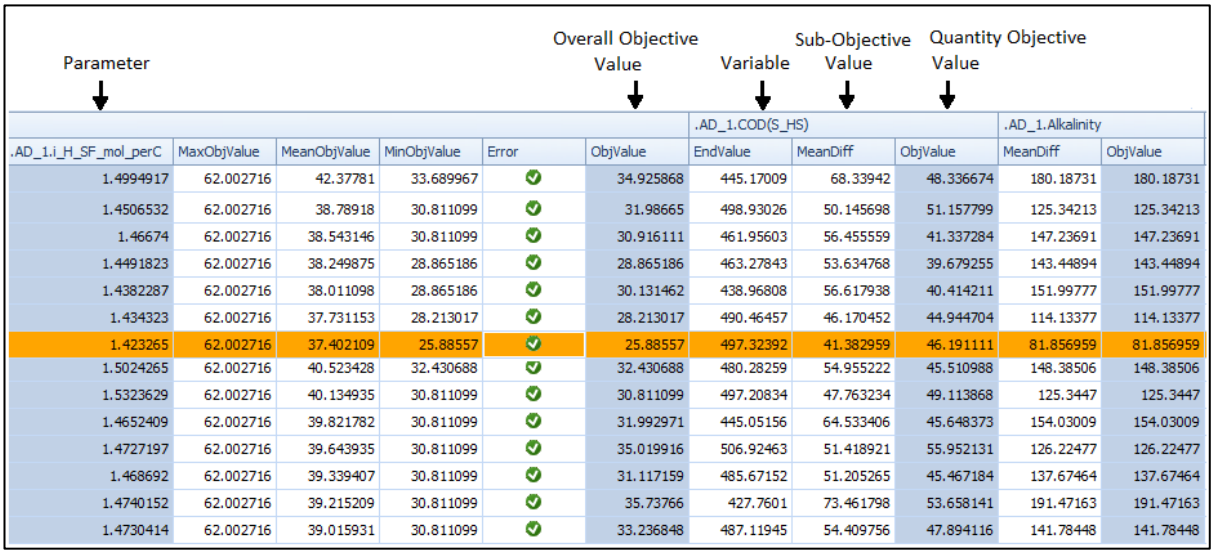

						.AD_1.COD(S_HS)			.AD_1.Alkalinity	
.AD_1.i_H_SF_mol_perC	MaxObjValue	MeanObjValue	MinObjValue	Error	ObjValue	EndValue	MeanDiff	ObjValue	MeanDiff	ObjValue
1.4994917	62.002716	42.37781	33.689967	✓	34.925868	445.17009	68.33942	48.336674	180.18731	180.18731
1.4506532	62.002716	38.78918	30.811099	✓	31.98665	498.93026	50.145698	51.157799	125.34213	125.34213
1.46674	62.002716	38.543146	30.811099	✓	30.916111	461.95603	56.455559	41.337284	147.23691	147.23691
1.4491823	62.002716	38.249875	28.865186	✓	28.865186	463.27843	53.634768	39.679255	143.44894	143.44894
1.4382287	62.002716	38.011098	28.865186	✓	30.131462	438.96808	56.617938	40.414211	151.99777	151.99777
1.434323	62.002716	37.731153	28.213017	✓	28.213017	490.46457	46.170452	44.944704	114.13377	114.13377
1.423265	62.002716	37.402109	25.88557	✓	25.88557	497.32392	41.382959	46.191111	81.856959	81.856959
1.5024265	62.002716	40.523428	32.430688	✓	32.430688	480.28259	54.955222	45.510988	148.38506	148.38506
1.5323629	62.002716	40.134935	30.811099	✓	30.811099	497.20834	47.763234	49.113868	125.3447	125.3447
1.4652409	62.002716	39.821782	30.811099	✓	31.992971	445.05156	64.533406	45.648373	154.03009	154.03009
1.4727197	62.002716	39.643935	30.811099	✓	35.019916	506.92463	51.418921	55.952131	126.22477	126.22477
1.468692	62.002716	39.339407	30.811099	✓	31.117159	485.67152	51.205265	45.467184	137.67464	137.67464
1.4740152	62.002716	39.215209	30.811099	✓	35.73766	427.7601	73.461798	53.658141	191.47163	191.47163
1.4730414	62.002716	39.015931	30.811099	✓	33.236848	487.11945	54.409756	47.894116	141.78448	141.78448

Figure 2. 5: Parameter estimation function in WEST

Chapter 3: Materials and Methods

3.1 Introduction

As highlighted in Chapter 1, the primary objective of this thesis is to determine the composition of the biodegradable particulate organics present in PSS. In order to achieve this, two different experimental approaches were used, a methanogenic approach and a sulphidogenic approach. Figure 3.1 describes the flow of Chapter 3, starting with the design and operation of the steady-state reactors used to grow the required inoculum. The feed storage and preparation are then discussed, followed by the design and operation of the AugBMP and AugBSP batch experiments. The analytical procedures used to collect the required data are then described, followed by the evaluation of the data collected, which made use of both conservation of mass and statistics. The influent fractionation method is then described for both the methanogenic and sulphidogenic system, followed by the methods used to identify the biodegradable organic composition. The methodology used to construct the virtual model of the steady-state reactors is then explained. Finally, the methods used to model the augmented batch test experiments, which includes the selection of parameters for the composition identification, are described.

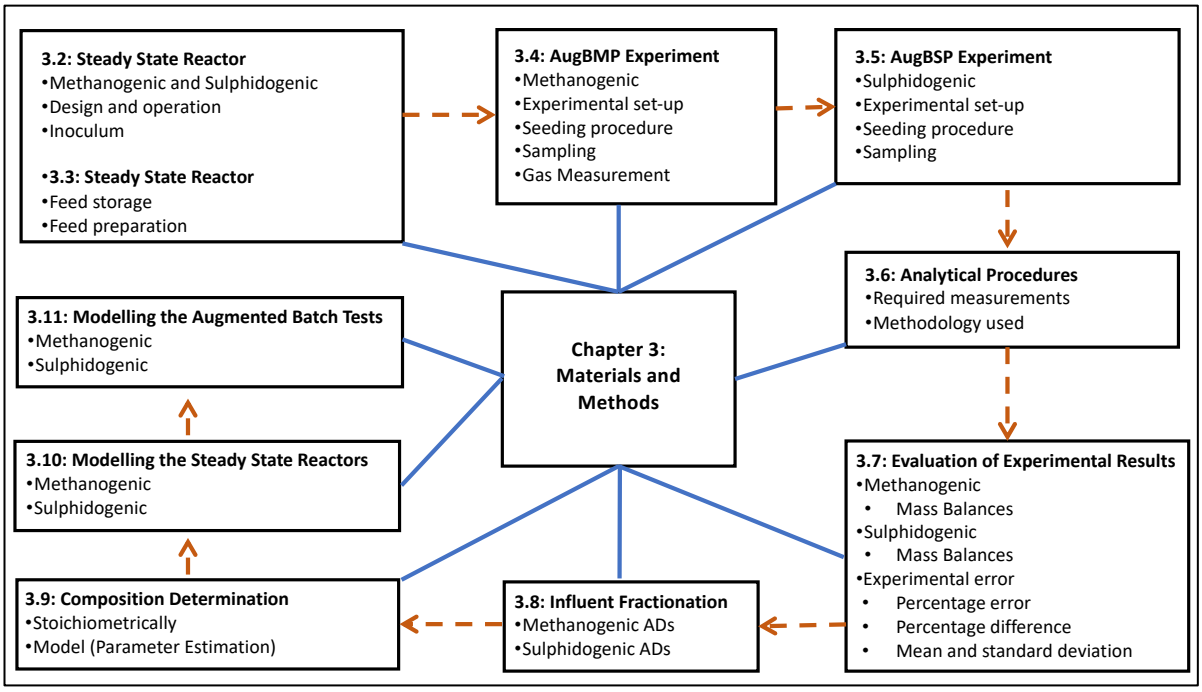

Figure 3. 1: Chapter 3 layout

3.2 Steady-state reactor design and operation

Both the AugBMP, and the AugBSP experiments required a stable inoculum. The inoculum needed to be taken from an active AD, which was fed a complex substrate such that a diverse range of microbes was present. In order to achieve this, a Steady-State Parent Anaerobic Digester (SSPAD) was required for each respective system, i.e. A methanogenic SSPAD (operated at a 20d sludge age) and a sulphidogenic SSPAD (operated at a 19d sludge age). Each of the SSPADs were fed the same macerated (shredded) PSS from Potsdam Wastewater Treatment Facility in the Western Cape, for at least three sludge ages (i.e., 20 × 3 = 60d) to allow for a steady-state to be achieved. A general rule for ensuring steady-state is to keep the flow rate and feed concentration constant for at least three sludge ages (i.e. in this case above 60 days). Steady-state was checked by measuring the influent and effluent concentrations of the SSPADs on different days. When the deviation in each respective measurement across the different days was not significant, the system was deemed to be at a steady-state.

3.2.1 Methanogenic Parent Digester

A single methanogenic SSPAD was operated in order to provide the required inoculum for the AugBMP experiment. The SSPAD was operated as a continuously stirred tank reactor (CSTR; completely mixed) under mesophilic conditions, 37°C. The digester was heated using a 200W submersible aquarium fish tank heater, and the temperature was regulated using an electric temperature controller. Furthermore, the digester was run as a continuously batch-fed digester, i.e. the digester was fed the same volume and concentration for a short period (2 minutes) once daily. The digester did not require additional alkalinity, and the pH was maintained around 7. The influent and effluent flow rates of the digester were fixed by feeding diluted PSS at 0.8*l*/d, which was prepared by mixing 0.6*l* of stored macerated PSS with 0.2*l* of warm (~40°C) tap water.

The methanogenic SSPAD consisted of a purpose-built Perspex digester with a liquid volume of 16*l* and a headspace volume of 4*l*. The digester had an electric motor fixed to the lid, which ensured that the contents were homogeneously mixed. The stirring also ensured that the liquid temperature was maintained at 37°C throughout the digester. The digester was fed through an inlet port on the lid, which could be sealed to maintain anaerobic conditions, and the effluent

was removed through an outlet port at the base of the digester. As previously mentioned, the same volume was fed to and wasted from the digester (0.8*l*/d); thereby fixing the sludge age of the digester to 20 days (i.e. 16*l* ÷ 0.8*l*/d). The layout of the methanogenic SSPAD is shown in Figure 3.2.

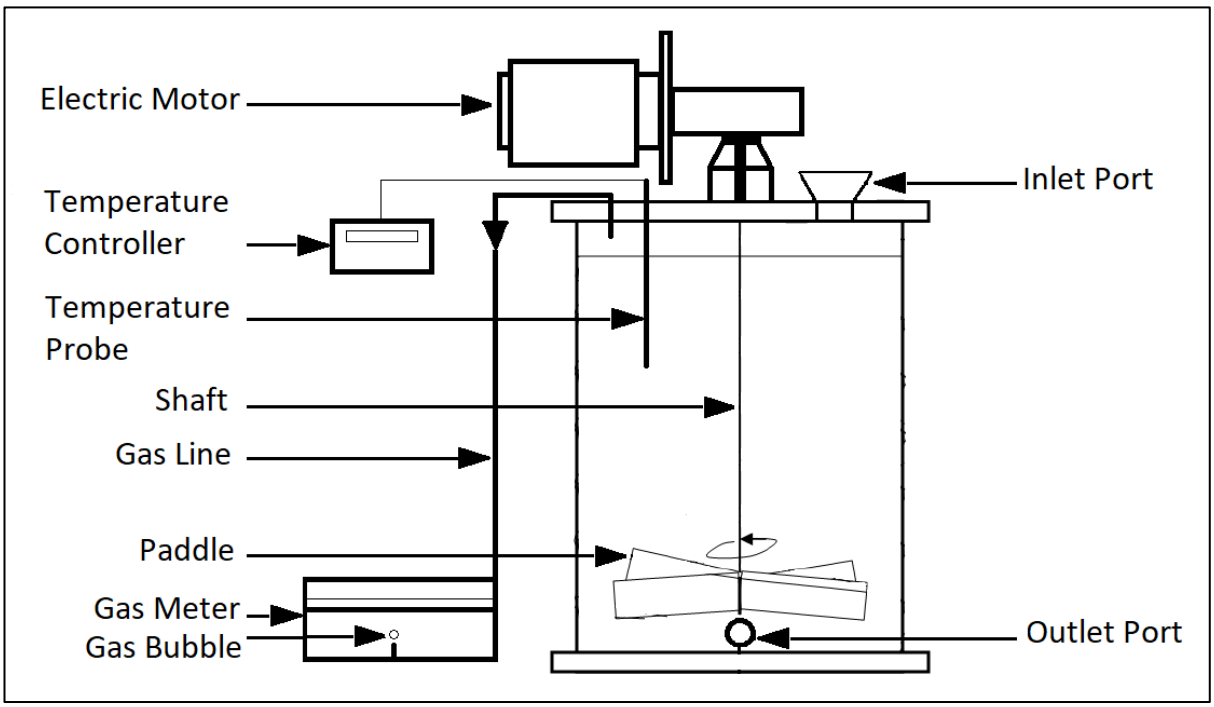

Figure 3. 2: Methanogenic Steady-State Parent Anaerobic Digester (SSPAD)

The biogas produced by the digester was measured using a wet-tip gas meter (http://wettipgasmeter.com/). The biogas escaped through a gas port on the lid of the digester and then flowed through a gas line to the base of the wet-tip gas meter. The gas then bubbled through water and collected in the tipping mechanism of the gas meter. The tipping mechanism on the meter was constructed of plastic and was set on a central pivot. Once 45m*l* of gas had been collected, the tipping mechanism became buoyant (due to the collected gas), and the mechanism pivoted, releasing the trapped gas. An electric counter was used to tally the number of pivots, and the total daily gas production was determined. Figure 3.3 shows a photograph of the experimental set-up, and the wet-tip gas meter is shown in Figure 3.4.

Figure 3. 3: Methanogenic SSPAD Photograph

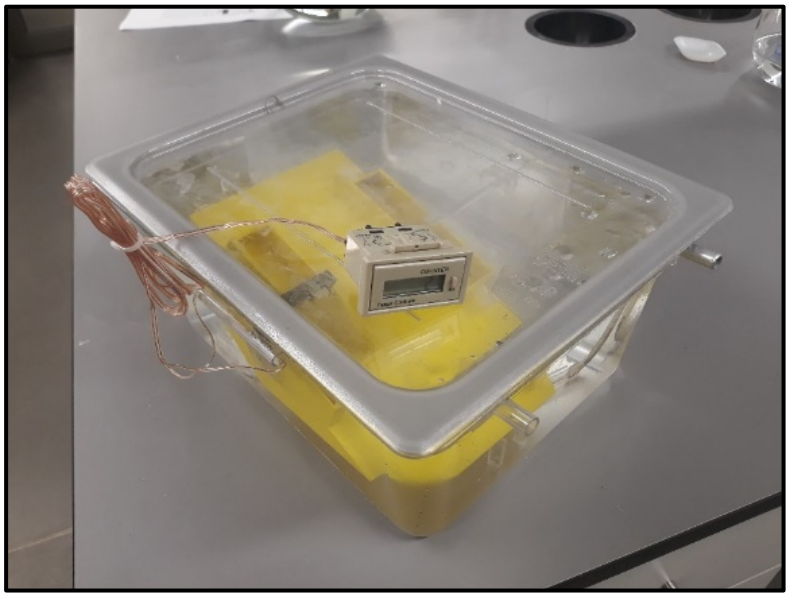

Figure 3. 4: Wet-tip gas meter

3.2.2 Sulphidogenic Parent Digester

Two sulphidogenic SSPADs were operated simultaneously to provide the required inoculum for the AugBSP experiment. Two SSPADs were required to keep the inoculum as stable as possible, as repeatably sourcing SRB was challenging. One of the SSPADs would need to be drained entirely to inoculate the AugBSP experimental reactors due to the low operating concentrations of the sulphidogenic system.

For the sulphidogenic system, the feed was diluted to avoid sulphide inhibition, as sulphide was not stripped out of the digester. Subsequently, the diluted feed produced lower constituent concentrations in the bulk liquid of the sulphidogenic system. As a result of the lower constituent concentrations, the sulphidogenic SSPAD effluent could not be diluted before inoculating the AugBSP experiment. Therefore, the second SSPAD was used to maintain the culture of SRB and restart the first SSPAD once it had been drained at the start of the AugBSP experiments.

The sulphidogenic SSPAD consisted of a 25*l* aspirator bottle fitted and sealed with a rubber stopper at the top and bottom orifices to ensure that anaerobic conditions were maintained. The SSPAD was operated as a continuously stirred tank reactor (CSTR; completely mixed) under mesophilic conditions, 35°C. The digester was heated using a 200W submersible aquarium fish tank heater, and the temperature was regulated using an electric temperature controller. Furthermore, the digester was run as a continuously batch fed digester, i.e. the digester was fed the same volume and concentration for a short period (2min) once daily. The digester did not require additional alkalinity, as sufficient alkalinity was generated by the sulphate reduction process, and the pH was maintained around 7. The influent and effluent flow rates of the digester were fixed by feeding 1*l*/d. The first sulphidogenic SSPAD consisted of a commercially available glass aspirator bottle and the second consisted of a commercially available plastic aspirator bottle. Both SSPADs were operated with a liquid volume of 19*l* and a headspace volume of 6*l*. The digesters were placed on a magnetic stirrer which ensured that the contents were homogeneously mixed. The stirring also ensured that the liquid temperature was maintained at 35°C throughout the digester. The temperature of the sulphidogenic system differed slightly from that of the methanogenic system due to the heating element and temperature controller used. However, consistent mesophilic conditions were maintained in both reactors, as minimal temperature fluctuations occurred.

When feeding the digesters, the effluent from the previous twenty-four hours was first removed. Nitrogen gas was sparged into the digester whilst draining the effluent to avoid a negative pressure and maintain atmospheric pressure in the digester. Positive pressure was prevented by allowing the excess gas to leave the digester via a gas line, which passed through the rubber stopper at the top of the digester. After the effluent was removed, the digester was fed by pumping the feed mixture through a feed line, which ran through the rubber stopper at the top of the digester. As previously mentioned, the same volume was fed to and wasted from the digester (1*l*/d); therefore, fixing the sludge age of the digester to 19 days (i.e. 19*l* ÷ 1*l*/d).

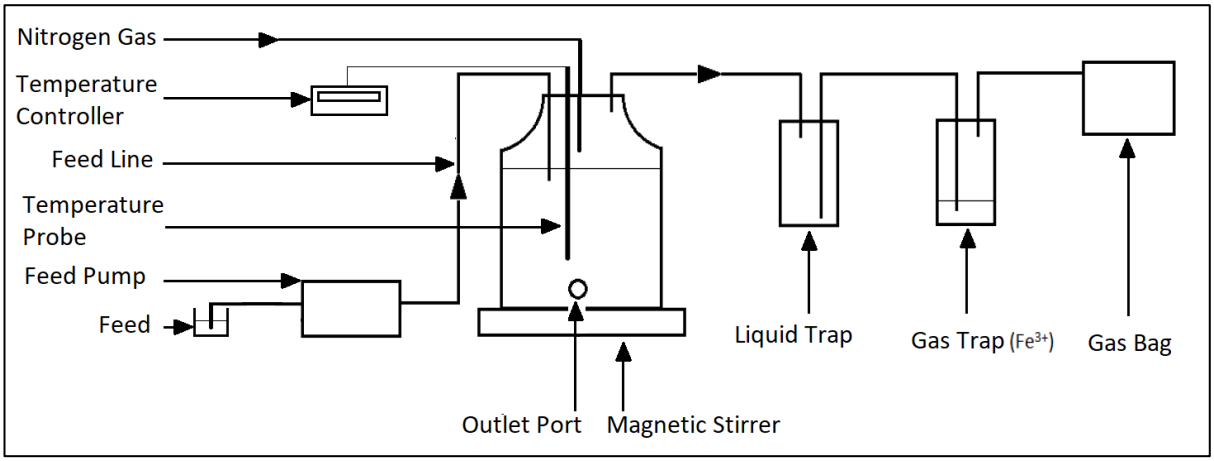

Figure 3. 5: Sulphidogenic Steady-State Parent Anaerobic Digester (SSPAD)

The sulphidogenic SSPAD produced hydrogen sulphide as a by-product, which can be toxic and lethal in high concentrations; therefore, the system was placed inside a fume cabinet to reduce exposure in the event of H_2S gas escape. The H_2S produced was removed from the digester via a gas line, which passed through the rubber stopper at the top of the digester. After leaving the digester headspace, the gas passed into a liquid trap, which ensured that no liquid could be sucked back into the digester due to negative pressure. Following the liquid trap, the gas passed into a gas trap where it bubbled through ferric chloride. The ferric chloride aimed to capture all the H_2S gas by forming ferrous iron (Fe^{2+}) from the reduction of ferric iron (Fe^{3+}). Equation 3.1 shows the reduction of Fe^{3+} to Fe^{2+} when H_2S is bubbled through the solution.

$$Fe^{3+}\,(aq) + H_2S\,(g) = Fe^{2+}\,(aq) + S^0\,(ppt) + 2H^+\,(aq) \qquad (3.1)$$

Finally, the gas was captured in a gas bag and disposed of accordingly. Figure 3.6 shows a photograph of the two sulphidogenic SSPADs run in parallel.

Figure 3. 6: Sulphidogenic SSPAD Photograph

3.3 Feed

The PSS used for the entire duration of the experiment was collected from Potsdam Wastewater Treatment Facility (Western Cape, South Africa). The PSS was collected from the bottom of the PST in 2 x 50*l* drums and transported back to the UCT Water Quality Lab. The PSS in the first 50*l* drum was then macerated in a blender to ensure homogenous distribution of the solid material. Following this maceration process, the PSS was transferred into 10 x 5*l* drums. The second 50*l* drum, as well as nine of the 5*l* drums, were stored in the freezer at -20°C. The PSS that was used for feeding the digesters was stored in the fridge at 4°C. Subsequently, when a 5*l* drum was empty, a frozen 5*l* drum was removed from the freezer, thawed in the fridge at 4°C, stored in the fridge and used for daily feeding. This process continued until the feed was utilised entirely, at which point, more PSS was collected from Potsdam. Furthermore, the PSS was tested occasionally while under storage to ensure consistency in the feed characteristics.

3.3.1 Methanogenic system feed preparation

The macerated PSS used to feed the methanogenic SSPAD was taken directly from the 5*l* drum, which was stored in the fridge. The PSS, 0.6*l*, was mixed with warm (~40°C) tap water, 0.2*l*, making a total of 0.8*l* methanogenic SSPAD PSS feed. The warm water was added to increase the temperature of the PSS before being fed to the digester. This addition of warm water caused the PSS to become slightly diluted (75% of its original concentration). This dilution was taken into consideration for all subsequent calculations and modelling performed on the methanogenic SSPAD.

3.3.2 Sulphidogenic system feed preparation

The sulphidogenic SSPAD was not capable of treating undiluted PSS without stripping H_2S out of the digester, as inhibition would have occurred. Undissociated H_2S is generally considered to be the sulphide species that is toxic when in high concentrations, accumulating in the undissociated form for digesters with a pH below 7 (Koster *et al.,* 1986). Therefore, even though the digesters were operated at a pH above 7, in order to avoid having to strip out the H_2S gas from the digester, the COD of the PSS was diluted such that the sulphide concentration did not exceed 500 mgH_2S-S/*l* (Ristow *et al.*, 2005). Therefore, for this experiment, the sulphate concentration was fixed at 1.5gSO4/*l*. Subsequently, the PSS was diluted to ensure that a COD/SO_4^{2-} ratio of 0.67 was maintained. Therefore 1gCOD/*l* of biodegradable organics needed to be fed to the digester. It was assumed that the biodegradable organics made up approximately 2/3 of the total COD in the PSS; therefore, the PSS was diluted to 1.5gCOD/*l* before being fed to the digester.

The amount of dilution required for the sulphidogenic SSPAD PSS feed was dependent on the COD concentration of the undiluted PSS. However, in general, the sulphidogenic SSPAD PSS feed was prepared by taking approximately 500m*l* undiluted PSS and diluting with 11*l* of tap water. Therefore, 11.5*l* of diluted PSS was prepared each time and stored in the fridge at 4°C.

For sulphate reduction, the biodegradable organics present in the PSS act as the electron donor, and sulphate is used as the electron acceptor, producing H_2S. Therefore, additional sulphate needed to be added to the sulphidogenic SSPAD PSS feed. The sulphate was added before

feeding, i.e. the sulphidogenic SSPAD PSS feed that was stored in the fridge did not contain sulphate.

Sulphate was added to the sulphidogenic SSPAD PSS feed as a blend of two mixtures, sulphuric acid (H_2SO_4) and sodium sulphate (Na_2SO_4). Both the sulphuric acid and the sodium sulphate were prepared beforehand, and the SO_4^{2-} was tested to ensure a concentration of 3 gSO_4^{2-}/l. The sulphate mixture, used for adding sulphate to the feed, did not contain any COD, as sulphate is in the most oxidised state. Therefore, adding the sulphate mixture to the sulphidogenic SSPAD PSS feed would further dilute it. Likewise, mixing the sulphidogenic SSPAD PSS feed with the sulphate mixture would dilute the sulphate concentration, as the PSS contained negligible sulphate. To compensate for this, the macerated PSS from Potsdam was diluted to a concentration of 3gCOD/*l* and the sulphate solution was diluted to a concentration of $3gSO_4/l$. Therefore, by adding 500m*l* of each, the resulting feed had a total volume of 1*l* and contained 1.5 gCOD/*l* and 1.5 gSO_4/l.

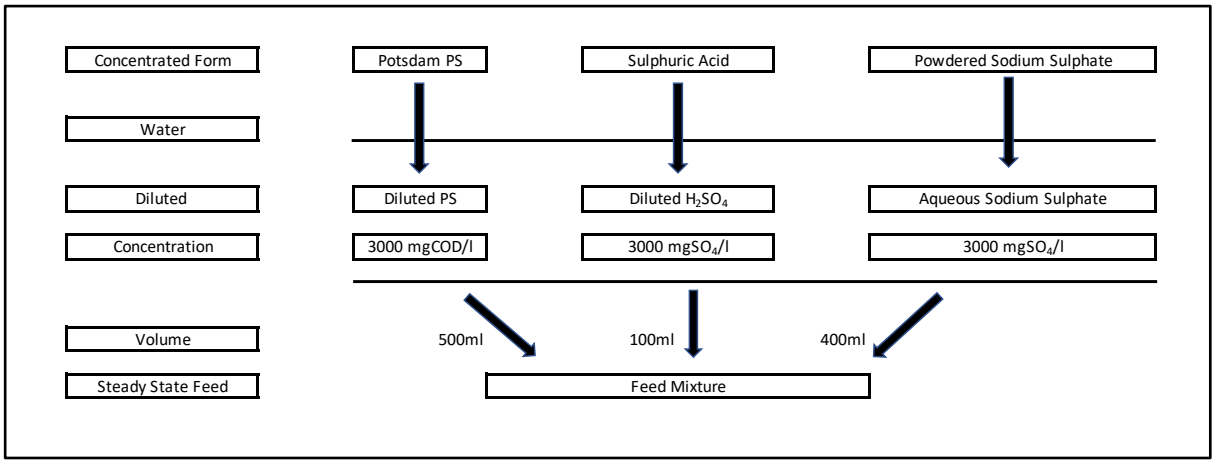

Figure 3. 7: Sulphidogenic SSPAD feed mixture

The final feed mixture fed to the sulphidogenic SSPAD was 5-parts sulphidogenic SSPAD PSS with 1-part diluted sulphuric acid and 4-parts sodium sulphate. The addition of the diluted sulphuric acid ensured a low feed pH of 2.6, as the sulphidogenic reaction generates alkalinity. Subsequently, even with the low feed pH, the sulphidogenic SSPAD was maintained at an operating pH of 7.1 without the addition of external alkalinity.

3.4 Augmented BMP Experiment

3.4.1 Overview

The AugBMP experiment consisted of the two usual seeding conditions, as specified by Angelidaki *et al.* (2009) and Holliger *et al.* (2016). The first seeding condition was a control batch reactor, in which only the methanogenic SSPAD effluent (inoculum) was inserted. The second seeding condition was a test batch reactor, in which both methanogenic SSPAD effluent (inoculum) and the organic substrate (in this case, casein/PSS, as described in Section 2.5 and Section 2.6) was inserted.

3.4.2 Experimental set-up

In order to achieve reliable results, the experiment was conducted in triplicate. i.e. utilising three control reactors and three test reactors; therefore, requiring six reactor vessels in total. The control reactors were labelled C1, C2, C3 and the test reactors T1, T2, T3, respectively. The reactor vessel chosen for the AugBMP experiment was a 6*l* glass aspirator bottle. The aspirator bottle consisted of two orifices, one at the top of the bottle, and the other near the base. A rubber stopper, with two holes drilled into it, was used to seal the orifice at the top of the bottle. The first hole in this top rubber stopper was used as a feeding tube (to get liquid into the bottle during seeding), and the second hole was to allow for the biogas to escape. The feeding tube was sealed with a clamped rubber hose for the duration of the experiment to ensure that anaerobic conditions, as well as a gas-tight environment, were maintained. The orifice at the bottom of the glass aspirator bottle was sealed with a rubber stopper and a syringe. The syringe was used for sampling and ensured that the accumulation of residual liquid in the outlet port was avoided. Therefore, when a sample was taken, the syringe was pulled out to allow for the effluent to leave the reactor. After a sufficient sample volume had been taken, the syringe was then pushed back in, subsequently forcing the liquid back into the reactor.

Each reactor included a 100W submersible aquarium fish tank heater (which was smaller than the 200W used in the SSPAD) to maintain mesophilic conditions, 35°C. The reactor was manually stirred by picking the vessel up and moving it in a horizontal, circular motion. This mixing regime was used as six magnetic stirrers were not available. The reactor was manually stirred 4-5 times daily to ensure homogenous mixing.

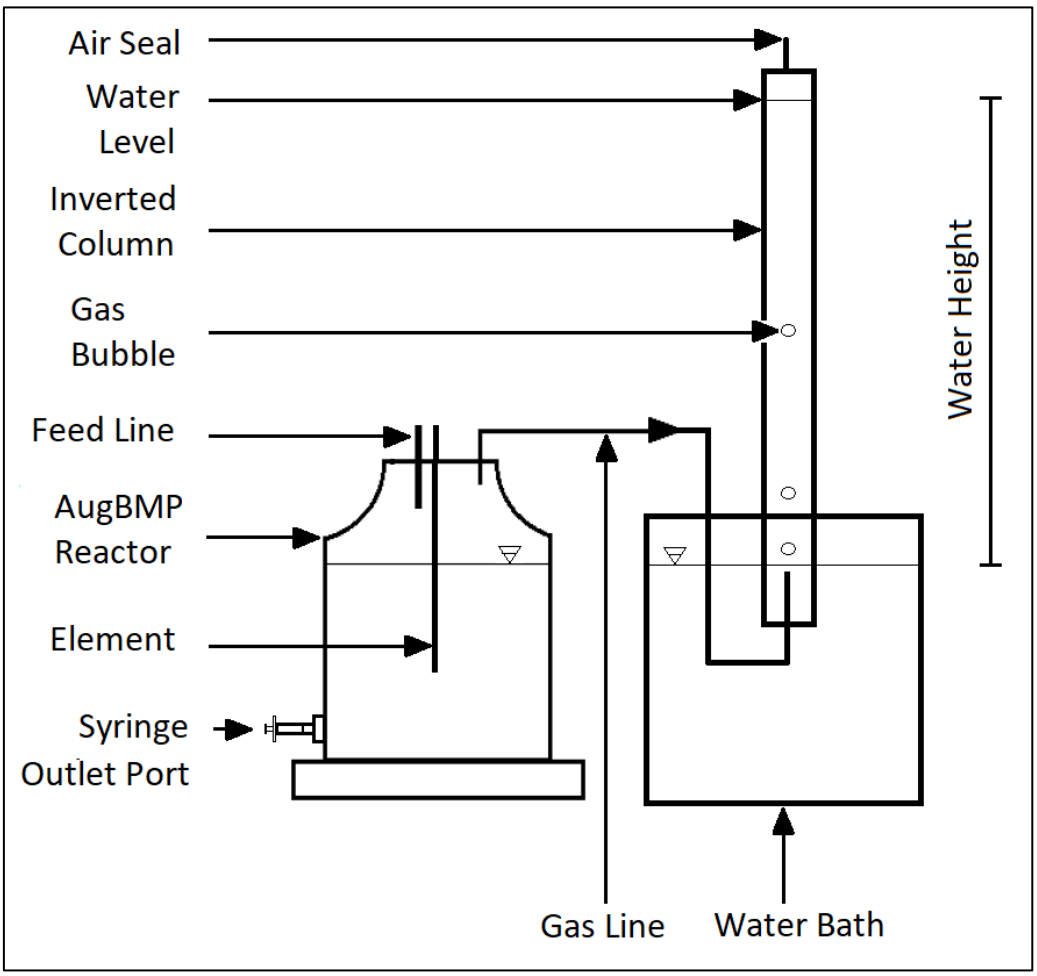

Figure 3. 8: AugBMP experiment set-up

The experiment was set up for volumetric measurement of the biogas, i.e. maintaining a neutral pressure inside the reactor, as shown in Figure 3.8. The rubber stopper used to seal the top of the reactor contained a gas port. The gas port was connected via silicon gas tubing to the base of an inverted water column. The inverted column was made from Perspex with a height of 2000mm and an internal diameter of 60mm. A measuring tape was placed along the outside of the column. Subsequently, the gas volume and production rate were determined using the internal diameter and the measuring tape. The inverted water column was mounted on a purpose-built rig and was submerged into the water bath. The water bath was filled with tap water, which was kept at ambient lab temperature (21°C). The column was filled using a vacuum pump connected at the top of the column, which sucked the water from the bath into the upright column. The columns were tested for leaks before the start of the experiments.

Figure 3. 9: AugBMP experiment photograph

3.4.3 Seeding Procedure

The inoculum used for seeding the AugBMP experiment was wasted directly from the methanogenic SSPAD on the day the experiment began. Therefore, a degassing period was not

utilised as the inoculum needed to be as fresh as possible to maintain the SSPAD effluent characteristics. Degassing is a pre-incubation step that removes any residual biodegradable material present in the inoculum (Angelidaki *et al*., 2009). The degradation of the residual biodegradable material present in the inoculum was accounted for by the AugBMP control reactor. The steady-state AD model of Sötemann *et al*. (2005), tailored for the SSPAD conditions, was used to estimate the active biomass concentration present in the methanogenic SSPAD effluent, that was used to inoculate the AugBMP experiment. It was crucial to correctly estimate the biomass concentrations at the start of the modelled AugBMP experiment, as the biomass concentrations were used as an input for the PWM_SA_AD model and would affect the material released into the AugBMP due to biomass decay, as well as the substrate degradation rates.

The AugBMP control reactor contained inoculum and water only. The starting mix consisted of 7.5*l* of inoculum and 7.5*l* of tap water (the mix resulted in the inoculum being diluted to half the original SSPAD effluent concentration). This 15*l* starting mix was stirred in a large container. Once the contents were homogenously mixed, 5*l* was transferred from the container to each of the three AugBMP control reactors through the feed line. The mixing process was performed as quickly as possible to limit exposure to oxygen. Furthermore, each AugBMP control reactor was flushed with nitrogen gas before the starting mix was transferred, which ensured anaerobic conditions inside the reactor.

The AugBMP test reactor contained inoculum, water and organic substrate (casein/PSS). The 15*l* starting mix contained 3.75*l* of inoculum, 10*l* of tap water and 1.25*l* of the substrate. Hence, this mix resulted in the inoculum being diluted to a quarter the original SSPAD effluent concentration, and half the AugBMP control concentration. Therefore, the influence (gas production and the release of inorganics) of the AugBMP control reactor due to the breakdown of residual organics was halved when using it as the baseline for analysis of the AugBSP test reactor. The starting procedure was identical to that of the AugBMP control, i.e. the 15*l* starting mix was stirred in a large container, and then 5*l* was transferred to each of the AugBMP test reactors. The starting mix for each of the AugBMP experiment reactors is summarised in Table 3.1

Table 3. 1: AugBMP experiment starting mixture

Total Mix			
Component Volumes	Unit	Control Reactors	Test Reactors
Biomass	l	7.5	3.75
Water	l	7.5	10
Substrate	l	0	1.25
Total Volume	l	15	15
Individual Reactor Mix			
Component Volumes	Unit	Control Reactor	Test Reactor
Biomass	l	2.5	1.25
Water	l	2.5	3.33
Substrate	l	0	0.42
Total Volume	l	5	5

3.4.4 Sampling Procedure

The sampling was conducted regularly to generate data that would be useful to determine kinetic parameters such as the hydrolysis rate and substrate uptake rates relative to the biogas production. The AugBMP reactors were sampled daily for the first ten days of the experiment, after which the reactors were sampled every second day for the remainder of the experiment. After the first ten days, the sampling frequency was decreased to every second day (this was because the hydrolysis rate and substrate uptake rates were expected to have decreased). The sampling continued until the activity in the reactor had stabilised, i.e. there was no significant change in COD or biogas production.

The AugBMP sampling was conducted using a gasbag and a sampling cup. The reactor was thoroughly mixed before sampling. The sample was removed from the syringe outlet port at the base of the reactor, as shown in Figure 3.8. The syringe was used to ensure that no residual effluent remained in the outlet port after sampling. During sampling, a gasbag containing biogas from the methanogenic SSPAD, was connected to the feed line at the top of the reactor. The gasbag ensured that the pressure remained constant, as a negative pressure occurred in the reactor if it was sealed when the sample was removed. The gasbag contained biogas from the methanogenic SSPAD in order to keep the headspace conditions anaerobic. Nitrogen gas was considered; however, biogas was used instead, as the gas in the AugBMP reactor headspace was sent for analysis to determine the methane content. A 120m*l* sample was taken from the

reactor, and the pH and conductivity were measured immediately after sampling (before significant loss of CO_2 occurred), after which, the sample was tested for a diverse range of constituents, which is further explained in Section 3.6.

3.4.5 Gas Measurement

The biogas produced by each of the reactors was captured in the inverted water columns. The water level in the column was checked frequently to accurately capture the methane potential curve. Each column was the same size in diameter and marked with a measuring tape, which allowed for the gas volume and production rate to be monitored with time. However, the gas volume in the inverted column was influenced by the column water level relative to the bath surface level. Therefore, when determining the molar equivalent, and subsequently, the COD equivalent of the biogas produced, adjustments for column pressure needed to be made. The pressure exerted on the gas inside the column varies with height above the water level of the bath. The surface of the water bath is at atmospheric pressure (ambient laboratory pressure). However, the gas inside the column has a pressure lower than atmospheric. This lower pressure is caused as the column water level is above that of the bath water level. As a result, the higher the column water level above the bath water level, the larger the volume the gas occupies. Equation 3.2 below illustrates that at the height of 1.8m above the water level of the bath, the pressure in the column is 17 623 Pa lower than atmospheric. Therefore, at room temperature (20°C) and atmospheric pressure (101.325kPa), 1 mol of gas would occupy 24l. However, at the height of 1.8m above the bath water level, 1 mol of gas would occupy 29l.

$$P = \rho g h \quad \text{Pa (3.2)}$$

$$P = (998 kg/m^3)(9.81 m/s^2)(-1.8 m)$$

$$P = -17622.68\ Pa$$

3.5 Augmented BSP Experiment

3.5.1 Overview

Similar to the AugBMP, the AugBSP experiment consisted of the two seeding conditions, specified by Angelidaki *et al.* (2009) and Holliger *et al.* (2016). The first seeding condition was a control batch reactor, in which only the sulphidogenic SSPAD effluent (inoculum) was inserted. The second seeding condition was a test batch reactor, in which both sulphidogenic SSPAD effluent (inoculum) and the organic substrate (casein/PSS) was inserted. The primary goal of the AugBSP test was to alleviate the gas measurement error experienced with the AugBMP test, as all measurements are conducted in the aqueous phase. Therefore, the approach for the AugBSP experiment was similar to that of the AugBMP test.

3.5.2 Experimental set-up

In order to achieve reliable results, the AugBSP experiment was conducted in duplicate. i.e. utilising two control reactors and two test reactors; therefore, requiring four reactor vessels in total. The control reactors were labelled C1 and C2, and the test reactors T1 and T2, respectively. The reason the experiment was not conducted in triplicate (similar to the AugBMP), was that the accuracy and precision of the results was expected to improve significantly when all measurements were performed on the aqueous solution, i.e. with the gas uncertainty removed.

The reactor vessel chosen for the AugBSP experiment was a 7.9*l* purpose-built Perspex reactor, which was completely sealed with a zero headspace, as shown in Figures 3.10 and 3.11. The reactor had an internal diameter of 186mm and a height of 290mm. The reactor incorporated a sealed plunger-mechanism which allowed a sample to be taken from the reactor while keeping a zero headspace. The plunger was constructed of a circular Polyvinyl Chloride (PVC) plate (184mm in diameter), with a groove cut along the circumference, such that a rubber O-ring could be fitted to ensure a gas-tight seal. The PVC plate was attached to a threaded bar, which rotated through a nut fixed to a horizontal bar. The horizontal bar was attached to the flange of the reactor vessel. At the top of the threaded bar was a handle. The handle allowed the user to screw the plunger up or down. The reactor and its sample mechanism resembled that of a large syringe, pushing a sample out of the reactor while maintaining a zero headspace.

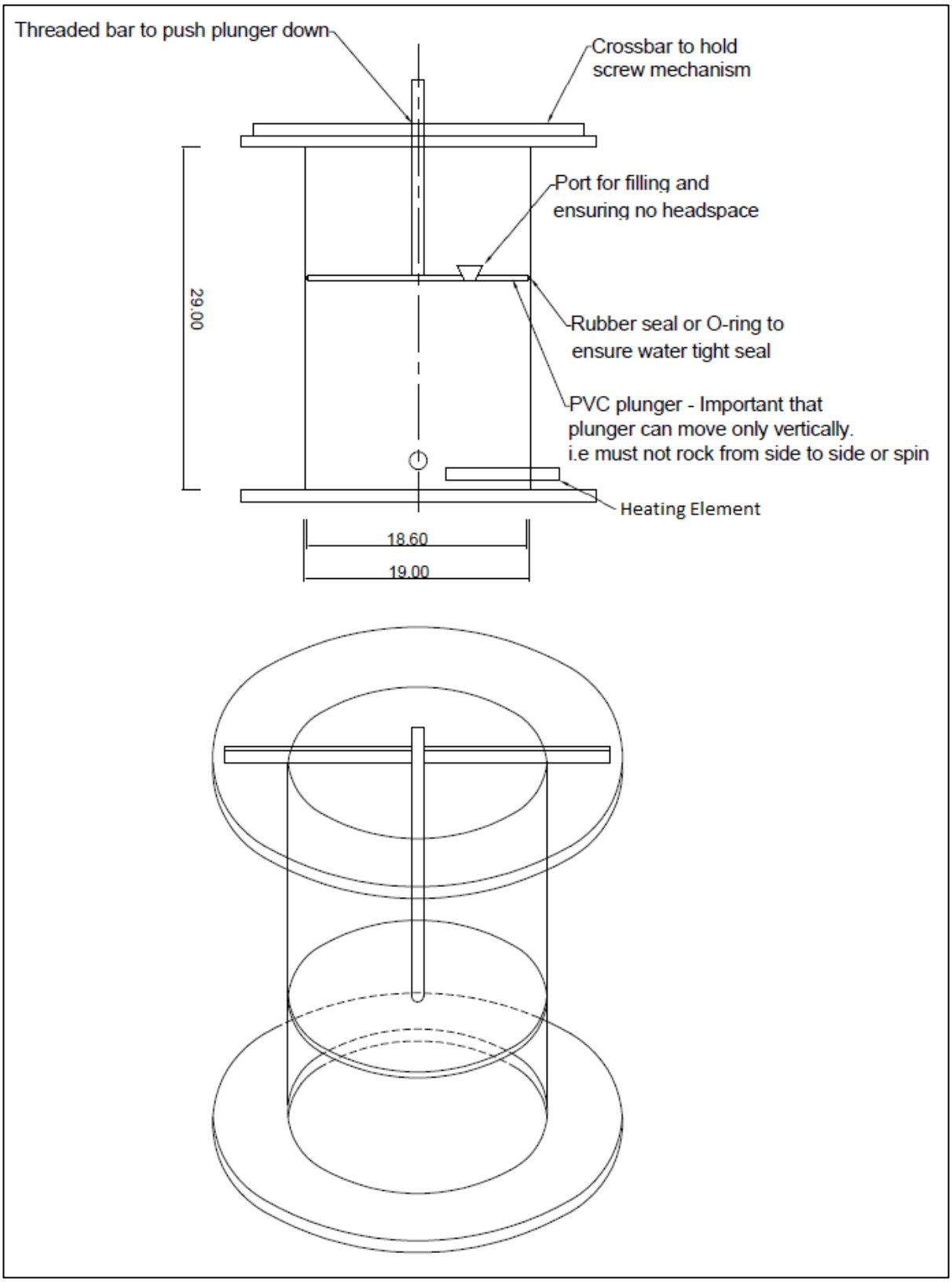

Figure 3. 10: AugBSP experiment design

Each reactor included a 100W submersible aquarium fish tank heater to maintain mesophilic conditions, 35°C. The heating element was inserted into the sidewall of the reactor close to the base. The heating element was placed horizontally and did not interfere with the plunger. The reactor was placed on top of a magnetic stirrer to ensure homogenous mixing. As with the AugBMP reactor vessel, the outlet port of the AugBSP reactor was sealed with a rubber stopper and a syringe. The syringe was used for sampling and ensured that the accumulation of residual liquid in the outlet port was avoided.

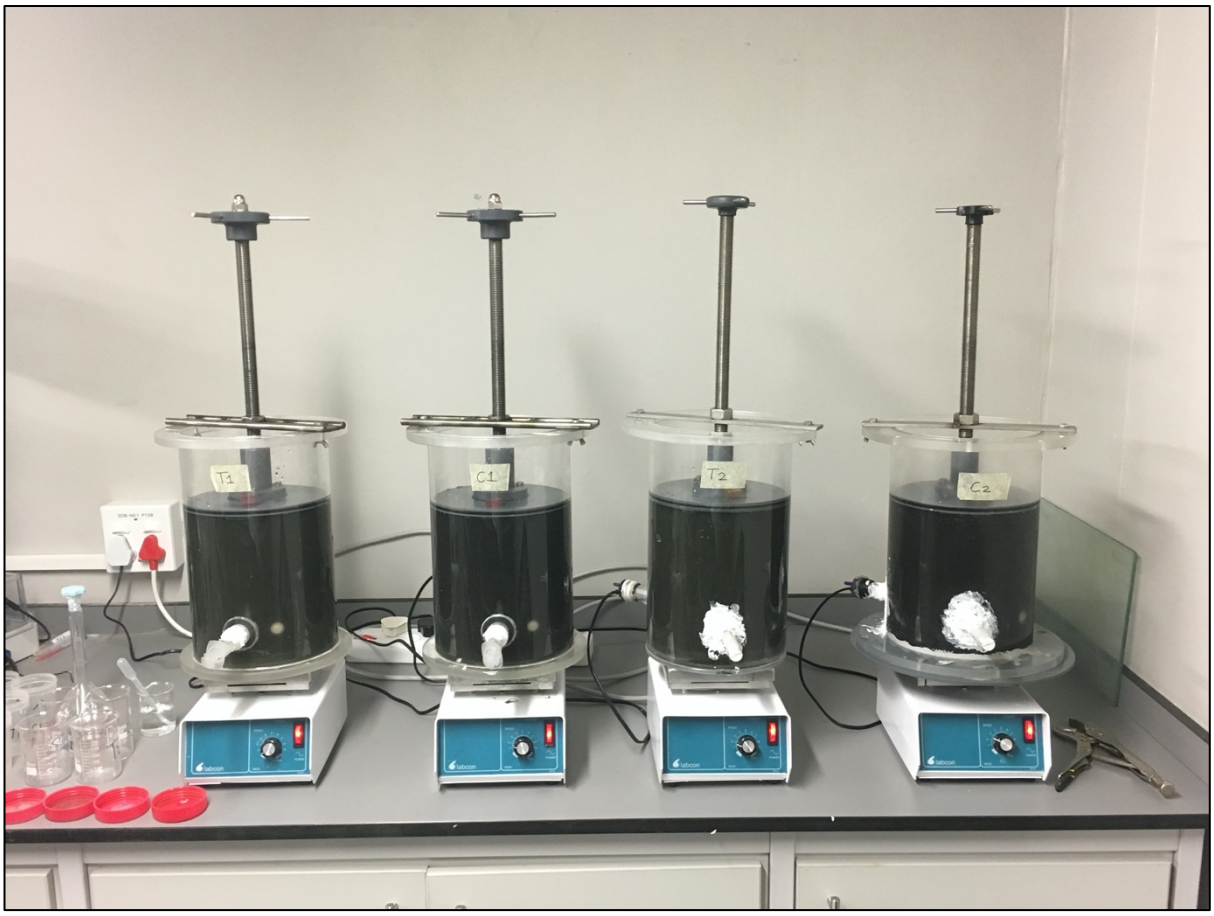

Figure 3. 11: AugBSP experiment photograph

3.5.3 Seeding Procedure

The inoculum used for seeding the AugBSP experiment was wasted directly from the sulphidogenic SSPAD on the day the experiment began. Therefore, as was the case with the AugBMP experiment, the inoculum had to be as fresh as possible (to maintain a SSPAD effluent that could be characterised using steady-state model equations). Likewise, the steady-state AD model of Sötemann *et al.* (2005) was used to estimate the active biomass

concentration present in the sulphidogenic SSPAD effluent, which was subsequently used to inoculate the AugBSP experiment. The degradation of the residual biodegradable material present in the inoculum was accounted for by the AugBSP control reactor. Furthermore, the concentration of biomass at the start of the modelled AugBSP experiment needed to be estimated as it was used as an input for the PWM_SA_AD model and would affect the sulphide produced due to biomass decay, as well as the substrate degradation rates.

The AugBSP control reactor contained inoculum only. The starting mix consisted of 12*l* of inoculum without the addition of tap water (i.e., the starting mix was at the same concentration as the SSPAD effluent). The 12*l* starting mix was then divided equally, such that 6*l* was transferred into each of the two AugBSP control reactors through an inlet port on the plunger. The transfer process was performed as quickly as possible to limit exposure to oxygen. Furthermore, each AugBSP control reactor was flushed with nitrogen gas before the starting mix was transferred, which ensured anaerobic conditions inside the reactor. However, due to the zero headspace in the reactor, anaerobic conditions were easier to ensure, compared to that of the AugBMP experiment. The inlet port was sealed with a rubber stopper immediately after transferring the 6-litre starting reactor mix.

The AugBSP test reactor contained inoculum and organic substrate (casein/PSS). The 12*l* starting mix contained 6*l* of inoculum, 3*l* of the substrate, 2.5*l* of Na_2SO_4 solution and 0.5*l* of H_2SO_4 solution. Each of the sulphate solutions (Na_2SO_4 and H_2SO_4) used was identical to the sulphate solutions described in Section 3.3.2. Subsequently, this mix resulted in the inoculum being diluted to half the original SSPAD effluent concentration, and subsequently, half of the AugBSP control concentration. Therefore, the influence (H_2S production, the release of inorganics) of the AugBSP control reactor due to the breakdown of residual organics was halved when using it as the baseline for analysis of the AugBSP test reactor results. The starting procedure was identical to that of the AugBSP control, i.e. the 12*l* starting mix was stirred in a large container and then 6*l* was transferred to each of the AugBSP test reactors. The starting mix for each of the AugBSP experiment reactors is summarised in Table 3.2.

Table 3. 2: AugBSP starting mixture

Total Mix			
Component Volumes	Unit	Control Reactors	Test Reactors
Biomass	l	12	6
Water	l	0	0
Substrate	l	0	3
Na_2SO_4 Solution	l	0	2.5
H_2SO_4 Solution	l	0	0.5
Total Volume	l	12	12
Individual Reactor Mix			
Component Volumes	Unit	Control Reactor	Test Reactor
Biomass	l	6	3
Water	l	0	0
Substrate	l	0	1.5
Na_2SO_4 Solution	l	0	1.25
H_2SO_4 Solution	l	0	0.25
Total Volume	l	6	6

3.5.4 Sampling Procedure

Similar to the AugBMP, the AugBSP reactors were sampled daily for the first ten days of the experiment, after which the reactors were sampled every second day. The regular sampling was useful to determine kinetic parameters such as the hydrolysis rate and substrate uptake rates relative to the H_2S production. After the first ten days, the sampling frequency was decreased to every second day as the hydrolysis rate and substrate uptake rates decreased. The sampling continued until the activity in the reactor had stabilised, i.e. there was no significant change in COD or H_2S production.

A sample was removed from the AugBSP test reactor by turning the handle at the top of the threaded bar. Turning the handle caused the plunger to move downwards towards the base of the reactor. This downwards motion of the plunger resulted in a brief positive pressure in the reactor, which pushed the sample out of the outlet port. A syringe was used to ensure that no residual effluent remained in the outlet port after sampling.

Two separate sample streams were removed from each of the AugBSP reactors. The first 100m*l* sample stream was collected directly into a glass beaker containing 8 drops of 10M NaOH. The

NaOH was added to the sample to raise the pH above 10. The increase in pH ensured that as much sulphide as possible remained in its dissociated form (HS^-). Raising the pH was necessary as the dissolved sulphide concentration was measured using the open-flux COD method. This method of sulphide measurement was confirmed by Poinapen *et al*. (2009) and is discussed further in Section 3.6.3. Consequently, achieving a sulphur balance over the AugBSP reactor was directly influenced by the amount of dissociated HS^- that remained in solution, as shown in Section 3.7.4.

The second 100m*l* stream, with no chemical additives, was collected in a plastic sampling cup. This second stream was used to determine the remaining constituents, such as pH, conductivity, FSA, OP, alkalinity and solids. Furthermore, the pH and conductivity of the sample were measured immediately (before significant loss of H_2S or CO_2 occurred).

3.6 Analytical Procedures

3.6.1 Overview

The concentrations of the constituents present in the substrate (casein/PSS), the effluent from the SSPADs for both the methanogenic and sulphidogenic systems, and the AugBMP and AugBSP reactors were determined using wet chemistry analysis. Additionally, the methane content of the biogas produced by the methanogenic systems was identified using gas chromatography. The measurements required differed between the methanogenic system and the sulphidogenic system. The sulphidogenic system required two additional measurements to quantify the sulphate and H_2S concentrations. This section describes the measurements performed.

3.6.2 Measurements performed

Table 3.3 shows the 'standard' measurements that were conducted. The term standard aims to highlight the fundamental measurements that were performed on everything, i.e. the feed (casein/PSS), the methanogenic systems (SSPAD and AugBMP) and the sulphidogenic systems (SSPAD and AugBSP).

Table 3. 3: Standard measurements performed

Standard Measurements								
Constituent	COD	Nitrogen	Phosphorus	Solids	Alkalinity	Species	pH	Conductivity
1	Unfiltered	TKN	TP	TSS	Carbonate	C_T	pH	Conductivity
2	Filtered	FSA	OP	VSS	Ammonium	A_T		
3				ISS	Phosphate			
4					VFA			
5					Sulphide			
6					Total			

The sulphidogenic SSPAD and the AugBSP experiment required two additional measurements above that of the standard measurements, as both sulphate and H_2S were present in the aqueous solution. The sulphate and H_2S concentrations were determined by including the organic COD concentration and a direct sulphate assay. These additional measurements are summarised in Table 3.4.

Table 3. 4: Additional sulphidogenic system measurements

Additional Measurements		
Constituent	COD	Sulphate
1	Organic	Sulphate

3.6.3 COD

The procedure used for the COD assay was the sulphuric acid open-flux COD method, followed by titration with ferrous ammonium sulphate (FAS), as defined by Standard Methods (1985). Both the unfiltered and filtered COD concentrations were determined. In general, the unfiltered sample was used to determine the total concentrations (including particulates) for COD, TKN and TP. The filtered sample was used to determine the soluble concentrations for the soluble COD, VFA, alkalinities, FSA and OP. Therefore, the terms unfiltered COD and total COD, as well as the terms filtered COD and soluble COD, are interchangeable.

The sample (substrate/effluent) was filtered using a series of filtration steps. The first step was to pour the sample into a 50m*l* centrifuge tube and centrifuge for 10 minutes at 3500 rpm. Following the centrifuge, the supernatant was poured from the centrifuge tube into a vacuum filter. The sample was filtered through a glass fibre (S&S GF 52) and then a 0.45 μm membrane

(S&S ME 25/21 ST) filter papers. After filtering, the sample was diluted to the appropriate dilution for the required measurement.

For the sulphidogenic SSPAD and the AugBSP experiment, an additional COD measurement was performed to determine the concentration of dissolved H_2S. The method, which was confirmed by Poinapen *et al*. (2009), retains all the sulphide in solution by converting the un-dissociated H_2S into the HS^- species by raising the sample pH using 10M NaOH. Minimal H_2S is lost during sample handling, which includes vacuum filtration. The method requires three COD measurements. The first two are the unfiltered and filtered COD, as specified above, and the third is the soluble organic COD.

The soluble organic COD is the COD associated with the dissolved organics without the influence of sulphide. Therefore, the soluble organic COD is determined by removing the sulphide COD from the sample. The filtered (total soluble) COD is the sum of the soluble organic COD and the soluble sulphide COD. Therefore, by removing the soluble sulphide COD from the sample, the soluble organic COD is isolated.

If the filtered (total soluble) COD concentration is measured, and the soluble organic COD concentration is isolated by removing the sulphide, the dissolved sulphide COD concentration can be determined as the difference between the filtered (total soluble) and the soluble organic COD.

$$H_2S\ COD = filtered\ COD - soluble\ organic\ COD \qquad \text{mgCOD/}l \quad (3.3)$$

Excess zinc sulphate ($ZnSO_4$) was used to remove the dissolved H_2S COD from the sample. The addition of excess zinc sulphate precipitates the dissolved H_2S out of solution as zinc sulphide (ZnS). Therefore, for the sulphidogenic systems, the COD effluent sample was split into three sub-streams. As previously mentioned, the sulphidogenic system was sampled into a beaker containing 8 drops of 10M NaOH. The first sub-stream was used to determine the unfiltered COD concentrations. The second sub-stream was used to determine the filtered COD concentration and underwent the same filtering procedure described above. The third sub-stream had excess zinc sulphate added to it. Following the addition of excess zinc sulphate, the third sub-stream was centrifuged for 10 minutes at 3500 rpm and then vacuum filtered through a 0.45 μm membrane filter paper to remove the precipitated zinc sulphide. The third sub-stream

was then tested for COD concentration using the procedure defined by Standard Methods (1985). Therefore, the third sub-stream quantified the soluble organic COD concentration.

3.6.4 TKN and FSA

The TKN and the FSA concentrations were determined using the micro-Kjeldahl method (4500-Norg (C)) and titrimetric method (4500-NH_3 (B), (E)) respectively, as outlined in Standard Methods (1985, Method 420B).

3.6.5 TP and OP

The TP concentration was determined using the sulphuric/persulphate digestion at 100°C (Standard Methods, 1985, Method 424C *III*). The acid digested TP sample, as well as the OP sample, were tested using the molybdate-vanadate colour development for ortho-phosphate using a spectrophotometer (Standard Methods, 1985, vanadomolybdophosphoric acid colorimetric method). The ThermoFisherScientific Gallery was used as a spectrophotometer, with a wavelength set to 470 μm, in order to measure the colour intensity of the sample.

3.6.6 Solids

The total suspended solids (TSS) concentration was measured by taking a 50m*l* sample and centrifuging in a centrifuge tube at 3500 rpm for 10 minutes. The supernatant was poured out, and the solids that settled at the bottom of the centrifuge tube were transferred to a crucible. The crucible was then oven-dried at 95°C for 24 hours. The inorganic suspended solids (ISS) concentration was measured by placing the oven-dried crucible in an incinerator at 550°C for 20 minutes. The empty crucible, the oven-dried crucible and the incinerated crucible was weighed on a mass balance. The volatile suspended solids (VSS) concentration was determined as the difference between the TSS and ISS mass. The method is described in Standard Methods (1985, 2540(D) for TSS and 2540(E) for VSS).

$$VSS = TSS\ (Oven\ dried\ mass) - ISS\ (incinerated\ mass) \qquad \text{mgVSS/}l \quad (3.4)$$

3.6.7 Alkalinity

The alkalinity was measured using the 5-pH point titration method (Moosbrugger *et al.*, 1993). The method allows for the total alkalinity and subspecies alkalinities to be determined. Furthermore, the method also allows for the VFA (as acetate, A_T) and the dissolved carbon (C_T) concentrations to be determined. Five pH points are required to determine the alkalinity, VFA (A_T) and C_T concentrations. A brief outline of the procedure is given below:

1. Pour a filtered sample (10-50m*l*) into a 50m*l* volumetric flask. If the sample is less than 50m*l*, fill the remaining volume in the flask with distilled water such that a total volume of 50m*l* is achieved. The dilution is taken into account by the 5-point titration software.
2. Measure the conductivity and temperature of the sample
3. The 50m*l* sample is gently stirred to avoid gas loss (CO_2 or H_2S)
4. The five pH points are the original sample pH (say 7.2) and four set pH points, 6.70, 5.90, 5.20, and 4.30.
5. Diluted HCl with known normality is added to lower the sample pH. The cumulative volume of acid added to reach each of the set points above is recorded.
6. The total ammonia, phosphate and sulphide system concentrations (N_T, P_T and S_T) need to be known.
7. The cumulative values of HCl acid added, as well as the pH points closest to the setpoints are then entered into the 5-point titration program.
8. The outcome gives the H_2CO_3 alkalinity, from which C_T is determined, theVFA (as acetate, A_T) and the total alkalinity concentrations.

The addition of acid for the 5-point titration method was conducted using the HI 902 Color, an automatic potentiometric titrator by Hanna Instruments. The automatic titrator contained a pH probe, a stirring paddle and a titration jet, from which the acid was added to the stirred sample. The titrator was programmed to discharge acid slowly while recording the sample pH. The acid was added at a moderate rate, such that the titration took approximately 10 minutes to complete. The titration concluded at an endpoint of 4.30, as specified above, and the data was stored digitally on a removable drive. The data was then extracted, and the required pH points and cumulative acid volumes were entered into the 5-point titration program.

The mixed weak acid/base species present in both the methanogenic and sulphidogenic systems were the carbonate (C_T), the ammonium (N_T), the phosphate (P_T) and the VFA (A_T) systems. The sulphidogenic system contained one additional species, sulphide (S_T), which was negligible in the methanogenic system. Therefore, to correctly determine the alkalinities for each of the species present, the concentration of ammonia, phosphate and sulphide needed to be known. The ammonia was measured using the FSA method, the phosphate was measured using the OP method, and the sulphide was measured using the COD method.

For the methanogenic system, the release of ammonia into the bulk liquid was significant. Furthermore, for the sulphidogenic system, the release of ammonia, as well as the production of sulphide, in the bulk liquid was significant. Therefore, in order to obtain the correct H_2CO_3 alk. and VFA concentrations from the titration program, it was crucial that the correct ammonia and sulphide concentrations were entered. Furthermore, the total alkalinity concentration is not affected by H_2S or CO_2 loss, as it is determined by the cumulative volume of acid added to the sample.

When determining the alkalinity of the PSS substrate using the 5-point titration method, a small volume of base was added to the sample to raise the starting pH. The PSS was acidic (pH of 5.4), and subsequently, the starting pH point was below the first set point of 6.7. Therefore, diluted NaOH was added to raise the pH of the solution. However, this addition of NaOH increased the total alkalinity of the PSS externally, i.e. buffer capacity was added to the PSS. Therefore, to determine the PSS alkalinity accurately, the alkalinity determined using the 5-point titration method needed to be adjusted back to the that of the original PSS alkalinity, i.e. before the addition of the base. The original PSS alkalinity was determined using the following steps:

1. The activity coefficients of each subspecies (carbonate, ammonia, phosphate, sulphide, acetate and water) needed to be adjusted based on the solution temperature. This concept was thoroughly explained by Loewenthal *et al.* (1989), in which the Davies equation (Butler, 1964) is used to calculate the activity coefficients.

2. The C_T and A_T species concentrations were calculated using the 5-point titration program for the PSS sample containing the NaOH solution, with N_T, P_T and S_T known. The addition of NaOH does not affect the subspecies concentrations. The addition of

NaOH only raises the solution pH and total alkalinity, as NaOH does not contain C, N, P or S.

3. With C_T and A_T determined from the solution containing the NaOH, the subspecies alkalinities for the original PSS sample can be determined using the equations described by Loewenthal *et al*. (1991). These equations allow for the sub-species alkalinities to be determined by knowing the total species concentration and the solution pH. For example, the Alk H_2CO_3 concentration of the PSS before the addition of NaOH can be determined using Equation 3.5 below, as C_T and the original sample pH of the PSS were known.

$$[Alk\ H_2CO_3] = C_T \frac{1 + 2X}{(1 + W + X)} \quad \text{mol (3.5)}$$

Where:

$W = 10^{pK\prime_1 - pH}$

$X = 10^{pH - pK\prime_2}$

4. This calculation was repeated for the remaining subspecies' alkalinities, the equations for which are given in Appendix A. Subsequently, the total alkalinity of the original PSS sample is the sum of the subspecies alkalinities, which should be the same as subtracting the total alkalinity of the NaOH added.

$$Total\ Alkalinity = AlkH_2CO_3 + AlkNH_4^+ + AlkH_2PO_4^- + AlkH_2S + AlkHAc + AlkH_2O \quad \text{mol (3.6)}$$

3.6.8 pH

The pH was measured daily using both a benchtop pH meter, an Accsen (pH 8) with an Accsen (AEL32T) pH probe, as well as the pH meter fitted to the automatic potentiometric titrator. The pH was measured immediately after sampling to avoid excess CO_2 or H_2S loss.

3.6.9 Sulphate

The sulphate used for the sulphidogenic systems was measured in the influent and effluent streams for both the SSPAD and the AugBSP reactors. The sulphate was measured using a discrete analyser, the Gallery by ThermoFisherScientific. The Gallery used the barium chloride (SM 4500 SO4- E, ISBN 0117533406, EPA 375.4, DIN 38405-D, ISO 15923-1) method for analysis. The analysis was conducted using a 2nd order calibration curve.

3.6.10 Gas Chromatography

The biogas produced in the methanogenic SSPAD and the AugBMP experiment was analysed using a Perkin-Elmer Autosystem gas chromatograph equipped with a Supelco wax column (1.2 mm x 37mm). A flame ionisation detector (FID) was used for the determination of the CH_4 fraction of the biogas. Measurements were performed by injecting 100 µl of gas, with the FID and oven temperatures set at 280°C and 50°C, respectively. A standard curve was generated using 25% and 50% CH_4, and nitrogen was used as a carrier gas at a flow rate of 1.5ml/min. The balance of the biogas composition was assumed to be CO_2.

3.6.11 Summary

Table 3.5 summarises the required measurements for each respective system.

Table 3. 5: Required measurements

Measurement required										
			Methanogenic SSPAD		Sulphidogenic SSPAD		AugBMP		AugBSP	
Measurement	Definition	Unit	Influent	Effluent	Influent	Effluent	Influent	Effluent	Influent	Effluent
Unfiltered COD	Chemical Oxygen Demand	mgCOD/l	√	√	√	√	√	√	√	√
Filtered COD	Chemical Oxygen Demand	mgCOD/l	√	√	√	√	√	√	√	√
Organic Soluble COD	Chemical Oxygen Demand	mgCOD/l				√				√
TKN	Total Kjeldahl Nitrogen	mgN/l	√	√	√	√	√	√	√	√
FSA	Free and Saline Ammonia	mgN/l	√	√	√	√	√	√	√	√
TP	Total Phosphate	mgP/l	√	√	√	√	√	√	√	√
OP	Ortho-phosphate	mgP/l	√	√	√	√	√	√	√	√
TSS	Total Suspended Solids	mgTSS/l	√	√	√	√	√	√	√	√
ISS	Inorganic Suspended solids	mgISS/l	√	√	√	√	√	√	√	√
VSS	Volatile Suspended solids	mgISS/l	√	√	√	√	√	√	√	√
Alk H_2CO_3	Carbonate Alkalinity	mgCaCO3/l	√	√	√	√	√	√	√	√
Alk NH_4^+	Ammonium Alkalinity	mgCaCO3/l	√	√	√	√	√	√	√	√
Alk $H_2PO_4^-$	Phosphate Alkalinity	mgCaCO3/l	√	√	√	√	√	√	√	√
Alk HAc	VFA Alkalinity	mgCaCO3/l	√	√	√	√	√	√	√	√
Alk H_2S	Sulphide Alkalinity	mgCaCO3/l				√				√
Alk H_2O	Water Alkalinity	mgCaCO3/l	√	√	√	√	√	√	√	√
Total Alkalinity	Total Alkalinity	mgCaCO3/l	√	√	√	√	√	√	√	√
C_T	Carbonate Species	mg/l	√	√	√	√	√	√	√	√
A_T	Acetate Species	mg/l	√	√	√	√	√	√	√	√
pH	Power of hydrogen		√	√	√	√	√	√	√	√
SO_4^{2-}	Sulphate	mg/l			√	√			√	√
CH_4	Methane Gas	l, mol, gCOD		√				√		

3.7 Evaluation of Experimental Results

3.7.1 Overview

The accuracy and precision of the experimental data collected for the SSPADs and the augmented batch tests was evaluated using two approaches. The first approach was based on the fundamental principle of conservation of mass, which states that mass is conserved throughout the system. The second approach was based on experimental error and uncertainty.

Conservation of mass states that the flux of material entering the system (AD) should equal the flux of material exiting the system. Anaerobic digestion, both methanogenic and sulphidogenic, requires the participation/conversion of organic and inorganic compounds for the biochemical processes. These compounds can be tracked such that their uptake, conversion or release can be traced throughout the system by measuring the constituent concentrations entering and exiting the AD. The mass balance calculations are explained in Sections 3.7.2 to Section 3.7.5.

It was crucial to incorporate some statistical evaluation for the collected data, as it is not possible to measure physical quantities with perfect certainty (Carson, 2002). Multiple samples for the same data point were collected and analysed such that a greater certainty for each point was achieved. Measuring multiple samples for the same data point is crucial, especially when

working with particulate samples as a homogeneous distribution throughout the solution is difficult to achieve, and therefore; some of the samples may contain more material, and subsequently have higher concentrations than other samples. The statistical evaluation for the collected data is explained in Section 3.7.6.

3.7.2 Mass Balances

The results obtained during the experimental investigation required continuous review and evaluation to check their reliability and validity before further calculations were undertaken. This evaluation mainly involved performing material mass balance calculations over the systems.

Material mass balance calculations are a good way of checking the reliability and accuracy of experimental results. They are based on the principle that at steady state the flux of the material exiting the system must be equal to the flux entering the system. Therefore, mass balance checks on COD, N, P and S were determined immediately on completing a steady state test period and at the end of the AugBMP and AugBSP experiments. Material mass balances within the range of 90% - 110% are indicative of accurate and reliable experimental measurements. Therefore, a good COD balance is defined as achieving a balance within 10% above or below 100%. This 10% range is acceptable as obtaining 100% balance under experimental conditions is challenging to achieve and is influenced by systematic and random errors, which can include instrument calibration, poorly maintained equipment and even inaccurate readings from the user (such as parallax error).

In some cases, the mass balances within the range of 80% to 120% are also acceptable if the reasons for it can be determined. If the mass balances are outside this range, one or more of the measured parameters may be incorrect and the results require careful interpretation. The mass balances reported in this thesis are the values obtained after careful evaluation of the data. Furthermore, outlying and inconsistent data, which would otherwise alter the level of accuracy in the result, were removed for the identification of the biodegradable organic composition using the PE function in the modelled environments.

3.7.3 Methanogenic COD mass balance

3.7.3.1 Methanogenic SSPAD

In the methanogenic SSPAD and the AugBMP experiments, COD is converted from the influent organic substrate to biogas (consisting of methane and carbon dioxide), as well as some particulate AD biomass. Chemical oxygen demand (COD) is the electron donating capacity (EDC) of organic material, measured as the quantity of oxygen required for the chemical oxidation of the organic material to simple compounds such as carbon dioxide (CO_2) and water. Hence, the COD balance is expressed in mass equivalent units (of oxygen). However, by measuring the EDC, the COD provides an indication of the utilisable energy in the organic material. A COD balance was achieved by accounting for the COD present in the influent and effluent streams. Therefore, in order to obtain a COD balance over the system, the COD entering the system via the influent must equate to the COD present in the system liquid effluent and the biogas (the biodegradable COD is converted to COD of methane in biogas) produced.

The SSPAD COD balance was performed using the influent and effluent COD concentrations, the cumulative volume of biogas produced and the flowrates in and out of the system. The balance is conducted using the material flux through the system, which is determined by multiplying the unfiltered COD concentration of the influent/effluent by the influent/effluent flowrate.

$$\mathrm{COD}_{in-flux} = COD_{in-conc} \times Q_{in} \quad \text{mgCOD/d} \quad (3.7)$$

$$COD_{out-flux} = COD_{out-conc} \times Q_{out} \quad \text{mgCOD/d} \quad (3.8)$$

The remaining COD required for the balance was contained in the methane gas produced by the methanogenic bioprocess. The difference in COD between the influent and effluent fluxes was contained in the methane gas, assuming a 100% COD balance.

$$\mathrm{COD}_{in-flux} = COD_{out-flux} + \mathrm{COD}_{CH_4} \quad \text{mgCOD/d} \quad (3.9)$$

The methane equivalent COD was required to perform the COD balance. As previously mentioned, the total volume of biogas produced was measured using the wet-tip gas meter connected to the SSPAD. The partial pressure of the methane gas in the SSPAD was determined using a gas chromatograph. Therefore, by multiplying the cumulative biogas volume by the fraction of methane present, the daily methane gas production was determined. The daily methane gas production was then converted to the molar equivalent using the universal gas law. The methane COD equivalent was then determined by multiplying the daily molar production of methane gas by 64 000 mgCOD/mol.

$$n = \frac{RT}{PV} \quad \text{mol (3.10a)}$$

$$COD = 64000n \quad \text{mgCOD(3.10b)}$$

Balancing the COD throughout the methanogenic AD is a crucial objective as it also ensures an energy balance across the system. As previously mentioned, the biodegradable COD is converted to COD of methane in biogas which is further utilisable for energy recovery in systems such as combined heat and power (CHP).

3.7.3.2 AugBMP experiment

The AugBMP experiment was performed as a batch test. Subsequently, the flux of COD entering the system was fixed by the starting COD concentration and starting liquid volume. Furthermore, each AugBMP reactor was sampled daily for the first ten days and then every second day until the end of the experiment. As a result, COD was removed from the batch test during sampling. Therefore, for the AugBMP batch test, in order for the COD to balance, the influent COD must equal the sum of the methane gas COD, the remaining COD in the reactor at the end of the experiment, and the COD present in the sample. The conservation of COD in the AugBMP system is shown in Equation 3.11 and Figure 3.12.

$$MCOD_{Inf} = MCOD_{CH_4} + MCOD_{Rem} + MCOD_{Samp} \quad \text{mgCOD (3.11)}$$

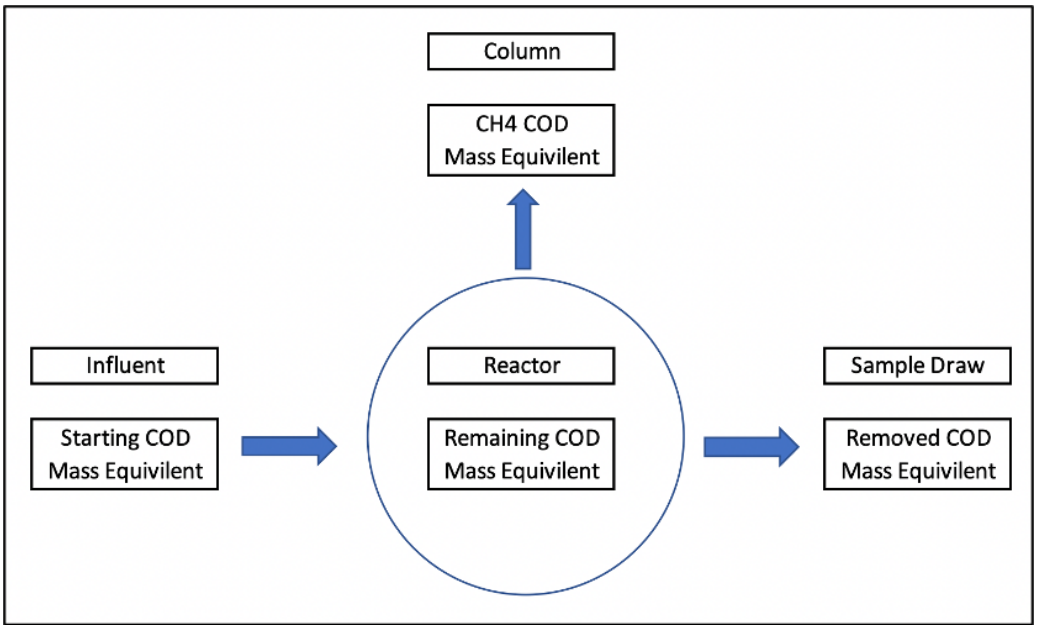

Figure 3. 12: AugBMP COD distribution

The calculation of the COD flux for the AugBMP experiment had a higher level of complexity. The COD that was removed from the AugBMP reactor during sampling needed to be accounted for. Therefore, the total COD in the influent was equal to the starting COD concentration multiplied by the total liquid volume in the reactor at the start. The total COD exiting the reactor was equivalent to the COD present in the methane gas collected in the inverted columns, plus the COD concentration remaining in the reactor at the end of the experiment multiplied by the remaining liquid volume, plus the accumulation of COD removed daily in the sample, which was determined by taking the COD concentration present in the sample multiplied by the volume of the sample drawn. Equation 3.11 has been expanded to Equation 3.12 to demonstrate the calculation.

$$COD_{Inf} \times Vol_{Inf} = MCOD_{CH_4} + (COD_{Rem} \times Vol_{Rem}) + \sum_{i=Day\ 1}^{Last\ day} (COD_{Samp} \times Vol_{Samp}) \quad \text{mgCOD (3.12)}$$

3.7.3.3 AugBMP virtual experiment environment

In tracking the COD for the simulated AugBMP, the PWM_SA_AD model code was adjusted accordingly to account for the sample draw. The adjustment accounted for the time at which the sample was taken, which was identical to that of the laboratory sample time. Subsequently,

120ml of reactor liquid, as well as each of the model components' mass, were removed from the modelled AugBMP experiment for each respective sample draw. A COD balance was then conducted for each of the laboratory AugBMP reactors, as well as the modelled AugBMP reactors, to quantify and compare the COD present in the influent, sample, remaining reactor volume and methane gas. The comparison aimed to highlight potential sources of error, as the modelled AugBMP reactor was mass balanced.

The PWM_SA_AD model usually maintains a liquid balance throughout the experiment. However, this liquid balance does not account for a sample drawn from the AugBMP reactor. Therefore, the code was altered to allow for 120m*l* of the sample to be removed from the reactor on the days that the laboratory reactor was sampled. The sample draw was included in the model by decreasing the equivalent mass of each model component contained in the 120m*l* sample from the total component masses. The mass removal included the mass of H_2O in the model. Consequently, the volume of the reactor, as well as the mass of each component decreased in equal proportions, which subsequently kept the concentration of each component in the reactor the same; therefore, replicating the laboratory conditions. The adjusted PWM_SA_AD model for the AugBMP reactor is shown in Figure 3.13 (which shows the decrease in H_2O mass due to sample draw), Figure 3.14 (which shows the decrease in COD mass due to sample draw) and Figure 3.15 (which shows that the COD concentration was not affected by the sample draw).

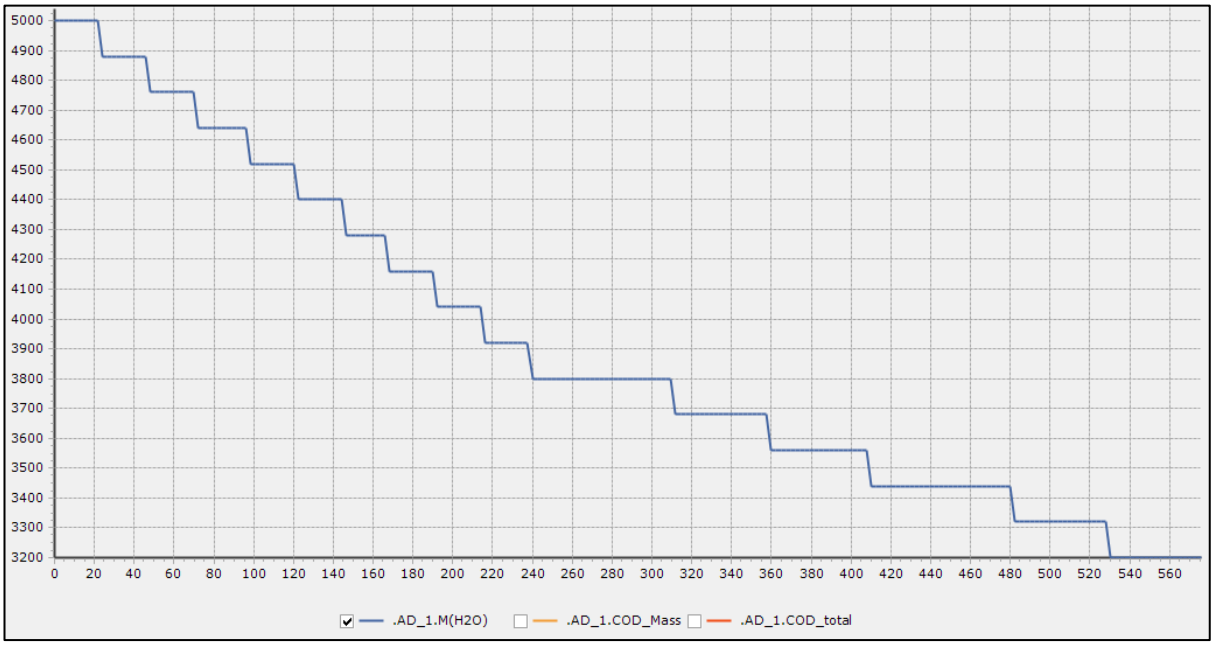

Figure 3. 13: Water mass in AugBMP M2 experiment (x-axis = hours; y-axis = grams)

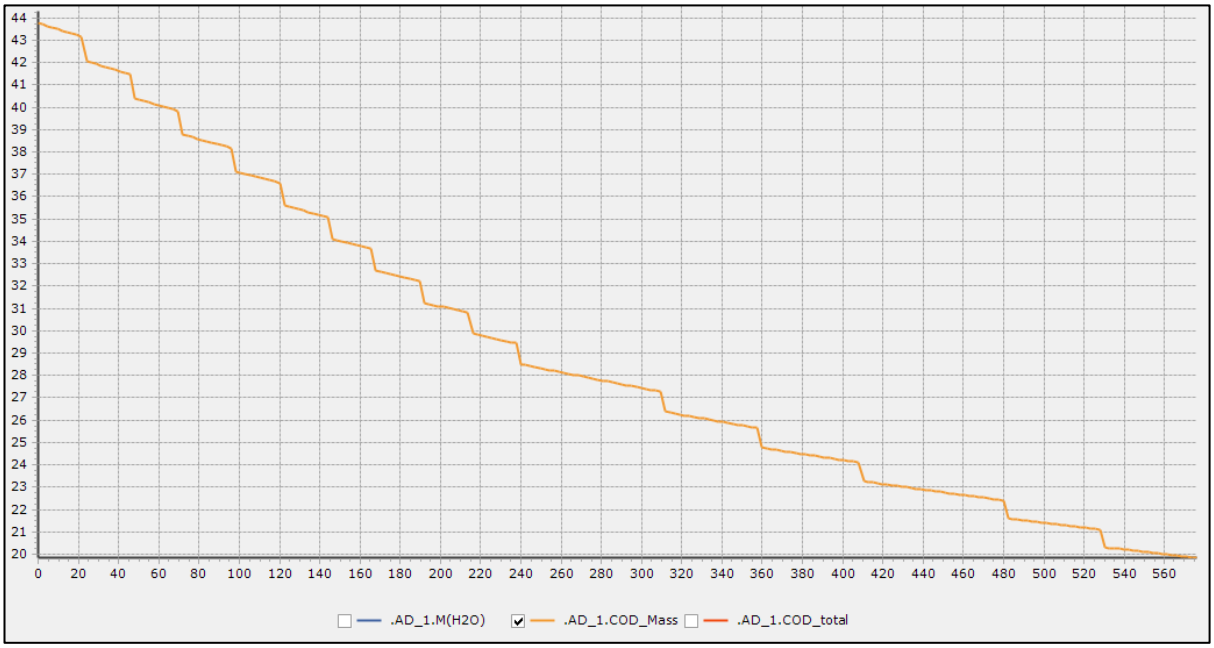

Figure 3. 14: COD mass in AugBMP M2 Experiment (x-axis = hours; y-axis = grams)

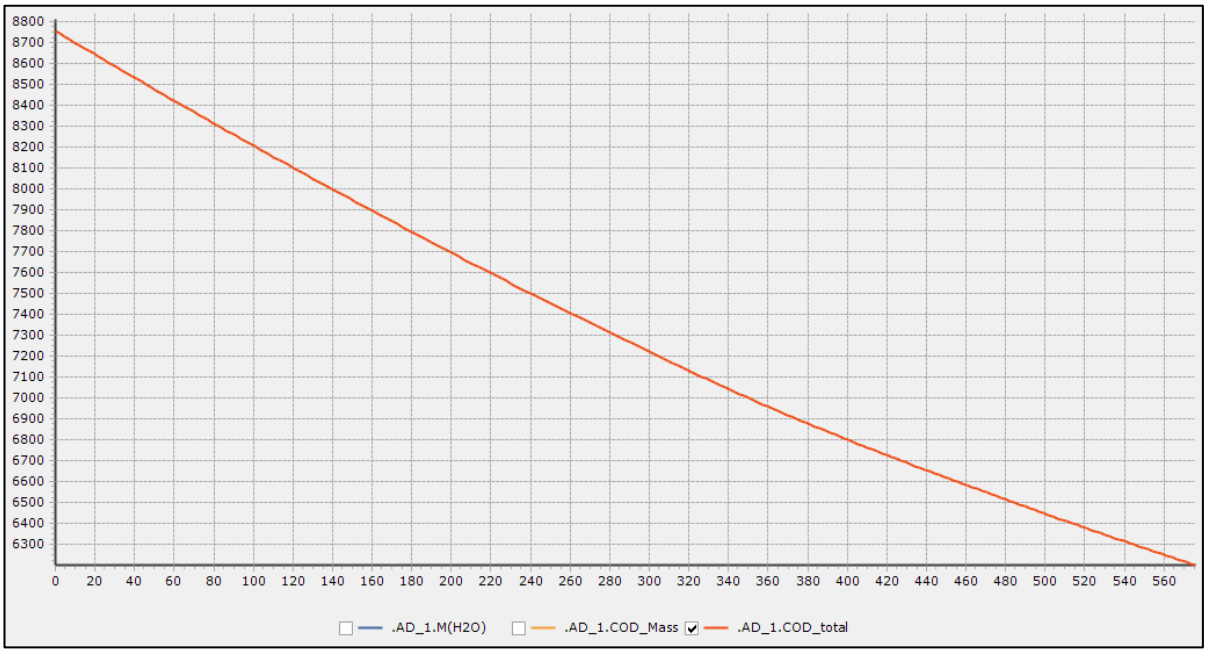

Figure 3. 15: COD concentration in AugBMP M2 Experiment (x-axis = hours; y-axis = mgCOD/l)

3.7.4 Sulphidogenic COD mass balance

3.7.4.1 Sulphidogenic SSPAD

A COD balance was also conducted for each of the sulphidogenic systems. The sulphidogenic system differs from that of the methanogenic system, as the conversion of COD from the influent organic substrate produces H_2S instead of methane. In the sulphidogenic SSPAD, the headspace of the reactor allows for H_2S to diffuse from the aqueous solution to reach equilibrium. However, the SSPAD headspace was sparged with nitrogen gas during feeding. The sparging of nitrogen gas forced H_2S gas out of the headspace and into the ferric chloride gas trap. The COD present in the precipitated ferrous sulphide, which accumulated in the gas trap, was challenging to account for accurately. Instead, the H_2S present in the digester headspace was estimated using the modelled sulphidogenic SSPAD, which was mass balanced.

3.7.4.2 AugBSP experiment COD Balance

In the AugBSP experiment, the total COD present in the reactor remained constant. The constant COD occurred as the reactor was completely sealed with a zero headspace, and subsequently, no COD escaped from the reactor. The H_2S gas remained in solution as HS^- and was measured using the COD determination method of Poinapen *et al.* (2009), as described in Section 3.6.3. It is important to note that concentration was used for the balances instead of mass flux, as all measurements for the sulphidogenic system were in the aqueous phase (mg*/l*), as opposed to the methanogenic system, in which the CH_4 gas produced resulted in a liquid to gas phase change.

3.7.4.3 AugBSP Sulphur Balance

The H_2S COD concentration was used to perform a sulphur balance over the AugBSP experiment. The equivalent sulphur concentration of the H_2S in the aqueous phase was calculated by dividing the H_2S COD concentration by 2. The division by 2 occurs as sulphide can donate 8 electrons per mol, and 1 electron is equivalent to 8 gCOD (Henze *et al.,* 2008). Therefore, 64 gCOD can be donated from 1 mol of sulphur (32g as S), equivalent to 2 gCOD/gS.

The equivalent sulphur uptake from the electron acceptor, sulphate, was calculated for the sulphur balance. The sulphur equivalent from the sulphate required was determined by taking the sulphate concentration and dividing by 3. The division by 3 occurs as sulphur makes up a third of the total mass of sulphate (SO_4^{2-}, 32g of the total 96g per mol). Therefore, the sulphur balance was performed by:

$$S\ Balance = \frac{3}{2} \times \frac{H_2S\ COD\ produced}{SO_4^{2-}\ uptake} \times 100 \quad \% \text{ (3.13)}$$

Equation 3.13 above assumes that all of the sulphur taken up from the sulphate is converted to H_2S. Subsequently, other intermediates such as sulphite (SO_3^{2-}) or thiosulphate ($S_2O_3^{2-}$) were not considered.

3.7.5 TKN and TP Balance

The mass flux of other compounds present in the entering and exiting streams for both the methanogenic and sulphidogenic systems, such as the Total Kjeldahl Nitrogen (TKN) and Total Phosphate (TP), were also checked using the mass balance approach. The total mass of these two constituents should remain constant even though FSA and OP were released into the bulk liquid during the breakdown of the influent organics. The mass remains constant as the unfiltered TKN and TP measurements account for the total flux of nitrogen and phosphorus, which includes both the organic and inorganic concentrations. Therefore, as the organics in the substrate are utilised, and inorganics are released, the total mass does not change.

$$MassBalance = \frac{Mass\ Flux_{eff}}{Mass\ Flux_{inf}} \times 100 \quad \% \text{ (3.14)}$$

3.7.6 Experimental error and uncertainty

Experimental error occurs as the difference between a measured value and the actual value (Carlson, 2002). The experimental error is measured based on its accuracy (which measures how close the measured value is to the actual value) and its precision (which measures how repeatable the measurement was). The errors experienced in the laboratory involve both systematic errors, which can occur due to faulty or poorly maintained instruments, and random

errors, which can occur due to instrument resolution. The error in this project was evaluated using calculations that determined the percentage error, the percentage difference, and the mean and standard deviation (Carlson, 2002).

3.7.6.1 Percentage error

The percentage error, also referred to as relative error in this thesis, assesses the accuracy of the measurement by comparing the difference between an experimental value (E) and the actual value (A).

$$\%error = \frac{|E - A|}{A} \quad \% \text{ (3.14)}$$

3.7.6.2 Percentage difference

The percentage difference assesses the difference between two measured values as a fraction of their average.

$$\%difference = \frac{|E_1 - E_2|}{\left(\frac{E_1 + E_2}{2}\right)} \quad \% \text{ (3.15)}$$

3.7.6.3 The mean and standard deviation

The mean measures the central value for multiple samples collected for a particular data point. The standard deviation measures the deviation of the measured values around the centre point. This mean and standard deviation was of particular importance for this thesis as multiple samples were collected and analysed for each data point throughout each experiment. Therefore, instead of presenting the values obtained from each individual sample, the mean was used to represent the central point of all the samples analysed for each required data point. The mean is determined by summing each of the values obtained and dividing by the number of samples analysed.

$$\langle x \rangle = \frac{1}{N} \sum_{i=1}^{N} x_i \quad \text{(3.16)}$$

The standard deviation is also referred to as the mean square deviation and measures the spread of the collected data relative to the mean (central point).

$$\sigma_x = \sqrt{\frac{1}{N-1}\sum_{i=1}^{N}(x_i - \langle x \rangle)^2} \tag{3.17}$$

For this thesis, the experimentally measured values presented in the tables represent the mean of the samples analysed for that particular data point. Therefore, when discussing values of significance in the text, the mean and standard deviation will be presented as follows:

$$x = \langle x \rangle \pm \sigma_x \tag{3.18}$$

3.8 Influent fractionation

3.8.1 Overview

The influent substrate can be subdivided into four main categories depending on physical and biological characteristics.

1. Biodegradable soluble organics (BSO), consisting of:
    a. Readily fermentable biodegradable soluble organics (FSBO)
    b. Volatile fatty acids (VFA)
2. Biodegradable particulate organics (BPO)
3. Unbiodegradable soluble organics (USO)
4. Unbiodegradable particulate organics (UPO)

Each of the four organic material subgroups, can be given a corresponding COD, C, H, O, N and P mass (or concentration). Therefore, the biodegradable particulate organics can be given a unique CHONP composition. The application of this comprehensive organic characterisation concept was important to meet the objectives of the project, which required the identification of the biodegradable organics composition. In this project, the viability of using the AugBMP and AugBSP experiments towards obtaining data that allows for the application of this

comprehensive organic characterisation concept is investigated for both a soluble organic (casein, which had a known elemental composition) and a particulate organic (PSS, which is a complex substrate containing a wide array of constituents). It should be noted that the PSS used as the substrate for the feed to the SSPADs was also used to seed the AugBMP and AugBSP experiments (See Section 3.3).

This project utilised both a stoichiometric calculation, shown in Section 3.9.2, as well as the PE function (the PWM_SA_AD model facilitates this by assigning each group (BSO, BPO, USO, UPO), a unique CHONP composition), shown in Section 3.10.4, to identify this CHONP composition of the biodegradable organics using the laboratory measurements conducted on the AugBMP and AugBSP experiments. The organic fractionation for COD is summarised in Figure 3.16.

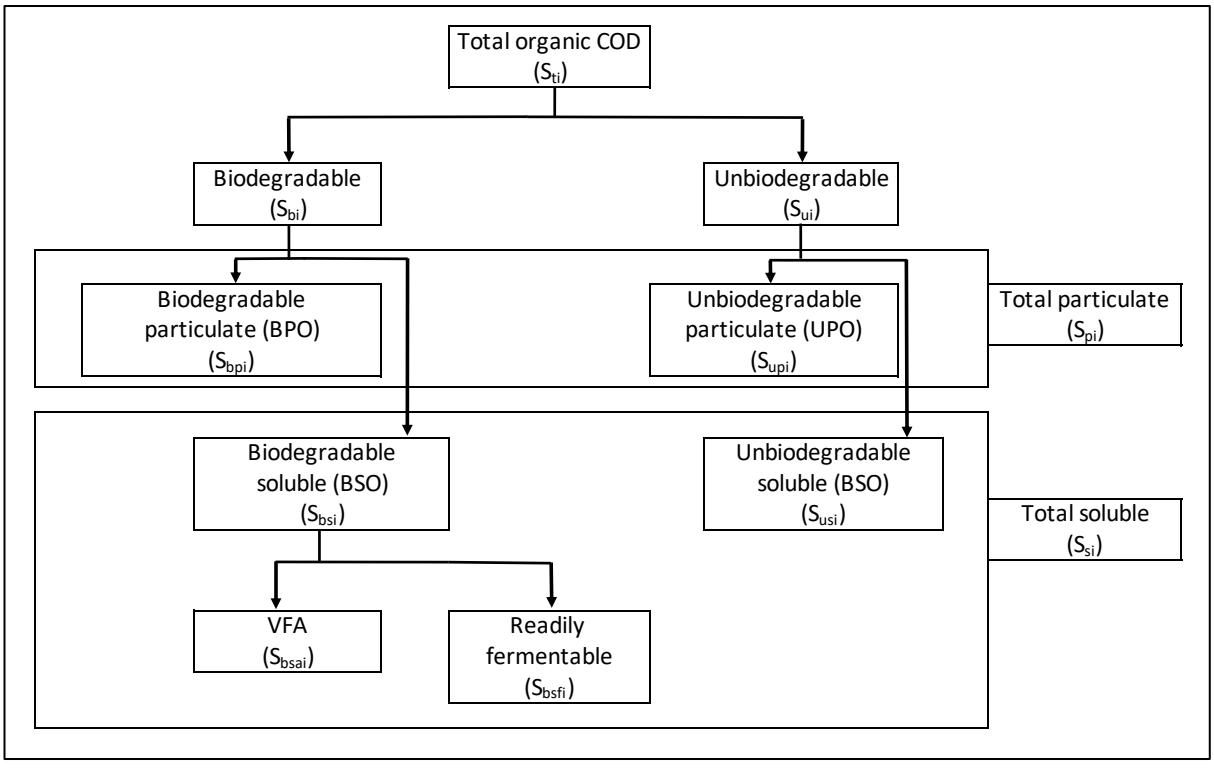

Figure 3. 16: COD fractionation

Accurately fractionating the influent COD in the substrate is imperative as the biodegradable organics behave differently in the AD. Furthermore, soluble organics behave differently to the particulate organics. For instance, the BSOs are hydrolysed faster than the BPOs, whereas the USOs and the UPOs are not hydrolysed at all, and consequently, are not utilised in the reaction.

The presence of unbiodegradable organics increases the total COD concentration in the AD but does not affect the biogas production (methanogenic) or H_2S production (sulphidogenic).

3.8.2 Methanogenic SSPAD

The method used for fractionating the PSS used in the modelled methanogenic SSPAD differed to that of the modelled sulphidogenic SSPAD. The primary difference was that the methanogenic SSPAD contained residual biodegradable organic material (the influent organics that are not degraded in AD, hence exit the PSSAD in the effluent stream). Therefore, because the SSPAD effluent is used to inoculate the AugBMP, the residual biodegradable organics are part of the organic mass to be further degraded. Conversely, the sulphidogenic SSPAD had negligible residual biodegradable organics as the COD concentration was lowered to maintain the COD/S ratio to prevent inhibition, which resulted in the substrate being completely utilised.

The following assumptions were made when fractionating the PSS that was used as the influent substrate for the methanogenic SSPAD:

1. All of the FBSOs were entirely utilised by the SSPAD within the 20-day sludge age, such that the concentration of FBSO in the effluent sample stream was zero. Therefore, the filtered effluent contained no FBSOs and was made up almost entirely of USOs, with a low concentration of measured VFAs.

2. The effluent COD concentration of the UPOs was equal to the influent COD concentration of UPOs, i.e. the endogenous residue accumulating in the reactor (generated from death and decay of the anaerobic organisms (Ze)) in the effluent was negligible.

$$S_{upi} = S_{upe} \qquad \text{mgCOD/}l \quad (3.19)$$

3. The particulate organics (S_{pe}) present in the SSPAD effluent comprised of three groups:
    a. UPOs
    b. Biomass (Z_{AD})
    c. Residual biodegradable organics (S_{bp})

Subsequently, the total particulate COD concentration exiting the SSPAD was the sum of these three groups.

The interaction that each specific organic group had on the methanogenic system is summarised as:

1. The USO and the UPO were inert and did not influence the quantity of methane produced by the reaction.

2. The BSO and BPO were degraded by the organisms to form biomass (Z_{AD}) and methane (S_m). The total methane produced (S_m) evolved from the liquid phase into the gaseous phase as CH_4 inside the reactor headspace.
   a. The gas in the reactor headspace comprised primarily of CH_4 and CO_2, with a small portion of N_2 and water vapour.

3. The particulate COD present in the effluent stream consisted of three groups: The UPO group, which was equal to the influent UPO concentrations, the biomass concentration (Z_{AD}) (which grew by degrading the influent BPO and BSO, producing negligible unbiodegradable organics (Z_e)) and the residual biodegradable organics (S_{bp}), that were not utilised and remained in the effluent.

The influent and effluent COD groups for the methanogenic SSPAD are summarised in Figure 3.17.

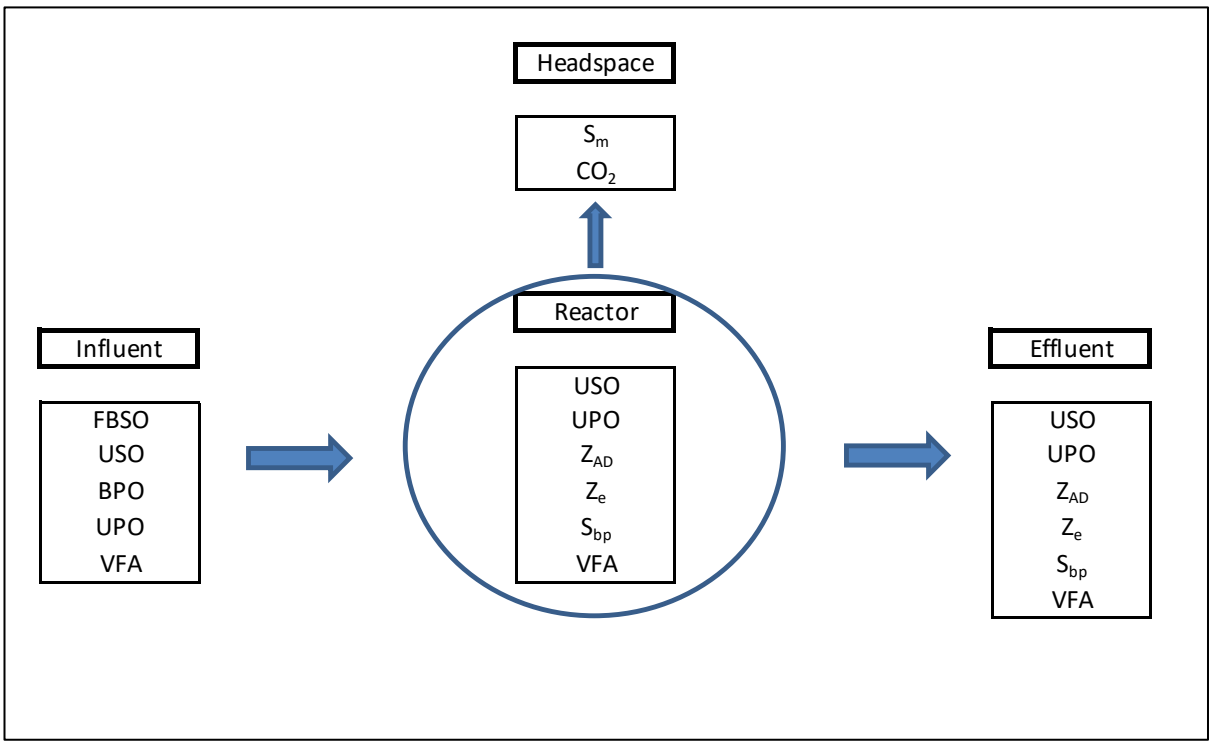

Figure 3. 17: Methanogenic SSPAD COD groups

3.8.2.1 Methanogenic SSPAD influent fractionation

The PSS substrate that was fed to the methanogenic SSPAD was fractionated using the influent and effluent COD measurements performed on the SSPAD, as well as the measurements performed on the AugBMP control reactor. The fractionation was completed using the following steps:

1. The total COD (S_{ti}) concentration entering the SSPAD was equivalent to the unfiltered COD concentration of the PSS.

2. The total soluble COD (S_{si}) concentration entering the SSPAD was equivalent to the filtered COD concentration of the PSS.

3. The total particulate COD (S_{pi}) concentration entering the SSPAD was equivalent to the total COD (S_{ti}) minus the total soluble COD (S_{si}).

$$S_{ti} = S_{si} + S_{pi} \qquad \text{mgCOD}/l \quad (3.20)$$

4. The USO COD (S_{usi}) concentration was equal to the effluent filtered COD (S_{se}) concentration minus the effluent VFA COD (S_{bsae}) concentration:

$$S_{se} = S_{usi} + S_{bsae} \quad \text{mgCOD}/l \quad (3.21)$$

5. The BSO COD (S_{bsi}) concentration was equal to the total soluble COD (S_{si}) concentration minus the USO COD (S_{usi}) concentration:

$$S_{si} = S_{bsi} + S_{usi} \quad \text{mgCOD}/l \quad (3.22)$$

6. The readily fermentable biodegradable soluble COD (S_{bsfi}) was equal to the BSO COD (S_{bsi}) concentration minus the influent VFA COD (S_{bsai})

$$S_{bsi} = S_{bsai} + S_{bsfi} \quad \text{mgCOD}/l \quad (3.23)$$

7. The particulate effluent COD (S_{pe}) concentration was the sum of the UPO COD (S_{upi}) concentration, the acidogen biomass COD (Z_{AD}) concentration and the residual biodegradable organics COD (S_{bp}) concentration.

$$S_{pe} = S_{upi} + Z_{AD} + S_{bp} \quad \text{mgCOD}/l \quad (3.24)$$

8. The Z_{AD} COD concentration was determined using the following equations established by Sötemann *et al.* (2005).

    a. Based on a reactor at steady-state and a mass balance on the acidogen biomass, the hydrolysis rate of the organics was determined by:

$$r_h = \frac{Z_{AD}}{Y_{AD}} \left(\frac{1}{R} + b_{AD} \right) \quad \text{mgCOD}/(l.\text{d}) \quad (3.25)$$

Where:

Y_{AD} = Biomass yield (gCOD biomass/ gCOD organics)
R = Sludge age (d)
b_{AD} = Biomass death rate (1/d)

b. Similarly, the hydrolysis rate could also be determined based on a reactor at steady-state and a mass balance of the biodegradable organics flowing through the reactor:

$$r_h = \frac{S_{bpi} - S_{bp}}{R} + b_{AD} Z_{AD} \quad \text{mgCOD/}(l.\text{d}) \quad (3.26)$$

c. The concentration of biomass present in the reactor could then be determined by:

$$Z_{AD} = \frac{Y_{AD}(S_{bpi} - S_{bp})}{[1 + b_{AD} R(1 - Y_{AD})]} \quad \text{mgCOD/}l \quad (3.27)$$

d. Finally, the COD concentration of methane, assuming that all of it remains dissolved in the solution was calculated by:

$$S_m = (1 - Y_{AD})\, R\, r_h \quad \text{mgCOD/}l \quad (3.28)$$

e. By using the four equations shown above, the COD concentration of biomass grown inside the reactor was calculated based on the daily concentration of methane produced by the reaction. Therefore, the Z_{AD} concentration in the effluent stream was calculated using the daily methane production (S_m). S_m was determined by taking the difference between the unfiltered influent and effluent COD concentrations, which should equal the biogas COD in a mass balanced system.

$$Z_{AD} = \frac{Y_{AD} S_m}{(1 + b_{AD} R(1 - Y_{AD}) + Y_{AD} R b_{AD})(1 - Y_{AD})} \quad \text{mgCOD/}l \quad (3.29)$$

9. The UPO COD (S_{upi}), acidogen biomass (Z_{AD}) and the residual biodegradable organics (S_{bp}) concentrations were challenging to separate. However, the Z_{AD} and S_{bp} are biodegradable and will subsequently be degraded during further anaerobic digestion (extended digestion). Extended digestion occurs inside the AugBMP control reactor as it only contains the SSPAD effluent (hence the SRT is extended from the SSPAD one

to the extra days added with the retainment in the AugBMP reactor). Therefore, the combined COD concentration for the of Z_{AD} lost (undergoing biomass decay) and the S_{bp} concentration was determined using the total COD change in the AugBMP control reactor ($\Delta S_{t\,(ABMP\cdot C)}$), excluding the AugBMP control reactor VFA COD concentration ($S_{bsai\,(ABMP\cdot C)}$).

$$\Delta S_{t(ABMP\cdot C)} - S_{bsai(ABMP\cdot C)} = Z_{AD(lost)} + S_{bp} \qquad \text{mgCOD}/l \quad (3.30)$$

10. The Z_{AD} COD loss was calculated using the modelled AugBMP control reactor, whereby the substrate uptake, as well as the biomass growth and decay reactions are simultaneously calculated at each timestep of the simulation. The S_{bp} COD concentration is calculated as the difference between the total COD change (excluding VFA) in the AugBMP control reactor (shown in Equation 3.31) and the Z_{AD} COD loss. This process involves multiple iterations of influent characterisation for the SSPAD, as well as running the modelled AugBMP control experiment, to determine the Z_{AD} COD model-calculated loss. Each iteration required the influent PSS characterisation process to be repeated, as the change in S_{bp} affects the UPO COD concentration.

$$S_{bp} = \Delta S_{t(ABMP\cdot C)} - S_{bsai(ABMP\cdot C)} - Z_{AD(lost)} \qquad \text{mgCOD}/l \quad (3.31)$$

11. With the Z_{AD} and S_{bp} concentration determined, the UPO COD (S_{upi}) was then calculated.

$$S_{upi} = S_{pe} - Z_{AD} - S_{bp} \qquad \text{mgCOD}/l \quad (3.32)$$

12. With the UPO COD (S_{upi}) known, the BPO COD (S_{bpi}) was determined using the total particulate COD (S_{pi}).

$$S_{pi} = S_{bpi} + S_{upi} \qquad \text{mgCOD}/l \quad (3.33)$$

13. The UPO VSS concentration was determined using the UPO COD (S_{upi}), and the literature stated f_{CV} value of 1.481 (Marais and Ekama, 1976).

$$UPO\ VSS = \frac{S_{upi}}{f_{CV}} \quad \text{mgVSS/}l \text{ (3.34)}$$

14. Finally, the BPO VSS concentration was determined using the total influent VSS (VSS_i) concentration minus the UPO VSS concentration.

$$VSS_i = BPO\ VSS + UPO\ VSS \quad \text{mgVSS/}l \text{ (3.35)}$$

Following this fractionation method, the characterised PSS was converted into the correct format for the PWM_SA model and used in the modelled methanogenic SSPAD to determine the active biomass present in the AugBMP inoculum.

3.8.3 Sulphidogenic SSPAD

The PSS fed to the sulphidogenic SSPAD used the same influent fractionation method as the methanogenic system above, with a few exceptions. As previously stated, the S_{bp} for the sulphidogenic SSPAD was negligible. When fractionating the PSS that was used as the influent substrate for the sulphidogenic SSPAD, two of the three primary assumptions made were the same as the methanogenic SSPAD:

1. All of the FBSOs were entirely utilised by the SSPAD within the 19-day sludge age, such that the concentration of FBSO in the effluent sample stream was zero. Therefore, the filtered effluent contained no FBSOs and was made up almost entirely of USOs, with a low concentration of measured VFAs.

2. The effluent COD concentration of the UPOs was equal to the influent COD concentration of UPOs, i.e. the endogenous residue accumulating in the reactor and subsequently, the effluent, due to the decay of the anaerobic organisms (Z_e) was negligible.

$$S_{upi} = S_{upe} \quad \text{mgCOD/}l \text{ (3.36)}$$

The third assumption stated that the sulphidogenic SSPAD had negligible residual biodegradable organics in the effluent as the influent COD concentration was lowered to

maintain the COD/S ratio to prevent inhibition, which resulted in the substrate being completely utilised.

3. The effluent particulate stream comprised entirely of UPO and biomass (Z_{AD}). The small quantity of BPOs were completely utilised within the 19-day sludge age. This assumption was founded based on the AugBSP control experiment data. In general, the total change in particulate COD concentration throughout the AugBSP control experiment was negligible (<10mgCOD/*l*). Therefore, the concentration of S_{bp} was taken to be zero in the effluent stream, and subsequently, the formation of H_2S in the AugBSP control reactor was due to organism decay.

The interaction that each specific organic group had on the sulphidogenic system is summarised as:

1. The USO and the UPO were inert and did not influence the concentration of sulphide produced by the reaction.

2. The BSO and BPO were degraded by the organisms to form biomass (Z_{AD}) and total sulphide (S_{ts}).

3. The total sulphide produced (S_{ts}) was in both the liquid phase as dissolved sulphide (S_{ds}) and in the gaseous phase as H_2S gas (S_{gs}), evolving into the reactor headspace.

4. The effluent UPO COD concentration was equal to that of the influent UPO COD concentration.
    a. The endogenous residue (Z_e) accumulating in the reactor and subsequently in the effluent due to the decay of the anaerobic organisms, was negligible.

5. The particulate COD present in the effluent stream consisted of two groups:
    a. The UPO concentration.
    b. The Biomass concentration (Z_{AD}).

The influent and effluent COD groups for the sulphidogenic SSPAD are summarised in Figure 3.18.

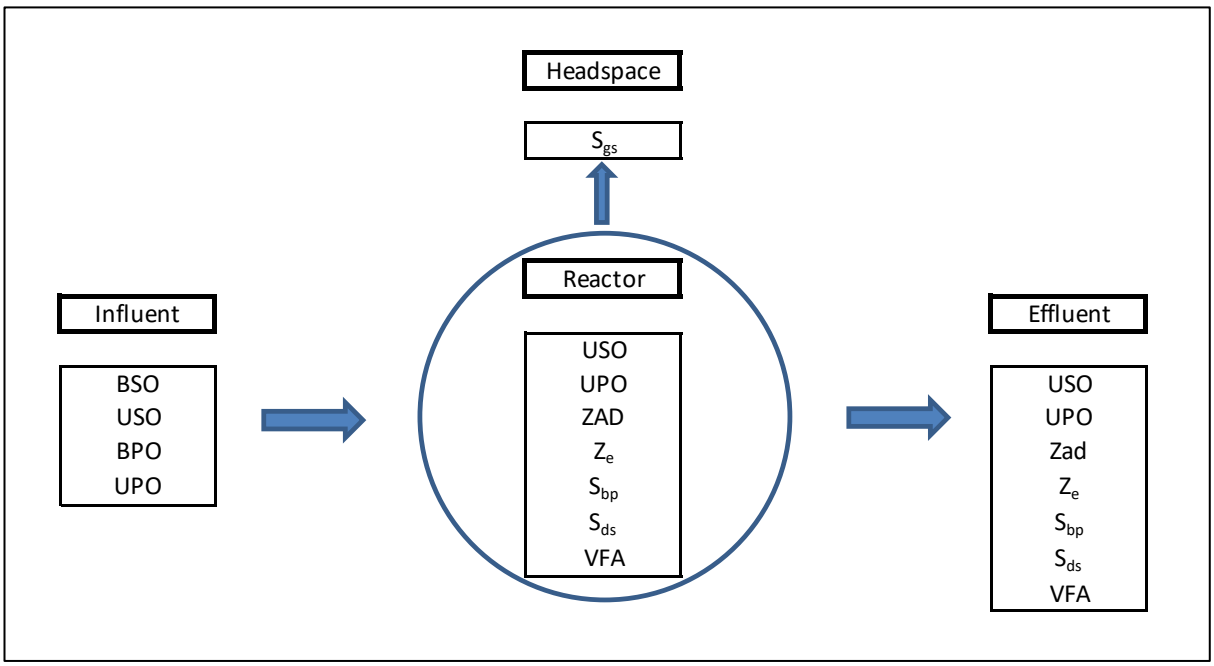

Figure 3. 18: Sulphidogenic SSPAD COD groups

3.8.3.1 Sulphidogenic SSPAD influent fractionation

The diluted PSS substrate that was fed to the sulphidogenic SSPAD was fractionated using the same steps, 1 to 6, as shown for the methanogenic SSPAD above, i.e. Section 3.8.2.1. However, a few steps were altered to account for the production of sulphide, as well as the negligible S_{bp} concentration. The exceptions were as follows:

1. The particulate effluent COD (S_{pe}) is the sum of the UPO COD (S_{upi}) and the acidogen biomass (Z_{AD}), as S_{bp} was taken to be zero.

$$S_{pe} = S_{upi} + Z_{AD} \quad \text{mgCOD/}l \quad (3.37)$$

2. The Z_{AD} concentration was determined using the same equations as in the methanogenic system, derived by Sötemann *et al.* (2005). However, the equations were adjusted to accommodate sulphide instead of methane.

$$Z_{AD} = \frac{Y_{AD} S_{ts}}{(1 + b_{AD} R(1 - Y_{AD}) + Y_{AD} R b_{AD})(1 - Y_{AD})} \quad \text{mgCOD/}l \quad (3.38)$$

3. With the Z_{AD} concentration determined in Step 2, the UPO COD (S_{upi}) was calculated.

$$S_{upi} = S_{pe} - Z_{AD} \quad \text{mgCOD}/l \quad (3.39)$$

4. With the UPO COD (S_{upi}) known, the BPO COD (S_{bpi}) was determined using the total particulate COD (S_{pi}).

$$S_{pi} = S_{bpi} + S_{upi} \quad \text{mgCOD}/l \quad (3.40)$$

5. The UPO VSS concentration was determined using the UPO COD (S_{upi}), and the literature stated f_{CV} value of 1.481 (Marais and Ekama, 1976).

$$UPO\ VSS = \frac{S_{upi}}{f_{CV}} \quad \text{mgVSS}/l \quad (3.41)$$

6. Finally, the BPO VSS concentration was determined using the total influent VSS (VSS_i) concentration minus the UPO VSS concentration.

$$VSS_i = BPO\ VSS + UPO\ VSS \quad \text{mgVSS}/l \quad (3.42)$$

3.8.4 Augmented batch tests

3.8.4.1 Overview

For the AugBMP and AugBSP experiments, the substrate fractionation was based on the observations made on the control and test reactors. The augmented batch reactors were separated into the two usual seeding conditions:

1. A control reactor in which only the inoculum (SSPAD effluent) was inserted.
2. A test reactor in which the inoculum (SSPAD effluent) and the substrate were inserted.

The biodegradable organics were broken down during the reaction, releasing organic and inorganic material into both the aqueous and gas phases in the reactors. Therefore, the observed

changes in the various constituent concentrations in the reactor were attributed to the breakdown of the biodegradable organics. The characterisation of the biodegradable organics in the control reactor was achieved by measuring the difference in the various constituent concentrations at the end and start of the experiment.

1. The carbon content:
   By using mixed weak acid/base chemistry (speciation methods of Loewenthal *et al*., 1991) and the 5-point titration method (of Moosbrugger *et al*., 1993), the H_2CO_3 alkalinity was identified. Therefore, the release of C was determined by calculating the change in concentration of CO_2, CH_4 (if methanogenic), and the H_2CO_3 alkalinity at the end and start of the experiment.

2. The nitrogen and phosphorus content:
   The N and P content of the biodegradable organics in the control were determined by calculating the change in concentration of FSA and OP at the end and start of the experiment, as the increase in these constituents was attributed to the breakdown of the biodegradable organics.

3. The COD:
   The change in COD throughout the experiment indicated the COD concentration of biodegradable organics present.

4. The VSS:
   The decrease in the VSS throughout the experiment indicated the mass of biodegradable organics present.

The same procedure was repeated in the test reactor. The results indicated the concentrations of the various elements transferred to the gas and aqueous phases for both the inoculum and substrate. The concentrations of the products released by the substrate were isolated by taking the difference between the test batch reactor and the control batch reactor:

$$[(Test_{end} - Test_{start}) - (Control_{end} - Control_{start})] \quad (3.43)$$

3.8.4.2 Fractionation

The bioprocesses that occurred in the control reactor were due to the breakdown of residual biodegradable organics (negligible in the AugBSP) and the cellular oxidation of biomass. Therefore, the change in concentration of the COD, FSA, OP, alkalinity, VFA, VSS and biogas/sulphide in the control reactor were due to the remaining biodegradable material present in the inoculum. The release of these products into the control reactor set the baseline for the products released into the test reactor due to the inoculum. Therefore, in the test reactor, the concentration of products released above this baseline were due to the breakdown of the biodegradable organics present in the substrate, as seen in Figure 3.19.

As a general rule for the augmented batch experiments conducted in this project, the inoculum in the test reactor was always diluted to half the concentration of the control reactor. Therefore, the concentration of the reactants taken up, as well as the products released into the test reactor due to the inoculum, were half that of the control reactor. The remaining concentration of the products released into the test reactor was due to the breakdown of the substrate. The rate of the reaction, as well as the concentration of the reactants/products that were taken up/released during the reaction stabilised after sufficient time (>20 days), had passed. The change in COD and VSS throughout the control reactor quantified the biodegradable material present in the inoculum. The concentration of COD and VSS remaining at the end of the experiment indicated the unbiodegradable material present in the inoculum. Likewise, the change in COD and VSS throughout the test reactor quantified the biodegradable material present in both the inoculum and the chosen substrate. Furthermore, the concentration of COD and VSS remaining at the end of the test experiment quantified the unbiodegradable material present in both the inoculum and the chosen substrate. Therefore, the influence of the substrate was determined as the difference between the test reactor concentrations (at the end and beginning of the experiment), and the control reactor concentrations (at the end and beginning of the experiment). Figure 3.19 shows the contribution of each organic group to both the control and test augmented batch reactors.

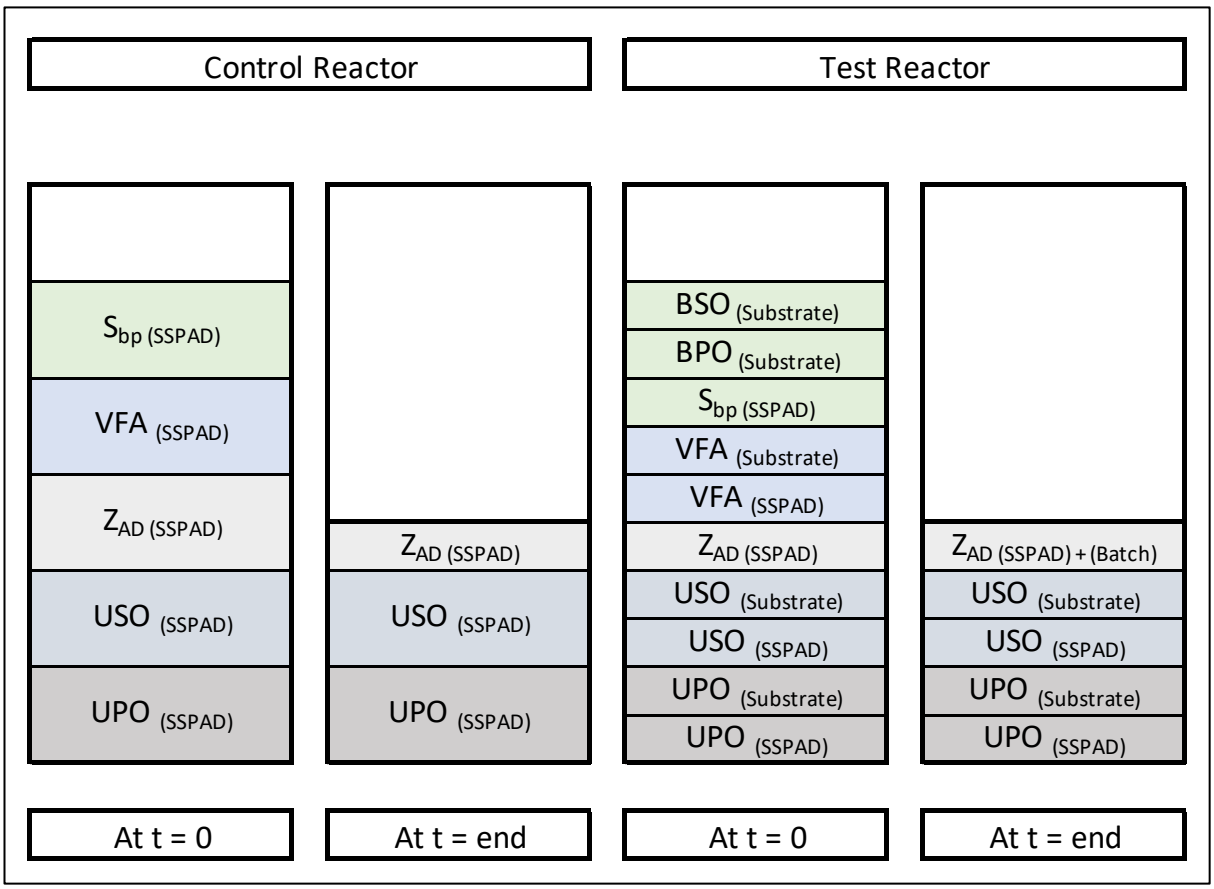

Figure 3. 19: Augmented batch test COD fractionation

In summary, the following observations for the augmented batch reactors were made:

1. The change in COD concentration (excluding the VFA COD) throughout the experiment, quantified the biodegradable COD concentration of the BPOs.

    a. In the control reactor, the change in COD concentration quantified the biomass and residual COD ($Z_{AD} + S_{bp}$) that was degraded.

    b. In the test reactor, the change in COD concentration quantified the biomass, residual and the substrate COD that was degraded.

    c. The difference between the test reactor COD and the control reactor COD isolated the BPO COD in the substrate.

d. If the substrate was soluble, the decrease in soluble COD in the test reactor quantified the biodegradable COD portion of the substrate. However, the VSS concentration was determined based on the mass of substrate added to the reactor, e.g. 5g of a powdered substrate (casein).

2. Likewise, the same applied to the VSS concentration, as mentioned in point 1a-1c.

3. The release of inorganics such as FSA and OP into the bulk liquid quantified the N and P that was organically bound in the BPOs.

4. The filtered COD concentration at the end of each experiment quantified the USO COD concentration present in the reactors.

5. The difference between the unfiltered COD concentration and the filtered COD concentration at the end of the experiment quantified the UPO COD concentration present in the reactors, as this COD was not biologically degraded.

6. The remaining VSS present in each of the reactors at the end of the experiment quantified the VSS concentration of the UPOs present in the reactors.

3.9 Calculating the organic composition

3.9.1 Overview

The composition of the biodegradable organics was identified by calculating the change in elemental concentrations between two measured data points. The data points required were the ending and the starting concentrations of the augmented batch experiments. The resultant composition of the biodegradable organics identified was directly dependent on the accuracy and validity of the laboratory measurements taken. This calculation is imperative to the augmented batch experiments, as it is relatively straight forward and allows for a mass balanced composition to be determined without the need for mathematical modelling.

3.9.2 Composition determination using stoichiometry

In general, there are two unknowns present in the bioprocess stoichiometry: the organic (reactant/substrate) and the biomass (product from growth stoichiometry), as shown in Section 2.5.3, Equation 2.1 and Section 2.5.4, Equation 2.2. However, via the mass balanced stoichiometry, the composition of these two unknowns directly influences the concentrations of the compounds in both the aqueous and gas phases. Therefore, the changes in the aqueous and gas-phase concentrations caused by these two unknowns allow for their compositions to be determined (Ekama and Brouckaert, 2020 in preparation).

The influence on the aqueous and gas-phase concentrations caused by the biomass present in the inoculum ($Z_{AD} + S_{bp}$) was quantified using the control reactor. The influence on the aqueous and gas-phase concentrations caused by the biomass, as well as the influent organic substrate was quantified using the test reactor. The difference between the test and control reactors isolated the influence of the organic substrate. By accurately measuring the changes in aqueous and gas-phase concentrations (COD, VSS, FSA, OP, H_2CO_3 Alk and biogas/sulphide) caused by both the biomass and the influent organic substrate, the compositions of the unknowns were calculated.

3.9.2.1 Mass ratio equations

In order to determine the elemental composition of the electron donor in the form of $C_xH_yO_zN_aP_b$, five element mass ratios needed to be known. The charge of the biodegradable organic, as well as the S content, was not considered for this project but can be included if necessary. The five elemental mass ratios represent the mass of each element relative to the total mass of the organic compound (g element/g compound) and correspond with the elements present in CHONP. Therefore, the elemental mass ratios are defined as: f_C (gC/gVSS), f_H (gH/gVSS), f_O (gO/gVSS), f_N (gN/gVSS) and f_P (gP/gVSS). The mass ratios are identical to the $\alpha_{C,i}$, $\alpha_{H,i}$, $\alpha_{O,i}$, $\alpha_{N,i}$ and $\alpha_{P,i}$ of Grau *et al*. (2007) and Volcke *et al.* (2006). An elemental mass balance specifies that the sum of the mass fractions must equate to 1.

$$f_C + f_H + f_O + f_N + f_P = 1 \tag{3.44}$$

Some of the mass ratios are more straightforward to determine than others and can be calculated directly from the measurements. In practice, the oxygen and hydrogen concentrations are not routinely measured, which results in unknown f_O and f_H mass fractions. However, it is still possible to determine the f_O and f_H mass fractions using the COD/VSS mass ratio (f_{CV}), which is routinely measured. The mass ratios required were calculated using the change in concentration of the COD, the C (which comes from the H_2CO_3 alk, CO_2 and CH_4), the N (from FSA released), the P (from OP released) and the VSS. The changes in these concentrations between the start and end of the augmented batch experiment isolated the influence of the biodegradable material. Therefore, f_O and f_H were calculated in terms of the 4 measured mass ratios (f_{CV}, f_C, f_N and f_P) using the following equations (Ekama and Brouckaert, 2020 in preparation):

$$f_O = \frac{16}{18}\left(1 - \frac{1}{8}f_{CV} - \frac{8}{12}f_C - \frac{17}{14}f_N - \frac{26}{31}f_P\right) \tag{3.45}$$

And

$$f_H = \frac{1}{9}\left(1 + f_{CV} - \frac{44}{12}f_C + \frac{10}{14}f_N - \frac{71}{31}f_P\right) \tag{3.46}$$

Equation 3.45 and Equation 3.46 above are aligned with the electron donating capacity (EDC) of the selected oxidation products. As shown in Section 2.5.3 and Section 2.5.4, the products selected for both the methanogenic system and sulphidogenic system bioprocesses were: $H_2PO_4^-$, HPO_3^{2-}, NH_4^+ and HCO_3^-. Additionally, the methanogenic system produced CH_4 and CO_2, and the sulphidogenic system produced H_2S. However, the S content of the organics was not included, and the required S was provided in the form of SO_4^{2-}.

In general, Equation 3.45 and Equation 3.46 are not fixed but can vary depending on the reaction products (Ekama and Brouckaert, 2020 in preparation). For example, if nitrate (NO_3^-) was selected as the oxidation product instead of NH_4^+, the f_N term in Equation 3.40, would be -9/14 f_N. However, even with an adjusted f_N term, the f_O and f_H mass ratios of the e^- donor (biodegradable organic) remain unchanged, as the f_N coefficients in Equation 3.45 and Equation 3.46 change by the same amount but with the opposite sign.

The advantage of basing the f_O and f_H mass ratio equations on the mass balance allows for any of the mass ratios to be set to zero, if negligibly small while maintaining the mass balance. Once the mass ratios for each element have been established, the elemental composition of the organic in question was calculated by:

$$C_{\frac{f_C}{12}} H_{\frac{f_H}{1}} O_{\frac{f_O}{16}} N_{\frac{f_N}{14}} P_{\frac{f_P}{31}} \tag{3.47}$$

Where:

$\frac{f_C}{12} = x \quad \frac{f_H}{1} = y \quad \frac{f_O}{16} = z \quad \frac{f_N}{14} = a \quad \frac{f_P}{31} = b$

The format of the elemental composition was adjusted to that of 1 mol of carbon (x=1). Therefore, the elemental composition was multiplied through by $12/f_C$.

$$C_1 H_{\frac{y}{x}} O_{\frac{z}{x}} N_{\frac{a}{x}} P_{\frac{b}{x}} \tag{3.48}$$

3.9.3 Composition determination using mathematical models

Identifying the organic composition using the stoichiometric calculation above is valid provided that the two required data points (the ending and the starting concentrations of the augmented batch experiments) are measured accurately. However, in practice, the measurements performed for these two data points are subject to error. Therefore, in some cases, the outcome of the stoichiometric calculation may not be valid, as the composition determined contains an unexpected or negative value. This invalid composition is directly affected by inaccurate measurements taken at the end or the start of the augmented batch experiments and is not due to the stoichiometric calculation. Therefore, in order to alleviate the potential error associated with only utilising two data points (the measured ending and starting concentrations), the data set as a whole was considered. As previously mentioned, daily measurements were performed on the augmented batch reactors for the first 10 days, after which measurements were taken every second day. The additional measurements taken increased the available data points significantly and encouraged the use of mathematical models to identify the composition, as well as determine the dynamics of the reaction.

The determination of the composition was extended using mass balanced mathematical bioprocess models which utilised the entire data set. The bioprocess models allow for the simultaneous calculation of substrate uptake, organism death and the presence of inert material. This simultaneous calculation allows for the composition identification to be based more in reality, as the possibility of an invalid outcome due to measurement error is decreased. Models were used in the identification of the composition for two reasons:

1. The models made use of the entire data set, and the PE function identified the composition of the biodegradable organics using the weighted mean of the measured data throughout the experiment. The PE identified the composition of the biodegradable organics by minimising the error across the measurements taken. Therefore, the organic composition identified using PE reflected the data collected throughout the experiment, and not only the beginning and end measurements.

2. By using the entire data set, dynamic parameters, such as the hydrolysis rate and substrate uptake rates, could be determined. The data points collected throughout the augmented batch experiments represented the rate at which the substrate was broken down, the rate at which inorganics were released into the aqueous phase, the accumulation of intermediates such as acetate and the subsequent uptake rates and half-saturation coefficients of the acetoclastic organisms.

Therefore, the use of mathematical bioprocess models was useful when analysing the collected data set as a whole. The use of intermediate points was good to alleviate errors with individual measurements as the weighted mean across the experiments could be used. Furthermore, the kinetics associated with the bioprocesses could be determined using the larger data set.

3.10 Modelling the Steady-State digesters

3.10.1 Overview

The anaerobic digestion model used throughout this project was the PWM_SA_AD model (Ikumi *et al.*, 2015). The PWM_SA_AD model is a three-phase plant-wide model that extends the UCTADM1 model of Sötemann *et al.* (2005), to include the hydrolysis of multiple organic types (PS, ND WAS, NDEBPR WAS and PS-WAS blends), the Ekama and Wentzel (2004) ISS model and the Brouckaert *et al.* (2010) speciation model which facilitates ionic speciation and multiple mineral precipitation and calculation of pH. The model has recently been extended further by Ghoor *et al.* (2020) to include BSR. The PWM_SA_AD model has been coded into WEST® (Vanhooren *et al.*, 2003) wastewater modelling software. Subsequently, WEST® was used as the primary modelling software tool throughout the project.

The main focus of the project was to determine the composition of the biodegradable organics present in the chosen substrate (casein/PSS). However, the starting concentrations of the active biomass in both the AugBMP/AugBSP were not known and needed to be estimated. Therefore, the methanogenic and sulphidogenic SSPADs were replicated as accurately as possible using steady-state models, such that the concentrations of active biomass present in the effluent was estimated.

The concentration of active biomass in the inoculum affects the production of biogas/sulphide due to biomass decay (control reactors), as well as the kinetic rates of bioprocesses occurring in the AugBMP/AugBSP experiment (test reactors), hence the quantity of products generated by the system. It is imperative to note that in practice, biomass is part of the VSS concentration measured. However, the active biomass, as an isolated component, is virtually impossible to measure and is subsequently, a modelling concept rather than a physical reality.

The modelled SSPAD required specific input parameters and variables in order to run. The parameters that were essential for correctly modelling the SSPAD using the PWM_SA_AD model were:

1. The elemental compositions for the:
    a. biomass and endogenous residue in the AD
    b. PSS (substrate) organics in the influent.
2. The saturation kinetics hydrolysis rate constants for the breakdown of biodegradable particulate organics (BPO), shown in Equation 3.50.
3. Monod growth kinetic constants, yield coefficients and death rates of the four AD organism groups.

3.10.2 Influent fractionation

The operating conditions of the SSPADs were replicated in WEST using an influent generator and a virtual AD, as shown in Figure 3.20. The PWM_SA_AD model coded into WEST reads the influent wastewater concentrations as a text file, which contains each input concentration at each required time interval. The model then uses the influent generator to supply the required daily AD influent load on the SSPAD for the duration of the virtual experiment (simulation). The SSPAD simulations ran at steady-state for 300 days and 150 days for the methanogenic and sulphidogenic SSPADs, respectively. The minimum time required to reach a steady state is 3x the digester's sludge age. Therefore, the simulation can be conducted for any duration, as long as it is longer than 3x the sludge age. The chosen simulation time for the methanogenic and sulphidogenic systems differed based on the computation time of the simulation.

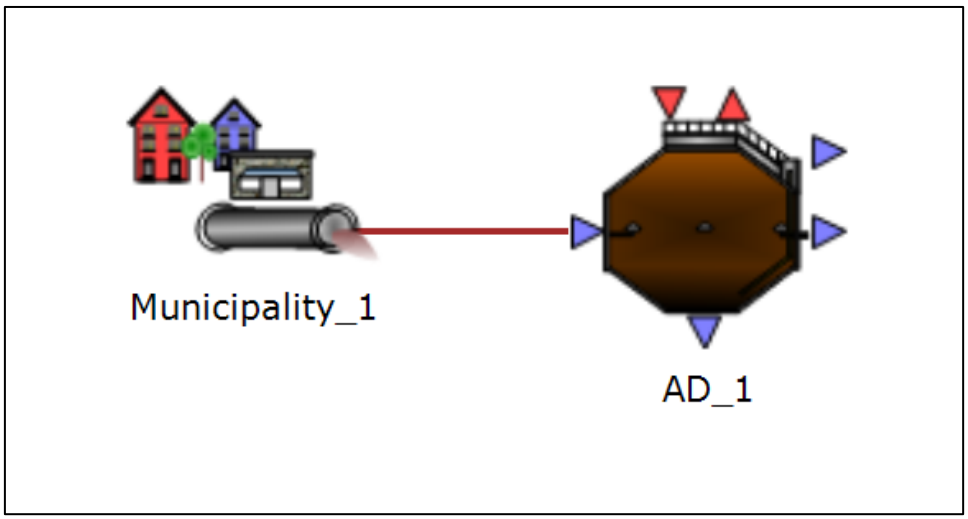

Figure 3. 20: SSPAD layout

The PWM_SA_AD model is a plant-wide model, and therefore all the model components are available in all unit operations of the plant as they move between specific plant unit operations (i.e., the supermodel approach of Jones and Takacs, 2004). This flow between unit operations requires a generalised mass concentration format for each component variable. Therefore, the measured lab data concentrations needed to be transformed to the mass basis (i.e., units of mg/*l*) required by PWM_SA_AD, which is accomplished by an influent pre-processor (Ekama and Brouckaert, 2020; Ekama *et al.*, 2020). An example of the mass conversions required by the PWM_SA_AD model, with example values, is shown in Table 3.6. However, during simulations, the component concentrations of COD, N, P and mols could also be calculated as model variables, using the component's given simulated mass concentrations and parameterised elemental compositions (i.e., the x,y,z,a,b values of $C_xH_yO_zN_aP_b$).

Table 3. 6: Conversion for WEST influent generator

Organics					
Component	Initial Unit	COD Conc	fcv	Final Unit	Mass Concentration
UPO	mgCOD/l	10889	1.48	mgVSS/l	7352
USO	mgCOD/l	4108	1.42	mgVSS/l	2893
BPO	mgCOD/l	21736	2.30	mgVSS/l	9450
RFSO	mgCOD/l	604	1.42	mgVSS/l	425
VFA	mgCOD/l	578	0.94	mgVFA/l	542
Inorganics					
Component	Initial Unit	Concentration	Conversion factor	Final Unit	Mass Concentration
NH4	mgFSA-N/l	228	1.29	mgNH4/l	293
PO4	mgPO4-P/l	29	3.07	mgPO4/l	89
CO3	mg/l as C	109	5.00	mgCO3/l	545

An example of the converted concentrations, as determined from the pre-processor, for the first ten days is shown in Figure 3.21, which is in the correct format for the influent generator of the PWM_SA_AD model. It can be seen that the same respective influent value was repeated each day, and subsequently, the steady-state achieved by the model was based on average values and did not account for cyclic variations.

%%BeginHeader																		
t	H2O	S_H	S_Na	S_K	S_Ca	S_Mg	S_NH	S_Cl	S_VFA	S_Pr	S_CO3	S_SO4	S_PO4	S_H2	S_U	S_F	S_Glu	X_U_In
d	m3/d	mg/L	mg/L	mg/L	mg/L	mg/L	mg/L	mg/L	mg/L	mg/L	mg/L	mg/L	mg/L	mg/L	mg/L	mg/L	mg/L	mg/L
%%EndHeader																		
1	8E-04	18.9	47.1	10	10	10	293.3	72.7	541.5	0.001	580.5	0.001	88.9	0.001	2893.3	425.7	0.00	7352.3
2	8E-04	18.9	47.1	10	10	10	293.3	72.7	541.5	0.001	580.5	0.001	88.9	0.001	2893.3	425.7	0.0010	7352.3
3	8E-04	18.9	47.1	10	10	10	293.3	72.7	541.5	0.001	580.5	0.001	88.9	0.001	2893.3	425.7	0.0010	7352.3
4	8E-04	18.9	47.1	10	10	10	293.3	72.7	541.5	0.001	580.5	0.001	88.9	0.001	2893.3	425.7	0.0010	7352.3
5	8E-04	18.9	47.1	10	10	10	293.3	72.7	541.5	0.001	580.5	0.001	88.9	0.001	2893.3	425.7	0.0010	7352.3
6	8E-04	18.9	47.1	10	10	10	293.3	72.7	541.5	0.001	580.5	0.001	88.9	0.001	2893.3	425.7	0.0010	7352.3
7	8E-04	18.9	47.1	10	10	10	293.3	72.7	541.5	0.001	580.5	0.001	88.9	0.001	2893.3	425.7	0.0010	7352.3
8	8E-04	18.9	47.1	10	10	10	293.3	72.7	541.5	0.001	580.5	0.001	88.9	0.001	2893.3	425.7	0.0010	7352.3
9	8E-04	18.9	47.1	10	10	10	293.3	72.7	541.5	0.001	580.5	0.001	88.9	0.001	2893.3	425.7	0.0010	7352.3
10	8E-04	18.9	47.1	10	10	10	293.3	72.7	541.5	0.001	580.5	0.001	88.9	0.001	2893.3	425.7	0.0010	7352.3

Figure 3. 21: WEST influent file

3.10.3 Hydrolysis kinetics

The steady-state model that was used to virtually replicate the SSPAD aimed to predict the observed SSPAD effluent as accurately as possible. In order to achieve this, specific kinetic constants needed to be determined, the most crucial being the value of K_M, represented by the PWM_SA_AD model as mu_AD. K_M is the kinetic constant that affects the hydrolysis rate of the biodegradable organics by the acidogen biomass. Additionally, K_M influences the concentration of the residual biodegradable organics (S_{bp}) in the SSPAD effluent (Ikumi, 2020).

The steady-state primary sludge model by Sötemann *et al.* (2005) was used to determine K_M, with the K_S value taken to be 7.98, a value determined for PSS by Izzett *et al*. (1992). The steady-state model by Sötemann *et al.* (2005) allows the residual BPO to be determined for a selected BPO hydrolysis kinetic rate equation (1st order, specific 1st order, Monod or Saturation) with a set of defined equations. The kinetics chosen for the PSS were saturation (Contois) kinetics, as the PWM_SA_AD used saturation kinetics for the breakdown of particulate influent organics. The hydrolysis rate was determined based on the daily production of methane/sulphide COD for the methanogenic and sulphidogenic SSPADs, respectively. The hydrolysis rate was calculated using Equation 3.49. Table 3.7 shows a range of observed hydrolysis rates for the treatment of primary sludge adapted from the steady-state anaerobic digestion model of Sötemann *et al.* (2005).

$$r_h = \frac{S_{Product}}{(1 - Y_{AD})\, R} \quad \text{mgCOD/}l \quad (3.49)$$

Where:
rh = Hydrolysis rate (gCOD/*l*.d)
$S_{Product}$= Daily COD production of product (methane/sulphide)
Y_{AD} = Yield coefficient of acidogen biomass
R = Sludge age

Table 3. 7: Observed hydrolysis rate adapted from Sötemann et al. (2005)

Izzett et al. (1992) 7 to 20 d retention time (R) anaerobic digester observed hydrolysis rate (rh)	
R	rh
d	g/(l.d)
7	2.871
10	2.064
12	1.663
15	1.548
20	1.204

With r_h calculated, and S_{bp} and Z_{AD} determined from the influent fractionation, the value of K_M was calculated. As mentioned, a K_S value of 7.98 gCOD/*l*, was used for the saturation kinetics of PSS.

$$r_h = \frac{K_M\left(\frac{S_{bp}}{Z_{AD}}\right)}{K_S + \left(\frac{S_{bp}}{Z_{AD}}\right)} Z_{AD} \quad \text{gCOD/(}l\text{.d)(3.50)}$$

Where:
K_M = Kinetic constant (gCOD organics / gCOD biomass.d)
K_S = Kinetic constant (gCOD/*l*)
S_{bp} = Residual biodegradable organics (gCOD/*l*)
Z_{AD} = Acidogen biomass concentration (gCOD/*l*)

Table 3.8 shows a range of K_M for the treatment of primary sludge adapted from the three-phase plant-wide model of Ikumi *et al.* (2015).

Table 3. 8: K_M and K_S values adapted from Ikumi et al. (2015)

	Saturation Kinetics	
	K_M	K_S
PS	1.796	7.962
PS-MLE	1.919	7.723
MLE 1	1.603	5.387
MLE 2	1.524	4.838
NDBEPR	1.951	9.109
PS (1)	5.27	7.98
PS (2)	2.047	0.263
PS (3)	11.2	13
Where: PS (1) is from Sötemann et al. (2005a), determined using data from Izzett et al. (1992). PS (2) is from Sötemann et al. (2005a), determined using data from O'Rourke (1968). PS (3) is from Ristow et al. (2004).		

3.10.4 Composition Determination

The concentrations of the products released into the SSPAD bulk liquid by the influent PSS are dependent on the elemental composition and VSS mass of the biodegradable organics present in the PSS, the flowrates in/out of the SSPAD and the liquid volume of the SSPAD. The organic groups present in the PSS were divided into four main categories (BSO, BPO, USO and UPO). The PWM_SA_AD model included an additional group, a shared composition for the biomass. The compositions of these organics needed to be estimated based on literature values, as well as the measured effluent concentrations. Therefore, the model needed to assign a unique composition to each of the following groups:

1. UPO
2. Biomass
3. BPO and BSO
4. USO

3.10.4.1 UPO

The elemental composition of the UPO was determined using mass ratio values from the literature. The mass ratios for UPO have been used for decades in activated sludge models

since the steady-state model of Marais and Ekama (1976), but there is evidence that it may need revision (Wentzel *et al.*, 2006). Nevertheless, the values were used to determine the composition of the UPO and may lead to some error.

Table 3. 9: Mass fractions for UPO

f_{CV}	1.481
f_C	0.515
f_N	0.1
f_P	0.025

With 4 of the 5 mass fractions known and assuming 100% mass balance, the unknown mass fractions for f_H and f_O were calculated using the equations from Section 3.9.2. Therefore, the UPO elemental composition of the influent PSS was calculated to be $C_1H_{1.571}O_{0.426}N_{0.166}P_{0.019.}$

3.10.4.2 Biomass

The composition of the biomass was assumed to be $C_5H_7O_2N$, a typical biomass composition used in AS and AD modelling initially measured by Porges and Hoover (1952). This composition was adjusted to the correct format using Section 3.9.2. The result was a biomass composition of $C_1H_{1.4}O_{0.4}N_{0.2}$

3.10.4.3 BPO and BSO

Identifying the composition of the BPO in the influent PSS for the SSPADs required some trial and error, as literature stated values for the BPO in the PSS were scarce and did not match the measured SSPAD effluent concentrations sufficiently well. Therefore, an approximate composition of the BPO was determined from the laboratory measurements on the SSPAD by accepting COD, C, N and P mass balances over the system like Sötemann *et al.* (2005) did. This was possible because the COD of the methane gas, the C in the methane, CO_2 and H_2CO_3 alk, and the FSA and OP in the effluent originated from the COD, C, N and P of the degraded BPOs. A small proportion (<3%) of the COD, C, N and P are taken up into AD biomass growth, but this can be taken into account if required.

The BPO and BSO were grouped as one component, effectively becoming the total biodegradable organics (S_{bi}), excluding the VFA contribution (which was accounted for separately), which simplified the elemental composition, as four fewer parameters were required for modelling the SSPAD when accepting a single composition for the biodegradable organics. This is shown in the organic compositions for the biodegradable organics in Table 4.13 in Section 4.2.3.4. Grouping both the BSO and BPO together was justified as the BPO contributed more than 95% of the biodegradable organic COD present in the PSS.

The BPO composition was estimated based on the observed change in concentrations of the constituents between the influent and effluent. The difference between the VSS entering and exiting the SSPAD gave a reasonable estimate of VSS concentration utilised by the SSPAD. Therefore, the BPO CHONP composition was adjusted until the desired SSPAD effluent concentrations were achieved.

3.10.4.4 USO

Identifying the composition of the USO was difficult as it is inert with no measurable mass concentration. The USO also has no interaction with the bioprocesses and aqueous phase, other than adding a small concentration of unbiodegradable dissolved COD and nitrogen to the bulk liquid. Furthermore, the USO has no P content. From many years of research on EBPR activated sludge systems, an unbiodegradable effluent OrgP has not been detected. Usually, the filtered effluent TP and OP are almost equal. Therefore, the composition of the USO was estimated based on the observed SSPAD soluble effluent COD concentration and some assumed mass ratios after the compositions of the other groups had been determined.

3.10.5 Modelled SSPAD evaluation

The PWM_SA_AD model for the methanogenic and sulphidogenic SSPADs were run under steady-state conditions for 300 days and 150 days, respectively. The models made use of all the required parameters and variables determined above, i.e. the hydrolysis rates and elemental compositions of the organics in the PSS substrate. The modelled SSPAD effluent was compared to the observed SSPAD effluent using relative error (percentage error), as described in Section 3.7.6.1. The relative error was calculated using Equation 3.51 below:

$$\%error = \frac{(modelled\ value - observed\ value)}{observed\ value} \times 100 \quad \% \quad (3.51)$$

The parameters for the SSPAD were adjusted in an attempt to get the relative error measured on each constituent to lower than 10%. However, this was not always possible, and in these cases, the parameters were adjusted to get a best-fit. The active biomass concentration present in the SSPAD effluent was then used as the inoculum for the modelled AugBMP and AugBSP experiment reactors, after the appropriate seeding dilutions had been applied.

3.10.6 Modelled methanogenic SSPAD

The modelled methanogenic SSPAD was run using measurements performed on both the influent and effluent streams. The main focus of the model was to as accurately as possible replicate the laboratory observations on the methanogenic SSPAD. The motivation for replicating the SSPAD as accurately as possible was to estimate the concentrations of the four different active organism groups present in the effluent stream, that would be used to inoculate the AugBMP experiment reactors. The active biomass in the methanogenic SSPAD was separated into four main groups of organisms:

1. Acidogens
2. Acetogens
3. Acetoclastic Methanogens
4. Hydrogenotrophic Methanogens

3.10.7 Modelled Sulphidogenic SSPAD

The sulphidogenic SSPAD was virtually replicated using the same model library that was used to model the methanogenic SSPAD, i.e. PWM_SA_AD model (Ikumi *et al.*, 2015). This could be done as the model was extended further by Ghoor *et al.* (2020) to include biological sulphate reduction (BSR). The model contains the identical stoichiometry for the hydrolysis reaction of the influent organics, but differs after the formation of glucose, splitting into two distinct pathways of either methanogenesis or sulphidogenesis.

As with the methanogenic SSPAD, the active biomass in the sulphiodogenic SSPAD was separated into four main groups of organisms:

1. Acidogens
2. Sulphidogenic Acetogens
3. Acetoclastic Sulphidogens
4. Hydrogenotrophic Sulphidogens

3.10.7.1 Sulphide steady-state model modification

The PWM_SA_AD model extended by Ghoor *et al.* (2020) has been coded in such a way that all of the sulphide remains dissolved in solution, i.e. there is no sulphide evolution from the liquid phase into the gas phase. The model was developed for simulating the AugBSP experiment, which takes place in a completely sealed reactor with no headspace, and subsequently, all the sulphide remains dissolved in the reactor liquid.

The missing sulphide evolution was problematic when modelling the sulphidogenic SSPAD, as the laboratory scale SSPAD had a headspace into which H_2S could evolve, and was additionally sparged with nitrogen during feeding and wasting, causing H_2S to evolve into the headspace. The model developed by Ghoor *et al.* (2020) needed to be modified to account for the H_2S evolution in the SSPAD. This modification only applied to the steady-state model, as the AugBSP experiments would use the extended PWM_SA_AD model in its intended form.

The only modification to the model developed by Ghoor *et al.* (2020) was allowing for H_2S to evolve from the liquid phase. The modification was made purely for establishing the required SSPAD dissolved sulphide (S_{ds}) concentration and pH. It is important to note that the modification was not intended as a realistic permanent fix for sulphide evolution inside the model, but rather as a way to remove the H_2S at a constant rate from the SSPAD liquid phase.

The modification was implemented without introducing a gaseous H_2S term to the model, but rather by using two existing model components: the dissolved HS^- concentration and the H^+ concentration. A new adjustable parameter was added to the model: the H_2S_molrate. This new parameter allowed the user to adjust the rate at which H_2S evolved from the solution. This rate

was applied to both HS^- and H^+, such that they were removed from the solution in equal parts, simulating the effect that a constant sulphide evolution rate would impose on the SSPAD, as shown by Equation 3.52.

$$HS^- + H^+ = H_2S \quad \text{mol} \quad (3.52)$$

3.11 Modelling the augmented batch experiments

3.11.1 Overview

The anaerobic digestion model used throughout this project was the PWM_SA_AD model (Ikumi *et al.*, 2015). The augmented batch experiments were modelled as AD batch reactors, as shown in Figure 3.22. Therefore, an influent generator was not necessary, as the selected feeding mode was once-off batch fed. Subsequently, the starting mass of each component was entered directly (as starting mass of the virtual reactor in the simulated experimental environment) into the PWM_SA_AD model in WEST®. The starting liquid volume of the augmented batch experiments were fixed at 5*l* and 6*l* for the AugBMP and AugBSP reactors, respectively. Therefore, the modelled AugBMP and AugBSP reactors had a starting liquid volume of 5*l* and 6*l*, respectively.

The starting constituent concentrations for the modelled augmented batch reactors were set to the observed starting constituent concentrations by adjusting the mass of each component in the PWM_SA_AD model, as the starting volume in each reactor was fixed. The concentrations that were adjusted to that of the observed starting concentrations were the FSA, OP, VFA, H_2CO_3 Alk and H^+ (pH). Therefore, where possible, the starting concentrations for the modelled augmented batch experiments began at the same concentrations to that of the observed augmented batch experiments. The PE function was used to determine the COD and VSS concentrations of the BPOs (above that of the unbiodegradable material), as the starting COD concentration was directly influenced by the BPOs composition and mass.

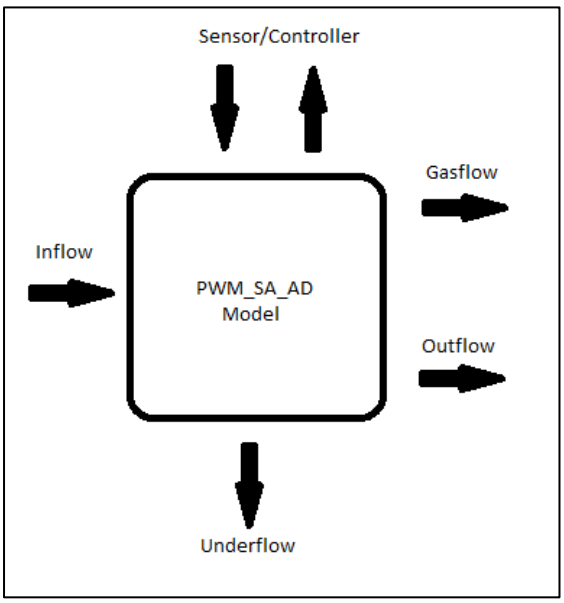

Figure 3. 22: Virtual augmented batch test layout

3.11.2 Control reactors

The augmented batch control reactors were used to identify the residual biodegradable material present in the SSPAD effluent. Therefore, the control reactors set the baseline for the test reactors, which contained the organic substrate in question. As discussed in Section 3.8.4.2, the control reactors contained residual biodegradable organics, VFAs, biomass, USO and UPO. In the PWM_SA_AD model, the biomass and biodegradable particulate material (BPO) are represented as two separate components.

The PWM_SA_AD model required a unique composition for both the biomass and the biodegradable organic material. The composition of the biomass was set to $C_1H_{1.4}O_{0.4}N_{0.2}$, as shown in Section 3.10.4.2. Therefore, the release of inorganics (such as FSA and OP) into the reactor liquid, as well as the generation of AD products (methane/sulphide), was directly influenced by the chosen biomass composition, the mass of biomass present in the batch reactor at the start of the experiment and the death rates of the biomass. Furthermore, the composition of the biomass was fixed. Therefore, the concentration of products released into the reactor liquid above that of the concentrations released due to the cellular oxidation of the biomass was due to the BPO present in the SSPAD effluent (with the VFAs accounted for separately).

However, for the sulphidogenic AugBSP reactors, the residual biodegradable organics present in the sulphidogenic SSPAD effluent was taken to be negligible. Therefore, the change in concentration of the specific components was due entirely to the biomass decay. Subsequently, the AugBSP control reactor was relatively straight forward to model and did not require PE to identify the composition of the biodegradable organics.

3.11.2.1 AugBMP Control Reactor Parameter Estimation

The fractionation procedure used to determine the specific organic groups was discussed in Section 3.8.4.2. The parameter estimation (PE) procedure required for coding of the PWM_SA_AD model to specify the biomass and biodegradable organics as two separate model component groups. With this in place, the PE was used to identify the composition of the BPO that was present in the methanogenic SSPAD effluent. To initiate this process, it was required to quantify the three organic groups of USO, BSO and UPO in order to identify the BPO group present. The steps to this process are listed below:

1. The USO concentration present in the AugBMP control reactor was quantified using the filtered (soluble) COD concentration that remained in the control reactor at the end of the experiment. The filtered COD concentration at the end of the experiment quantified the soluble material that did not degrade throughout the experiment, i.e unbiodegradable soluble. Therefore, the mass (in the simulated reactor) of USO was adjusted until the modelled filtered COD concentration at the end of the experiment reflected the observed filtered COD concentration.

2. The concentration of the BSO present in the AugBMP control reactor was quantified using the difference between the starting and ending filtered COD concentrations (excluding the VFAs present). The filtered COD concentration at the end of the experiment quantified the unbiodegradable soluble material. Therefore, the difference between the starting and ending filtered COD concentrations quantified the biodegradable soluble COD that was utilised throughout the experiment. Therefore, the mass of BSO in the modelled AugBMP control reactor was adjusted to reflect this starting concentration.

3. The composition of the UPO was fixed at $C_1H_{1.571}O_{0.426}N_{0.166}P_{0.019}$, as shown in Section 3.10.4.1. Furthermore, the COD and VSS concentrations of the UPO were related by an f_{CV} value of 1.48. This relationship fixed the COD concentration relative to the VSS concentration remaining at the end of the experiment. The COD and VSS concentration at the end of the experiment quantified the particulate material that did not degrade over the duration of the experiment (i.e unbiodegradable particulate), but also included the COD and VSS concentration of the biomass at the end of the experiment due to the low organism death rates. Therefore, the mass of UPO (which affects both the COD and VSS concentrations) was used as an unknown parameter in the PE. The PE took into account the mass of biomass that grew and degraded throughout the experiment and assigned the remaining mass (at the end of the batch reactor experiment) to the UPO, such that the observed COD and VSS concentrations at the end of the modelled experiment reflected the observed concentrations.

4. The concentration of biomass at the start of the experiment was determined using the modelled SSPAD effluent concentrations.

With four of the organic groups identified, as well as the presence of VFAs taken into account (the concentration of the VFAs at the start of the virtual experiment were entered as a direct input), the influence of the biodegradable organics present in the AugBMP control reactor was determined using the PE function. The PE estimation adjusted the BPO composition and mass by completing hundreds of iterations until the error across the prediction of measurements were minimised. The following measurements affected how the composition and mass of the BPO were determined.

1. The COD and VSS concentrations at the start of the AugBMP control were used as the objective values, which were associated with the BPOs, as the concentrations of the COD and VSS relating to the UPO and biomass were taken into consideration of values quantified (as shown in (3) and (4) above). Therefore, (with VFA COD accounted for separately) the COD and VSS concentrations present at the start of the experiment, above that of the UPO and biomass, were due to the BPOs.

2. The release of FSA and OP into the bulk liquid of the AugBMP control reactor, above that of the concentrations released due to biomass decay, quantified the N and P content of the BPO, respectively.

3. The release of alkalinity and the change in reactor pH, above that of the influence caused by biomass decay, were a result of the products released into the reactor due to the breakdown of the BPO.

In addition to identifying the composition and mass of the BPO, the PE was used to identify the hydrolysis rate of the BPO, the substrate uptake rate of the acetoclastic methanogens and the half-saturation coefficient of the acetoclastic methanogens. Table 3.10 shows the target parameters used in the modelled AugBMP control reactor for the PE. The best solution was achieved by the PE through multiple iterations. The iterations adjusted the selected parameters until the lowest objective value was achieved. This process is explained in detail in Section 2.7.2.

Table 3. 10: AugBMP PE parameters

PWM_SA Parameter	Description
i_H_XBInf_mol_perC	The H content of the BPO (y)
i_O_XBInf_mol_perC	The O content of the BPO (z)
i_N_XBInf_mol_perC	The N content of the BPO (a)
i_P_XBInf_mol_perC	The P content of the BPO (b)
M(X_B_Inf)	The mass of the BPO
M(X_U_Inf)	The mass of the UPO
kM_BInf_AD_hyd	The saturation hydrolysis constant for BPO breakdown.
mu_AM	The growth rate of the acetoclastic methanogens
KS_AM	The half-saturation coefficient of the acetoclastic methanogens

The composition and mass of the BPO identified using the PE function was then used as the baseline for the modelled AugBMP test reactor, above which the release of products into the reactor liquid was a direct result of chosen the biodegradable substrate (either PSS or casein).

3.11.3 Test reactors

The augmented batch test reactors were used to identify the composition of the biodegradable organic material present in a chosen substrate. For this project, both a soluble and a particulate substrate were selected:

1. The soluble substrate used was a powdered casein hydrolysate, which was dissolved into an aqueous solution.

2. The particulate substrate used was the biodegradable material present in the PSS, which was mostly (>95%) in the particulate form.

The properties of the biodegradable organic (soluble or particulate) had a significant effect on how the augmented batch test reactors were modelled, as well as the parameters used for the PE. The augmented batch test reactors used the same model as the control reactors. Therefore, the same biomass and UPO compositions from Section 3.11.2.1 were present in the test reactors. Furthermore, the organic groups present in the AugBMP/AugBSP test reactors were determined using the fractionation principles described in Section 3.8.4.2.

The mass and composition of the BPO present in the AugBMP control reactors was identified using PE and was subsequently entered into the model for the AugBMP test reactor (with the correct dilution applied). Furthermore, the composition of the biomass was fixed at $C_1H_{1.4}O_{0.4}N_{0.2}$. Therefore, the mass, and subsequently, the concentration of active biomass present in the AugBMP test reactor inoculum was determined using the modelled SSPAD and was entered into the model for the AugBMP test reactor (with the correct dilution applied). The release of products above the entered BPO and biomass mass in the modelled AugBMP test reactor was due to the biodegradable organics present in the selected substrate.

The AugBSP reactor contained negligible BPOs, and the subsequent release of products into the bulk liquid of the AugBSP control reactor was due entirely to the biomass decay. For the modelled AugBSP test reactor, the composition of the biomass was fixed at $C_1H_{1.4}O_{0.4}N_{0.2}$. The mass, and subsequently, the concentration of active biomass present in the AugBSP test reactor inoculum was determined using the modelled SSPAD and was entered into the model for the AugBSP test reactor (with the correct dilution applied).

3.11.3.1 Identifying the Soluble Substrate using Parameter Estimation

The soluble substrate selected was casein hydrolysate, an organic compound with a well-documented composition. Casein was selected with the primary aim of comparing the compositions identified by the AugBMP and AugBSP experiments. This comparison was possible as a laboratory-grade casein was utilised, and subsequently, the compositions identified by each of the augmented batch reactors (AugBMP/AugBSP) should be similar. The biodegradable organic present in PSS varies depending on the time of collection, and subsequently, was not ideal for comparing the compositions identified by each of the augmented batch experiments.

As previously mentioned, the PWM_SA_AD model comprises of different components. For instance, the USO, BSO, UPO, BPO and biomass are separated, and each given a unique composition and starting mass. The augmented batch control reactor was used to determine the concentration of the BPOs present in the inoculum. Therefore, the composition and mass of the BPOs determined using the modelled augmented batch control reactors were entered directly into the modelled augmented batch test reactors (as inputs in the modelling environment).

For this particular type of substrate (soluble), the composition of the BSO in the influent was unknown. However, the remaining organic groups were determined using a similar approach to Section 3.11.2.1.

1. The concentration of USO in the augmented test reactors were determined by the filtered COD concentration remaining at the end of the experiment.

2. The concentration of the BSO was the difference between the starting and ending filtered COD concentration.

3. The composition of the UPOs were fixed at $C_1H_{1.571}O_{0.426}N_{0.166}P_{0.019}$. The COD and VSS concentration at the end of the experiment quantified the particulate material that did not degrade throughout the experiment.

4. The composition and concentration of the BPOs present in the inoculum were taken from the control reactor (negligible for AugBSP). The BPO concentration was diluted accordingly based on the starting mixtures for the augmented batch experiments.

5. The VSS at the end of the experiment represented the UPOs and active biomass, as a soluble substrate was utilised.

The soluble substrate chosen presented some challenges to the modelling procedure as casein hydrolysate is a micelle. As explained in Section 2.6, a micelle is a colloidal particle, which contains a hydrophobic head and a hydrophilic tail. Subsequently, casein hydrolysate has difficulty dissolving in water as it tends to be hydrophobic. For this reason, it was believed that, although the best efforts were made to completely dissolve the casein into solution, a fraction of the casein remained in its particulate form and did not hydrolyse during the experiment. To compensate for this property of casein, an additional term was added to both the AugBMP and AugBSP models, f_S_F_dis, which took into account the fraction of casein that dissolved in solution. The f_S_F_dis term only applied to the PE done for casein and was not present in the models used to determine the composition of the BPO in PSS.

The mass of BSO present in the augmented batch test reactors at the start of the experiment was determined by the dry mass of the casein hydrolysate powder that was added to water to form the feed solution. Therefore, the BSO mass was fixed at the start of the modelled experiment as it depended on the mass entered into the model. The mass of BSO that was hydrolysed and used throughout the modelled experiment was depended on the f_S_F_dis term. The remaining casein hydrolysate that did not dissolve into solution became UPO. The f_S_F_dis term, as well as the BSO composition was adjusted using multiple iterations by the PE until the observed COD, VSS, FSA, OP, alkalinity and pH was achieved by the model. The parameters adjusted by the PE for the casein experiment are shown in Table 3.11.

Table 3. 11: AugBMP/AugBSP test PE parameters for casein

PWM_SA Parameter	Description
i_H_SF_mol_perC	The H content of the BSO (y)
i_O_SF_mol_perC	The O content of the BSO (z)
i_N_SF_mol_perC	The N content of the BSO (a)
i_P_SF_mol_perC	The P content of the BSO (b)
f_S_F_dis	The fraction of casein hydrolysate that dissolved into solution
M(X_U_Inf)	The mass of the UPO
K_H_f	The saturation hydrolysis constant for BSO breakdown.
mu_AM/mu_AS	The growth rate of the aceticlastic organisms (either methanogenic or sulphidogenic)
Ks_AM/Ks_AS	The half saturation coefficient of the aceticlastic organisms (either methanogenic or sulphidogenic)

3.11.3.2 Identifying the Particulate Substrate using Parameter Estimation in the modelled AugBMP test experiment

The particulate substrate chosen for this project was the biodegradable organics present in PSS, which was taken from Potsdam Wastewater Treatment Plant. The fractionation procedure used to determine the specific organic groups was discussed in Section 3.8.4.2. The PWM_SA_AD model specifies the biomass and biodegradable organics as two separate groups. The AugBMP control reactor was used to identify the composition of the residual biodegradable particulate organics in the methanogenic SSPAD effluent. The composition of the biomass, as well as the composition of the biodegradable organics, were fixed (to be the same as for the control AugBMP) for the duration of the modelled AugBMP test experiment.

The fixed BPO composition for the residual biodegradable organics in the SSPAD effluent presented a problem when running a PE for the AugBMP test reactor, as the composition of the biodegradable particulates in the PSS could not be isolated. Therefore, in order to identify the composition of the biodegradable particulate organics present in the PSS, an additional component was added to the PWM_SA_AD model. The additional component, named PSS particulate organics (X_B_PSS), was identical to the biodegradable particulate component (X_B_Inf), already in the model, in every way, i.e. it used the same stoichiometric and kinetic equations. The new PSS particulate component allowed for the composition of the

biodegradable particulate organics in the PSS (X_B_PSS) to be identified above that of the residual particulate organics (X_B_Inf) present in the modelled SSPAD inoculum.

Therefore, PE was used to identify the composition of the biodegradable particulate organics in the PSS. In order to identify the biodegradable particulate organics in the PSS, the other three organic groups, USO, BSO and UPO, needed to be quantified.

1. The concentration of the USO present in the AugBMP test reactor was determined using the filtered COD concentration that remained in the test reactor at the end of the experiment, which quantified the soluble material that did not degrade throughout the experiment, i.e unbiodegradable soluble. Therefore, the mass of USO was adjusted until the modelled soluble COD concentration at the end of the experiment reflected the observed soluble COD concentration.

2. The concentration of the BSO present in the AugBMP test reactor was quantified using the difference between the starting and ending soluble COD concentrations (excluding the VFAs present). The soluble COD concentration at the end of the experiment quantified the unbiodegradable soluble material. Therefore, the difference between the starting and ending soluble COD concentrations quantified the biodegradable soluble COD that was utilised throughout the experiment. Therefore, the mass of BSO in the modelled AugBMP test reactor was adjusted to reflect this starting concentration.

3. The composition of the UPO was fixed at $C_1H_{1.571}O_{0.426}N_{0.166}P_{0.019}$. Therefore, the COD and VSS concentrations of the UPO were related by an f_{CV} value of 1.48. This relationship fixed the COD concentration relative to the VSS concentration remaining at the end of the experiment. The COD and VSS concentration at the end of the experiment quantified the particulate material that did not degrade throughout the experiment (i.e unbiodegradable particulate), but also included the COD and VSS concentration of the biomass at the end of the experiment due to the low organism death rates. Therefore, the mass of UPO was used as an unknown parameter in the PE. The PE took into account the mass of biomass that grew and degraded throughout the experiment and assigned the remaining mass to the UPO, such that the observed COD and VSS concentrations at the end of the modelled experiment reflected the observed concentrations.

4. The concentration and composition of the BPO present in the SSPAD inoculum was identified using the modelled AugBMP control experiment.

5. The concentration of biomass at the start of the experiment was determined using the modelled SSPAD effluent concentrations.

With five of the organic groups identified as well as the presence of VFAs taken into account, the influence of the biodegradable particulate organics in the PSS was determined using the PE function. The following measurements affected how the composition and mass of the biodegradable particulate organics in the PSS was determined using the same approach as described in Section 3.11.2.1 The parameters used to determine the X_B_PSS characteristics (including its elemental composition and kinetics of hydrolysis) are listed in Table 3.12.

Table 3. 12: AugBMP test PE parameters for PSS

PWM_SA Parameter	Description
i_H_XBPSS_mol_perC	The H content of the particulate organics in the PSS (y)
i_O_XBPSS_mol_perC	The O content of the particulate organics in the PSS (z)
i_N_XBPSS_mol_perC	The N content of the particulate organics in the PSS (a)
i_P_XBPSS_mol_perC	The P content of the particulate organics in the PSS (b)
M(X_B_PSS)	The mass of the particulate organics in the PSS
M(X_U_Inf)	The mass of the UPO
kM_BPSS_AD_hyd	The saturation hydrolysis constant for particulate organics in the PSS breakdown.
mu_AM	The growth rate of the acetoclastic methanogens
KS_AM	The half-saturation coefficient of the acetoclastic methanogens

3.11.3.3 Identifying the Particulate Substrate using Parameter Estimation in the modelled AugBSP test experiment

The AugBSP test PE used the same alterations made to the PWM_SA_AD model, such that the particulate organics in the PSS were represented by (X_B_PSS). However, the AugBSP experiment did not have any residual biodegradable organics present in the inoculum. Therefore, the BPO component in the PWM_SA_AD model could have been used to represent the particulate organics in the PSS; however, (X_B_PSS) was used for consistency. The procedure for identifying the composition of the particulate organics in the PSS was identical to that of the AugBMP test, as described in Section 3.11.3.2. The only exception was that the mass of BPO was set to zero.

The parameters used to determine the X_B_PSS composition were the same as listed in Table 3.12, however, the growth rate and half-saturation coefficient for acetoclastic sulphidogenesis was used instead, as shown in Table 3.13.

Table 3. 13: AugBSP test PE parameters for PSS

PWM_SA Parameter	Description
i_H_XBPSS_mol_perC	The H content of the particulate organics in the PSS (y)
i_O_XBPSS_mol_perC	The O content of the particulate organics in the PSS (z)
i_N_XBPSS_mol_perC	The N content of the particulate organics in the PSS (a)
i_P_XBPSS_mol_perC	The P content of the particulate organics in the PSS (b)
M(X_B_PSS)	The mass of the particulate organics in the PSS
M(X_U_Inf)	The mass of the UPO
kM_BPSS_AD_hyd	The saturation hydrolysis constant for particulate organics in the PSS breakdown.
mu_AS	The growth rate of the acetoclastic sulphidogens
KS_AS	The half-saturation coefficient of the acetoclastic sulphidogens

Chapter 4: Steady-state parent anaerobic digester results and modelling

4.1 Introduction

The identification of the composition of the biodegradable organics present in the selected substrates, casein and PSS, was explained over three chapters (Chapter 4, 5 and 6). Chapter 4 presents the analysis of results obtained from both the methanogenic and sulphidogenic SSPADs, Chapter 5 identifies the composition of residual BPOs present in the inoculum using the augmented batch control reactors, and Chapter 6 identifies the composition of the biodegradable organics present in the chosen substrates using the augmented batch test reactors.

This Chapter 4 presents the analysis of the results for the methanogenic and sulphidogenic SSPADs used to provide the inoculum for the AugBMP and AugBSP experiments, respectively. This included the data collected, the data evaluation using mass balances performed and the modelling results. This chapter was important for establishing that the SSPADs were running at steady state, as well as confirming that mass was conserved throughout the system, using the mass balance checks.

Further, to determine the concentrations of the active biomass (which is represented by a separate and unique composition to that of the substrate) that were used for the modelled augmented batch experiments, steady state models were applied to the data generated by the SSPADs.

This chapter has been separated into two main sections. Each section described the results, mass balances and modelling for the SSPADs used to grow the inoculum for the AugBMP and AugBSP experiments.

4.2 The methanogenic SSPAD

4.3 The sulphidogenic SSPAD

Both the AugBMP and the AugBSP experiments required a stable inoculum, which was grown using SSPADs for each respective system, i.e. A methanogenic SSPAD and a sulphidogenic SSPAD. Each respective system was fed the same organic substrate, in this case, stored PSS from Potsdam Wastewater Treatment Facility in the Western Cape.

Both the AugBMP and the AugBSP experiments were repeated four times each. One of the experiments was used to identify the composition of the organics in the soluble substrate, casein, and the remaining three experiments were used to identify the composition of the organics in the particulate substrate, PSS. The same respective SSPAD, either methanogenic or sulphidogenic, was used throughout the experiments conducted to provide the inoculum required, however, the dates at which the experiments were conducted differed. Therefore, an inoculum was required for each of the AugBMP and AugBSP experiments conducted on the casein, labelled MC1 and SC1, as well as the experiments conducted on the PSS, labelled MP1, MP2, MP3, and SP1, SP2, SP3, respectively.

Table 4. 1: Experiment Periods

Label	Type of Experiment	Date of Experiment
MC1	Methanogenic Casein	February – March 2019
MP1	Methanogenic PSS	February – March 2018
MP2	Methanogenic PSS	May-June 2018
MP3	Methanogenic PSS	December 2018
SC1	Sulphidogenic Casein	March 2019
SP1	Sulphidogenic PSS	November 2018
SP2	Sulphidogenic PSS	January – February 2019
SP3	Sulphidogenic PSS	April 2019

The procedure used to analyse and model the methanogenic SSPAD for each experiment period, MC1, MP1, MP2, and MP3 was the same. Likewise, the procedure used to analyse and model the sulphidogenic SSPAD for each experiment period, SC1, SP1, SP2, and SP3 was the same.

4.2 Methanogenic SSPAD

As previously mentioned, the same methanogenic SSPAD was used throughout the experiments conducted, however, the dates at which the experiments were conducted differed. The operation of the methanogenic SSPAD is given in Section 3.2.1. The measured constituent concentrations present in the influent PSS feed and the effluent from the methanogenic SSPAD during the MC1, MP1, MP2 and MP3 experiments are summarised in Table 4.2. The details for the preparation of the influent PSS are given in Section 3.3.1. The concentrations presented in Table 4.2 for the influent PSS accounted for the dilution that occurred when adding warm tap water to the PSS before feeding the digester.

Table 4.2 illustrates the aqueous concentrations for a range of constituents present in the influent and effluent streams of the SSPAD during the four experiment periods, from which the inoculum for each AugBMP reactor experiment was taken. The values listed in the table are the averaged values determined from conducting multiple measurements over at least four consecutive days. The analytical procedures used to measure each constituent is given in Section 3.6.

Table 4. 2: Methanogenic SSPAD results

Methanogenic SSPAD		MC1			MP1			MP2			MP3		
Constituent	**Unit**	Influent	Effluent	Change (△)	Influent	Effluent	Change (△)	Influent	Effluent	Change (△)	Influent	Effluent	Change (△)
COD													
Total	mgCOD/l	37916	20107	-17809	49749	18423	-31326	52093	16854	-35239	58519	23957	-34562
Soluble	mgCOD/l	5291	4409	-882	6593	4947	-1646	6470	3006	-3464	7220	4626	-2594
Particulate	mgCOD/l	32625	15698	-16927	43155	13476	-29680	45623	13848	-31776	51299	19330	-31969
Nitrogen													
TKN	mgTKN-N/l	924	999	75	1066	1251	185	1327	1254	-73	938	1019	81
FSA	mgFSA-N/l	228	508	280	74	536	463	218	660	443	174	602	428
Phosphate													
TP	mgTP-P/l	119	126	7	145	186	40	152	186	34	198	185	-14
OP	mgOP-P/l	29	26	-3	84	24	-60	41	13	-29	61	41	-20
Solids													
TSS	mgTSS/l	20742	12169	-8573	26415	12984	-13432	27238	10488	-16751	34268	15275	-18992
VSS	mgVSS/l	16783	9154	-7629	21579	9670	-11909	24058	8028	-16030	27817	11921	-15897
ISS	mgISS/l	3958	3015	-943	4836	3313	-1523	4251	2460	-1791	6090	3355	-2735
pH													
pH		5.45	6.96	1.51	5.50	7.00	1.50	5.39	7.09	1.70	5.06	7.11	2.05
Alkalinty													
Carbonate + H2O	mg/l as CaCO3	59	2352	2293	2.1	2001	1999	108	2681	2574	71	2501	2430
Ammonia	mg/l as CaCO3	0	10	10	0	13	13	0	17	17	0	16	16
Phospahte	mg/l as CaCO3	1.3	22.3	21.0	3.5	23	20	0.5	14	14	0.3	49	48
Sulphide	mg/l as CaCO3	0	0	0	0	0	0	0	0	0	0	0	0
VFA	mg/l as CaCO3	383	234	-150	957	8	-949	1	2	1	1	2	1
Total	mg/l as CaCO3	443	2618	2175	962	2045	1083	109	2715	2605	74	2568	2494
Species Concentration													
CT	mg/l as C	109	674	565	0.4	553	553	409	727	318	535	683	148
VFA	mg/l as acetate	542	282	-260	1328	9	-1319	2	2	1	2	3	1

The total influent COD concentration differed between 37916± 2700 and 58519± 3351 mgCOD/*l*, a range of 20603mgCOD/*l*. The soluble influent COD concentration differed from 5291± 585 to 7220± 254 mgCOD/*l*, a range of 1390mgCOD/*l*. The concentration of the influent soluble COD was low relative to the total COD concentration (12.3 – 14%), indicating that the particulate material present in the PSS had a significant impact on the total COD concentration. However, different batches of PSS were collected from Potsdam WWTP throughout the year, subsequently affecting the PSS characteristics at different experiment periods. The influent PSS concentrations for MC1 suggested that the PSS was more dilute than during the remaining three experiment periods.

The total effluent COD concentration fluctuated between 16854± 2215 and 23957± 1177 mgCOD/*l*, a range of 7103 mgCOD/*l*. The soluble effluent COD concentration had a range of 1941mgCOD/*l*. It was assumed that all of the biodegradable soluble COD was utilised by the methanogenic SSPAD over the 20-day sludge age; therefore, the soluble COD exiting the SSPAD consisted of unbiodegradable soluble COD and some VFA. The biodegradable soluble COD concentration was calculated using the change in soluble COD concentration between the influent and effluent streams. Subsequently, the biodegradable soluble COD in the PSS varied between 882 and 3464 mgCOD/*l*. This fluctuation indicated a change in the biodegradable soluble COD entering the WWTP, which may have been caused by dilution during wet weather.

Interestingly, the concentration of particulate COD utilised by the SSPAD remained relatively constant for the MP1, MP2 and MP3 experiment periods. The particulate COD concentration was calculated as the difference between the total and soluble COD concentrations. The particulate COD concentration used by the digester for the experiments MP1, MP2 and MP3 were 29680, 31776 and 31969 mgCOD/*l* respectively. This indicated a range of 2289mgCOD/*l*, which suggested that the biodegradability of the PSS remained relatively consistent, with varying unbiodegradable constituents.

Constituents such as TKN and TP were relatively consistent for all four experiments, while the influent FSA concentration in the PSS differed significantly. However, the concentration of FSA released into the SSPAD during the breakdown of the biodegradable organics for the

MP1, MP2 and MP3 experiments were consistent at 463, 443 and 428 mgFSA-N/*l*, respectively.

The OP concentration decreased from the influent to the effluent stream, the reason for this is not known; however, it may be caused by chemical processes such as struvite precipitation. The implications of struvite precipitation are not considered for this project as it was highly unlikely that struvite precipitation occurred in the AugBMP experiment reactors, as the reactors contained very low OP and metals, as shown in Table 4.2. PSS has been known to have low phosphate and metal concentrations, making struvite precipitation unlikely. Furthermore, the influence of OP on the system was negligible in comparison to the other weak acid/bases present, as the concentration of OP entering the AugBMP reactors in the inoculum was less than 18mgOP-P/*l*. However, a parallel project by Maake *et al.* (2020), is exploring the influence of high phosphate concentrations on the AugBMP test method.

The TSS and VSS concentrations of the influent PSS also differed significantly between the four experimental periods. The change in the VSS concentration between the influent and effluent streams highlighted the fluctuation of the biodegradable particulate organics present in the PSS. This observation emphasises the varying nature of PSS and the importance of correct substrate characterisation in modelling WRRFs.

The pH of the influent PSS remained relatively constant at a value between 5 - 5.5. Interestingly, the PSS collected for MC1 and MP1 appears to have undergone fermentation during storage, as a high concentration of VFA, 542± 102 and 1328± 218 mg/*l* as acetate respectively, was present in the influent stream, compared to both MP2 and MP3. This fermentation did not significantly affect the pH of the influent PSS as it remained around 5.31± 0.2 for all four experiments.

4.2.1 Gas Chromatography

The partial pressure of methane inside the digester headspace was an important parameter necessary for determining COD flux balances. The reactor headspace consists of an array of different gases, of which the most prominent are methane and carbon dioxide, along with negligible quantities of hydrogen, hydrogen sulphide and water vapour. The partial pressure of

the methane present in the digester headspace was especially important for the COD balance, as methane is the only gas that has a COD (assuming negligible hydrogen sulphide production).

Therefore, to close the COD balance, the volume and equivalent COD of the methane produced by the reaction was calculated. The calculation required that the partial pressure of methane be known. The partial pressure of methane in the headspace was determined using a gas chromatograph, fitted with a methane column, as described in Section 3.6.10. The equipment was not directly available to the Water Research Lab and needed to be accessed through an agreement with the Chemical Engineering Department at UCT. For this reason, the data regarding the partial pressure of methane in the headspace was limited. Nevertheless, the headspaces for the methanogenic SSPAD, the AugBMP control reactors and the AugBMP test reactors were analysed when possible. Table 4.3 shows the average methane partial pressures for the testing periods when the equipment was available.

Table 4. 3: Gas chromatography results

		Period	
Experiment Type	**Unit**	**MP2**	**MP3**
Methanogenic SSPAD	% Methane	59.2± 1.7	57.2± 2.7
AugBMP Control	% Methane	57.5± 9	50.3± 8.7
AugBMP Test	% Methane	62.8± 6.5	54.7± 4.5

4.2.2 Mass Balances

Conservation of mass states that, at steady state, the flux of material entering the AD should equal the flux of material exiting the AD. Methanogenic anaerobic digestion requires organic and inorganic compounds for biochemical processes, such as catabolism and anabolism. The uptake and release of these compounds can be traced throughout the system by measuring the component concentrations entering and exiting the AD. For instance, the conversion of COD from the influent organic substrate produces biogas, consisting of methane and carbon dioxide, as well as some particulate biomass, as a by-product. The influent and effluent flowrates for the methanogenic SSPAD were both 0.8*l*/d. The COD fluxes were calculated using Equations 3.7, 3.8 and 3.9 from Section 3.7.3.1.

The remaining COD required for the balance was that of the methane gas produced by the methanogenic bio-process. The difference in COD flux between the influent and liquid effluent should be that of the methane gas, assuming a 100% COD balance, and is illustrated in Figure 4.1 below for the methanogenic SSPAD MC1 experiment.

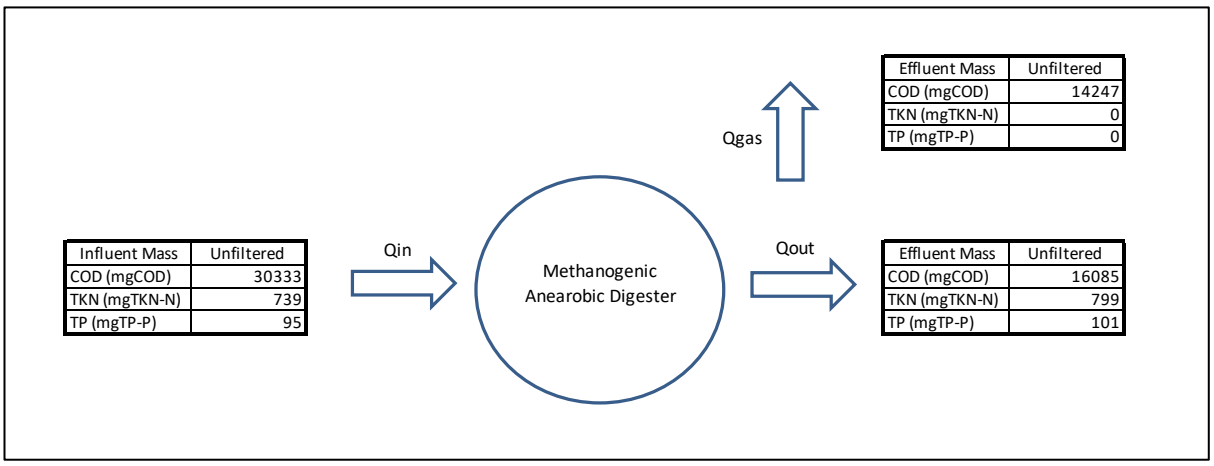

Figure 4. 1: Methanogenic SSPAD mass flux MC1 SSPAD

The daily methane production was measured using a wet-tip gas meter, which is further explained in Section 3.2.1. Therefore, the daily recorded gas tips were converted to the equivalent daily methane production. The number of gas tips varied daily. The reason for this was most likely due to the nature of the PSS substrate, as a homogenous mixture was difficult to achieve. Therefore, the COD balance was conducted by taking the COD value required for a 100% balance and then calculating the number of gas tips required to achieve it.

The partial pressure of the methane gas in the MC1 SSPAD headspace was taken to be 60%, a value close to that of the MP2 and MP3 SSPADs. Therefore, assuming that the majority of the headspace gas was made up of CH_4 and CO_2, the total expected biogas production, for the MC1 SSPAD, over a 24-hour cycle was 9.32 *l/d*. The wet-tip gas meter was calibrated to measure 45m*l* of gas per tip. Therefore, assuming a 100% COD balance, the expected number of tips per day was 207. The observed gas tips for a 24hour cycle varied between 180-220 depending on the AD feeding time, as well as the homogeneity of the PSS. Therefore, the COD balances varied from 94% to 103%. This calculation was then repeated for the remaining experiments, MP1, MP2 and MP3. The results are summarised in Table 4.4. However, a COD balance could not be conducted for MP3, as the wet-tip gas meter was undergoing repairs.

The methane gas production by MC1, MP1, MP2 and MP3 was 184, 247, 266 and 232 $mlCH_4/gCOD$. O'Rourke (1967) identified a methane gas production of 330 $mlCH_4/gCOD$ when treating primary and humus sludge at a retention time of 15 days, and Izzett et al. (1992) identified a gas production of 371 $mlCH_4/gCOD$ when treating a mixture of primary and humus sludge at a retention time of 20 days. The difference in methane gas production between MC1, MP1, MP2 and MP3 and the literature values is due to the variability of the biodegradable organics present in the primary sludge. The primary sludge consists of both biodegradable and unbiodegradable COD. Therefore, the characteristics of the sludge, such as the ratio of biodegradable organics to unbiodegradable organics and the composition of these organics, influence the potential biogas production.

Table 4. 4: Methanogenic SSPAD COD balance

COD Balance	MC1	MP1	MP2	MP3
COD In				
Average Influent COD Flux (mgCOD)	30333	39799	41674	46815
COD Out				
Average Effluent COD Flux (mgCOD)	16085	14738	13483	19165
Methane COD (mgCOD)	14247	25061	28191	27650
Total COD	30333	39799	41674	46815
COD Balance (%)	**100**	**100**	**100**	**100**
Gas Volume Equivilent				
Gaseous CH4 COD (mgCOD)	14247	25061	28191	27650
Mol CH4 (mol)	0.223	0.392	0.440	0.432
Volume Methane (l)	5.6	9.8	11.1	10.9
Volume Methane (ml)	5592	9837	11066	10853
Partial Pressure	0.60	0.60	0.59	0.57
Total Gas Volume (ml)	9321	16395	18692	18974
Volume of Tip (ml)	45	45	45	45
Gas Tips	207	364	415	422
Gas Production (ml CH_4/gCOD)	184	247	266	232
Observed				
Observed Tips	180 - 220	381 - 409	490 - 666	-
Observed Gaseous COD (mgCOD)	12381-15133	26207-28133	33255-45200	-
COD Balance Range (%)	94-103	105 - 112	118-160	-

Consequently, it was accepted with certainty that a good COD balance was achieved over the methanogenic SSPAD for the MC1 and MP1 experiments, as the balances were within 10%, as explained in Section 3.7.2. The COD balance for the MP2 experiment was significantly high, between 118-160%. The reason for the high observation of methane gas produced during the

MP2 experiment was unclear, as the expected gas production agreed well with the MP1 experiment.

The mass flux of other constituents present in the entering and exiting streams such as the TKN and TP were also checked using the mass balanced approach. The total mass of these two constituents should remain constant throughout the experiment. The TKN and TP mass fluxes were calculated using Equation 3.14 from Section 3.7.5. The TKN and TP balances are shown in Table 4.5.

Table 4. 5: Methanogenic SSPAD TKN/TP balance

	MC1	MP1	MP2	MP3
TKN Balance				
TKN In				
Influent Average (mgTKN-N)	739	853	1062	750
TKN out				
Effluent Average (mgTKN-N)	799	1001	1003	815
Balance (%)	**108**	**117**	**94**	**109**
TP Balance				
TP In				
Influent Average (mgTP-P)	95	116	122	159
TP out				
Effluent Average (mgTP-P)	101	149	149	148
Balance (%)	**106**	**128**	**122**	**93**

A TKN balance for the SSPAD for the MC1, MP2 and MP3 experiments was accepted, as the balances were within 10%, as explained in Section 3.7.2. The TKN balance from the MP1 experiment was high at 117%, indicating that more material was present in the effluent than the influent. The discrepancy for the MP1 TKN balance was most likely caused by measurement error.

A TP balance for the MC1 and MP3 experiments was accepted. However, the TP balances from the MP1 and MP2 experiments were high at 128% and 122%, indicating that more material was present in the effluent than the influent. The discrepancy was most likely due to the spectrophotometry method, as described in Section 3.6.5, which highlighted a variance

among the collected phosphate results. The variance was most likely caused by the set dilution intervals of the discrete analyser used.

4.2.3 Modelling the Methanogenic SSPAD

The methanogenic SSPAD was modelled using the PWM_SA_AD model coded into WEST® wastewater software (Vanhooren *et al.*, 2003). Correctly modelling the SSPAD allowed for the mass of active biomass present in the SSPAD effluent to be estimated. The methanogenic SSPAD effluent was used as the inoculum in both the AugBMP control and test reactors. However, modelling the SSPAD was not required for identifying the biodegradable composition using the stoichiometric method explained in Section 3.9.2.

The main focus of the modelled SSPAD was to, as accurately as possible, replicate the laboratory observations on the methanogenic SSPAD. By accurately replicating the observed SSPAD, the concentrations of each active biomass group were estimated. The active biomass groups considered by the PWM_SA_AD model were the acidogens, acetogens, acetoclastic methanogens and hydrogenotrophic methanogens. The active biomass estimation was achieved by characterising the influent PSS and then adjusting the model parameters such that the effluent concentrations of the modelled SSPAD replicated the observed SSPAD effluent concentrations.

4.2.3.1 Influent Fractionation

In order to run the model, it was necessary to characterise the influent COD of the PSS into the correct COD fractions. The organic groups present in the influent PSS were BSO, consisting of FSBO and VFA, BPO, USO and UPO. The influent fractionation procedure used to characterise the influent PSS is thoroughly explained in Section 3.8.1. and Section 3.8.2.

A crucial characteristic of the methanogenic system was that it contained residual biodegradable organics (S_{bp}), as well as active biomass (Z_{AD}), in the effluent stream. In contrast, the sulphidogenic system contained negligible S_{bp}, and only active Z_{AD} in the effluent stream. Equations 3.20 to 3.35 in Section 3.8.2.1 were used to characterise the influent PSS.

The Z_{AD} concentration was determined using the steady-state equations of Sötemann *et al.* (2005). Sötemann *et al.* (2005) stated that the acidogens have the highest yield coefficient (Y_{AD} = 0.089 gCOD biomass/ gCOD substrate). However, the acetoclastic methanogens also contribute significantly to the concentration of biomass present. Therefore, determining the concentration of biomass present can be simplified by increasing the Y_{AD} from 0.089 to 0.113. This increase of Y_{AD} takes into account the formation of the other organism groups. Furthermore, this simplification is acceptable as the death rates for these two organisms (acidogen and aceticlastic methanogens; b_{AD} = 0.041/d, and b_{AC} = 0.037/d) are similar. Therefore, the Y_{AD} value was increased to 0.129 based on the standard yield coefficients (Y_{AD} = 0.0895, and Y_{AC} = 0.039) used by the PWM_SA_AD model.

Equation 3.29 in Section 3.8.2.1 was used to determine the Z_{AD} concentration based on the daily methane production. The daily methane production was calculated as the difference between the total influent COD and total effluent COD concentrations. Equation 3.29 has been structured such that only the daily COD production of methane, the yield coefficient, the collective biomass death rate and the sludge age of the reactor is required. The calculated biomass concentrations are summarised in Table 4.6.

Table 4. 6: Calculated methanogenic SSPAD biomass COD concentration

COD	Unit	MC1	MP1	MP2	MP3
Unfiltered Influent	mgCOD/l	37916	49749	52093	58519
Unfiltered Effluent	mgCOD/l	20107	18423	16854	23957
Daily Methane Production (S_m)	mgCOD/l	17809	31326	35239	34562
Constants					
Y_{AD}		0.129	0.129	0.129	0.129
b_{AD}	/d	0.041	0.041	0.041	0.041
R	days	20	20	20	20
Biomass					
Z_{AD}	mgCOD/l	1446	2544	2861	2806

With the Z_{AD} COD concentration determined, the change in COD observed in the AugBMP control reactors was calculated. The change in COD concentration (excluding the VFA) indicated the residual biodegradable material present in the SSPAD effluent, as the AugBMP control reactor allowed for extended digestion of the SSPAD effluent to occur. The biodegradable organics present in the SSPAD effluent comprised of three main groups: The residual biodegradable organics (S_{bp}), the active biomass (Z_{AD}) and the VFAs. The total change

in COD was calculated using Equation 3.30 from Section 3.8.2.1. The change in COD concentration in the AugBMP control reactor, as shown in Table 4.7, was due to both the breakdown of S_{bp} and biomass decay.

It was difficult to estimate the concentration of Z_{AD} COD that was lost due to biomass decay during the AugBMP control experiment, as it is a slow process. A good approximation was achieved by modelling the AugBMP control experiment at different Z_{AD} COD losses. The process of determining the Z_{AD} COD loss involved multiple iterations, which required the influent PSS characterisation process to be repeated, as the change in S_{bp} affected the UPO COD concentration. The Z_{AD} COD loss was determined using the modelled AugBMP control reactor, as the substrate uptake, as well as the biomass growth and decay reactions are calculated for each timestep in the model. The dilution of the SSPAD effluent due to the AugBMP control starting mixture was accounted for in the model.

Table 4. 7: Total COD change in AugBMP control reactors

AugBMP Control Reactors	Unit	Start	End	Change (Δ)
MC1				
Time	days	0	28	28
Total COD	mgCOD/l	10401	8333	2068
VFA COD	mgCOD/l	206	0	206
Total COD (excluding VFA)	mgCOD/l	10196	8333	1862
MP1				
Time	days	0	28	28
Total COD	mgCOD/l	8730	6308	2422
VFA COD	mgCOD/l	1	5	-4
Total COD (excluding VFA)	mgCOD/l	8729	6303	2426
MP2				
Time	days	0	22	22
Total COD	mgCOD/l	9545	8907	638
VFA COD	mgCOD/l	38	0	38
Total COD (Excluding VFA)	mgCOD/l	9507	8907	600
MP3				
Time	days	0	19	19
Total COD	mgCOD/l	13306	11493	1813
VFA COD	mgCOD/l	89	150	-61
Total COD (Excluding VFA)	mgCOD/l	13218	11343	1875

Once the estimation of the Z_{AD} COD loss was confirmed by the modelled AugBMP control reactor, the S_{bp} COD concentration was calculated as the difference between the total COD change (excluding VFA) and the Z_{AD} COD loss, as shown in Equation 3.31 in Section 3.8.2.1.

The outcome of the Z_{AD} loss approximation and S_{bp} COD concentrations is summarised in Table 4.8.

The Z_{AD} COD loss differed due to the duration of the AugBMP experiment. The AugBMP experiment for MC1, MP1, MP2 and MP3 were run for 19, 29, 24 and 19 days, respectively. Table 4.8 shows that the estimate of 25%, 50% and 35% Z_{AD} COD loss for MC1, MP1 and MP3, respectively, closely matched that of the model. The S_{bp} value determined in Table 4.8 was then multiplied by 2 to account for the dilution when characterising the influent PSS.

Table 4. 8: Methanogenic SSPAD residual biodegradable organics

		MC1			**MP1**		
		25% Z_{AD} COD Loss			50% Z_{AD} COD Loss		
Observed Experiment	**Unit**	Z_{AD}	S_{bp}	Change (Δ)	Z_{AD}	S_{bp}	Change (Δ)
Starting Value	mgCOD/l	723	1682	-	1272	1790	-
Ending Value	mgCOD/l	542	0	-	636	0	-
Observed COD Change	mgCOD/l	181	1682	1862	636	1790	2426
COD loss	%	25	100	-	50	100	-
Modelled		Z_{AD}	S_{bp}	Total	Z_{AD}	S_{bp}	Total
Starting Value	mgCOD/l	729	1734	-	1439	1619	-
Ending Value	mgCOD/l	544	2	-	697	0	-
Model COD Change	mgCOD/l	185	1732	1918	741	1618	2360
COD loss	%	25	100	-	52	100	-
		MP2			**MP3**		
		35% Z_{AD} COD Loss			35% Z_{AD} COD Loss		
Observed Experiment	**Unit**	Z_{AD}	S_{bp}	Change (Δ)	Z_{AD}	S_{bp}	Change (Δ)
Starting Value	mgCOD/l	1431	99	-	1403	1383	-
Ending Value	mgCOD/l	930	0	-	912	0	-
Observed COD Change	mgCOD/l	501	99	600	491	1383	1875
COD loss	%	35	100	-	35	100	-
Modelled		Z_{AD}	S_{bp}	Total	Z_{AD}	S_{bp}	Total
Starting Value	mgCOD/l	1556	697	-	1658	1380	-
Ending Value	mgCOD/l	802	3	-	1064	416	-
Model COD Change	mgCOD/l	753	693	1447	595	964	1559
COD loss	%	48	100	-	36	70	-

The estimated Z_{AD} COD loss was well represented by the model, except for the MP2 experiment. Table 4.8 shows that the total change in COD for MP2 was lower than the other experiments, at 600mgCOD/*l*. Therefore, it was initially assumed that the Z_{AD} COD loss was low, at 35%. However, in the modelled AugBMP control for MP2, it was observed that 48%

of the biomass concentration was degraded. However, if the Z_{AD} loss was set to 50% for the observed results, the S_{bp} value became negative, which was not possible. Therefore, the Z_{AD} COD loss was set to 35% to allow for a low concentration (99mgCOD/*l*) of S_{bp} to be present in the AugBMP control reactor. This low concentration of S_{bp} allowed for a PE to be conducted on the BPO present in the AugBMP control reactor at the beginning of the MP2 experiment. However, it was later shown in Section 5.2 that the MP2 experiment contained inconsistencies between the observed experimental data and the modelled data. The S_{bp} COD concentration, and consequently, the total COD concentration change was increased by the PE from 600mgCOD/*l* to 1447mgCOD/*l* to minimise the error on the methane gas measurements for the AugBMP control MP2 experiment.

With the concentration of the residual biodegradable particulate COD (S_{bp}) determined, the concentration of the unbiodegradable particulate COD was calculated by subtracting the biomass COD and residual biodegradable particulate COD concentrations from the total particulate COD concentration in the effluent, as shown in Equation 3.32 in Section 3.8.2.1. With the COD concentration of UPO determined, the influent wastewater was then fractionated. The fractionation for the SSPAD for each experiment is summarised in Table 4.9.

Table 4. 9: Methanogenic SSPAD influent fractionation

Constituent	Unit	MC1	MP1	MP2	MP3
VFA	mgCOD/l	578	1417	2	2
FSBO	mgCOD/l	604	239	3464	2594
Total BSO	**mgCOD/l**	**1182**	**1656**	**3466**	**2597**
USO	mgCOD/l	4108	4937	3004	4624
Total Soluble	**mgCOD/l**	**5291**	**6593**	**6470**	**7220**
BPO	mgCOD/l	21736	35804	36036	37542
UPO	mgCOD/l	10889	7351	9588	13757
Total Particulate	**mgCOD/l**	**32625**	**43155**	**45623**	**51299**
Total COD	**mgCOD/l**	**37916**	**49749**	**52093**	**58519**

However, it was observed that the VSS concentration in the effluent was not well represented by the modelled SSPAD using the fractionated influent in Table 4.9. The discrepancy was most likely caused by the UPO composition used, as it was previously stated that the UPO composition needs revision. However, it was not in the scope of this investigation to change the UPO composition, as the project focused on the biodegradable organic composition.

However, changing the composition of the UPOs is discussed in the recommendations. Instead, the UPO concentrations were adjusted to align the modelled SSPAD effluent VSS concentration to that of the observed effluent VSS concentration.

Consequently, adjusting the UPO concentration affected the BPO concentration, as the sum of UPO and BPO equated to the total particulate COD in the influent. However, the composition of the BPO was also adjusted to account for this. Therefore, the BPO composition determined for the modelled SSPAD was the best fit for the observed values. However, this did not affect the identification of the biodegradable organics in the AugBMP control and test reactors, as the modelled SSPAD was only used to estimate the active biomass concentrations in the inoculum. The adjusted UPO COD concentrations are shown in Table 4.10.

Table 4. 10: Adjusted methanogenic SSPAD influent fractionation

Constituent	Unit	MC1	MP1	MP2	MP3
VFA	mgCOD/l	578	1417	2	2
FSBO	mgCOD/l	604	239	3464	2594
Total BSO	**mgCOD/l**	**1182**	**1656**	**3466**	**2597**
USO	mgCOD/l	4108	4937	3004	4624
Total Soluble	**mgCOD/l**	**5291**	**6593**	**6470**	**7220**
BPO	mgCOD/l	23146	35804	37923	39299
UPO	mgCOD/l	9479	7351	7700	12000
Total Particulate	**mgCOD/l**	**32625**	**43155**	**45623**	**51299**
Total COD	**mgCOD/l**	**37916**	**49749**	**52093**	**58519**

The VSS concentrations for the unbiodegradable and biodegradable particulates was then calculated using Equations 3.34 and 3.35 in Section 3.8.2.1. The UPO VSS concentration was calculated with a COD/VSS ratio (f_{CV}) of 1.481 gCOD/gVSS. This ratio for UPO has been used for decades in activated sludge models since the steady-state model of Marais and Ekama (1976) but there is evidence that it may need revision (Wentzel *et al*., 2006). Nevertheless, this UPO COD/VSS ratio was adopted for this research and based on this ratio, the f_{CV} ratio of the BPO was determined using the BPO COD concentration and the remaining measured VSS concentration. The f_{CV} mass ratios determined are summarised in Table 4.11.

Table 4. 11: Methanogenic SSPAD influent COD/VSS fractions

Constituent	Unit	MC1	MP1	MP2	MP3
UPO COD	mgCOD/l	9479	7351	7700	12000
UPO VSS	mgVSS/l	6405	4967	5203	8108
UPO fcv	mgCOD/mgVSS	1.48	1.48	1.48	1.48
BPO COD	mgCOD/l	23146	35804	37923	39299
BPO VSS	mgVSS/l	10383	16615	18859	19715
BPO fcv	mgCOD/mgVSS	2.23	2.15	2.01	1.99

Therefore, the f_{CV} ratio of the BPOs in the influent PSS from Potsdam remained relatively consistent, around 2.1 ± 0.1 gCOD/gVSS.

4.2.3.2 Hydrolysis Kinetics

The PWM_SA_AD model required specific kinetic constants as inputs, of which the value of K_M (mu_AD) was the most important. K_M is the kinetic constant that affects the hydrolysis rate of the biodegradable organics by the acidogen biomass, which subsequently influences the concentration of S_{bp} in the SSPAD. K_M was calculated using Equation 3.49 from Section 3.10.3, using a K_S value of 7.98 gCOD/*l*, a value supported by Sötemann *et al.* (2005) for the hydrolysis of PSS using saturation kinetics. Table 4.12 summarises the K_M values determined for the methanogenic SSPAD.

Table 4. 12: Methanogenic SSPAD hydrolysis rate constants

COD	Unit	MC1	MP1	MP2	MP3
Daily Methane Production (S_m)	mgCOD/l	17809	31326	35239	34562
Residual Biodegradable Organics (S_{bp})	mgCOD/l	3363	3581	1394	2767
Biomass (Z_{AD})	mgCOD/l	1446	2544	2861	2806
Hydrolysis Rate					
r_h	mgCOD/(l .d)	1022	1798	2022	1983
Constants					
Y_{AD}		0.129	0.129	0.129	0.129
b_{AD}	/d	0.041	0.041	0.041	0.041
R	days	20	20	20	20
K_S	gCOD/l	7.98	7.98	7.98	7.98
K_M	gCOD organics/ gCOD biomass.d	3.13	4.71	12.24	6.43

The daily methane production of MC1 was significantly low relative to the remaining three experiments. The lower methane production of MC1 was due to a lower concentration of

biodegradable COD available in the influent PSS, which subsequently resulted in a lower concentration of Z_{AD}. The K_M values calculated highlight the relationship between the S_{bp} and Z_{AD} concentrations. Table 4.12 shows that MC1 and MP1 had similar S_{bp} concentrations, but the concentration of Z_{AD} for each differed. The higher Z_{AD} concentration in MP1 was due to more biodegradable organics being utilised, however, the resulting S_{bp} was the same for each. Therefore, the K_M rate in MP1 was greater than in MC1, as more biodegradable organics were used over the same sludge age (R, 20 days). Table 4.12 shows that the MP2 and MP3 experiments had similar Z_{AD} concentrations, but the concentration of S_{bp} differed. The K_M value determined for MP2 was high, at 12.24 gCOD/gCOD.d as the S_{bp} concentration was low, and therefore, a significant concentration of S_{bp} was utilised over the 20 day sludge age. The rh and KM values obtained in Table 4.12 differ from the values obtained by Sötemann *et al*. (2005) as shown in Table 3.7 and Ikumi *et al* (2015), as shown in Table 3.8 in Section 3.10.3. The kinetic parameters are substrate-specific and depend on the characteristics of the substrate. Therefore, the kinetic parameters differ for each substrate as different organics degrade at different rates. Furthermore, given the variability of the biodegradable particulates present in the PSS, the kinetic parameters for each experiment were expected to differ.

4.2.3.3 Model Influent

The organic groups determined in Table 4.10, as well as the required inorganics (FSA, OP) were then converted into the correct format for the PWM_SA_AD model and entered into the WEST® influent generator. The WEST® influent generator ensures that the correct mass of each component in the influent PSS stream was added to the modelled SSPAD daily. An example of the required conversions is given in Table 3.6 and Figure 3.21 in Section 3.10.2.

4.2.3.4 Composition Determination

In the PWM_SA_AD model, the concentration of constituents released into the bulk liquid of the digester is dependent on the elemental composition, and the mass of the organics present in the influent substrate. Therefore, an elemental composition for each group of organics was required. There are five groups of organics, and subsequently, the model requires five separate elemental compositions, i.e one each for BSO, BPO, USO, UPO and Biomass. The

composition determination for each specific organic was described in Section 3.10.4. Table 4.13 shows the compositions used for the methanogenic SSPAD model.

Table 4. 13: Methanogenic SSPAD organic compositions

Group	**MC1**	**MP1**
BSO:	$C_1H_{2.5}O_{0.361}N_{0.08}P_0$	$C_1H_{1.5}O_{0.148}N_{0.055}P_0$
BPO:	$C_1H_{2.5}O_{0.361}N_{0.08}P_0$	$C_1H_{1.5}O_{0.148}N_{0.055}P_0$
USO:	$C_1H_{1.3}O_{0.6}N_{0.01}P_0$	$C_1H_{1.3}O_{0.6}N_{0.01}P_0$
UPO:	$C_1H_{1.571}O_{0.426}N_{0.166}P_{0.019}$	$C_1H_{1.571}O_{0.426}N_{0.166}P_{0.019}$
Biomass:	$C_1H_{1.4}O_{0.4}N_{0.2}$	$C_1H_{1.4}O_{0.4}N_{0.2}$
Group	**MP2**	**MP3**
BSO:	$C_1H_{2.5}O_{0.361}N_{0.064}P_0$	$C_1H_{2.5}O_{0.348}N_{0.064}P_0$
BPO:	$C_1H_{2.5}O_{0.361}N_{0.064}P_0$	$C_1H_{2.5}O_{0.348}N_{0.064}P_0$
USO:	$C_1H_{1.3}O_{0.6}N_{0.01}P_0$	$C_1H_{1.3}O_{0.6}N_{0.01}P_0$
UPO:	$C_1H_{1.571}O_{0.426}N_{0.166}P_{0.019}$	$C_1H_{1.571}O_{0.426}N_{0.166}P_{0.019}$
Biomass:	$C_1H_{1.4}O_{0.4}N_{0.2}$	$C_1H_{1.4}O_{0.4}N_{0.2}$

4.2.3.5 Modelled SSPAD and observed SSPAD comparison

The PWM_SA_AD model was run under steady-state conditions using the parameters and variables determined above, i.e. the hydrolysis rates and elemental compositions of the organics in the PSS substrate. The modelled data was compared to the observed data and evaluated using relative error. Therefore, the closer the value of error was to zero, the more accurate the modelled results. The relative error (percentage error) for each of the SSPAD variables was calculated using Equation 3.51 from Section 3.10.5.

Table 4.14 shows that a low relative error was achieved for the modelled COD groups when compared to the observed COD groups, as the relative error for each group was lower than 10%. However, the modelled biomass concentrations for MP1, MP2 and MP3 were higher than the observed (calculated) concentrations. As mentioned, the Y_{AD} value for the biomass was increased to 0.129 based on the standard yield coefficients (Y_{AD} = 0.0895, and Y_{AC} = 0.039) used by the PWM_SA_AD model. Therefore, increasing the Y_{AD} value when calculating the biomass concentrations using the equations by Sötemann *et al.* (2005) aimed to account for the

combined biomass COD concentration (i.e. the COD concentration of all four groups). The Z_{AD} concentrations in the model may have been higher as the PWM_SA_AD model assigns individual yield coefficients to each organism group. The sum of the yield coefficients in the PWM_SA_AD model for all four groups is greater than the sum of Y_{AD} and Y_{AC}. Therefore, the Z_{AD} COD concentration calculated using the equations by Sötemann *et al.* (2005) may have underpredicted the Z_{AD} COD concentration present in the modelled methanogenic SSPAD. The COD and VSS concentrations were well represented by the modelled SSPAD, which increased the validity of the Z_{AD} concentrations determined by the model.

The rate of daily methane gas production in the MP1, MP2 and MP3 experiments was higher than observed. However, the total gas production rate for all four experimental periods was lower in the modelled SSPAD than was observed. The lower gas production rate may have been due to the CO_2 evolution in the model, as well as the selected compositions of each component. The modelled C_T concentrations in MC1, MP2 and MP3 were lower than was observed, and the rate of total daily gas production was low. However, in MP1, the modelled C_T concentration was higher than observed, which may have caused more CO_2 to evolve in the model, increasing the total gas production. Table 4.13 shows that more C was present in the composition of the MP1 BPO relative to the other elements.

Table 4. 14: Modelled methanogenic SSPAD results

Methanogenic SSPAD	MC1			MP1			MP2			MP3		
COD (mgCOD/l)	**Observed**	**Modelled**	**% error**	**Observed**	**Modelled**	**% error**	**Observed**	**Modelled**	**% error**	**Observed**	**Modelled**	**% error**
Total	20107	18885	-6.1	18423	19396	5.3	16854	16110	-4.4	23957	23464	-2.1
Soluble	4409	4349	-1.4	4947	4981	0.7	3006	3019	0.4	4626	4638	0.2
USO	4108	4094	-0.4	4937	4961	0.5	3004	2999	-0.2	4624	4616	-0.2
RFSO	0	0	-	0	0	-	0	0	-	0	0	-
UPO	9479	9490	0.1	7351	7422	1.0	7700	7724	0.3	12000	12037	0.3
BPO	3363	3298	-2.0	3581	3542	-1.1	1399	1378	-1.5	2767	2814	1.7
Biomass (ZAD)	1446	1459	0.9	2544	2877	13.1	2861	3327	16.3	2806	3317	18.2
Gas Molrate (mol/d)												
Methane Gas Molrate	0.223	0.221	-0.9	0.392	0.439	12.2	0.440	0.496	12.5	0.432	0.494	14.4
Total Gas Molrate	0.371	0.287	-22.6	0.653	0.638	-2.2	0.747	0.661	-11.5	0.758	0.661	-12.8
Nitrogen (mgN/l)												
TKN	999	1454	45.5	1251	1377	10.1	1254	1631	30.1	1019	1877	84.2
FSA	508	558	9.9	536	485	-9.5	660	720	9.0	602	643	6.9
Phosphate (mgP/l)												
TP	126	190	50.3	186	210	13.1	186	172	-7.6	185	264	43.1
OP	26	29	15.2	24	85	259.9	13	41	226.2	41	61	50.8
Acetate (mg/l as acetate)												
VFA	282	217	-23.0	9	1	-93.4	2	1	-74.4	3	2	-27.2
Alkalinity (mg/l as CaCO3)												
Carbonate + H2O	2352	1542	-34.4	2001	2693	34.6	2681	1941	-27.6	2501	1813	-27.5
Total	2618	1796	-31.4	2045	2901	41.8	2715	2045	-24.7	2568	1962	-23.6
Species Concentration (mg/l)												
CT	674	441	-34.7	553	743	34.4	727	543	-25.3	683	514	-24.8
Solids (mgVSS/l)												
VSS	9154	9246	1	9670	8919	-8	8028	8693	8	11921	12256	3
pH												
pH	6.96	6.94	-3.8	7.00	7.04	8.5	7.09	6.99	-24.0	7.11	6.96	-40.2

The TKN and TP concentrations were significantly higher in the modelled SSPAD than in the observed SSPAD. The reason for this was due to the chosen UPO composition. The FSA concentrations released into the modelled SSPAD agreed well with the observed SSPAD FSA concentrations. Furthermore, the FSA concentration was adjusted accordingly, by either increasing or decreasing the concentration, such that the error on the H_2CO_3 alkalinity improved. The H_2CO_3 alkalinity and the FSA concentrations are related as the increase in FSA in the reactor liquid increases the alkalinity of the system. The organic N stored in the BPO is released into the bulk liquid as NH_3. However, due to the pH of the reactor (~7), the NH_3 (p_{ka} ~ 9) cannot exist in this form and subsequently picks up a proton from the aqueous solution to form NH_4^+. The proton taken from the water results in the formation of HCO_3^-, which increases the carbonate alkalinity. However, the low carbonate alkalinity in MC1, MP2 and MP3 was most likely caused by the C content of the BPO organic, which affected the C_T concentration.

The OP concentration released was higher in the modelled SSPAD than in the SSPAD, even with the biodegradable organic P composition set to 0. As previously mentioned, the decrease in OP concentration from the influent to the effluent stream may be caused by chemical processes such as struvite precipitation. However, the implications of struvite precipitation are not considered for this project as it was highly unlikely that struvite precipitation occurred in the AugBMP experiment reactors.

The residual concentration of VFAs in the modelled SSPAD represented the observed VFA concentrations. Furthermore, in an attempt to achieve the high residual VFA concentration in the MC1 effluent, the half-saturation coefficient of the acetoclastic methanogens (KS_AM) was increased from 0.013 to 180 mg*/l*.

The operating pH of the modelled SSPAD reactor for MC1 and MP1 was well represented by the model. However, the operating pH of MP2 and MP3 was lower for the modelled SSPAD. The modelled SSPAD had an operating pH close to 7 for all four experiments. However, the lower operating pH of the modelled SSPAD for MP2 and MP3 may have been due to the low alkalinity generated by the modelled SSPAD compared to the observed SSPAD. Finally, the effluent VSS concentration in the modelled SSPAD agreed well with the observed effluent VSS concentration.

In general, the results for the observed SSPAD were challenging to replicate using the modelled SSPAD. The reason that replicating the observed SSPAD results was challenging to do accurately, was due entirely to the difficulty of adjusting the fractionation of the organic groups in the model. It was not possible to use the PE function for characterising the influent in the modelled SSPAD as the fractionated groups were passed into the model using a text file. The values of the input components required by the model were determined using a separate pre-processor spreadsheet, which converted the laboratory measurements into a text file containing the equivalent model component masses. The text file was then loaded into the influent generator and passed into the PWM_SA_AD model. The text file could not be altered by PE.

Therefore, the equations in Section 3.8.2 were developed to fractionate the organic groups as accurately as possible. However, for every additional adjustment made, the organic groups needed to be re-fractionated and then passed through the pre-processor to get a new text file that was then passed into the model. This made modelling the SSPADs tedious and required trial and error. The accuracy of the modelled SSPAD can be greatly improved by modifying the way in which the influent is passed into the PWM_SA_AD model. However, these changes were too significant for the scope of this project and are discussed in the recommendations.

Therefore, the results obtained in the modelled SSPAD were focused towards accurately representing the active biomass concentrations that were used as inputs for the modelled AugBMP control and test reactors.

4.2.3.6 Active Biomass present in the inoculum

The SSPAD was modelled to estimate the concentrations of active biomass present in the SSPAD effluent as accurately as possible. The concentrations for each group of active biomass present in the inoculum for MC1, MP1 MP2 and MP3 is summarised in Table 4.15 below.

Table 4. 15: Methanogenic SSPAD active biomass concentrations

COD (mgCOD/l)	MC1	MP1	MP2	MP3
Acidogens (X_AD)	975	1911	2235	2228
Acetogens (X_AC)	4	8	10	9
Acetoclastic Methanogens (X_AM)	279	565	622	620
Hydrogenotrophic Methanogens (X_HM)	201	394	460	459
Total Biomass Concentration	1459	2877	3327	3317

4.3 Sulphidogenic SSPAD

As previously mentioned, the same sulphidogenic SSPAD was used throughout the experiments conducted, however, the dates at which the experiments were conducted differed. The operation of the sulphidogenic SSPAD is described in Section 3.2.2. The measured constituent concentrations present in the influent feed solution and the effluent from the sulphidogenic SSPAD during the SC1, SP1, SP2 and SP3 experiments are summarised in Table 4.16. The details for the preparation of the influent feed solution are given in Section 3.3.2.

Table 4.16 illustrates the aqueous concentrations for a range of constituents present in the influent and effluent streams of the sulphidogenic SSPAD during the four experiments, from which the inoculum for each AugBSP reactor experiment was taken. The values listed in the table are the averaged measured values for the measurements performed on the SSPAD during each experiment. The analytical procedures used to measure each constituent is given in Section 3.6.

The total influent COD concentrations for SP1, SP2 and SP3 were relatively consistent at values of 1441± 48, 1643± 116 and 1543± 43 mgCOD/*l*. The desired total COD concentration in the influent was 1500mg COD/*l*, for a sulphate concentration of 1500mgSO_4/*l*. It was assumed that the biodegradable organics made up approximately 2/3 of the total COD in the PSS. Therefore, the COD and sulphate influent solutions were prepared such that a COD/SO_4^{2-} ratio of 0.67 was maintained. However, the COD concentration for the SC1 experiment was lower than the other experiments. The low COD concentration coincides with the low COD concentration of the PSS feed experienced during the MC1 experiment, as shown in Table 4.2 in Section 4.2. The PSS used in both the SC1 and MC1 experiments was the same batch collected from the Potsdam WWTP in February 2019.

The concentration of the influent soluble COD was low relative to the total COD concentration (6 – 8%), indicating that the particulate material present in the PSS had a significant impact on the total COD concentration. The percentage of soluble COD concentration relative to the total COD agreed with the values obtained for the PSS fed to the methanogenic SSPAD (12-14%), as shown in Table 4.2 in Section 4.2.

Table 4. 16: Sulphidogenic SSPAD results

Sulphidogenic SSPAD		SC1			SP1			SP2			SP3		
Constituent	**Unit**	Influent	Effluent	Change (Δ)	Influent	Effluent	Change (Δ)	Influent	Effluent	Change (Δ)	Influent	Effluent	Change (Δ)
COD													
Total	mgCOD/l	646	748	102	1441	1782	341	1643	1705	61	1543	936	-606
Soluble	mgCOD/l	54	466	411	113	691	577	143	796	653	91	411	320
Organic	mgCOD/l	-	109	-	-	66	-	-	112	-	-	102	-
Sulphide	mgCOD/l	-	357	-	-	625	-	-	684	-	-	309	-
Sulphate													
Total	mgSO4/l	1500	617	-883	1500	97	-1403	1500	129	-1371	1500	624	-876
Nitrogen													
TKN	mgTKN-N/l	22	22	1	46	48	2	29	33	4	38	24	-13
FSA	mgFSA-N/l	3	7	4	3	14	12	4	16	12	4	8	4
Phosphate													
TP	mgTP-P/l	3	4	1	7	8	0	5	7	2	6	4	-2
OP	mgOP-P/l	0	2	2	3	4	1	2	4	2	1	3	1
Solids													
TSS	mgTSS/l	468	364	-104	849	778	-71	883	494	-389	1027	448	-579
VSS	mgVSS/l	390	211	-179	773	547	-226	776	342	-434	841	246	-595
ISS	mgISS/l	79	153	75	84	231	147	118	152	34	186	202	16
pH													
pH		2.60	7.21	5	2.68	7.24	5	2.30	7.24	5	2.79	7.04	4
Alkalinty													
Carbonate	mg/l as CaCO3	0	605	605	0.0	925	925	0	947	947	0	606	606
Ammonia	mg/l as CaCO3	0	0	0	0	1	1	0	1	1	0	0	0
Phosphate	mg/l as CaCO3	-0.1	2.6	3	-0.8	4	5	-1.2	4	5	-0.3	2	3
Sulphide	mg/l as CaCO3	0	192	192	0	326	326	0	335	335	0	138	138
VFA	mg/l as CaCO3	0	0	0	0	0	0	0	139	139	0	0	0
H20	mg/l as CaCO3	1971	0	-1971	1679	0	-1679	4573	0	-4573	1252	0	-1252
Total	mg/l as CaCO3	1971	800	-1171	1678	1256	-422	4572	1426	-3146	1252	746	-505
Species Concentration													
CT	mg/l as C	10	158	148	11.3	243	232	8	254	246	16	167	151
VFA	mg/l as acetate	0	0	0	24	0	-24	37	167	130	21	0	-21

For the SC1, SP1 and SP2 experiments, the total COD concentration in the effluent was higher than the total COD concentration in the influent. Therefore, additional COD was generated inside the SSPAD. A portion of sulphide COD was removed from the reactor headspace during feeding, as nitrogen gas was sparged into the reactor. Consequently, the total COD concentration should have decreased as sulphide COD was removed from the SSPAD. However, the source of the error was not identified, but suggested that a measurement error occurred. The removal of sulphide COD did not occur during the AugBSP experiments, as a completely sealed reactor with zero headspace was utilised. Therefore, in future, it was recommended that the sulphidogenic SSPAD should be run with zero headspace, which would retain all the COD in the system.

The soluble COD concentration increased between the influent and effluent streams due to the generation of hydrogen sulphide by the SRB bioprocess. The particulate organics present in the influent PSS feed were broken down to produce soluble sulphide in the digester liquid. The organic and sulphide COD present in the digester effluent was identified using the COD method proposed by Poinapen *et al*. (2009), as described in Section 3.6.3.

The sulphate utilised by the sulphidogenic SSPAD differed between 883 to 1403mgSO_4^{2-}/*l*. The concentration of sulphate utilised by the reaction was related to the concentration of sulphide produced by the bioprocess. Therefore, the greater the sulphide concentration produced, the greater the sulphate concentration utilised, which was expected as S was conserved in the system.

The TKN and the TP concentrations differed for all four experiments. However, the TKN concentration change between the influent and effluent streams of SC1, SP1 and SP2 was low. The low TKN concentration change indicated that a good N balance over the SSPAD was achieved. Similarly, the change in TP concentration between the influent and effluent streams for all four experimental periods was low. The low TP concentration change indicated that a good P balance over the SSPAD was achieved. The release of FSA into the sulphidogenic SSPAD was low (4-12mgN/*l*). Similarly, the release of OP into the sulphidogenic SSPAD was low (1-2mgP/*l*)

The change between the influent and effluent TSS and VSS concentrations differed significantly between the four experimental periods. The change in the VSS concentration between the influent and effluent streams highlighted the fluctuation of the biodegradable particulate organics present in the PSS. This observation emphasises the varying nature of PSS and the importance of correctly characterising the substrate.

The pH of the prepared feed solution remained relatively constant at a value between 2.3 – 2.79. The low feed pH was due to the addition of sulphuric acid, as described in Section 3.3.2. However, even with a low feed pH, the sulphidogenic SSPAD maintained a neutral operating pH of 7.04 – 7.24. This pH change highlights the sulphidogenic system's ability to treat acidic wastewater streams containing sulphate, as the SRB process is efficient at generating alkalinity within the digester. The alkalinity of the feed solution was adjusted to reflect the low pH conditions. This adjustment was calculated by performing the 5-point titration on the diluted PSS feed mixture without the addition of acid, and then recalculating the alkalinity of each reference species based on the dropped pH value of the feed solution pH, due to the addition of the sulphuric acid. It was observed that at a low pH of 2.5, the alkalinity was represented entirely by the buffer capacity of the water. The C_T concentration present in the feed solution was determined using the 5-point titration method for the diluted PSS feed mixture before the addition of the sulphuric acid and was then diluted accordingly.

4.3.1 Mass Balances

Conservation of mass states that, at steady state, the flux of material entering the AD should equal the flux of material exiting the AD. Completing a COD balance over the sulphidogenic SSPAD was difficult as the sulphide gas that evolved into the SSPAD headspace was challenging to measure accurately. Unlike the methanogenic SSPAD, in which the volume of biogas was measured using a wet-tip gas meter, the sulphidogenic SSPAD required a ferric chloride gas trap to capture the sulphide leaving the digester via the gas port. Additionally, the SSPAD headspace was sparged with nitrogen daily during feeding and wasting to ensure that the required anaerobic conditions were maintained. Therefore, measuring the amount of sulphide exiting the system daily was challenging to do accurately. If a complete sulphur balance is an important objective in the sulphidogenic SSPAD, it is advised that a digester without a headspace be used in future.

Therefore, an S balance was conducted based on the observed influent and effluent SO_4^{2-} concentration, as it was assumed that all of the SO_4^{2-} was taken up for H_2S production. It was also important to note that concentration could be used for the balances instead of mass flux, as all measurements for the sulphidogenic SSPAD, apart from the H_2S gas, were taken in the liquid phase. Subsequently, the concentration of each constituent could be used instead of flux, unlike the methanogenic SSPAD, in which the CH_4 gas produced was measured as COD flux (mgCOD/d).

The S balance was performed using the daily aqueous sulphide COD concentration produced, and the sulphate concentration utilised, by the sulphidogenic SSPAD. As explained in Section 3.7.4.3, sulphide can donate 2 gCOD/gS, and subsequently, the S present in the sulphide was determined by dividing the sulphide COD concentration by 2. Furthermore, the S present in the sulphate was determined by dividing the sulphate concentration utilised by the reaction by 3. The results for the COD and S balances for SC1, SP1, SP2 and SP3 are given in Table 4.17.

Table 4. 17: Sulphidogenic SSPAD Sulphur Balance

		SC1	SP1	SP2	SP3
COD Balance					
Average COD influent concentration	mgCOD/l	646	1441	1643	1543
Average COD effluent concentration	mgCOD/l	748	1782	1705	936
COD balance	**%**	**116**	**124**	**104**	**61**
Sulphur Balance					
Influent sulphate concentration	mgSO4/l	1500	1500	1500	1500
Average sulphate effluent concentration	mgSO4/l	617	97	129	624
Sulphate utilised by reactor	mgSO4/l	883	1403	1371	876
Sulphur equivilant of sulphate utilised	mgSO4-S/l	294	468	457	292
Average sulphide COD in effluent	mgCOD/l	357	625	684	309
Sulphur equivilant from sulphide COD effluent	mgCOD-S/l	178	312	342	154
Sulphur balance	**%**	**61**	**67**	**75**	**53**
Assuming 100% Sulphur Balance					
Sulphur lost in headspace and sparging	mgH2S-S/l	116	155	115	138
COD of sulphur lost	mgCOD/l	232	310	230	276
Total Sulphide COD produced	mgCOD/l	588	935	914	584

As previously observed, the effluent COD concentrations were higher than the influent COD concentrations for SC1, SP1, and SP2, and consequently, the COD balances were greater than 100%. However, the COD balance for SP3 was lower than 100%, which was expected as H_2S COD was lost from the aqueous solution and was present in the headspace of the digester.

In contrast to the COD balances, Table 4.17 shows that a significant concentration of H_2S evolved from the SSPAD liquid into the digester headspace. The concentration of sulphur lost by evolution into the headspace, as well as from sparging the reactor with nitrogen gas was calculated as the difference between the S equivalent of sulphate utilised and the S equivalent from the sulphide COD in the SSPAD effluent stream. The sulphur lost was then converted to the COD equivalent by multiplying by 2. The total sulphide produced by the SSPAD was then calculated as the sum of the measured aqueous sulphide COD, and the H_2S COD lost in the headspace.

The mass flux of other constituents present in the entering and exiting streams such as the TKN and TP were also checked using the mass balanced approach. The total mass of these two constituents should remain constant throughout the experiment. The TKN and TP mass fluxes were calculated using Equations 3.14, as described in Section 3.7.5.

Table 4.18 shows that a TKN balance for the SC1 and SP1 experiments was accepted, as the balances were within 10%. The TKN balance from the SP2 testing period was high at 113%, indicating that more material was present in the effluent than the influent. Furthermore, the TKN balance from the SP3 testing period was low at 65%, indicating that less material was present in the effluent than the influent. The discrepancy was most likely caused by measurement error.

Table 4. 18: Sulphidogenic SSPAD TKN/TP Balance

		SC1	SP1	SP2	SP3
Nitrogen Balance					
Average TKN influent concentration	mgTKN-N/l	21.6	46.0	28.8	37.5
Average TKN effleunt concentration	mgTKN-N/l	22.3	48.2	32.7	24.5
Nitrogen balance	**%**	**103**	**105**	**113**	**65**
Phosphorus Balance					
Average TP influent concentration	mgTP-P/l	2.8	7.2	5.3	6.4
Average TP effleunt concentration	mgTP-P/l	3.9	7.6	7.3	4.5
Phosphorus balance	**%**	**139**	**105**	**138**	**70**

Finally, Table 4.18 highlighted that the TP balance showed fluctuations between the concentrations of the influent and effluent streams. However, the concentration of TP in the SSPAD was low. Therefore, the error was most likely inflated due to the resolution and

accuracy of the analytical procedure, such as the set dilution intervals of the spectrophotometer (discrete analyser) used.

4.3.2 Modelling the Sulphidogenic SSPAD

The sulphidogenic SSPAD was virtually replicated using the same model library that was used to model the methanogenic SSPAD, i.e. PWM_SA_AD model (Ikumi *et al*., 2015). The model was extended further by Ghoor *et al*. (2020) to include biological sulphate reduction (BSR) and includes a switching function that allows the user to select either a methanogenic or sulphidogenic bioprocess. The model contains the identical stoichiometry for the hydrolysis reaction of the influent organics, but differs after the formation of glucose, splitting into two distinct pathways of either methanogenesis or sulphidogenesis.

Modelling the sulphidogenic SSPAD allowed for the mass, and therefore, the concentration of active biomass present in the SSPAD effluent to be correctly estimated. The Sulphidogenic SSPAD effluent was used as the inoculum in both the AugBSP control and test reactors. As with the methanogenic SSPAD, modelling the sulphidogenic SSPAD was not required for identifying the biodegradable composition using the stoichiometric method explained in Section 3.9.2.

The main focus of the modelled SSPAD was to, as accurately as possible, replicate the laboratory observations on the sulphidogenic SSPAD. The active biomass considered by the PWM_SA_AD model were the acidogens, sulphidogenic acetogens, acetoclastic sulphidogens and hydrogenotrophic sulphidogens, as discussed in Section 3.10.7. The active biomass estimation was achieved by characterising the influent PSS and then adjusting the model parameters such that the effluent concentrations of the modelled SSPAD replicated the observed SSPAD effluent concentrations.

4.3.2.1 Influent Fractionation

In order to run the model, it was necessary to characterise the influent COD of the diluted PSS into the correct COD fractions. The organic groups present in the influent PSS were BSO,

consisting of FSBO and VFA, BPO, USO and UPO. The influent fractionation procedure used to characterise the influent PSS is thoroughly explained in Section 3.8.1. and Section 3.8.3.

The sulphidogenic system contained negligible S_{bp} in the effluent stream. Subsequently, the particulates present in the SSPAD effluent were either UPO or Z_{AD}. This simplification allowed for both the influent fractionation and sulphidogenic SSPAD modelling to be relatively straight forward, compared to that of the methanogenic SSPAD. The characterisation of the influent PSS was performed using Equations 3.20 to 3.23 in Section 3.8.2.1 and Equations 3.37 to 3.42 in Section 3.8.3.1.

As explained in Section 3.10.7.1, the PWM_SA_AD model extended by Ghoor *et al.* (2020) was coded in such a way that all of the sulphide produced by the SRB bioprocess remained in solution. This model characteristic was useful when modelling the AugBSP reactors, as all sulphide remained in the aqueous solution; however, for the sulphidogenic SSPAD, H_2S gas evolved from the liquid phase to the gas phase. This evolution of H_2S gas from the liquid phase was illustrated in Table 4.17, as the S balances were below 100%. Therefore, the model was modified to account for the H_2S that evolved from the SSPAD liquid. This modification was done without introducing a new gaseous H_2S term to the model, but instead using the dissolved HS^- concentration and the H^+ concentration. The removal of HS^- and H from solution was controlled by an adjustable parameter added to the model, the H_2S_molrate. Therefore, both HS^- and H^+ were removed from solution in equal parts.

The removal of HS^- allowed for the sulphide to evolve from the aqueous solution. Furthermore, the removal of H^+ from the aqueous solution affected the pH of the system, which subsequently increased. The pH increase was comparable to an acid being removed from the aqueous phase, driving the solution pH up. However, it is critical to note that the removal of H_2S gas from the aqueous phase did not affect the total alkalinity of the system. Consequently, the total system alkalinity is a latent parameter influenced by the composition of the organic, as well as the BSR process. Therefore, as the organic degrades due to the bioprocess, organic and inorganic material is released into the aqueous solution. The release of this material into the solution, as well as the sulphide produced, increases the system alkalinity. However, the evolution of subspecies such as CO_2 or H_2S from the aqueous solution does not change the total alkalinity of the system, only the species that represent it. Therefore, the total alkalinity of the system can

be used as an objective value for validating the chosen organic composition of the BPO in the sulphidogenic SSPAD.

This concept was imperative to understand when modelling the sulphidogenic SSPAD, as removing H_2S from the liquid phase affected the solution pH. Therefore, in some cases it was observed that, if a significant amount of H_2S evolved into the digester headspace, the pH in the modelled SSPAD exceeded a value of 8. This observation occurred in both SC1 and SP1, as the modelled SSPAD pH was significantly high when the H_2S COD, as calculated using the S balance in Table 4.17, was removed. Therefore, to rectify the modelled SSPAD pH for SC1 and SP1, the BPO composition, as well as the H_2S evolution (via the daily sulphide production) was adjusted such that the pH and the total alkalinity in the modelled SSPAD agreed with the observed SSPAD values. The adjustment was based on trial and error, using multiple iterations until the desired solution pH was achieved. The adjusted H_2S concentrations are summarised in Table 4.19.

Table 4. 19: Sulphidogenic SSPAD sulphide concentrations

		SC1	SP1	SP2	SP3
Calculated					
Soluble Sulphide (S_{ds})	mgCOD/l	357	625	684	309
Headspace Sulphide (S_{gs})	mgCOD/l	232	310	230	276
Daily Sulphide Production (S_{ts})	mgCOD/l	588	935	914	584
Adjusted					
Soluble Sulphide (S_{ds})	mgCOD/l	357	625	684	309
Headspace Sulphide (S_{gs})	mgCOD/l	149	123	230	276
Daily Sulphide Production (S_{ts})	mgCOD/l	506	748	914	584
Percentage of original	**%**	**86**	**80**	**100**	**100**

The Z_{AD} concentration was calculated using the steady-state equations of Sötemann *et al.* (2005), as shown in Equation 3.38 in Section 3.8.3.1. Furthermore, Z_{AD} was determined using the same assumptions as stated in Section 4.2.3.1, which simplified the calculation by increasing the $Y_{AD,}$ from 0.089 to 0.113, to account for the formation of the other organism groups. The Z_{AD} concentration was calculated based on the daily sulphide production, which was adjusted for SC1 and SP1, as shown in Table 4.19. The biomass concentrations calculated using Equation 3.38 are summarised in Table 4.20.

Table 4. 20: Calculated sulphidogenic SSPAD biomass COD concentration

COD	Unit	SC1	SP1	SP2	SP3
Soluble Sulphide (S_{ds})	mgCOD/l	357	625	684	309
Headspace Sulphide (S_{gs})	mgCOD/l	149	123	230	276
Daily Sulphide Production (S_{ts})	mgCOD/l	506	748	914	584
Constants					
Y_{AD}		0.129	0.129	0.129	0.129
b_{AD}	/d	0.041	0.041	0.041	0.041
R	days	19	19	19	19
Biomass					
Z_{AD}	mgCOD/l	42	62	76	49

With the Z_{AD} concentration determined, the UPO concentration was calculated as the difference between the particulate COD concentration in the effluent and the Z_{AD} COD concentration, as shown in Equation 3.39 in Section 3.8.3.1. With the concentration of UPO determined, the diluted influent PSS was then fractionated. The summary of this fractionation for the SSPAD for each experiment is given in Table 4.21

Table 4. 21: Sulphidogenic SSPAD influent fractionation

Constituent	Unit	SC1	SP1	SP2	SP3
VFA	mgCOD/l	0	25	31	0
FSBO	mgCOD/l	0	22	0	0
Total BSO	**mgCOD/l**	**0**	**48**	**31**	**0**
USO	mgCOD/l	109	66	112	102
Total Soluble	**mgCOD/l**	**109**	**113**	**143**	**102**
BPO	mgCOD/l	351	299	667	975
UPO	mgCOD/l	241	1029	833	477
Total Particulate	**mgCOD/l**	**592**	**1328**	**1500**	**1452**
Total COD	**mgCOD/l**	**701**	**1441**	**1643**	**1554**

However, as seen in the methanogenic SSPAD in Section 4.2.3.1, the observed VSS concentration in the SSPAD effluent was not well represented in the modelled SSPAD using the fractionated influent in Table 4.21. The discrepancy was caused by the UPO composition. Therefore, for the modelled SSPAD reactor to better reflect the VSS concentrations present in the observed SSPAD effluent, the UPO concentrations were adjusted, such that the modelled SSPAD VSS concentration effluent replicated the observed VSS concentration. The change in

UPO concentration affected the BPO concentration. Therefore, the BPO composition determined for the modelled SSPAD was the best fit for the observed values. However, this did not affect the identification of the biodegradable organics in the AugBSP control and test reactors, as the SSPAD was only used to estimate the biomass concentrations in the inoculum. The adjusted UPO COD concentrations are shown in Table 4.22.

Table 4. 22: Adjusted sulphidogenic SSPAD influent fractionation

Constituent	Unit	SC1	SP1	SP2	SP3
VFA	mgCOD/l	0	25	31	0
FSBO	mgCOD/l	0	22	0	0
Total BSO	**mgCOD/l**	**0**	**48**	**31**	**0**
USO	mgCOD/l	109	66	112	102
Total Soluble	**mgCOD/l**	**109**	**113**	**143**	**102**
BPO	mgCOD/l	351	636	1040	1113
UPO	mgCOD/l	241	692	460	339
Total Particulate	**mgCOD/l**	**592**	**1328**	**1500**	**1452**
Total COD	**mgCOD/l**	**701**	**1441**	**1643**	**1554**

The mass of the unbiodegradable and biodegradable particulates was then calculated using Equations 3.41 and 3.42 in Section 3.8.3.1 and are shown in Table 4.23. The UPO VSS concentration was calculated with a COD/VSS ratio (f_{CV}) of 1.481 gCOD/gVSS. This ratio for UPO has been used for decades in activated sludge models since the steady-state model of Marais and Ekama (1976) but there is evidence that it may need revision (Wentzel *et al*., 2006).

Table 4. 23: Sulphidogenic SSPAD influent COD/VSS fractions

Constituent	Unit	SC1	SP1	SP2	SP3
UPO COD	mgCOD/l	241	692	460	339
UPO VSS	mgVSS/l	162	467	311	229
UPO fcv	mgCOD/mgVSS	1.48	1.48	1.48	1.48
BPO COD	mgCOD/l	351	636	1040	1113
BPO VSS	mgVSS/l	227	306	466	612
BPO fcv	mgCOD/mgVSS	1.55	2.08	2.23	1.82

4.3.2.2 Hydrolysis Kinetics

The kinetics used in the sulphidogenic SSPAD were calculated just as they were in the methanogenic SSPAD, using the steady-state calculations used by Sötemann *et al.* (2005), as shown in Section 3.10.3. However, the S_{bp} in the sulphidogenic SSPAD was negligible. Consequently, the value of K_M needed to be sufficiently high, such that all the biodegradable organics were completely utilised by the SSPAD. Therefore, the value of K_M was set high for all four experiments (>150 gCOD organics/gCOD biomass.d). Additionally, a K_S value of 7.98 gCOD/*l* was used, a value supported by Sötemann *et al.* (2005) for the hydrolysis of PSS using saturation kinetics.

4.3.2.3 Model Influent

The organic groups determined in Table 4.22 above, as well as the required inorganics (FSA, OP) were then converted into the correct format for the PWM_SA_AD model and entered into the WEST® influent generator, which ensured that the correct mass of each component in the influent PSS stream was added to the SSPAD daily. An example of the required conversions is given in Table 3.6 and Figure 3.21 in Section 3.10.2.

4.3.2.4 Composition Determination

In the PWM_SA_AD model, the release of constituents into the bulk liquid of the digester is dependent on the elemental composition and mass of the organics present in the influent substrate. Therefore, an elemental composition for each group of organics was required. There are five groups of organics, and subsequently, the model requires five separate elemental compositions, i.e. one each for BSO, BPO, USO, UPO and Biomass. The composition determination for each specific organic was described in Section 3.10.4. Table 4.24 shows the compositions used for the modelled sulphidogenic SSPAD.

Table 4. 24: Sulphidogenic SSPAD influent organic compositions

Group	**SC1**	**SP1**
BSO:	$C_1H_{1.211}O_{0.073}N_{0.046}P_{0.004}$	$C_1H_{1.2}O_{0.07}N_{0.064}P_{0.002}$
BPO:	$C_1H_{1.211}O_{0.729}N_{0.046}P_{0.004}$	$C_1H_{1.2}O_{0.07}N_{0.064}P_{0.002}$
USO:	$C_1H_{1.3}O_{0.6}N_{0.01}P_0$	$C_1H_{1.3}O_{0.6}N_{0.01}P_0$
UPO:	$C_1H_{1.571}O_{0.426}N_{0.166}P_{0.019}$	$C_1H_{1.571}O_{0.426}N_{0.166}P_{0.019}$
Biomass:	$C_1H_{1.4}O_{0.4}N_{0.2}$	$C_1H_{1.4}O_{0.4}N_{0.2}$
Group	**SP2**	**SP3**
BSO:	$C_1H_{1.4}O_{0.23}N_{0.058}P_{0.002}$	$C_1H_{2.2}O_{0.98}N_{0.035}P_{0.002}$
BPO:	$C_1H_{1.4}O_{0.23}N_{0.058}P_{0.002}$	$C_1H_{2.2}O_{0.98}N_{0.035}P_{0.002}$
USO:	$C_1H_{1.3}O_{0.6}N_{0.01}P_0$	$C_1H_{1.3}O_{0.6}N_{0.01}P_0$
UPO:	$C_1H_{1.571}O_{0.426}N_{0.166}P_{0.019}$	$C_1H_{1.571}O_{0.426}N_{0.166}P_{0.019}$
Biomass:	$C_1H_{1.4}O_{0.4}N_{0.2}$	$C_1H_{1.4}O_{0.4}N_{0.2}$

4.3.2.5 Modelled SSPAD and observed SSPAD comparison

The PWM_SA_AD model was run under steady-state conditions using the parameters and variables determined above, i.e. the hydrolysis rates and elemental compositions of the organics in the PSS substrate. The modelled data was compared to the observed data and evaluated using relative error. Therefore, the closer the value of error was to zero, the more accurate the modelled results were, when compared to that of the observed results. The relative error for each of the SSPAD variables was calculated using Equation 3.51 from Section 3.10.5.

Table 4.25 shows that the total COD concentrations in the modelled SSPAD were lower than the observed total COD concentrations. The inconsistency was previously highlighted in Table 4.17, which showed that the COD balances were greater than 100%, indicating that more material was leaving the SSPAD via the effluent than entering via the influent. Therefore, the modelled SSPAD did not reflect the high total COD concentration in the observed SSPAD effluent, as the PWM_SA model was mass balanced.

Table 4. 25: Modelled sulphidogenic SSPAD results

Sulphidogenic SSPAD	SC1			SP1			SP2			SP3		
COD (mgCOD/l)	**Observed**	**Modelled**	**% error**	**Observed**	**Modelled**	**% error**	**Observed**	**Modelled**	**% error**	**Observed**	**Modelled**	**% error**
Total	748	791	5.7	1782	1473	-17.4	1705	1383	-18.9	936	841	-10.2
Soluble	466	492	5.8	691	698	1.1	796	822	3.3	411	435	5.9
USO	109	108	-0.6	66	65	-0.6	112	111	-0.6	102	102	-0.6
BSO	0	0	-	0	0	-	0	0	-	0	0	-
UPO	241	240	-0.1	692	691	-0.1	460	460	-0.1	339	339	-0.1
BPO	0	1	-	0	2	-	0	2	-	0	2	-
Biomass (Zad)	42	47	12.0	62	66	7.0	76	81	6.8	49	54	11.0
Dissolved Sulphide	357	360	0.8	625	612	-2.1	684	690	0.9	309	313	1.4
Headspace Sulphide	232	147	-36.7	310	127	-59.0	230	214	-6.8	276	286	3.6
Total Sulphide	588	506	-14.0	935	739	-21.0	914	904	-1.0	584	598	2.4
Sulphate (mgSO4/l)												
SO4 remaining	617	734	18.9	97	390	301.4	129	138	6.7	624	598	-4.1
SO4 Utilised	883	766	-13.2	1403	1110	-20.9	1371	1362	-0.6	876	902	2.9
Sulphide Evolution (mol/d)												
H2S molrate	-	0.0024	-	-	0.002	-	-	0.0034	-	-	0.0045	-
Nitrogen (mgN/l)												
TKN	22	28	24.5	48	66	37.6	33	54	64.6	24	36	45.7
FSA	7	7	1.5	14	14	0.9	16	16	2.6	8	8	0.5
Phosphate (mgP/l)												
TP	4	6	59.8	8	15	102.6	7	12	58.6	4	8	83.6
OP	2	2	-2.3	4	4	-3.4	4	4	1.3	3	2	-2.9
Acetate (mg/l as acetate)												
VFA	0	5	-	0	1	-	167	1	-	0	1	-
Alkalinity (mg/l as CaCO3)												
Carbonate + H2O	605	598	-1.2	925	872	-6	947	1088	15	606	817	35
Total	800	809	1.1	1256	1216	-3.2	1426	1488	4.3	746	967	29.6
Species Concentration (mg/l)												
CT	158	159	0.5	243	234	-3.9	254	289	13.6	167	232	39.2
Solids (mgVSS/l)												
VSS	211	191	-9.2	547	508	-7.2	342	360	5.3	246	263	7.1
pH												
pH	7.21	7.21	0.0	7.24	7.17	15.8	7.24	7.22	3.4	7.04	6.96	20.0

The USO, BSO, UPO and BPO COD concentrations of the modelled SSPAD agreed well with the observed values. The Z_{AD} COD concentration for all four of the modelled SSPAD experiments was higher than the observed SSPAD concentrations. As previously mentioned in Section 4.2.3.1, the Y_{AD} value for the biomass was increased to 0.129 based on the standard yield coefficients used by the PWM_SA_AD model, as recommended by Sötemann *et al.* (2005). Therefore, the measured biomass concentration represented the four active biomass groups present in the SSPAD. As explained for the methanogenic SSPAD, the Z_{AD} concentrations in the model may have been higher as the PWM_SA_AD model assigns individual yield coefficients to each organism group. Consequently, the modelled Z_{AD} COD concentrations were accepted as a good approximation of the active biomass present in the SSPAD effluent.

As shown in Table 4.19, the total daily sulphide production in the SSPAD was adjusted for SC1 and SP1 such that the modelled SSPAD total alkalinity reflected the observed total alkalinity. Consequently, the modelled SSPAD for SC1 and SP1 produced a lower total sulphide concentration, with less H_2S gas evolving into the digester headspace. However, the observed dissolved (aqueous) sulphide COD concentration for all experiments was well represented by the modelled SSPAD.

The sulphate utilised in the SSPAD reflected the total sulphide concentration produced by the bioprocess. Therefore, the sulphate utilised by the modelled SSPAD for SC1 and SP1 was lower than what was observed. However, for SP2 and SP3, the sulphate concentration utilised by the modelled SSPAD had lower error relative to the observed SSPAD. The lower error was expected as the total sulphide concentration produced by the SSPAD for SP2 and SP3 was calculated using the utilised sulphate concentration. As previously mentioned, the removal of HS^- and H^+ from solution was controlled by an adjustable parameter added to the model, the H_2S_molrate.

The TKN and TP concentrations were significantly higher in the modelled SSPAD than in the observed SSPAD. The reason for this was due to the UPO composition. It was previously mentioned that the mass fractions used to calculate the UPO composition in Section 3.10.4.1 might need revision. However, determining the UPO composition was not in the scope of this project.

Both the FSA and OP concentrations in the observed SSPAD effluent were well represented by the modelled SSPAD, indicating that the BPO and BSO compositions were accurate in representing the observed influent organics. The total alkalinity in the observed SC1, SP1 and SP2 experiments were well replicated by the modelled SSPAD. However, the total alkalinity in the modelled SSPAD for SP3 was greater than the observed total alkalinity. The total alkalinity concentration in SP3 was challenging to replicate as the correct concentration of sulphide was produced by the model. Furthermore, the correct sulphide evolution was achieved by the model. However, the modelled SSPAD pH was low, even with a high alkalinity.

Therefore, the issue may have come from the modelled CT concentration, which was 39% higher than was observed. The additional CT increased the carbonate alkalinity, which subsequently increased the total alkalinity in the modelled SSPAD. However, changing the C term in the BPO was challenging as the convention used in the PWM_SA model to represent the biodegrade organic composition sets the C term equal to 1. Therefore, the remaining terms (HONP) need to be adjusted accordingly. However, adjusting the other terms resulted in errors occurring elsewhere in the modelled SSPAD, such as the FSA and OP concentrations. Finally, the observed VSS concentration, as well as the digester pH, was well represented by the modelled SSPAD.

4.3.2.6 Active Biomass present in the inoculum

The SSPAD was modelled to estimate the concentrations of active biomass present in the SSPAD effluent as accurately as possible. The concentrations for each group of active biomass present in the inoculum for SC1, SP1 SP2 and SP3 is summarised in Table 4.26.

Table 4. 26: Sulphidogenic SSPAD active biomass concentrations

COD (mgCOD/l)	SC1	SP1	SP2	SP3
Acidogens (X_AD)	30	42	51	34
Acetogens (X_ACS)	0	0	0	0
Acetoclastic Sulphidogens (X_AS)	11	16	20	13
Hydrogenotrophic Sulphidogens (X_HS)	6	8	10	7
Total Biomass Concentration	47	66	81	54

4.4 Conclusions

The effluent from the methanogenic SSPAD was used as an inoculum for the AugBMP control and test reactors. However, in order to understand the impact that the biodegradable organics present in the inoculum had on the modelled AugBMP control and test reactors, the SSPAD needed to be modelled. As previously mentioned, understanding the source of the inoculum was not required when determining the composition of the organics using the stoichiometric calculation in Section 3.9.2. However, in order to correctly model the AugBMP experiment using the PWM_SA_AD model, understanding the SSPAD was important.

The PWM_SA_AD model separates the biomass and biodegradable organics into two groups, each with their unique composition. Furthermore, the breakdown and decay of these two organic groups are represented using different rates and stoichiometry in the model. Therefore, while it was possible to group all of the biodegradable material in the AugBMP control (biomass) and test (substrate) reactors into one, collective composition and mass for each when using the stoichiometric composition calculation of Section 3.9.2, it was not possible to do so with the PWM_SA_AD model. The model is specific regarding the rates and stoichiometry of the growth and decay of the components present. Furthermore, the composition of the biomass and UPO groups were 'fixed' in the model used for this investigation. This does not imply that they are always fixed, as they can be adjusted freely. However, the number of unknowns increased significantly to a point where solving the parameters of each group was not possible within the boundaries of this thesis.

Therefore, determining the concentrations of the residual biodegradable organics (S_{bp}) and the biomass (Z_{AD}) was crucial for determining the composition of the selected substrates in the modelled AugBMP control and test reactors, as the model required the mass of these two groups as an input. Furthermore, the procedure for modelling the sulphidogenic SSPAD differed from that of the methanogenic SSPAD. The most crucial differences were the negligible S_{bp} concentration and the evolution of H_2S gas from the liquid phase of the digester. However, in both the modelled methanogenic and sulphidogenic SSPADs, the compositions of the UPO, USO and biomass were fixed. Therefore, the SSPADs were modelled as accurately as possible within the scope of the investigation.

However, accurately modelling the SSPAD was complex and time consuming to do based on the current method of passing the influent feed component masses into the PWM_SA_AD model. As mentioned, making any adjustments to the influent characteristics of the steady-state model was tedious and required trial and error. Ideally, the active biomass concentrations should be determined using the PE function, instead of trial and error. The influent generator requires a text file containing the measured concentrations of each component as an input, which subsequently generates the organic load onto the anaerobic digester. This configuration makes PE challenging as the variables cannot be changed within the optimisation simulation. The accuracy of the modelled SSPAD can be greatly improved by modifying the way in which the influent is passed into the PWM_SA_AD model. However, these changes were too significant for the scope of this project and are discussed in the recommendations.

Currently, the biomass and the biodegradable organics are separated into two unique compositions in the PWM_SA_AD model, as the rates at which the organisms grow and decay within the digester need to be represented separately to that of the biodegradable organics. However, for the purpose of conducting an augmented batch test experiment, merging the composition of the biomass and biodegradable organics into one grouped composition may be useful as the biological activity present in the control reactor will be represented by one group instead of two. This merger of compositions follows the same principles as the stoichiometric composition determination explained in Section 3.9.2. Furthermore, determining the concentration of active biomass present in the AugBMP control reactor using PE will be easier to do accurately, as fewer unknown parameters will be present.

If the primary aim of the investigation is to identify the composition of the biodegradable organics, a steady inoculum is not critical. The augmented batch control reactor accounts for the products released due to the residual organics present in the inoculum, setting the baseline for the test reactor. However, the experiment should be run for an extended period of time (>30 days) to ensure that all biodegradable organics are utilized regardless of the hydrolysis rates.

Chapter 5: Augmented batch control reactor results and modelling

5.1 Introduction

The augmented batch control reactors were used for establishing the baseline that quantified the products released due to the breakdown of biodegradable organics present in the SSPAD effluent, which was used as the inoculum. The products released above this baseline inside the augmented batch test reactors were due to the chosen organic substrate (casein and PSS), the composition of which could then be identified, using methods shown in Section 3.9. Establishing the baseline included analysing mass balances and identifying the composition of residual BPO present in the inoculum, using the stoichiometric calculation, as well as the modelled control reactors, which used the PE function.

As previously mentioned, both the AugBMP and the AugBSP experiments required a stable inoculum, which was grown using steady-state parent anaerobic digesters (SSPAD) for each respective system, i.e. a methanogenic SSPAD and a sulphidogenic SSPAD. The details for the operation and testing of these systems is given in Section 3.2 and Section 3.6, and the results and their modelling in Chapter 4. The modelled SSPADs (using mass balanced steady state equations as shown in Section 3.8.2 and Section 3.8.3) allow for the mass, and therefore, the concentration of the active biomass groups to be estimated, which were used as inputs (of biomass concentrations) for the modelled AugBMP and AugBSP experiment reactors.

As described in Chapter 4, both the AugBMP and the AugBSP experiments were repeated four times each. Therefore, the four augmented batch control experiments corresponded to the four SSPAD experiments described in Chapter 4. The experiment in which the AugBMP and AugBSP control reactors were used as the baseline for identifying the casein composition were labelled MC1 and SC1, respectively. Furthermore, the experiments in which the AugBMP and AugBSP control reactors were used as the baseline for identifying the PSS composition were labelled MP1, MP2, MP3, and SP1, SP2, SP3, respectively. This is summarised in Table 5.1.

Table 5. 1: Experiment Periods

Label	Type of Experiment	Date of Experiment
MC1	Methanogenic Casein	February – March 2019
MP1	Methanogenic PSS	February – March 2018
MP2	Methanogenic PSS	May-June 2018
MP3	Methanogenic PSS	December 2018
SC1	Sulphidogenic Casein	March 2019
SP1	Sulphidogenic PSS	November 2018
SP2	Sulphidogenic PSS	January – February 2019
SP3	Sulphidogenic PSS	April 2019

5.2 AugBMP Control Reactors

The AugBMP control experiments were conducted as specified in Section 3.4. In order to achieve reliable results, the experiment was conducted in triplicate, using three control reactors. The control reactors were labelled C1, C2, and C3 for all four experiments (i.e., MC1, MP1, MP2 and MP3).

The AugBMP control reactors were seeded with inoculum, taken directly from the SSPAD, and tap water (the seeding procedure is described in Section 3.4.3). The tap water was added such that the inoculum from the methanogenic SSPAD was diluted to half the original concentration. The dilution was required, as the SSPAD waste volume was not sufficient to conduct the AugBMP control and AugBMP test experiments in triplicate. The starting mix for the AugBMP control experiment is given in Table 3.1 in Section 3.4.3.

The concentration of each constituent in the AugBMP control reactor was measured using the analytical procedures described in Section 3.6. The measured values in each of the AugBMP control reactors (C1, C2 and C3) were then combined into one value by calculating the average constituent value between the reactors. Table 5.2 summarises the combined averaged measurements, taken at the start and end of the experiment, for the AugBMP control reactor for the MC1, MP1, MP2 and MP3 experiments.

Table 5. 2: AugBMP control results

		MC1			MP1			MP2			MP3		
	Unit	Start	End	Change (△)	Start	End	Change (△)	Start	End	Change (△)	Start	End	Change (△)
Time	hours	0	456	456	0	695	695	0	576	576	0	452	452
Total COD	mgCOD/l	10401	8333	-2068	8730	6308	-2422	9545	8907	-638	13306	11493	-1813
Soluble COD	mgCOD/l	1084	1104	20	2078	1116	-962	831	1027	195	1834	1333	-501
VFA COD	mgCOD/l	206	0	-206	1	5	4	38	0	-38	89	150	61
TKN	mgN/l	581	532	-48	533	537	4	604	618	13	649	676	28
FSA	mgN/l	235	217	-18	172	256	85	254	297	42	273	330	57
TP	mgP/l	87	99	12	84	72	-12	101	111	10	117	113	-4
OP	mgP/l	13	23	10	14	19	5	5	14	8	13	23	11
VSS	mgVSS/l	4476	4497	21	5019	3987	-1032	5634	4530	-1104	5911	5299	-612
pH	pH	7.31	7.20	-0.11	7.27	7.16	-0.11	7.38	7.31	-0.07	7.38	7.18	-0.19
Carbonate Alk	mg/l as $CaCo_3$	1113	1428	315	1139	1353	214	1339	1674	335	1225	1526	301
Total Alk	mg/l as $CaCo_3$	1297	1462	165	1166	1386	220	1388	1704	316	1323	1678	355
CT	mgC /l	296	378	83	299	363	64	347	439	92	317	410	93
CH4 COD	mgCOD	0	2816	2816	0	2205	2205	0	6916	6916	0	4697	4697
Carbon in Gas	mgC	0	880	880	0	719	719	0	2255	2255	0	1751	1751

The total COD concentration change for MC1, MP1 and MP3 ranged between 1813mgCOD/*l* to 2422mgCOD/*l*, a difference of 609mgCOD/*l*. The total COD concentration change in the MP2 experiment was low at 638mgCOD/*l*. The low change in total COD of 638mgCOD/*l* for MP2 indicated a low concentration of biodegradable organics present in the inoculum. The soluble COD concentration present at the start of all four experiments varied significantly. This variance was due to the USO concentration in the inoculum (as all the BSO was deemed to have been utilised within the 20d sludge age of the methanogenic SSPAD).

The concentration of VFA present in the inoculum varied between the experiments. The VFA concentration at the end of the MC1, MP1 and MP2 experimental periods was low (0± 0, 5± 8 and 0± 0 mgCOD/*l*, respectively), indicating that the VFAs were utilised by the acetoclastic methanogens throughout the AugBMP control experiment. However, the VFA concentration at the end of the MP3 AugBMP control experiment was higher (150± 11 mgCOD/*l*) than at the start (89± 20 mgCOD/*l*).

The change in TKN and TP throughout the experiment was not significant in all four experiments. The FSA and OP in MP1, MP2 and MP3 increased over the duration of the experiment, indicating the breakdown of organics, which subsequently released inorganics into the AugBMP control reactor liquid. However, the FSA change in MC1 was negative, indicating that FSA was taken up during the experiment. The uptake of FSA was possible, however very unlikely for the augmented batch experiments. The decrease in FSA during the MC1 AugBMP experiment was most likely due to measurement error. The expected FSA release for MC1 is shown in Figure 5.13 in Section 5.2.6.3.

The VSS concentration for the MP1, MP2 and MP3 experimental periods decreased throughout the AugBMP control experiment. The decrease in VSS throughout the experiment was a good indicator of the biodegradable particulate material present in the inoculum. However, in the MP2 experiment, the total change in COD concentration was significantly low compared to the VSS concentration utilised, with a f_{CV} (COD/VSS) ratio of 0.58. This discrepancy in MP2 suggested that one of the measurements, either the COD or the VSS was inaccurate. In addition to the error experienced in MP2, the VSS in MC1 increased throughout the experiment. However, when analysing the entire data set, it was observed that a decrease in VSS throughout

the experiment occurred, and the source of the error was due to the observed starting VSS concentration, as shown in Figure 5.29 in Section 5.2.6.7.

The cumulative CH_4 COD produced by the experiment, which was measured using the inverted columns, as explained in Section 3.4.5, varied significantly between the four experiments. This was a good example of the gas measurement error experienced by the BMP test, and consequently, the AugBMP experiment. A COD balance was performed using the modelled AugBMP control reactor to determine the error associated with the gas measurement, as the model was mass balanced. The total carbon in the gas was calculated using the total volume of gas produced, as the gas composition was assumed to be made up of CO_2 and CH_4. The total carbon in the gas was used to determine the BPO composition using the stoichiometric method explained in Section 3.9.2.

5.2.1 Gas Measurement

The gas produced by the AugBMP control experiment was captured inside of an inverted water column. The setup and specifications of the water columns are given in Section 3.4.2. The gas produced by the AugBMP control reactor was quantified by the volume of water displaced in the column. The water from the bath was sucked into the gas column using a vacuum pump. However, as the water level in the column was above the water level in the bath, the partial pressure in the column was less than atmospheric.

Consequently, the gas occupied a larger volume in the column than at atmosphere. However, this additional volume was accounted for using the universal gas law, as explained in Section 3.4.5. The volume of methane present in the biogas was calculated using the methane partial pressure, which was determined using gas chromatography, as explained in Section 3.6.10. The molar equivalent of methane produced was then calculated using the universal gas law. Finally, the COD contained in the methane was calculated by multiplying the number of moles by 64gCOD/mol, as explained in Equation 3.10 in Section 3.7.3.1. The cumulative methane COD for MC1, MP1, MP2 and MP3 are shown in Figures 5.1, 5.2, 5.3 and 5.4.

In Figure 5.2 for MP1, two of the AugBMP control reactors, C2 and C3, had a significantly larger amount of COD collected in the inverted column compared to C1, indicating a possible

gas leak. Furthermore, the gas data for all four experiments indicated that the control reactor C1 had a lower cumulative CH_4 COD than C2 and C3.

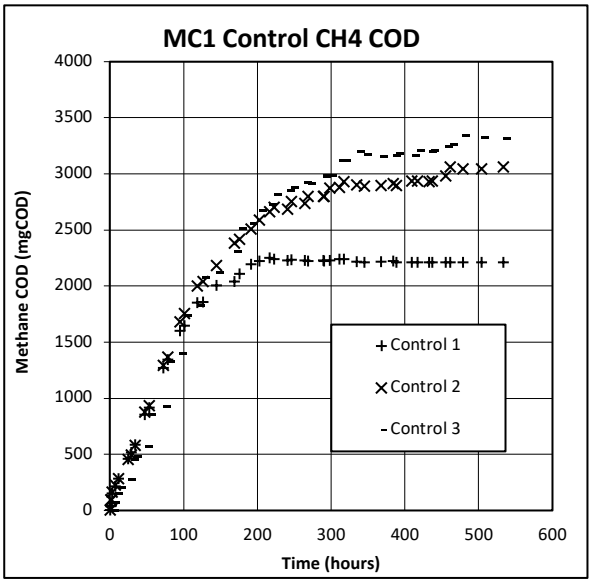

Figure 5. 1: MC1 AugBMP control CH_4 COD

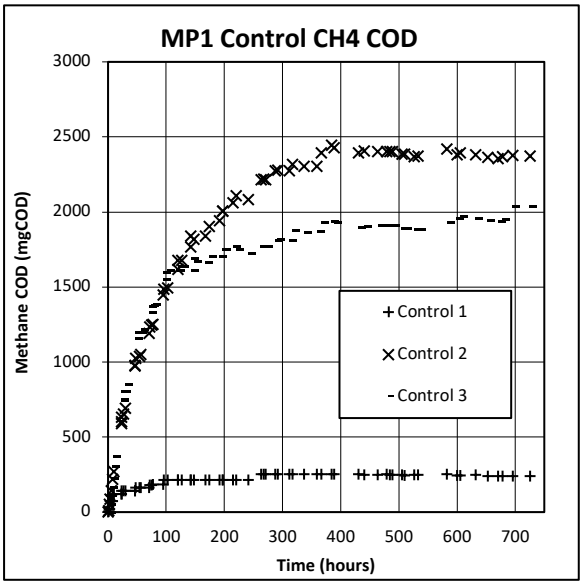

Figure 5. 2: MP1 AugBMP control CH_4 COD

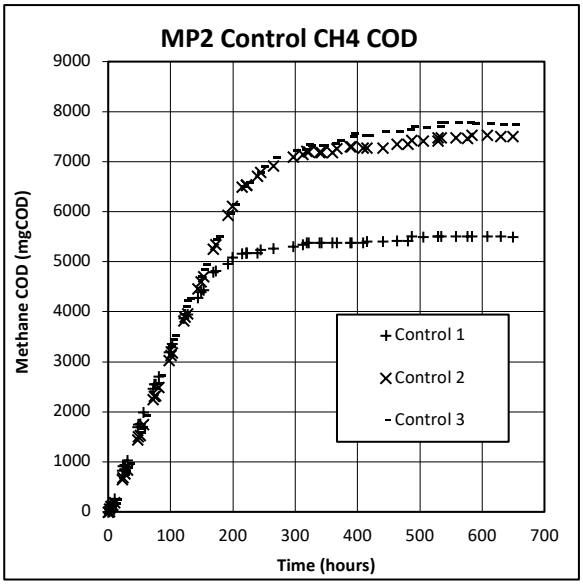

Figure 5. 3: MP2 AugBMP control CH_4 COD

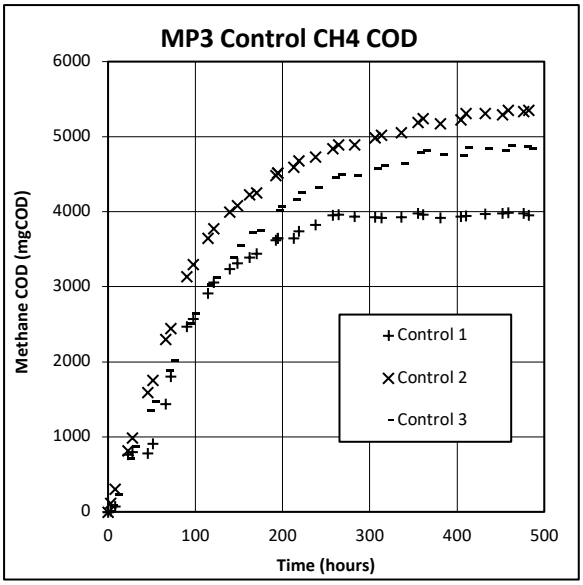

Figure 5. 4: MP3 AugBMP control CH_4 COD

5.2.2 Mass Balances

The mass of material entering the AugBMP control reactor should equate to the mass of material leaving the reactor, as mass was conserved within the system, and the AugBMP control reactor was completely sealed for the duration of the experiment. Furthermore, the gas produced throughout the experiment was captured by the inverted water column. The COD

entering the AugBMP reactor was contained inside the inoculum, which was taken from the methanogenic SSPAD effluent, and the COD leaving the reactor was either in the liquid effluent stream or in the methane gas produced.

Therefore, the starting COD in the reactor must equate to the sum of COD removed from the reactor during sampling, the methane COD in the inverted column, and the remaining COD in the reactor at the end of the experiment. This is shown in Equation 3.12, and summarised in Figure 3.12, in Section 3.7.3.2.

The methane partial pressure in the AugBMP control reactor for MP2 and MP3 was measured using a gas chromatograph. However, due to limited data availability, the average methane partial pressures obtained for the AugBMP control reactors were used to calculate the COD mass of methane present in the inverted columns (the data for which can be found in Appendix A). The summarised data obtained from the GC is shown in Table 5.3 below.

Table 5. 3: Gas chromatography results

		Period	
Experiment Type	**Unit**	**MP2**	**MP3**
Methanogenic SSPAD	% Methane	59.2± 1.7	57.2± 2.7
AugBMP Control	% Methane	57.5± 9	50.3± 8.7
AugBMP Test	% Methane	62.8± 6.5	54.7± 4.5

The methane partial pressure present in MC1 and MP1 was not available, however, based on the data available for MP2 and MP3, the partial pressure of MC1 was set to 60% and MP1 set to 57.5% methane. Therefore, the methane partial pressure for the AugBMP control reactors for experiments MC1, MP1, MP2 and MP3 were 60%, 57.5%, 57.5% and 50.3%, respectively. With the partial pressure of methane determined, a COD balance was performed to check if the COD entering the system equated to the COD exiting the system.

The COD flux in the AugBMP control reactor was calculated using Equation 3.12 in Section 3.7.3.2. The COD in the influent was equal to the starting COD concentration multiplied by the total liquid volume in the reactor. The total COD leaving the reactor was equivalent to the cumulative COD in the methane gas (collected by the inverted columns), the cumulation of COD present in the daily sample, which was calculated by summing the COD concentration

multiplied by the volume of the sample, for each sample drawn, and the COD concentration remaining in the reactor at the end of the experiment multiplied by the volume remaining.

5.2.2.1 MC1 COD Balance

Based on Equation 3.12 in Section 3.7.3.2, the COD balances for the AugBMP control reactors for the MC1 experiment are shown in Table 5.4.

Table 5. 4: MC1 AugBMP control COD balance

MC1 AugBMP Control Mass Balance (60% Methane Partial Pressure)						
	Starting Mass	Mass Removed	Remaining Mass	Gas Mass	Total Effluent	Balance
Unit	mgCOD	mgCOD	mgCOD	mgCOD	mgCOD	%
C1	49397	12361	28308	2208	42877	86.8
C2	53915	13185	29809	2980	45974	85.3
C3	52710	13402	30881	3259	47543	90.2

Table 5.4 indicated that a poor COD balance in the AugBMP control reactor for MC1 was achieved, as the balances for C1, C2 and C3 were 87%, 85% and 90%. The COD balances lay outside of the 10% tolerance required for a good balance, as explained in Section 3.7.2. As previously mentioned, the partial pressure of methane for MC1 was not analysed, and subsequently the methane partial pressure was set to 60%. Therefore, in an attempt to identify the cause of the low COD balance, the methane partial pressure was adjusted to the highest possible value of 100%. The results for 100% methane partial pressure is shown in Table 5.5.

Table 5. 5: Adjusted MC1 AugBMP control COD balance

MC1 AugBMP Control Mass Balance (100% Methane Partial Pressure)						
	Starting Mass	Mass Removed	Remaining Mass	Gas Mass	Total Effluent	Balance
Unit	mgCOD	mgCOD	mgCOD	mgCOD	mgCOD	%
C1	49397	12361	28308	3679	44349	89.8
C2	53915	13185	29809	4966	47961	89.0
C3	52710	13402	30881	5432	49716	94.3

However, even with the methane partial pressure set to the highest possible value, the COD balance did not improve significantly. Therefore, it was concluded that the low COD balance was not a result of the methane partial pressure, but rather a gas measurement error.

5.2.2.2 MP1 COD Balance

The COD balances for the AugBMP control reactors for the MP1 experiment was calculated using Equation 3.12 from Section 3.7.3.2. The COD balance is summarised in Table 5.6.

Table 5. 6: MP1 AugBMP control COD balance

MP1 AugBMP Control Mass Balance (57.5% Methane Partial Pressure)						
	Starting Mass	Mass Removed	Remaining Mass	Gas Mass	Total Effluent	Balance
Unit	mgCOD	mgCOD	mgCOD	mgCOD	mgCOD	%
C1	46552	16440	17920	239	34599	74.3
C2	43718	16964	18852	2374	38191	87.4
C3	40682	16347	16677	2036	35059	86.2

Table 5.6 indicated that a poor COD balance in the AugBMP control reactor for MP1 was achieved, as the balances for C1, C2 and C3 were 74%, 87% and 86%. The COD balances lay outside of the 10% tolerance required for a good balance, as explained in Section 3.7.2. As for MC1, in an attempt to identify the cause of the poor COD balance, the methane partial pressure was set to 100%. The results for 100% methane partial pressure is shown in Table 5.7.

Table 5. 7: Adjusted MP1 AugBMP control COD balance

MP1 AugBMP Control Mass Balance (100% Methane Partial Pressure)						
	Starting Mass	Mass Removed	Remaining Mass	Gas Mass	Total Effluent	Balance
Unit	mgCOD	mgCOD	mgCOD	mgCOD	mgCOD	%
C1	46552	16440	17920	416	34776	74.7
C2	43718	16964	18852	4129	39945	91.4
C3	40682	16347	16677	3540	36564	89.9

However, even when the partial pressure of the methane in the column was increased to 100%, the COD in the reactor did not balance. This was a repeat of the result in MC1 above and was a strong indication that measuring gas was tedious and lead to measurement error.

5.2.2.3 MP2 COD Balance

The same procedure that was used to check the COD balances in MC1 and MP1 was used in MP2. The partial pressure of the reactor was measured using the GC. Table 5.8 shows that the COD balance exceeded 100%. A balance over 100% indicated that more COD was remaining

at the end of the experiment than at the start of the experiment. This observation was challenging to explain as poor balances for MC1 and MP1 were achieved, and suggested gas measurement error. However, the balances for C1 and C2 were 107% and 107%, respectively, which lay within the 10% error tolerance for a good balance. However, the COD balance for C3 was high at 120% and suggested aqueous COD measurement error.

Table 5. 8: MP2 AugBMP control COD balance

MP2 AugBMP Control Mass Balance (57.5% Methane Partial Pressure)						
	Starting Mass	Mass Removed	Remaining Mass	Gas Mass	Total Effluent	Balance
Unit	mgCOD	mgCOD	mgCOD	mgCOD	mgCOD	%
C1	46586	16821	27350	5506	49677	106.6
C2	49999	17413	28829	7470	53712	107.4
C3	46586	18158	29814	7773	55746	119.7

5.2.2.4 MP3 COD Balance

The same procedure that was used to check the COD balances in the first three experiments was used in MP3, as shown in Table 5.9. The partial pressure of methane in the reactor headspace was measured as 50.3%. Consequently, C1, C2 and C3 had COD balances of 96%, 97% and 94%, which all lay within 10%, indicating that the majority of COD was tracked through the system. This COD balance was the most accurate of the four AugBMP control reactor experiments and indicated that the gas measurement error in the experiment was reduced as much as possible.

Table 5. 9: MP3 AugBMP control COD balance

M3 AugBMP Control Mass Balance (50.3% Methane Partial Pressure)						
	Starting Mass	Mass Removed	Remaining Mass	Gas Mass	Total Effluent	Balance
Unit	mgCOD	mgCOD	mgCOD	mgCOD	mgCOD	%
C1	66264	20496	39043	3983	63522	95.9
C2	67067	21567	38246	5290	65104	97.1
C3	66264	20530	37184	4818	62532	94.4

5.2.2.5 TKN and TP Balance

The mass flux of other constituents present in the entering and exiting streams such as the TKN and TP were also checked using the mass balanced approach. The total mass of these two

constituents should remain constant throughout the experiment. The TKN and TP mass fluxes were calculated using Equation 3.14, as described in Section 3.7.5.

Table 5.10 confirms that, in general, good mass balances for TKN and TP were achieved for the four experiments. However, there were also some outliers. For instance, the TKN balance for C1 during MC1 was low, as the starting concentration of C1 was higher than both C2 and C3. The remaining outliers followed the same pattern, that is, either the starting or ending concentrations differed from the other reactors' concentrations, resulting in a poor TKN or TP balance.

Table 5. 10: AugBMP control TKN/TP balance

Reactor	TKN in	TKN out	**Balance**	TP in	TP out	**Balance**
	mgTKN-N/l		**%**	mgTP-P/l		**%**
MC1						
C1	643	542	**84**	78	90	**115**
C2	554	489	**88**	105	94	**90**
C3	563	552	**98**	78	112	**143**
MP1						
C1	490	562	**115**	83	72	**87**
C2	523	534	**102**	86	71	**83**
C3	586	516	**88**	83	73	**88**
MP2						
C1	606	603	**100**	99	113	**114**
C2	595	616	**104**	101	108	**107**
C3	612	633	**103**	103	113	**110**
MP3						
C1	647	685	**106**	120	119	**99**
C2	659	672	**102**	115	114	**99**
C3	640	671	**105**	117	106	**91**

5.2.3 Stoichiometric Composition Identification

The composition of the biodegradable organics was identified by calculating the change in elemental concentrations, together with COD and VSS between the end and the start of the augmented batch experiments. The calculation involves mass ratios for each element (f_{CV}, f_C,

f_N and f_P), which allow for f_O and f_H to be calculated. The calculation is explained in detail in Section 3.9.2.

Therefore, the change in COD, C, N, P and VSS throughout the experiment was required. The change in the required components was previously shown in Table 5.2. The stoichiometric identification of the biodegradable composition for the AugBMP control experiments is shown in Table 5.11, which illustrates how the composition of the biodegradable organics was identified using the stoichiometric calculation described in Section 3.9.2. The change between the ending and starting concentrations of each constituent quantified the material contained in the biodegradable organics. The total COD concentration decreased throughout all four experiments. The total COD concentration change quantified the COD available in the biodegradable organic material including the BPO, BSO and VFA COD concentrations. Therefore, the BPO COD concentration available in the organics of the AugBMP control reactor was calculated as the difference between the total COD and the VFA COD concentration changes. The contribution of VFAs towards the total methane production must be included for systems in which the COD in the biogas was conserved. However, due to inaccuracies in the measured methane volume, the methane COD produced by the experiment was not used in the calculation, instead the total COD change was used to identify the available COD in the biodegradable organics.

Table 5. 11: AugBMP control stoichiometric composition determination as explained in Section 3.9. The compositions were identified stoichiometrically using the measured variables. The composition identified is based on an elemental mass balance between the reactants and products.

		MC1	MP1	MP2	MP3
Measured	**Unit**	Change (∆)	Change (∆)	Change (∆)	Change (∆)
Total COD	mgCOD/l	-2068	-2422	-638	-1813
VFA COD	mgCOD/l	-206	4	-38	61
FSA	mgN/l	-18	85	42	57
OP	mgP/l	10	5	8	11
VSS	mgVSS/l	21	-1032	-1104	-612
Carbonate Alk	mg/l as $CaCo_3$	315	214	335	301
CH_4 COD	mgCOD	2816	2205	6916	4697
C in Gas	mgC	880	719	2255	1751
COD Change					
Biodegradable COD	mgCOD/l	1862	2422	600	1813
COD in Methane	mgCOD/l	563	441	1383	939
Carbon Change					
C in Gas	mgC/l	176	144	451	350
C in H_2CO_3 Alk	mgC/l	76	51	81	72
Total C	mgC/l	252	195	532	422
VSS Change					
Biodegradable VSS	mgVSS/l	-21	1032	1104	612
Mass Ratio	Unit	g/g	g/g	g/g	g/g
f_{CV}	gCOD/gVSS	-90.116	2.347	0.544	2.962
f_C	gC/gVSS	-12.177	0.189	0.482	0.690
f_N	gN/gVSS	0.894	0.082	0.038	0.093
f_P	gP/gVSS	-0.471	0.005	0.007	0.017
f_H	gH/gVSS	-4.750	0.300	-0.023	0.162
f_O	gO/gVSS	17.504	0.424	0.496	0.037
Compostion	Unit	mol	mol	mol	mol
C	-	1	1	1	1
H	-	4.681	19.059	-0.585	2.816
O	-	-1.078	1.681	0.773	0.040
N	-	-0.063	0.373	0.068	0.116
P	-	0.015	0.010	0.006	0.010

The total carbon change in the system was the sum of the carbon in the gas and the carbon in the aqueous solution. The mass of carbon in the gas was calculated by multiplying the cumulative mols of biogas produced, measured using the inverted columns, by 12gC/mol. This conversion from mol to carbon was based on CO_2 and CH_4 (which were assumed to make up the majority of biogas) both having 1 mol of carbon. The total concentration of carbon in the gas was then determined by taking this calculated mass of carbon in the gas (mgC) and dividing

it by the starting reactor volume (5*l*). However, due to the inaccuracies experienced relating to the biogas measurement, the total carbon in the gas had a high level of error. The change in carbon in the aqueous phase was quantified by the change in H_2CO_3 alkalinity, which was calculated by taking the change in measured H_2CO_3 alkalinity and dividing by 50 (alkalinity was measured in mg/*l* as $CaCO_3$, which has an equivalence of 50mg $CaCO_3$/mol). The mols of alkalinity were then multiplied by 12gC/mol to get the carbon equivalent.

The VSS change was determined as the change in the VSS concentration between the end and the start of the experiment. As seen in MC1, the VSS concentration change was positive between the end and the start of the experiment. This indicated that the VSS increased, which was unlikely as the total COD decreased, and the AugBMP control reactor contained negligible soluble COD. The change in VSS concentration quantified the biodegradable VSS (which changed the sign of the VSS from negative to positive)

The mass ratios were then calculated by taking the change in each respective constituent and dividing by the VSS concentration. i.e., the biodegradable COD/VSS (f_{CV}), the total C/VSS (f_C), the FSA/VSS (f_N) and the OP/VSS (f_P). The mass ratios for f_O and f_H were calculated using Equations 3.45 and 3.46 in Section 3.9.2.1. Finally, the composition of the biodegradable organic present in the AugBMP control reactor was identified using the mass ratios and Equations 3.47 and 3.48 in Section 3.9.2.1.

The compositions determined in Table 5.11 suggested that an error occurred in the proposed stoichiometric composition calculation. The error was due to the measured starting and ending concentrations in the AugBMP control reactor. The measurements are prone to error, and the error increases significantly if only two data points are used. Instead, the entire data set (containing daily measurements) should be used, as explained in Section 3.9.3.

The use of mathematical models and the PE function introduced a data reconciliation aspect into the thesis, as the composition of the biodegradable organics were identified by minimising the error across the observed results.

5.2.4 Modelling the AugBMP control experiment

The AugBMP control experiment was modelled using the biomass concentrations determined in the modelled SSPAD as inputs. The biomass concentrations were previously shown in Table 4.15 in Section 4.2.3.6. The remaining constituent concentrations such as the FSA, OP, VFA, H_2CO_3 alkalinity, as well as the reactor pH, were adjusted to the averaged observed starting values for the AugBMP control reactor. The procedure used for modelling the AugBMP control reactor is described in Section 3.11.

The biomass and the UPO compositions used were the same as in the SSPAD, i.e. $C_1H_{1.4}O_{0.4}N_{0.2}$ and $C_1H_{1.571}O_{0.426}N_{0.166}P_{0.019}$, respectively. Therefore, the composition of the BPO (S_{bp}) was an unknown parameter. The S_{bp} COD concentration in the AugBMP control reactor was previously calculated in Table 4.8 in Section 4.2.3.1.

The COD and VSS concentrations present in the modelled AugBMP control reactor were dependent on the chosen compositions for each of the particulate groups (biomass, UPO and BPO), the mass of each group, and the AugBMP reactor liquid volume. Therefore, the composition and mass of the BPO directly related to the COD and VSS concentrations utilised throughout the modelled AugBMP control experiment.

The composition and mass of the UPO, as well as the biomass, affected the COD and VSS concentrations remaining at the end of the AugBMP control experiment. The composition and mass of the biomass influenced the uptake and release of material into the reactor's liquid and gas phases due to growth and decay.

The composition of the BPO, as well as the mass of the BPO and the UPO, were used in the PE as unknown parameters. Additionally, the saturation hydrolysis constant for the breakdown of the BPO (kM_BInf_AD_hyd), the growth rate of the acetoclastic methanogens (mu_AM), and the half-saturation coefficient of the acetoclastic methanogens (Ks_AM) were adjusted by the PE. The PE conducted hundreds of iterations until the lowest error across the observed measurements was achieved. The parameters used by the PE for determining the composition of the BPO are summarised in Table 3.10 in Section 3.11.2.1

The concentration of constituents released, such as the FSA, OP, H_2CO_3 alkalinity, as well as the reactor pH, were dependent on the composition and mass of the BPO degraded during the experiment. However, the biomass decay also contributed to the release of these constituents. Therefore, the model isolated the BPO group, as the composition and mass of the biomass was fixed, and the release of constituents above that of the biomass decay were due to the BPO degradation. The measured (observed) variables used by the PE are shown in Table 5.12.

Table 5. 12: Modelled AugBMP control variables

Variable	Description	Weighting			
		MC1	MP1	MP2	MP3
Alkalinity	The total alkalinity generated	1	1	1	1
COD_total	The unfiltered COD concentration	2	1	1	1
COD_soluble	The filtered COD concentration	1	1	1	1
COD_(X_B_Inf)	The S_{bp} COD concentration	1	1	5	5
FSA	The Free and Saline Ammonia concentration	1	1	1	1
$H2CO_3$ alkalinity	The carbonate alkalinity generated	1	1	1	2
OrthoP	The Orthophosphate concentration	5	5	5	5
VFA	The Volatile Fatty Acids concentration	3	1	1	5
VSS	The Volatile Suspended Solids concentration	5	5	1	5
p_H_s	The reactor pH	5	1	1	1

The weighting shown in Table 5.12 above was determined using multiple iterations and simulations. The PE environment can be run using four different error criteria: absolute, absolute squared, relative or relative squared, as explained in Section 2.7.2. The error criteria used for this project was absolute squared; although relative squared was also thoroughly checked, the most accurate outcome for fitting the modelled data to that of the observed data was achieved using absolute squared error. Therefore, the weighting factor for constituents with lower concentrations were given a higher weighting factor, such that they were considered by the parameter estimation when minimising the error between measurements for the entire data set. The weighting of each variable was entered at the start of the PE and the simulation was left to run until the error was minimised and an outcome determined. The accuracy of the outcome was checked by plotting the modelled data against the observed data, and if required, the weighting was adjusted for a specific variable and the PE was run again. This iterative

process allowed for the weighting to be carefully adjusted, considering each variable individually.

5.2.5 Modelled Composition Identification

The PE ran hundreds of iterations until a combination of parameters, which achieved the desired results with the lowest error was determined. The parameters determined by the PE for each of the AugBMP experiments are summarised in Table 5.13. The kinetic parameters differ for each substrate as different organics degrade at different rates. Consequently, given the variability of the biodegradable particulates present in the PSS, the kinetic parameters for each experiment were expected to differ. Therefore, the kinetic parameters are substrate-specific and depend on the characteristics of the substrate.

Table 5. 13: The modelled AugBMP control composition identification using the PWM_SA_AD model and parameter estimation. The compositions were identified by using the entire data set of measurements collected and minimising the error between the measurements, such that a best fit was determined.

Parameter	**Unit**	**MC1**	**MP1**
BPO Composition	mol	$C_1H_{2.706}O_{0.239}N_{0.036}P_{0.011}$	$C_1H_{2.959}O_{0.323}N_{0.001}P_{0.008}$
kM_BInf_AD_hyd	gCOD/gCOD.d	3	8
mu_AM	gCOD/gCOD.d	0.065	4.93
KS_AM	gCOD/l	0.4	1
Parameter	**Unit**	**MP2**	**MP3**
BPO Composition	mol	$C_1H_{3.931}O_{0.062}N_{0.012}P_{0.024}$	$C_1H_{3.273}O_{0.055}N_{0.041}P_{0.02}$
kM_BInf_AD_hyd	gCOD/gCOD.d	0.619	0.562
mu_AM	gCOD)/gCOD.d	4.39	2.77
KS_AM	gCOD/l	0.013	499

5.2.6 Modelled AugBMP Results

The observed (measured) results from the C1, C2 and C3 AugBMP control reactors were summarised by averaging the values obtained for each measurement taken. For instance, the unfiltered COD measurements were performed in duplicate for each control reactor (C1, C2, C3); therefore, 6 COD data points are available each day for the total COD concentration. The value used by the modelled AugBMP control PE for the total COD concentration was the

average of the 6 unfiltered COD measurements. The values used for the remaining constituents were also the averaged measured values.

Table 5.14 and Table 5.15 summarise the results obtained for the starting and ending concentrations for each constituent in the modelled AugBMP control experiments. The results obtained from the model were then compared to that of the observed results. Furthermore, the results have been compared visually in Section 5.2.6.1 (Figure 5.5) to Section 5.2.6.10 (Figure 5.44). The visual comparison between the modelled and observed results evaluated the dynamic parameters established by the PE. As previously mentioned, the parameters with the most significant impact on the dynamics of the AugBMP control experiment were the BPO hydrolysis rate (kM_BInf_AD_hyd), the uptake rate of the acetoclastic methanogens (mu_AM) and the half-saturation coefficient of the acetoclastic methanogens (KS_AM)

Table 5.14 and Table 5.15 both show that the modelled AugBMP control reactor replicated the total COD concentration change well for the MC1, MP1 and MP3 experiments. However, the total COD concentration change in the MP2 experiment differed to the other experiments. The observed total COD change in MP2 was significantly lower, as only 638mgCOD/*l* was utilised during the experiment. However, both the methane production, as well as the VSS concentration utilised, suggested that the change in total COD throughout the MP2 experiment was higher than measured. Therefore, the concentration of the BPO in MP2 was increased by the PE, as the error across the remaining observed measurements was minimised. This increased BPO concentration was considered in the methanogenic SSPAD for MP2, as shown in Table 4.8 in Section 4.2.3.1.

The soluble COD concentration change in the modelled AugBMP control reactor differed from the observed soluble COD concentration change. As previously mentioned, the USO concentration in the modelled AugBMP control reactor was adjusted such that the soluble COD concentration at the end of the experiment was entirely due to the USO concentration, except for MP3, in which the soluble COD at the end of the experiment comprised of USO and VFA. Therefore, Table 5.14 and Table 5.15 illustrate that the soluble COD concentration at the end of the modelled control experiments replicated the soluble COD concentration at the end of the observed control experiments. The discrepancies in the soluble COD concentration is explained visually in Section 5.2.6.2 (see Figures 5.9, 5.10, 5.11 and 5.12)

Table 5. 14: Modelled MC1 and MP1 AugBMP control results

MC1 Control Model Results								MP1 Control Model Results					
		Start		End		Change		Start		End		Change	
COD	**Unit**	**Observed**	**Modelled**	**Observed**	**Modelled**	**Observed**	**Modelled**	**Observed**	**Modelled**	**Observed**	**Modelled**	**Observed**	**Modelled**
Total COD	mgCOD/l	10401	9857	8333	7773	**-2068**	**-2084**	8730	9274	6308	6843	**-2422**	**-2432**
Soluble COD	mgCOD/l	1084	1302	1104	1090	**20**	**-213**	2078	1260	1116	1164	**-962**	**-97**
Gas													
Methane	mgCOD	0	0	2816	9546	**2816**	**9546**	0	0	2205	10882	**2205**	**10882**
Nitrogen													
FSA	mgFSA/l	235	235	217	266	**-18**	**30**	172	171	256	240	**85**	**68**
Phosphate													
OP	mgOP/l	13.2	13.2	23.0	24.7	**9.7**	**11.5**	14.4	14.4	19.5	22.1	**5.1**	**7.7**
Alkalinity													
Carbonate	mg/l as CaCO3	1113	1139	1428	1384	**315**	**245**	1139	1141	1353	1373	**214**	**232**
Total	mg/l as CaCO3	1297	1337	1462	1446	**165**	**109**	1166	1181	1386	1424	**220**	**244**
Species													
VFA Conc	mg/l as acetate	193.0	193.0	0.0	1.9	**-193**	**-191**	0.7	0.7	4.9	0.1	**4**	**-1**
CT	mgC/l	296	296	378	390	**83**	**94**	299	299	363	410	**64**	**111**
Solids													
VSS	mgVSS/l	4476	5319	4497	4540	**21**	**-779**	5019	5028	3987	3870	**-1032**	**-1158**
pH													
pH		7.31	7.31	7.20	6.99	**-0.11**	**-0.32**	7.27	7.27	7.16	6.84	**-0.11**	**-0.43**

Table 5. 15: Modelled MP2 and MP3 AugBMP control results

MP2 Control Model Results								MP3 Control Model Results					
		Start		End		Change		Start		End		Change	
COD	**Unit**	**Observed**	**Modelled**	**Observed**	**Modelled**	**Observed**	**Modelled**	**Observed**	**Modelled**	**Observed**	**Modelled**	**Observed**	**Modelled**
Total COD	mgCOD/l	9545	9632	8907	8215	**-638**	**-1417**	13306	11598	11493	9429	**-1813**	**-2169**
Soluble COD	mgCOD/l	831	1099	1133	1053	**302**	**-47**	1834	2015	1333	1350	**-501**	**-665**
Gas													
Methane	mgCOD	0	0	6916	5784	**6916**	**5784**	0	0	4697	9464	**4697**	**9464**
Nitrogen													
FSA	mgFSA/l	254	254	297	325	**42**	**71**	273	273	330	364	**57**	**90**
Phosphate													
OP	mgOP/l	5.4	5.4	13.6	12.2	**8.2**	**6.8**	12.7	12.7	23.4	23.0	**10.7**	**10.3**
Alkalinity													
Carbonate	mg/l as CaCO3	1339	1350	1674	1621	**335**	**270**	1225	1235	1526	1533	**301**	**298**
Total	mg/l as CaCO3	1388	1399	1704	1654	**316**	**254**	1323	1343	1678	1666	**355**	**323**
Species													
VFA Conc	mg/l as acetate	35.6	35.5	0.0	0.0	**-36**	**-36**	83.0	83.2	140.6	90.7	**58**	**7**
CT	mgC/l	347	347	439	446	**92**	**100**	317	317	410	428	**93**	**111**
Solids													
VSS	mgVSS/l	5634	5554	4530	4832	**-1104**	**-723**	5911	6027	5299	5351	**-612**	**-676**
pH													
pH		7.38	7.38	7.31	7.06	**-0.07**	**-0.33**	7.38	7.38	7.18	7.01	**-0.19**	**-0.37**

The methane produced in the modelled AugBMP control experiments was significantly higher than the observed methane produced for MC1, MP1 and MP3. The methane produced by the modelled AugBMP control reactor was based on a 100% COD balance, as mass was conserved in the model. Therefore, the COD utilised during the experiment was conserved in the methane gas produced. The discrepancy between the observed cumulative methane production and the methane produced by the model highlights the gas measurement error experienced in the BMP test. However, as previously explained, the total COD change in the MP2 experiment was low relative to the methane produced and VSS utilised. Therefore, the methane produced in the modelled AugBMP control for the MP2 experiment was a best fit by the PE function (which considered all of the measurements taken).

The change in FSA, OP, H_2CO_3 alkalinity, total alkalinity and VSS were replicated well by the model for all four experiments. However, the FSA change, as well as the VSS change, in MC1 differed significantly between the modelled AugBMP control and the observed control. The discrepancy in the MC1 FSA and VSS values are explained visually in Section 5.2.6.3 (Figure 5.13) and Section 5.2.6.7 (Figure 5.29), respectively. Table 5.16 below shows the various issues associated with the measured data and explains how the issues were overcome such that the research objectives were still achieved.

Table 5. 16: Measurement error associated with data set and manner in which error was handled for modelling

Data set	Measurement Error	Solution to error
MC1 FSA (Figure 5.13).	Drop in FSA concentration.	Lower FSA concentration values ignored by simulation and trajectory maintained from first 5 points.
MC1 FSA (Figure 5.29).	Low starting VSS concentration.	Starting VSS concentration determined by PE to fit remaining data set.
Soluble COD concentration in all four reactors (Figures 5.9 to 5.12).	High variance in soluble COD concentrations between start and end.	Soluble COD concentration at end of experiment determined using USO concentration and PE used to determine soluble COD fluctuation based on observed data.
Methane COD in all four reactors (Figures 5.41 to 5.44).	Mismatch between observed methane production and modelled methane production.	Change in COD used to determine methane gas production as PWM_SA_AD model is mass balanced.

5.2.6.1 Total COD

The total COD concentration change in the modelled AugBMP control reactor for the MC1, MP1 and MP2 experiments (Figures 5.5, 5.6 and 5.7) replicated the total COD change in the observed AugBMP control reactor well. However, for the MP3 experiment (Figure 5.8), the total COD concentration in the model started lower than what was observed. The low starting COD concentration in the modelled MP3 experiment was due to the low starting value of the UPO COD and VSS concentrations (determined based on the fixed UPO composition). However, Figure 5.32 in Section 5.2.6.7 shows that the VSS concentration in the modelled MP3 experiment agreed well with the observed VSS concentration. Hence, the low starting total COD concentration was noted to be a consequence of the fixed UPO elemental composition, which subsequently affected the VSS and COD concentrations.

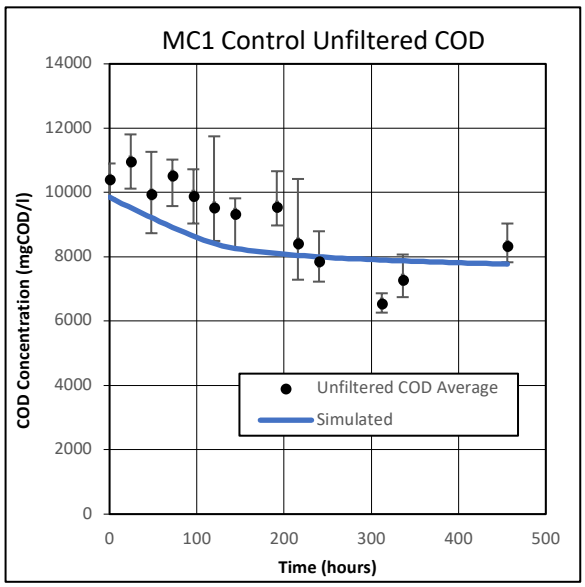

Figure 5. 5: MC1 AugBMP control total COD

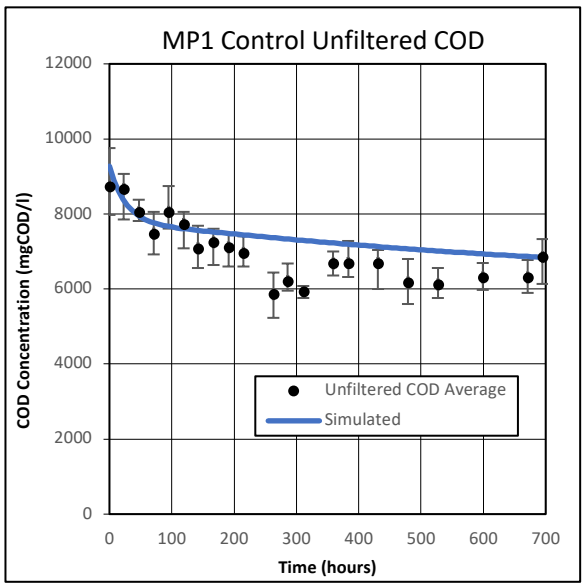

Figure 5. 6: MP1 AugBMP control total COD

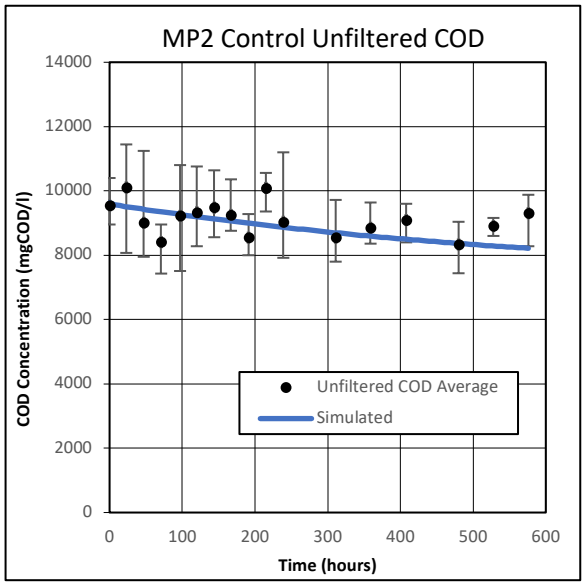

Figure 5. 7: MP2 AugBMP control total COD

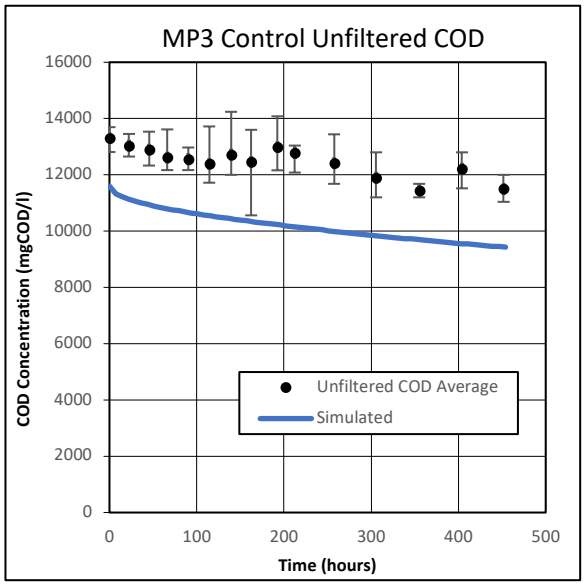

Figure 5. 8: MP3 AugBMP control total COD

5.2.6.2 Soluble COD

The soluble COD concentration comprises of BSO, USO and VFA. The FBSO and VFA is deemed to all be used by the end of the AugBMP experiment. However, some VFA is generated as an intermediate product of the AD environment, which results in small concentrations of VFA at the effluent generated from the AD system. However, the soluble COD concentration at the end of the observed AugBMP control experiments was used to set the USO COD concentration in the modelled control reactor (since the USO is deemed not to degrade during the AugBMP control experiment). The VFA present in the AugBMP control reactor also contributes to the soluble COD concentration – hence the presence of this VFA COD was the reason for the mismatch of the soluble COD concentration for the modelled MC1 experiment (Figure 5.9), which was higher than observed.

The values used in the modelled AugBMP control were the averaged observed values for all three control reactors (C1, C2 and C3). Therefore, the starting soluble COD concentration in the MP1 experiment (Figure 5.10) was skewed by an outlier, which consequently raised the average starting soluble COD concentration of the observed results. However, this outlier was not considered in the modelled MP1 AugBMP control experiment.

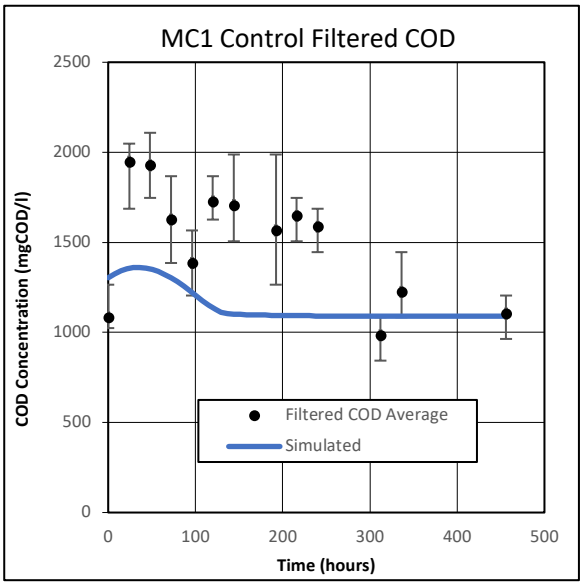

Figure 5. 9: MC1 AugBMP control soluble COD

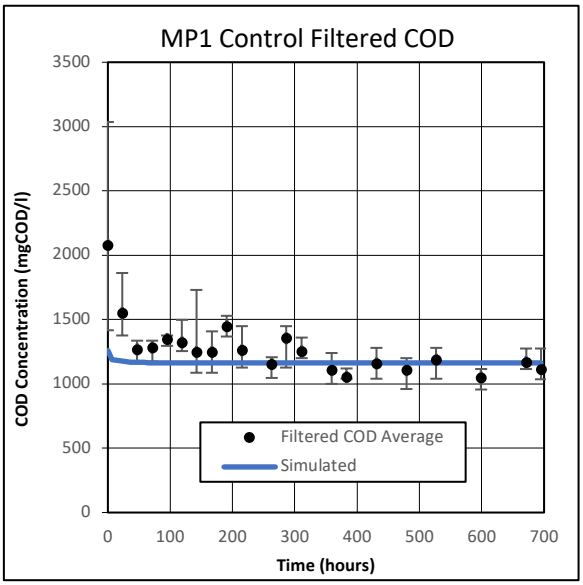

Figure 5. 10: MP1 AugBMP control soluble COD

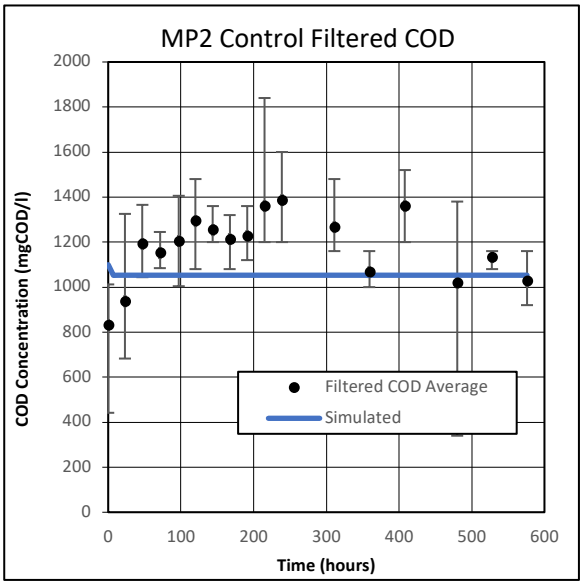

Figure 5. 11: MP2 AugBMP control soluble COD

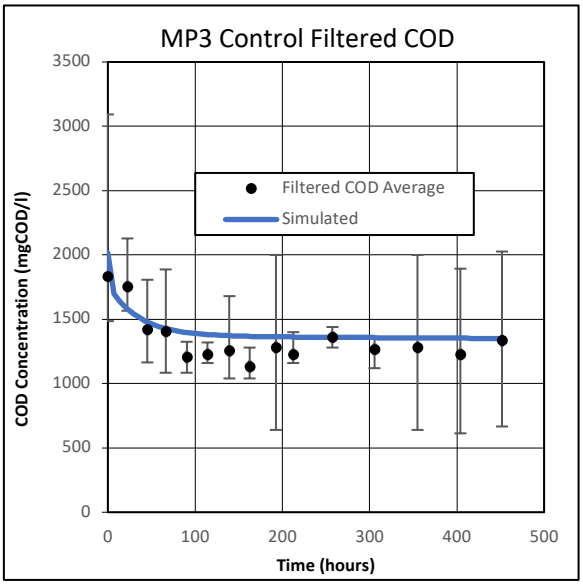

Figure 5. 12: MP3 AugBMP control soluble COD

5.2.6.3 Free and Saline Ammonia (FSA)

The FSA concentration in the modelled AugBMP control reactor replicated the FSA concentrations observed in the MP1, MP2 and MP3 experiments (Figures 5.14, 5.15 and 5.16) well. The rate at which the FSA was released into the aqueous phase was a good indication of the BPO hydrolysis rate, as the organic N contained in the BPO was released as FSA during the breakdown of the organics.

Furthermore, the release of FSA into the bulk liquid also impacted the H_2CO_3 alkalinity in the reactor. The FSA was released into the reactor liquid as NH_3. However, due to the operating pH of the AugBMP reactor, the NH_3 re-speciates into NH_4^+. Therefore, this re-speciation requires an additional H^+ ion, which is subsequently taken from the aqueous phase. The uptake of the H^+ ion from the aqueous solution forms HCO_3^-, which is carbonate alkalinity. Therefore, the PE identified the BPO composition by minimising the error between the observed FSA and carbonate alkalinity concentrations.

The MC1 FSA (Figure 5.13) concentration decreased rapidly after the first 100 hours of the experiment. However, this rapid decrease in FSA concentration was most likely due to measurement error, such as the normality of the reagent used in the analytical procedure changing. However, the modelled FSA concentration for the MC1 experiment followed the expected trajectory.

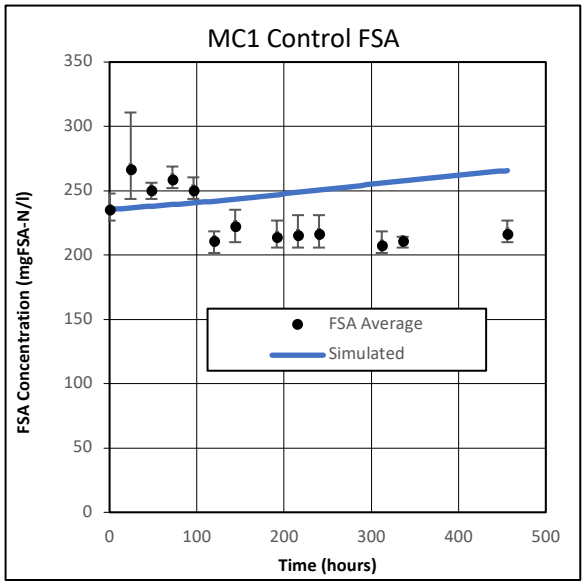

Figure 5. 13: MC1 AugBMP control FSA

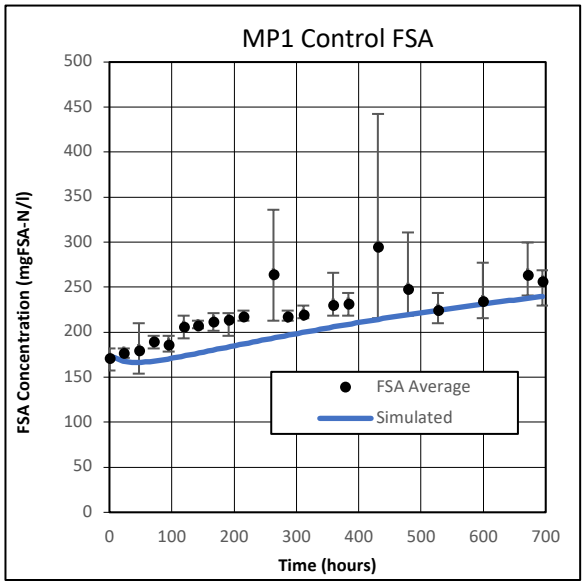

Figure 5. 14: MP1 AugBMP control FSA

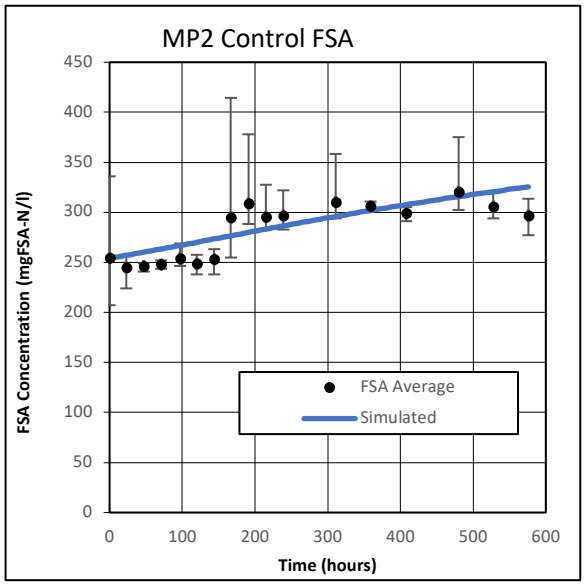

Figure 5. 15: MP2 AugBMP control FSA

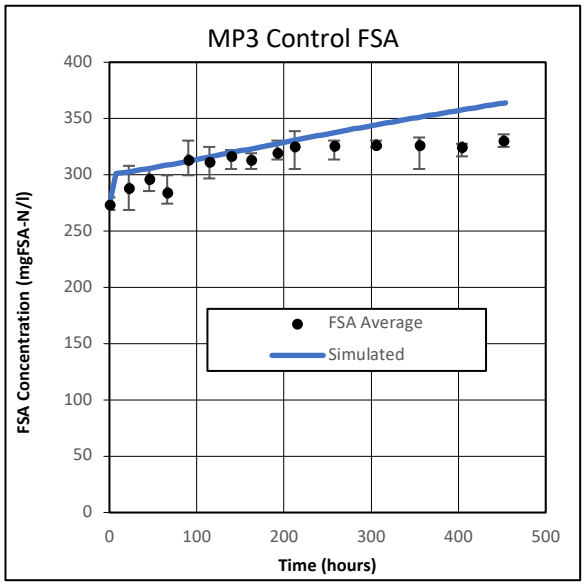

Figure 5. 16: MP3 AugBMP control FSA

5.2.6.4 Orthophosphate (OP)

The release of OP into the AugBMP control reactor liquid for all for experiments was relatively low (5 to 11mgOP/*l*), compared to the other constituents released, which indicated that the organic P content in the BPO was low. Furthermore, as with the FSA, the rate at which the OP was released into the AugBMP control reactor liquid was a good indication of the hydrolysis rate of the BPO. The modelled AugBMP control reactor replicated the OP released into the observed AugBMP control reactor for all four experiments well.

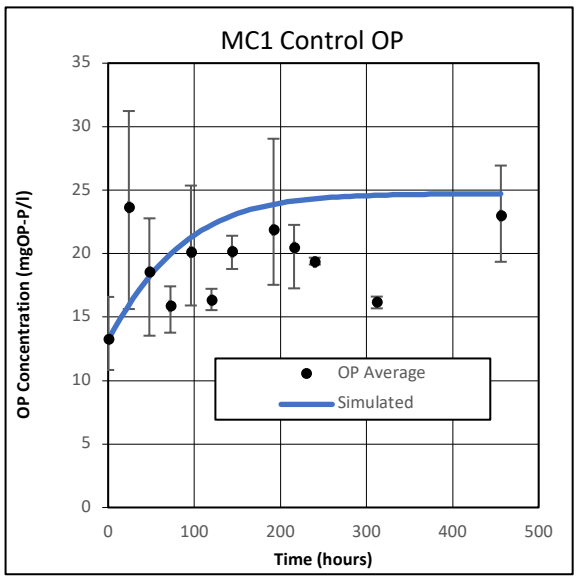

Figure 5. 17: MC1 AugBMP control OP

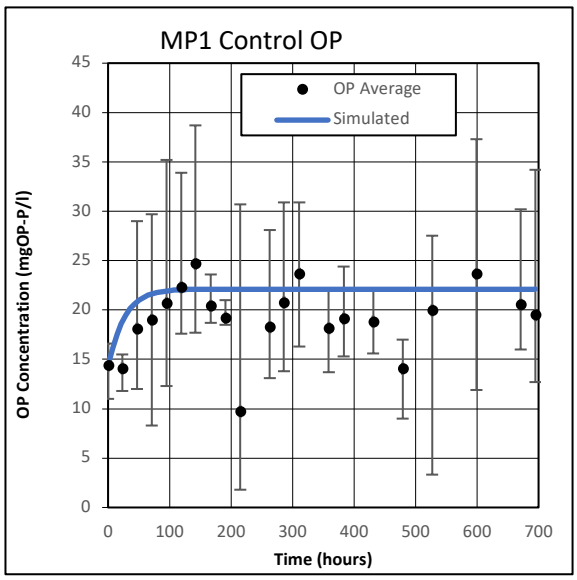

Figure 5. 18: MP1 AugBMP control OP

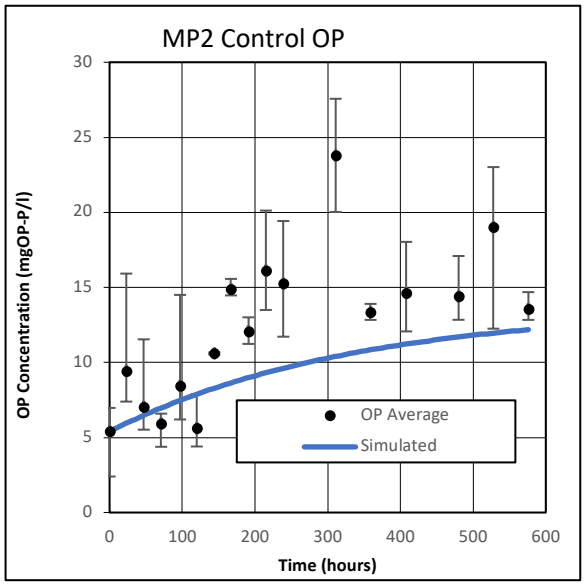

Figure 5. 19: MP2 AugBMP control OP

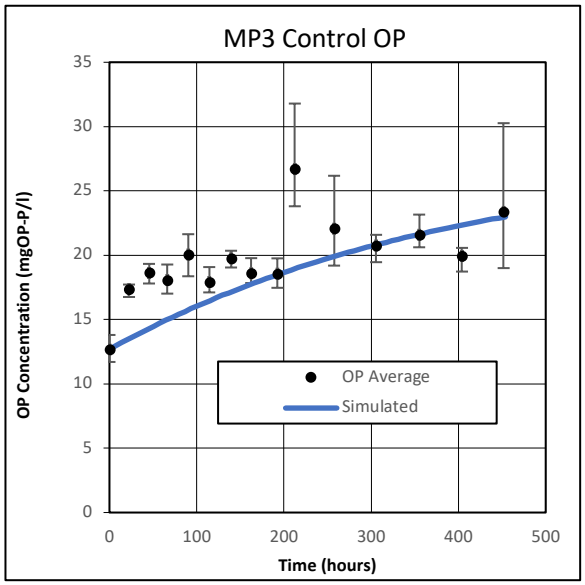

Figure 5. 20: MP3 AugBMP control OP

5.2.6.5 Carbonate Alkalinity

As mentioned for the FSA in Section 5.2.6.3, the increase in carbonate alkalinity in the AugBMP control reactor was dependent on the release of FSA into the reactor liquid. However, the release of OP also affected the carbonate alkalinity, as OP was released into the reactor as H_3PO_4, which subsequently re-speciated into $H_2PO_4^-$ and HPO_4^{2-}. The additional H^+ ions released into solution due to the re-speciation of H_3PO_4, decreased the carbonate alkalinity concentration, but increased the H_3PO_4 alkalinity by the same amount. This is explained further in Section 5.2.6.6 below. Therefore, the BPO composition determined by the PE minimised the error across these measurements. Subsequently, the results obtained from the modelled AugBMP control reactors for MC1, MP1, MP2 and MP3 (Figures 5.21, 5.22, 5.23 and 5.24) agreed well with the observed results.

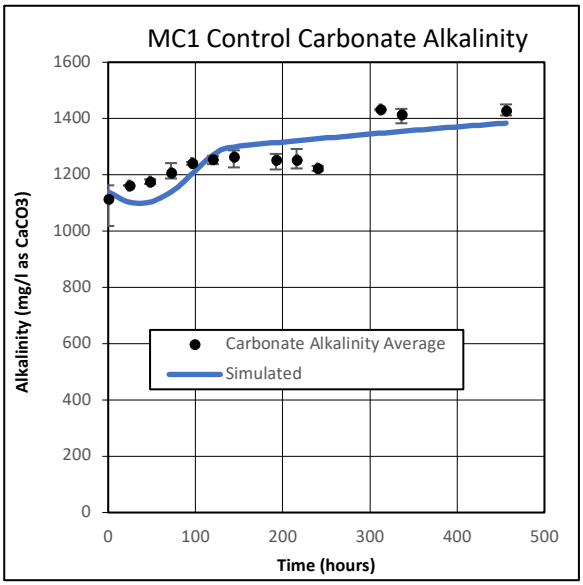

Figure 5. 21: MC1 AugBMP control carbonate alkalinty

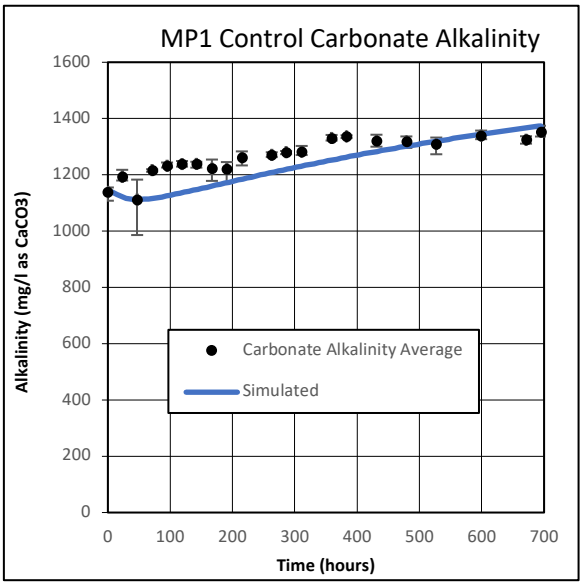

Figure 5. 22: MP1 AugBMP control carbonate alkalinty

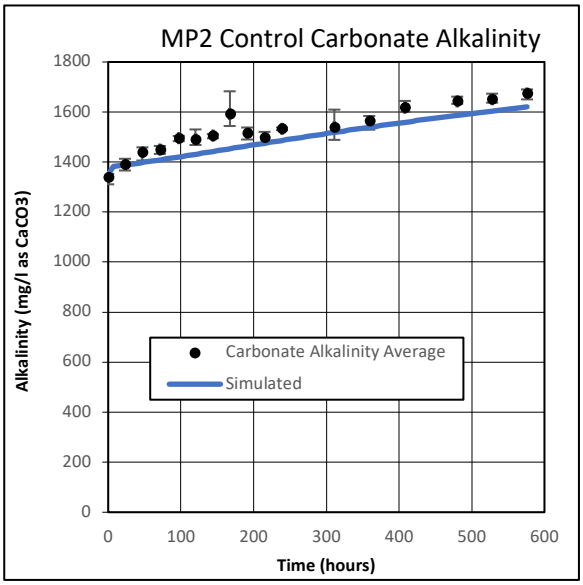

Figure 5. 23: MP2 AugBMP control carbonate alkalinty

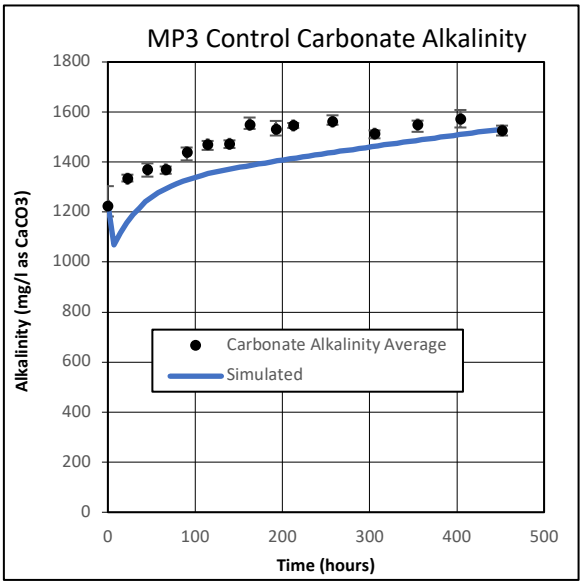

Figure 5. 24: MP3 AugBMP control carbonate alkalinty

5.2.6.6 Total Alkalinity

The total alkalinity of the system is a conservative parameter (it is dependent on the composition of the influent organics fed to the AD). The release of FSA into the reactor liquid increases the total alkalinity through the re-speciation of NH_3 to NH_4^+; therefore, making the N content of the influent organics intrinsic alkalinity.

The release of OP into the bulk liquid results in a re-speciation of H_3PO_4, into $H_2PO_4^-$ and HPO_4^{2-}. The release of OP into the reactor liquid does not affect the total alkalinity of the

system, as H_3PO_4 is the reference species. The re-speciation of H_3PO_4, decreases the HCO_3^- by forming H_2CO_3, which evolves from solution as CO_2 gas. However, the decrease in H_2CO_3 alkalinity (caused by the decrease in HCO_3^-) is equal to the increase of H_3PO_4 alkalinity by the increase of $H_2PO_4^-$ and HPO_4^{2-}. Therefore, the total alkalinity released by the organics remains unchanged even though the species that represent it change. The total alkalinity change serves as a check to evaluate the chosen BPO composition. However, the total alkalinity change is unable to identify individual elements. The modelled AugBMP control reactor replicated the change in observed total alkalinity well for MC1, MP1, MP2 and MP3 (Figures 5.25, 5.26, 5.27 and 5.28), indicating that the compositions determined by the model were a good fit for the observed data.

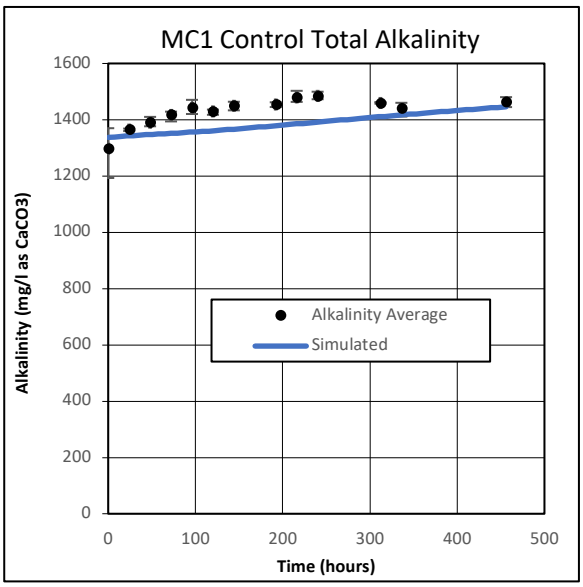

Figure 5. 25: MC1 AugBMP control total alkalinty

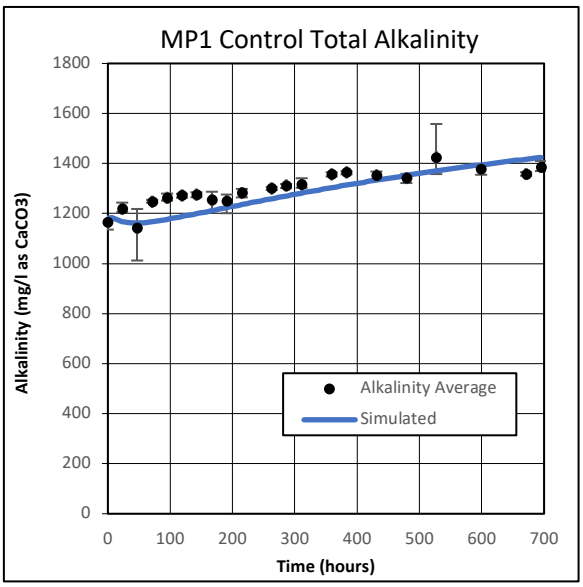

Figure 5. 26: MP1 AugBMP control total alkalinty

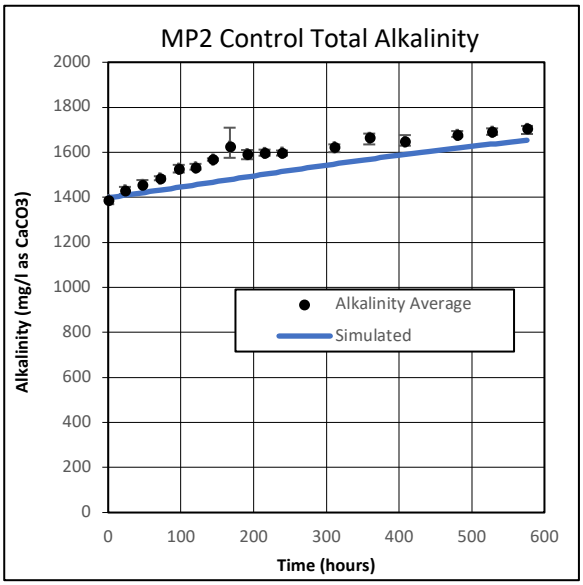

Figure 5. 27: MP2 AugBMP control total alkalinty

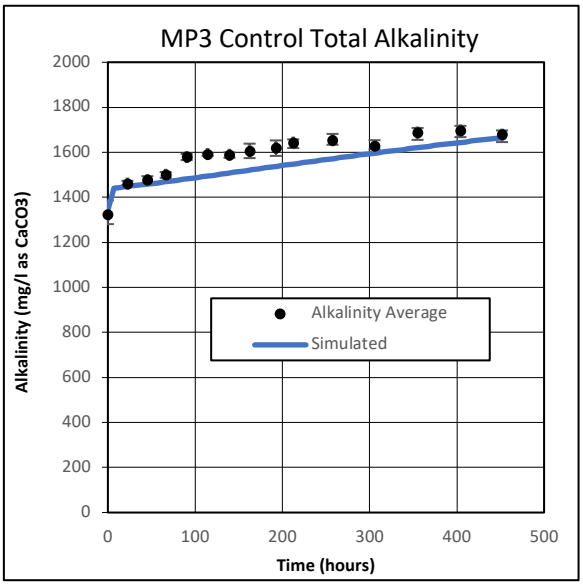

Figure 5. 28: MP3 AugBMP control total alkalinty

5.2.6.7 Volatile Suspended Solids (VSS)

The change in VSS concentration throughout the AugBMP control experiment was a good indication of the particulate biodegradable material present in the inoculum. The starting VSS concentration in MC1 (Figure 5.29) was lower than the ending VSS concentration. However, the VSS data collected throughout the experiment suggested that the observed starting concentration was incorrect, as the VSS gradually decreased after 24hours. The PE accounted for the decrease in VSS concentration over the entire data set, and subsequently estimated a starting BPO mass for the MC1 experiment based on all of the measurements taken. The modelled AugBMP reactor replicated the observed VSS concentrations for the AugBMP control experiments, MP1, MP2 and MP3 (Figures 5.30, 5.31 and 5.32) well.

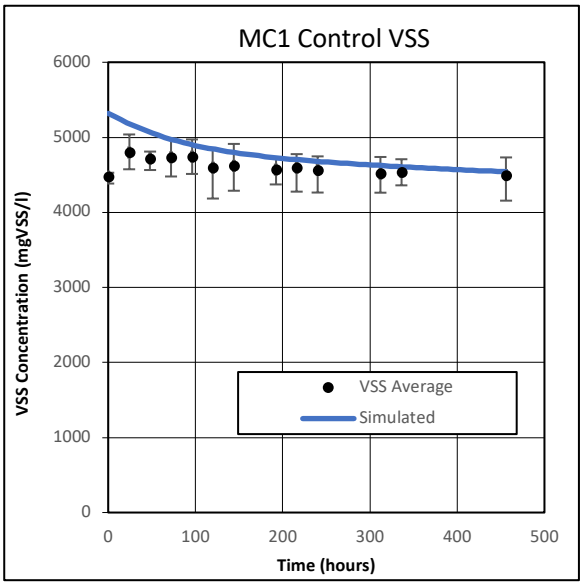

Figure 5. 29: MC1 AugBMP control VSS

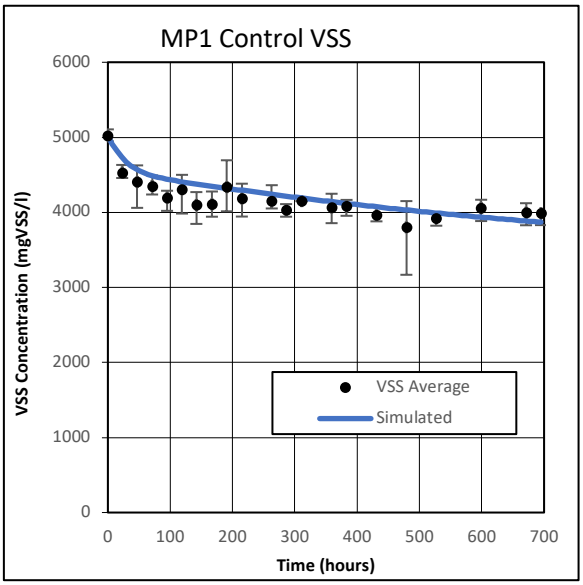

Figure 5. 30: MP1 AugBMP control VSS

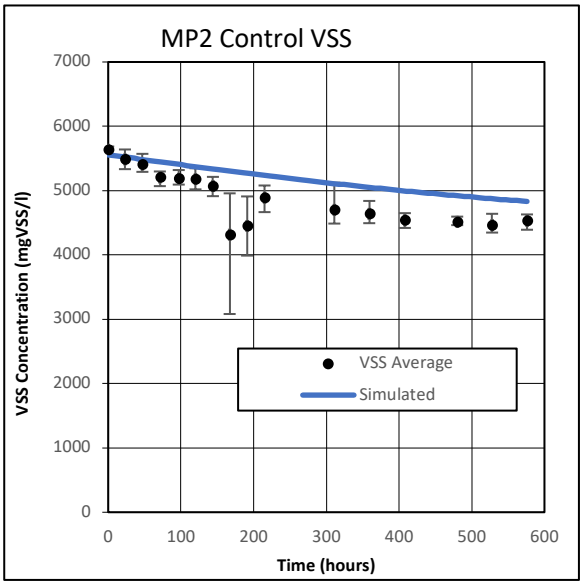

Figure 5. 31: MP2 AugBMP control VSS

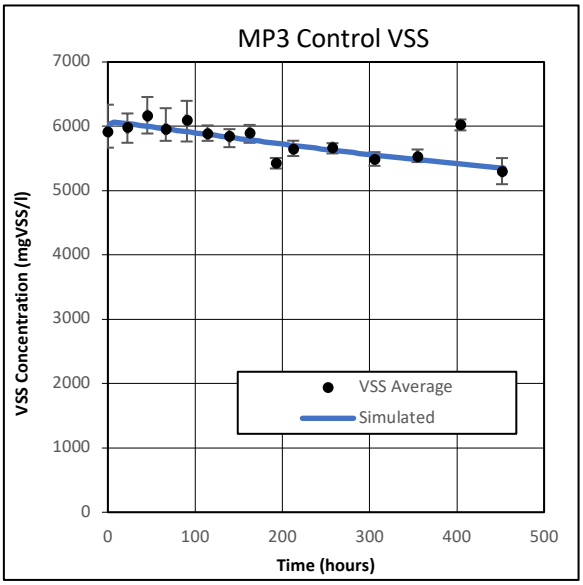

Figure 5. 32: MP3 AugBMP control VSS

5.2.6.8 Volatile Fatty Acids (VFA)

The VFA present in the modelled AugBMP control reactor was an intermediate product formed by the degradation of glucose (which formed from the hydrolysis of the biodegradable organics). The accumulation of VFA in the modelled AugBMP control reactor was dependent on the BPO hydrolysis rate, the substrate uptake rate of the acetoclastic methanogens and the half-saturation coefficient of the acetoclastic methanogens. The PE adjusted these parameters, as well as the composition of the BPO, until the parameters that best represented the observed data set were determined. It is imperative to note that the concentrations of soluble constituents

such as VFA only influence the kinetics of the experiment and not the identification of the composition of the biodegradable particulate organics.

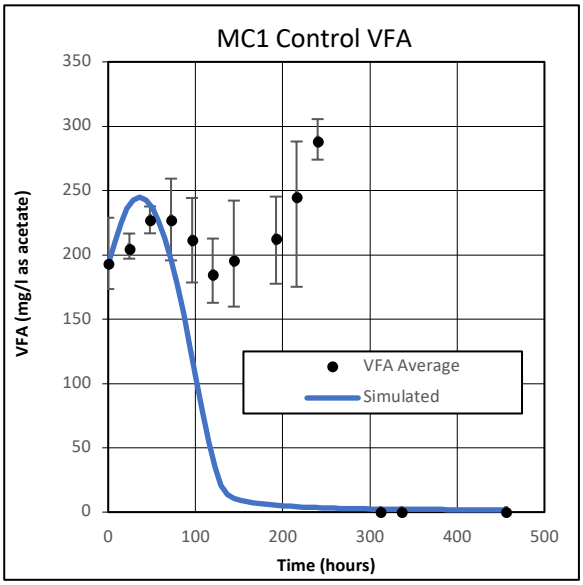

Figure 5. 33: MC1 AugBMP control VFA

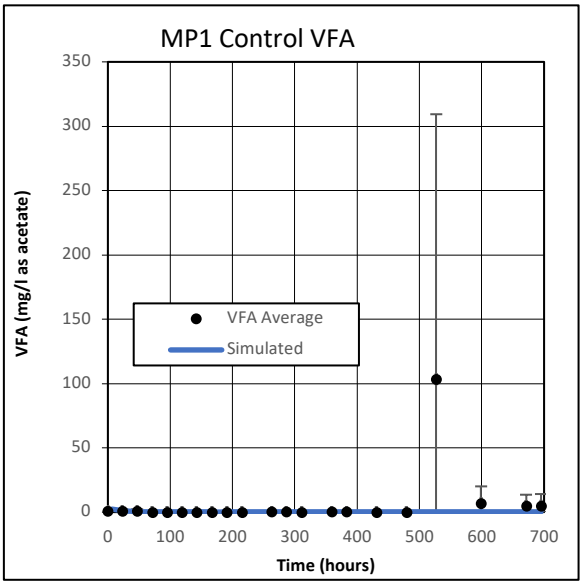

Figure 5. 34: MP1 AugBMP control VFA

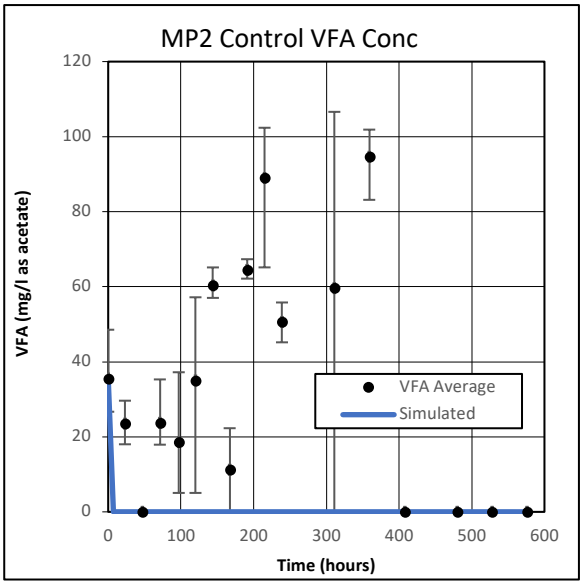

Figure 5. 35: MP2 AugBMP control VFA

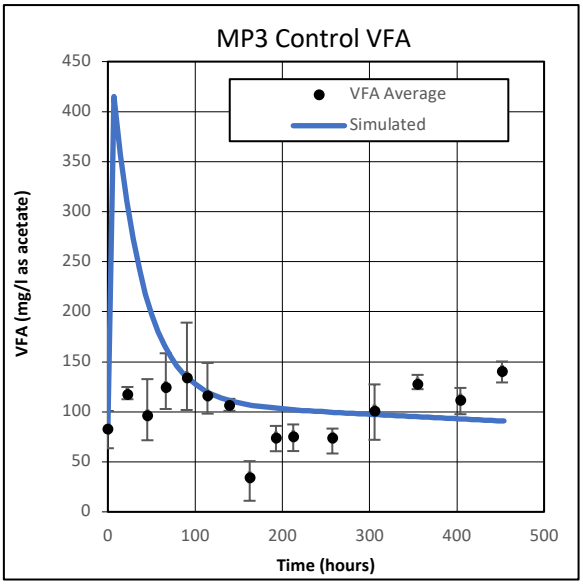

Figure 5. 36: MP3 AugBMP control VFA

5.2.6.9 pH

The pH of the AugBMP control reactor was affected by the total alkalinity generated, as well as the increased CO_2 partial pressure (p_{CO2}), due to the breakdown of the organics. The methane produced throughout the AugBMP experiment was fixed by the available biodegradable COD concentration. Therefore, the C from the organics that was not included in the methane became

CO_2, (as either dissolved HCO_3^-, or gaseous CO_2). Consequently, the evolution of CO_2 from the reactor liquid increased the p_{CO2} in the reactor headspace, which decreased the aqueous phase pH. The change in pH for the MC1, MP2 and MP3 experimental periods (Figure 5.37, 5.39 and 5.40), was well represented by the modelled AugBMP control reactor. However, the pH in the modelled MP1 (Figure 5.38) experiment dropped below the observed pH, which suggested that the composition determined by the PE was not entirely correct. However, the determined composition accurately replicated the other aqueous constituents.

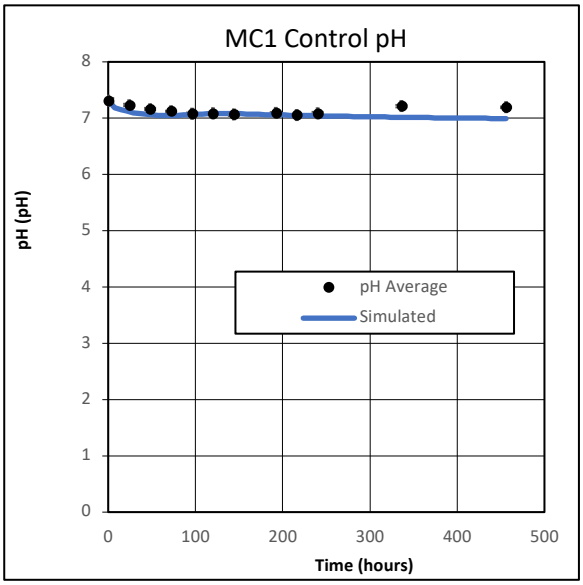

Figure 5. 37: MC1 AugBMP control pH

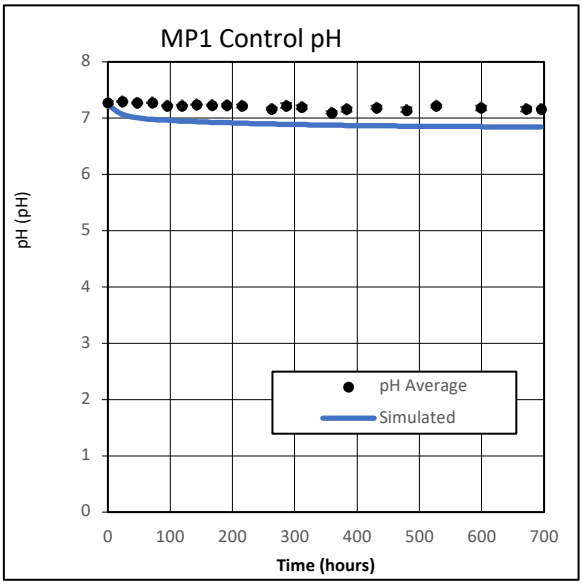

Figure 5. 38: MP1 AugBMP control pH

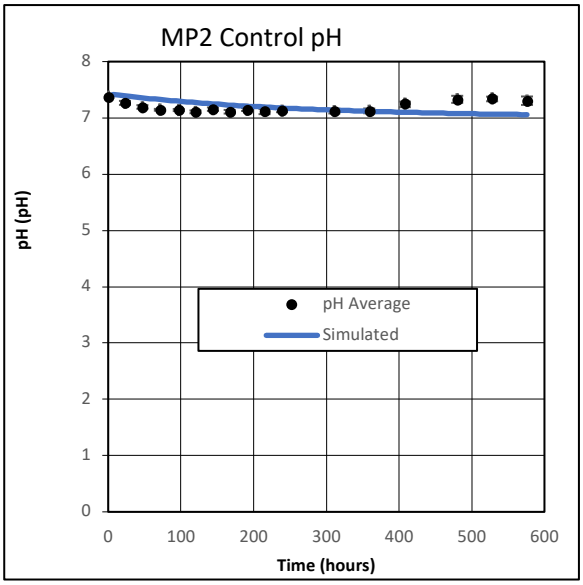

Figure 5. 39: MP2 AugBMP control pH

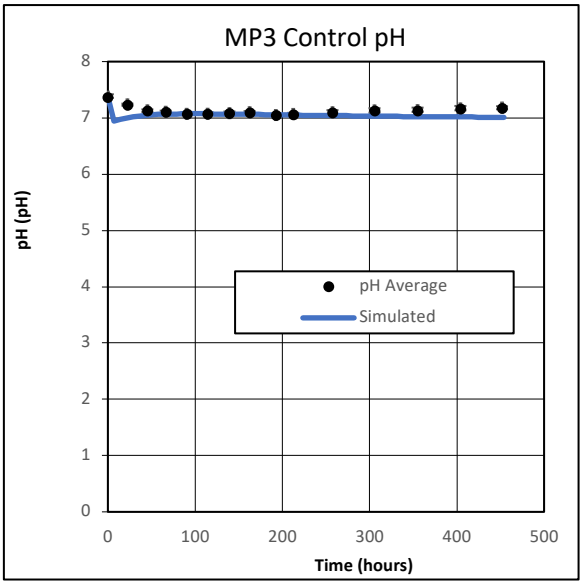

Figure 5. 40: MP3 AugBMP control pH

5.2.6.10 Methane

The methane produced by the modelled AugBMP control for the MC1, MP1 and MP3 experiments (Figures 5.41, 5.42 and 5.44) significantly exceeded the observed methane production. As previously mentioned, the modelled AugBMP control experiment was mass balanced. Therefore, the COD of the biodegradable organics utilised throughout the modelled AugBMP control experiment were conserved in either the biomass or the methane gas produced.

It was shown in Section 5.2.2, that the COD balances for MC1, MP1 and MP3 were below 100%. The low COD balances indicated that the COD flux through the system was not conserved, as more COD entered the AugBMP reactor than was accounted for in the liquid effluent and methane gas. The inverted water column was used to measure the total gas produced during the reaction; however, the result suggested that this method of biogas measurement was inaccurate. Therefore, in order to explore this further, COD balances were performed on the modelled AugBMP control reactor, which are explained in Section 5.2.6.11 below.

The methane produced by the modelled MP2 experiment (Figure 5.43) was lower than the observed methane. However, it was previously shown in Table 5.2, that the total COD change for the MP2 experiment was low relative to the methane produced and the VSS consumed. Therefore, the methane produced by the modelled MP2 experiment was dependent on the composition determined by the PE, which minimised the error across all of the measurements taken.

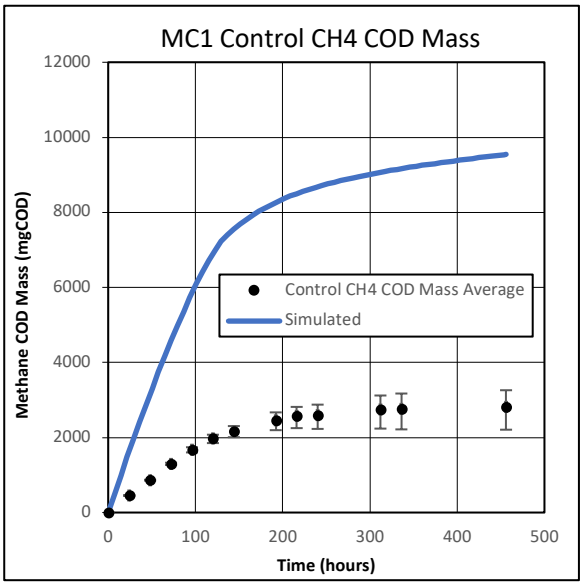

Figure 5. 41: MC1 AugBMP control methane

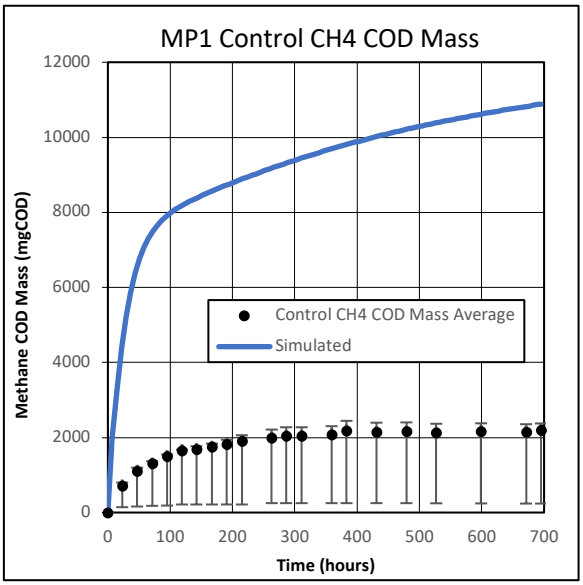

Figure 5. 42: MP1 AugBMP control methane

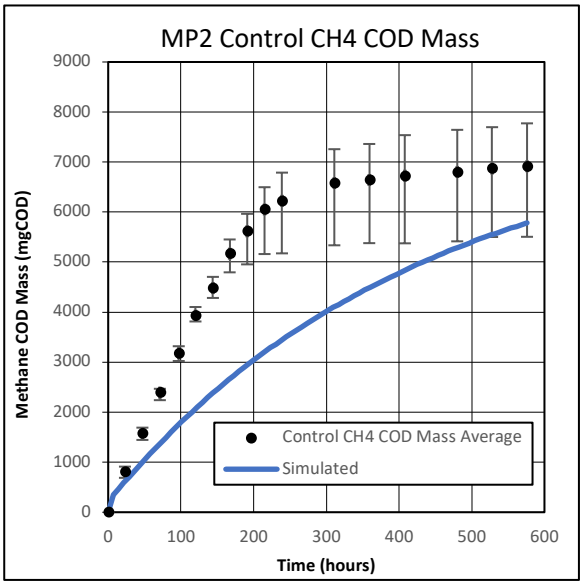

Figure 5. 43: MP2 AugBMP control methane

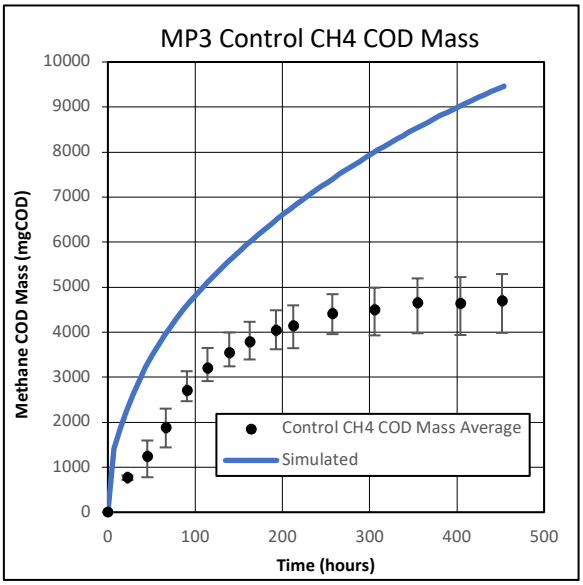

Figure 5. 44: MP3 AugBMP control methane

5.2.6.11 Model Mass Balances

As explained in Section 5.2.2, the mass of material entering the AugBMP control reactor should equate to the mass of material leaving the reactor, as mass was conserved within the system, and the AugBMP control reactor was completely sealed for the duration of the experiment. However, a COD balance for the observed AugBMP control reactors for MC1 and MP1 had COD balances of 87 ± 2% and 83 ± 6%, which lay outside the 10% tolerance for accurate COD balances.

Therefore, to account for the COD removed from the modelled AugBMP reactor during sampling, the PWM_SA_AD model code was adjusted to allow for 120ml of the sample to be removed from the reactor on the days that the laboratory reactor was sampled. An example of the sample drawn from the modelled MP2 experiment is shown in Figure 13, 14 and 15 in Section 3.7.3.3.

Table 5.17 shows that the modelled AugBMP control reactor for all four experiments had a 100% COD balance, which was expected as the models are mass balanced. The COD in the methane gas for the modelled MC1, MP1 and MP3 experiments was significantly higher than the observed methane COD, which was collected using the inverted water columns. The significant discrepancy between the observed and the modelled methane gas COD strongly suggested that the gas measurements were a substantial source of error for the AugBMP test, and consequently, the BMP test. Therefore, the aqueous COD measurements were taken to be more accurate than the biogas COD when identifying the composition of the BPO.

Table 5. 17: Modelled AugBMP control COD balance

	MC1			MP1		
	Observed	Model	%error	Observed	Model	%error
Unit	mgCOD	mgCOD	%	mgCOD	mgCOD	%
Starting	**52007**	**49286**	-5	**43651**	**46372**	6
Removed	12983	11150	-14	16584	16893	2
Remaining	29666	28603	-4	17816	18609	4
Gas	2816	9546	239	2205	10882	394
Total Effluent	**45465**	**49299**	8	**36605**	**46385**	27
Unit	%	%		%	%	
Balance	**87**	**100**	**-**	**84**	**100**	-
	MP2			MP3		
	Observed	Model	%error	Observed	Model	%error
Unit	mgCOD	mgCOD	%	mgCOD	mgCOD	%
Starting	**47723**	**48158**	1	**66532**	**57992**	-13
Removed	17464	16103	-8	20864	17250	-17
Remaining	28665	26285	-8	38158	31301	-18
Gas	7622	5784	-24	4697	9464	101
Total Effluent	**53750**	**48172**	-10	**63719**	**58015**	-9
Unit	%	%		%	%	
Balance	**113**	**100**	**-**	**96**	**100**	-

5.3 AugBSP Control Reactors

The AugBSP control experiment was conducted as specified in Section 3.5. In order to achieve reliable results, the experiment was conducted in duplicate, utilising two control reactors. The control reactors were labelled C1 and C2 for all four experiments. The inoculum was removed from the sulphidogenic SSPAD on the day that the experiment started and was inserted directly into the AugBSP reactors.

The seeding procedure is described in Section 3.5.3. The AugBSP control reactors were seeded with inoculum only. Therefore, the effluent from the sulphidogenic SSPAD, that was used as the inoculum, was not diluted at the start of the AugBSP experiment. Dilution was not necessary, as the volume of effluent generated from the two SSPADs was sufficient to provide inoculum for both the AugBSP control and AugBSP test experiments, each in duplicate. The starting mix for the AugBSP control experiment is given in Table 3.2 in Section 3.5.3.

The concentration of each constituent in the AugBSP control reactor was measured using the analytical procedures described in Section 3.6. The measured concentrations for each constituent in each of the AugBSP reactors (C1 and C2) were combined into one value by taking the average between the reactors. Table 5.18 summarises the combined averaged measurements, taken at the start and end of the experiment, for the AugBSP control reactor for the SC1, SP1, SP2 and SP3 experiments.

The total COD concentration in the AugBSP control reactor should remain constant as the system was completely sealed with zero headspace. The total COD concentration change for the SC1, SP2 and SP3 experiments was low (19 to 35mgCOD/*l*). The total COD concentration in SP1 increased throughout the experiment. However, this should not have been possible as additional COD was not added to the reactor during the experiment. Therefore, the observed change was most likely due to measurement error.

Table 5. 18: AugBSP control results

AugBSP Control		SC1			SP1			SP2			SP3		
	Unit	Start	End	Change (Δ)	Start	End	Change (Δ)	Start	End	Change (Δ)	Start	End	Change (Δ)
Time	hours	0	384	384	0	430	430	0	552	552	0	382	382
Total COD	mgCOD/l	755	731	-24	1492	1759	267	1194	1229	35	917	936	19
Soluble COD	mgCOD/l	418	405	-13	621	700	79	604	684	80	412	396	-16
Soluble Organic COD	mgCOD/l	117	91	-26	53	90	38	83	123	40	87	44	-43
Soluble Sulphide COD	mgCOD/l	300	313	13	568	609	41	521	560	39	324	351	27
VFA COD	mgCOD/l	0	11	11	0	79	79	0	109	109	0	0	0
Sulphate	mgSO_4/l	686	573	-113	-	-	-163	324	169	-154	446	416	-30
TKN	mgN/l	23	23	0	51	48	-3	29	30	1	24	23	0
FSA	mgN/l	8	9	1	15	19	4	14	16	2	7	9	2
TP	mgP/l	4	4	0	7	7	0	6	5	-1	5	5	0
OP	mgP/l	2.3	2.1	-0.1	3.6	3.9	0.4	3.0	3.4	0.4	2.7	3.8	1.1
VSS	mgVSS/l	213	254	41	536	721	185	333	351	18	287	626	339
pH	pH	7.55	7.46	-0.09	7.57	7.48	-0.09	7.57	7.55	-0.02	7.50	7.32	-0.18
Carbonate Alk	mg/l as $CaCo_3$	502	583	80	875	950	75	897	967	70	573	699	127
Total Alk	mg/l as $CaCo_3$	692	779	87	1230	1387	157	1223	1401	177	771	895	123
CT	mgC /l	126	149	22	221	242	21	226	245	19	145	182	37

The total soluble COD concentration in Table 5.18 increased throughout the SP1 and SP2 experiments. The total soluble COD contained both the soluble organic COD (i.e. the total soluble COD with the sulphide COD removed, as explained in Section 3.6.3) and the soluble sulphide COD. The increase in total soluble COD indicated the breakdown of particulate organics, which were broken down via hydrolysis and converted to soluble sulphide COD, increasing the total soluble COD concentration. Furthermore, influent S_{bp} was assumed to be zero, and subsequently, the particulate organics utilised were the biomass in the inoculum.

The total soluble COD in the AugBSP control reactor should remain constant in the absence of particulate COD material, as the soluble organic COD should decrease by the same amount as the increase in soluble sulphide COD, keeping the total soluble COD concentration unchanged. However, the soluble COD concentration in SC1 and SP3 decreased throughout the experiment. This observation was unexpected, as the soluble sulphide COD concentration in all four experiments increased.

The VFA COD increased for the SC1, SP1 and SP2 experiments, indicating the accumulation of VFA from the hydrolysis step. The sulphate concentration for all four experiments decreased, which was expected as sulphide was produced during the experiment. For the SP1 experiment, the sulphate was completely utilised after 94 hours. Therefore, additional sulphate was added to the AugBSP control reactor, which resulted in a total sulphate uptake of 163mgSO_4/*l*.

The TKN and TP concentrations did not differ significantly between the start and end of the AugBSP control experiment, indicating that the N and P were conserved. The change in FSA (1 to 4mgFSA-N/*l*) and the change in OP (0.4 to 1mgOP-P/*l*) were low for all four experiments, indicating a low N and P content in the biomass. The VSS concentration increased between the start and end of the AugBSP control experiment in all four experiments. However, this increase in VSS was most likely caused by measurement error, as the modelled AugBSP control reactor showed a decrease in VSS throughout the experiment. A decrease in VSS was expected as biomass decay occurred. The VSS data is represented in Figures 5.77 to 5.80 in Section 5.3.4.9.

The pH of the AugBMP control reactor had a low decrease (0.02 to 0.18) throughout the experiment and maintained a neutral pH. (~pH of 7.5). The carbonate and total alkalinity of the

AugBSP control reactor increased throughout all four experiments due to the release of FSA from the organic N, as well as the production of sulphide.

5.3.1 Mass Balances

The AugBSP control experiment was conducted in a purpose-built reactor with zero headspace. The zero headspace should ensure that the products produced by the reaction remain in the aqueous phase. Therefore, unlike the methanogenic AugBMP experiment, the mass of the products is conserved within the aqueous solution, as no gas evolution occurs. Table 5.19 shows the mass balances achieved for the four AugBSP control experiments. The S balance was explained in Equation 3.13 in Section 3.7.4.3. The sulphur-in was the S equivalent concentration of sulphate used, and the sulphur-out was the S equivalent concentration of sulphide produced.

Table 5. 19: AugBSP control mass balance

AugBSP	S in	S out	**Balance**	TKN in	TKN out	**Balance**	TP in	TP out	**Balance**
Control	mgS/l		**%**	mgTKN-N/l		**%**	mgTP-P/l		**%**
SC1									
C1	27	9	**34**	23	22	**99**	3.8	4.1	**107**
C2	54	4	**7**	23	24	**102**	3.8	3.5	**91**
SP1									
C1	52	12	**24**	51	49	**97**	6.5	6.7	**104**
C2	49	29	**59**	51	47	**93**	6.7	6.8	**103**
SP2									
C1	55	28	**52**	36	37	**103**	7.1	5.1	**71**
C2	51	11	**22**	39	37	**94**	4.6	4.6	**100**
SP3									
C1	17	9	**52**	27	29	**110**	4.9	4.9	**99**
C2	7	18	**270**	29	31	**106**	5.2	5.0	**96**

Table 5.19 illustrates that the S was not conserved by the AugBSP control reactor. It was observed that in all of the AugBSP control reactors for all four of the experiments, with the exception of SP3 C2, that more S was utilised by the uptake of sulphate than the S produced by the formation of sulphide. The source of this discrepancy was difficult to identify, as the measured decrease in sulphate may have been overpredicted by the discrete analyser. Alternatively, sulphide may have escaped the sample during the analytical testing procedure.

The loss of sulphide during the COD test was minimised by raising the pH of the sample above 10 using NaOH, as recommended by Poinapen *et al.* (2009). Another possible explanation was the formation of other compounds containing S, such as thiosulphate ($S_2O_3^{2-}$), which were not measured, as they were not expected to form in the AugBSP reactors. Additionally, some volatile inorganic salts are also lost at 500°C (ex: ammonium carbonate), which may overestimate the organics.

The TKN and TP balances for all four experiments were within 10%, except for the TP balance of SP2 C1. The TKN and TP mass balances illustrate that the N and P were conserved throughout the experiment.

5.3.2 Stoichiometric Composition Identification

The composition of the biodegradable organics was identified by calculating the change in elemental concentrations between two measured data points. The data points required were the ending and the starting concentrations of the augmented batch experiments. The calculation is explained in detail in Section 3.9.2. The mass ratios for each element (f_{CV}, f_C, f_N and f_P) needed to be determined in order to calculate the unknown mass ratios (f_O and f_H).

Therefore, the change in COD, C, N, P and VSS throughout the experiment was required. The change in the required components was previously shown in Table 5.18. The identification of the biodegradable composition for the AugBMP control experiments is shown in Table 5.20. Table 5.20 illustrates how the composition of the biodegradable organics was identified using the stoichiometric calculation described in Section 3.9.2. The change between the ending and starting concentrations of each constituent quantified the material released by the biodegradable organics.

Table 5. 20: AugBSP control stoichiometric composition determination

AugBSP Control		SC1	SP1	SP2	SP3
Measured	**Unit**	Change (∆)	Change (∆)	Change (∆)	Change (∆)
Soluble Sulphide COD	mgCOD/l	13	41	39	27
VFA COD	mgCOD/l	11	79	109	0
FSA	mgN/l	1	4	2	2
OP	mgP/l	-0.1	0.4	0.4	1.1
VSS	mgVSS/l	41	185	18	339
Carbonate Alk	mg/l as $CaCo_3$	80	75	70	127
COD Change					
Biodegradable COD	mgCOD/l	24	120	148	27
Carbon Change					
C in Gas	mgC/l	-	-	-	-
C in H_2CO_3 Alk	mgC/l	19	18	17	30
Total C	mgC/l	19	18	17	30
VSS Change					
Biodegradable VSS	mgVSS/l	-41	-185	-18	-339
Mass Ratio					
f_{CV}	gCOD/gVSS	-0.590	-0.652	-8.244	-0.080
f_C	gC/gVSS	-0.471	-0.097	-0.927	-0.090
f_N	gN/gVSS	-0.028	-0.019	-0.127	-0.006
f_P	gP/gVSS	0.003	-0.002	-0.020	-0.003
f_H	gH/gVSS	0.234	0.077	-0.432	0.139
f_O	gO/gVSS	1.262	1.041	2.506	0.960
Compostion					
C	-	1	1	1	1
H	-	-5.971	-9.526	5.597	-18.602
O	-	-2.010	-8.033	-2.028	-8.024
N	-	0.052	0.171	0.117	0.061
P	-	-0.003	0.008	0.008	0.014

The sulphide COD produced by the reaction quantified the concentration of COD available in the biodegradable organics. The S_{bp} in the AugBSP control reactor was taken to be negligible and the sulphide COD produced in the reaction was due to the biomass decay. The influence of the VFAs on the total sulphide COD concentration produced should be taken into account in the calculation. However, in the SC1, SP1 and SP2 AugBSP control experiments, the concentration of VFA COD increased between the start and end of the experiment. Therefore, the total available COD in the biodegradable organics was the sum of the COD used to produce sulphide, and the COD used to produce VFAs.

The change in H_2CO_3 alkalinity quantified the change in carbon in the aqueous phase, which was calculated by taking the change in H_2CO_3 alkalinity and dividing by 50 (alkalinity was measured in mg/*l* as $CaCO_3$, which has an equivalence of 50mg $CaCO_3$/mol). The alkalinity (mols) was then multiplied by 12gC/mol to get the carbon equivalent. The AugBSP reactor did not produce any CO_2 gas; therefore, the total carbon change in the system was determined using the H_2CO_3 alkalinity.

The VSS change was determined as the difference between the VSS concentration at the end and the start of the experiment. However, the VSS concentration in all four experiments increased between the measured starting and ending concentrations. This increase in VSS resulted in a negative biodegradable VSS for the BPO (biomass). This outcome was challenging to explain, as the sulphide COD, the FSA, the OP and the H_2CO_3 alkalinity all increased throughout the experiment. Therefore, caution should be taken when measuring only the starting and ending concentrations as measurement error may occur, and subsequently, taking the entire data set into consideration allows for the error across the measurements to be minimised. However, another explanation for the increase in these constituents may have been caused by a biodegradable soluble substrate present in the inoculum, which was unlikely because the sulphidogenic SSPAD had a sludge age of 19 days, and subsequently, the BSOs were completely utilised.

Consequently, the compositions determined using the negative biodegradable VSS resulted in negative terms. However, for the modelled AugBSP control experiment, the sulphidogenic SSPAD effluent (inoculum) was inserted directly into the modelled reactor and run without using the PE function. The model indicated that the VSS concentration should have decreased throughout the AugBSP control experiment. The VSS for the modelled AugBSP experiment is shown in Section 5.3.4.9, in Figures 5.77 to 5.80.

The mass ratios were calculated by taking the change in each respective constituent and dividing by the VSS concentration. Therefore, the mass ratios were determined as the biodegradable COD/VSS (f_{CV}), the total C/VSS (f_C), the FSA/VSS (f_N) and the OP/VSS (f_P). The mass ratios for f_O and f_H were calculated using Equations 3.45 and 3.46 in Section 3.9.2.1. Finally, the composition of the biodegradable organic present in the AugBSP control reactor was identified using the mass ratios and Equations 3.47 and 3.48 in Section 3.9.2.1.

The compositions determined in Table 5.20 suggested that a calculation error occurred in the proposed mass balanced stoichiometric composition calculation. This error was due to the measured starting and ending concentrations in the AugBSP control reactor. The measurements are prone to error, and the error increases significantly if only two data points are used. Instead, the entire data set (containing daily measurements) should be used, as explained in Section 3.9.3.

Therefore, the AugBSP control experiment was modelled using the PWM_SA_AD model. The use of mathematical models introduced a data reconciliation aspect into the thesis, as the models aimed to predict the changes in the AugBSP control reactor using mass balanced stoichiometry, which minimised the measurement error. However, this does not suggest that the model was correct, and the measurements in the experiment were incorrect. The model serves as a useful tool for identifying possible sources of error.

5.3.3 Modelling the AugBSP control experiment

The AugBSP control experiment was modelled using the biomass concentrations determined in the modelled SSPAD, as shown in Table 4.26 in Section 4.3.2.6. The remaining constituent concentrations such as the sulphide COD, FSA, OP, VFA, sulphate and H_2CO_3 alkalinity concentrations, as well as the reactor pH, were adjusted to the averaged observed starting values for each of the experiments. The procedure used for modelling the AugBSP control reactor is described in Section 3.11.2. Furthermore, the S_{bp} concentration present in the sulphidogenic SSPAD was taken to be negligible. Therefore, the observed changes in the AugBSP experiment were due entirely to the biomass decay. Consequently, the PE function was not utilised for the AugBSP control reactor, as the mass of the BPOs were equated to zero, and therefore the composition of the BPO was irrelevant. Hence, a modelled (via the PE process) composition identification was not conducted for the AugBSP control experiment.

The biomass and the UPO compositions used were the same as in the SSPAD, i.e. $C_1H_{1.4}O_{0.4}N_{0.2}$ and $C_1H_{1.571}O_{0.426}N_{0.166}P_{0.019}$, respectively. As mentioned, the starting concentrations of the sulphide COD, FSA, OP, VFA, sulphate and H_2CO_3 alkalinity, as well as the reactor pH, were adjusted to the averaged measured (observed) starting values for the experiments. However, the COD and the VSS concentration of the UPOs were not adjusted at

all. Therefore, the amount of UPO COD and VSS entering the modelled AugBSP control reactor was the same amount of UPO COD and VSS exiting the modelled sulphidogenic SSPAD effluent. The only COD adjustment done was the starting soluble sulphide COD.

5.3.4 Modelled AugBSP Results

The observed results from the C1 and C2 AugBSP control reactors were summarised by averaging the values obtained for each measurement taken. For instance, the unfiltered COD measurements were performed in duplicate for each control reactor; therefore, 4 unfiltered COD data points were available for each day. The value used by the modelled AugBSP control PE was the average of the 4 unfiltered COD concentrations. The values used for the remaining constituents were the averaged measured values.

Table 5.21 and Table 5.22 summarise the results obtained for the starting and ending concentrations for each constituent in the modelled AugBSP control reactor for all four experiments. The results obtained from the model were compared to that of the observed (measured) results. Furthermore, the results have been compared from Section 5.3.4.1 (from Figure 5.45) to Section 5.3.4.11 (to Figure 5.88), which allows for a visual comparison between the modelled and observed results and evaluates the accuracy of the PWM_SA_AD to replicate the dynamics of the AugBSP control reactor.

Table 5.21 and Table 5.22 show that the total COD concentration in the modelled AugBSP control reactor remained constant throughout the experiment. This outcome was expected, as the COD was conserved by the modelled AugBSP control reactor, due to the zero headspace. In the modelled AugBMP control reactor, the change in the total soluble COD concentration was equal to the change in the soluble sulphide COD concentration. Therefore, the biomass decay increased the sulphide COD concentration, as particulate organics were degraded, which subsequently increased the total soluble COD concentration by the same amount. The modelled AugBMP control reactor replicated the sulphide COD concentration change well.

Table 5. 21: Modelled SC1 and SP1 AugBSP control results

SC1 Control Model Results								SP1 Control Model Results					
		Start		End		Change		Start		End		Change	
COD	**Unit**	**Observed**	**Modelled**	**Observed**	**Modelled**	**Observed**	**Modelled**	**Observed**	**Modelled**	**Observed**	**Modelled**	**Observed**	**Modelled**
Total COD	mgCOD/l	755	708	731	708	**-24**	**0**	1492	1409	1759	1409	**267**	**0**
Total Soluble COD	mgCOD/l	418	409	405	429	**-13**	**20**	621	635	700	666	**79**	**31**
Sulphide	mgCOD/l	300	301	313	319	**13**	**19**	568	568	609	599	**41**	**31**
Sulphate													
Sulphate	mgSO4/l	694	687	573	659	**-121**	**-28**	143	143	0	96	**-143**	**-47**
Nitrogen													
FSA	mgFSA/l	7.6	7.6	8.8	9.3	**1.2**	**1.7**	15.2	15.1	18.7	17.8	**3.6**	**2.6**
Phosphate													
OP	mgOP/l	2.3	2.3	2.1	2.3	**-0.1**	**0.0**	3.6	3.6	3.9	3.6	**0.4**	**0.0**
Alkalinity													
Carbonate	mg/l as CaCO3	502	501	583	527	**80**	**25**	875	874	950	916	**75**	**42**
Total	mg/l as CaCO3	692	706	779	741	**87**	**35**	1230	1263	1387	1320	**157**	**57**
Species													
VFA Conc	mg/l as acetate	0	0	12	0	**12**	**0**	0	1	85	0	**85**	**-1**
CT	mgC/l	126	126	149	133	**22**	**7**	221	221	242	232	**21**	**11**
Solids													
VSS	mgVSS/l	213	191	254	182	**41**	**-9**	536	508	721	494	**185**	**-14**
pH													
pH		7.6	7.6	7.5	7.5	**-0.1**	**0.0**	7.6	7.6	7.5	7.5	**-0.1**	**0.0**

Table 5. 22: Modelled SP2 and SP3 AugBSP control results

SP2 Control Model Results								SP3 Control Model Results					
		Start		End		Change		Start		End		Change	
COD	**Unit**	**Observed**	**Modelled**	**Observed**	**Modelled**	**Observed**	**Modelled**	**Observed**	**Modelled**	**Observed**	**Modelled**	**Observed**	**Modelled**
Total COD	mgCOD/l	1194	1194	1229	1194	**35**	**0**	917	833	936	833	**19**	**0**
Total Soluble COD	mgCOD/l	604	633	684	679	**80**	**46**	412	427	396	450	**-16**	**23**
Sulphide	mgCOD/l	521	521	560	566	**39**	**45**	324	324	351	347	**27**	**23**
Sulphate													
Sulphate	mgSO4/l	324	323	169	255	**-154**	**-68**	595	595	559	561	**-36**	**-34**
Nitrogen													
FSA	mgFSA/l	13.8	13.8	16.1	17.6	**2.3**	**3.8**	7.1	7.1	9.3	9.0	**2.2**	**1.9**
Phosphate													
OP	mgOP/l	3.0	3.0	3.4	3.0	**0.4**	**0.0**	2.7	2.7	3.8	2.7	**1.1**	**0.0**
Alkalinity													
Carbonate	mg/l as CaCO3	897	896	967	957	**70**	**61**	573	572	699	602	**127**	**31**
Total	mg/l as CaCO3	1223	1251	1401	1335	**177**	**84**	771	790	895	832	**123**	**42**
Species													
VFA Conc	mg/l as acetate	0	1	116	0	**116**	**-1**	0	1	0	0	**0**	**-1**
CT	mgC/l	226	226	245	243	**19**	**17**	145	145	182	154	**37**	**8**
Solids													
VSS	mgVSS/l	333	360	351	339	**18**	**-21**	287	263	626	252	**339**	**-11**
pH													
pH		7.6	7.6	7.5	7.5	0.0	-0.1	7.5	7.5	7.3	7.5	-0.2	0.0

The sulphate concentration decreased throughout the experiment, as sulphate was the electron acceptor for the production of sulphide. However, for the SC1, SP1 and SP2 experiments, the observed sulphate uptake was significantly higher than the modelled sulphate uptake. The PWM_SA_AD model is mass balanced; therefore, the modelled sulphate uptake was balanced with the sulphide produced. However, a good S balance was achieved in SP3 as the sulphide produced equated to the sulphate required in both the observed and modelled AugBSP control reactors.

The change in FSA and OP concentrations throughout all four experiments was low (<4mg/*l*). Moreover, in the modelled AugBSP control reactor, the observed change in the FSA concentration was well represented by the SC1, SP2 and SP3 experiments, and the observed change in OP was well represented for the SC1, SP1 and SP2 experiments. The higher OP ending concentration in the observed SP3 experiment was due to measurement error (this error was resolved in the modelled AugBSP control reactor by allowing the OP concentration to remain at the starting OP concentration, as shown in Figure 5.68). The visual comparison between the observed and modelled AugBSP experiments for the FSA and OP concentrations is given in Section 5.3.4.5 and Section 5.3.4.6, respectively.

The change in the carbonate alkalinity and the total alkalinity in the modelled AugBSP control reactor was lower than was observed for all four experiments. This discrepancy was noted despite the reasonably good match in sulphide COD concentration, as well as the FSA concentration produced in the observed and modelled AugBSP control reactor. This indicated towards the possibility of low C_T production being the cause of the simulated low carbonate alkalinity. This low C_T production is strongly linked to the carbon content of the biomass (i.e within the chosen composition of the biomass). However, the composition of the biomass was not changed during this investigation and remained fixed at the composition determined by Porges and Hoover (1952).

The total alkalinity generated in the AugBSP control reactor was dependent on the composition of the biodegradable organics. The production of sulphide by the SRB generates alkalinity within the system. The sulphate utilised in the modelled AugBSP reactor was lower than was observed for the SC1, SP1 and SP2 experiments. As the modelled AugBSP control reactor was mass balanced, the sulphide produced by the model influenced the sulphate uptake, as well as the total alkalinity generated.

The modelled AugBSP control reactor replicated the sulphide COD concentration produced in the observed experiments well. However, the observed AugBSP reactor may have produced more sulphide than was measured, which would explain the higher observed sulphate usage, as well as the higher observed total alkalinity. However, in the SP3 experiment, even though the sulphide COD concentration, as well as the sulphate concentration, was well replicated by the modelled AugBSP control reactor, the total alkalinity generated by the model remained low.

The observed SC1, SP1 and SP2 experiments produced VFA throughout the experiment. This production of VFA in the modelled AugBSP control reactor was not replicated, as the uptake rate of the acetoclastic sulphidogens (mu_AS), as well as the half-saturation coefficient of the acetoclastic sulphidogens (KS_AS), was not changed. The production of VFA in the observed AugBSP control reactor was challenging to explain. The biomass decay did not rapidly produce glucose, as the death rate of the organism was low. Therefore, the increase in VFA throughout the observed AugBSP control experiment may have been due to error involved in the 5-point titration method, or alternatively, a missing intermediate in the PWM_SA_AD model.

To virtually replicate the experimental set up, whereby the sulphidogenic SSPAD was used to seed the AugBSP reactors, the starting VSS concentration of the modelled AugBSP control experiment was entirely dependent on the VSS concentration of the modelled sulphidogenic SSPAD effluent (i.e. the starting AugBSP VSS was modelled to stay the same as the effluent from the SSPAD). The modelled AugBSP reactor replicated the observed VSS concentration well for all four experiments when using the entire data set, which is shown visually in Section 5.3.4.9 (Figures 5.77 to 5.80). As noted in the Figures 5.77 to 5.80, the VSS concentration in the modelled AugBSP control reactor decreased throughout the experiment, which was expected as the biomass decayed.

5.3.4.1 Total COD

The only COD concentration adjustment made in the modelled AugBSP control reactor at the start of each experiment was the sulphide COD concentration. The remaining COD concentrations were unchanged and were taken directly from the modelled sulphidogenic

SSPAD effluent. Consequently, the total COD concentration in the observed AugBSP control reactor was replicated by the modelled AugBMP control reactor for all four experiments well.

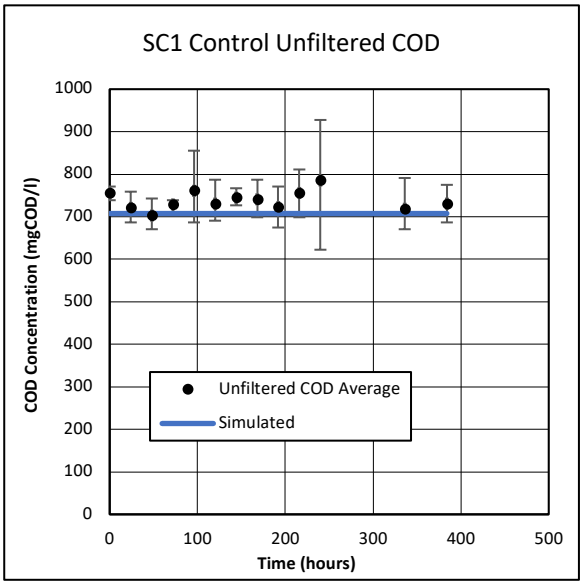

Figure 5. 45: SC1 AugBSP control total COD

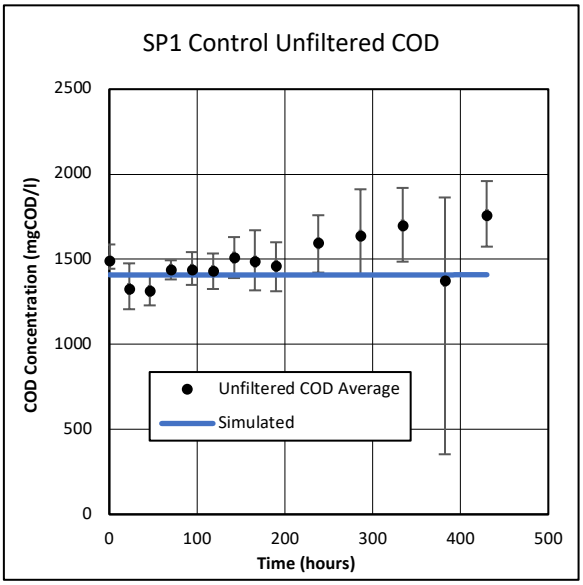

Figure 5. 46: SP1 AugBSP control total COD

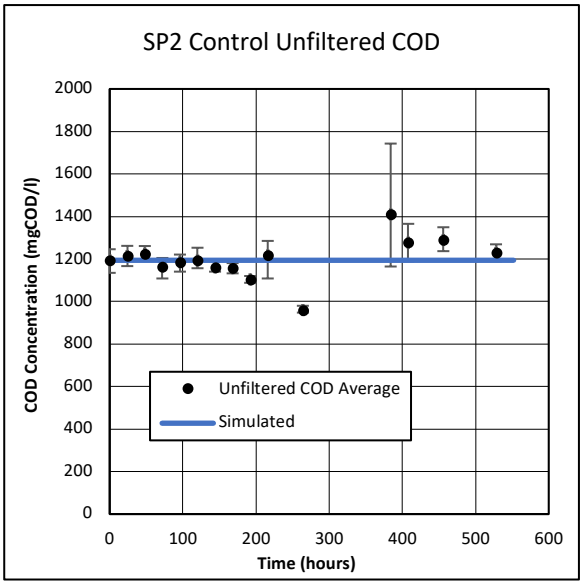

Figure 5. 47: SP2 AugBSP control total COD

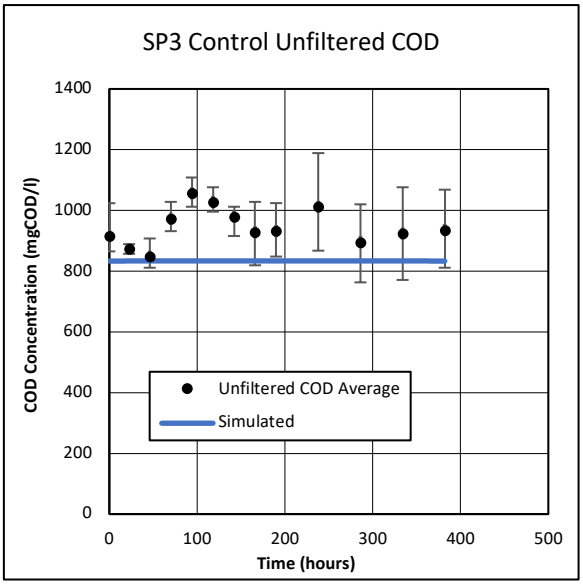

Figure 5. 48: SP3 AugBSP control total COD

5.3.4.2 Soluble COD

The starting soluble COD concentration in the modelled AugBSP control reactor depended on the soluble organic COD, the soluble sulphide COD and the USO COD concentrations. As mentioned, the soluble sulphide COD concentration in the modelled AugBSP control reactor was adjusted to the observed starting concentration, while the remaining COD concentrations

remained unchanged. The production of sulphide due to the biomass decay increased the total soluble COD. Consequently, the soluble COD concentrations were replicated by the model well, indicating that the soluble COD and the USO COD concentrations in the modelled sulphidogenic SSPAD effluent were accurate.

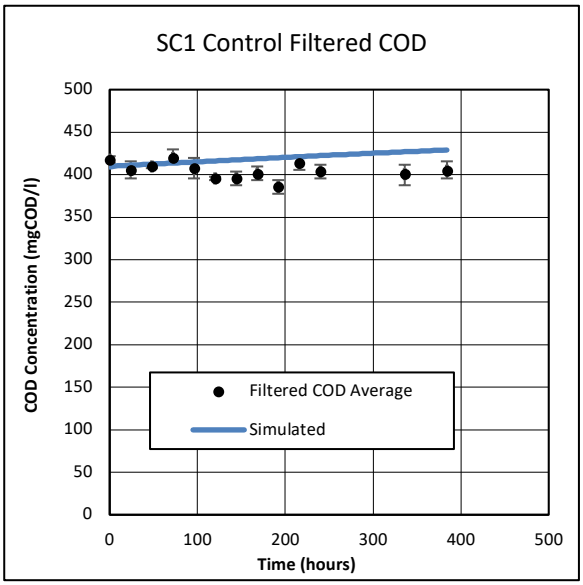

Figure 5. 49: SC1 AugBSP control soluble COD

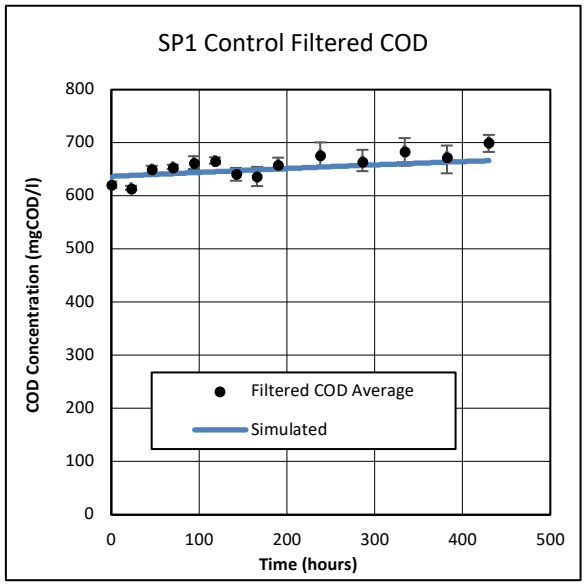

Figure 5. 50: SP1 AugBSP control soluble COD

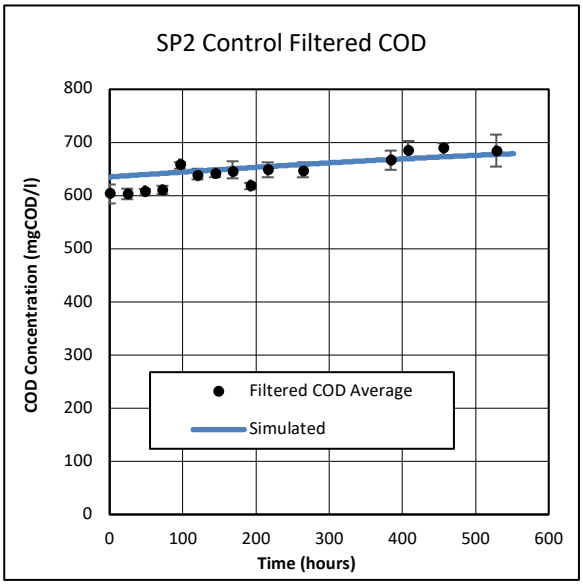

Figure 5. 51: SP2 AugBSP control soluble COD

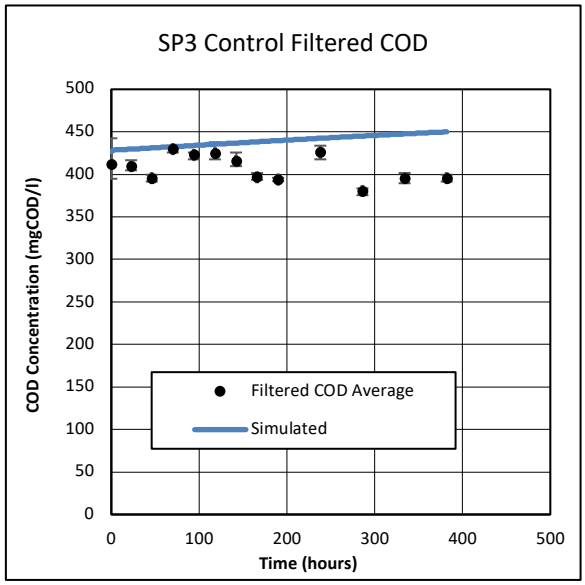

Figure 5. 52: SP3 AugBSP control soluble COD

5.3.4.3 Soluble Sulphide COD

The observed soluble sulphide COD concentration change was well replicated by the modelled AugBSP control reactor for all four experiments. The increase in sulphide COD concentration

due to the biomass decay indicated that the biomass composition of Porges and Hoover (1952), as well as the biomass death rate in the model, were a good representation of the organics present in the sulphidogenic SSPAD in terms of electron donating capacity (COD).

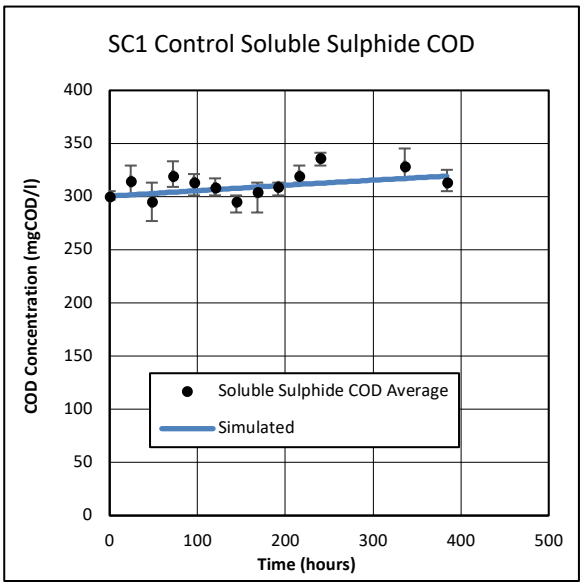

Figure 5. 53: SC1 AugBSP control soluble sulphide COD

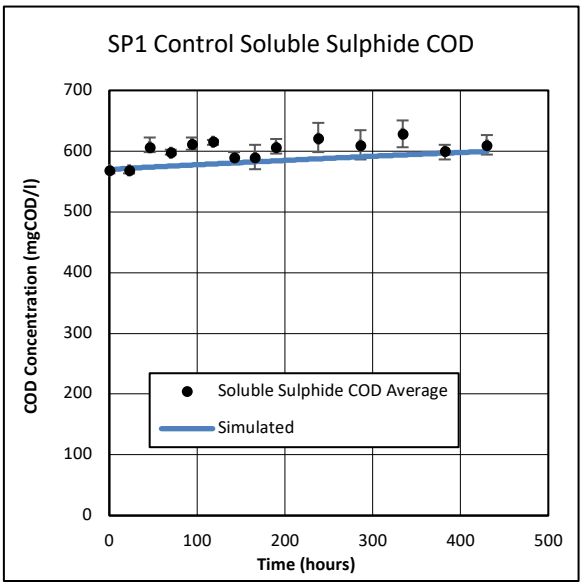

Figure 5. 54: SP1 AugBSP control soluble sulphide COD

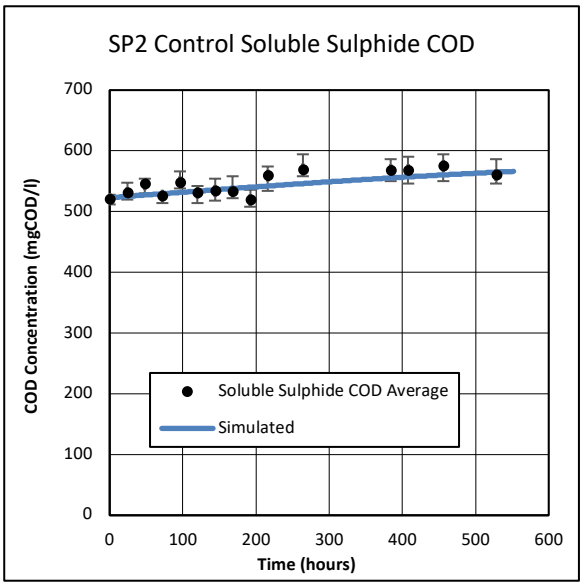

Figure 5. 55: SP2 AugBSP control soluble sulphide COD

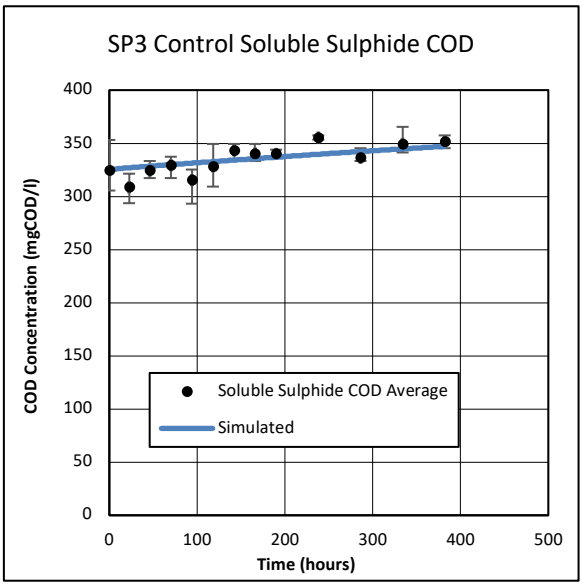

Figure 5. 56: SP3 AugBSP control soluble sulphide COD

5.3.4.4 Sulphate

The sulphate concentration utilised during the modelled AugBSP control experiments was replicated by the concentration of sulphide produced, as the PWM_SA_AD model was mass balanced. The sulphate utilised by the modelled AugBSP in SC1 (Figure 5.57) followed the

trajectory of the observed sulphate concentration for the first 100 hours, after which the observed sulphate concentration dropped by 112 $mgSO_4/l$ over 24 hours. This rapid drop in sulphate concentration was not reflected in the sulphide COD measurements, making the source of the error challenging to identify.

The sulphate concentration in the observed SP1 experiment (Figure 5.58) dropped rapidly over the first 100 hours until it was completely utilised. Following the complete utilisation of sulphate in both control reactors (C1 and C2), additional sulphate was added to the C2 reactor. Subsequently, the C2 control reactor concentration decreased slightly (18$mgSO_4/l$) and then stabilised (~270$mgSO_4/l$). However, the modelled AugBSP control reactor did not completely utilise the available sulphate, which gradually decreased. Furthermore, the gradual decrease in sulphate was reflected by the gradual increase in sulphide.

The sulphate concentration decrease in the modelled SP2 experiment (Figure 5.59) was also gradual when compared to that of the observed sulphate concentration decrease in SP2. However, in the modelled SP3 experiment (Figure 5.60), the decrease in the sulphate concentration between the start and end of the experiment agreed well with the observed SP3 sulphate decrease, which suggested that S was conserved between the sulphate utilised and the sulphide produced.

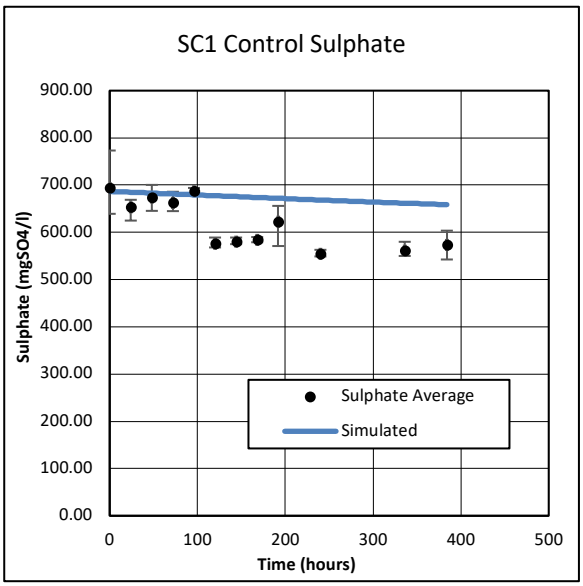

Figure 5. 57: SC1 AugBSP control sulphate

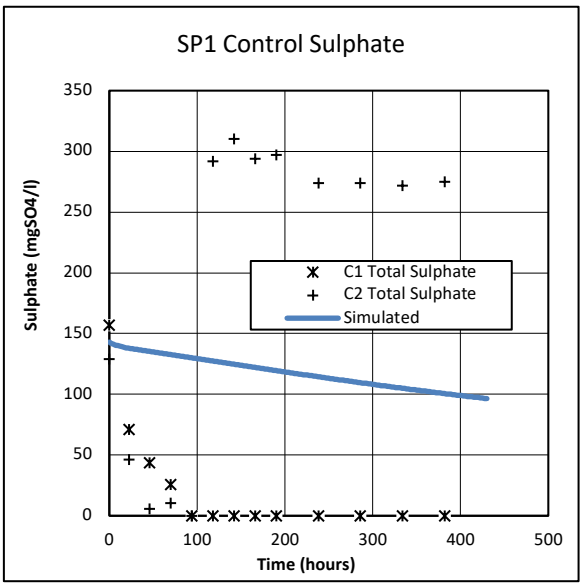

Figure 5. 58: SP1 AugBSP control sulphate

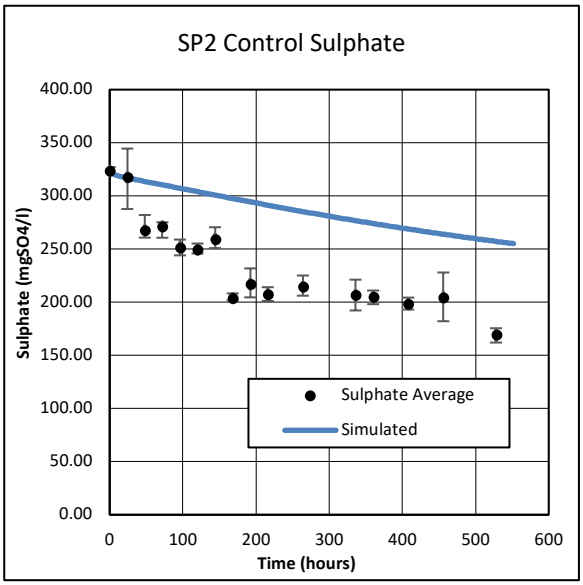

Figure 5. 59: SP2 AugBSP control sulphate

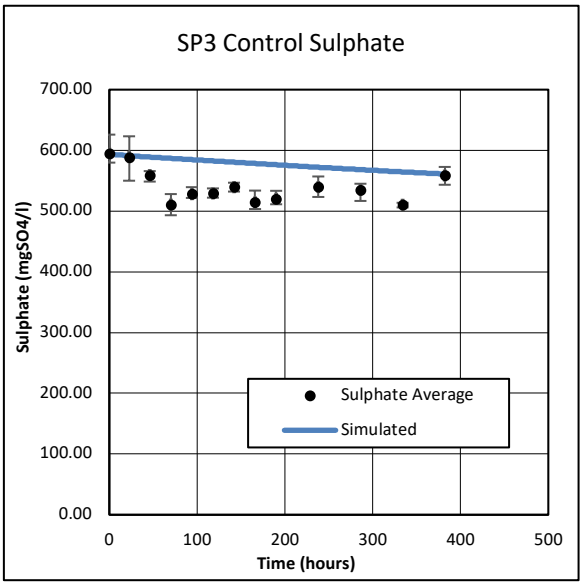

Figure 5. 60: SP3 AugBSP control sulphate

5.3.4.5 Free and Saline Ammonia (FSA)

Figures 5.61, 5.62, 5.63 and 5.64 show that the observed FSA concentration increase was replicated by the modelled AugBSP control reactor well for all four experiments. The rate at which the FSA was released into the aqueous phase was a good indication of the particulate organics hydrolysis rate (which in this case was the death rate of the organisms) as the organic N contained in the BPO subsequently became FSA during the breakdown of the organics.

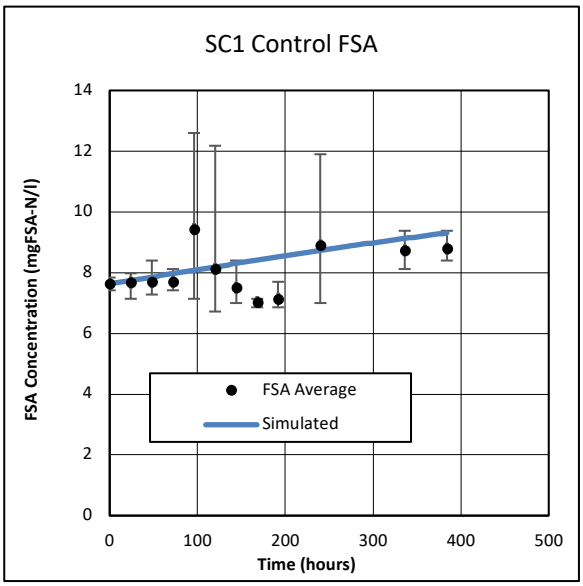

Figure 5. 61: SC1 AugBSP control FSA

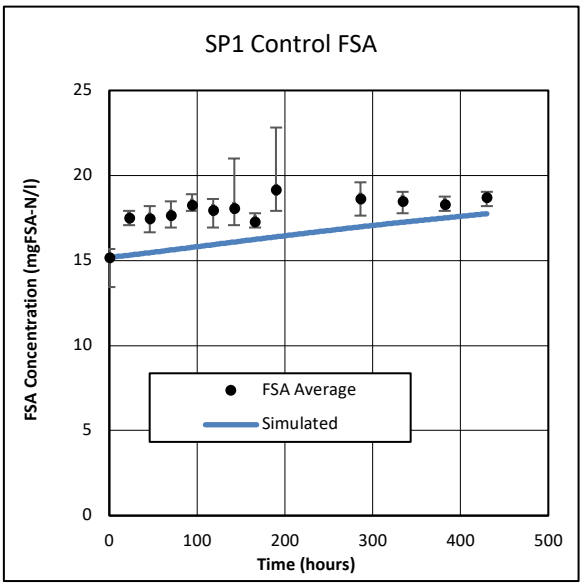

Figure 5. 62: SP1 AugBSP control FSA

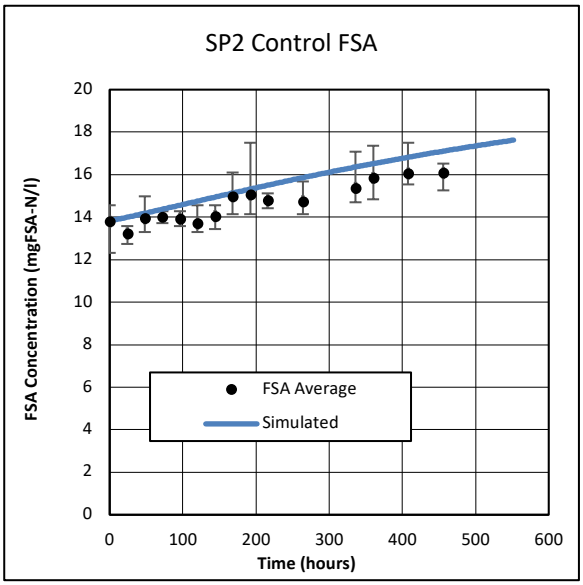

Figure 5. 63: SP2 AugBSP control FSA

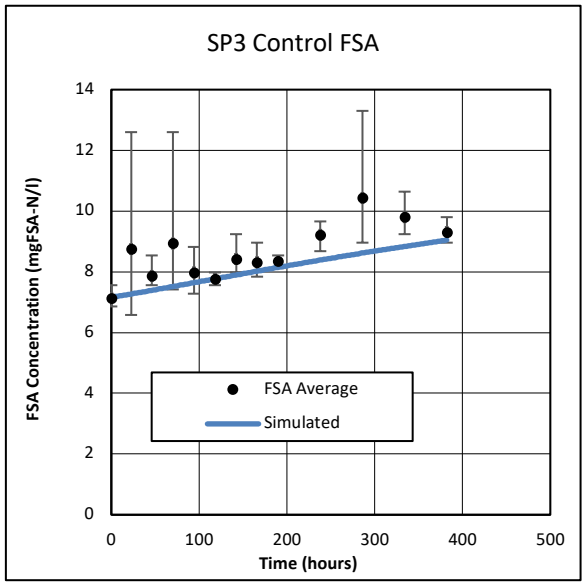

Figure 5. 64: SP3 AugBSP control FSA

5.3.4.6 Orthophosphate (OP)

Figures 5.65, 5.66, 5.67 and 5.68 show that the release of OP into the AugBMP control reactor liquid for all for experiments was relatively low (0 to 1mgOP/*l*), which indicated that the organic P content in the biodegradable organics was low. The low P release due to the biodegradable organics was expected as the biomass composition of Porges and Hoover (1952) did not contain any P ($C_1H_{1.4}O_{0.4}N_{0.2}$).

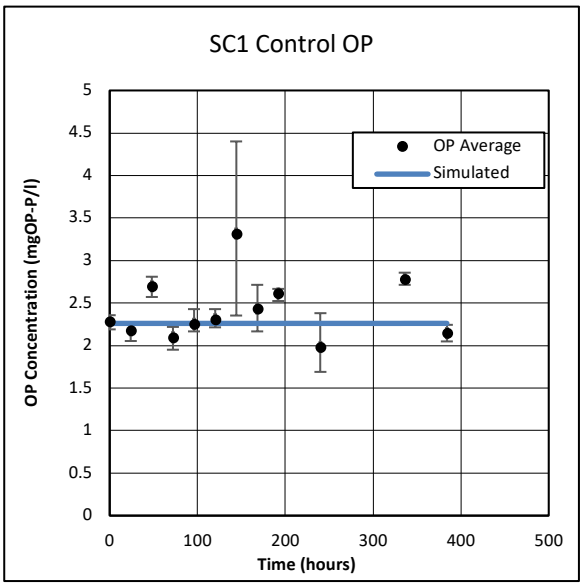

Figure 5. 65: SC1 AugBSP control OP

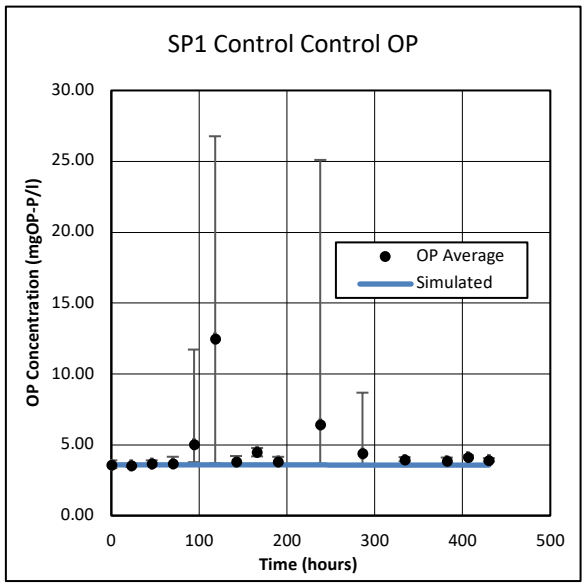

Figure 5. 66: SP1 AugBSP control OP

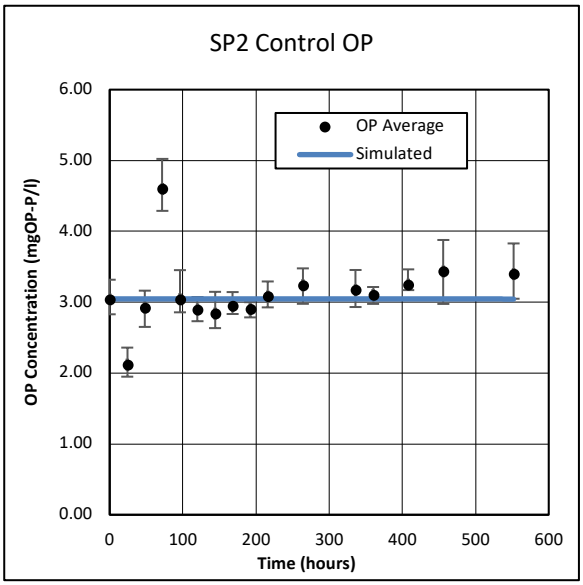

Figure 5. 67: SP2 AugBSP control OP

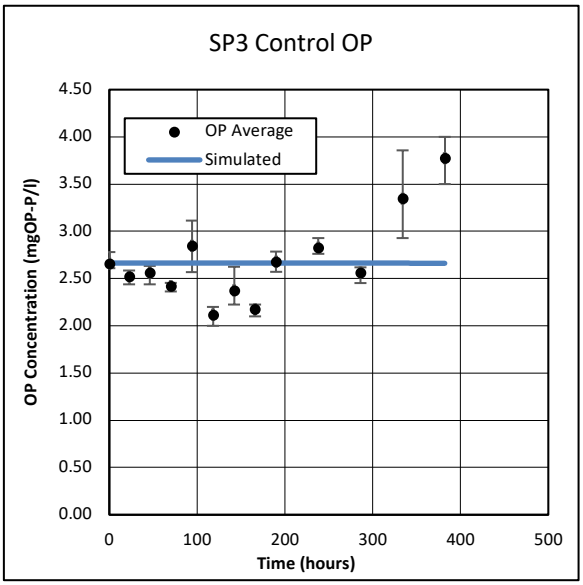

Figure 5. 68: SP3 AugBSP control OP

5.3.4.7 Carbonate Alkalinity

As mentioned in Section 5.2.6.3, the release of FSA into the reactor liquid due to the breakdown of organics directly influences the carbonate alkalinity concentration. The carbonate alkalinity concentrations for the observed SP1 and SP2 experiments (Figures 5.70 and 5.71) were replicated by the modelled AugBSP control reactor well. However, the observed carbonate alkalinity concentrations for SC1 and SP3 (Figures 5.69 and 5.72) were higher than the carbonate alkalinity increase predicted by the model. The reason for this was possibly due to the higher C_T concentration present in the observed AugBSP control reactor, which was influenced by the composition of the biodegradable organics.

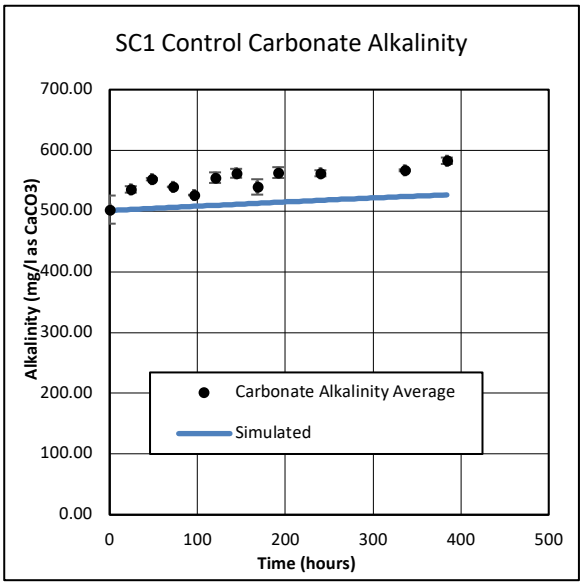

Figure 5. 69: SC1 AugBSP control carbonate alkalinity

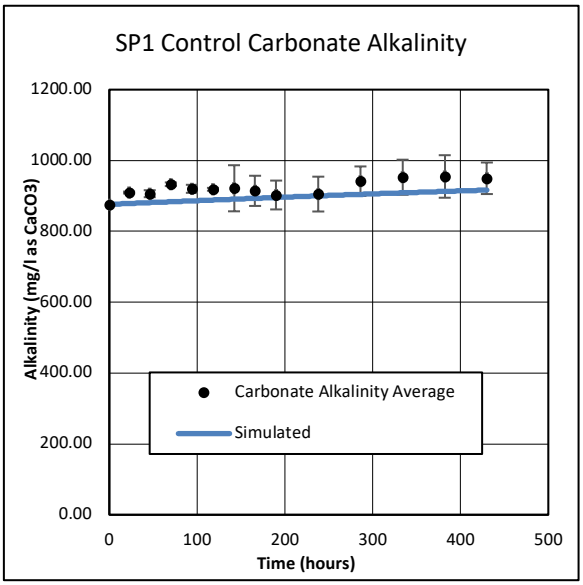

Figure 5. 70: SP1 AugBSP control carbonate alkalinity

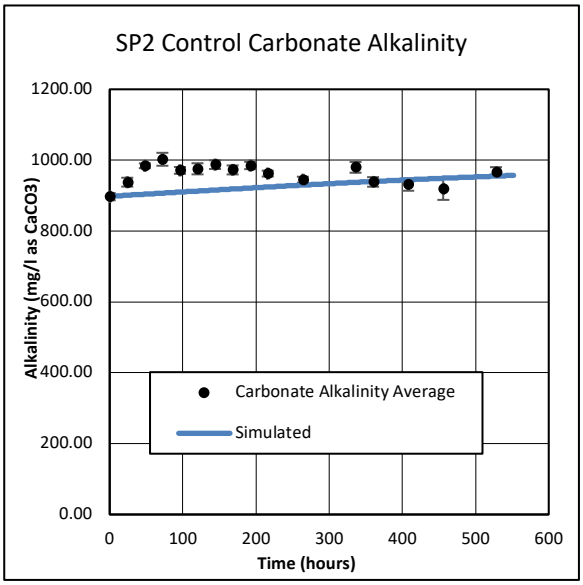

Figure 5. 71: SP2 AugBSP control carbonate alkalinity

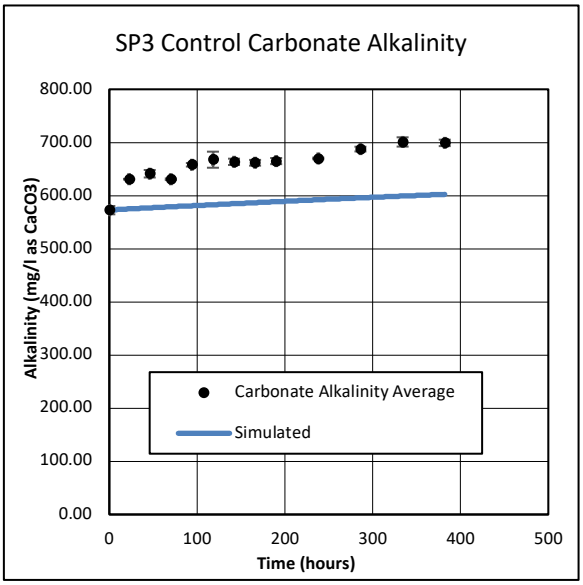

Figure 5. 72: SP3 AugBSP control carbonate alkalinity

5.3.4.8 Total Alkalinity

The total alkalinity of the system is a conservative parameter. In BSR systems, the total alkalinity is influenced by the release of material into the reactor liquid, due to the breakdown of organics, as well as the alkalinity generated by the conversion of sulphate to sulphide. Therefore, the total increase in alkalinity observed in the AugBSP control reactor was entirely defined by the composition of organics fed to it, which controlled the concentration of sulphide produced, as the available electron donating capacity (COD) was a consequence of the biodegradable organics.

As mentioned in Section 5.2.6.3, the release of FSA into the reactor liquid increases the total alkalinity through the re-speciation of NH_3 to NH_4^+; therefore, making the N content of the influent organics intrinsic alkalinity. As mentioned in Section 2.5.4, most organics found in wastewater are 'carbon deficient'. Therefore, another system has to provide the shortfall for the required alkalinity increase. For BSR, the sulphide system provides the required alkalinity in the form of HS^-.

The observed total alkalinity generated in the SP1 experiment (Figure 5.74) was replicated by the modelled AugBSP control reactor well, indicating that the composition of the organics was accurately represented in the model. However, this outcome was interesting, as the modelled SP1 experiment correctly replicated the FSA increase, as well as the sulphide concentration increase, but underpredicted the sulphate concentration used by the reaction. Therefore, even though the sulphate concentration was completely utilised in the observed SP1 experiment (which was not reflected in the model), the model was still able to predict the increase in carbonate alkalinity, as well as the increase in total alkalinity, accurately. The discrepancy suggests an error for the sulphate measurements.

However, the total alkalinity for the modelled SC1 (Figure 5.73), SP2 (Figure 5.75) and SP3 (Figure 5.76) experiments were lower than what was observed. This outcome suggested that not enough alkalinity was generated by the modelled AugBSP control reactor relative to the observed reactor. The reason for the low total alkalinity generated may be due to the carbon content of the biodegradable organics, that form part of the biomass, for which the composition was taken to be $C_1H_{1.4}O_{0.4}N_{0.2}$ (Porges and Hoover, 1952).

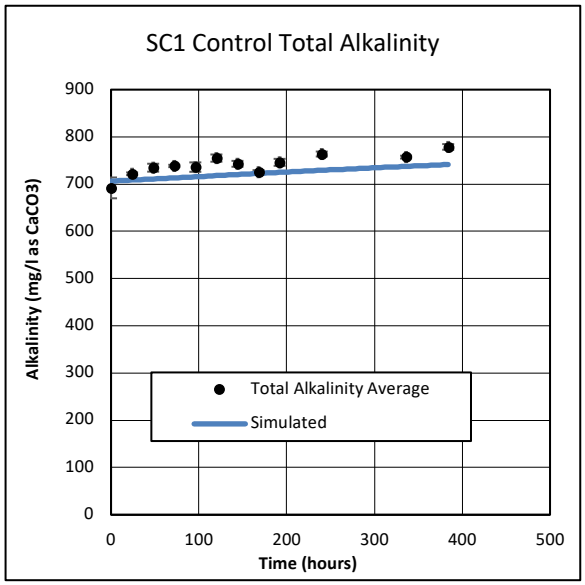

Figure 5. 73: SC1 AugBSP control total alkalinity

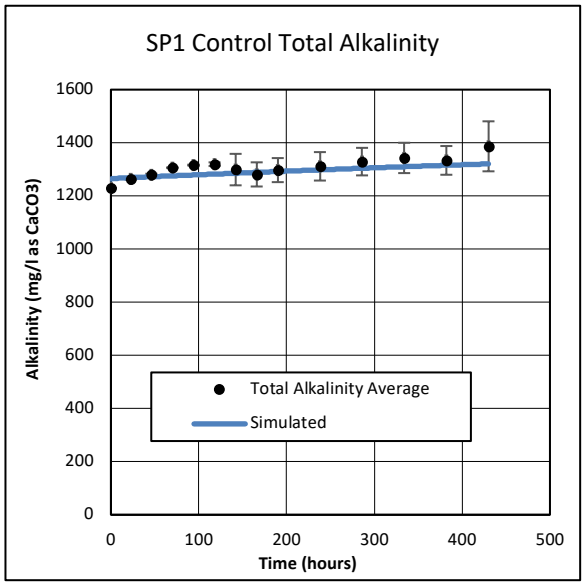

Figure 5. 74: SP2 AugBSP control total alkalinity

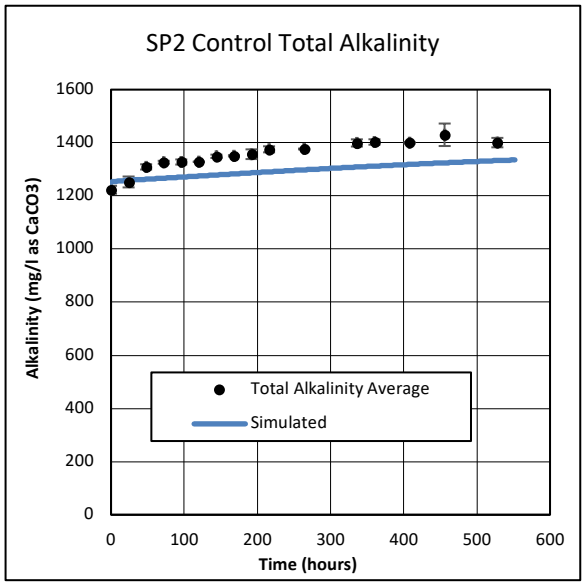

Figure 5. 75: SP2 AugBSP control total alkalinity

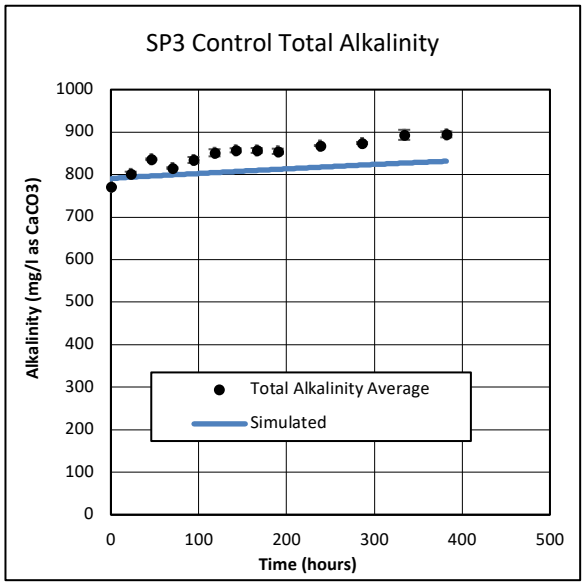

Figure 5. 76: SP3 AugBSP control total alkalinity

5.3.4.9 Volatile Suspended Solids (VSS)

Figures 5.77, 5.78, 5.79 and 5.80 show that the VSS concentration in the observed AugBSP control reactor fluctuated throughout the experiment. Furthermore, the variance of the observed VSS concentrations was high. However, the PSS concentration fed to the sulphidogenic experiments was diluted to avoid sulphide inhibition within the system. Therefore, it is possible, that due to the low concentrations used in the sulphidogenic experiments, the accuracy of the method used to determine the VSS concentration was negatively affected. The

decrease in accuracy may have occurred as the mass intervals used became smaller. Therefore, precise equipment was required to increase the resolution of the measurement, to 4 decimal places of a gram (0.1mg), for instance. Consequently, the calibration, the age, the maintenance and the operation of the equipment becomes essential in order to provide accurate measurements. Therefore, the high variance associated with the VSS concentration may have been caused by an experimental error when working with samples containing a low solid mass.

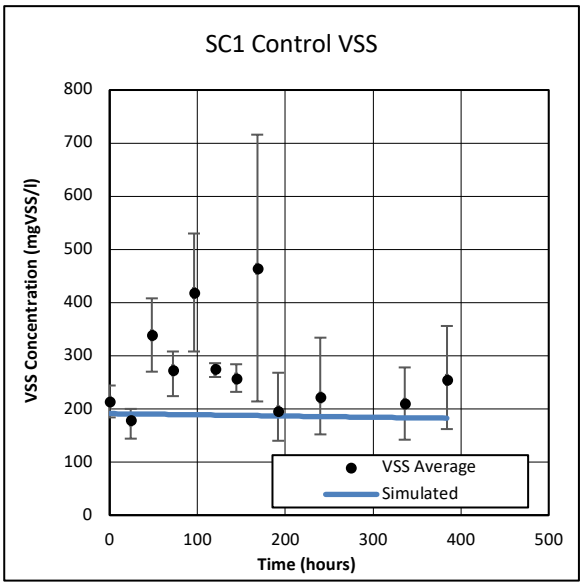

Figure 5. 77: SC1 AugBSP control VSS

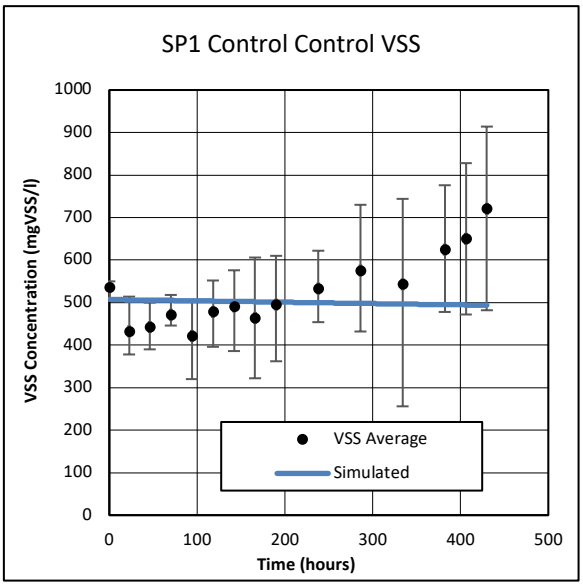

Figure 5. 78: SP1 AugBSP control VSS

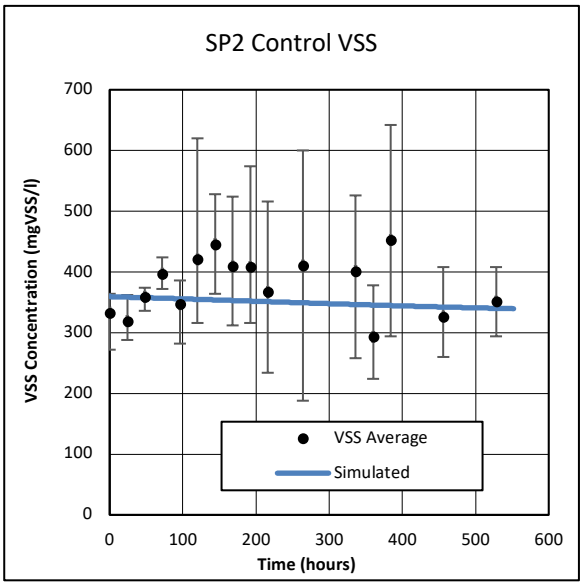

Figure 5. 79: SP2 AugBSP control VSS

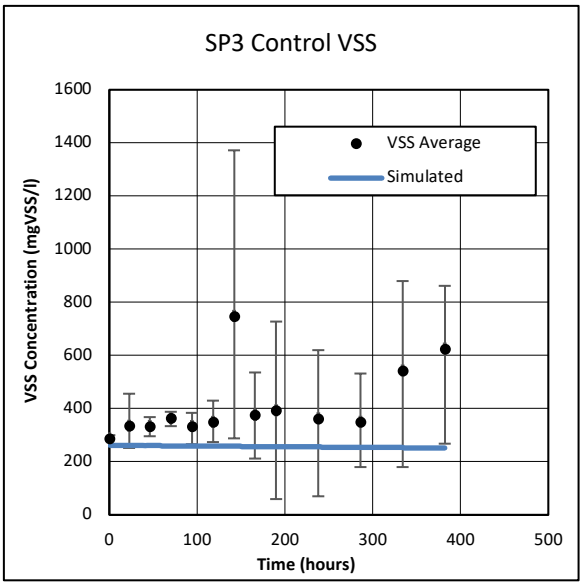

Figure 5. 80: SP3 AugBSP control VSS

However, the modelled AugBSP control reactor replicated the starting VSS concentrations of the observed AugBSP reactor well. As mentioned, the VSS concentration was not adjusted at

the start of the modelled experiments and was taken directly from the modelled sulphidogenic SSPAD effluent.

5.3.4.10 Volatile Fatty Acids (VFA)

Figures 5.81, 5.82, 5.83 and 5.84 show the VFA concentrations for both the observed and modelled experiments. The VFA concentration was determined using the 5-point titration method, as described in Section 3.6.7. The modelled SC1 and SP3 experiments replicated the observed experiments well, as the VFA concentration remained low, except for a few outliers. However, the increase in VFA for the SP2 experiment (Figure 5.83) was significant (>100mgCOD/*l*, converted by taking mg/*l* as acetate and multiplying by 64/60). This increase in VFA COD was not reflected in the increase in soluble COD concentration (80mgCOD/*l*, of which 40mgCOD/*l* was due to sulphide COD).

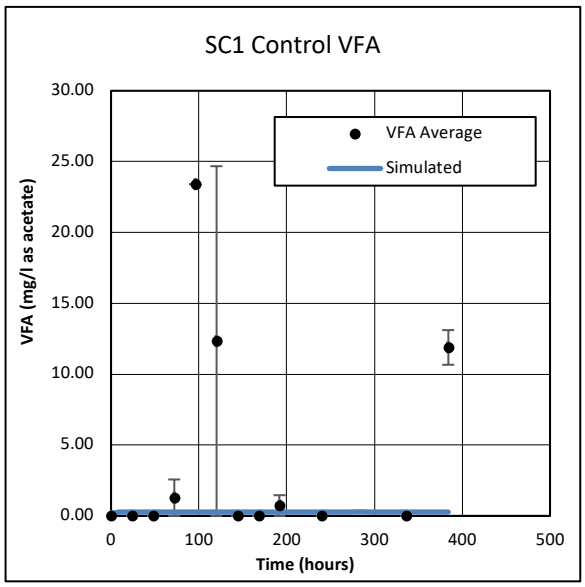

Figure 5. 81: SC1 AugBSP control VFA

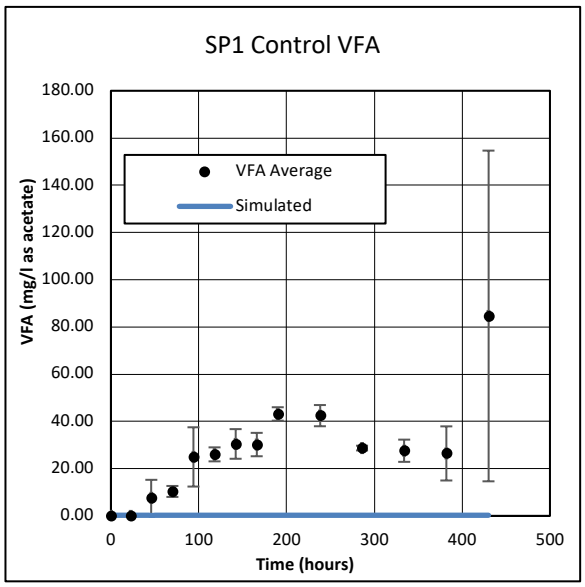

Figure 5. 82: SP1 AugBSP control VFA

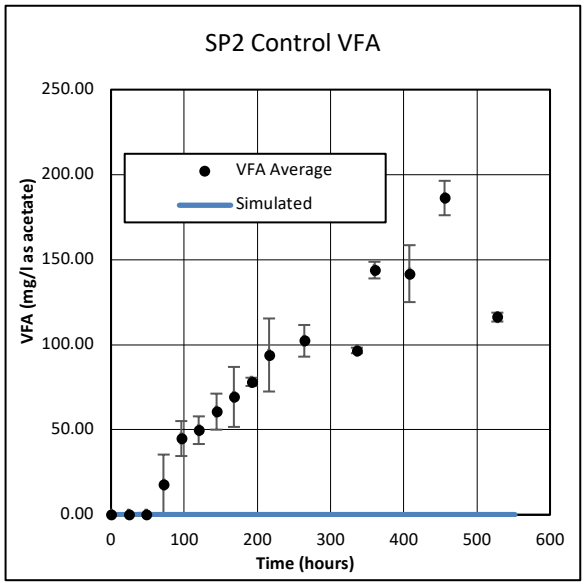

Figure 5. 83: SP2 AugBSP control VFA

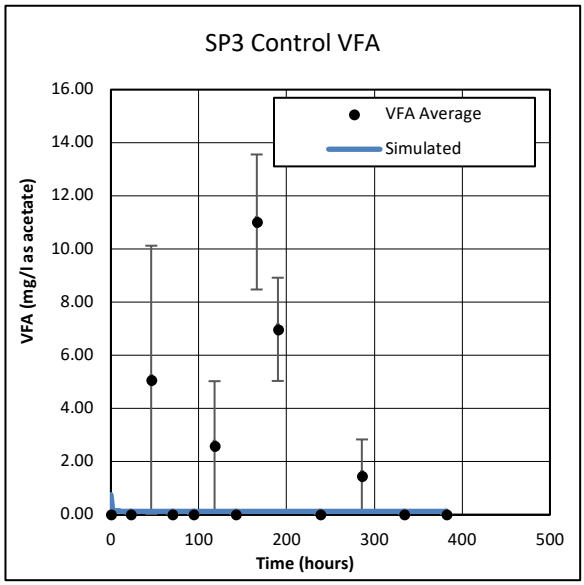

Figure 5. 84: SP3 AugBSP control VFA

Figure 5.83 shows an increase in VFA concentration throughout the observed SP2 AugBSP control experiment. The increase in VFA was challenging to explain as it was believed that the only biodegradable material present was that of the biomass in the SSPAD effluent. Therefore, this increase in VFA was not considered by the modelled SP2 control experiment.

5.3.4.11 pH

Figures 5.85, 5.86, 5.87 and 5.88 show the reactor pH for both the observed and modelled experiments. The pH of the observed AugBSP remained constant (pH of 7.50) throughout all four experiments. The modelled AugBSP control replicated the observed reactor well for the pH measurements.

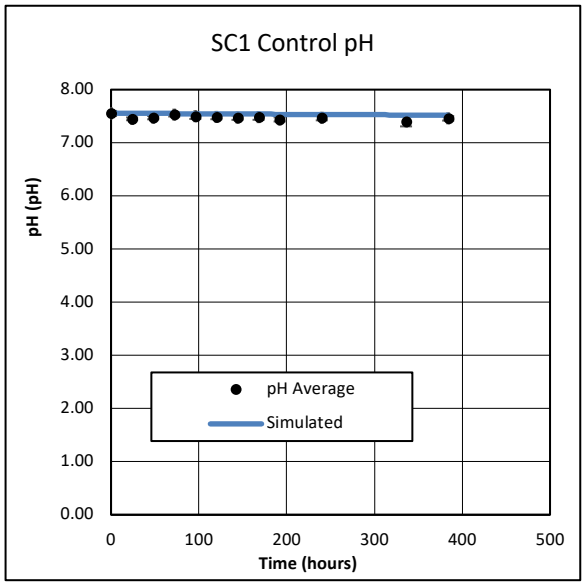

Figure 5. 85: SC1 AugBSP control pH

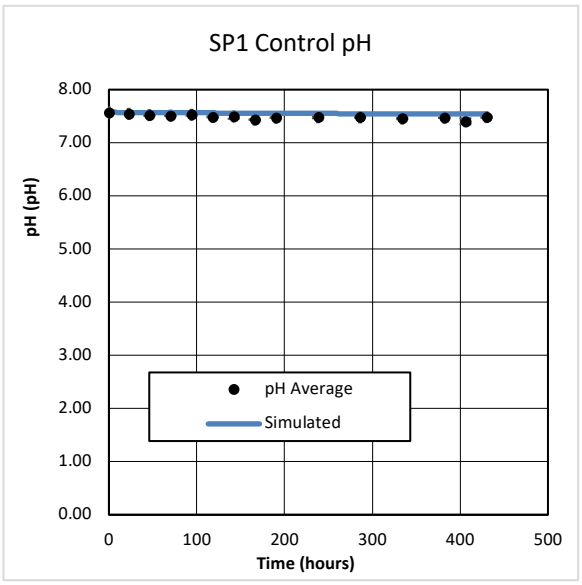

Figure 5. 86: SP1 AugBSP control pH

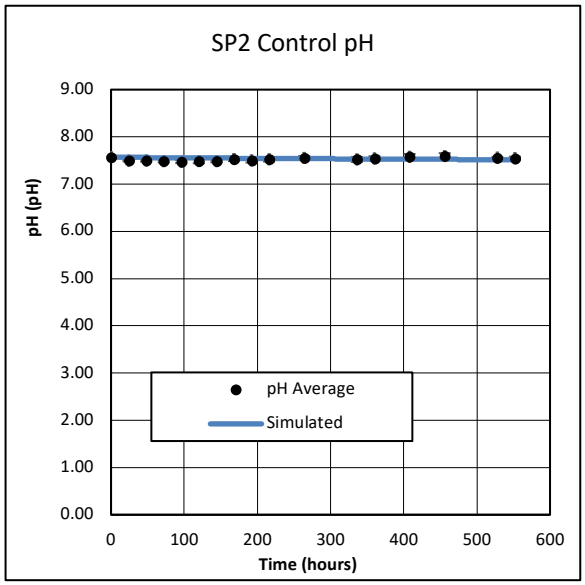

Figure 5. 87: SP2 AugBSP control pH

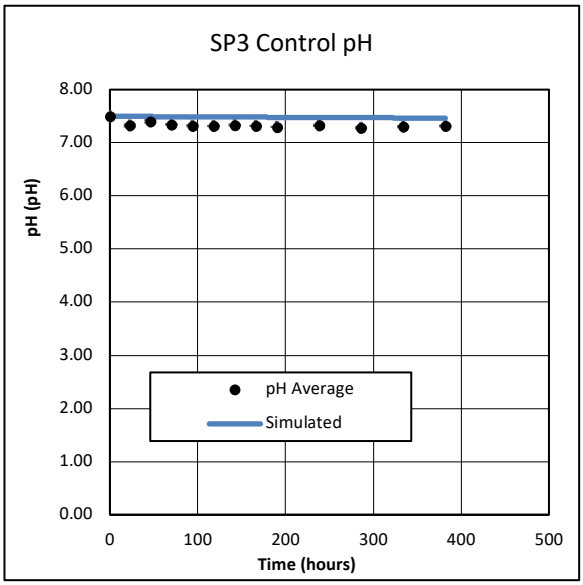

Figure 5. 88: SP3 AugBSP control pH

5.4 Conclusions

The augmented control reactors were used to establish the baseline for the biodegradable material present in the inoculum. The release of material above this baseline was due to the breakdown of the organics in the chosen substrate. The stoichiometric composition identification calculation highlighted the influence that measurement error had on accurately determining the biodegradable material present in the control reactors (baseline). Therefore,

the PWM_SA_AD model was used for data reconciliation, as the entire data set could be utilised to identify the composition of the organics, minimising the measurement error. The ability of the models to replicate and predict the observed measurements for the augmented control reactors highlighted the value of using computer modelling to reconcile the results, especially when measurement error occurred.

The AugBMP control reactor was modelled differently to the AugBSP control reactor, as it contained residual biodegradable organics and biomass, whereas the modelled AugBSP control reactor only contained biomass. The modelled AugBMP control reactor utilised the PE function to identify the composition of residual biodegradable organics present in the inoculum. The modelled AugBMP control replicated the observed results by adjusting the mass and composition of the residual biodegradable organic, as well as the uptake rate and half-saturation coefficient of the acetoclastic methanogens. Therefore, the modelled AugBMP control reactor had more flexibility than the modelled AugBSP control reactor, as the parameters could be adjusted to replicate the desired results. Consequently, this allowed for a higher acceptable error for the active biomass concentrations determined by the modelled methanogenic SSPAD, as the parameters in the model were adjusted to compensate for any error in the active biomass.

However, the modelled AugBSP control reactor was entirely dependent on the concentrations of the biomass determined in the modelled sulphidogenic SSPAD, as well as the chosen composition. The PE function was not used for the AugBSP control reactor, and subsequently, the release of material into the reactor liquid was completely dependent on the biomass decay. Therefore, the accuracy of the modelled AugBSP control reactor depended on the accuracy of the active biomass concentrations determined by the modelled sulphidogenic SSPAD. The outcome of the modelled AugBSP control experiments confirmed that the sulphidogenic SSPAD was modelled accurately.

It is important to note that it was not suggested that the models were correct, and the observations were incorrect. The models were a useful tool in assessing the accuracy of the methods used, as well as the parameters determined. Furthermore, the composition of the biodegradable organics was identified using the modelled control reactor as the measurement error was minimised by using the PE function for the entire data set.

Furthermore, the composition of the biodegradable material in the augmented control reactors should be grouped into one collective composition, which includes both the biomass and residual organics. This grouped composition would significantly decrease the parameters required for determining the baseline for the augmented test reactors, as the PE function could be used on the augmented control reactors to determine the required parameters without the need for modelling the SSPADs from which the inoculum was taken.

Chapter 6: Augmented batch test reactor results and modelling

6.1 Introduction

The augmented batch test reactors were used to identify the composition of the biodegradable organics present in the chosen substrates. Two different substrates were used in the augmented batch test experiments, a soluble substrate (casein) and a particulate substrate (PSS). The approach for each was the same, i.e. the inoculum was taken from each respective SSAPD. Furthermore, the augmented batch control reactors were used to identify the breakdown of residual material present in the SSPAD effluent, which quantified the baseline, above which the material released into the augmented test reactors was due to the breakdown of the chosen organic substrates. The augmented batch test experiments differed with regards to the chosen substrate, as casein hydrolysate was used in the MC1 and SC1 experiments, and PSS was used in the MP1, MP2, MP3, and the SP1, SP2, SP3 experiments.

Therefore, this chapter involved the analysis of results obtained by both the methanogenic and sulphidogenic augmented test experiments. It has two main sections (1) the analysis is performed for results where casein was used as an organic substrate and (2) the analysis is performed for results where PSS is used as the organic substrate. The analytical process included: data evaluation by checking material mass balances, using mass balanced stoichiometry and mathematically modelled augmented batch tests towards identifying the substrate composition (as shown in Sections 3.92 and 3.93).

As described in Chapter 4 and in Chapter 5, both the AugBMP and the AugBSP experiments were repeated four times each. Therefore, the four augmented batch test experiments corresponded to the four SSPAD experiments described in Chapter 4, and the four augmented control experiments described in Chapter 5. This is summarised in Table 6.1.

Table 6. 1: Experiment Periods

Label	Type of Experiment	Date of Experiment
MC1	Methanogenic Casein	February – March 2019
MP1	Methanogenic PSS	February – March 2018
MP2	Methanogenic PSS	May-June 2018
MP3	Methanogenic PSS	December 2018
SC1	Sulphidogenic Casein	March 2019
SP1	Sulphidogenic PSS	November 2018
SP2	Sulphidogenic PSS	January – February 2019
SP3	Sulphidogenic PSS	April 2019

The AugBMP test and the AugBSP test experiments were conducted as specified in Section 3.4 and Section 3.5, respectively. In order to achieve reliable results, the AugBMP test experiment was conducted in triplicate, using three test reactors, and the AugBSP test experiment was conducted in duplicate, using two test reactors. The test reactors were labelled T1, T2 and T3 for the AugBMP test, and T1 and T2 for the AugBSP test. The inoculum was removed from each of the respective SSPADs on the day that the experiment started and was inserted directly into the AugBMP/AugBSP reactors. However, it is important to note that the AugBMP and AugBSP tests for casein were not conducted simultaneously, but rather consecutively, starting with the AugBMP experiment.

The seeding procedure for the AugBMP and AugBSP tests is described in Section 3.4.3 and Section 3.5.3, respectively. The AugBMP test reactors were seeded with inoculum, tap water and substrate. The AugBSP test reactors were seeded with inoculum, substrate and the sulphate solution (prepared using sodium sulphate and sulphuric acid). The volume of inoculum added to each respective augmented test reactor was half the volume of inoculum added to the augmented control reactor. Therefore, the influence of the inoculum (i.e. the products released into solution/ the gas generated) as measured by the augmented control reactors, was halved in the augmented test reactors.

The concentration of each constituent in the AugBMP and AugBSP test reactors was measured using the analytical procedures described in Section 3.6. The measured values in each of the AugBMP reactors (T1, T2 and T3) were combined into one value by calculating the average

constituent value between the reactors. Similarly, the measured values in each of the AugBSP reactors (T1 and T2) were combined into one value by calculating the average constituent value between the reactors.

6.2 Casein Experiment

The purpose of this experiment was to evaluate the accuracy of the augmented batch experiments when characterising a known stable organic substrate, casein, into its elemental composition represented by CHONP. Furthermore, the experiment utilised a soluble substrate, as opposed to that of a particulate substrate. Therefore, diversifying the biodegradable substrate used in the augmented batch experiments. The properties of casein were described in Section 2.6.

The chemical composition of the biodegradable substrate impacts the mass of COD available, the alkalinity generated, and the organic carbon available. Casein is one of the primary protein sources present in cow's milk. Casein was chosen for this experiment as it contains organically bound nitrogen (N) and phosphorus (P), similar to the N and P contained in the biodegradable organics present in Primary Sewage Sludge (PSS). The experiment described in this section aimed to achieve the following:

- Determine the elemental composition of casein using both the AugBMP and AugBSP experiments, which included utilising the PE function within the PWM_SA_AD model.
- Compare the composition identified by the AugBMP and AugBSP experiments to that of the literature stated composition for casein.
- Compare the concentrations of the products released by casein into the bulk liquid of each experiment.
- Conclude on the accuracy and usability of each test (AugBMP and AugBSP) as a means for substrate characterisation.
- Conclude if the dynamics of each experiment can be virtually replicated using the proposed PWM_SA_AD model.
- Identify the error associated with the proposed testing methods or modelling procedure.

6.2.1 AugBMP test casein mixture

The casein hydrolysate was available in a powder form, and was subsequently added to water to form a casein solution. The prepared casein solution was stirred using a magnetic stirrer until the powder was homogenously mixed. The casein solution for the AugBMP test experiment (MC1) was prepared by adding 70g of powdered casein hydrolysate into 1.5l of deionised water. After 15 minutes of stirring, 1.25l of the casein solution was added to the AugBMP test reactor starting mix, as shown in Section 3.4.3. The 70g of casein hydrolysate was used to achieve a COD concentration consistent with that of the PSS fed to the methanogenic SSPAD. The casein hydrolysate used was tested using the analytical procedures described in Section 3.6, the results for which are given in Section 6.2.9. The casein solution was further diluted by the 10l of tap water added to the starting mix for the AugBMP test reactor. The mass of casein present in the AugBMP test reactor at the start of the experiment was calculated by:

Initial Casein mix:

$$Concentration_{Casein} = 70g/1.5l \qquad (6.1)$$
$$Concentration_{Casein} = 46.67g/l$$

Test reactor starting mix:

$$Concentration_{Casein} = \frac{(1.25l)(46.67g/l)}{15l} \qquad (6.2)$$
$$Concentration_{Casein} = 3.9g/l$$

Therefore, the mass of casein in each test reactor at the start of the experiment:

$$Mass_{Casein} = (3.9g/l)(5l) \qquad (6.3)$$
$$Mass_{Casein} = 19.5g$$

The solubility of the casein hydrolysate used in this experiment was specified by Merck to be 310 g/l (Sigmaaldrich.com).

6.2.2 AugBSP test casein mixture

As described in Section 6.2.1, the casein hydrolysate was available in a powder form, and was subsequently added to water to form a casein solution. The required mass of casein hydrolysate in the AugBSP test experiment was lower than the mass required in the AugBMP test experiment, due to the lower concentrations in the AugBSP test reactor. The casein solution for the AugBSP test experiment (SC1) was prepared by adding 3.75g of powdered casein hydrolysate into 3l of deionised water. After 15 minutes of stirring, the entire 3l casein solution was added to the AugBSP test reactor starting mix, as shown in Section 3.5.3. The mass of casein present in the AugBSP test reactor at the start of the experiment was calculated by:

Initial Casein mix:

$$Concentration_{Casein} = 3.75g/3l$$
$$Concentration_{Casein} = 1.25g/l \quad (6.4)$$

Test reactor starting mix:

$$Concentration_{Casein} = \frac{(3l)(1.25g/l)}{12l}$$
$$Concentration_{Casein} = 0.3125g/l \quad (6.5)$$

Therefore, the mass of casein in each AugBSP test reactor at the start of the experiment:

$$Mass_{Casein} = (0.3125g/l)(6l)$$
$$Mass_{Casein} = 1.875g \quad (6.6)$$

6.2.3 Results for augmented batch test experiments using casein

The results for the starting and ending values for the AugBMP and AugBSP test reactors for the MC1 and SC1 experiments, which used casein as an organic substrate, are shown in Table 6.2.

Table 6. 2: AugBMP/AugBSP test results for casein

Casein Experiment		MC1			SC1		
	Unit	Start	End	Change (△)	Start	End	Change (△)
Time	hours	0	456	456	0	384	384
Total COD	mgCOD/l	13193	8273	-4920	781	763	-18
Soluble COD	mgCOD/l	5542	1847	-3695	604	578	-26
Soluble Organic COD	mgCOD/l	-	-	-	468	132	-336
Soluble Sulphide COD	mgCOD/l	-	-	-	137	447	310
VFA COD	mgCOD/l	301	221	-80	16	8	-8
Sulphate	$mgSO_4/l$	-	-	-	1096	679	-417
TKN	mgN/l	859	860	1	54	55	0
FSA	mgN/l	168	558	390	6	36	29
TP	mgP/l	105	110	5	4	5	0
OP	mgP/l	20	44	24	3	3	0
VSS	mgVSS/l	4291	3869	-422	129	143	14
pH	pH	7.1	7.3	0.2	6.8	7.2	0.4
Carbonate Alk	mg/l as $CaCo_3$	645	2357	1712	174	677	503
Total Alk	mg/l as $CaCo_3$	903	2608	1705	235	910	675
CT	mgC /l	177	610	432	52	181	128
CH_4 COD	mgCOD	0	11060	11060	-	-	-
Carbon in Gas	mgC	0	3456	3456	-	-	-

Both the total COD concentration and the soluble COD concentration for MC1 decreased throughout the experiment. The decrease in the COD concentrations for MC1 were expected, as the substrate was utilised by the biomass and converted to methane gas. However, the soluble COD concentration used was not equal to the total COD concentration used. This indicated that particulate COD was also consumed throughout the MC1 experiment. The particulate COD was due to the S_{bp} present in the methanogenic SSPAD effluent, as well as the casein that did not dissolve into solution. The assumption that not all of the casein dissolved into solution is further explained in Section 6.2.7.

The total COD concentration in SC1 remained constant throughout the experiment, which was expected, as the COD was conserved by the AugBSP reactor, which contained a zero headspace. The total soluble COD remained relatively constant, even though soluble sulphide

COD was produced. The constant total soluble COD concentration was expected, as the use of a soluble substrate should decrease the soluble organic COD by the same amount as the increase in soluble sulphide COD, keeping the total soluble COD concentration unchanged.

The starting VFA concentrations for both MC1 and SC1 were higher than expected, as the AugBMP and AugBSP control reactors had lower starting VFA COD concentrations (206mgCOD/*l* and 0mgCOD/*l*, respectively). This higher concentration of COD indicated that the casein began to hydrolyse rapidly in the samples taken from the starting mix for both the AugBMP and AugBSP test experiments.

The TKN and TP concentrations remained unchanged throughout the experiment, indicating that N and P were conserved. The change in FSA in both MC1 and SC1 was significant, at 390mgFSA-N/*l* and 29mgFSA-N/*l*, respectively. The significant change in FSA indicated that casein contained a high organic N content, which was subsequently degraded and released as FSA into the test reactor liquid. The change in OP in both MC1 and SC1 was not as high, at 24mgOP-P/*l* and 0mgOP-P/*l*, respectively. The change in OP indicated that casein contained a low organic P content, which was released as OP with the breakdown of the organic material.

The VSS concentration in MC1 decreased throughout the experiment. This decrease in VSS concentration was related to the decrease in particulate COD in the AugBMP test reactor. The VSS concentration in SC1 increased by 14mgVSS/*l* throughout the experiment. This increase in VSS concentration was due to the growth of new biomass. For the AugBSP SC1, the soluble organic COD utilised was 336mgCOD/*l*, which produced 310mgCOD/*l* of sulphide. The remaining 26mgCOD/*l* is equivalent to 18mgVSS/*l* (i.e. 26/1.42, where 1.42 is the f_{CV} for biomass), which was close to the observed VSS increase of 14mgVSS/*l*.

The pH for both MC1 and SC1 increased throughout the experiment. The increase in pH was related to the FSA produced in MC1, and the FSA and sulphide produced in SC1. The increase in total alkalinity in MC1 was due to the increase in carbonate alkalinity in the system. As mentioned, the release of FSA into the bulk liquid increased the carbonate alkalinity through the re-speciation of NH_3 to NH_4^+, which subsequently took an H^+ ion from the water, forming HCO_3^-. The increase in total alkalinity in SC1 was due to the increase in carbonate alkalinity, as well as the alkalinity generated by the production of sulphide.

6.2.4 Gas Measurement

The gas produced by the MC1 AugBMP test experiment was captured inside of an inverted water column. The setup and specifications of the water columns are given in Section 3.4.2. The gas produced by the MC1 AugBMP test reactor was quantified by the volume of water displaced in the column. The procedure for calculating the mass of COD contained in the methane was described in Section 3.7.3.

Figure 6.1 shows the cumulative methane COD produced by the MC1 experiment, which had a low variance between all three AugBMP test reactors. The low variance between all three test reactors indicated that the cumulative methane COD collected was repeatable. Furthermore, this repeatability suggested that the gas measurements were accurate.

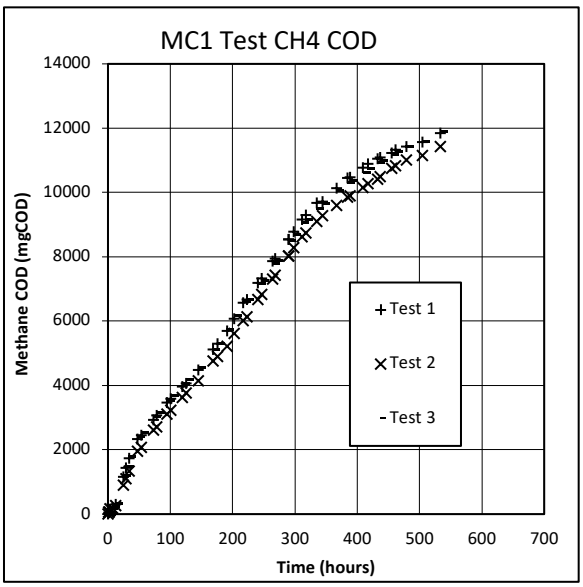

Figure 6. 1: MC1 AugBMP test CH_4 COD

6.2.5 Mass Balances

The mass of material entering the AugBMP test reactor should equate to the mass of material leaving the reactor, as mass was conserved within the system. The COD entering the AugBMP test reactor was contained inside the inoculum and the substrate, and the COD leaving the AugBMP test reactor was either in the liquid effluent stream or in the methane gas produced. As described in Section 3.7.3, the starting COD in the AugBMP reactor must equate to the sum of COD removed from the reactor during sampling, the methane COD in the inverted water

column and the remaining COD in the reactor at the end of the experiment. The methane partial pressure for the MC1 AugBMP test experiment was not measured. However, the methane partial pressure in the AugBMP test reactor for MP2 and MP3 was measured using a gas chromatograph. The results for the methane partial pressure in MP2 and MP3 are given in Table 6.3. Therefore, the methane partial pressure in the MC1 AugBMP test reactor headspace was approximated to be 60%.

Table 6. 3: Gas chromatography results

		Period	
Experiment Type	**Unit**	**MP2**	**MP3**
Methanogenic SSPAD	% Methane	59.2± 1.7	57.2± 2.7
AugBMP Control	% Methane	57.5± 9	50.3± 8.7
AugBMP Test	% Methane	62.8± 6.5	54.7± 4.5

The SC1 AugBSP test experiment was conducted in a purpose-built reactor with zero headspace. The zero headspace ensured that the products produced by the reaction remained in the aqueous phase. Therefore, unlike the methanogenic AugBMP experiment, the mass of the products entering and exiting the system are conserved within the aqueous solution, as no gas evolution occurred. Furthermore, due to the zero headspace in the AugBSP test reactor, the total COD concentration remains constant.

6.2.5.1 MC1 COD Balance

The COD balance for the MC1 AugBMP test experiment was calculated using Equation 3.12 from Section 3.7.3.2. The COD balance for MC1 with a headspace methane partial pressure of 60% is shown in Table 6.4.

Table 6. 4: MC1 AugBMP test COD balance

MC1 AugBMP Test COD Balance (60% Methane Partial Pressure)						
	Starting Mass	Mass Removed	Remaining Mass	Gas Mass	Total Effluent	Balance
Unit	mgCOD	mgCOD	mgCOD	mgCOD	mgCOD	%
T1	65360	15043	29809	11242	56094	85.8
T2	66264	15007	28951	10747	54706	82.6
T3	66264	16099	29595	11191	56884	85.8

Table 6.4 indicated that COD balances in the MC1 AugBMP test reactor were in the region of 83% to 86%, which were not within the required range for a good mass balance (see Section 3.7.2). Therefore, in an attempt to evaluate the impact of methane COD on the low COD balance, the methane partial pressure was set to the maximum possible value of 100%. The Table 6.5 below shows the results obtained with this adjustment.

Table 6. 5: Adjusted MC1 AugBMP test COD balance

MC1 AugBMP Test COD Balance (100% Methane Partial Pressure)						
	Starting Mass	Mass Removed	Remaining Mass	Gas Mass	Total Effluent	Balance
Unit	mgCOD	mgCOD	mgCOD	mgCOD	mgCOD	%
T1	65360	15043	29809	18737	63589	97.3
T2	66264	15007	28951	17912	61871	93.4
T3	66264	16099	29595	18652	64345	97.1

Table 6.5 shows that only when the methane partial pressure in the MC1 AugBMP test reactor headspace was set to 100%, was a COD balance within 7% achieved. However, a 100% COD headspace partial pressure in the laboratory AugBMP test reactor was unlikely. The methane partial pressure was only increased to 100% for the basis of checking the mass balance, as the gas measurements were suspected to be the source of error in the COD balance. The increase in methane partial pressure to 100% highlights that less COD was present in the methane gas than was expected for the COD balance.

6.2.5.2 SC1 Sulphur Balance

The sulphur utilised in the sulphate and produced in the sulphide should be conserved throughout the AugBSP test experiment, assuming that no other S compounds formed. The sulphur balance is explained in Section 3.7.4.3. A sulphur balance was achieved in the SC1 T2 AugBSP reactor. However, for the T1 AugBSP reactor, more S was produced in the sulphide than was taken up in the sulphate. The test sulphur balance is shown in Table 6.6.

Table 6. 6: SC1 AugBSP test sulphur balance

SC1 S Balance			
	S in	S out	**Balance**
Reactor	mgS/l		**%**
T1	124	165	**132**
T2	154	146	**95**

6.2.5.3 TKN and TP balance

The mass flux of other constituents present in the entering and exiting streams such as the TKN and TP were also checked using the mass balanced approach. The total mass of these two constituents should remain constant throughout the experiment. The TKN and TP mass fluxes were calculated using Equation 3.14, as described in Section 3.7.5. Table 6.7 confirms that, in general, good mass balances for TKN and TP were achieved for the MC1 and SC1 experiments.

Table 6. 7: MC1/SP1 AugBMP/AugBSP test TKN/TP balance

	MC1			SC1	
Reactor	T1	T2	T3	T1	T2
Nitrogen					
TKN in	897	867	813	55	54
TKN out	857	876	848	56	54
Balance	**96**	**101**	**104**	**101**	**99**
Phosphorus					
TP in	104	123	88	5	4
TP out	105	118	106	5	5
Balance	**101**	**96**	**120**	**111**	**109**

6.2.6 Stoichiometric Composition Identification

The composition of the biodegradable organics was identified by calculating the change in elemental concentrations between two measured data points. The data points required were the ending and the starting concentrations of the augmented batch experiments. The calculation is explained in detail in Section 3.9.2. The mass ratios for each element (f_{CV}, f_C, f_N and f_P) needed to be determined in order to calculate the unknown mass ratios (f_O and f_H).

Therefore, the change in COD, C, N, P and VSS throughout the experiment was required. The change in the required components was previously shown in Table 6.2. The identification of the biodegradable composition for the AugBMP control experiments is shown in Table 6.8.

Table 6. 8: AugBMP and AugBSP test stoichiometric composition identification for casein

Casein Experiment		MC1			SC1		
		Control	Test	Test - Control	Control	Test	Test - Control
Measured	**Unit**	Change (Δ)	Change (Δ)	Change (Δ)	Change (Δ)	Change (Δ)	Change (Δ)
Total COD	mgCOD/l	-1034	-4920	-3885	-	-	-
VFA COD	mgCOD/l	-103	-80	23	5.6	-7.7	-13.32
Soluble Sulphide COD	mgCOD/l	-	-	-	7	310	304
FSA	mgN/l	-9	390	399	1	29	29
OP	mgP/l	5	23.5	19	0	-0.1	0
VSS	mgVSS/l	10	-3900	-3910	20	-313	-333
Carbonate Alk	mg/l as $CaCo_3$	158	1712	1554	40	503	463
CH_4 COD	mgCOD	1408	11060	9652	-	-	-
C in Gas	mgC	440	3456	3016	-	-	-
COD Change							
Biodegradable COD	mgCOD/l	-	-	3885	-	-	290
Carbon Change							
C in Gas	mgC/l	-	-	603	-	-	-
C in H_2CO_3 Alk	mgC/l	-	-	373	-	-	111
Total C	mgC/l	-	-	976	-	-	111
VSS Change							
Biodegradable VSS	mgVSS/l	-	-	3910	-	-	333
Mass Ratio							
f_{CV}	gCOD/gVSS	-	-	0.994	-	-	0.872
f_C	gC/gVSS	-	-	0.250	-	-	0.334
f_N	gN/gVSS	-	-	0.102	-	-	0.086
f_P	gP/gVSS	-	-	0.005	-	-	0.000
f_H	gH/gVSS	-	-	0.127	-	-	0.079
f_O	gO/gVSS	-	-	0.517	-	-	0.501
Compostion							
C	-	-	-	1	-	-	1
H	-	-	-	6.088	-	-	2.835
O	-	-	-	1.552	-	-	1.125
N	-	-	-	0.350	-	-	0.222
P	-	-	-	0.007	-	-	0.000

Table 6.8 presents the data used towards the identification of the casein composition using the stoichiometric calculation described in Section 3.9.2. The change between the ending and starting concentrations of each constituent in the control reactor quantified the products released due to the residual biodegradable organics present in the inoculum. Furthermore, the change between the ending and starting concentrations of each constituent in the test reactor quantified the products released due to the residual biodegradable organics present in the

inoculum, as well as the casein substrate. The concentrations observed in the control reactors were divided by two, as the inoculum used in the test reactors was diluted to half the concentration of the control reactors. Therefore, the difference between the test reactor and the control reactor isolated the products released due to the casein substrate.

The total COD concentration change in the MC1 experiment was used to quantify the casein COD available in the AugBMP test reactor. This is with the acceptance that the solids retention time is long enough for the breakdown of all the complex biodegradable organics in the substrate (i.e., casein) and taking into consideration the VFA COD generated as an intermediate product of AD bioprocesses. The VFA generated in this case between the AugBMP control and test reactors was calculated to be 23mgCOD/*l* (a very small value relative to the influent COD). Hence, the COD that was not used to generate methane gas would be the small quantity of COD that forms VFA in the effluent. This was considered during analysis of the results.

The sulphide COD concentration produced in SC1 was used to quantify the COD change for the AugBSP reactors (as described in Section 3.6.3). However, the VFA COD concentration affected the total sulphide COD produced. It was observed that an additional 5mgCOD/*l* of VFAs were produced in the AugBSP control, and 8mgCOD/*l* of VFA was consumed in the AugBSP test. Therefore, a total VFA COD of 13mgCOD/*l* was utilised in the AugBSP test reactor for sulphide production. Therefore, the COD available in the organics was adjusted to 290mgCOD/*l*.

The total carbon in the gas for the MC1 AugBMP reactor was determined by multiplying the cumulative mols of biogas produced, measured using the inverted columns, by 12gC/mol. The change in H_2CO_3 alkalinity quantified the change in carbon in the aqueous phase for both the AugBMP and AugBSP reactors. The change in carbon present in the aqueous phase was calculated by taking the change in H_2CO_3 alkalinity concentration and dividing by 50, which gave the mols of alkalinity (the alkalinity was measured in mg/*l* as $CaCO_3$, which has an equivalence of 50mg $CaCO_3$/mol). The mols of alkalinity were then multiplied by 12gC/mol to get the carbon equivalent.

In the AugBMP reactor, the total carbon change in the system was the sum of the carbon in the gas and the carbon in the aqueous solution. In the AugBSP reactor the total carbon change was the carbon in the aqueous solution.

The VSS change was determined as the change in the VSS concentration between the end and the start of the experiment. The VSS for the control reactors was measured using the VSS method as described by Standard Methods. The VSS in the test reactors was the concentration of powdered casein hydrolysate present in each respective reactor at the start of the experiment, as shown in Equation 6.2 in Section 6.2.1, and Equation 6.5 in Section 6.2.2. Therefore, it was assumed that the casein hydrolysate was completely utilised by the test reactors at the end of the experiment.

The mass ratios were then calculated by taking the change in each respective constituent and dividing by the VSS concentration. Therefore, the mass ratios were determined as the biodegradable COD/VSS (f_{CV}), the total C/VSS (f_C), the FSA/VSS (f_N) and the OP/VSS (f_P). The mass ratios for f_O and f_H were calculated using Equations 3.45 and 3.46 in Section 3.9.2.1. Finally, the composition of casein was identified using the mass ratios and Equations 3.47 and 3.48 in Section 3.9.2.1.

The casein compositions identified in Table 6.8 for the AugBMP and AugBSP tests were not the same. The mass ratios for each experiment were different, which affected the calculated compositions. As previously shown in Section 5.2.3 and Section 5.3.2, the compositions identified using the stoichiometric calculation for the AugBMP and AugBSP control reactors were inaccurate. The inaccuracies were due to the limited data points used, i.e. only the starting and ending concentrations. Therefore, this inaccuracy carried through into the casein composition identification. Furthermore, it was assumed that all of the casein was soluble and that it was completely utilised during the AugBMP and AugBSP test experiments.

Therefore, the MC1 and SC1 augmented batch test experiment were modelled using the PWM_SA_AD model. The use of mathematical models and the PE function introduced a data reconciliation aspect into the thesis, as the composition of the casein, as well as additional physical parameters, were identified by minimising the error across the observed results. It was observed that, when using the entire data set in the modelled AugBMP and AugBSP test reactors, the model found inconsistencies in the collected data and it was later determined, that in order for the model to replicate the observed data set, a portion of the casein hydrolysate remained insoluble and was not utilised during the experiment.

6.2.7 Modelling the casein experiment

The procedure used to identify the composition of a soluble substrate using the PE function was described in Section 3.11.3.1. The inoculum used in both the modelled AugBMP and AugBSP test experiments was taken from the modelled methanogenic and sulphidogenic SSPADs, respectively. The modelled AugBMP control reactor was used to identify the composition of the residual biodegradable organics. Subsequently, the mass and composition of the residual organics determined by the modelled AugBMP control reactor was used as an input for the modelled AugBMP test reactor. The starting concentration of the biomass, as well as the starting concentration of the residual organics, was halved for the modelled AugBMP test reactor to account for the dilution used.

The AugBSP control experiment did not use the PE estimation function, as the modelled sulphidogenic SSPAD effluent achieved the observed AugBSP control values without adjusting the model parameters. The concentration of biomass in the modelled SSPAD effluent was halved to account for the starting dilution of the AugBSP test experiment.

The compositions of the biomass and the UPOs remained fixed at $C_1H_{1.4}O_{0.4}N_{0.2}$ and $C_1H_{1.571}O_{0.426}N_{0.166}P_{0.019}$, respectively, for both the modelled AugBMP and AugBSP test experiments. The casein was believed to be soluble; therefore, the composition of the BSO was set as the unknown parameter for the modelled casein experiment PE (for which the aim was to identify the casein composition). The starting mass of the BSO in both the modelled AugBMP and AugBSP test reactors was set to the starting mass of casein in each reactor (19.5g and 1.875g, respectively), as determined in Section 6.2.1. and Section 6.2.2.

For the initial PE, for both the modelled AugBMP and AugBSP test experiments, the parameters determined by the model inaccurately replicated the observed AugBMP and AugBSP test values. The composition identified by the initial PE for the modelled AugBMP and AugBSP test experiments did not agree well with the literature stated casein compositions. Furthermore, the VSS concentrations in the modelled AugBMP and AugBSP test experiments were significantly lower than the observed VSS concentrations.

In order to minimise the error, the modelling approach was adjusted such that the fraction of casein that dissolved into solution could be adjusted by the PE. Therefore, the mass of casein

at the start of the experiment remained the same for the AugBMP and AugBSP test reactors, 19.5g and 1.875g, respectively. However, the mass of casein used during the experiment was adjusted by introducing a new parameter. The new parameter, f_S_F_dis, set the fraction of the total casein that became soluble and was therefore utilised during the experiment. The remaining casein that did not dissolve into solution became unbiodegradable particulate VSS. Therefore, if f_S_F_dis was set to 1, all of the casein became BSO and was utilised, however, if f_S_F_dis was set to 0.5, half the casein became BSO and was utilised, and the remaining half became unbiodegradable VSS.

The starting concentrations of constituents such as FSA, OP, VFA, H_2CO_3 alkalinity, as well as the reactor pH, in the modelled AugBMP test experiment were adjusted to the averaged observed starting values for the AugBMP test experiment. Furthermore, the starting concentrations of constituents such as sulphide COD, FSA, OP, VFA, sulphate and H_2CO_3 alkalinity, as well as the reactor pH, in the modelled AugBSP test experiment were adjusted to the averaged observed starting values for the AugBSP test experiment.

The mass of UPO, the f_S_F_dis and the BSO (casein) composition were used as unknown parameters for the modelled AugBMP and AugBSP experiments. Additionally, the saturation hydrolysis constant for the breakdown of BSO (K_H_f), the growth rate of the acetoclastic organisms (mu_AM/mu_AS), and the half-saturation coefficient of the acetoclastic organisms (Ks_AM/Ks_AS) were adjusted by the PE. The PE conducted hundreds of iterations until the lowest error across the observed measurements was achieved. The parameters used by the PE for determining the casein composition are summarised in Table 3.11 in Section 3.11.3.1.

The observed measurements used to determine the casein composition for the AugBMP and AugBSP tests differed. The AugBMP test reactor had measurements conducted on both the liquid and gas phases, whereas, the AugBSP reactor had all the measurements taken in the aqueous phase. The observed measurements used for the modelled AugBMP test reactor is given in Table 6.9, and the observed measurements used for the modelled AugBSP test reactor is given in Table 6.10.

Table 6. 9: Modelled AugBMP test variables for casein

Variable	Description	Weighting
Alkalinity	The total alkalinity generated	1
COD_total	The unfiltered COD concentration	1
COD_soluble	The filtered COD concentration	1
FSA	The Free and Saline Ammonia concentration	1
$H2CO_3$ alkalinity	The carbonate alkalinity generated	1
OrthoP	The Orthophosphate concentration	1
VFA	The Volatile Fatty Acids concentration	1
VSS	The Volatile Suspended Solids concentration	1
p_H_s	The reactor pH	1

Table 6. 10: Modelled AugBSP test variables for casein

Variable	Description	Weighting
Alkalinity	The total alkalinity generated	1
C(S_SO4)	The sulphate concentration	1
COD(S_HS)	The sulphide COD concentration	3
COD_total	The unfiltered COD concentration	1
COD_soluble	The filtered COD concentration	1
FSA	The Free and Saline Ammonia concentration	5
$H2CO_3$ alkalinity	The carbonate alkalinity generated	1
OrthoP	The Orthophosphate concentration	5
VFA	The Volatile Fatty Acids concentration	1
VSS	The Volatile Suspended Solids concentration	2
p_H_s	The reactor pH	1

The weighting for the variables in Table 6.9 and 6.10 were determined as was described in Section 5.2.4.

6.2.8 Modelled Composition Identification

The PE ran hundreds of iterations until the correct combination of parameters, which achieved the desired results with the lowest error was determined. The parameters determined by the PE for the AugBMP and AugBSP test experiments using casein are summarised in Table 6.11.

Table 6. 11: Modelled AugBMP and AugBSP test composition identification for casein

Parameter	**MC1**	**SC1**
BSO Composition	$C_1H_{1.588}O_{0.596}N_{0.249}P_{0.004}$	$C_1H_{1.406}O_{0.577}N_{0.22}P_{0.001}$
f_S_F_dis	0.83	0.87
M(X_U_Inf)	14.764	0.409
kH_F_AD_hyd	0.0009	0.05
mu_AM	0.7	-
mu_AS	-	0.331
KS_AM	34.09	-
KS_AS	-	0.3747

The PE results for both the MC1 and SC1 experiments indicated that, in order for the modelled AugBMP and AugBSP test reactors to accurately replicate the observed results, a small fraction of the total casein added at the start of the experiments (0.17 and 0.13, respectively) remained as unbiodegradable particulate VSS throughout the experiment, and subsequently did not dissolve into solution. The casein composition determined by the PE for the modelled AugBMP and AugBSP test experiments was then compared to the literature stated casein compositions, which were described in Section 2.6. The casein compositions are compared in Table 6.12.

Table 6. 12: Casein composition comparison to the literature stated values

Source	**Casein Composition**
Hoover and Porges (1952)	$C_1H_{1.47}O_{0.35}N_{0.25}$
Schrieke and Winter (2011)	$C_1H_{1.59}O_{0.31}N_{0.25}P_{0.005}$
MC1	$C_1H_{1.588}O_{0.596}N_{0.249}P_{0.004}$
SC1	$C_1H_{1.406}O_{0.577}N_{0.22}P_{0.001}$

The casein compositions determined by the PE for MC1 and SC1 agreed well with the literature values. However, the O content of the casein composition identified by the PE for both MC1 and SC1 was higher at $O_{0.596}$ and $O_{0.577,}$ respectively. The O content affects the total COD concentration (electron donating capacity of the organic), as well as the total molar mass of the organic. Therefore, the higher the O content, the lower the available COD for the organic. The elevated O content for the MC1 and SC1 casein compositions, compared to the literature stated compositions, indicated that the available COD in the casein needed to be lowered by the PE for the mass of casein available. The observed VSS concentrations for the MC1 and SC1 experiments were replicated by the modelled AugBMP and AugBSP test experiments well, which are shown in Section 6.2.10.7 in Figures 6.16 and 6.17. Therefore, the higher O content in the casein hydrolysate used in the experiment may have been caused by the casein source or the preparation methods used by the manufacturer.

6.2.9 Casein hydrolysate analysis

The casein hydrolysate used for the AugBMP and AugBSP experiments was tested independently using the analytical procedures described in Section 3.6. The casein substrate was analysed by mixing 1g of casein hydrolysate powder into 1*l* of deionised water. The solution was then stirred for 10min, after which measurements for COD, TKN, FSA, TP and OP, as well as the alkalinity (5-point titration), were performed. The casein measurements were performed in duplicate once per day, at three different dilutions, for three consecutive days. The dilutions used were 0x, 10x and 15x. The organic N and the organic P in the casein were determined by taking the difference between the TKN and FSA concentrations, and the TP and OP concentrations, respectively. The detailed results for the casein analysis are shown in Appendix G. The summarised results for the casein analysis are shown in Table 6.13.

Table 6. 13: Casein hydrolysate powder analysis

Casein Analysis (1g/l)		
Constituent	**Unit**	**Measured**
Total COD	mgCOD/l	1252
VFA COD	mgCOD/l	43
TKN	mgN/l	139
FSA	mgN/l	14
OrgN	mgN/l	125
TP	mgP/l	8
OP	mgP/l	3
OrgP	mgP/l	5
VSS	mgVSS/l	1000
Carbonate Alk	mg/l as $CaCo_3$	21
Total Alk	mg/l as $CaCo_3$	59

A common unit needed to be established in order to compare the measured casein hydrolysate to that of the casein identified in the PE for the modelled MC1 and SC1 experiments. The common unit chosen was the constituent concentrations (mg*/l*) for COD, FSA and OP. Therefore, the casein composition identified by the PE was converted into the equivalent constituent concentrations. The conversion was calculated using the mass fractions (f_{CV}, f_N and f_P) of the casein composition identified by the PE for MC1 and SC1. The mass fractions were determined using the molar mass of the casein composition identified by the PE. The molar mass of each composition ($C_xH_yO_zN_aP_b$) was calculated using Equation 6.7.

$$MM = 12x + y + 16z + 14a + 31b \tag{6.7}$$

The electron donating capacity (COD) for each casein composition identified by the PE for MC1 and SC1 was calculated using Equation 6.8.

$$COD = 8(4x + y - 2z - 3a + 5b) \tag{6.8}$$

The f_{CV} mass fraction was calculated by taking the COD and dividing by the molar mass. The f_N mass ratio was calculated by taking the N portion of the identified casein composition and multiplying by 14gN/mol divided by the molar mass. The f_P mass ratio was calculated by taking the P portion of the identified casein composition and multiplying by 31gP/mol divided by the molar mass. Finally, the COD, OrgN and OrgP concentrations, present in 1g*/l* of the casein identified by the PE, were calculated by multiplying the mass ratios by 1000mgVSS*/l*. The

measured concentrations for casein hydrolysate powder, determined by mixing 1g of casein hydrolysate powder into 1*l* of deionised water, as shown in Table 6.13, was then compared to the constituent concentrations calculated from the PE for the MC1 and SC1, which were determined in Table 6.14.

Table 6. 14: Casein hydrolysate powder COD, OrgN and OrgP content

	Unit	MC1	SC1
Composition			
C	-	1	1
H	-	1.588	1.406
O	-	0.596	0.577
N	-	0.249	0.22
P	-	0.004	0.001
Molar Mass	gVSS/mol	26.69	25.74
COD	gCOD/mol	29.35	28.78
Mass Fractions			
f_{CV}	COD/VSS	1.0996	1.1180
f_N	N/VSS	0.1306	0.1197
f_P	P/VSS	0.0046	0.0012
Concentration (1000mgVSS/l)			
COD	mgCOD/l	1100	1118
OrgN	mgN/l	130.6	119.7
OrgP	mgP/l	4.6	1.2

Table 6.15 shows that the casein composition identified using the modelled AugBMP and AugBSP experiments, which was converted to the equivalent constituent concentrations, had low error compared to that of the measured casein concentrations. This outcome strengthened the accuracy of the modelled AugBMP and AugBSP test experiment's ability to determine the composition of an unknown organic.

Table 6. 15: Casein hydrolysate powder comparison with AugBMP/AugBSP PE Casein (1g/l)

1g/l casein		Analysed	MC1		SC1	
Constituent	Unit	Casein	PE	%error	PE	%error
COD	mgCOD/l	1252	1100	**-12**	1118	**-11**
OrgN	mgN/l	125	131	**4**	120	**-5**
OrgP	mgP/l	4.8	4.6	**-4.2**	1.2	**-75**

6.2.10 Modelled casein experiment results

The observed results from the T1, T2 and T3 AugBMP test reactors, as well as the observed results from the T1 and T2 AugBSP test reactors were summarised by averaging the values obtained for each measurement taken. Table 6.16 and Table 6.17 summarise the results obtained for the starting and ending concentrations for each constituent in the modelled AugBMP and AugBSP test experiments for casein. The results obtained from the model were compared to that of the observed results. Furthermore, the results have been compared visually in Section 6.2.10.1 (Figure 6.2) to Section 6.2.10.10 (Figure 6.22). The visual comparison between the modelled and observed results evaluated the accuracy of the dynamic parameters determined by the PE.

Table 6. 16: Modelled MC1 AugBMP test results for casein

MC1 Test Model Results							
		Start		End		Change	
COD	**Unit**	**Observed**	**Modelled**	**Observed**	**Modelled**	**Observed**	**Modelled**
Total COD	mgCOD/l	13193	12417	8273	8080	**-4920**	**-4337**
Soluble COD	mgCOD/l	5542	5766	1847	2007	**-3695**	**-3759**
Gas							
Methane	mgCOD	0	0	11060	19149	**11060**	**19149**
Nitrogen							
FSA	mgFSA/l	168	168	558	569	**390**	**401**
Phosphate							
OP	mgOP/l	20.3	20.2	43.8	41.1	**23.5**	**20.9**
Alkalinity							
Carbonate	mg/l as CaCO3	645	656	2357	2237	**1712**	**1581**
Total	mg/l as CaCO3	903	928	2608	2360	**1705**	**1432**
Species							
VFA Conc	mg/l as acetate	282.1	281.9	207.3	19.3	**-75**	**-263**
CT	mgC/l	177	177	610	617	**432**	**439**
Solids							
VSS	mgVSS/l	4291	4264	3869	4128	**-422**	**-137**
pH							
pH		7.14	7.14	7.31	7.04	**0.17**	**-0.10**

The modelled MC1 AugBMP test reactor replicated the observed test reactor well, as shown in Table 6.16. However, the methane COD in the modelled MC1 AugBMP test was higher (by 8089mgCOD) than the observed methane COD. This highlighted the error associated with the

gas measurements, as the model was mass balanced. The increase in total alkalinity was due to the increase in carbonate alkalinity. However, the increase in the modelled total alkalinity was lower than the increase in the observed total alkalinity. The VSS concentration change for the modelled AugBMP reactor was lower than the observed VSS concentration change. However, the additional 285mgVSS/*l* in the observed AugBMP test reactor may have been due to some of the undissolved casein being hydrolysed later in the experiment, which was not considered by the adjustments made to the model. Finally, the pH of the modelled AugBMP test was lower than the observed pH. The source of this error was not determined but may arise as a result of the lower total alkalinity generated by the modelled experiment compared to the observed experiment.

Table 6. 17: Modelled SC1 AugBSP test results for casein

SC1 Test Model Results							
		Start		End		Change	
COD	**Unit**	**Observed**	**Modelled**	**Observed**	**Modelled**	**Observed**	**Modelled**
Total COD	mgCOD/l	781	781	763	781	**-18**	**0**
Total Soluble COD	mgCOD/l	604	589	578	565	**-26**	**-24**
Sulphide	mgCOD/l	137	137	447	439	**310**	**303**
Sulphate							
Sulphate	mgSO4/l	1096	1096	679	642	**-417**	**-454**
Nitrogen							
FSA	mgFSA/l	6.4	6.4	35.8	36.7	**29.4**	**30.2**
Phosphate							
OP	mgOP/l	3.4	3.4	3.3	3.8	**-0.1**	**0.3**
Alkalinity							
Carbonate	mg/l as CaCO3	174	168	677	613	**503**	**444**
Total	mg/l as CaCO3	235	238	910	813	**675**	**575**
Species							
VFA Conc	mg/l as acetate	15	17	8	1	**-7**	**-16**
CT	mgC/l	52	52	181	178	**128**	**126**
Solids							
VSS	mgVSS/l	129	124	143	137	**14**	**13**
pH							
pH		6.8	6.8	7.2	6.9	**0.4**	**0.2**

The modelled AugBSP test reactor replicated the observed test reactor well, as shown in Table 6.17. However, as was seen with the AugBMP test reactor above, the alkalinity generated by the model was lower than what was observed, which may have caused the lower pH in the

modelled reactor. Nevertheless, the parameters determined by the PE were accurate for replicating the observed results in the modelled AugBSP test reactor.

6.2.10.1 Total COD

The total COD concentration in the observed MC1 experiment (Figure 6.2) was well replicated by the modelled AugBMP test reactor. The total COD concentration was dependent on the mass and composition of the casein present in the reactor, as well as the COD of the UPOs present. The total COD in the observed SC1 experiment (Figure 6.3) remained constant, which was replicated by the modelled AugBSP test reactor well.

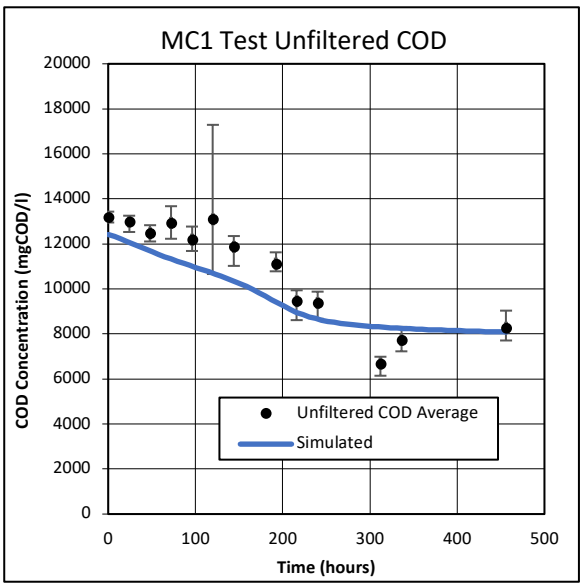

Figure 6. 2: MC1 AugBMP test total COD

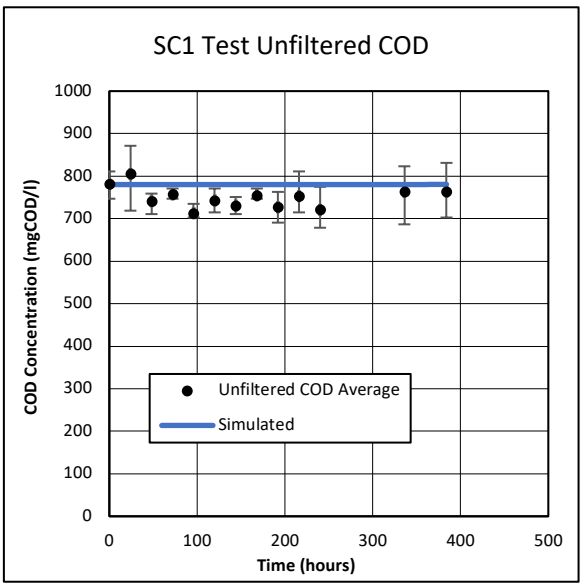

Figure 6. 3: SC1 AugBSP test total COD

6.2.10.2 Soluble COD

The soluble COD concentrations in both the observed MC1 (Figure 6.4) and SC1 (Figure 6.5) experiments were replicated by the modelled AugBMP and AugBSP test reactors, respectively. The soluble COD concentration was dependent on the USO COD, the VFA COD, and the casein COD (BSO) that dissolved into solution. Therefore, the soluble COD compositions achieved by the modelled AugBMP and AugBSP test reactors suggested that the f_S_F_dis term, which was determined using the PE, was accurate.

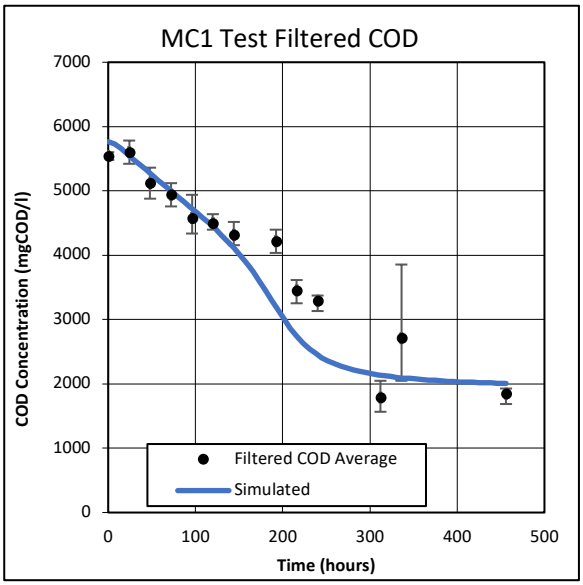

Figure 6. 4: MC1 AugBMP test soluble COD

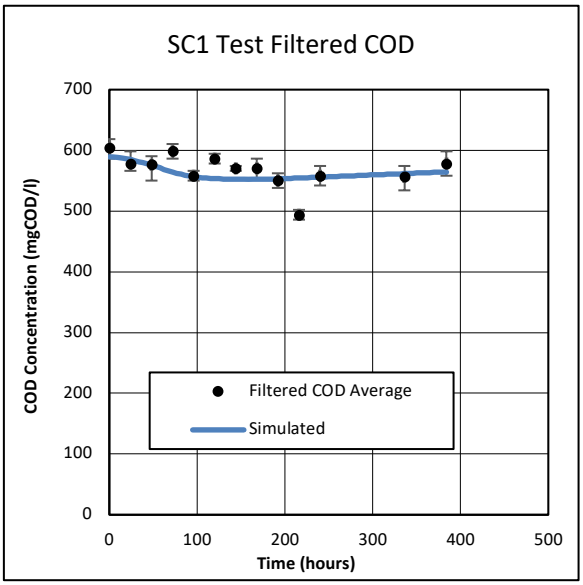

Figure 6. 5: SC1 AugBSP test soluble COD

6.2.10.3 Sulphide COD and Sulphate

The sulphide COD concentration produced by the modelled SC1 AugBSP experiment (Figure 6.6) replicated the observed sulphide COD concentration well. Furthermore, the sulphate concentration utilised (Figure 6.7) by the modelled AugBSP experiment replicated the observed sulphate concentration well. This was a good indication that the sulphur was balanced throughout the experiment, and that all of the sulphate utilised was subsequently converted to sulphide.

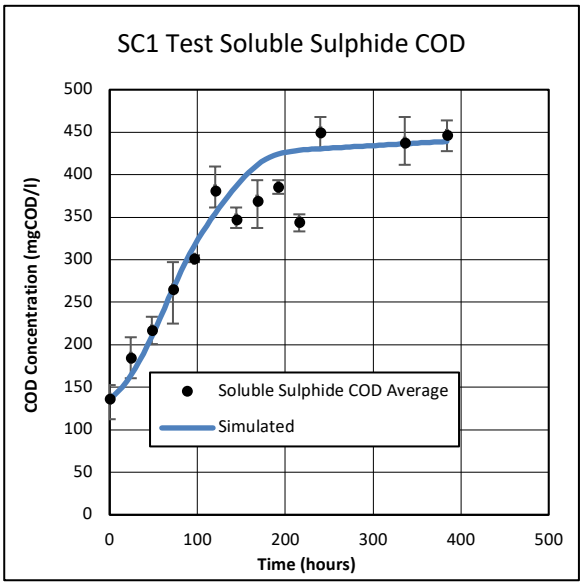

Figure 6. 6: SC1 AugBSP test soluble sulphide COD

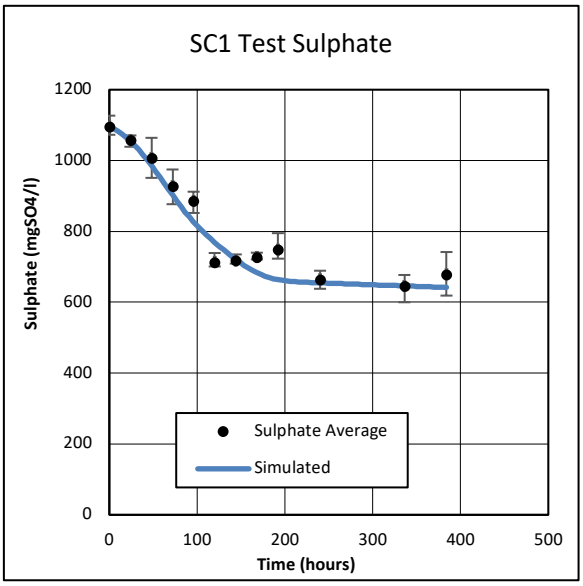

Figure 6. 7: SC1 AugBSP test sulphate

6.2.10.4 Free and Saline Ammonia (FSA) and Orthophosphate (OP)

The FSA concentration, as well as the OP concentration released into the aqueous solution in the modelled MC1 AugBMP (Figure 6.8 and 6.10) and SC1 AugBSP (Figure 6.9 and 6.11) test reactors, replicated the observed concentrations well. However, the rate at which the FSA and OP were released into the modelled MC1 AugBMP test reactor was slower than was observed. The release of FSA and OP into the reactor liquid was dependent on the BSO hydrolysis constant, as the breakdown of the organic material released inorganics such as FSA and OP into the aqueous solution. However, the rate at which the soluble COD concentration was broken down in the observed MC1 experiments (Figure 6.4) was well replicated by the model. Therefore, the discrepancy experienced between the rate at which the soluble COD concentration decreased and the rate at which the FSA and OP were released into the reactor liquid may indicate that an intermediate product was missing from the PWM_SA_AD model for the digestion of casein. However, it was not in the scope of this thesis to identify and include such intermediates.

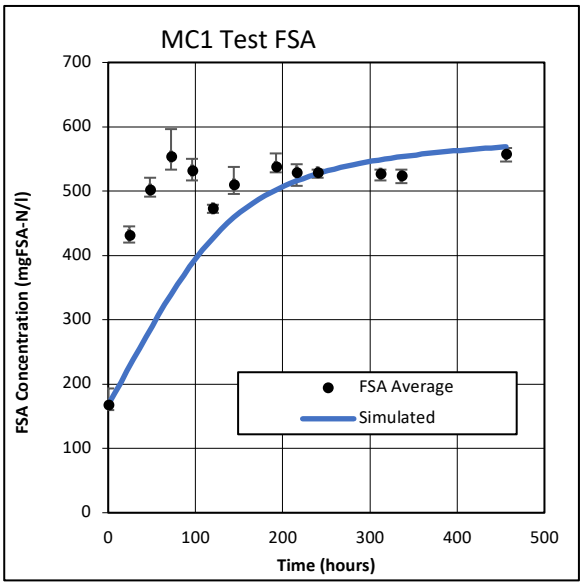

Figure 6. 8: MC1 AugBMP test FSA

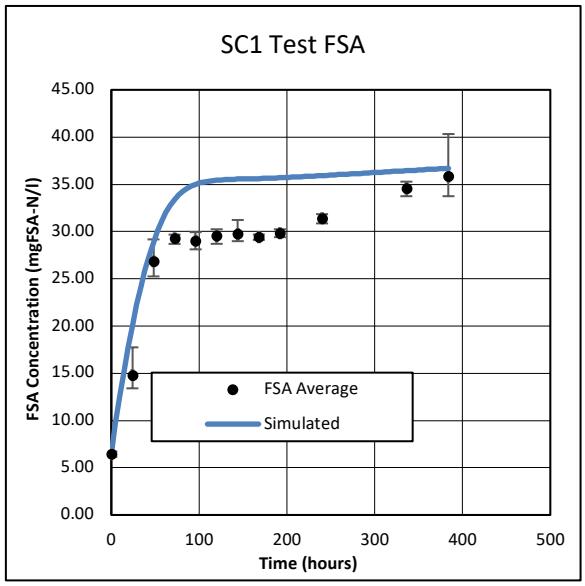

Figure 6. 9: SC1 AugBSP test FSA

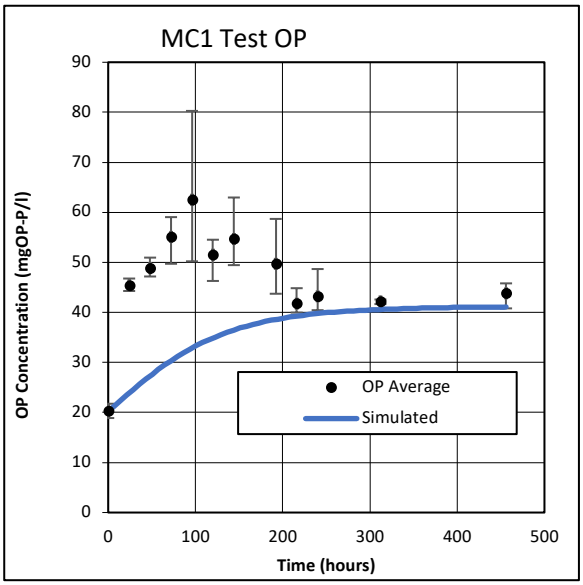

Figure 6. 10: MC1 AugBMP test OP

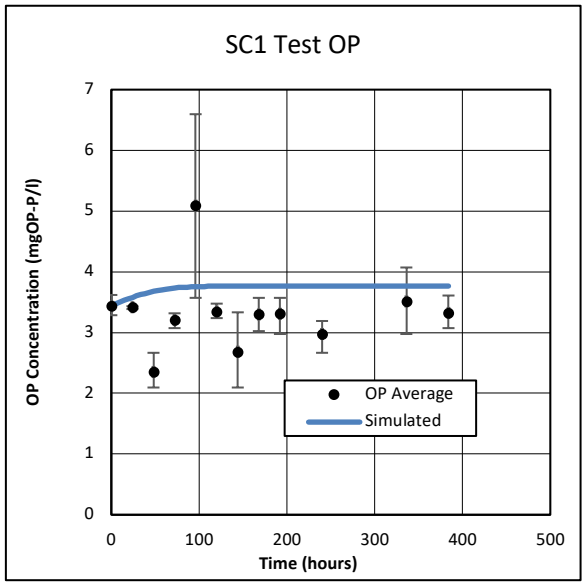

Figure 6. 11: SC1 AugBSP test OP

6.2.10.5 Carbonate Alkalinity

As previously mentioned in Section 5.2.6.3, the increase in carbonate alkalinity in the AugBMP and AugBSP reactors was influenced by the release of FSA into the reactor liquid. The casein composition was identified using the PE function, which minimised the error across the observed FSA and carbonate alkalinity measurements. Consequently, the observed carbonate alkalinity concentration in the MC1 AugBMP (Figure 6.12) and SC1 AugBSP (Figure 6.13) test reactors were replicated by the model well.

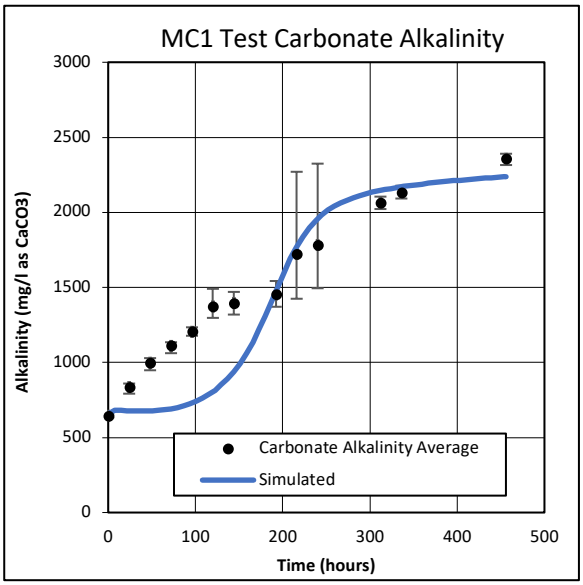

Figure 6. 12: MC1 AugBMP test carbonate alkalinity

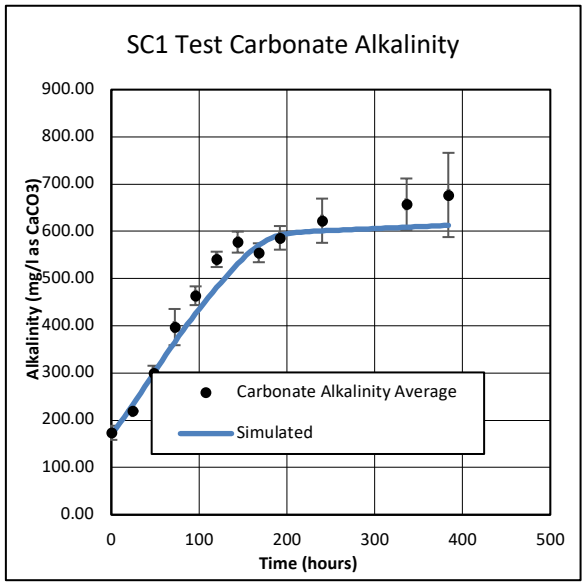

Figure 6. 13: SC1 AugBSP test carbonate alkalinity

6.2.10.6 Total Alkalinity

The total alkalinity concentration in the modelled MC1 experiment (Figure 6.14) was lower than the observed total alkalinity concentration. The discrepancy in the total alkalinity for the modelled MC1 experiment was due to the model pH, as the increase in the C_T concentration, as well as the FSA concentration, were correctly replicated in the modelled AugBMP test reactor. However, the lower reactor pH caused the carbonate alkalinity, and consequently, the total alkalinity concentration to be lower than was observed. Nevertheless, the casein composition identified by the PE was still valid, as the C_T and FSA concentrations were accurately replicated by the model.

The modelled SC1 experiment (Figure 6.15) replicated the observed total alkalinity concentration relatively well. However, the concentration of the total alkalinity in the observed SC1 experiment was higher than the modelled total alkalinity. As for the MC1 experiment above, the C_T concentration, as well as the FSA concentration, were correctly replicated in the modelled AugBSP test reactor. However, the lower reactor pH caused the carbonate alkalinity, and consequently, the total alkalinity concentration to be lower than was observed.

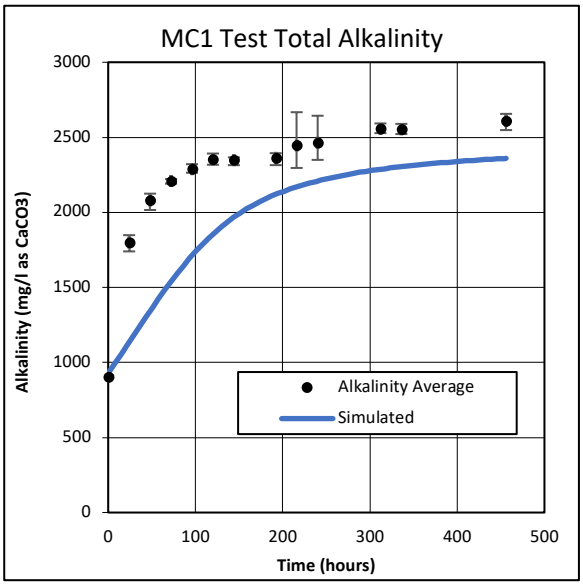

Figure 6. 14: MC1 AugBMP test total alkalinity

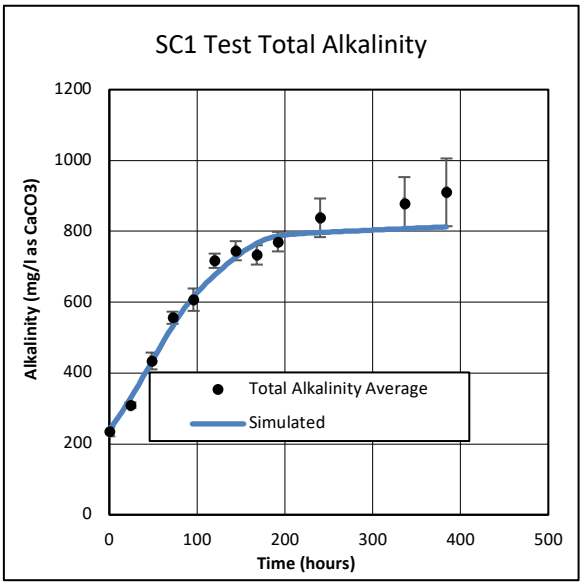

Figure 6. 15: SC1 AugBSP test total alkalinity

6.2.10.7 Volatile Suspended Solids (VSS)

The VSS concentrations in both the AugBMP and AugBSP test reactors were a good indication of the particulate material present. The VSS concentration consisted of the particulate material from the biomass, the UPOs, the residual biodegradable organics, and the portion of the casein that did not dissolve into solution. Therefore, the VSS concentrations in the MC1 AugBMP (Figure 6.16) and SC1 AugBSP test (Figure 6.17) reactors were used to identify the fraction of casein that dissolved into solution (f_S_F_dis), with the remaining portion becoming UPO VSS. Consequently, the PE function adjusted the parameters that influenced the VSS concentrations, as well as the COD concentrations of the particulate material, until the parameters that achieved the lowest error across the measurements were determined. Figures 6.16 and 6.17 show that the data contained some outliers which were most likely due to error caused by the mass balance used to measure the mass of the solids. Subsequently, the data points were taken to be non-sensical and excluded from the modelled experiments.

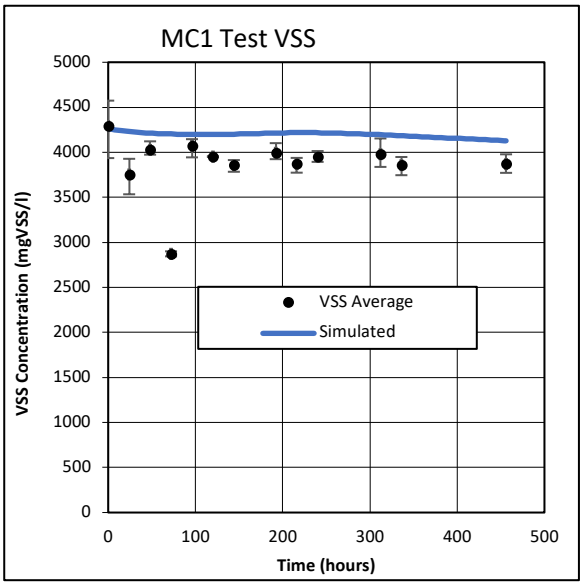

Figure 6. 16: MC1 AugBMP test VSS

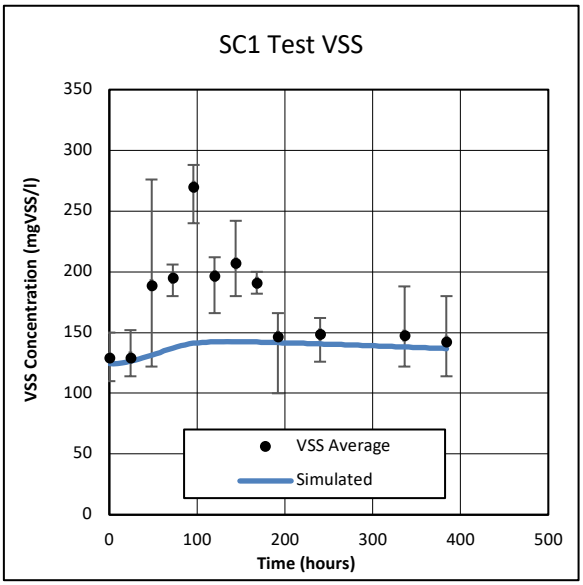

Figure 6. 17: SC1 AugBSP test VSS

6.2.10.8 Volatile Fatty Acids (VFA)

The VFA present in the modelled MC1 AugBMP (Figure 6.18) and SC1 AugBSP (Figure 6.19) test reactors was an intermediate product formed by the degradation of glucose (which formed from the hydrolysis of the biodegradable organics). The accumulation of VFA in the modelled MC1 AugBMP and SC1 AugBSP test reactors was dependent on the BSO hydrolysis rate, the substrate uptake rate of the acetoclastic organisms and the half-saturation coefficient of the acetoclastic organisms used in the model. The PE adjusted these parameters, as well as the composition of the BSO (casein), until the parameters with the lowest error across the observed measurements was achieved.

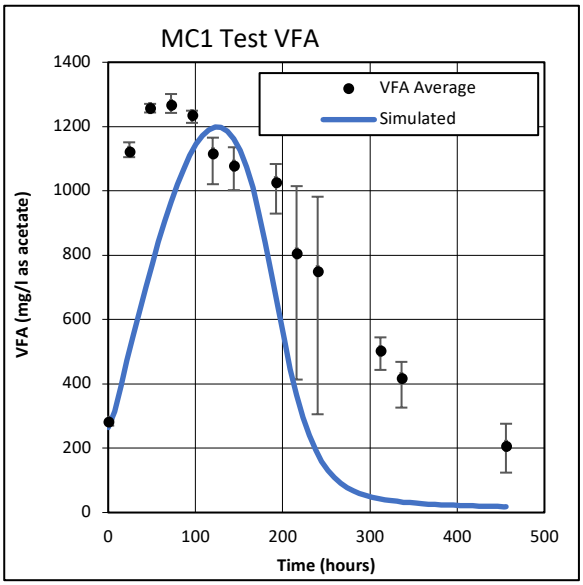

Figure 6. 18 : MC1 AugBMP test VFA

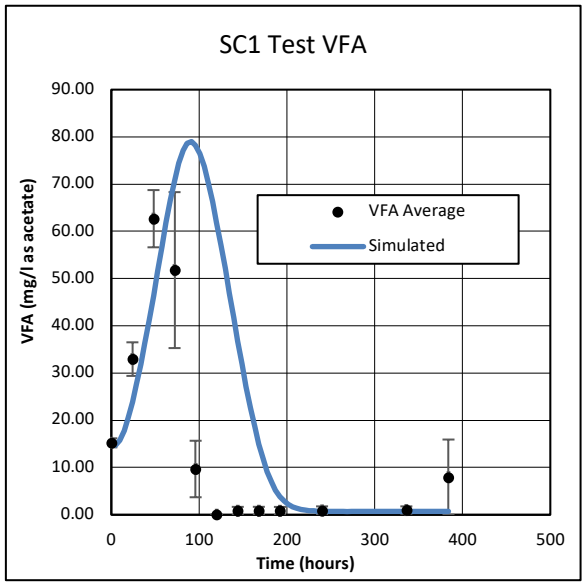

Figure 6. 19: SC1 AugBSP test VFA

6.2.10.9 pH

The decrease in pH in the MC1 AugBMP (Figure 6.20) test experiment over the first 24 hours was due to the production and accumulation of VFAs, as shown in Figure 6.18. The rapid formation of VFAs was caused by the fast hydrolysis rate of casein. The pH of the MC1 and SC1 experiments increased as the VFAs were consumed by the acetoclastic organisms. Furthermore, the pH of the SC1 AugBSP test reactor increased throughout the experiment, as sulphide was produced, which generated alkalinity in the system. However, as discussed in section 6.2.10.6, the total alkalinity concentrations in both the modelled MC1 AugBMP and SC1 AugBSP test reactors were lower than was observed due to the model pH. The source of the low final pH in the model may be due to the O/H ratio in the substrate formula.

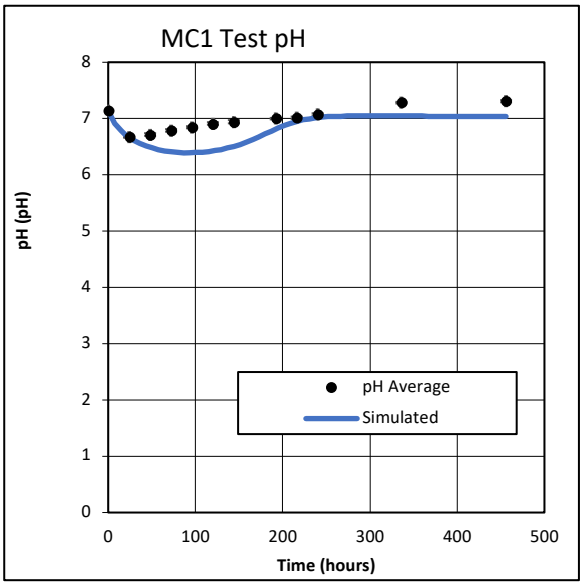

Figure 6. 20: MC1 AugBMP test pH

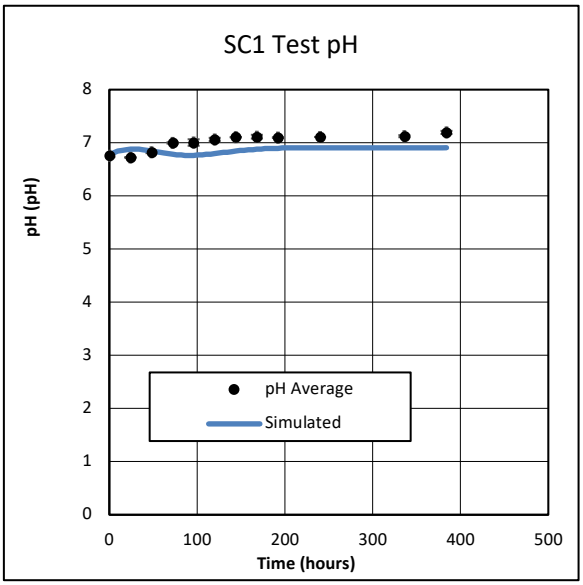

Figure 6. 21: SC1 AugBSP test pH

6.2.10.10 Methane

The methane produced by the modelled MC1 AugBMP test (Figure 6.22) reactor significantly exceeded the observed methane production. As previously mentioned, the modelled AugBMP test reactor was COD balanced. It was shown in Section 6.2.5.1, that the COD balance for the MC1 test experiment was below 100%, which indicated that the COD flux through the system was not conserved. It was believed that the error was due to the observed gas measurement. However, the methane production was not used as a variable for determining the composition of the biodegradable organics in the casein. Instead, the composition was determined using the change in COD, as the production of methane in the model is balanced by the COD consumed, as well as the aqueous carbonate alkalinity. Furthermore, the outcome of the experiment shows that the composition of casein was still accurately determined by the PE, even though the biogas data was not used. This outcome further strengthens the PWM_SA_AD model's ability, when used together with the parameter estimation function, to reconcile input parameters, even when inaccurate measurements are present, as the error is spread across the remaining measurements taken.

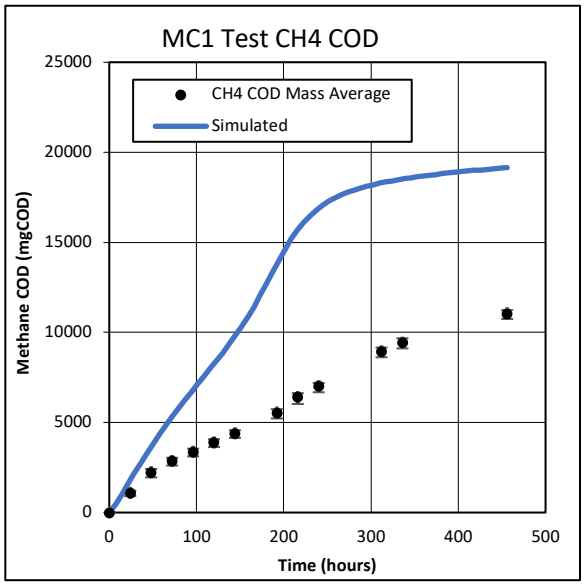

Figure 6. 22: MC1 AugBMP test methane

6.2.10.11 MC1 Model COD Balance

The COD balance for the AugBMP experiment is explained in Section 3.7.3.2. and Section 3.7.3.3. The PWM_SA_AD model code was adjusted to account for the COD removed from the modelled AugBMP reactor during sampling. The adjusted code did not affect the kinetics or the stoichiometry of the bioprocesses, but rather the liquid balance of the PWM_SA_AD model. The modelled COD balances were included in an attempt to identify the COD error experienced with the gas measurements. The modelled COD balance was compared to the observed COD balance, as shown in Table 6.18.

Table 6. 18: Modelled MC1 AugBMP test COD balance

	MC1		
	Observed	Model	%error
Unit	mgCOD	mgCOD	%
Starting	**65963**	**62087**	-6
Removed	15383	13288	-14
Remaining	29452	29729	1
Gas	11060	19149	73
Total Effluent	**55895**	**62166**	11
Unit	%	%	
Balance	**85**	**100**	**-**

Table 6.18 shows that the observed and modelled COD balances agreed well except for the methane gas COD. The modelled methane COD was significantly higher than the observed methane COD. The significant discrepancy between the observed and the modelled methane COD strongly suggested that the gas measurements are a substantial source of error for the AugBMP test, and subsequently, the BMP test.

6.2.11 Conclusions from the casein experiment

The primary objective of the casein experiment was to assess the accuracy of the AugBMP and AugBSP experiments when identifying the composition of a known organic. Furthermore, the casein experiment allowed for a direct comparison between the AugBMP and AugBSP tests, as the identical substrate was used in each test.

The casein composition identified by the modelled AugBMP and AugBSP tests accurately resembled the literature stated values, except for the larger O term. However, the composition determined by both the modelled AugBMP and AugBSP tests was similar, i.e. each with an elevated O term. Furthermore, the casein compositions determined by the modelled AugBMP and AugBSP test reactors were converted into a COD, FSA and OP concentration equivalent and compared to the measurements performed on the casein hydrolysate powder. The comparison showed that a low error was achieved between the modelled casein and the measured casein, and suggested that the composition determined by the PE for both the modelled MC1 and SC1 experiments was accurate.

Furthermore, the outcome showed that either the AugBMP test or the AugBSP test could be performed to determine the casein composition and suggested that the AugBSP test could accurately replace the AugBMP test, and consequently, the BMP test. However, in order to definitively prove this hypothesis, additional comparisons for a range of substrates should be conducted for the AugBMP and AugBSP tests. For this thesis, the casein experiment was used to validate the comparability between the AugBMP and AugBSP tests in the context of identifying the composition of the biodegradable particulates in PSS.

The PWM_SA_AD model's ability to accurately determine the casein composition using results from the AugBMP and AugBSP tests, highlighted the strength of incorporating

mathematical models for data reconciliation. The model was able to accurately reconcile the data and fit parameters that minimised the error across the observed measurements. Furthermore, the dynamics of the PWM_SA_AD model accurately represented the component concentration changes for each time step throughout the observed experiment. However, future investigations into the model intermediates should be performed, as components such as the VFA, due to the rapid hydrolysis of the casein, was challenging to replicate accurately.

6.3 PSS Experiments

The purpose of this experiment was to accurately identify the elemental composition of Primary Sewage Sludge (PSS), represented by CHONP, using the augmented batch test reactors.

The chemical composition of PSS impacts the mass of COD available, the alkalinity generated and the availability of organic carbon. The basis for this investigation is the prevention of AD failure. Under stable operating conditions, the products exiting an AD and the pH inside, are directly dependent on the composition (CHONP) of the biodegradable organics fed to it, in particular the protein content, which adds alkalinity and therefore pH buffer capacity to the aqueous phase. Identifying the composition of the influent wastewater organics will allow designers and plant operators to track the various elements and materials through the entire system and predict AD pH, allowing the digester to be operated at greater levels of efficiency and closer to capacity. This will also improve the effluent quality and the nutrient recovery potential from the AD products. The composition of the influent organics directly affects the digester pH. If the influent characteristics can be identified accurately, digester failure can be anticipated and prevented by simply changing the composition of the fed organics (more proteins). The experiments described in this chapter aimed to achieve the following:

- Determine the elemental composition of PSS using both the AugBMP and AugBSP tests, which includes utilising Parameter Estimation (PE) within the PWM_SA_AD model.
- Compare the PSS compositions determined by each respective test.
- Conclude on the accuracy and usability of each test as a means for substrate characterisation.
- Conclude if the dynamics of each experiment can be virtually replicated using the proposed PWM_SA_AD model.
- Identify the error associated with the proposed testing methods or modelling procedure.

The AugBMP test experiment results, as well as the AugBSP test experiment results, for the PSS substrate, will be explained simultaneously in this section.

6.3.1 Starting mixture

The PSS used for both the AugBMP and AugBSP test experiments was collected from Potsdam Wastewater Treatment Facility. The collection and storage of the PSS was explained in Section 3.3. The AugBMP test experiment was seeded using the starting mix shown in Table 3.1 in Section 3.4.3. Therefore, 1.25*l* of PSS and 10*l* of water was added to 3.75*l* of biomass from the methanogenic SSPAD effluent. The 15*l* starting mixture was then divided by three (5*l* each) into each AugBMP test reactors (T1 T2, and T3). The starting procedure was the same for the MP1, MP2 and MP3 experiments. The AugBSP test experiment used the starting mix as described in Table 3.2 in Section 3.5.3. Therefore, 3*l* of the diluted PSS mixture (3000mgCOD/*l*), 2.5*l* of the Na_2SO_4 solution and 0.5*l* of the H_2SO_4 solution was added to 6*l* of biomass from the sulphidogenic SSPAD effluent. The 12*l* starting mixture was then divided by two (6*l* each) into each AugBSP test reactor (T1 and T2). The starting procedure was the same for the SP1, SP2 and SP3 experiments.

6.3.2 Results for augmented batch test experiments on PSS

The results for the starting and ending values for the AugBMP and AugBSP test reactors for the MP1, MP2 and MP3, as well as the SP1, SP2 and SP3 experiments, which used PSS as an organic substrate, are shown in Table 6.19 and Table 6.20, respectively.

Table 6. 19: AugBMP test results for PSS

AugBMP Test		MP1			MP2			MP3		
	Unit	Start	End	Change (Δ)	Start	End	Change (Δ)	Start	End	Change (Δ)
Time	hours	0	695	695	0	576	576	0	452	452
Total COD	mgCOD/l	11429	6813	-4616	8822	6627	-2195	15207	11440	-3767
Soluble COD	mgCOD/l	2011	969	-1041	1151	1120	-31	1821	1307	-514
Particulate COD	mgCOD/l	9418	5843	-3575	7671	5507	-2164	13387	10133	-3253
VFA COD	mgCOD/l	205	0	-205	143	0	-143	247	112	-135
TKN	mgN/l	435	438	4	448	467	19	422	426	4
FSA	mgN/l	90	213	123	167	219	52	159	239	81
TP	mgP/l	75	74	-2	68	84	17	101	106	4
OP	mgP/l	18	23	5	8	14	6	14	21	7
VSS	mgVSS/l	6502	3839	-2663	4146	2963	-1183	6994	4915	-2079
pH	pH	6.94	6.92	-0.02	7.04	7.13	0.09	6.81	6.93	0.12
Carbonate Alk	mg/l as $CaCo_3$	473	1019	546	649	1193	544	511	1157	646
Total Alk	mg/l as $CaCo_3$	648	1042	394	771	1215	443	715	1266	551
CT	mgC /l	136	291	154	183	325	142	156	336	180
CH4 COD	mgCOD	0	11953	11953	0	11331	11331	0	12325	12325
Carbon in Gas	mgC	0	3569	3569	0	3383	3383	0	4225	4225

Table 6. 20: AugBSP test results for PSS

AugBSP Test		SP1			SP2			SP3		
	Unit	Start	End	Change (∆)	Start	End	Change (∆)	Start	End	Change (∆)
Time	hours	0	430	430	0	552	552	0	382	382
Total COD	mgCOD/l	1508	1715	207	1631	1582	-49	1167	1185	18
Soluble COD	mgCOD/l	414	734	320	397	819	422	268	557	289
Soluble Organic COD	mgCOD/l	69	91	22	91	127	35	92	48	-44
Soluble Sulphide COD	mgCOD/l	344	643	298	306	693	387	176	509	333
Particulate COD	mgCOD/l	1094	981	-113	1234	763	-471	899	628	-271
VFA COD	mgCOD/l	2	12	10	0	120	120	3	0	-3
Sulphate	$mgSO_4/l$	948	146	-802	-	-	-981	974	474	-500
TKN	mgN/l	49	48	-1	35	36	1	26	31	5
FSA	mgN/l	10	17	7	9	17	7	6	8	3
TP	mgP/l	7	7	0	6	7	1	6	5	-1
OP	mgP/l	3.0	4.0	1.0	3.0	3.7	0.7	2.4	3.7	1.4
VSS	mgVSS/l	581	616	36	565	381	-184	530	267	-263
pH	pH	7.39	7.31	-0.08	7.00	7.13	0.14	6.78	7.09	0.31
Carbonate Alk	mg/l as $CaCo_3$	366	1034	667	408	1015	606	217	789	572
Total Alk	mg/l as $CaCo_3$	554	1388	835	534	1435	901	278	1034	756
CT	mgC /l	96	271	175	116	275	159	66	213	147

6.3.2.1 AugBMP test experiments results

The AugBMP test results for the MP1, MP2 and MP3 experiments are shown in Table 6.19. The total COD concentrations at the start of the MP1, MP2 and MP3 experiments fluctuated. The total COD fluctuation was due to the total COD concentration in the PSS, which was collected in three separate batches from Potsdam. Consequently, the change in total COD concentration between the three experiments fluctuated, which indicated that the biodegradable organics present in the PSS differed between the three batches. Furthermore, the soluble COD utilised in the AugBMP test reactor differed between the three PSS experiments. The fluctuations in COD usage were a good indication of the variance of the organics present in PSS and highlighted the importance of correct characterisation.

The TKN concentrations remained consistent throughout the three experiments. The FSA concentration increased for all three experiments, but by different amounts. The FSA in the MP1 experiment was the highest, which correlated with the high COD and VSS change, indicating a high concentration of available biodegradable organics. The TP concentrations for MP1 and MP3 remained constant, while the MP2 TP concentration varied by 17mgP/*l*. A low OP concentration increase occurred in all three experiments. Furthermore, the OP increase was relatively constant (5-7 mgP/*l*) for all three experiments, indicating that the organic P content of the PSS was low.

The VSS concentration change was the highest in MP1. The larger VSS concentration change in the MP1 experiment, compared to the MP2 and MP3 experiments, indicated a larger concentration of biodegradable particulate organics in MP1. Furthermore, the MP1 experiment had the largest total COD concentration change. However, MP1 also had the largest soluble COD concentration change; therefore, the COD change associated with the particulate organics was calculated as the difference between the total COD and soluble COD concentrations and was determined to be 3575mgCOD/*l*. However, even though the particulate COD change was higher in MP1 than in MP2 and MP3, the f_{CV} ratio (COD/VSS) of MP2 (1.83) was greater than MP1 (1.34).

The change in carbonate alkalinity was greater than the change in total alkalinity for all three experiments. The reason that the carbonate alkalinity change was greater than the total

alkalinity change was that VFAs were consumed during the reaction. The VFA subspecies adds to the total alkalinity concentration. Therefore, the total alkalinity concentration is the sum of the subspecies that represent it. Furthermore, if the alkalinity of one subspecies decreases, the alkalinity of another subspecies increases such that the total alkalinity is conserved, which was the case for the carbonate alkalinity concentration.

6.3.2.2 AugBSP test experiments results

The AugBSP test results for the SP1, SP2 and SP3 experiments are shown in Table 6.20. The total COD concentration in the AugBSP test reactor should remain constant, as the system was completely sealed with zero headspace. The increase in the total COD concentration in SP1 was due to measurement error, as the total COD concentration in one of the test reactors increased, which subsequently increased the average total COD concentration between the T1 and T2 test reactors. The total soluble COD concentration increased throughout all three experiments, which indicated that biodegradable particulate material was being broken down and converted to soluble sulphide COD, consequently increasing the total soluble COD concentration.

Sulphate was consumed by the AugBSP reactor for all three experiments. However, the sulphate in the AugBSP test reactor for SP2 was completely utilised after 380 hours. Therefore, additional sulphate was added to one of the SP2 AugBSP reactors (T2). Therefore, the total change in sulphate by the AugBSP test reactor for SP2 was 981mgSO_4*/l*.

The TKN and TP concentrations remained constant throughout the experiment, indicating that N and P were conserved. Both the FSA and OP concentrations increased for all three experiments. Due to the diluted PSS used for the AugBSP test experiment, the increase in FSA and OP concentrations for the AugBSP test reactor were lower than observed in the AugBMP test reactor.

The VSS concentration decreased in the SP2 and SP3 reactors throughout the experiment. However, the VSS data set for SP1, (shown visually in Table 6.80 in Section 6.3.10.9) was seen to decrease for the first 200 hours, after which it began to increase, however, this increase in VSS was not considered by the PE conducted.

6.3.3 AugBMP test gas measurement

The gas produced by the AugBMP test experiment was captured inside of an inverted water column. The setup and specifications of the water columns are given in Section 3.4.2. The gas produced by the AugBMP test reactor was quantified by the volume of water displaced in the column. The procedure for calculating the mass of COD contained in the methane was described in Section 3.7.3. The cumulative methane COD for MP1, MP2 and MP3 is shown in Figures 6.23, 6.24 and 6.25.

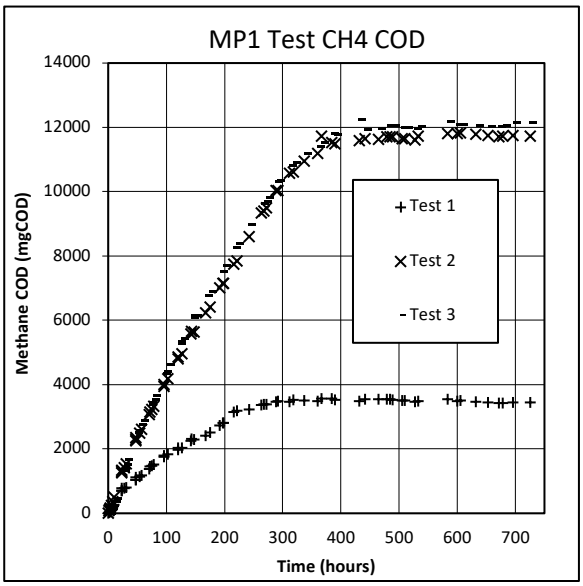

Figure 6. 23: MP1 AugBMP test CH_4 COD

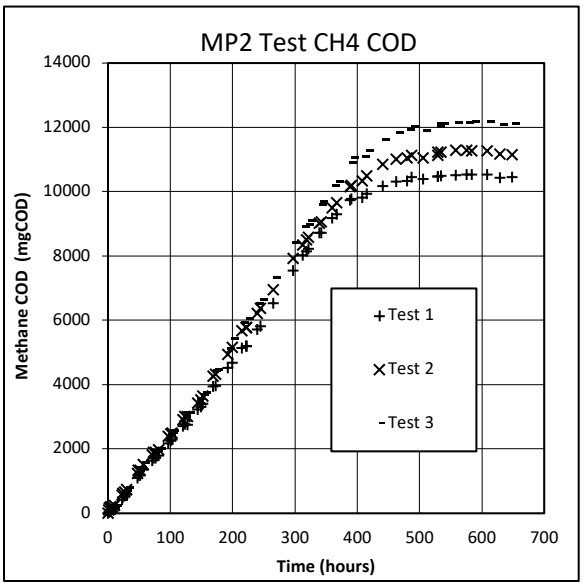

Figure 6. 24: MP2 AugBMP test CH_4 COD

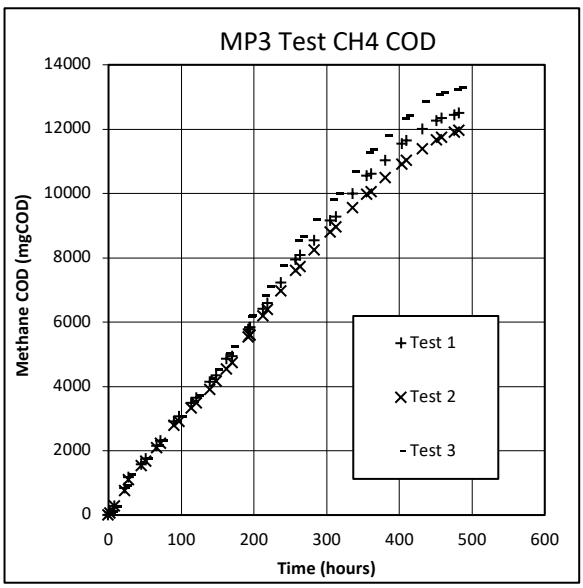

Figure 6. 25: MP3 AugBMP test CH_4 COD

The cumulative methane COD produced by the MP2 (Figure 6.24) and MP3 (Figure 6.25) experiments had a low variance between the T1, T2 and T3 test reactors. The low variance indicated that the cumulative methane COD collected by the inverted columns was repeatable for MP2 and MP3. However, the gas collected in the T1 column for MP1 (Figure 6.23) suggested that a gas leak occurred.

6.3.4 AugBMP test mass balances

The mass of material entering the AugBMP test reactor should equate to the mass of material leaving the reactor, as mass was conserved within the system. The COD entering the AugBMP test reactor was contained inside the inoculum and the substrate, and the COD leaving the AugBMP test reactor was either in the liquid effluent stream or in the methane gas produced. As described in Section 3.7.3.2, the total COD at the start of the AugBMP reactor must equate to the sum of COD removed from the reactor during sampling, the methane COD contained in the inverted water column, and the COD remaining in the reactor at the end of the experiment. The results for the methane partial pressure in MP2 and MP3 are given in Table 6.21. The methane partial pressure in the MP1 experiment was not measured, however, the partial pressure for MP1 was set to the same methane partial pressure as MP2 (62.8%). Therefore, the methane partial pressures used for MP1, MP2 and MP3 were 62.8%, 62.8% and 54.7%, respectively.

Table 6. 21: Gas chromatography results

		Period	
Experiment Type	**Unit**	**MP2**	**MP3**
Methanogenic SSPAD	% Methane	59.2± 1.7	57.2± 2.7
AugBMP Control	% Methane	57.5± 9	50.3± 8.7
AugBMP Test	% Methane	62.8± 6.5	54.7± 4.5

6.3.4.1 MP1 COD Balance

The COD balance for the MP1 AugBMP test experiment was calculated using Equation 3.12 from Section 3.7.3.2. Table 6.22 indicated that a poor COD balance (as described in Section 3.7.2) in the MP1 AugBMP test reactor was achieved, as the balances were 70%, 86% and 85%.

Table 6. 22: MP1 AugBMP test COD balance

MP1 AugBMP Test Mass Balance (62.8% Methane Partial Pressure)						
	Starting Mass	Mass Removed	Remaining Mass	Gas Mass	Total Effluent	Balance
Unit	mgCOD	mgCOD	mgCOD	mgCOD	mgCOD	%
T1	55053	18311	16677	3439	38427	69.8
T2	58494	19828	18749	11731	50307	86.0
T3	57886	19378	17713	12066	49156	84.9

6.3.4.2 MP2 COD Balance

The COD balance for the MP2 AugBMP test experiment was calculated using the same procedure used for the MP1 AugBMP test reactor. Table 6.23 indicated that a good COD balance for MP2 was achieved for the T1 and T2 reactors, as the balances were within 10% at 102% and 96%, respectively.

Table 6. 23: MP2 AugBMP test COD balance

MP2 AugBMP Test Mass Balance (62.8% Methane Partial Pressure)						
	Starting Mass	Mass Removed	Remaining Mass	Gas Mass	Total Effluent	Balance
Unit	mgCOD	mgCOD	mgCOD	mgCOD	mgCOD	%
T1	42369	13232	19342	10537	43111	101.8
T2	47991	14260	20574	11294	46129	96.1
T3	41967	15155	21314	12162	48631	115.9

6.3.4.3 MP3 COD Balance

The COD balance for the MP3 AugBMP test experiment was calculated using the same procedure used for the MP1 and MP2 AugBMP test reactors. Table 6.24 indicated that a good COD balance for MP3 was achieved for the T1 and T2 reactors, as the balances were 103% and 100%, respectively.

Table 6. 24: MP3 AugBMP test COD balance

MP3 AugBMP Test Mass Balance (54.7% Methane Partial Pressure)						
	Starting Mass	Mass Removed	Remaining Mass	Gas Mass	Total Effluent	Balance
Unit	mgCOD	mgCOD	mgCOD	mgCOD	mgCOD	%
T1	69075	21905	36918	12256	71079	102.9
T2	75300	23400	40106	11653	75159	99.8
T3	83734	22833	36918	13064	72816	87.0

6.3.4.4 TKN and TP balance

The mass flux of other constituents present in the entering and exiting streams such as the TKN and TP were also checked using the mass balanced approach. The total mass of these two constituents should remain constant throughout the experiment. The TKN and TP mass fluxes were calculated using Equation 3.14, as described in Section 3.7.5, and are summarised in Table 6.25.

Table 6. 25: AugBMP test TKN/TP balance for PSS

Reactor	TKN in	TKN out	**Balance**	TP in	TP out	**Balance**
	mgTKN-N/l		**%**	mgTP-P/l		**%**
MP1						
T1	443	443	**100**	75	95	**127**
T2	460	453	**98**	76	63	**83**
T3	401	418	**104**	76	63	**84**
MP2						
C1	470	496	**105**	68	85	**126**
C2	423	480	**114**	69	83	**120**
C3	428	440	**103**	66	85	**129**
MP3						
C1	447	560	**125**	85	125	**147**
C2	515	552	**107**	99	95	**96**
C3	521	524	**101**	117	103	**88**

The TKN data for the AugBMP test reactor exhibited internal consistency in the conservation of N (indicated by the good mass balances achieved of 100%, 98%, and 104% for T1, T2 and T3 respectively) for all three PSS experiments. However, the TP balances experienced error. The source of the error was difficult to determine as the AugBMP test reactors were completely sealed and the substrate was only added to the reactor once, during the seeding procedure. Furthermore, P could not leave the reactor via the gas stream. Therefore, the P in the system should have been conserved, and the discrepancy was most likely caused by measurement error. However, the TP balances did not affect the determination of the composition, as the change in OP concentration indicated the release of organically bound phosphorus.

6.3.5 AugBSP test mass balances

The AugBSP test experiment was conducted in a purpose-built reactor with zero headspace. The zero headspace ensured that the products produced by the reaction remained in the aqueous phase. Therefore, unlike the methanogenic AugBMP experiment, the mass of the products entering and exiting the system are conserved within the aqueous solution, as no gas evolution occurred. Furthermore, due to the zero headspace in the AugBSP test reactor, the total COD concentration remains constant. Therefore, the mass balances were performed for sulphur, TKN and TP.

6.3.5.1 Sulphur, TKN and TP balance

The sulphur, N and P balance is explained in Section 3.7.4 and Section 3.7.5. The sulphur utilised in the sulphate, and sulphur produced in the sulphide should be conserved throughout the AugBSP test experiment, assuming that no other S compounds formed. Furthermore, the total mass of TKN and TP should remain constant throughout the experiment. The TKN and TP mass fluxes were calculated using Equation 3.14, as described in Section 3.7.5. The AugBSP test mass balances are shown in Table 6.26.

Table 6. 26: AugBSP test mass balance for PSS

AugBSP	S in	S out	**Balance**	TKN in	TKN out	**Balance**	TP in	TP out	**Balance**
Control	mgS/l		**%**	mgTKN-N/l		**%**	mgTP-P/l		**%**
SP1									
T1	261	167	**64**	48	48	**100**	7.2	6.5	**90**
T2	273	132	**48**	50	47	**95**	6.7	6.8	**101**
SP2									
T1	286	177	**62**	41	43	**107**	5.9	6.5	**109**
T2	326	210	**65**	43	44	**104**	5.5	6.9	**126**
SP3									
T1	171	175	**102**	34	35	**102**	6.1	5.1	**84**
T2	163	159	**98**	34	35	**103**	5.8	5.3	**93**

A good S balance was achieved in the AugBSP test reactor for the SP3 experiment, as the balance for T1 and T2 was 102% and 98%, respectively. However, a poor S balance was achieved in the SP1 and SP2 experiments. The source of the discrepancy between the S-in and S-out concentrations in the SP1 and SP2 experiments was difficult to identify, as the S should

have been conserved within the completely sealed reactor with zero headspace. Therefore, the error may lie with either the sulphate, or the sulphide measurement. However, for this thesis, the sulphide values were taken to be accurate and the models were fitted to the sulphide data.

The TKN and TP in the AugBSP test reactor had good balances for all three experiments, except for the TP in the T2 SP2 reactor, as well as the TP in the T1 SP3 reactor.

6.3.6 Stoichiometric Composition Identification

The composition of the biodegradable particulate organics present in the PSS was identified by calculating the change in elemental concentrations between the ending and the starting concentrations of the augmented batch test experiments. The calculation is explained in detail in Section 3.9.2. The mass ratios for each element (f_{CV}, f_C, f_N and f_P) needed to be determined in order to calculate the unknown mass ratios (f_O and f_H). Therefore, the change in COD, C, N, P and VSS throughout the experiment was required.

6.3.6.1 AugBMP test experiment

The results for the stoichiometric composition calculation for PSS in the AugBMP test reactors are shown in Table 6.27. The stoichiometric calculation used to identify the composition of the biodegradable organic for the AugBMP experiment was previously described in Section 6.2.6. The procedure used to identify the PSS composition was identical, however, the change in concentrations between the test and control reactors isolated the influence of the PSS in the AugBMP test experiment. The concentrations observed in the AugBMP control reactor were divided by two, as the inoculum used in the AugBMP test reactor was diluted to half the concentration of the AugBMP control reactor.

The VSS concentration decreased in all three experiments, which was due to the breakdown of particulate organics in the PSS. Strictly speaking, the concentration of soluble COD utilised by the AugBMP control and test reactors should be subtracted from the total COD concentration when identifying the composition of the particulate organics. However, the soluble COD concentration contributes to the total volume of biogas produced by the experiment. Furthermore, the total volume of biogas was used to determine the carbon content in the gas

phase. Therefore, subtracting the influence of the soluble biodegradable organics was challenging, as the equivalent COD needed to be subtracted from the biogas produced. Consequently, the composition identified by the stoichiometric calculation included the influence of the biodegradable soluble organics. Therefore, the use of computer models allows for the particulate organics group in the PSS to be isolated, as described in Section 3.11.3.2

6.3.6.2 AugBSP test experiment

The results for the stoichiometric composition calculation for PSS in the AugBSP test reactors are shown in Table 6.28. The stoichiometric calculation used to identify the composition of the biodegradable organic for the AugBSP experiment was previously described in Section 6.2.6. The procedure used to identify the PSS composition was identical, however, the change in concentrations between the test and control reactors isolated the influence of the PSS in the AugBSP test experiment. As was done for the AugBMP test experiment, the concentrations observed in the AugBSP control reactor were divided by two, as the inoculum used in the AugBSP test reactor was diluted to half the concentration of the AugBSP control reactor.

The biodegradable COD available in the PSS for the SP1 and SP3 experiments was determined using the soluble sulphide COD and the VFA COD concentrations. For the SP1 and SP3 experiments, VFAs were consumed throughout the reaction; therefore, the VFAs consumed contributed to the total sulphide COD concentration produced. Subsequently, the VFA COD utilised was subtracted from the sulphide COD in order to isolate the sulphide COD produced due to the biodegradable organics in the PSS. For the SP2 reactor, VFAs were produced throughout the experiment. The sum of the VFA COD and sulphide COD quantified the total COD available in the biodegradable organics present in the PSS.

As mentioned above for the AugBMP test experiment, the concentration of the soluble organic COD utilised should be subtracted from the available biodegradable COD, such that the biodegradable particulate COD is isolated. However, this was not possible for the SP1 and SP2 due to the increase in soluble organic COD (which contributed to the total sulphide COD production) throughout the experiment. The use of the mass balanced model allowed for the particulate organic group in the PSS to be isolated as described in Section 3.11.3.3.

Table 6. 27: AugBMP test stoichiometric composition identification for PSS

PSS Experiment		MP1			MP2			MP3		
		Control	Test	Test - Control	Control	Test	Test - Control	Control	Test	Test - Control
Measured	**Unit**	Change (Δ)	Change (Δ)	Change (Δ)	Change (Δ)	Change (Δ)	Change (Δ)	Change (Δ)	Change (Δ)	Change (Δ)
Total COD	mgCOD/l	-1211	-4616	-3405	-319	-2195	-1876	-907	-3767	-2861
VFA COD	mgCOD/l	2	-205	-207	-19	-143	-124	31	-135	-166
FSA	mgN/l	42	123	80	21	52	31	28	81	52
OP	mgP/l	3	5.5	3	4	6.4	2	5	6.9	2
VSS	mgVSS/l	-516	-2663	-2147	-552	-1183	-631	-306	-2079	-1773
Carbonate Alk	mg/l as $CaCo_3$	107	546	439	168	544	376	151	646	495
CH_4 COD	mgCOD	1102	11953	10851	3458	11331	7873	2348	12325	9976
C in Gas	mgC	359	3569	3209	1128	3383	2255	875	4225	3349
COD Change										
Biodegradable COD	mgCOD/l	-	-	3198	-	-	1752	-	-	2695
Carbon Change										
C in Gas	mgC/l	-	-	642	-	-	451	-	-	670
C in H_2CO_3 Alk	mgC/l	-	-	105	-	-	90	-	-	119
Total C	mgC/l	-	-	747	-	-	541	-	-	789
VSS Change										
Biodegradable VSS	mgVSS/l	-	-	2147	-	-	631	-	-	1773
Mass Ratio										
f_{CV}	gCOD/gVSS	-	-	1.490	-	-	2.776	-	-	1.520
f_C	gC/gVSS	-	-	0.348	-	-	0.858	-	-	0.445
f_N	gN/gVSS	-	-	0.037	-	-	0.049	-	-	0.029
f_P	gP/gVSS	-	-	0.001	-	-	0.004	-	-	0.001
f_H	gH/gVSS	-	-	0.137	-	-	0.073	-	-	0.101
f_O	gO/gVSS	-	-	0.476	-	-	0.017	-	-	0.424
Compostion										
C	-	-	-	1	-	-	1	-	-	1
H	-	-	-	4.739	-	-	1.023	-	-	2.722
O	-	-	-	1.025	-	-	0.014	-	-	0.715
N	-	-	-	0.092	-	-	0.049	-	-	0.057
P	-	-	-	0.002	-	-	0.002	-	-	0.001

Table 6. 28: AugBSP test stoichiometric composition identification for PSS

PSS Experiment		SP1			SP2			SP3		
		Control	Test	Test - Control	Control	Test	Test - Control	Control	Test	Test - Control
Measured	**Unit**	Change (Δ)	Change (Δ)	Change (Δ)	Change (Δ)	Change (Δ)	Change (Δ)	Change (Δ)	Change (Δ)	Change (Δ)
Soluble Sulphide COD	mgCOD/l	21	298	278	20	387	368	14	333	320
VFA COD	mgCOD/l	40	10	-30	54	120	66	0	-3	-3
FSA	mgN/l	2	7	5	1	7	6	1	3	1
OP	mgP/l	0	1.0	1	0	0.7	1	1	1.4	1
VSS	mgVSS/l	92	36	-56	9	-184	-193	169	-263	-432
Carbonate Alk	mg/l as $CaCo_3$	37	667	630	35	606	572	63	572	508
COD Change										
Biodegradable COD	mgCOD/l	-	-	248	-	-	433	-	-	317
Carbon Change										
C in Gas	mgC/l	-	-	-	-	-	-	-	-	-
C in H_2CO_3 Alk	mgC/l	-	-	151	-	-	137	-	-	122
Total C	mgC/l	-	-	151	-	-	137	-	-	122
VSS Change										
Biodegradable VSS	mgVSS/l	-	-	56	-	-	193	-	-	432
Mass Ratio										
f_{CV}	gCOD/gVSS	-	-	4.412	-	-	2.245	-	-	0.733
f_C	gC/gVSS	-	-	2.687	-	-	0.711	-	-	0.283
f_N	gN/gVSS	-	-	0.097	-	-	0.033	-	-	0.003
f_P	gP/gVSS	-	-	0.015	-	-	0.003	-	-	0.002
f_H	gH/gVSS	-	-	-0.489	-	-	0.073	-	-	0.077
f_O	gO/gVSS	-	-	-1.310	-	-	0.181	-	-	0.635
Compostion										
C	-	-	-	1	-	-	1	-	-	1
H	-	-	-	-2.186	-	-	1.230	-	-	3.278
O	-	-	-	-0.366	-	-	0.191	-	-	1.685
N	-	-	-	0.031	-	-	0.040	-	-	0.010
P	-	-	-	0.002	-	-	0.001	-	-	0.003

6.3.7 Modelling the PSS experiment

The procedure used to identify the particulate substrate composition using the PE function was described in Section 3.11.3.2. The inoculum used in both the modelled AugBMP and AugBSP test experiments was taken from the modelled methanogenic and sulphidogenic SSPADs, respectively. The concentration of biomass in the modelled SSPAD effluent was correctly adjusted to account for the starting dilutions of the augmented batch test experiments.

The compositions of the biomass and the UPOs remained fixed at $C_1H_{1.4}O_{0.4}N_{0.2}$ and $C_1H_{1.571}O_{0.426}N_{0.166}P_{0.019}$, respectively, for both the modelled AugBMP and AugBSP test experiments. The composition and concentration of the residual biodegradable organics were previously identified using the modelled AugBMP control reactor. Therefore, the composition of the residual biodegradable organics (X_B_Inf) was used as an input for the modelled AugBMP test experiment. However, this presented a problem, as the PWM_SA_AD model only included one biodegradable particulate component. Consequently, there was no additional component available that could be used to identify the composition of the biodegradable particulates present in the PSS. Therefore, in order to identify the composition of the biodegradable particulate organics present in the PSS, an additional component was added to the PWM_SA_AD model. The additional component, named PSS particulate organics (X_B_PSS), was identical to the biodegradable particulate component (X_B_Inf) already in the model. This is further explained in Section 3.11.3.2.

The starting concentrations of constituents such as FSA, OP, VFA, H_2CO_3 alkalinity, as well as the reactor pH in the modelled augmented batch test experiments were adjusted to the averaged starting values for the observed augmented batch test experiments. The mass of the BSO, USO, UPO and PSS particulate organics, as well as the composition of the PSS particulate organics, were used as unknown parameters for the modelled AugBMP and AugBSP experiments. Additionally, the saturation hydrolysis constant for the breakdown of PSS particulate organics (KM_BPSS_AD_hyd), the growth rate of the acetoclastic organisms (mu_AM/mu_AS), and the half-saturation coefficient of the acetoclastic organisms (Ks_AM/Ks_AS) were adjusted by the PE. The PE conducted hundreds of iterations until the lowest error across the observed measurements was achieved. The parameters used by the PE for identifying the composition of the biodegradable particulates in the PSS for the modelled

AugBMP test experiment are summarised in Table 3.12 in Section 3.11.3.2, and the parameters used by the PE in the modelled AugBSP test experiment are summarised in Table 3.13 in Section 3.11.3.3

The observed measurements used to identify the composition of the biodegradable particulate organics present in the PSS for the AugBMP and AugBSP tests differed. The AugBMP test reactor had measurements conducted on both the liquid and gas phases, whereas, the AugBSP reactor had all the measurements taken in the aqueous phase. The observed measurements used for the modelled AugBMP test reactor is given in Table 6.29, and the observed measurements used for the modelled AugBSP test reactor is given in Table 30.

Table 6. 29: Modelled AugBMP test variables for PSS

Variable	Description	Weighting		
		MP1	MP2	MP3
Alkalinity	The total alkalinity generated	1	1	1
COD_total	The unfiltered COD concentration	1	1	2
COD_soluble	The filtered COD concentration	5	1	5
FSA	The Free and Saline Ammonia concentration	1	1	5
$H2CO_3$ alkalinity	The carbonate alkalinity generated	1	1	5
OrthoP	The Orthophosphate concentration	5	5	5
VFA	The Volatile Fatty Acids concentration	10	5	1
VSS	The Volatile Suspended Solids concentration	1	1	5
p_H_s	The reactor pH	1	1	1

Table 6. 30: Modelled AugBSP test variables for PSS

Variable	Description	Weighting		
		SP1	SP2	SP3
Alkalinity	The total alkalinity generated	1	1	1
C(S_SO4)	The sulphate concentration	1	1	1
COD(S_HS)	The sulphide COD concentration	10	10	1
COD_total	The unfiltered COD concentration	1	1	1
COD_soluble	The filtered COD concentration	1	1	1
FSA	The Free and Saline Ammonia concentration	10	10	50
$H2CO_3$ alkalinity	The carbonate alkalinity generated	1	1	1
OrthoP	The Orthophosphate concentration	10	10	1
VFA	The Volatile Fatty Acids concentration	1	1	1
VSS	The Volatile Suspended Solids concentration	10	10	3
p_H_s	The reactor pH	10	10	10

The weighting for the variables in Table 6.29 and 6.30 were determined as was described in Section 5.2.4.

6.3.8 Modelled Composition Identification

The PE ran hundreds of iterations until the correct combination of parameters, which achieved the desired results with the lowest error was determined.

6.3.8.1 AugBMP test experiment

The parameters determined by the PE for the AugBMP test experiments using PSS are summarised in Table 6.31.

Table 6. 31: Modelled AugBMP test composition identification for PSS

Parameter	MP1	MP2
PSS Composition	$C_1H_{2.964}O_{0.829}N_{0.071}P_0$	$C_1H_{2.654}O_{0.236}N_{0.18}P_{0.002}$
M(X_B_PSS)	11.669	9.912
M(X_U_Inf)	15.63	6.447
kM_BPSS_AD_hyd	1.542	0.377
mu_AM	0.387	0.025
KS_AM	1	0.023

Parameter	MP3
PSS Composition	$C_1H_{1.056}O_{0.048}N_{0.093}P_{0.001}$
M(X_B_PSS)	17.451
M(X_U_Inf)	11.431
kM_BPSS_AD_hyd	0.558
mu_AM	4
KS_AM	0.508

The parameters determined by the PE for the PSS in the modelled AugBMP test experiment differed as was expected. One of the primary objectives for identifying the composition of the biodegradable particulates present in the PSS was due to the varying nature of the PSS, which was directly affected by the influent stream entering the treatment plant. The influent stream is subject to cyclic and seasonal variations. Therefore, each batch of PSS collected from Potsdam WWTW was expected to differ. Subsequently, the augmented batch tests were developed to identify and characterise the PSS.

6.3.8.2 AugBSP test experiment

The parameters determined by the PE for the AugBSP test experiments using PSS are summarised in Table 6.32:

Table 6. 32: Modelled AugBSP test composition identification for PSS

Parameter	SP1	SP2
PSS Composition	$C_1H_{1.856}O_{0.555}N_{0.0707}P_{0.004}$	$C_1H_{2.365}O_{0.323}N_{0.0723}P_{0.004}$
M(X_B_PSS)	1.32	1.112
M(X_U_Inf)	2.102	2.198
kM_BPSS_AD_hyd	8.976	6.575
mu_AS	6.536	2.932
KS_AS	0.162	0.047

Parameter	SP3
PSS Composition	$C_1H_{1.004}O_{0.431}N_{0.032}P_0$
M(X_B_PSS)	1.484
M(X_U_Inf)	1.64
kM_BPSS_AD_hyd	10.926
mu_AS	400
KS_AS	0.003

As was shown for the modelled AugBMP test experiment results in Section 6.3.8.1 above, the parameters determined by the PE for the PSS in the modelled AugBSP test experiment differed. However, as previously mentioned, the biodegradable particulates in the PSS do not remain constant and are subject to fluctuations of the treatment plant.

6.3.9 Modelled AugBMP test PSS experiment results

The observed results from the T1, T2 and T3 AugBMP test reactors were summarised by averaging the values obtained for each measurement taken. Table 6.33 and Table 6.34 summarise the results obtained for the starting and ending concentrations for each constituent in the modelled AugBMP test experiments for PSS. The results obtained from the model were compared to that of the observed results. Furthermore, the results have been compared visually for the AugBMP test experiment in Section 6.3.9.1 (Figure 6.26) to Section 6.3.9.10 (Figure 6.55). The visual comparisons between the modelled and observed results were used to evaluate the accuracy of the dynamic parameters established by the PE.

The total COD concentration change for all three observed AugBMP test experiments were replicated by the modelled test reactor well. The total cumulative methane COD produced by MP1 and MP3 were significantly higher (>6000mgCOD) than the observed methane COD produced. However, the cumulative methane for the observed MP2 experiment was replicated by the modelled AugBMP test reactor well.

The FSA concentration released by the modelled MP2 and MP3 experiments was higher than the observed FSA concentration released. However, the PE minimised the error between the FSA and carbonate alkalinity measurements; therefore, the additional FSA concentration released in the modelled AugBMP test experiments was required for the model to replicate the observed carbonate alkalinity concentrations well.

The increase in the observed total alkalinity was replicated by the modelled AugBMP test reactor for all three experiments well. The increase in the carbonate alkalinity was greater than the increase in total alkalinity. As explained in Section 6.3.2.1, the reason that the carbonate alkalinity change was greater than the total alkalinity change, was due to the consumption of VFAs during the reaction. The decrease in alkalinity of one subspecies results in the increase in alkalinity of another subspecies, such that the total alkalinity is conserved.

It was crucial that the total COD and VSS concentration change for the observed AugBMP test experiment was well replicated by the model, as the substrate used was a biodegradable particulate organic. Subsequently, the modelled AugBMP test reactor replicated the VSS concentration in the observed test reactor well, indicating that the parameters determined by the PE accurately represented the particulate organics.

Table 6. 33: Modelled MP1 and MP2 AugBMP test results for PSS

MP1 Test Model Results								MP2 Test Model Results					
		Start		End		Change		Start		End		Change	
COD	**Unit**	**Observed**	**Modelled**	**Observed**	**Modelled**	**Observed**	**Modelled**	**Observed**	**Modelled**	**Observed**	**Modelled**	**Observed**	**Modelled**
Total COD	mgCOD/l	11429	11546	6813	6677	**-4616**	**-4869**	8822	8755	6627	6201	**-2195**	**-2554**
Soluble COD	mgCOD/l	2011	1999	969	1216	**-1041**	**-783**	1151	1244	1120	1106	**-31**	**-138**
Gas													
Methane	mgCOD	0	0	11953	21077	**11953**	**21077**	0	0	11331	10235	**11331**	**10235**
Nitrogen													
FSA	mgFSA/l	90	90	213	203	**123**	**113**	167	167	219	293	**52**	**126**
Phosphate													
OP	mgOP/l	17.7	17.7	23.2	22.5	**5.5**	**4.8**	7.6	7.6	13.9	14.1	**6.4**	**6.5**
Alkalinity													
Carbonate	mg/l as CaCO3	473	472	1019	1025	**546**	**552**	649	656	1193	1194	**544**	**539**
Total	mg/l as CaCO3	648	672	1042	1075	**394**	**403**	771	786	1215	1236	**443**	**450**
Species													
VFA Conc	mg/l as acetate	191.8	191.8	0.0	2.7	**-192**	**-189**	133.8	133.8	0.0	4.5	**-134**	**-129**
CT	mgC/l	136	136	291	339	**154**	**203**	183	183	325	327	**142**	**144**
Solids													
VSS	mgVSS/l	6502	6397	3839	3718	**-2663**	**-2679**	4146	4076	2963	2956	**-1183**	**-1120**
pH													
pH		6.94	6.94	6.92	6.66	**-0.02**	**-0.28**	7.04	7.04	7.13	7.08	**0.09**	**0.04**

Table 6. 34: Modelled MP3 AugBMP test results for PSS

MP3 Test Model Results							
		Start		End		Change	
COD	**Unit**	**Observed**	**Modelled**	**Observed**	**Modelled**	**Observed**	**Modelled**
Total COD	mgCOD/l	15207	15482	11440	11115	**-3767**	**-4368**
Soluble COD	mgCOD/l	1821	1800	1307	1361	**-514**	**-439**
Gas							
Methane	mgCOD	0	0	12325	18388	**12325**	**18388**
Nitrogen							
FSA	mgFSA/l	159	159	239	289	**81**	**130**
Phosphate							
OP	mgOP/l	14.2	14.2	21.1	23.3	**6.9**	**9.1**
Alkalinity							
Carbonate	mg/l as CaCO3	511	510	1157	1147	**646**	**636**
Total	mg/l as CaCO3	715	734	1266	1198	**551**	**464**
Species							
VFA Conc	mg/l as acetate	231.7	231.7	105.3	0.4	**-126**	**-231**
CT	mgC/l	156	156	336	373	**180**	**217**
Solids							
VSS	mgVSS/l	6994	6689	4915	5181	**-2079**	**-1508**
pH							
pH		6.81	6.81	6.93	6.68	**0.12**	**-0.13**

6.3.9.1 Total COD

The unfiltered COD concentrations for the observed and modelled experiments are shown in Figures 6.26, 6.27 and 6.28. The total COD concentration for all three of the observed AugBMP experiments was well replicated by the modelled AugBMP test reactor. The total COD concentration was dependent on the mass and composition of the biodegradable particulates present in the PSS, as well as the mass of the UPOs. The PE minimised the error between the total COD concentration and the VSS concentration by adjusting the mass and composition of the biodegradable particulates and the mass of the UPOs.

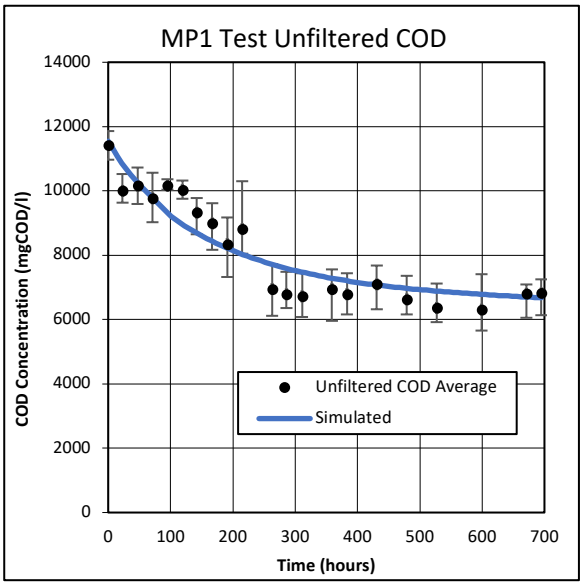

Figure 6. 26: MP1 AugBMP test total COD

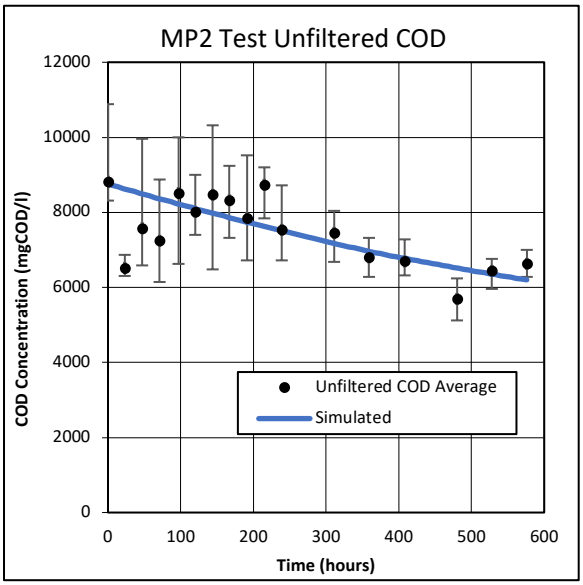

Figure 6. 27: MP2 AugBMP test total COD

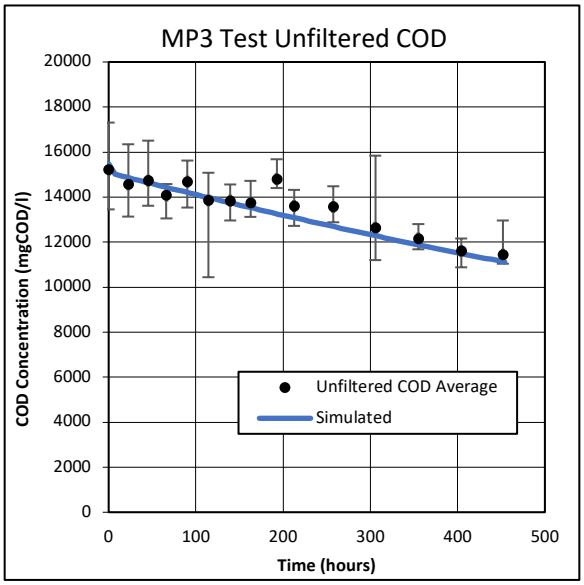

Figure 6. 28: MP3 AugBMP test total COD

6.3.9.2 Soluble COD

The filtered COD concentrations for the observed and modelled experiments are shown in Figures 6.29, 6.30 and 6.31. The soluble COD concentration for all three observed AugBMP test reactors decreased throughout the experiment. As mentioned in Section 6.3.6.1, the influence of the soluble organics was challenging to remove when calculating the compositions stoichiometrically. However, the modelled AugBMP test reactors took the concentration of the soluble organics into account (see Section 3.11.3.2) when identifying the composition of the biodegradable particulate organics in the PSS. Therefore, it can be seen, that the PSS contained

a portion of soluble organics, as both RFBSO and VFAs, which were also degraded during the AugBMP test experiment. However, the influence of these soluble organics was accounted for well in the modelled AugBMP test reactor.

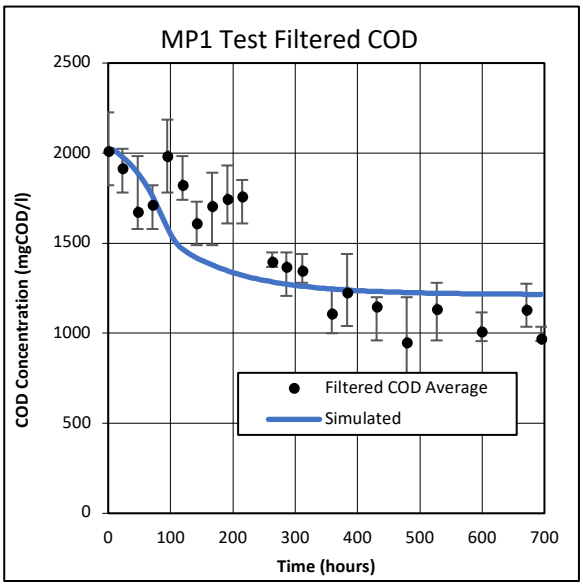

Figure 6. 29: MP1 AugBMP test soluble COD

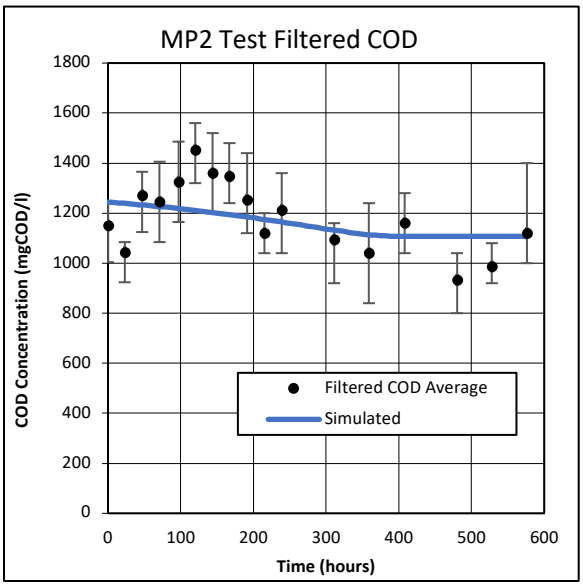

Figure 6. 30: MP2 AugBMP test soluble COD

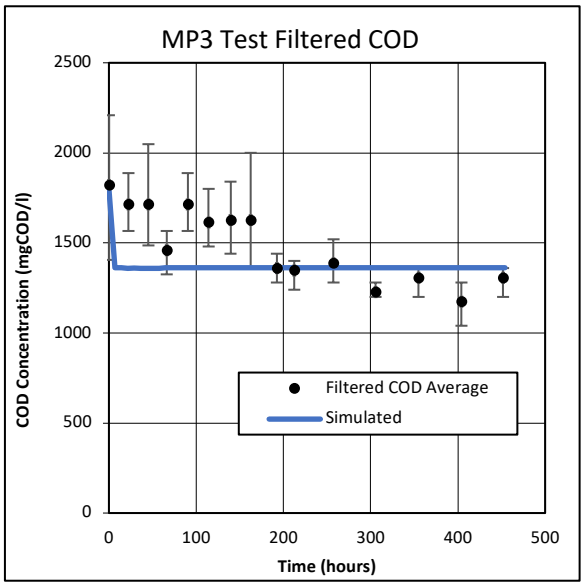

Figure 6. 31: MP3 AugBMP test soluble COD

6.3.9.3 Free and Saline Ammonia (FSA)

The observed FSA concentration, as well as the rate at which the FSA was released in the MP1 experiment (Figure 6.32), was well replicated by the modelled AugBMP test reactor. The FSA concentration in the modelled MP2 and MP3 experiments (Figures 6.33 and 6.34) was higher

than the observed FSA concentrations. However, the rate at which the FSA was released into the modelled MP2 AugBMP test reactor (Figure 6.33) was accurate. As previously mentioned in Section 5.2.6.3, the PE minimised the error between the FSA and carbonate alkalinity measurements, as the two were related. Therefore, the higher FSA concentrations in the modelled AugBMP test reactor for MP2 and MP3 were as a result of the PE fitting the carbonate alkalinity concentrations.

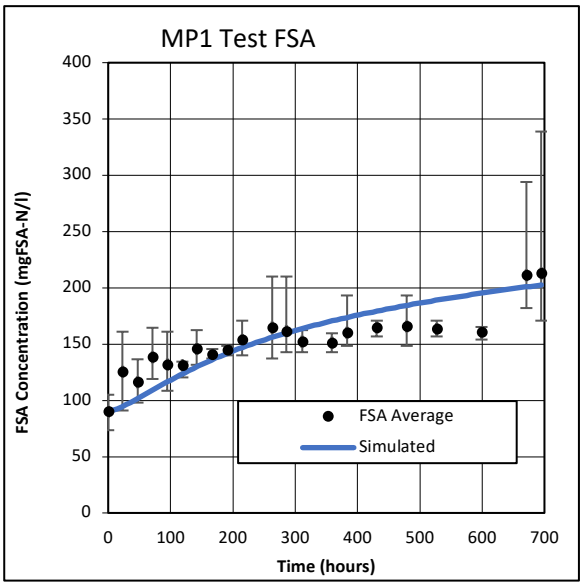

Figure 6. 32: MP1 AugBMP test FSA

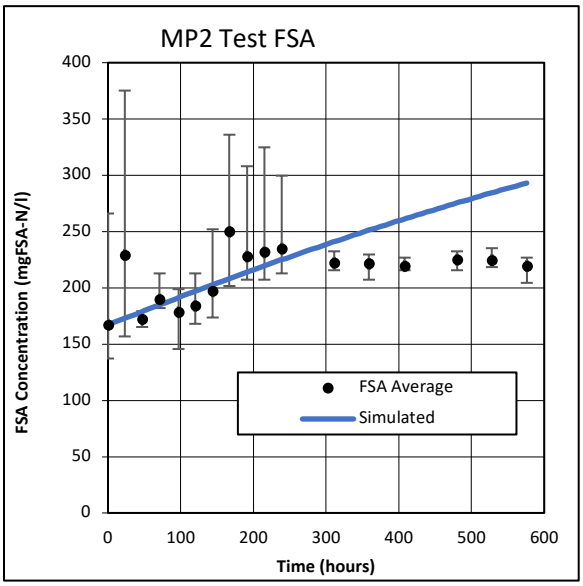

Figure 6. 33: MP2 AugBMP test FSA

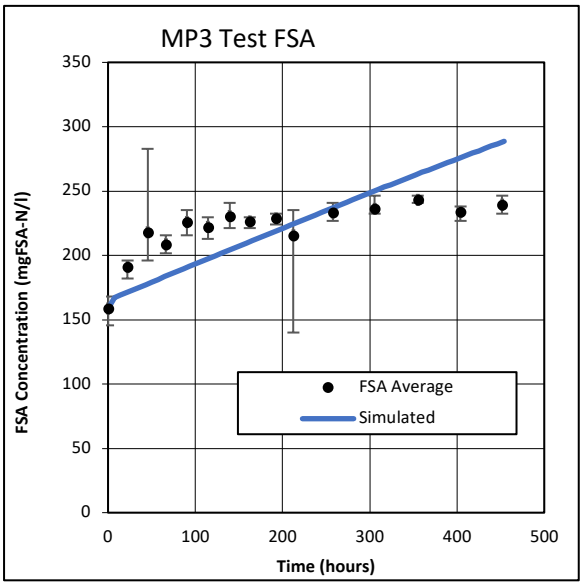

Figure 6. 34: MP3 AugBMP test FSA

6.3.9.4 Orthophosphate (OP)

The OP concentrations for the observed and modelled experiments are shown in Figures 6.35, 6.36 and 6.37. The concentration of OP release in the AugBMP test experiment was low (~7mgP/*l*), which indicated that the P content of the biodegradable particulates in the PSS was low. The observed AugBMP test OP concentrations were replicated by the modelled AugBMP test reactor well. However, the rate at which the OP was released in the modelled MP3 AugBMP test reactor (Figure 6.37) compared to the observed test reactor was inaccurate and suggested that the hydrolysis rate of the organics was higher than the rate determined by the PE. However, the model replicated the rate at which the COD decreased in MP3 (Figure 6.28) well. Therefore, the release of OP into the AugBMP test reactor liquid for MP3 was not adjusted.

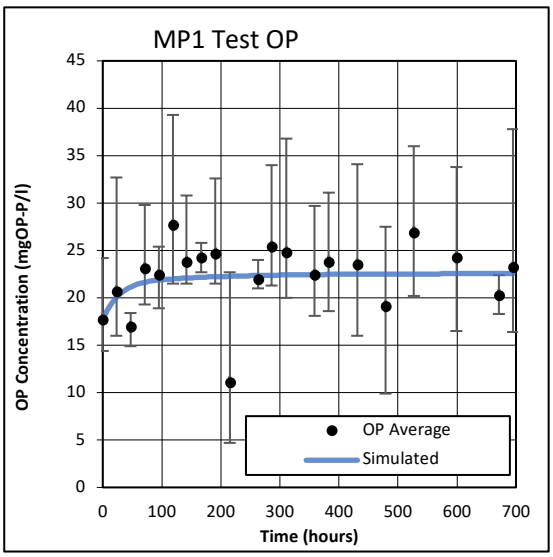

Figure 6. 35: MP1 AugBMP test OP

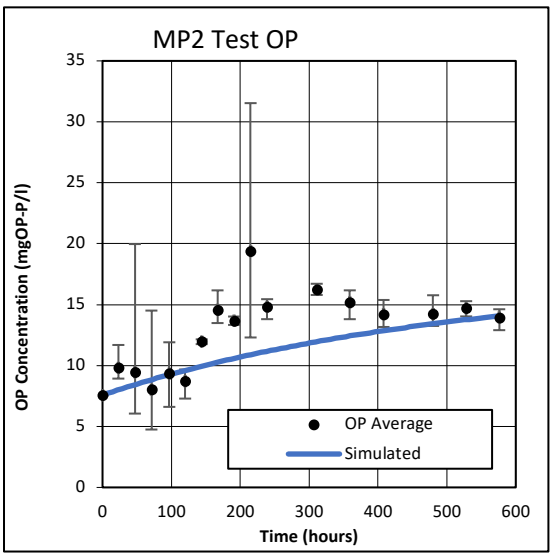

Figure 6. 36: MP2 AugBMP test OP

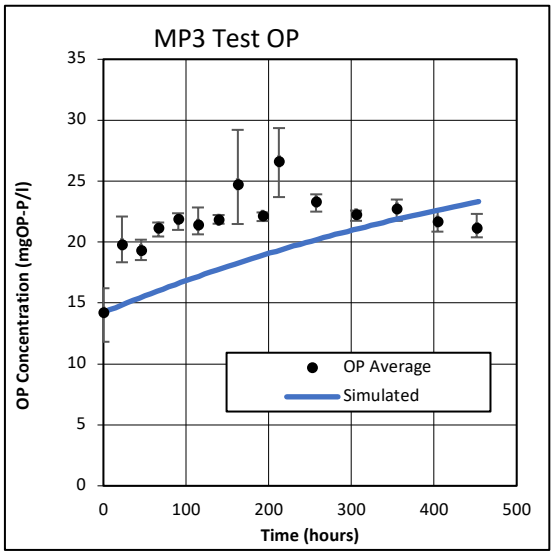

Figure 6. 37: MP3 AugBMP test OP

6.3.9.5 Carbonate Alkalinity

The carbonate alkalinity concentrations for the observed and modelled experiments are shown in Figures 6.38, 6.39 and 6.40. As previously mentioned, the increase in carbonate alkalinity in the AugBMP reactor was influenced by the release of FSA and C_T into the reactor liquid. The composition of the biodegradable particulate organics in the PSS identified by the PE minimised the error across the observed FSA and H_2CO_3 alkalinity measurements.

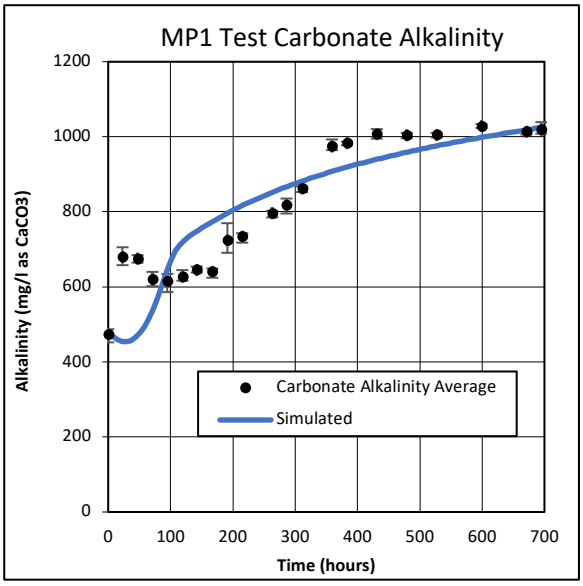

Figure 6. 38: MP1 AugBMP test carbonate alkalinity

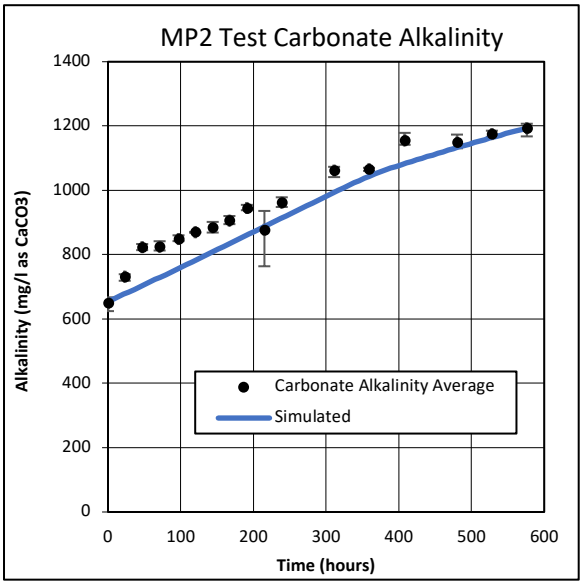

Figure 6. 39: MP2 AugBMP test carbonate alkalinity

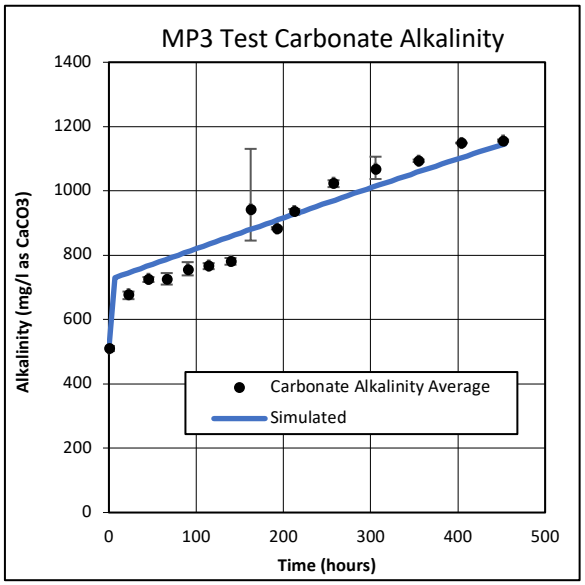

Figure 6. 40: MP3 AugBMP test carbonate alkalinity

6.3.9.6 Total Alkalinity

As mentioned, the total alkalinity of the system is a conservative parameter. Therefore, the total increase in alkalinity observed in the AugBMP test reactor was dependent on the composition of organics fed to it. The modelled AugBMP test experiment replicated the observed increase in total alkalinity for the MP1 (Figure 6.41) and MP2 (Figure 6.42) experiments well. However, the total alkalinity in the modelled MP3 (Figure 6.43) experiment was lower than the observed total alkalinity. The source of this discrepancy was challenging to identify, as the increase in carbonate alkalinity in MP3 was well represented by the modelled AugBMP test reactor. However, the lower total alkalinity in the modelled MP3 experiment may have been due to the lower pH achieved by the model. The lower pH in the modelled AugBMP test affected the carbonate alkalinity concentration. However, the modelled AugBMP test reactor compensated for the lower reactor pH by releasing a higher concentration of C_T into the reactor liquid; therefore, correctly establishing the carbonate alkalinity. However, even with the correct concentration of carbonate alkalinity released, the modelled total alkalinity remained lower than was observed for MP3. Furthermore, the source of this discrepancy should be further investigated as the model's calculations for total alkalinity may need checking for certainty.

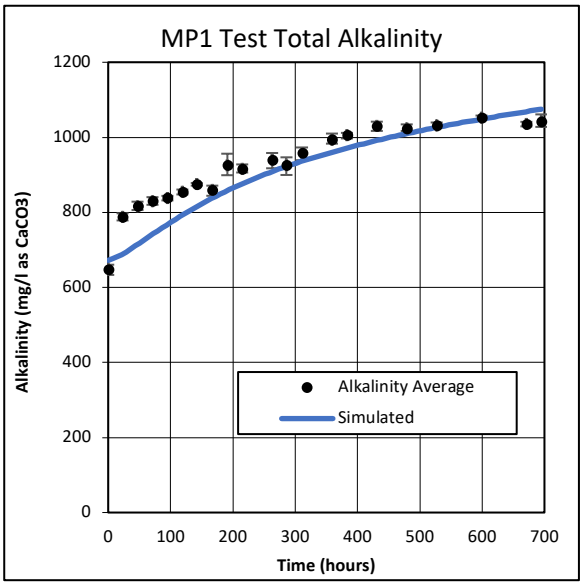

Figure 6. 41: MP1 AugBMP test total alkalinity

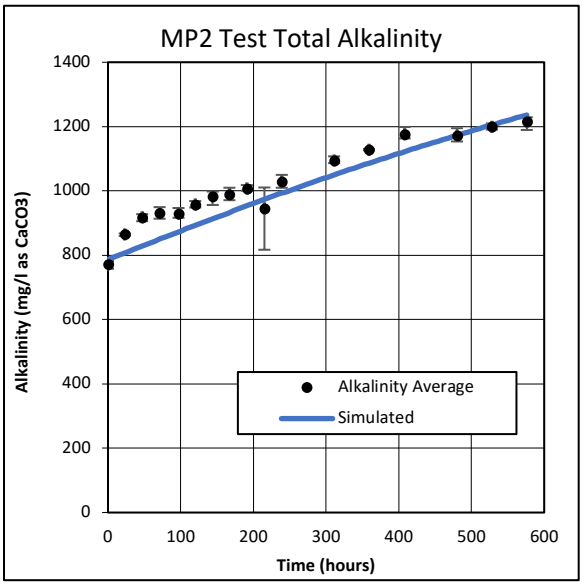

Figure 6. 42: MP2 AugBMP test total alkalinity

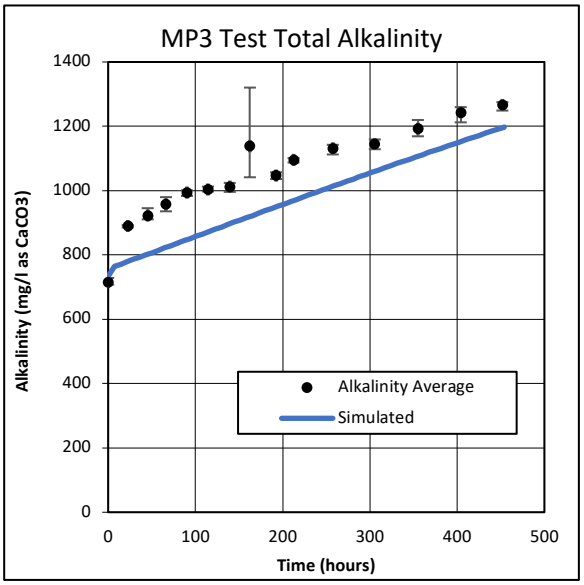

Figure 6. 43: MP3 AugBMP test total alkalinity

6.3.9.7 Volatile Suspended Solids (VSS)

The VSS of the UPO, residual biodegradable organics, biomass and the particulate organics in the PSS were considered. The VSS concentration of the residual biodegradable organics and biomass was fixed, as these concentrations were previously determined in the AugBMP control reactor. However, the mass and therefore, the concentration of the UPOs and biodegradable particulate organics were adjusted by the PE to fit the observed data. Consequently, the modelled AugBMP test reactor replicated the observed VSS concentrations for all three

experiments well (Figures 6.44, 6.45 and 6.46). This indicated that the parameters determined by the PE were accurate for describing the observed AugBMP test experiments.

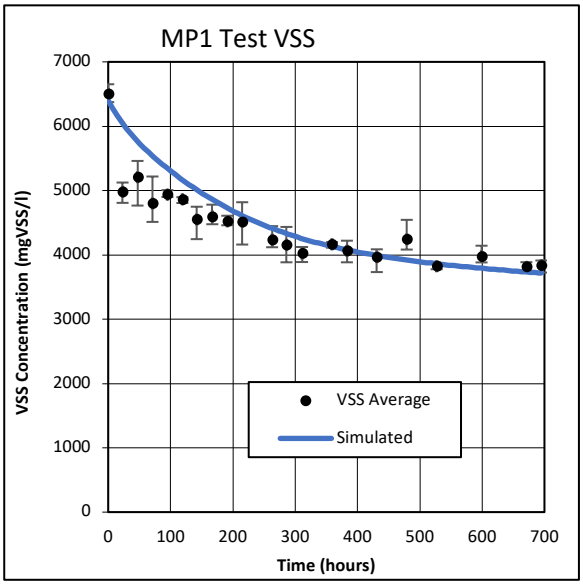

Figure 6. 44: MP1 AugBMP test VSS

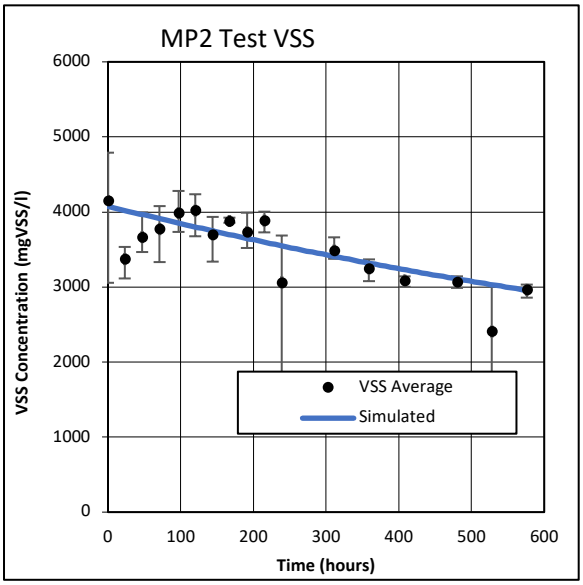

Figure 6. 45: MP2 AugBMP test VSS

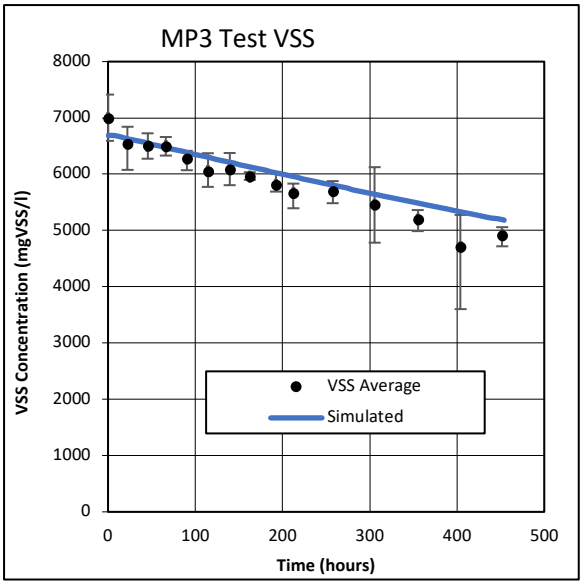

Figure 6. 46: MP3 AugBMP test VSS

6.3.9.8 Volatile Fatty Acids (VFA)

The VFA concentrations for the observed and modelled experiments are shown in Figures 6.47, 6.48 and 6.49. VFAs were produced in the modelled AugBMP test reactor as an intermediate product due to the degradation of glucose (which was produced from the hydrolysis of the biodegradable organics). The accumulation of VFA in the modelled AugBMP test reactor was

dependent on the organic substrate hydrolysis rate (kM_BPSS_AD_hyd), the substrate uptake rate of the acetoclastic organisms, and the half-saturation coefficient of the acetoclastic organisms. The PE adjusted these parameters, as well as the composition of the biodegradable particulate organics in the PSS until the parameters with the lowest error across the observed data were achieved.

However, the observed VFA concentration for the MP1 (Figure 6.47) and MP3 (Figure 6.49) experiments was not represented well by the modelled AugBMP test reactor. The dynamics of the VFA accumulation was challenging to achieve accurately. This discrepancy in the model may need some future work to identify other possible intermediates in the model that represent the observed accumulation of VFAs. Additionally, the accumulation may be caused by substrate inhibition for the acetoclastic organisms. The pathways of the PWM_SA_AD model may need additional data on the formation of possible intermediates. Therefore, future work is suggested in the recommendations.

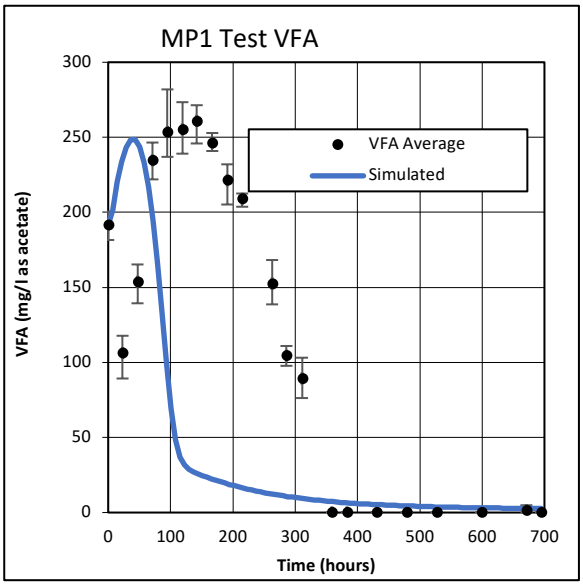

Figure 6. 47: MP1 AugBMP test VFA

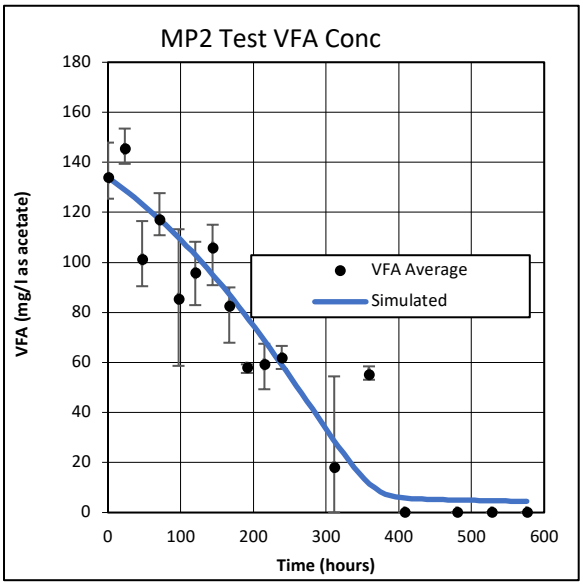

Figure 6. 48: MP2 AugBMP test VFA

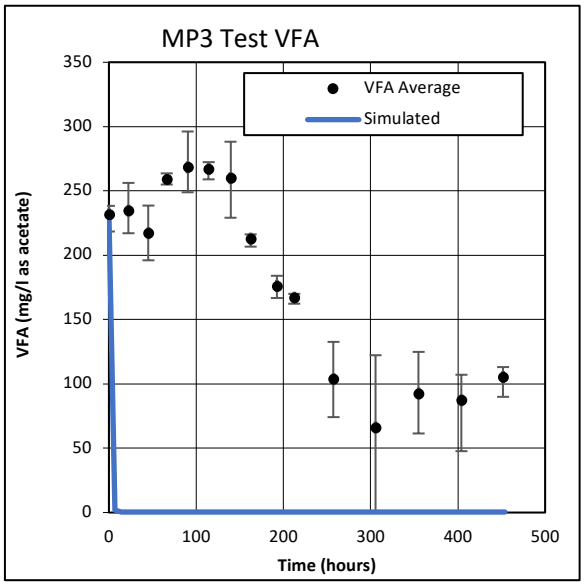

Figure 6. 49: MP3 AugBMP test VFA

6.3.9.9 pH

The decrease in pH in the AugBMP test experiments was due to the formation of VFAs, after which the pH began to increase and stabilise around pH 7. The modelled AugBMP test reactor replicated the both the initial drop in pH, as well as the pH stabilisation towards the end of the experiment well for all three experiments (Figures 6.50, 6.51 and 6.52).

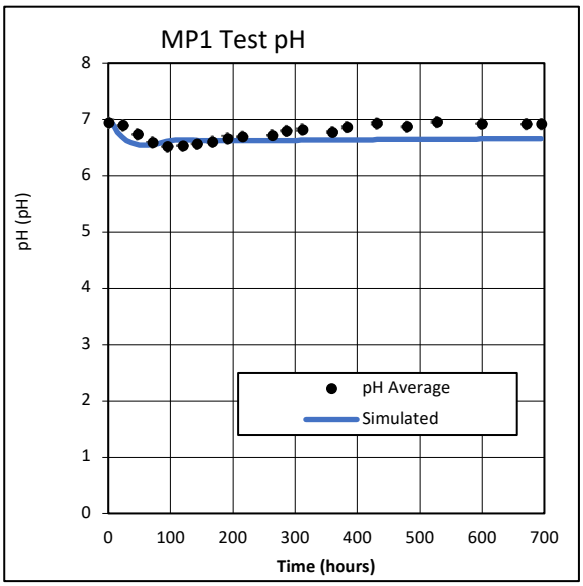

Figure 6. 50: MP1 AugBMP test pH

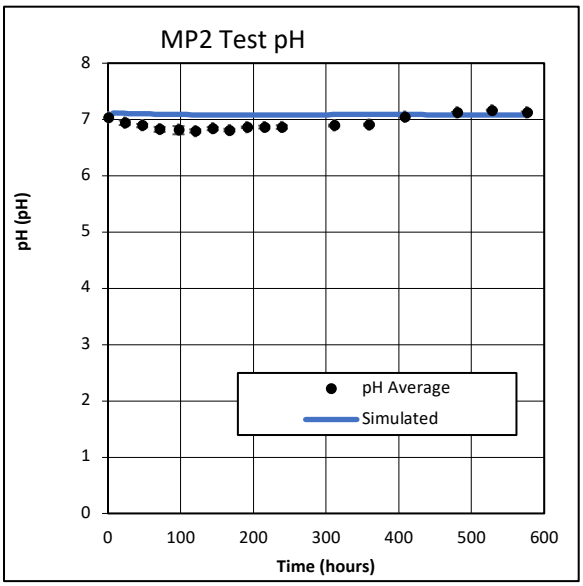

Figure 6. 51: MP2 AugBMP test pH

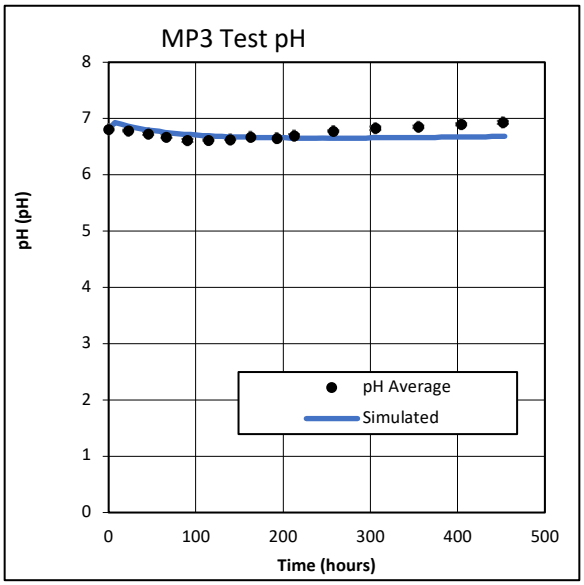

Figure 6. 52: MP3 AugBMP test pH

6.3.9.10 Methane

The methane produced by the modelled AugBMP test reactor for MP1 (Figure 6.53) and MP3 (Figure 6.55) significantly exceeded the observed methane production. This outcome, as well as the poor COD balances obtained in Section 6.3.4 strongly suggested that the observed gas measurements were inaccurate. The outcome was challenging to explain as Figure 6.23, and Figure 6.25 in Section 6.3.3 illustrated that the gas measured in the inverted water columns for the AugBMP test reactor was repeatable. However, the methane produced in the observed MP2 (Figure 6.54) experiment was well replicated by the modelled AugBMP test experiment. However, the methane production was not used as a variable for determining the composition of the biodegradable organics in the PSS. Instead, the composition was determined using the change in COD, as the production of methane in the model is balanced by the COD consumed, as well as the aqueous carbonate alkalinity.

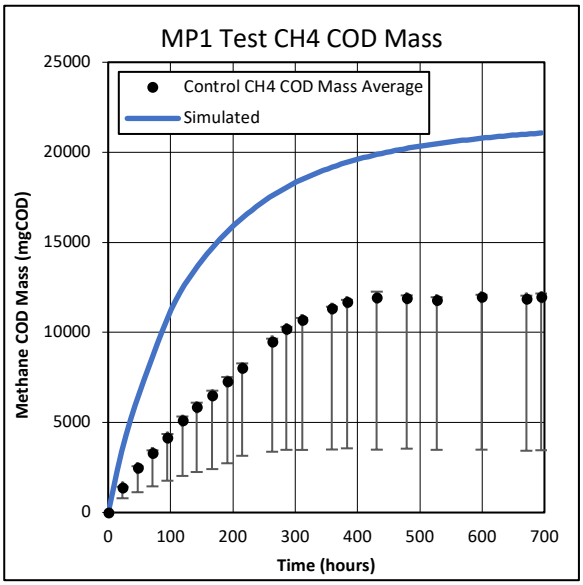

Figure 6. 53: MP1 AugBMP test methane

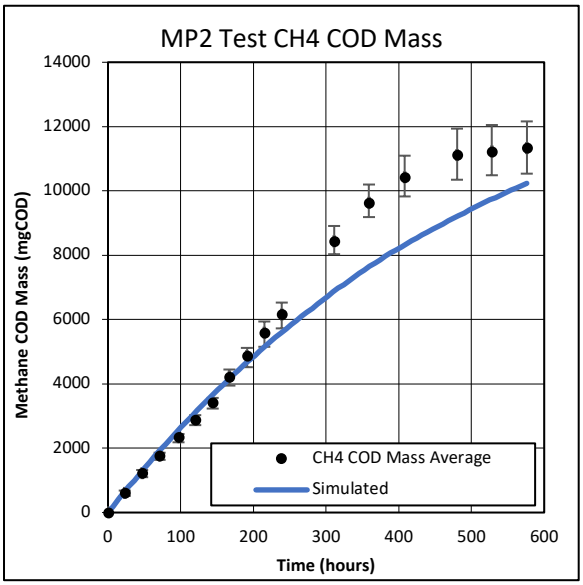

Figure 6. 54: MP2 AugBMP test methane

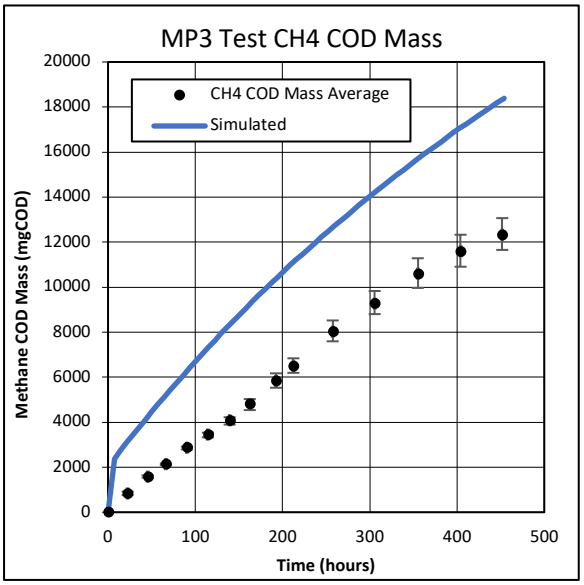

Figure 6. 55: MP3 AugBMP test methane

6.3.9.11 Model COD Balance

The COD mass balance for the AugBMP experiment is explained in Section 3.7.3.3. The PWM_SA_AD model code was adjusted to account for the COD removed from the modelled AugBMP reactor during sampling. The adjusted code did not affect the kinetics or the stoichiometry of the bioprocesses, but rather the liquid balance of the PWM_SA_AD model. The modelled COD balances were included in an attempt to identify the COD error experienced with the gas measurements.

The modelled COD balances were compared to the observed COD balances, as shown in Table 6.35. The observed and modelled COD balances for all three experiments agreed well, with the exception of the methane gas COD. The modelled COD in MP1 and MP3 was significantly higher than the observed COD. As was noted earlier, the significant discrepancy between the observed and the modelled methane COD strongly suggested that the gas measurements are a substantial source of error for the AugBMP test, and subsequently, the BMP test.

Table 6. 35: Modelled AugBMP test COD balance for PSS

	MP1			MP2		
	Observed	Model	%error	Observed	Model	%error
Unit	mgCOD	mgCOD	%	mgCOD	mgCOD	%
Starting	**57144**	**57732**	1	**44109**	**43775**	-1
Removed	19172	18506	-3	14216	13714	-4
Remaining	17713	18156	3	20410	19842	-3
Gas	11898	21077	77	11728	10235	-13
Total Effluent	**48783**	**57740**	18	**46354**	**43791**	-6
Unit	%	%		%	%	
Balance	**85**	**100**	**-**	**105**	**100**	-

	MP3		
	Observed	Model	%error
Unit	mgCOD	mgCOD	%
Starting	**76036**	**77412**	2
Removed	22713	22223	-2
Remaining	37981	36892	-3
Gas	12359	18388	49
Total Effluent	**73052**	**77503**	6
Unit	%	%	
Balance	**96**	**100**	**-**

6.3.10 Modelled AugBSP test PSS experiment results

The observed results from the T1 and T2 AugBSP test reactors were summarised by averaging the values obtained for each measurement taken. Table 6.36 and Table 6.37 summarise the results obtained for the starting and ending concentrations for each constituent in the modelled AugBSP test experiments for PSS. The results obtained from the model were compared to that of the observed results. Furthermore, the results have been compared visually in Section 6.3.10.1 (Figure 6.56) to Section 6.3.10.11 (Figure 6.88). The visual comparisons between the modelled and observed results were used to evaluate the accuracy of the dynamic parameters established by the PE.

The total COD concentration for the modelled AugBSP test reactor remained constant as COD was conserved within the system. The increase in the total soluble COD concentration, as well as the sulphide COD concentration, for the observed SP1 and SP2 experiments, was represented well by the modelled AugBSP test reactor. However, the total soluble COD concentration for the modelled SP3 experiment was higher than observed. The elevated total soluble COD concentration in the modelled SP3 experiment was due to the elevated sulphide COD concentration. The sulphide concentration in the modelled SP3 experiment was increased by the PE such that the sulphate concentration utilised by the observed AugBSP reactor was replicated by the model. The sulphate concentration utilised by the modelled SP1 and SP2 experiments was lower than that utilised in the observed AugBSP test reactor. The PWM_SA_AD model was mass balanced; therefore, the sulphur required to produce sulphide was taken from the sulphate. Subsequently, the observed SP1 and SP2 experiments were not S balanced. However, the S in the SP3 experiment was conserved, which indicated that the SP3 experiment was S balanced.

Table 6. 36: Modelled SP1 and SP2 AugBSP test results for PSS

SP1 Test Model Results								SP2 Test Model Results					
		Start		End		Change		Start		End		Change	
COD	**Unit**	**Observed**	**Modelled**	**Observed**	**Modelled**	**Observed**	**Modelled**	**Observed**	**Modelled**	**Observed**	**Modelled**	**Observed**	**Modelled**
Total COD	mgCOD/l	1508	1310	1715	1310	**207**	**0**	1631	1388	1582	1388	**-49**	**0**
Total Soluble COD	mgCOD/l	414	415	734	730	**320**	**315**	397	400	819	781	**422**	**382**
Sulphide	mgCOD/l	344	344	643	679	**298**	**335**	306	306	693	697	**387**	**391**
Sulphate													
Sulphate	mgSO4/l	948	948	146	445	**-802**	**-503**	883	883	81	296	**-802**	**-587**
Nitrogen													
FSA	mgFSA/l	10.2	10.2	17.5	17.7	**7.3**	**7.5**	9.5	9.5	16.9	17.3	**7.5**	**7.8**
Phosphate													
OP	mgOP/l	3.0	3.0	4.0	4.0	**1.0**	**1.1**	3.0	3.0	3.7	4.0	**0.7**	**1.0**
Alkalinity													
Carbonate	mg/l as CaCO3	366	373	1034	764	**667**	**392**	408	411	1015	820	**606**	**409**
Total	mg/l as CaCO3	554	595	1388	1141	**835**	**546**	534	562	1435	1198	**901**	**636**
Species													
VFA Conc	mg/l as acetate	2	2	11	0	**9**	**-2**	0	1	113	0	**113**	**0**
CT	mgC/l	96	96	271	206	**175**	**110**	116	116	275	222	**159**	**106**
Solids													
VSS	mgVSS/l	581	591	616	382	**36**	**-208**	565	576	381	399	**-184**	**-177**
pH													
pH		7.4	7.4	7.3	7.2	**-0.1**	**-0.2**	7.0	7.0	7.1	7.1	**0.1**	**0.1**

Table 6. 37 :Modelled SP3 AugBSP test results for PSS

SP3 Test Model Results							
		Start		End		Change	
COD	**Unit**	**Observed**	**Modelled**	**Observed**	**Modelled**	**Observed**	**Modelled**
Total COD	mgCOD/l	1167	1093	1185	1093	**18**	**0**
Total Soluble COD	mgCOD/l	268	262	557	623	**289**	**361**
Sulphide	mgCOD/l	176	176	509	546	**333**	**370**
Sulphate							
Sulphate	mgSO4/l	974	974	474	419	**-500**	**-556**
Nitrogen							
FSA	mgFSA/l	5.7	5.7	8.2	8.2	**2.5**	**2.5**
Phosphate							
OP	mgOP/l	2.4	2.4	3.7	2.4	**1.4**	**0.0**
Alkalinity							
Carbonate	mg/l as CaCO3	217	216	789	662	**572**	**446**
Total	mg/l as CaCO3	278	287	1034	872	**756**	**585**
Species							
VFA Conc	mg/l as acetate	3	0	0	0	**-3**	**0**
CT	mgC/l	66	66	213	203	**147**	**137**
Solids							
VSS	mgVSS/l	530	538	267	307	**-263**	**-231**
pH							
pH		6.8	6.8	7.1	6.8	0.3	0.0

The increase in the FSA and the OP concentrations for the observed AugBSP test experiments were replicated well by the modelled AugBMP test reactor. However, the carbonate and total alkalinity concentrations in the modelled AugBSP test reactors were lower than the observed concentrations. The low carbonate alkalinity was most likely caused by the low C_T production in the modelled AugBSP reactors, which was influenced by the composition of the biodegradable organics. However, the sulphide and FSA concentrations and the reactor pH were well replicated by the model. Therefore, the composition determined by the PE minimised the error across the range of components, and the alkalinity values determined were as a result of the PE. However, as mentioned in Section 6.3.9.6, the source of this discrepancy should be further investigated as the model's calculations for alkalinity may need checking for certainty.

The change in VSS concentration for the observed MP2 and MP3 experiments was well replicated by the modelled AugBSP test reactor. However, it is shown in Figure 6.80 in Section 6.3.10.9, that the modelled AugBSP test reactor replicated the observed MP1 VSS

concentrations for the first 200 hours of the experiment well, and subsequently, the increase in VSS concentration was not considered by the PE.

6.3.10.1 Total COD

The total COD concentration in the modelled AugBSP test reactors remained constant throughout the experiments (Figures 6.56 to 6.58). The modelled AugBSP test reactor represented the total COD concentration in the observed test reactor well for all three experiments. The PE minimised the error across the COD concentrations (total COD, soluble COD and sulphide COD) and the VSS concentrations in order to determine the mass and composition of the biodegradable particulate organics in the PSS.

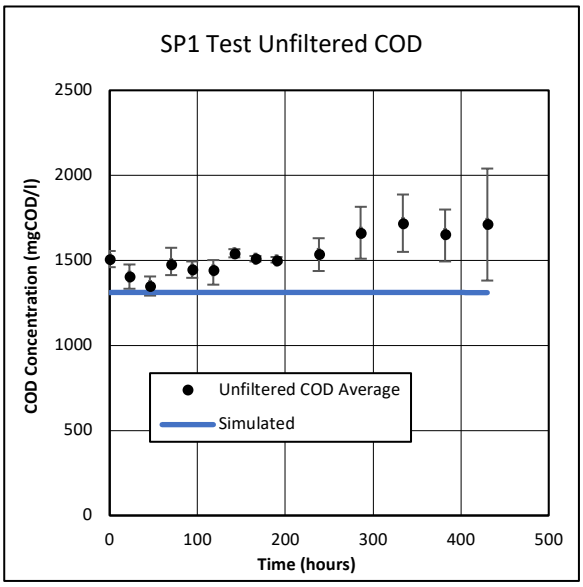

Figure 6. 56: SP1 AugBSP test total COD

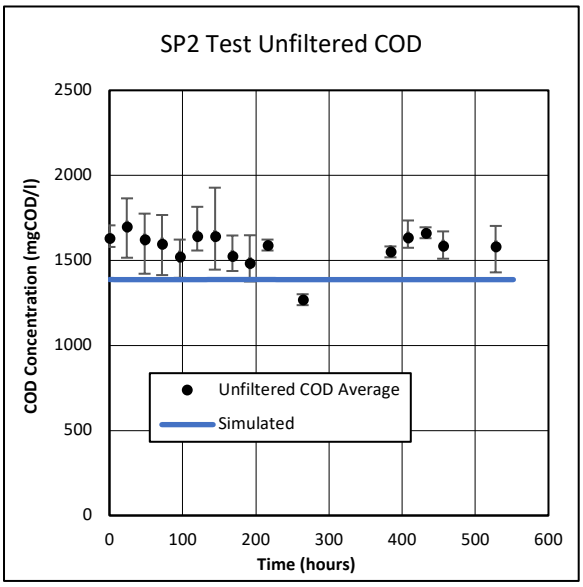

Figure 6. 57: SP2 AugBSP test total COD

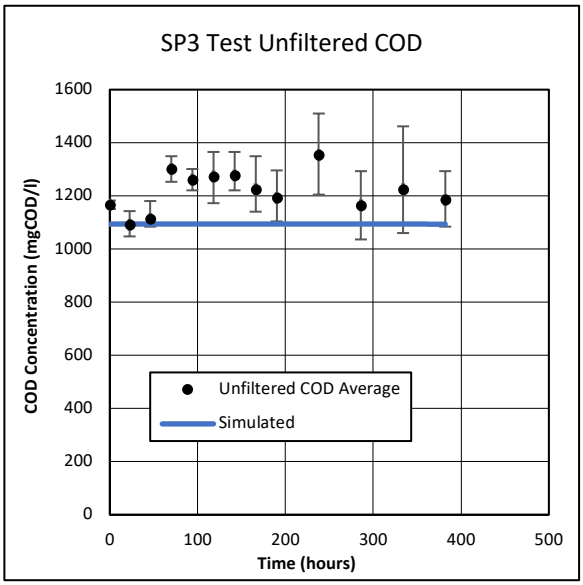

Figure 6. 58: SP3 AugBSP test total COD

6.3.10.2 Soluble COD

The soluble COD concentration comprised of the soluble organic COD and the soluble sulphide COD. The biodegradable particulate organics in the PSS were broken down and converted to soluble sulphide COD. Therefore, the increase in soluble COD was a good indication of the COD contained in the biodegradable particulates in the PSS. The observed soluble COD for the SP1 and SP2 experiments (Figures 6.59 and 6.60) were replicated well by the modelled AugBSP test reactor. However, the soluble COD concentration in the SP3 (Figure 6.61) experiment was slightly overpredicted by the modelled AugBSP test reactor. This elevated soluble COD prediction may have been caused by the sulphate concentration utilised by the modelled SP3 AugBSP test experiment, as shown in Figure 6.67.

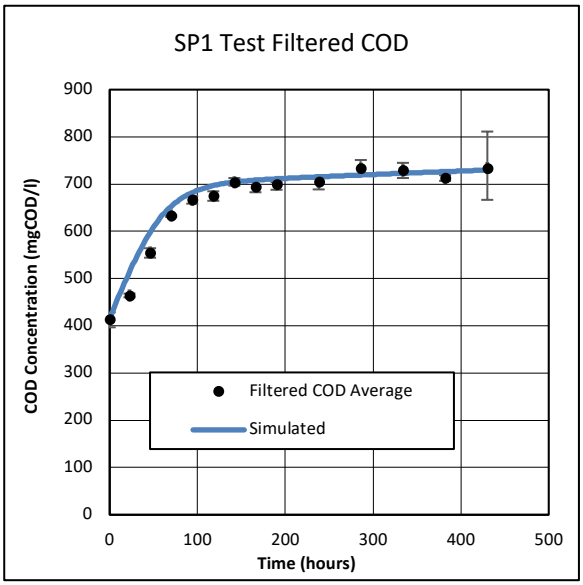

Figure 6. 59: SP1 AugBSP test soluble COD

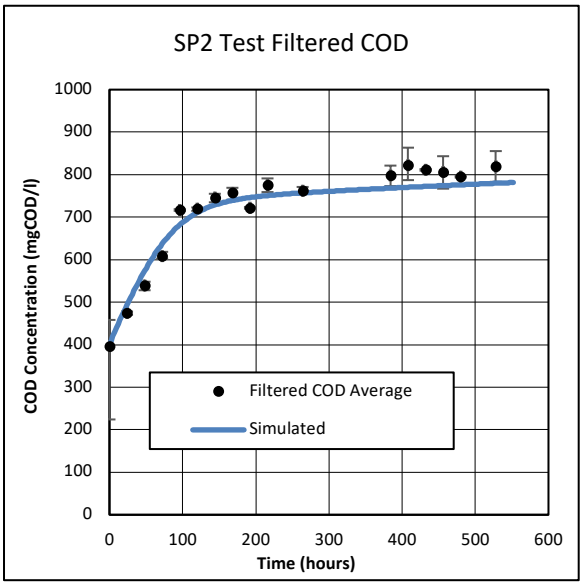

Figure 6. 60: SP2 AugBSP test soluble COD

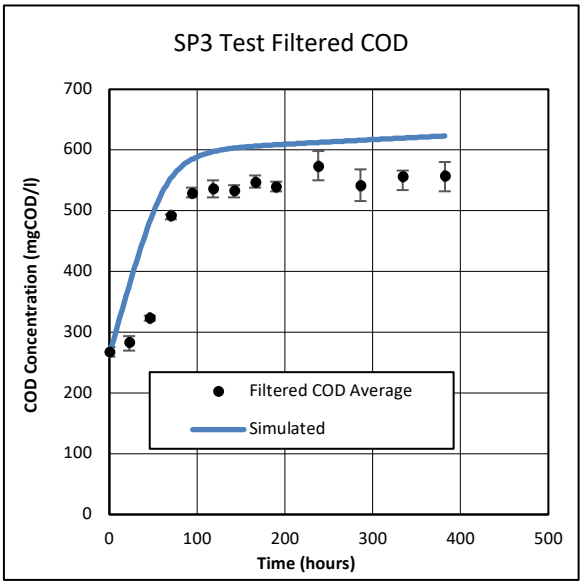

Figure 6. 61: SP3 AugBSP test soluble COD

6.3.10.3 Sulphide COD

The increase in soluble sulphide COD was dependent on the COD contained in the biodegradable particulates in the PSS, as well as the small soluble organic COD component. This was because the biodegradable organics present in the PSS were converted to sulphide COD by the SRB (Poinapen *et al.*, 2010). The modelled AugBSP test reactor replicated the soluble sulphide COD concentrations in the SP1 (Figure 6.62) and SP2 (Figure 6.63) experiments well. However, the soluble sulphide COD in SP3 (Figure 6.64) was overpredicted by the model, which was a result of the sulphate concentration utilised.

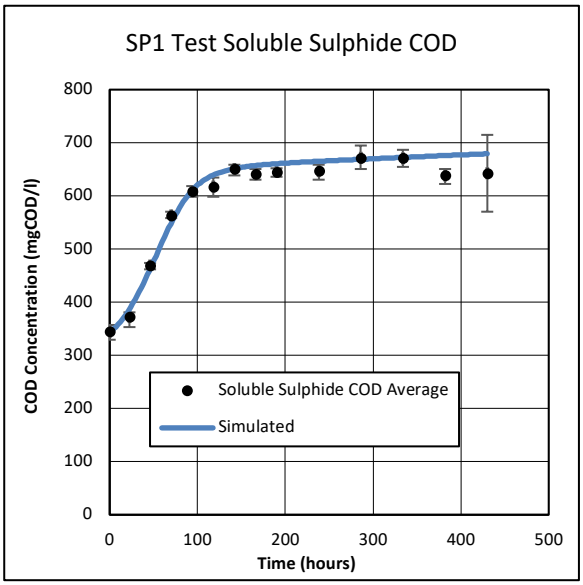

Figure 6. 62: SP1 AugBSP test soluble sulphide COD

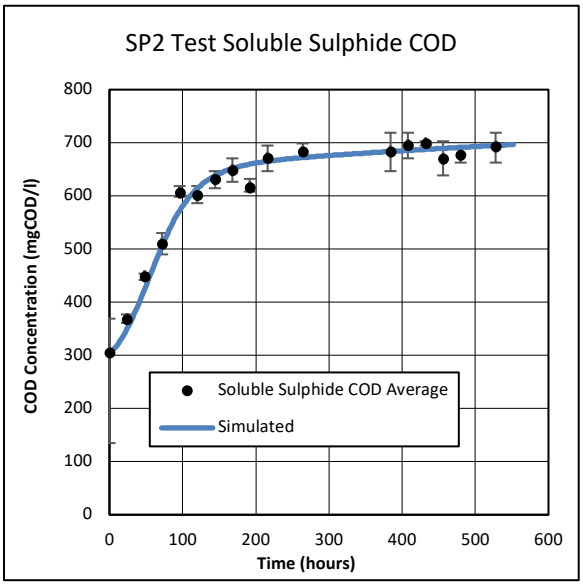

Figure 6. 63: SP2 AugBSP test soluble sulphide COD

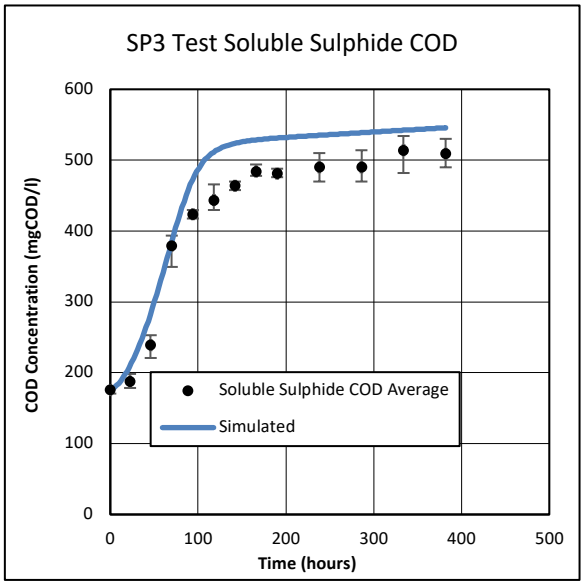

Figure 6. 64: SP3 AugBSP test soluble sulphide COD

6.3.10.4 Sulphate

The AugBSP test was conducted in a sealed reactor with zero headspace (all the products remained in the aqueous phase). Hence it was reasonable for the PWM_SA_AD model to convert the sulphate utilised to sulphide and not consider the formation of other sulphur compounds. Furthermore, in the event of a sulphide gas leak in the AugBSP test reactor, the total COD concentration would decrease. The modelled SP1 (Figure 6.65) and SP2 (Figure 6.66) experiments utilised a lower concentration of sulphate than was observed. The observed sulphate concentration in the SP2 test experiment (Figure 6.66) was completely utilised within

250 hours. However, the modelled SP2 test experiment showed that, for the concentration of sulphide produced by the reaction, the available sulphate would not be completely utilised in a mass balanced system. The source of the sulphate concentration error in the SP2 experiment was challenging to identify or explain.

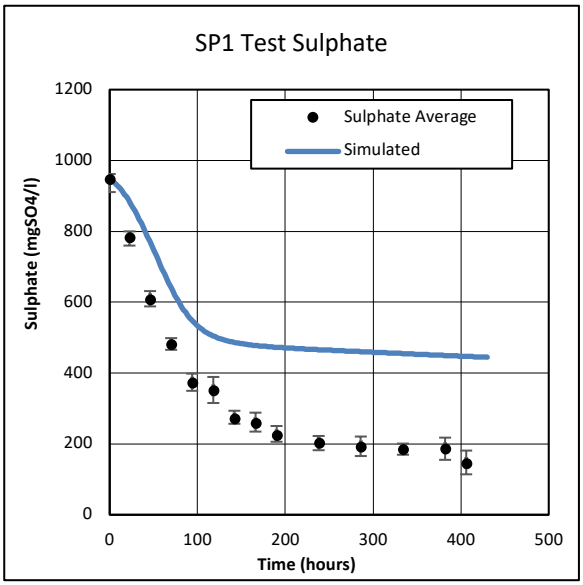

Figure 6. 65: SP1 AugBSP test sulphate

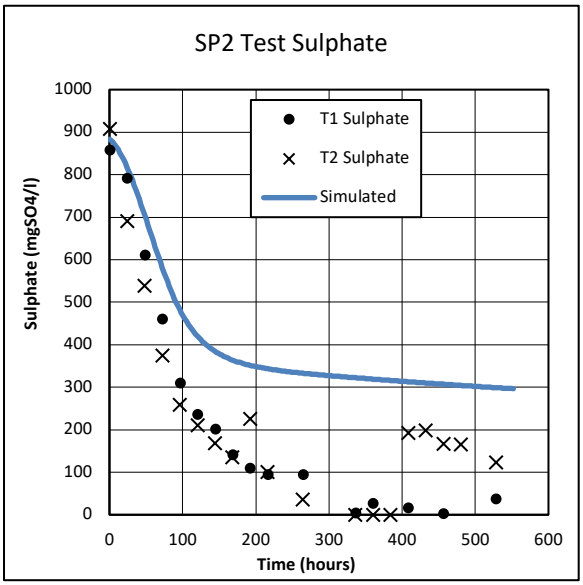

Figure 6. 66: SP2 AugBSP test sulphate

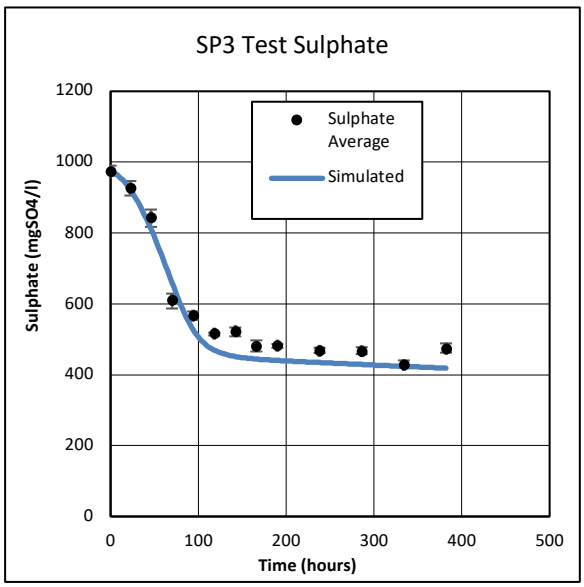

Figure 6. 67: SP3 AugBSP test sulphate

6.3.10.5 Free and Saline Ammonia (FSA)

The FSA concentrations for the observed and modelled experiments are shown in Figures 6.68, 6.69 and 6.70. The modelled AugBSP test reactor replicated both the total concentration of FSA released, as well as the rate at which the FSA was released with reasonable accuracy for all three experiments.

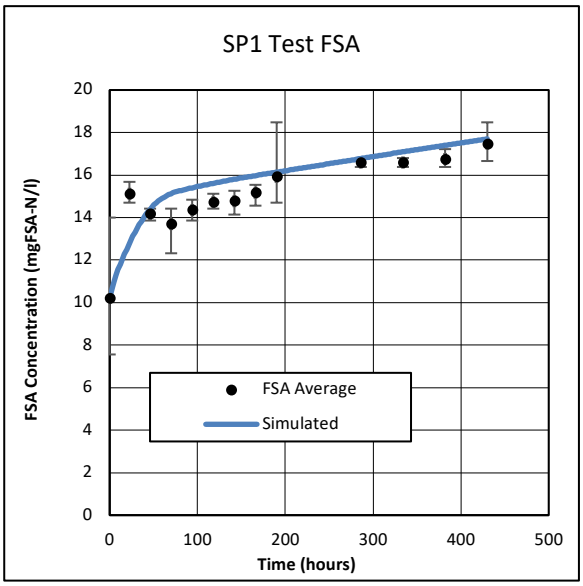

Figure 6. 68: SP1 AugBSP test FSA

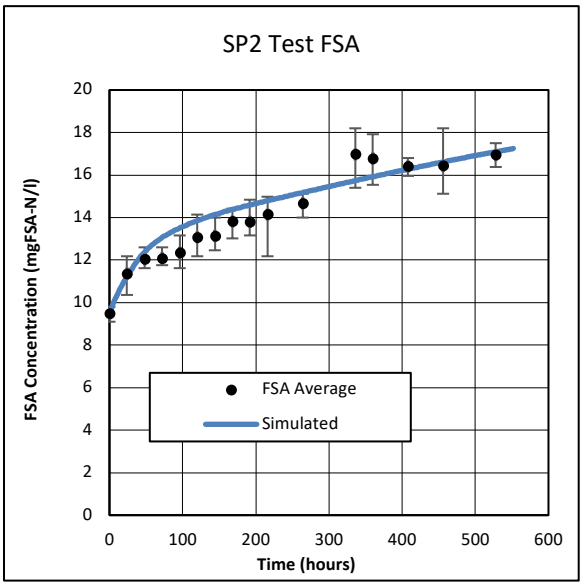

Figure 6. 69: SP2 AugBSP test FSA

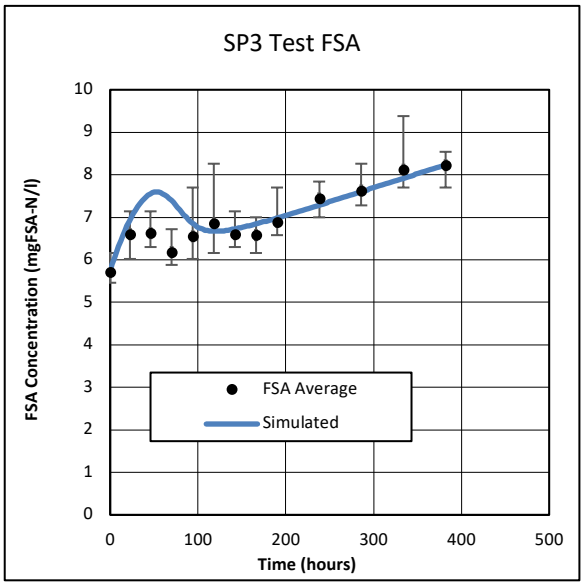

Figure 6. 70: SP3 AugBSP test FSA

6.3.10.6 Orthophosphate (OP)

The OP concentrations for the observed and modelled experiments are shown in Figures 6.71, 6.72 and 6.73. The modelled AugBSP test reactor replicated both the total concentration of OP released, as well as the rate at which the OP was released with reasonable accuracy for the observed SP1 (Figure 6.71) and SP2 (Figure 6.72) experiments.

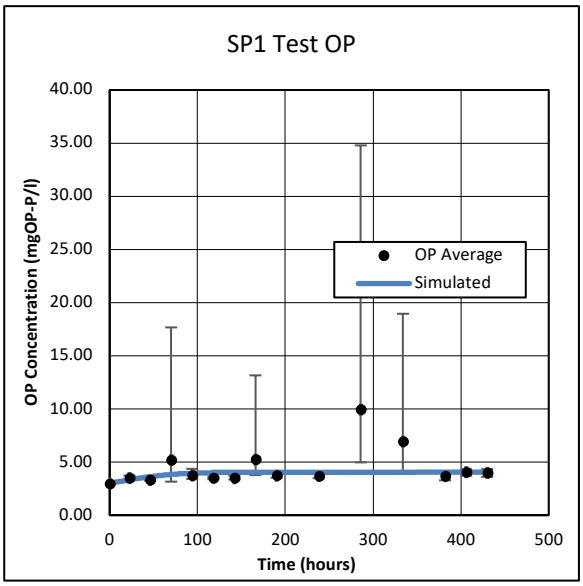

Figure 6. 71: SP1 AugBSP test OP

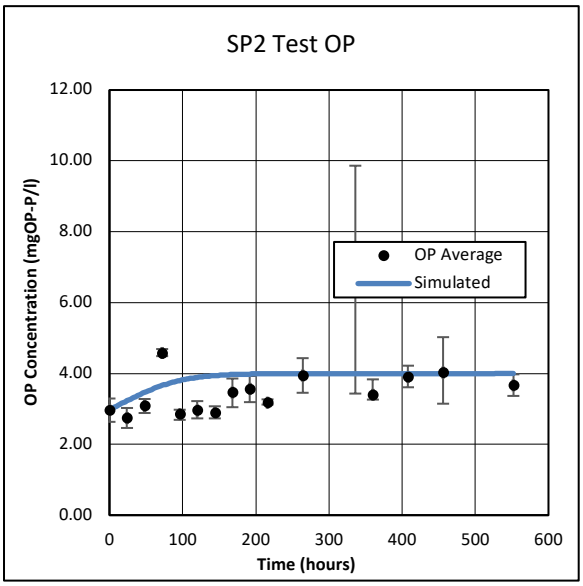

Figure 6. 72: SP2 AugBSP test OP

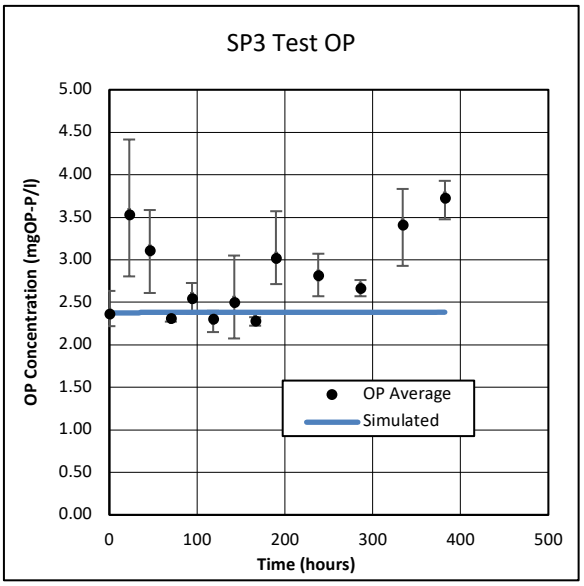

Figure 6. 73: SP3 AugBSP test OP

6.3.10.7 Carbonate Alkalinity

The carbonate alkalinity concentrations for the observed and modelled experiments are shown in Figures 6.74, 6.75 and 6.76. As previously mentioned, the increase in carbonate alkalinity in the AugBSP test reactor was influenced by the release of FSA and sulphide into the reactor liquid, as well as the C_T concentration released by the biodegradable organics. The observed carbonate alkalinity was poorly replicated by the modelled AugBSP test reactor for all three experiments. The source of the error was most likely due to the C_T concentration released by the biodegradable organics for SP1 and SP2, and the pH for SP3, as the observed FSA and sulphide concentrations were replicated by the model well.

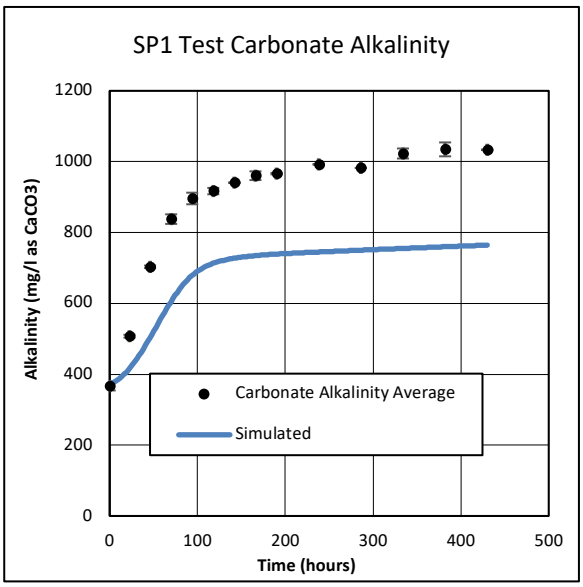

Figure 6. 74: SP1 AugBSP test carbonate alkalinty

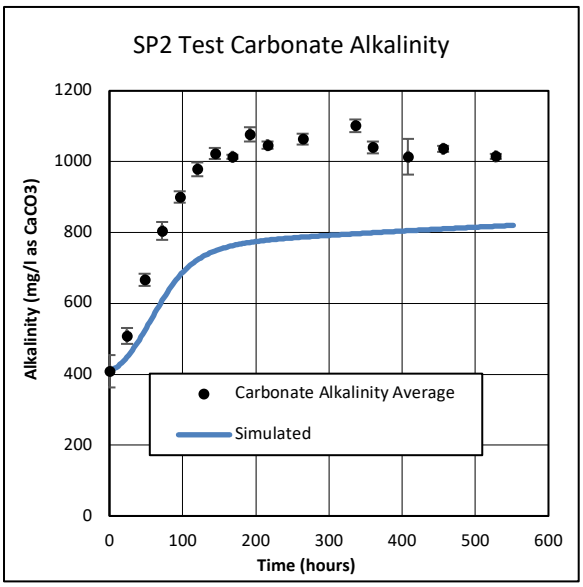

Figure 6. 75: SP2 AugBSP test carbonate alkalinty

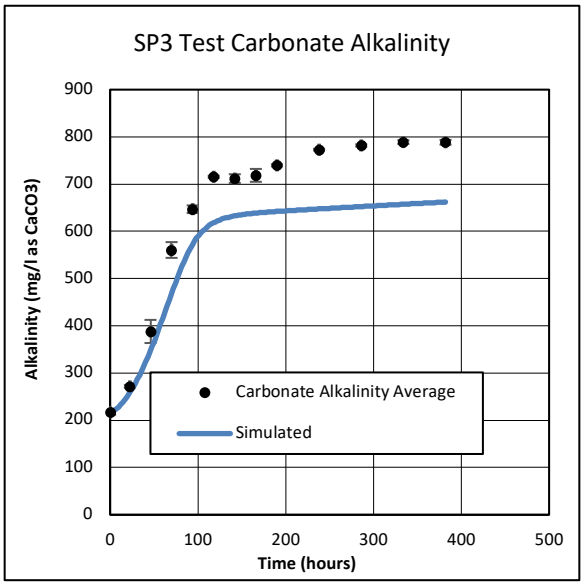

Figure 6. 76: SP3 AugBSP test carbonate alkalinty

6.3.10.8 Total Alkalinity

The total alkalinity concentrations for the observed and modelled experiments are shown in Figures 6.77, 6.78 and 6.79. The total alkalinity in the modelled AugBSP experiments was significantly lower than the total alkalinity observed in the test reactor. This outcome was related to the issue explained for the carbonate alkalinity above.

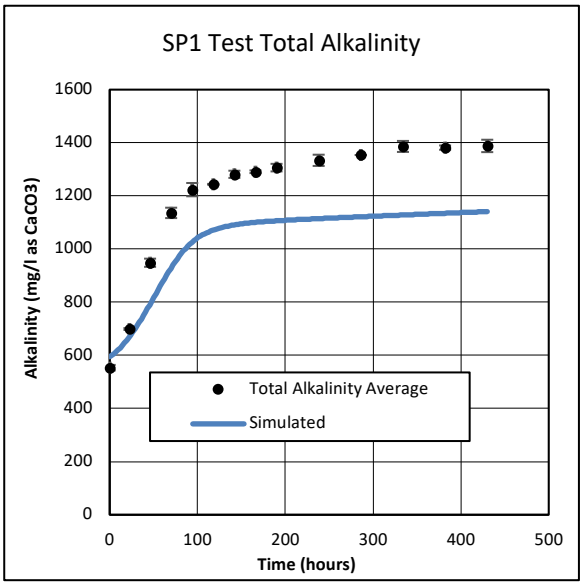

Figure 6. 77: SP1 AugBSP test total alkalinty

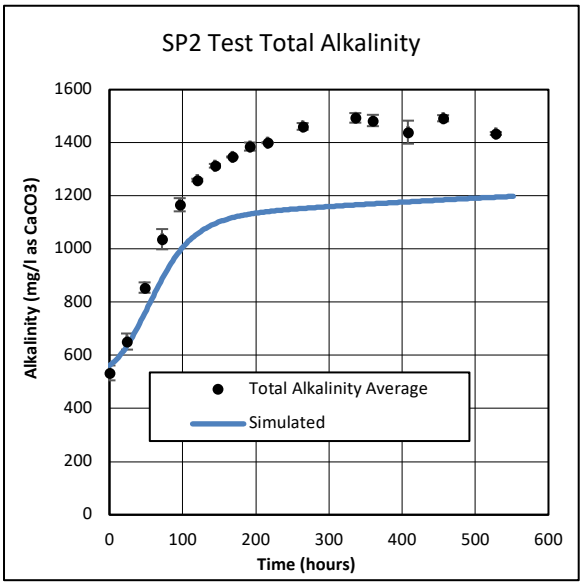

Figure 6. 78: SP2 AugBSP test total alkalinty

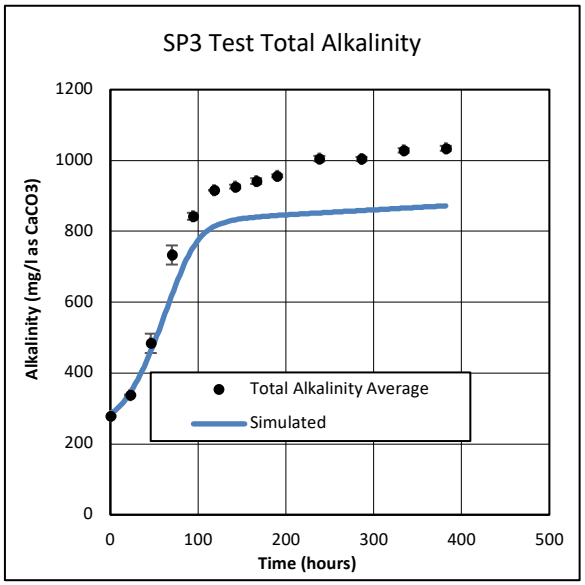

Figure 6. 79: SP3 AugBSP test total alkalinty

6.3.10.9 Volatile Suspended Solids (VSS)

The VSS concentrations for the observed and modelled experiments are shown in Figures 6.80, 6.81 and 6.82. The VSS concentration was dependent on both the composition and mass of the biomass, the UPOs, and the biodegradable particulate organics in the PSS. The composition of the biomass and UPOs were fixed. Therefore, the PE adjusted the mass and composition of the biodegradable particulate organics in the PSS, as well as the mass of the UPOs by minimising the error across the COD and VSS concentrations.

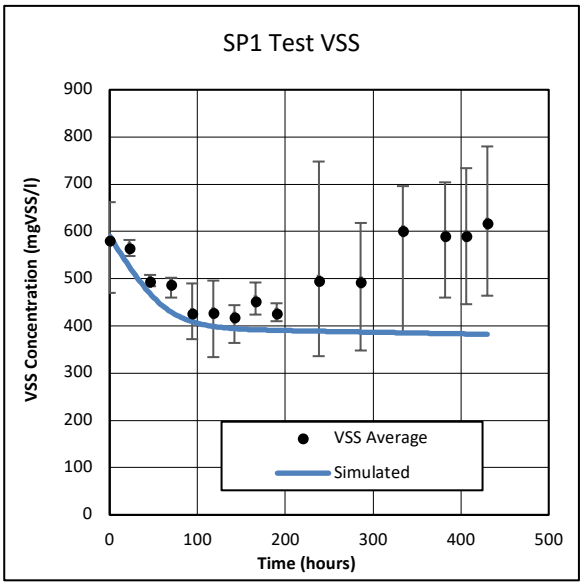

Figure 6. 80: SP1 AugBSP test VSS

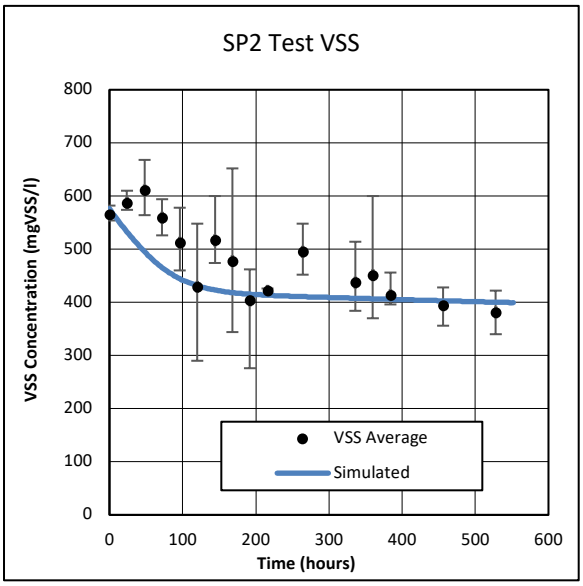

Figure 6. 81: SP2 AugBSP test VSS

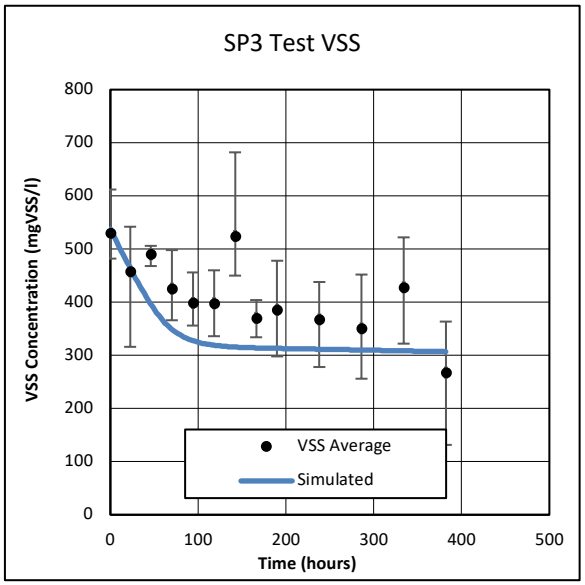

Figure 6. 82: SP3 AugBSP test VSS

6.3.10.10 Volatile Fatty Acids (VFA)

The VFA accumulation and uptake for SP1, SP2 and SP3 are shown in Figures 6.83, 6.84 and 6.85. However, the modelled AugBSP reactor was unable to replicate the observed VFA concentrations for all three test experiments. As previously mentioned, the discrepancy in the model may need some future work to identify other possible intermediates in the model that represent the observed accumulation of VFAs. Additionally, the accumulation may be caused by substrate inhibition for the acetoclastic organisms. However, the concentration of VFAs relative to the influent COD concentration was relatively low and did not impact the performance of the system significantly. Therefore, future work is suggested in the recommendations.

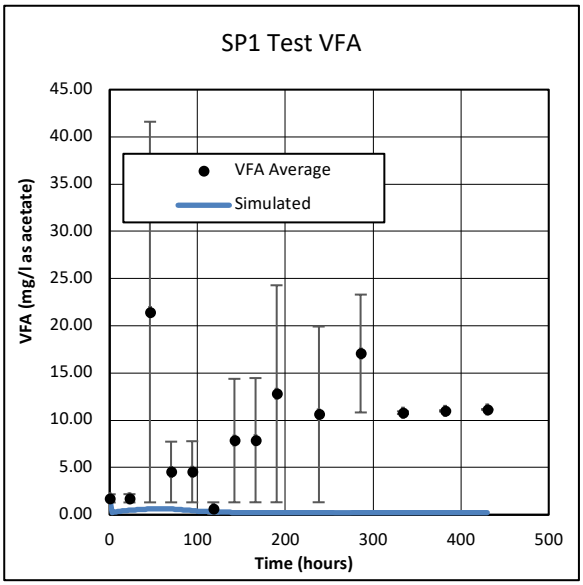

Figure 6. 83: SP1 AugBSP test VFA

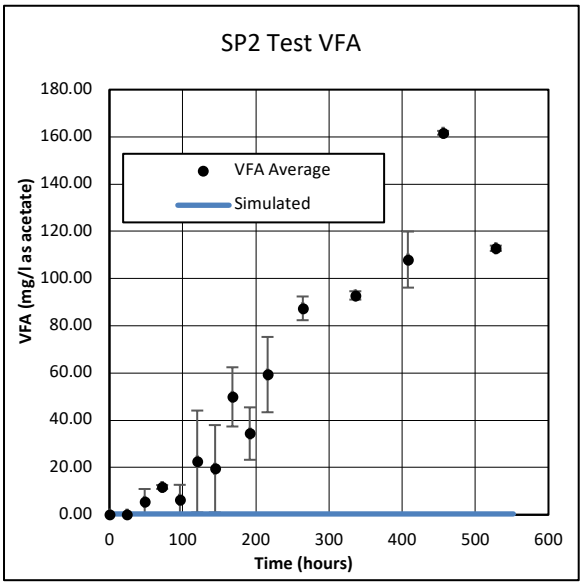

Figure 6. 84: SP2 AugBSP test VFA

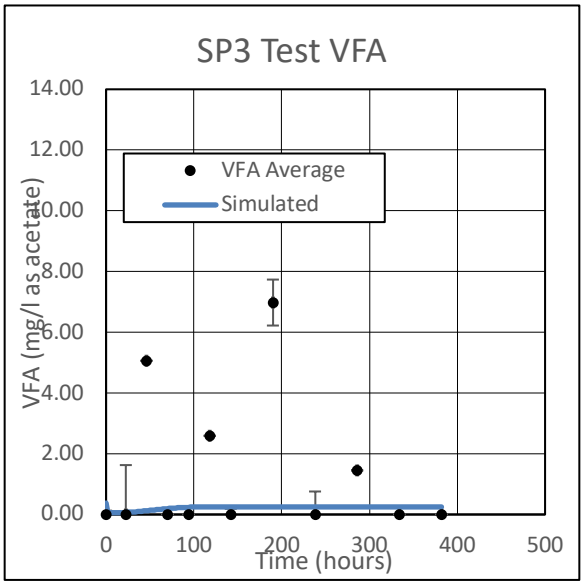

Figure 6. 85: SP3 AugBSP test VFA

6.3.10.11 pH

The modelled AugBSP test reactor replicated the observed pH for SP1 (Figure 6.86) and SP2 (Figure 6.87) accurately. However, the modelled pH in the SP3 (Figure 6.88) reactor was slightly lower than the observed pH. As discussed in Section 6.3.10.8, the total alkalinity concentration generated by the modelled AugBSP test reactor was lower than the observed total alkalinity generated. Therefore, the low pH at the end of the modelled SP3 experiment may have been caused by the O/H ratio in the composition determined, which subsequently influenced the low total alkalinity generated, as the carbonate alkalinity generated was low.

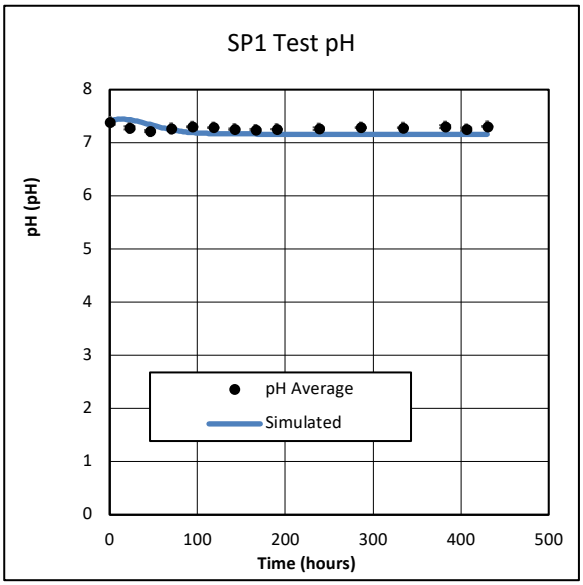

Figure 6. 86: SP1 AugBSP test pH

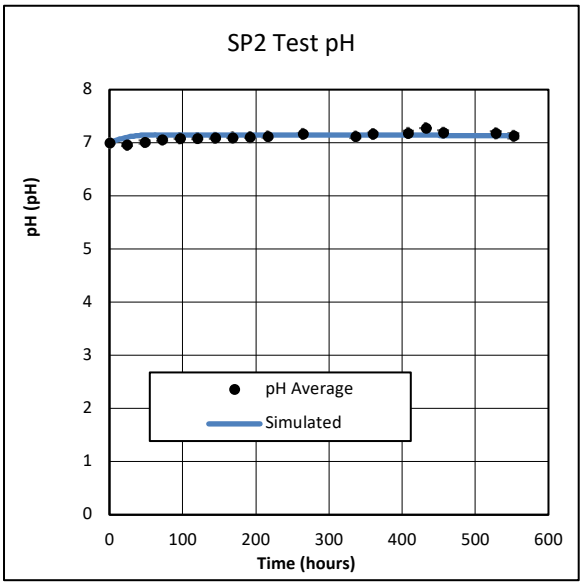

Figure 6. 87: SP2 AugBSP test pH

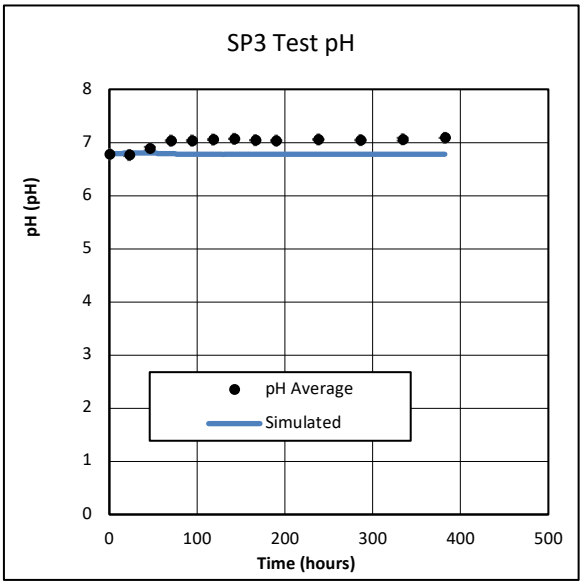

Figure 6. 88: SP3 AugBSP test pH

6.3.11 Conclusions from the PSS experiment

The primary objective of the PSS experiment was to accurately characterise the PSS into its elemental composition represented by CHONP. The composition of the PSS identified differed for the AugBMP and AugBSP tests. However, the compositions of the biodegradable organics present in the PSS were expected to differ, as the biodegradable particulates fluctuate based on the treatment plant and the collection time. Each of the six tests (AugBMP and AugBSP) used PSS taken from Potsdam at different times throughout the project. The variation in biodegradable organic composition across each of the six test highlights the variability of the

biodegradable particulate organics present in the AD influent. Consequently, the efficiency of anaerobic digestion modelling can be further improved by building a database of identified compositions for each treatment plant for varying periods throughout the year. The data set could then be used to predict historical or future events and scenarios occurring at the treatment plant using plantwide modelling.

The primary application of the augmented batch tests for this thesis was to identify and characterise the biodegradable particulate organics present in the PSS. The results obtained for both the AugBMP and AugBSP test reactors showed that the composition, as well as the dynamics regarding the breakdown of the PSS, could be accurately represented by the PWM_SA_AD model. However, even though there were discrepancies in the model for specific measurements, the PE was successful in determining an outcome that minimised the error across all of the observed measurements. The best fit achieved by the model was based on data reconciliation from a large data set containing multiple daily measurements.

Therefore, the augmented batch test coupled with mass balanced mathematical models could improve current analytical methods for substrate characterisation, and composition identification, with a specific focus on biodegradability. The biodegradability aspect of the augmented batch tests is appealing, especially for anaerobic digestion, as variables such as methane generation, or reactor pH could be determined for specific treatment plants or unit processes. However, future work is recommended and discussed in the recommendations regarding the gas measurements accuracy.

However, it was shown throughout the investigation that gas was not used as a measured variable in the modelled AugBMP experiment due to the measurement error. Instead, the error was minimised across the remaining measurements to obtain a best fit. This suggests that gas measurements may not even be necessary for the AugBMP test experiments. However, removing the gas component from the biodegradability AugBMP test will need to be investigated further. Furthermore, as discussed for casein, future investigations into the model intermediates should be performed, as components such as the VFAs were challenging to replicate accurately.

Chapter 7: Conclusions and Recommendations

7.1 Conclusions

This project proposed and developed a methodology for characterising and identifying the composition of the biodegradable organics present in an unknown substrate (e.g., Primary Sewage Sludge; PSS). The proposed methodology included the development of two new analytical testing procedures: (i) The Augmented Biochemical Methane Potential (AugBMP) Test, which extended the commonly used Biochemical Methane Potential (BMP) test to include additional measurements for the identification of the biodegradable organics present in an unknown substrate, and (ii) The Augmented Biochemical Sulphide Potential (AugBSP) Test, a test based on the same principles as the BMP, but rather using sulphidogenic organisms in a completely sealed reactor with zero headspace such that all measurements were conducted in the aqueous phase, alleviating the gas measurement error associated with the BMP test.

In order to identify the biodegradable organics present in the substrate, a parent steady-state anaerobic digester for both methanogenic and sulphidogenic conditions needed to be operated and tested, such that an inoculum for the AugBMP and AugBSP tests could be provided. Both the methanogenic and sulphidogenic SSPADs were fed PSS from Potsdam Wastewater Treatment Plant in the Western Cape, South Africa. The PSS was collected on multiple occasions and carefully stored. The PSS collected from Potsdam showed a variance in the biodegradable organics present when fed to each of the respective SSPADs. The variance in biodegradability was expected as primary sludge has a high level of variability depending on the time at which the sample was taken.

Mass balances were performed on both the methanogenic and sulphidogenic SSPADs. The results from the methanogenic SSPAD indicated that good COD balances (within 10%) were obtained for both the MC1 and MP1 experiments (99 ± 3% and 108 ± 2%). Furthermore, balances for other constituents such as TKN and TP were also checked. The MC1, MP2 and MP3 (108%, 94% and 109%) experiments had good TKN balances (within 10%). The MC1 and MP3 (106% and 93%) experiments has good TP balances (within 10%). The good balances concluded that material was conserved over the methanogenic SSPADs that were used to seed the AugBMP control and test reactors.

The results from the sulphidogenic SSPAD showed that achieving both a COD balance, as well as an S balance was challenging to do accurately, as H_2S gas evolved from the aqueous solution and was captured by the ferric chloride solution contained inside the gas trap. Determining the concentration of H_2S gas present in the ferric chloride solution was challenging to do accurately, and consequently, the COD and S that were contained in the gaseous H_2S were not measured. However, the COD and S contained in the gas were accounted for by the PWM_SA_AD steady state model, which was mass balanced.

The methanogenic and sulphidogenic SSPADs were virtually replicated by the PWM_SA_AD model such that the concentration of active biomass present in the inoculum that was used to seed the modelled AugBMP and AugBSP experiments was determined. The active biomass makes up the total VSS concentration and is virtually impossible to separate from other volatile solids. Therefore, the active biomass concentration in the SSPAD was a modelling parameter that needed to be determined by the steady-state PWM_SA_AD model, such that the concentration of products released into the AugBMP and AugBSP reactors, as well as the substrate utilisation and growth rates, could be accounted for. It was observed in all cases (both methanogenic and sulphidogenic), that the modelled SSPADs accurately represented the COD and VSS concentrations present in the respective effluent streams. Most importantly, the collective biomass concentrations (determined using the steady-state equations of Sotemann *et al.* (2005)) were well represented by the individual (acidogen, acetogen, acetoclastic and hydrogenotrophic) organisms present in the modelled SSPAD effluent that was used to seed the modelled AugBMP and AugBSP experimental environments.

Modelling the SSPADs are of significant importance when virtually replicating the AugBMP and AugBSP experiments using the PWM_SA_AD model, as the concentrations of the various organism groups (acidogen, acetogen, acetoclastic and hydrogenotrophic) are required as an input. However, when using the stoichiometric method described in Section 3.9.2, the influences of the biomass and residual organics can be combined into one group representing the baseline, with the biodegradable organics in the substrate considered separately. Therefore, when using the stoichiometric identification method, modelling the SSPADs is not required and all measurements can be performed directly on the augmented batch control and test reactors. However, a good characterisation of the methanogenic and/or sulphidogenic SSPADs

is required such that the source of the inoculum used in the experiments is well documented and understood.

The augmented batch control reactors were used to set the baseline for the material that was released due to the anaerobic breakdown of the residual biodegradable organics and the biomass present in the SSPAD effluent. The data collected from the AugBMP control reactors showed that the total COD present decreased throughout the duration of the experiment. This decrease in total COD indicated that biodegradable material was present inside the methanogenic SSPAD effluent that was fed to the AugBMP control reactor. Therefore, the AugBMP control reactors were crucial for determining the breakdown of biodegradable organics in the SSPAD effluent, such that the influence of the chosen biodegradable organics (added for testing substrate composition) could be isolated in the AugBMP test reactors.

It is imperative to note that the PWM_SA_AD model was not taken to be correct and the collected data incorrect, however, as the model contains stoichiometry and kinetics that have been developed and evaluated over the years, the model provides a useful tool for reconciling the data collected and aids in the identification of possible sources of error in the measurements conducted. However, in some cases the outcomes determined by the PWM_SA_AD model was accurate. For instance, since the SSPAD effluent that was used to inoculate the AugBSP control reactor was deemed to comprise mainly of the mediating biomass (with no residual biodegradable organics present), the modelled AugBMP control experiment relied entirely on the biomass concentrations predicted from the SSPAD model. Consequently, it was observed that the estimated concentrations of active biomass in the sulphidogenic SSPAD effluent were accurate as the modelled AugBSP control reactor replicated the observed AugBSP control reactor well for all four experiments. This outcome emphasised the validity of the biomass composition determined by Porges and Hoover (1952), and further justified the assumption of negligible residual biodegradable organics in the sulphidogenic SSPAD effluent, as well as strengthend the proposed methodology for characterising the organics present in the sulphidogenic SSPAD.

The composition of the biodegradable material present in both the AugBMP and AugBSP control reactors was identified using the stoichiometric method, as described in Section 3.9.2. However, it was observed that in both cases (AugBMP and AugBSP), that an error in the composition determined occurred. When reviewing the collected data set as a whole, it was

observed that if any error in the measurements occurred for the starting or ending concentrations, the composition identified using the stoichiometric method was negatively affected. Therefore, it is advised that either more data points be collected for the starting and ending concentrations, which then need to be critically evaluated to determine their accuracy, or as was done in this thesis, more data points should be collected throughout the experiment to identify possible outliers and discrepancies in the data. The latter appears tedious, but will ensure accuracy in the long run, as the possible measurement error associated with the starting and ending concentrations will be minimised. In summary:

1. The measured beginning and ending points give a good indication of the composition and biodegradability of the unknown substrate used.
2. The intermediate points allow for the identification of the parameters used in the kinetics of the breakdown processes (e.g., hydrolysis rate). However, the validity of the kinetic rates should be assessed and compared to the literature. Furthermore, the data set as a whole allows for the measurement error to be spread throughout the experiment, minimising the error associated with the starting and ending points.

Casein hydrolysate was chosen, as a substrate worth investigating for both the AugBMP and AugBSP experiments, as it contains organically bound nitrogen and phosphorus, similar to that of the PSS; therefore, providing the ideal environment for determining the strengths and weaknesses of each of the proposed tests in the context of composition identification. It was seen that both the AugBMP and AugBSP tests were accurate in determining the casein composition, as the results reflected the literature stated values well. However, there was a slight discrepancy in the O term of the composition identified, as the value was higher than stated in the literature (MC1 and SC1 had $O_{0.596}$ and $O_{0.577}$, respectively, instead of $O_{0.35}$ or $O_{0.31}$, as shown in Hoover and Porges (1952), as $C_1H_{1.47}O_{0.35}N_{0.25}$, and Schrieke and Winter (2011) as $C_1H_{1.59}O_{0.31}N_{0.25}P_{0.005}$). The higher O term in the composition identified by the PE lowered the total electron donating capacity (COD) of the biodegradable organics relative to the mass of casein. However, the elevated O term was observed in both the AugBMP and AugBSP experiments, which subsequently suggested that the elevated O term, for the casein sample used, was accurate.

Furthermore, the casein hydrolysate was analysed using wet chemistry analysis (as described in Section 3.6) for a range of constituent concentration such as COD, TKN, FSA, TP and OP, which were then compared to the equivalent concentrations in the casein identified by the PE

for both the AugBMP and AugBSP tests. It was observed that the compositions identified by the PE replicated the measured constituent concentrations in the casein well. Therefore, it could be concluded that both the proposed AugBMP and AugBSP test methods were accurate when identifying the composition of a known organic. However, only one test using casein for the AugBMP and AugBSP test reactors was conducted. Furthermore, only one substrate with a known organic composition was tested. Therefore, there was not enough conclusive evidence to confirm that the AugBMP and AugBSP tests could determine the compositions of any substrate, as the casein was only used to validate the proposed tests for the context of identifying the composition of the biodegradable organics in PSS. Therefore, it is advised that more experiments using a diverse range of substrates with a known composition be tested, such that the accuracy of these tests can be confirmed.

The AugBMP test had a high level of error associated with the gas measurements taken, as the modelled AugBMP test reactor predicted a significantly higher methane gas production. However, the volume of methane gas produced was not used as a variable for the PE conducted on the AugBMP test experiment; nonetheless, the PE was still able to identify the composition of the casein accurately. However, accurate gas measurements were required when identifying the composition of the biodegradable organics using the stoichiometric method described in Section 3.9.2, as the total carbon released contained in both the gaseous and aqueous phases needed to be quantified. Therefore, the stoichiometric identification of the casein composition was negatively affected by inaccurate biogas measurements as the C content of the biodegradable organics was under predicted. However, for the PWM_SA_AD model, the production of methane is directly related to the COD of the biodegradable organics utilised throughout the reaction, as the model was COD balanced. Therefore, if the COD measurements are taken to be accurate (which in most cases they are as they are performed in the aqueous phase), the production of methane is accounted for via the conservation of COD within the model. Furthermore, the release of carbon present in the aqueous phase is determined by the model using the carbonate alkalinity concentration. Therefore, even though the PE did not incorporate the biogas volume produced throughout the experiment, the model was still able to identify the casein composition accurately. This outcome highlights the strength of the proposed AugBMP experiment, as well as the PWM_SA_AD model combined with the PE function as a tool for reconciling parameters from inaccurate gas measurement data, as a relatively accurate outcome can still be achieved by minimising the error across the other measurements taken.

The AugBSP test was proposed as a novel analytical procedure that could be used to identify the composition of the biodegradable organics by alleviating the gas measurement error associated with the BMP test. The results obtained from the casein experiment illustrate that the proposed AugBSP test is a viable substitute for the BMP and AugBMP tests as the composition of the biodegradable organics in the casein was accurately determined. However, as previously mentioned, it is advised that additional tests be conducted on a range of substrates using both the AugBMP and AugBSP methods, such that the strengths and weaknesses of each be thoroughly evaluated. However, it was not in the scope of this thesis to conduct these measurements as the thesis focused on identifying the composition of the biodegradable particulate organics present in PSS, and the casein experiment was conducted purely for validation of the proposed methods.

The AugBMP and AugBSP test experiments were then used to identify the composition of the biodegradable organics present in PSS, taken from Potsdam. It was observed that the compositions identified by each of the AugBMP and AugBSP test experiments differed, which was expected as the biodegradable particulates fluctuate based on the treatment plant and the collection time. Therefore, the composition of the organics present in sewage is not generic and hence specific to the source of the feed, and subsequently requires continuous measurement and analysis in order to predict the performance of the AD system to which it is fed.

The results obtained for both the AugBMP and AugBSP test reactors showed that the composition, as well as the dynamics regarding the breakdown of the PSS, could be accurately represented by the PWM_SA_AD model. However, even though there were discrepancies in the model for specific measurements, the PE was successful in determining an outcome that minimised the error across all of the observed measurements. Further investigations such as sensitivity and uncertainty analyses could be conducted on the PSS composition to ensure validity in the compositions identified. In conclusion, the augmented batch test coupled with mass balanced mathematical models could improve current analytical methods for substrate characterisation, and composition identification, with a specific focus on biodegradability.

7.2 Recommendations

Discrepancies were observed in the modelled SSPADs for some constituents such as TKN, TP and Alkalinity. The source of this discrepancy was related to (i) the chosen compositions of the UPOs in the feed stream, which were taken from the literature (Marais and Ekama, 1976), which were not adjusted, as identifying the composition of the inert organic particulates lay outside the scope of this investigation, and (ii) the chosen BPO and BSO compositions which were adjusted manually via trial and error, as it was not possible to conduct a parameter estimation due to the structure of the influent generator present in WEST. Therefore, accurately modelling the SSPAD was complex and time consuming to do based on the current method of passing the influent feed component masses into the PWM_SA_AD model. The influent generator requires a text file containing the measured concentrations of each component as an input, which subsequently generates the organic load onto the anaerobic digester. Therefore, any changes to the fractionation of the COD groups entering the steady-state AD requires that a new influent file be generated using the pre-processor. Ideally, the influent PSS characterisation for the residual biodegradable organics (S_{bp}), the biomass (Z_{AD}) and the UPO concentrations should be determined using the measured data for the influent and effluent streams combined with the PE function, instead of trial and error. The current configuration of passing a text file into the influent generator makes conducting a PE challenging, as the variables cannot be changed within the optimisation environment. Therefore, a future research project may be the development of tools that can connect influent generators to models such that the PE function can be implemented into the automatic pre-processing of the influent within the parameter estimation environment, ultimately introducing a better influent wizard for the platforms that lack it.

Combining the biomass and residual organics into one collective group, as was done when using the stoichiometric composition calculation of Section 3.9.2, is not possible within the current PWM_SA_AD model framework, The PWM_SA_AD separates the biomass and biodegradable organics into two groups, each with their unique composition. Furthermore, the breakdown and decay of these two organic groups are represented using different rates and stoichiometry in the model. Therefore, if the residual biodegradable organics and the biomass can be combined into one group of organics used to determine the baseline, a parameter estimation can be conducted for a grouped composition, removing the need to model the parent

steady-state anaerobic digesters, in order to determine the biomass concentrations, present in both the augmented control and test reactors.

The proposed analytical testing methods (AugBMP and AugBSP) were accurate in determining the composition of the biodegradable organics present in both a known and unknown substrate. However, the composition of the biomass and UPO groups were accepted to be from literature in the model used for this investigation. This does not imply that they are always fixed, as they can be adjusted freely. However, the number of unknowns increased significantly to a point where solving the parameters of each group was not possible within the boundaries of this thesis. Therefore, it is proposed that future work be conducted by devising an experiment such that the compositions of both the UPO and biomass can be identified and validated. Currently, the compositions of both the UPO and biomass used for modelling are taken to be the literature specified values. However, the proposed testing methodology allows for the composition of any group of organics to be identified, provided that sufficient 'known' parameters are supplied. Therefore, the compositions of the UPOs in primary sludge, waste activated sludge, or even a combined composition can be identified. Furthermore, the composition of individual biomass groups (Acidogens, Acetogens, Acetoclastic or Hydrogenotrophic) can be identified provided the correct adjustments to the model are made. This would greatly benefit processes such as thermophilic anaerobic digestion (TAD) or thermal hydrolysis process (THP), as the changes in composition and biodegradability of the substrates fed to the respective processes could be identified.

The AugBSP control and test reactors showed a discrepancy in the concentration of sulphide utilised to the concentration of sulphide produced. The discrepancy was highlighted in the S balances, in which the S equivalent from the COD concentration of sulphide produced was compared to that of the S equivalent of the sulphate consumed throughout the experiments. The discrepancy was further highlighted when modelling the AugBSP control and test reactors using the PWM_SA_AD model, as the model was mass balanced. Subsequently, in some cases the concentration of sulphide produced during the reaction did not align with the concentration of sulphate utilised. The reason for this discrepancy is challenging to identify with certainty, as the modelled AugBSP control and test reactors for the remaining constituents (such as FSA, OP etc.) were determined relatively accurately by minimising the error across the observed measurements. The method used for quantifying the sulphide concentration via the COD measurement was confirmed by Poinapen *et al*. (2009) and was subsequently taken to be

correct. Therefore, the error was taken to be due to the sulphate measurements performed using the spectrophotometer, as interference due to dissolved constituents may have occurred. The possibility of such interferences, within this testing method, is worth investigating further. Furthermore, the possibility of Fe^{3+} as an alternative electron acceptor (present in the primary substrate) is of interest and is worth investigating in future studies.

The results obtained in the thesis showed that the AugBMP and AugBSP test were accurate in identifying the biodegradable organics present in casein. However, this conclusion was achieved based on a single set of experiments on a single organic substrate with a known composition. Therefore, it is recommended that a diverse range of known compounds be tested using both the AugBMP and AugBSP tests, such that the validity and accuracy of each test be thoroughly investigated. The tested substrates should include a "synthetic" PSS made of a mixture of synthetic substrate cellulose, fat and proteins with a known elementary composition. This investigation will highlight the strengths and weaknesses associated with each respective test and identify the conditions in which one test may be favoured over another.

It was observed in both the AugBMP and AugBSP experiments, that the concentration of acetate (VFAs) accumulating in the modelled environment was challenging to replicate accurately. Therefore, additional experiments on the intermediates (glucose and acetate/propionate) in the PWM_SA_AD model should be investigated and validated. This investigation can be performed using the augmented batch tests and substrates with a known composition, as well as more advanced analytical procedures such as HPLC. Furthermore, the VFA concentration was determined using the 5-point titration method of Moosbrugger *et al.* (1993) and the accompanying speciation routine. Therefore, it is also recommended that the current methods used for determining the VFA concentration in both the methanogenic and sulphidogenic systems be checked for accuracy and validity. The investigation into improving the model intermediates would prove beneficial in the long run, as issues like substrate inhibition can be identified and resolved using the augmented batch tests, provided accurate measurements are collected, and the intermediates are correctly represented within the PWM_SA_AD model.

The data collected for the biogas measurements had a significantly high level of error. This high level of error affected the accuracy of the COD balances in the AugBMP control and test reactors, as well as the composition identification using the stoichiometric identification

method proposed in Section 3.9.2. Therefore, in order to achieve accurate gas measurements, additional work is required to determine an accurate and reliable method for quantifying the gas produced. A suggestion for improving the gas measurements is, instead of using the inverted gas columns submerged in a water bath, the wet-tip gas meter, as described in Section 3.2.1 should be used. The wet-tip gas meter uses a tipping mechanism to quantify the volume of methane gas produced. Furthermore, the wet-tip gas meter can be calibrated to measure the biogas produced in 45m*l* increments. Therefore, (i) the biogas produced is not exposed to pressure lower than that of atmospheric, as water was sucked into the inverted columns, and (ii) the diffusion of CO_2 and CH_4 into the water is minimised as the gas is only in contact with the water for a brief period of time before the gas meter tips (quantifying the gas produced and releasing it from the tipping mechanism).

The quantification of the model fit relative to the observed data can be investigated further, especially in the context of validating the chosen model for industrial-scale processes. A further research project could achieve this by consolidating an extensive data set for each of the unit processes of a treatment plant and assessing the accuracy of the model fitted data.

Chapter 8: References

Angelidaki, I., Alves, M., Bolzonella, D., Borzacconi, L., Campos, J.L., Guwy, A.J., Kalyuzhnyi, S., Jenicek, P. et al. 2009. Defining the biomethane potential (BMP) of solid organic wastes and energy crops: a proposed protocol for batch assays. Water Science and Technology. 59(5):927-934. DOI: https://doi.org/10.2166/wst.2009.040

Angelidaki, I., Ellegaard, L. & Ahring, B.K. 2003. Applications of the anaerobic digestion process. In Biomethanation II. Springer. 1-33. DOI: https://doi.org/10.1007/3-540-45838-7_1

Angelidaki, I., Karakashev, D., Batstone, D.J., Plugge, C.M. & Stams, A.J. 2011. Biomethanation and its potential. In Methods in enzymology. Elsevier. 327-351. DOI: https://doi.org/10.1016/B978-0-12-385112-3.00016-0

Apha. 1985. Standard methods for the examination of water and wastewater. Apha.

Astals, S., Venegas, C., Peces, M., Jofre, J., Lucena, F. & Mata-Alvarez, J. 2012. Balancing hygienization and anaerobic digestion of raw sewage sludge. Water Research. 46(19):6218-6227. DOI: https://doi.org/10.1016/j.watres.2012.07.035

Astals, S., Esteban-Gutie´rrez, M., Ferna´ndez-Are´valo, T., Aymerich, E., Garc´ıa-Heras, J.L. & Mata-Alvarez, J. 2013. Anaerobic digestion of seven different sewage sludges: A biodegradability and modelling study.
Available: http://www.sciencedirect.com/science/article/pii/S0043135413005939.

Batstone, D.J., Keller, J., Angelidaki, I., Kalyuzhnyi, S.V., Pavlostathis, S.G., Rozzi, A., Sanders, W.T., Siegrist, H., et al. 2002. The IWA Anaerobic Digestion Model No 1 (ADM1). Water Science and Technology. 45(10):65–73. DOI: https://doi.org/10.2166/wst.2002.0292

Benneouala, M., Bareha, Y., Mengelle, E., Bounouba, M., Sperandio, M., Bessiere, Y. & Paul, E. 2017. Hydrolysis of particulate settleable solids (PSS) in activated sludge is determined by the bacteria initially adsorbed in the sewage. Water Research. 125:400-409.
DOI: https://doi.org/10.1016/j.watres.2017.08.058
Available: https://www.sciencedirect.com/science/article/pii/S0043135417307224.

Biller, P., Johannsen, I., dos Passos, J.S. & Ottosen, L.D.M. 2018b. Primary sewage sludge filtration using biomass filter aids and subsequent hydrothermal co-liquefaction. Water Research. 130:58-68. DOI: https://doi.org/10.1016/j.watres.2017.11.048
Available: http://www.sciencedirect.com/science/article/pii/S0043135417309764.

Bodegom, P.M.v. & Stams, A.J.M. 1999. Effects of alternative electron acceptors and temperature on methanogenesis in rice paddy soils. Chemosphere. 39(2):167-182.
DOI: https://doi.org/10.1016/S0045-6535(99)00101-0
Available: https://www.sciencedirect.com/science/article/pii/S0045653599001010.

Boland, M. 2011. Whey proteins. Woodhead Publishing Limited
DOI: https://doi.org/10.1533/9780857093639.30

Botha, R. 2015. Characterization of organics for anaerobic digestion by modelling augmented biochemical methane potential test results. University of Cape Town

Brouckaert, C.J., Ikumi, D.S. & Ekama, G.A. 2010. A 3 phase anaerobic digestion model. In 12th IWA AD conference. Guadalajara, Mexico.

Carlson, G.A. 2002. Experimental Errors and Uncertainty.2000-2002.
Available: www.ece.rochester.edu/courses/ECE111/error_uncertainty.pdf.

Chynoweth, D.P., Owens, J.M. & Legrand, R. 2001. Renewable methane from anaerobic digestion of biomass. Renewable Energy. 22(1-3):1-8.
DOI: https://doi.org/10.1016/S0960-1481(00)00019-7

Claeys, F. 2008. A generic software framework for modelling and virtual experimentation with complex biological systems. PhD thesis. Dept. of Applied Mathematics, Biometrics and Process Control, Ghent University, Belgium.

Dalgleish, D.G. 1998. Casein micelles as colloids: surface structures and stabilities. Journal of Dairy Science. 81(11):3013-3018. DOI: https://doi.org/10.3168/jds.S0022-0302(98)75865-5

Dalgleish, D.G. 2011. On the structural models of bovine casein micelles—review and possible improvements. Soft Matter. 7(6):2265-2272. DOI: https://doi.org/10.1039/C0SM00806K

De Vrieze, J., Raport, L., Willems, B., Verbrugge, S., Volcke, E., Meers, E., Angenent, L.T. & Boon, N. 2015. Inoculum selection influences the biochemical methane potential of agro-industrial substrates. Microbial Biotechnology. 8(5):776-786.
DOI: https://doi.org/10.1111/1751-7915.12268

Demirel, B. & Scherer, P. 2008. The roles of acetotrophic and hydrogenotrophic methanogens during anaerobic conversion of biomass to methane: a review. Reviews in Environmental Science and Bio/Technology. 7(2):173-190.
DOI: http://dx.doi.org/10.1007/s11157-008-9131-1

Ekama, G.A. & Wentzel, M.C. 2004. A predictive model for the reactor inorganic suspended solids concentration in activated sludge systems. Water Research. 38(19):4093-4106.
DOI: https://doi.org/10.1016/j.watres.2004.08.005

Ekama, G.A., Wentzel, M.C. & Sötemann, S.W. 2006. Tracking the inorganic suspended solids through biological treatment units of wastewater treatment plants. Water Research. 40(19):3587-3595.
DOI: https://doi.org/10.1016/j.watres.2006.05.034
Available: https://www.sciencedirect.com/science/article/pii/S0043135406003204.

Ekama, G.A., Brouckaert, C.J., Brouckaert, B.M. & Ikumi, D.S. 2020. Integration of complete elemental mass balanced stoichiometry and aqueous phase chemistry for bioprocess modelling of liquid and solid waste treatment systems: Part 2 - Bioprocess stoichiometry. Water SA, Accepted.

Ekama, G.A., Brouckaert, C.J., Brouckaert, B.M. & Ikumi, D.S. 2020. Integration of complete elemental mass balanced stoichiometry and aqueous phase chemistry for bioprocess modelling of liquid and solid waste treatment systems: Part 3 – Measuring the organics composition. Water SA, Accepted.

Elbeshbishy, E., Nakhla, G. & Hafez, H. 2012. Biochemical methane potential (BMP) of food waste and primary sludge: influence of inoculum pre-incubation and inoculum source. Bioresource Technology. 110:18-25. DOI: https://doi.org/10.1016/j.biortech.2012.01.025

Esposito, G., Frunzo, L., Liotta, F., Panico, A. & Pirozzi, F. 2012. Bio-methane potential tests to measure the biogas production from the digestion and co-digestion of complex organic substrates. The Open Environmental Engineering Journal. 5(1).
DOI: http://dx.doi.org/10.2174/1874829501205010001

Ghoor, T. 2020. Developments in anaerobic digestion. University of Cape Town.

Grau P, DE Gracia M, VAnrolleghem PA and Ayesa E (2007) A new plant wide methodology for WWTPs. Water Research 41 4357-4372.
DOI: https://doi.org/10.1016/j.watres.2007.06.019

Gujer, W. & Zehnder, A.J. 1983. Conversion processes in anaerobic digestion. Water Science and Technology. 15(8-9):127-167. DOI: https://doi.org/10.2166/wst.1983.0164

Hao, O.J., Chen, J.M., Huang, L. & Buglass, R.L. 1996. Sulfate-reducing bacteria. Critical Reviews in Environmental Science and Technology. 26(2):155-187.
DOI:10.1080/10643389609388489
Available: https://doi.org/10.1080/10643389609388489

Hao, T., Xiang, P., Mackey, H.R., Chi, K., Lu, H., Chui, H., van Loosdrecht, M.C. & Chen, G. 2014. A review of biological sulfate conversions in wastewater treatment. Water Research. 65:1-21. DOI: https://doi.org/10.1016/j.watres.2014.06.043

Henze, M., van Loosdrecht, M., Ekama, G. & Brdjanovic, D. 2008. Anaerobic Wastewater Treatment. In Biological Wastewater Treatment: Principles, Modelling and Design. M. Henze, Ed. illustrated, reprint ed. IWA Publishing. 415.
DOI: https://doi.org/10.2166/9781789060362_0701

Holliger, C., Alves, M., Andrade, D., Angelidaki, I., Astals, S., Baier, U., Bougrier, C., Buffière, P. et al. 2016. Towards a standardization of biomethane potential tests. Water Science and Technology. 74(11):2515-2522. DOI: https://doi.org/10.2166/wst.2016.336

Hoover, S.R. & Porges, N. 1952. Assimilation of dairy wastes by activated sludge: II. The equation of synthesis and rate of oxygen utilization. Sewage and Industrial Wastes. :306-312. DOI: https://www.jstor.org/stable/25031525

Ikumi, D.S. 2011. The development of a three phase plant-wide mathematical model for sewage treatment. University of Cape Town.

Ikumi, D.S., Harding, T.H. & Ekama, G.A. 2014. Biodegradability of wastewater and activated sludge organics in anaerobic digestion. Water Research. 56:267-279.
DOI: https://doi.org/10.1016/j.watres.2014.02.008
Available: https://www.sciencedirect.com/science/article/pii/S0043135414001183.

Izzett, H. 1992. The effect of thermophilic heat treatment on the anaerobic digestibility of primary sludge. University of Cape Town.

Jensen, P.D., Ge, H. & Batstone, D.J. 2011. Assessing the role of biochemical methane potential tests in determining anaerobic degradability rate and extent. Water Science and Technology. 64(4):880-886. DOI: https://doi.org/10.2166/wst.2011.662

Jimenez, J., Gonidec, E., Cacho Rivero, J.A., Latrille, E., Vedrenne, F. & Steyer, J. 2014. Prediction of anaerobic biodegradability and bioaccessibility of municipal sludge by coupling sequential extractions with fluorescence spectroscopy: Towards ADM1 variables characterization.
Water Research. 50:359-372. DOI: https://doi.org/10.1016/j.watres.2013.10.048
Available: http://www.sciencedirect.com/science/article/pii/S0043135413008543.

Jimenez, J., Charnier, C., Kouas, M., Latrille, E., Torrijos, M., Harmand, J., Patureau, D., Spérandio, M. et al. 2020. Modelling hydrolysis: Simultaneous versus sequential biodegradation of the hydrolysable fractions. Waste Management. 101:150-160.
DOI: https://doi.org/10.1016/j.wasman.2019.10.004
Available: https://www.sciencedirect.com/science/article/pii/S0956053X19306312.

Joseph, M. 2017. Peptide and protein-based therapeutic agents. Emerging nanotechnologies for diagnostics, drug delivery and medical devices.
DOI: https://doi.org/10.1016/B978-0-323-42978-8.00007-3

Kaspar, H.F. & Wuhrmann, K. 1978. Kinetic parameters and relative turnovers of some important catabolic reactions in digesting sludge. Applied and Environmental Microbiology. 36(1):1-7. DOI: https://doi.org/10.1128/aem.36.1.1-7.1978

Kleerebezem, R., Joosse, B., Rozendal, R. and Van Loosdrecht, M. C. M. 2015. Anaerobic digestion without biogas? Reviews in Environmental Science and Bio/Technology. Springer Netherlands, (October). DOI: 10.1007/s11157-015-9374-6.

Koster, I.W., Rinzema, A., De Vegt, A.L. & Lettinga, G. 1986. Sulfide inhibition of the methanogenic activity of granular sludge at various pH-levels. Water Research. 20(12):1561-1567. DOI: https://doi.org/10.1016/0043-1354(86)90121-1

Liamleam, W. & Annachhatre, A.P. 2007. Electron donors for biological sulfate reduction. Biotechnology Advances. 25(5):452-463.
DOI: https://doi.org/10.1016/j.biotechadv.2007.05.002

Loewenthal, R.E., Ekama, G.A. & Marais, G. v. R. 1989. Mixed weak acid/base systems Part I - Mixture characterisation. Water SA. 15(1):3–24.
DOI: https://hdl.handle.net/10520/AJA03784738_1550

Loewenthal, R.E., Wentzel, M.C., Ekama, G.A. & Marais, G. v. R. 1991. Mixed weak acid/base systems Part II: Dosing estimation, aqueous phase. Water SA. 17(2):107– 122.

Lovley, D.R. and Phillips E.P. 1987. Competitive mechanisms for inhibition of sulfate reduction and methane production in the zone of ferric iron reduction in sediments, Appl. Env. Microbiol. 53, 2636- 264.

Marais, G. & Ekama, G.A. 1976. The activated sludge process part I-steady state behaviour. Water Sa. 2(4):163-200.

McCarty, P.L. & Mosey, F.E. 1991. Modelling of anaerobic digestion processes (a discussion of concepts). Water Science and Technology. 24(8):17-33.
DOI: https://doi.org/10.2166/wst.1991.0216

McCarty, P.L. 1974. Anaerobic processes. Birmingham Short Course on Design Aspects of Biological Treatment, International Association of Water Pollution Research, Birmingham, England.

McMahon, D.J. & Oommen, B.S. 2013. Casein micelle structure, functions, and interactions. In Advanced dairy chemistry. Springer. 185-209.

Moody, L., Burns, R., Wu-Haan, W. & Spajic, R. 2009. Use of biochemical methane potential (BMP) assays for predicting and enhancing anaerobic digester performance. Proceedings of the 44th Croatian and the 4th International Symposium on Agriculture, Opatija, Croatia, 16-20 February 2009.

Moosbrugger, R., Wentzel, M., Ekama, G. & Marais, G. 1993a. Mixed weak acid base chemistry and pH in anaerobic digestion - A review. Water SA. 19(1):1–10.

Moosbrugger, R.E., Wentzel, M.C., Ekama, G.A. & Marais, G. v. R. 1993c. Alkalinity measurement: Part 1 - A 4 pH point titration method to determine the carbonate weak acid/base in an aqueous carbonate solution. Water SA. 19(1):11–22.

Moosbrugger, R.E., Wentzel, M.C., Ekama, G.A. & Marais, G. v. R. 1993d. A 5 pH point titration method for determining the carbonate and SCFA weak acid/bases in anaerobic systems. Water Science and Technology. 28(2):237–245.
DOI: https://doi.org/10.2166/wst.1993.0112

Mosey, F.E. 1983. Mathematical modelling of the anaerobic digestion process: Regulatory mechanisms for the formation of short-chain volatile acids from glucose. Water Science and Technology. 15(8–9):209–232. DOI: https://doi.org/10.2166/wst.1983.0168

O'Rourke, J.T. 1967. Kinetics of anaerobic treatment at reduced temperatures. Stanford University

Owen, W.F., Stuckey, D.C., Healy Jr, J.B., Young, L.Y. & McCarty, P.L. 1979. Bioassay for monitoring biochemical methane potential and anaerobic toxicity. Water Research. 13(6):485-492. DOI: https://doi.org/10.1016/0043-1354(79)90043-5

Parajuli, P. 2011b. Biogas measurement techniques and the associated errors.

Poinapen, J. & Ekama, G.A. 2010. Biological sulphate reduction with primary sewage sludge in an upflow anaerobic sludge bed reactor–Part 5: Steady-state model. SA Journal of Radiology. 36(3).

Poinapen, J., Ekama, G.A. & Wentzel, M.C. 2009. Biological sulphate reduction with primary sewage sludge in an upflow anaerobic sludge bed (UASB) reactor–Part 2: Modification of simple wet chemistry analytical procedures to achieve COD and S mass balances. Water SA. 35(5).

Raposo, F., De la Rubia, M A, Fernández-Cegrí, V. & Borja, R. 2012. Anaerobic digestion of solid organic substrates in batch mode: an overview relating to methane yields and experimental procedures. Renewable and Sustainable Energy Reviews. 16(1):861-877. DOI: https://doi.org/10.1016/j.rser.2011.09.008

Raposo, F., Fernández-Cegrí, V., De la Rubia, M A, Borja, R., Béline, F., Cavinato, C., Demirer, G., Fernández, B. et al. 2011. Biochemical methane potential (BMP) of solid organic substrates: evaluation of anaerobic biodegradability using data from an international interlaboratory study. Journal of Chemical Technology & Biotechnology. 86(8):1088-1098. DOI: https://doi.org/10.1002/jctb.2622

Ristow, N.E., Sötemann, S.W., Loewenthal, R.E., Wentzel, M.C. & Ekama, G.A. 2005. Hydrolysis of primary sewage sludge under methanogenic, acidogenic and sulphate reducing conditions. Water Research Commission Report. (1216/1):05.

Sam-Soon, P.A.L.N.S., Loewenthal, R.E., Wentzel, M.C. & Marais, G. v. R. 1991a. A long-chain fatty acid, oleate, as sole substrate in Upflow Anaerobic Sludge Bed (UASB) reactor systems. Water SA. 17(1):31–36. DOI: https://hdl.handle.net/10520/AJA03784738_1408

Sam-Soon, P.A.L.N.S., Wentzel, M.C., Dold, P.L., Loewenthal, R.E. & Marais, G. v. R. 1991b. Mathematical modelling of upflow anaerobic sludge bed (UASB) systems treating carbohydrate waste waters. Water SA. 17(2):91–106.
DOI: https://hdl.handle.net/10520/AJA03784738_1576

Schrieke, R.R. & Winter, G. 2011. Casein. Encyclopedia of Polymer Science and Technology.

Shin, S.G., Lee, S., Lee, C., Hwang, K. & Hwang, S. 2010. Qualitative and quantitative assessment of microbial community in batch anaerobic digestion of secondary sludge. Bioresource Technology. 101(24):9461-9470.
DOI: https://doi.org/10.1016/j.biortech.2010.07.081

Sötemann, S.W., Ristow, N.E., Wentzel, M.C. & Ekama, G.A. 2005a. A steady state model for anaerobic digestion of sewage sludges. Water SA. 31(4):511–528.
DOI: https://doi.org/10.4314/wsa.v31i4.5143

Sötemann, S.W., Van Rensburg, P., Ristow, N.E., Wentzel, M.C., Loewenthal, R.E. & Ekama, G.A. 2005b. Integrated chemical / physical and biological processes modelling Part 2 - Anaerobic digestion of sewage sludges. Water SA. 31(4):545–568.
DOI: https://doi.org/10.4314/wsa.v31i4.5145

Speece, R.E. 1983. Anaerobic biotechnology for industrial wastewater treatment. Environmental Science & Technology. 17(9):416A-427A.

Strömberg, S., Nistor, M. & Liu, J. 2014. Towards eliminating systematic errors caused by the experimental conditions in Biochemical Methane Potential (BMP) tests. Waste Management. 34(11):1939-1948. DOI: https://doi.org/10.1016/j.wasman.2014.07.018

Strömberg, S., Nistor, M. & Liu, J. 2015. Early prediction of Biochemical Methane Potential through statistical and kinetic modelling of initial gas production. Bioresource Technology. 176:233-241. DOI: https://doi.org/10.1016/j.biortech.2014.11.033

Vanhooren, H., Meirlaen, J., Amerlinck, Y., Claeys, F., Vangheluwe, H. & Vanrolleghem, P.A. 2003. WEST: modelling biological wastewater treatment. Journal of Hydroinformatics. 5(1):27-50. DOI: https://doi.org/10.2166/hydro.2003.0003

Volcke EIP, Van Loosdrecht MCM and Vanrolleghem PA. 2006. Continuity-based model interfacing for plant-wide simulation: A general approach. Water Research 40(15) 2817-2828. DOI: https://doi.org/10.1016/j.watres.2006.05.011

Wentzel, M.C., Ekama, G.A. & Sötemann, S.W. 2006. Mass balance-based plant-wide wastewater treatment plant models–Part 1: Biodegradability of wastewater organics under anaerobic conditions. Water SA. 32(3):269-275. DOI: https://doi.org/10.4314/wsa.v32i3.5261

Zhang, R., El-Mashad, H.M., Hartman, K., Wang, F., Liu, G., Choate, C. & Gamble, P. 2007. Characterization of food waste as feedstock for anaerobic digestion. Bioresource Technology. 98(4):929-935.
DOI:https://doi.org/10.1016/j.biortech.2006.02.039
Available: http://www.sciencedirect.com/science/article/pii/S0960852406000940.

Appendix A: Weak Acid/Base Chemistry

The equations used for determining the total alkalinity are described below (Loewenthal *et al*. (1991):

$$[Alk\ HAc] = A_T \frac{1}{(1 + W)} \quad \text{mol (A.1)}$$

$$[Alk\ NH_4^+] = N_T \frac{1}{(1 + W)} \quad \text{mol (A.2)}$$

$$[Alk\ H_3PO_4] = P_T \frac{1 + 2X + 3XY}{(1 + W + X + XY)} \quad \text{mol (A.3)}$$

$$[Alk\ H_2S] = S_T \frac{1 + 2X}{(1 + W + X)} \quad \text{mol (A.4)}$$

$$[Alk\ H_2O] = 10^{pH-pKw'} - \frac{10^{-pH}}{fm} \quad \text{mol (A.5)}$$

Where:

$W = 10^{pK'_1 - pH}$

$X = 10^{pH - pK'_2}$

$Y = 10^{pH - pK'_3}$

$pK' = -\log K'$

Appendix B: Gas Chromatography Data

Table B. 1: GC Data 04.05.2018

Date	04.05.2018					
Unit	Area injection displacement					%
Injection	1	2	3	4	Average	Partial Pressure
24.3% Standard	1096309	903604	947672	1056314	1000975	24.3
50% Standard	2512687	2495438	2422544	2340860	2442882	50
Headspace Sample	2899181	3089975	2887917	2963326	2960100	**59.2**

Table B. 2: GC Data 03.12.2018

Date	03.12.2018				
Unit	Area under injection displacement				%
Injection	1	2	3	Average	Partial Pressure
24.3% Standard	665492	589566	618942	624667	24.3
50% Standard	1216663	1184665	1192076	1197801	50
Headspace Sample	1400258	1310281	1312514	1341017	**56.4**
Date	04.12.2018				
Unit	Area under injection displacement				%
Injection	1	2	3	Average	Partial Pressure
24.3% Standard	584567	600129	570808	585168	24.3
50% Standard	1325783	1254023	1215654	1265153	50
Headspace Sample	1472575	1312539	-	1392557	**54.8**
Date	05.12.2018				
Unit	Area under injection displacement				%
Injection	1	2	3	Average	Partial Pressure
24.3% Standard	611687	577545	568562	585931	24.3
50% Standard	1227232	1206663	1309753	1247882	50
Headspace Sample	1433655	1520051	-	1476853	**58.9**
Date	06.12.2018				
Unit	Area under injection displacement				%
Injection	1	2	3	Average	Partial Pressure
24.3% Standard	1013127	1047450	1059630	1040069	24.3
50% Standard	2260162	2363626	2141767	2255185	50
Headspace Sample	2632358	2714554	-	2673456	**58.8**
Average Partial Pressure					**57.2**

Table B. 3: GC Data 22.05.2018

Date	22.05.2018				
Unit	Area under injection displacement				%
Injection	1	2	3	Average	Partial Pressure
24.3% Standard	1243110	1178765	1206035	1209303	24.3
50% Standard	2739003	2765663	2926128	2810265	50
Test Reactor 1	4142267	4144736	-	4143502	**71.6**
Test Reactor 2	3755893	3888876	-	3822385	**66.4**
Test Reactor 3	-	-	-	-	**-**
Control Reactor 1	3549985	3605828	-	3577907	**62.4**
Control Reactor 2	3797595	3598959	-	3698277	**64.4**
Control Reactor 3	-	-	-	-	**-**
Date	22.05.2018				
Unit	Area under injection displacement				%
Injection	1	2	3	Average	Partial Pressure
24.3% Standard	1431845	1342741	1427864	1400817	24.3
50% Standard	2745290	2650648	2792516	2729484	50
Test Reactor 1	3861398	3681289	-	3771343	**70.5**
Test Reactor 2	3684018	3820991	-	3752505	**70.1**
Test Reactor 3	-	-	-	-	**-**
Control Reactor 1	3068590	3193383	-	3130986	**57.9**
Control Reactor 2	3793309	3447406	-	3620357	**67.5**
Control Reactor 3	-	-	-	-	**-**
Date	22.05.2018				
Unit	Area under injection displacement				%
Injection	1	2	3	Average	Partial Pressure
24.3% Standard	1277059	1301429	1266178	1281555	24.3
50% Standard	2700368	2677600	2664119	2680696	50
Test Reactor 1	3125477	3023153	-	3074315	**57.3**
Test Reactor 2	3138884	2973157	-	3056021	**57.0**
Test Reactor 3	3148970	3012119	-	-	**57.5**
Control Reactor 1	2400254	2321061	-	2360657	**44.0**
Control Reactor 2	2671518	2586174	-	2628846	**49.0**
Control Reactor 3	1206275	1137029	-	-	**21.8***

Average Partial Pressures	
Test Reactor 1	**66.5**
Test Reactor 2	**64.5**
Test Reactor 3	**57.5**
Control Reactor 1	**54.8**
Control Reactor 2	**60.3**
Control Reactor 3	**-**

Table B. 4: GC Data 11.12.2018

Date	11.12.2018				
Unit	Area under injection displacement				%
Injection	1	2	3	Average	Partial Pressure
24.3% Standard	1146600	1315564	1269782	1243982	24.3
50% Standard	2673151	2715268	2687681	2692033	50
Test Reactor 1	2391732	2632846	-	2512289	**46.8**
Test Reactor 2	-	-	-	-	**-**
Test Reactor 3	-	-	-	-	**-**
Control Reactor 1	2817183	2656758	-	2736970	**50.8**
Control Reactor 2	-	-	-	-	**-**
Control Reactor 3	-	-	-	-	**-**
Date	12.12.2018				
Unit	Area under injection displacement				%
Injection	1	2	3	Average	Partial Pressure
24.3% Standard	1009764	883123	794323	895737	24.3
50% Standard	1964480	1991802	1897290	1951190	50
Test Reactor 1	-	-	-	-	**-**
Test Reactor 2	1889805	1785537	-	1837671	**47.2**
Test Reactor 3	-	-	-	-	**-**
Control Reactor 1	-	-	-	-	**-**
Control Reactor 2	2230600	2300797	-	2265699	**57.8**
Control Reactor 3	-	-	-	-	**-**
Date	13.12.2018				
Unit	Area under injection displacement				%
Injection	1	2	3	Average	Partial Pressure
24.3% Standard	1195405	1228749	1348124	1257426	24.3
50% Standard	2390810	2457498	2696249	2514852	50
Test Reactor 1	-	-	-	-	**-**
Test Reactor 2	-	-	-	-	**-**
Test Reactor 3	1971504	1990423	-	-	**38.9**
Control Reactor 1	-	-	-	-	**-**
Control Reactor 2	-	-	-	-	**-**
Control Reactor 3	1935391	1997383	-	-	**38.6**
Date	21.12.2018				
Unit	Area under injection displacement				%
Injection	1	2	3	Average	Partial Pressure
24.3% Standard	1312774	1392966	1307858	1337866	24.3
50% Standard	2625548	2785933	2615717	2675732	50
Test Reactor 1	3322616	3165618	-	3244117	**61.1**
Test Reactor 2	3421790	3958075	-	3689932	**69.8**
Test Reactor 3	3545195	3272013	-	3408604	**64.3**
Control Reactor 1	2498200	2592996	-	2545598	**47.5**
Control Reactor 2	2806728	2902467	-	2854598	**53.5**
Control Reactor 3	2865349	2848518	-	2856933	**53.5**

Average Partial Pressures	
Test Reactor 1	**53.9**
Test Reactor 2	**58.5**
Test Reactor 3	**51.6**
Control Reactor 1	**49.1**
Control Reactor 2	**55.6**
Control Reactor 3	**46.1**

Appendix C: Methanogenic Steady State Reactor Data

Table C. 1: Methanogenic Steady State Digester Data

		MP1										MP2										MP3									
		Steady State Methanogenic Influent					Steady State Methanogenic Effluent					Steady State Methanogenic Influent					Steady State Methanogenic Effluent					Steady State Methanogenic Influent						Steady State Methanogenic Effluent					
Constituent		Date				Average	Date				Average	Date				Average	Date				Average	Date					Average	Date					Average
COD	Unit	01.02.2018	03.02.2018	06.02.2018	20.02.2018		30.01.2018	02.02.2018	07.02.2018	20.02.2018		02.05.2018	03.05.2018	04.05.2018	05.05.2018		02.05.2018	03.05.2018	04.05.2018	05.05.2018		01.12.2018	03.12.2018	04.12.2018	05.12.2018	06.12.2018		01.12.2018	03.12.2018	04.12.2018	05.12.2018	06.12.2018	
Total 1	mgCOD/l	68988	45992	46894	44933		19238	18992	16678	17811		62800	61046	50477	38632		20080	16867	15903	15743		55214	57502	55761	60863	64872		22972	22490	23453	25702	23132	
Total 2	mgCOD/l	53958	39679	51703	45844		19238	19317	18621	17487		54969	62504	50112	52846		19437	17188	13654	14779		54486	57097	57948	56490	63779		24899	22811	24096	26024	23453	
Total 3	mgCOD/l	-	-	-	-	**49749**	-	-	-	-	**18423**	51053	48654	44281	47743	**52093**	19437	15903	19116	14136	**16854**	56672		58312	56855	63415	**58519**	23614	22490	23775	25381	25060	**23957**
Soluble 1	mgCOD/l	6463	6012	6613	6983		6012	6006	4048	4534		7078	7107	5649	5831		8193*	3373	2088	2570		7107	7289	7289	7289	6925		5622	3855	4819	4819	4177	
Soluble 2	mgCOD/l	6764	6313	6313	7286	**6593**	6012	4707	3724	4534	**4947**	6777	7836	5285	6196	**6470**	5301	3695	1767	2249	**3006**	7471	7694	6925	6925	7289	**7220**	5944	3855	4498	3855	4819	**4626**
TKN																																	
Total 1	mgTKN-N/l	1349	971	903	971		-	1295	1183	1197		1360	1432	1276	1288		1085	1141	1085	1141		1242	1317	1253	1242	1634		1267	1253	1281	1218	1183	
Total 2	mgTKN-N/l	1318	982	1171	866		-	1722	1218	1204		1155	1363	1299	1392		1680	1134	1078	1113		1265		1271	1299	1236		1127	973	1288		1218	
Total 3	mgTKN-N/l	-	-	-	-	**1066**	-	1211	1148	1085	**1251**	1323	1346	1305	1386	**1327**	2002	1288	1064	1232	**1254**	283	277	271	243	295	**938**		595	560	595	686	**1019**
FSA																																	
Total 1	mgFSA-N/l	58	89	42	121		581	497	441	637		278	202	133	219		735	840	455	651		133	110	127	116	104		525	1414	553	560	567	
Total 2	mgFSA-N/l	47	79	42	89		588	581	434	546		252	237	156	364		1106	567	469	700		162	347	156	104	121		518		532	532	546	
Total 3	mgFSA-N/l	241.5*	74	53	116	**74**	721	483	448	476	**536**	242	196	162	173	**218**	581	525	630	665	**660**	127	578	133		116	**174**	539	532	525	539	539	**602**
TP																																	
Total 1	mgTP-P/l	-	-	-	137		-	-	-	185			152	148	146			155	229	190		166	206	227	165	209		179	176	174	185	194	
Total 2	mgTP-P/l	-	-	-	154	**145**	-	-	-	187	**186**		152	147	145			155	224	190		158	205	229	167	211		188	176	191	186	190	
Total 3	mgTP-P/l												222	146	133			136	233	178		159	206	230	174	213		177	186	176	184	187	
Total 4	mgTP-P/l												154	146	134	**152**		135	226	179	**186**	161	205	236	165	273	**198**	181	181	193	188	186	**185**
OP																																	
Total 1	mgOP-P/l	95.4	95.4	95.4	54.7		20.0	20.0	20.0	23.9																							
Total 2	mgOP-P/l	76.6	76.6	76.6	-		27.1	27.1	27.1	-			36.8	42.4	44.3			19.2	4.4	16.4		65.5	55.4	60.5	59.5	62.7		49.1	41.6	40.4	36.5	35.9	
Total 3	mgOP-P/l	90.0	90.0	90.0	-	**84**	23.6	23.6	23.6	-	**23.6**		37.3	41.3	45.7	**41**		11.6	6.6	18.1	**13**	66.1	56.0	60.4	59.8	63.0	**61**	51.0	36.3	39.4	37.1	38.3	**41**
Solids																																	
TSS 1	mgTSS/l	28590	25767	26655	-		13384	12868	-	-		31997	27657	44535	25458		11998	11826	10656	11304		35523	37751	37517	37041	36049		17350	16156	16906	17506	15892	
TSS 2	mgTSS/l	26633	24334	26513	-	**26415**	13106	12576	-	-	**12984**	26039	26397	12717	23108	**27238**	9244	11338	8698	8836	**10488**	31770	32324	31529	32160	31016	**34268**	14006	13246	14028	14688	12976	**15275**
VSS 1	mgVSS/l	23730	20775	21557	-		9988	9614	-	-		26442	23270	39662	21631		9094	8812	7838	8456		28715	31131	16053*	30167	30138		13136	12444	12738	13220	11968	
VSS 2	mgVSS/l	22229	19637	21546	-	**21579**	9736	9342	-	-	**9670**	21977	22665	17027	19790	**24058**	7398	8986	6776	6861	**8028**	25301	26195	26592	25682	26436	**27817**	10336	11646	10772	12984	9962	**11921**
ISS 1	mgISS/l	4860	4992	5099	-		3396	3254	-	-		5555	4387	4873	3826		2904	3014	2818	2848		6809	6619	21463*	6875	5912		4214	3712	4168	4286	3924	
ISS 2	mgISS/l	4404	4698	4966	-	**4836**	3370	3234	-	-	**3313**	4062	3732		3318	**4251**	1846	2352	1922	1975	**2460**	6470	6129	4937	6478	4580	**6090**	3670	1600	3256	1704	3014	**3355**
pH																																	
pH		5.50	5.40	5.50	5.60	**5.50**	6.99	7.01	7	6.99	**7.00**	5.37	5.34	5.45	5.39	**5.39**	7.081	7.067	7.077	7.125	**7.09**	4.95	5.06	5.11	5.09	5.10	**5.06**	7.06	7.107	7.094	7.14	7.134	**7.11**
Alkalinity																																	
Carbonate + H2O	mg/l as CaCO3	1.8	2.3	2.4	2.0	**2.1**	1111	2208	2447	2237	**2001**	107.1	84.1	118.2	121.4	**107.7**	2754	2585	2745	2641	**2681**	61.2	74.1	74.8	73.9	78.3	**71.0**	2535	2401	2512	2577	2480	**2501**
Ammonia	mg/l as CaCO3	0.0	0.0	0.0	0.1	**0.0**	19.0	12.4	9.9	11.7	**13.2**	0.0	0.0	0.0	0.0	**0.0**	19.9	15.5	14.6	19.2	**17.3**	0.0	0.0	0.0	0.0	0.0	**0.0**	12.7	25.0	13.3	15.8	14.5	**16.3**
Phospahte	mg/l as CaCO3	3.8	2.9	4.4	3.1	**3.5**	25.6	22.9	23.2	22.3	**23.5**	0.5	0.3	0.5	0.6	**0.5**	16.4	15.7	5.8	19.4	**14.3**	0.3	0.3	0.3	0.3	0.3	**0.3**	50.3	61.3	53.6	39.6	38.5	**48.7**
Sulphide	mg/l as CaCO3	0	0	0	0	**0.0**	0	0	0	0	**0**	0	0	0	0	**0.0**	0	0	0	0	**0**	0	0	0	0	0	**0.0**	0	0	0	0	0	**0**
VFA	mg/l as CaCO3	757	983	926	1161	**956.6**	0	0	0	31	**8**	1	1	1	1	**1.2**	2	2	2	2	**2**	1	1	1	1	1	**1.1**	2	2	2	2	2	**2**
Total	mg/l as CaCO3	763	988	933	1166	**962.3**	1156	2243	2480	2303	**2045**	109	86	120	123	**109.4**	2792	2619	2767	2681	**2715**	62	75	76	75	80	**73.9**	2600	2490	2581	2635	2535	**2568**
Species Conc																																	
CT	mg/l as C	0	0	1	1	**0**	296	610	676	632	**553**	432	347	399	457	**409**	748	711	747	702	**727**	565	547	488	509	564	**535**	700	652	691	695	677	**683**
VFA	mg/l as Hac	1051	1413	1284	1567	**1328**	0	0	0	38	**9**	2	2	2	2	**2**	2	2	2	2	**2**	2	2	2	2	2	**2**	3	3	3	3	3	**3**

Appendix D: Sulphidogenic Steady State Reactor Data

Table D. 1: Sulphidogenic Steady State Digester Data

		SP1												SP2												SP3					
		Steady State Sulphideogenic Influent						Steady State Sulphidogenic Effluent						Steady State Sulphideogenic Influent						Steady State Sulphidogenic Effluent						Steady State Sulphide Influent			Steady State Sulphide Effluent		
Constituent		Date					Average	Date					Average	Date					Average	Date					Average	Date		Average	Date		Average
COD	**Unit**	**6.11.2018**	**7.11.2018**	**8.11.2018**	**9.11.2018**	**10.11.2018**		**6.11.2018**	**7.11.2018**	**8.11.2018**	**9.11.2018**	**10.11.2018**		**21.01.2019**	**22.01.2019**	**23.01.2019**	**24.01.2019**	**25.01.2019**		**21.01.2019**	**22.01.2019**	**23.01.2019**	**24.01.2019**	**25.01.2019**		**02.04.2019**	**03.04.2019**		**02.04.2019**	**03.04.2019**	
Total 1	mgCOD/l	1427	1538	1384	1438	1404	48	1635	1968	1992	1651	1674		1723	1726	1662	1681	1364	116	2000	1635	1706	1690	1405		1593	1557	43	1016	921	
Total 2	mgCOD/l	1459	1498	1414	1458	1394	**1441**	1714	1936	1960	1667	1627	**1782**	1713	1567	1562	1731	1701	**1643**	2127	1651	1674	1738	1421	**1705**	1493	1528	**1543**	936	873	**936**
Soluble 1	mgCOD/l	148	121	120	99	76	24	663	730	700	667	681		170	171	140	120	92	32	829	809	807	776	748		94	77	10	401	425	
Soluble 2	mgCOD/l	138	129	126	97	78	**113**	667	738	704	675	684	**691**	180	177	154	122	102	**143**	833	813	819	780	740	**796**	90	101	**91**	397	421	**411**
Organic 1	mgCOD/l	-	-	-	-	-		91	67	69	56	46		-	-	-	-	-		119	111	117	101	109		-	-		107	79	
Organic 2	mgCOD/l	-	-	-	-	-	-	79	79	65	56	50	**66**	-	-	-	-	-	-	127	115	113	105	101	**112**	-	-	-	103	119	**102**
Sulphide 1	mgCOD/l	-	-	-	-	-		571	663	631	611	635		-	-	-	-	-		710	698	690	675	639		-	-		294	345	
Sulphide 2	mgCOD/l	-	-	-	-	-	-	587	659	639	619	635	**625**	-	-	-	-	-	-	706	698	706	675	639	**684**	-	-	-	294	302	**309**
Sulphate																															
Total 1	mgSO4/l	1500	1500	1500	1500	1500		113	73	107	101	102		1500	1500	1500	1500	1500		-	144	85	175	121		1500	1500		643	606	
Total 2	mgSO4/l	1500	1500	1500	1500	1500	**1500**	100	-	92	94	91	**97**	1500	1500	1500	1500	1500	**1500**	-	142	81	171	117	**129**	1500	1500	**1500**	633	614	**624**
TKN																															
Total 1	mgTKN-N/l	42.0	38.2	43.4	91.0	21.1		45.8	49.8	51.8	42.8	51.8		43.8	41.6	40.5	39.8	40.2		31.2	54.8	52.1	60.5	46.2		36.7	38.1		20.4	31.5	
Total 2	mgTKN-N/l	37.0	39.9	44.5	86.8	20.4		49.0	47.9	52.5	46.3	49.8		39.3	36.7	40.6	40.7			32.5	24.6	47.0	11.5	-		37.8	37.5		28.3	17.6	
Total 3	mgTKN-N/l	41.0	38.0	42.1	85.1	20.0	**46.0**	47.2	47.6	50.8	43.3	47.2	**48.2**	6.6	9.1	11.7	7.3	6.0	**28.8**	9.5	15.8	17.9	21.8	-	**32.7**	5.8	5.9	**37.5**	10.5	5.9	**24.5**
FSA																															
Total 1	mgFSA-N/l	2.7	3.6	1.7	2.7	3.1		19.3	7.6	13.0	15.1	16.9		4.8	3.8	3.6	3.7	3.6		18.3	15.1	15.7	16.5	15.0		5.2	3.6		10.2	-	
Total 2	mgFSA-N/l	3.1	2.6	2.1	2.9	3.2		13.9	13.2	13.7	17.4	15.5		4.1	4.2	3.7	3.5	3.6		16.5	15.3	16.0	16.8	15.1		4.6	3.5		8.5	6.9	
Total 3	mgFSA-N/l	2.7	2.2	2.9	3.1	2.8	**2.76**	13.3	12.7	13.3	14.3	15.7	**14.3**	4.6		4.1	3.9		**3.9**	-	14.7	15.4	16.4	15.4	**15.9**	4.6	3.9	**4.2**	8.7	7.0	**8.3**
TP																															
Total 1	mgTP-P/l	9.0	7.6	6.8	6.8	6.3		8.3	8.0	7.5	6.9	7.5		5.3	5.9	5.4	4.6	5.2		6.8	6.6	8.1	7.2	5.7		5.6	8.6		4.6	4.5	
Total 2	mgTP-P/l	8.8	7.3	6.8	6.7	6.3	**7.2**	8.1	7.8	7.2	7.3	7.2	**7.6**	5.3	5.9	5.5	4.7	5.1		6.9	6.6	8.1	7.2	5.6		5.6	5.6	**6.4**	4.4	4.5	**4.5**
Soluble 1	mgTP-P/l	-	-	-	-	-		3.9	3.8	3.7	3.9	3.6		5	6	5	5	5		6.8	6.7	8.0	7.0	5.9		-	-		2.6	2.4	
Soluble 2	mgTP-P/l	-	-	-	-	-		4.1	3.5	3.8	4.1	3.7	**3.8**	5	6	5	5	5	**5.3**	6.8	6.8	8.1	14.4	6.1	**7.3**	-	-		2.6	2.6	**2.5**
OP																															
Total 1	mgOP-P/l	2.4	2.2	2.9	2.7	2.5		3.9	3.8	3.7	3.9	3.6		2.2	2.3	2.2	2.1	1.7		3.7	3.8	3.4	3.8	4.1		1.6	1.2		2.6	2.4	
Total 2	mgOP-P/l	2.3	2.3	2.9	2.7	2.4	**2.5**	4.1	3.5	3.8	4.1	3.7	**3.8**	2.2	2.3	2.2	2.0	1.7	**2.1**	3.7	3.7	3.2	3.8	4.1	**3.7**	1.7	1.2	**1.4**	2.6	2.6	**2.5**
Solids																															
TSS 1	mgTSS/l	824	899	866	862	830		844	834	1068	674	700		904	869	910	812	862		694	562	510	384	374		1168	981		400	452	
TSS 2	mgTSS/l	833	813	874	862	826	**849**	762	882	782	632	602	**778**	891	929	889	935	829	**883**	626	566	488	330	402	**494**	948	1009	**1027**	502	436	**448**
VSS 1	mgVSS/l	749	820	763	784	758		540	568	628	504	522		778	757	790	691	752		448	366	380	266	276		959	796		224	260	
VSS 2	mgVSS/l	753	723	776	775	826	**773**	556	636	562	460	494	**547**	785	808	771	801	829	**776**	368	408	358	242	308	**342**	778	831	**841**	250	248	**246**
ISS 1	mgISS/l	75	79	103	78	72		304	266	440	170	178		126	112	120	121	110		246	196	130	118	98		209	185		176	192	
ISS 2	mgISS/l	80	90	98	87	77	**84**	206	246	220	172	108	**231**	106	121	118	134	112	**118**	258	158	130	88	94	**152**	170	178	**186**	252	188	**202**
pH																															
pH		2.79	2.61	2.50	2.82	2.67	**2.68**	7.17	7.26	7.26	7.22	7.28	**7.24**	2.50	2.60	2.40	2.00	2.00	**2.30**	7.30	7.35	7.30	7.11	7.13	**7.24**	2.75	2.83	**2.79**	7.01	7.07	**7.04**
Alkalinity																															
Carbonate	mg/l as CaCO3	0.0	0.0	0.0	0.0	0.0	**0.0**	965.0	910.9	915.0	914.2	918.8	**924.8**	0.0	0.0	0.0	0.0	0.0	**0.0**	919.5	939.9	884.3	950.9	1040.1	**946.9**	0.0	0.0	**0.0**	607.1	604.7	**605.9**
Ammonia	mg/l as CaCO3	0.0	0.0	0.0	0.0	0.0	**0.0**	0.6	0.5	0.6	0.7	0.8	**0.6**	0.0	0.0	0.0	0.0	0.0	**0.0**	0.8	0.7	0.6	0.5	0.4	**0.6**	0.0	0.0	**0.0**	0.3	0.2	**0.3**
Phosphate	mg/l as CaCO3	-0.6	-0.8	-1.3	-0.6	-0.9	**-0.8**	4.3	4.2	4.3	4.5	4.2	**4.3**	-0.8	-0.8	-1.1	-1.8	-1.5	**-1.2**	4.2	4.3	3.5	3.6	3.9	**3.9**	-0.4	-0.3	**-0.3**	2.3	2.4	**2.4**
Sulphide	mg/l as CaCO3	0	0	0	0	0	**0.0**	288.4	354.7	332.5	320.0	336.7	**326.5**	0	0	0	0	0	**0.0**	373.0	378.9	345.4	295.5	284.6	**335.5**	0	0	**0.0**	126.6	149.1	**137.8**
VFA	mg/l as CaCO3	0.4	0.2	0.1	0.2	0.1	**0.2**	0.0	0.0	0.0	0.0	0.0	**0.0**	0.2	0.3	0.2	0.1	0.0	**0.2**	123.7	113.4	195.7	165.8	95.1	**138.7**	0.2	0.2	**0.2**	0.0	0.0	**0.0**
H20	mg/l as CaCO4	1250.4	1901.2	2426.8	1166.9	1648.3	**1678.7**	0.0	0.0	0.0	0.0	0.0	**0.0**	2438.0	1936.6	3069.3	7709.7	7709.7	**4572.6**	0.0	0.0	0.0	0.0	0.0	**0.0**	1371.0	1132.5	**1251.7**	0.0	0.0	**0.0**
Total	mg/l as CaCO3	1250.2	1900.7	2425.6	1166.5	1647.4	**1678.1**	1258.3	1270.3	1252.4	1239.4	1260.5	**1256.2**	2437.4	1936.0	3068.3	7708.0	7708.2	**4571.6**	1421.2	1437.3	1429.4	1416.2	1424.2	**1425.7**	1370.8	1132.5	**1251.6**	736.3	756.4	**746.3**
Species Concentration																															
CT	mg/l as C	5.8	8.8	11.5	15.0	15.2	**11.3**	257.2	237.8	240.5	240.7	240.7	**243.4**	4.3	6.5	7.3	9.8	12.1	**8.0**	241.3	244.6	236.1	263.2	286.4	**254.3**	15.2	16.1	**15.7**	169.0	164.9	**167.0**
VFA	mg/l as acetate	37.4	35.3	22.8	15.6	7.0	**23.6**	0.0	0.0	0.0	0.0	0.0	**0.0**	42.0	37.7	39.4	37.3	28.9	**37.0**	148.8	136.4	235.4	199.7	114.5	**167.0**	22.8	19.0	**20.9**	0.0	0.0	**0.0**

Appendix E: Methanogenic Batch Test (AugBMP) Data

Table E. 1: MC1 Data

MC1														
Date		21.02.19	22.02.19	23.02.19	24.02.19	25.02.19	26.02.19	27.02.19	01.03.19	02.03.18	03.03.18	06.03.19	07.03.19	12.03.19
Time		0	24	48	72	96	120	144	192	216	240	312	336	456
Control Reactor Average														
Total COD	mgCOD/l	10401.4	10963.7	9939.6	10521.9	9899.4	9538.0	9337.2	9558.1	8413.5	7851.3	6546.1	7289.0	8333.2
Soluble Organic COD	mgCOD/l	1084.3	1947.8	1927.7	1626.5	1385.5	1726.9	1706.8	1566.2	1646.6	1586.3	983.9	1224.9	1104.4
Carbonate Alk	mg/l as CaCO3	1113.1	1161.8	1175.9	1206.6	1241.8	1256.0	1263.8	1252.3	1252.6	1222.4	1432.1	1413.8	1428.5
VFA Conc	mg/l as Acetate	193.0	204.3	226.9	226.7	211.1	184.2	195.2	212.1	244.8	288.0	0.0	0.0	0.0
FSA	mgN/l	235.2	266.7	250.3	259.0	250.3	210.8	222.6	214.2	215.6	216.3	207.5	210.8	216.7
OP	mgP/l	13.2	23.7	18.5	15.9	20.1	17.5	20.1	21.9	20.5	27.8	16.2		63.8
OP Adjusted	mgP/l	13.2	23.7	18.5	15.9	20.1	16.3	20.1	21.9	20.5	19.3	16.2		23.0
VSS	mgVSS/l	4476.0	4797.3	4718.0	4733.0	4742.0	4595.3	4619.3	4569.3	4594.7	4564.0	4515.3	4538.7	4496.7
Carbon Gas Mass	mgC	0.0	141.8	268.5	404.9	523.0	617.1	676.5	767.8	804.7	811.1	857.9	863.5	879.9
CH4 mol	mol CH4	0.0	0.0	0.0	0.0	0.0	0.0	0.0	0.0	0.0	0.0	0.0	0.0	0.0
pH	pH	7.3	7.2	7.2	7.1	7.1	7.1	7.1	7.1	7.1	7.1		7.2	7.2
VFA COD	mgCOD/l	205.9	218.0	242.0	241.8	225.1	196.5	208.3	226.2	261.1	307.2	0.0	0.0	0.0
Total Alk	mg/l as CaCO3	1297.2	1365.0	1389.6	1417.1	1442.0	1429.6	1449.5	1454.2	1479.3	1484.9	1459.7	1441.5	1462.4
CT	mg/l	295.7	312.3	322.9	333.9	347.1	350.5	355.5	349.3	353.1	341.2	376.0	371.3	378.2
Test Reactor Average														
Total COD	mgCOD/l	13192.6	12991.8	12469.7	12931.5	12188.6	13092.2	11867.3	11124.3	9457.7	9377.4	6686.6	7730.8	8273.0
Soluble Organic COD	mgCOD/l	5542.1	5602.3	5120.4	4939.7	4578.2	4497.9	4317.2	4216.8	3453.8	3293.1	1787.1	2710.8	1847.4
Carbonate Alk	mg/l as CaCO3	644.6	836.0	998.0	1110.0	1204.1	1372.9	1395.4	1451.2	1722.5	1782.4	2064.0	2131.9	2356.8
VFA Conc	mg/l as Acetate	282.1	1121.5	1257.5	1266.9	1235.3	1116.9	1078.4	1027.3	805.7	750.6	502.1	418.1	207.3
FSA	mgN/l	168.0	431.9	502.3	553.7	532.0	473.2	510.3	537.6	529.2	529.2	527.1	523.6	557.9
OP	mgP/l	23.8	48.4	52.8	55.1	70.5	51.5	60.7	49.7	41.7	43.2	47.2		71.6
OP Adjusted	mgP/l	20.3	45.4	48.8	55.1	62.5	51.5	54.7	49.7	41.7	43.2	42.2		43.8
VSS	mgVSS/l	4291.3	3753.3	4026.7	2872.7	4070.7	3952.7	3858.0	3994.7	3868.7	3948.0	3978.7	3857.3	3869.3
Carbon Gas Mass	mgC	0.0	341.4	698.9	894.8	1055.1	1215.4	1375.4	1735.0	2003.5	2191.8	2796.6	2946.6	3456.3
CH4 mol	mol CH4	0.0	0.0	0.0	0.0	0.1	0.1	0.1	0.1	0.1	0.1	0.1	0.1	0.2
pH	pH	7.1	6.7	6.7	6.8	6.8	6.9	6.9	7.0	7.0	7.1		7.3	7.3
VFA COD	mgCOD/l	300.9	1196.2	1341.4	1351.4	1317.7	1191.4	1150.3	1095.7	859.4	800.6	535.6	445.9	221.1
Total Alk	mg/l as CaCO3	903.2	1798.7	2079.6	2209.3	2287.6	2352.3	2348.3	2363.3	2444.8	2464.1	2555.8	2553.3	2608.3
CT	mg/l	177.4	266.7	311.8	337.0	356.5	397.7	400.8	406.7	477.8	487.3	536.0	553.9	609.8

Table E. 2: MP1 Data

MP1																					
Date		22.02.18	23.02.18	24.02.18	25.02.18	26.02.18	27.02.18	28.02.18	01.03.18	02.03.18	03.03.18	05.03.18	06.03.18	07.03.18	09.03.18	10.03.18	12.03.18	14.03.18	16.03.18	19.03.18	22.03.18	23.03.18
Time		0	23	47	71	95	119	142	167	191	215	263	286	311	359	383	431	479	527	599	671	695
Control Reactor Average																						
Total COD	mgCOD/l	8730.2	8662.7	8042.0	7475.3	8055.5	7731.7	7082.2	7243.2	7109.1	6961.5	5861.6	6210.4	5933.3	6680.0	6693.3	6693.3	6173.3	6120.0	6308.0	6308.0	6852.5
Soluble Organic COD	mgCOD/l	2078.0	1551.7	1268.4	1281.9	1349.3	1322.3	1247.4	1247.4	1448.6	1260.9	1153.5	1354.7	1253.3	1106.7	1053.3	1160.0	1106.7	1186.7	1049.1	1168.6	1115.5
Carbonate Alk	mg/l as CaCO3	1139.4	1192.6	1112.1	1216.7	1232.1	1238.3	1238.9	1222.2	1220.2	1262.2	1271.0	1280.4	1282.5	1331.1	1336.4	1321.8	1318.9	1309.8	1339.6	1324.6	1352.9
VFA Conc	mg/l as Acetate	0.7	0.7	0.7	0.0	0.0	0.0	0.0	0.0	0.0	0.0	0.0	0.0	0.0	0.0	0.0	0.0	0.0	103.3	6.9	4.7	4.9
FSA	mgN/l	171.5	177.3	180.3	189.6	186.7	206.1	207.7	212.2	213.7	217.8	264.3	217.5	219.5	230.7	231.8	294.9	248.3	224.9	234.6	264.1	256.5
OP	mgP/l	14.4	14.1	18.1	19.0	20.7	22.3	24.7	20.4	19.2	9.7	18.3	20.8	23.7	18.2	19.1	18.8	14.1	20.0	23.7	20.5	19.5
VSS	mgVSS/l	5019.3	4530.0	4404.0	4349.3	4197.3	4308.7	4098.7	4107.3	4336.0	4184.7	4156.0	4031.3	4150.0	4064.0	4081.3	3960.7	3800.0	3920.7	4060.7	3995.3	3987.3
CH4 mol	mol CH4	0.000	0.011	0.017	0.020	0.023	0.026	0.026	0.027	0.028	0.030	0.031	0.032	0.032	0.033	0.034	0.034	0.034	0.033	0.034	0.034	0.034
pH	pH	7.3	7.3	7.3	7.3	7.2	7.2	7.2	7.2	7.2	7.2	7.2	7.2	7.2	7.1	7.2	7.2	7.1	7.2	7.2	7.2	7.2
VFA COD	mgCOD/l	0.8	0.8	0.8	0.0	0.0	0.0	0.0	0.0	0.0	0.0	0.0	0.0	0.0	0.0	0.0	0.0	0.0	110.2	7.4	5.1	5.2
Total Alk	mg/l as CaCO3	1166.2	1218.3	1142.3	1247.3	1263.0	1272.1	1275.6	1254.1	1250.1	1282.0	1300.3	1312.2	1315.9	1356.6	1364.6	1352.7	1341.9	1424.8	1378.4	1357.9	1385.9
CT	mg/l	299.0	310.0	289.9	318.0	325.2	326.2	325.6	321.9	322.0	334.2	338.6	338.9	341.1	360.2	357.2	351.5	354.7	347.8	358.6	357.2	363.0
Test Reactor Average																						
Total COD	mgCOD/l	11428.9	9998.6	10160.5	9769.2	10160.5	10025.5	9322.3	8986.9	8343.1	8812.6	6948.1	6787.1	6720.0	6946.7	6786.7	7093.3	6626.7	6360.0	6308.0	6799.4	6812.6
Soluble Organic COD	mgCOD/l	2010.5	1916.1	1673.2	1713.7	1983.5	1821.6	1609.6	1703.5	1743.7	1757.1	1395.0	1368.2	1346.7	1106.7	1226.7	1146.7	946.7	1133.3	1009.3	1128.8	969.4
Carbonate Alk	mg/l as CaCO3	473.0	679.8	675.2	620.5	615.5	627.2	644.8	639.9	724.2	733.5	796.5	817.9	862.5	974.3	983.0	1007.1	1004.1	1004.7	1028.5	1013.3	1018.7
VFA Conc	mg/l as Acetate	191.8	106.2	153.8	234.6	253.6	255.2	260.9	246.4	221.3	209.1	152.6	104.5	89.3	0.0	0.0	0.0	0.0	0.0	0.0	1.6	0.0
FSA	mgN/l	89.8	125.4	116.1	138.3	131.8	131.1	145.6	140.7	144.7	153.5	164.6	161.5	152.1	151.2	160.1	164.7	165.7	163.3	160.5	211.1	212.8
OP	mgP/l	17.7	20.7	16.9	23.1	22.4	27.7	23.8	24.3	24.7	11.1	22.0	25.4	24.8	22.4	23.8	23.5	19.1	26.9	24.3	20.3	23.2
VSS	mgVSS/l	6502.0	4980.7	5207.3	4799.3	4936.0	4862.7	4548.7	4594.7	4521.3	4514.0	4234.7	4156.7	4021.3	4163.3	4063.3	3964.0	4240.0	3823.3	3978.0	3812.7	3839.3
CH4 mol	mol CH4	0.000	0.022	0.038	0.052	0.065	0.080	0.091	0.102	0.114	0.125	0.148	0.159	0.167	0.177	0.182	0.186	0.186	0.184	0.187	0.186	0.187
pH	pH	6.9	6.9	6.7	6.6	6.5	6.5	6.6	6.6	6.7	6.7	6.7	6.8	6.8	6.8	6.9	6.9	6.9	7.0	6.9	6.9	6.9
VFA COD	mgCOD/l	204.6	113.3	164.0	250.3	270.5	272.2	278.3	262.8	236.1	223.0	162.7	111.5	95.3	0.0	0.0	0.0	0.0	0.0	0.0	1.7	0.0
Total Alk	mg/l as CaCO3	648.3	788.0	816.3	829.7	838.1	854.8	875.6	859.8	925.2	916.0	940.3	925.6	957.8	993.3	1005.8	1030.4	1023.6	1031.7	1052.3	1035.6	1042.2
CT	mg/l	136.4	194.4	204.8	202.7	209.0	209.5	213.0	207.6	228.8	229.4	245.9	245.8	256.0	291.6	283.4	286.5	289.9	285.1	294.1	291.7	290.7

Table E. 3: MP2 Data

MP2																		
Date		08.05.18	09.05.18	10.05.18	11.05.18	12.05.18	13.05.18	14.05.18	15.05.18	16.05.18	17.05.18	18.05.18	21.05.18	23.05.18	25.05.18	28.05.18	30.05.18	01.06.18
Time		0	23	47	71	97	120	144	167	191	215	239	311	359	408	480	528	576
Control Reactor Average																		
Total COD	mgCOD/l	9544.7	10106.9	9009.2	8406.8	9223.4	9333.3	9480.0	9253.3	8546.7	10093.3	9040.0	8546.7	8853.3	9093.3	8333.3	8906.7	9306.7
Soluble Organic COD	mgCOD/l	831.3	937.1	1191.4	1151.3	1204.8	1293.3	1253.3	1213.3	1226.7	1360.0	1386.7	1266.7	1066.7	1360.0	1020.0	1133.3	1026.7
Carbonate Alk	mg/l as CaCO3	1338.6	1390.7	1439.2	1449.8	1495.5	1491.2	1505.8	1592.0	1516.5	1498.9	1532.7	1539.7	1563.0	1617.3	1642.6	1651.3	1674.1
VFA Conc	mg/l as Acetate	35.6	23.5	0.0	23.7	18.6	35.0	60.3	11.2	64.5	89.0	50.6	59.6	94.6	0.0	0.0	0.0	0.0
FSA	mgN/l	254.3	245.0	246.4	247.8	253.9	248.7	252.9	294.9	308.9	295.4	296.8	310.3	306.1	299.0	320.6	305.9	296.8
OP	mgP/l	5.4	9.4	7.0	5.9	8.5	5.6	10.6	14.9	12.1	16.1	15.2	23.8	13.3	14.6	14.4	19.0	13.6
VSS	mgVSS/l	5634.0	5486.0	5404.7	5205.3	5184.0	5179.3	5071.3	4315.3	4450.0	4889.3	103740.7	4700.7	4638.7	4539.3	4515.3	4464.7	4530.0
CH4 mol	mol CH4	0.000	0.012	0.024	0.037	0.050	0.062	0.072	0.084	0.093	0.102	0.105	0.113	0.114	0.116	0.117	0.118	0.119
pH	pH	7.4	7.3	7.2	7.1	7.1	7.1	7.2	7.1	7.1	7.1	7.1	7.1	7.1	7.3	7.3	7.3	7.3
VFA COD	mgCOD/l	37.9	25.1	0.0	25.3	19.9	37.3	64.3	12.0	68.8	94.9	54.0	63.6	100.9	0.0	0.0	0.0	0.0
Total Alk	mg/l as CaCO3	1388.0	1430.7	1455.4	1483.7	1527.2	1532.8	1567.7	1625.1	1591.8	1597.4	1598.6	1622.3	1664.3	1648.1	1677.5	1691.3	1704.0
CT	mg/l	346.9	367.8	385.9	393.8	405.9	410.1	409.1	435.8	413.2	411.3	420.3	420.9	426.8	423.9	424.2	425.1	438.9
Test Reactor Average																		
Total COD	mgCOD/l	8821.8	6519.3	7576.9	7242.2	8513.9	8013.3	8466.7	8320.0	7840.0	8733.3	7533.3	7453.3	6800.0	6693.3	5693.3	6440.0	6626.7
Soluble Organic COD	mgCOD/l	1151.3	1044.2	1271.7	1245.0	1325.3	1453.3	1360.0	1346.7	1253.3	1120.0	1213.3	1093.3	1040.0	1160.0	933.3	986.7	1120.0
Carbonate Alk	mg/l as CaCO3	649.2	731.7	823.3	824.7	848.7	869.8	885.3	905.8	945.2	877.5	961.8	1061.4	1065.6	1155.1	1148.5	1175.0	1193.4
VFA Conc	mg/l as Acetate	133.8	145.4	101.2	117.1	85.4	95.7	105.9	82.5	57.9	59.2	61.8	18.1	55.2	0.0	0.0	0.0	0.0
FSA	mgN/l	167.1	229.1	171.9	189.5	178.3	183.9	196.9	249.7	227.7	231.5	234.7	222.1	221.2	219.3	224.9	224.6	219.3
OP	mgP/l	7.6	9.8	9.4	8.0	9.3	8.7	12.0	14.6	13.7	19.4	14.8	16.3	15.2	14.2	14.2	14.7	13.9
VSS	mgVSS/l	4146.0	3371.3	3664.7	3770.7	3984.7	4017.3	3700.7	3879.3	3730.0	3884.0	3061.3	3484.7	3247.3	3086.7	3068.0	2406.7	2962.7
CH4 mol	mol CH4	0.000	0.010	0.019	0.028	0.037	0.045	0.053	0.066	0.076	0.087	0.096	0.132	0.150	0.163	0.174	0.175	0.177
pH	pH	7.0	6.9	6.9	6.8	6.8	6.8	6.8	6.8	6.9	6.9	6.9	6.9	6.9	7.1	7.1	7.2	7.1
VFA COD	mgCOD/l	142.8	155.0	107.9	124.9	91.1	102.1	112.9	88.0	61.7	63.2	65.9	19.4	58.9	0.0	0.0	0.0	0.0
Total Alk	mg/l as CaCO3	771.4	864.7	917.9	930.9	929.2	957.8	982.3	988.8	1007.6	945.3	1028.6	1094.6	1128.0	1175.9	1171.5	1199.4	1214.8
CT	mg/l	182.8	213.6	242.6	249.0	256.4	268.2	266.5	275.7	282.6	262.7	286.2	306.5	311.6	316.4	308.5	313.2	324.9

Table E. 4: MP3 Data

MP3															
Date		07.12.18	08.12.18	09.12.18	10.12.18	11.12.18	12.12.18	13.12.18	14.12.18	15.12.18	16.12.18	18.12.18	20.12.18	22.12.18	24.12.18	26.12.18
Time		0	22	45	66	90	114	139	162	193	212	257	306	355	404	452
Control Reactor Average																
Total COD	mgCOD/l	13306.3	13038.6	12891.4	12610.2	12556.7	12386.7	12720.0	12453.3	12986.7	12773.3	12413.3	11893.3	11440.0	12213.3	11493.3
Soluble Organic COD	mgCOD/l	1834.0	1753.7	1419.0	1405.6	1204.8	1226.7	1253.3	1133.3	1280.0	1226.7	1360.0	1266.7	1280.0	1226.7	1333.3
Carbonate Alk	mg/l as CaCO3	1224.6	1333.1	1369.0	1370.6	1439.7	1470.4	1472.7	1549.0	1532.0	1546.3	1561.8	1513.2	1549.8	1572.8	1525.8
VFA Conc	mg/l as Acetate	83.0	118.0	96.4	124.7	134.6	116.2	106.7	34.5	74.3	75.5	74.0	101.3	128.1	112.2	140.6
FSA	mgN/l	273.5	287.9	296.3	284.2	313.1	311.7	316.9	313.1	319.2	325.3	325.7	326.5	326.2	324.3	330.4
OP	mgP/l	12.7	17.4	18.6	18.1	20.1	17.9	19.8	18.6	18.6	26.7	22.1	20.8	21.6	19.9	23.4
VSS	mgVSS/l	5911.3	5978.7	6164.7	5956.0	6092.7	5881.3	5841.3	5892.0	5428.7	5643.3	5668.0	5482.0	5528.7	6022.0	5299.3
CH4 mol	mol CH4	0.000	0.012	0.023	0.033	0.044	0.052	0.058	0.062	0.066	0.069	0.073	0.075	0.078	0.078	0.079
pH	pH	7.4	7.2	7.1	7.1	7.1	7.1	7.1	7.1	7.1	7.1	7.1	7.1	7.1	7.2	7.2
VFA COD	mgCOD/l	88.5	125.9	102.8	133.0	143.6	123.9	113.8	36.8	79.2	80.5	79.0	108.0	136.6	119.6	150.0
Total Alk	mg/l as CaCO3	1322.8	1460.9	1477.1	1500.0	1579.2	1592.2	1588.8	1604.9	1620.0	1643.1	1653.7	1628.3	1687.6	1697.1	1678.2
CT	mg/l	317.3	354.9	372.4	376.2	398.1	407.6	407.3	425.0	424.2	428.4	430.7	411.6	423.1	425.2	410.3
Test Reactor Average																
Total COD	mgCOD/l	15207.3	14564.7	14725.3	14069.4	14685.2	13853.3	13840.0	13733.3	14800.0	13600.0	13560.0	12640.0	12160.0	11600.0	11440.0
Soluble Organic COD	mgCOD/l	1820.6	1713.5	1713.5	1459.1	1713.5	1613.3	1626.7	1626.7	1360.0	1346.7	1386.7	1226.7	1306.7	1173.3	1306.7
Carbonate Alk	mg/l as CaCO3	511.0	678.7	726.7	726.8	756.6	768.0	782.4	942.7	883.6	937.5	1025.4	1068.9	1093.9	1149.0	1156.7
VFA Conc	mg/l as Acetate	231.7	234.7	217.2	259.2	268.4	266.9	259.9	212.9	176.2	166.9	103.7	66.1	92.5	87.2	105.3
FSA	mgN/l	158.7	190.9	217.9	208.6	225.9	222.1	230.5	226.3	228.7	215.6	233.3	236.1	243.1	233.8	239.4
OP	mgP/l	14.2	19.8	19.3	21.2	21.9	21.4	21.8	24.7	22.2	26.6	23.3	22.3	22.8	21.7	21.1
VSS	mgVSS/l	6994.0	6538.7	6500.7	6495.3	6272.7	6053.3	6087.3	5956.0	5810.0	5664.0	5697.3	5456.7	5192.7	4704.0	4915.3
CH4 mol	mol CH4	0.000	0.013	0.025	0.033	0.045	0.054	0.064	0.075	0.091	0.101	0.125	0.145	0.166	0.181	0.193
pH	pH	6.8	6.8	6.7	6.7	6.6	6.6	6.6	6.7	6.7	6.7	6.8	6.8	6.9	6.9	6.9
VFA COD	mgCOD/l	247.2	250.3	231.6	276.5	286.2	284.7	277.2	227.1	187.9	178.1	110.6	70.5	98.7	93.0	112.3
Total Alk	mg/l as CaCO3	715.4	890.0	922.7	957.1	993.9	1003.6	1012.6	1138.0	1046.8	1095.7	1131.5	1145.1	1192.3	1243.4	1266.3
CT	mg/l	156.1	207.7	226.1	232.7	248.2	253.3	257.6	297.7	279.7	297.1	313.6	317.0	325.9	336.1	335.6

Appendix F: Sulphidogenic Batch Test (AugBSP) Data

Table F. 1: SC1 Data

SC1														
Date		13.03.19	14.03.19	15.03.19	16.03.19	17.03.19	18.03.19	19.03.19	20.03.19	21.03.19	22.03.19	23.03.19	27.03.19	29.03.19
Time		0	24	48	72	96	120	144	168	192	216	240	336	384
Control Reactor Average														
Total COD	mgCOD/l	755.0	720.9	702.8	728.9	761.0	730.9	745.0	741.0	722.9	756.0	785.1	718.9	730.9
Total Soluble COD	mgCOD/l	417.7	405.6	409.6	419.7	407.6	395.6	395.6	400.6	385.5	413.6	403.6	400.6	404.6
Soluble Organic COD	mgCOD/l	117.5	91.4	114.5	100.4	94.4	87.3	100.4	96.4	76.3	94.4	67.3	72.3	91.4
Sulphide COD	mgCOD/l	300.2	314.3	295.2	319.3	313.2	308.2	295.2	304.2	309.2	319.3	336.3	328.3	313.2
Particulate COD	mgCOD/l	337.3	315.3	293.2	309.2	353.4	335.3	349.4	340.4	337.3	342.4	381.5	318.3	326.3
Carbonate Alk	mg/l as CaCO3	502.4	535.7	552.6	539.9	526.4	555.1	562.2	539.8	563.4	-	562.3	567.1	582.9
Sulphide Alk	mg/l as CaCO3	185.9	182.9	178.1	194.1	186.6	186.2	176.1	181.8	178.4	-	198.3	186.1	182.7
Total Alk	mg/l as CaCO3	692.0	721.8	734.7	738.4	736.0	755.0	742.9	725.2	746.0	-	763.7	757.1	778.7
FSA	mgN/l	7.6	7.7	7.7	7.7	9.4	8.1	7.5	7.0	7.1	-	8.9	8.7	8.8
OP	mgP/l	2.3	2.2	2.7	2.1	2.3	2.3	3.3	2.4	2.6	-	2.0	2.8	2.1
VSS	mgVSS/l	213.5	178.0	338.5	272.5	418.0	274.0	257.0	463.5	195.5	-	221.3	209.5	254.5
VFA Conc	mg/l as Acetate	0.0	0.0	0.0	1.3	23.4	12.3	0.0	0.0	0.7	-	0.0	0.0	11.9
pH	pH	7.6	7.5	7.5	7.5	7.5	7.5	7.5	7.5	7.4	-	7.5	7.4	7.5
Sulphate	mgSO4/l	693.9	652.9	673.6	662.3	687.0	575.8	580.3	584.0	622.5	-	554.5	561.3	573.4
CT	mgC/l	126.4	136.9	139.9	136.4	133.7	140.6	142.8	137.1	144.4	-	143.2	146.0	148.9
Test Reactor Average														
Total COD	mgCOD/l	781.1	805.2	741.0	757.0	712.8	743.0	730.9	755.0	726.9	753.0	720.9	763.0	763.0
Total Soluble COD	mgCOD/l	604.4	578.3	576.3	598.4	558.2	586.3	570.3	570.3	550.2	494.0	558.2	556.2	578.3
Soluble Organic COD	mgCOD/l	467.9	393.6	359.4	333.3	257.0	204.8	222.9	200.8	164.7	149.6	108.4	118.5	131.5
Sulphide COD	mgCOD/l	136.5	184.7	216.9	265.1	301.2	381.5	347.4	369.5	385.5	344.4	449.8	437.7	446.8
Particulate COD	mgCOD/l	176.7	226.9	164.7	158.6	154.6	156.6	160.6	184.7	176.7	259.0	162.6	206.8	184.7
Carbonate Alk	mg/l as CaCO3	173.5	219.6	300.3	397.3	463.7	540.7	577.1	554.6	586.2	-	622.5	657.2	677.0
Sulphide Alk	mg/l as CaCO3	46.2	59.9	79.5	112.1	129.9	172.1	163.7	173.7	179.8	-	210.9	215.4	221.6
Total Alk	mg/l as CaCO3	234.9	309.3	434.1	556.1	607.1	716.9	745.3	733.4	770.9	-	838.2	878.5	910.2
FSA	mgN/l	6.4	14.8	26.8	29.3	29.0	29.5	29.7	29.4	29.8	-	31.4	34.6	35.8
OP	mgP/l	3.4	3.4	2.4	3.2	5.1	3.3	2.7	3.3	3.3	-	3.0	3.5	3.3
VSS	mgVSS/l	129.0	129.5	189.0	195.0	270.0	196.5	207.0	191.0	146.5	-	148.5	147.5	142.5
VFA Conc	mg/l as Acetate	15.2	33.0	62.7	51.8	9.7	0.0	0.8	0.8	0.8	-	0.9	1.0	8.0
pH	pH	6.8	6.7	6.8	7.0	7.0	7.1	7.1	7.1	7.1	-	7.1	7.1	7.2
Sulphate	mgSO4/l	1096.0	1058.0	1007.3	927.8	886.0	713.5	717.8	727.9	748.5	-	664.8	646.0	678.8
CT	mgC/l	52.4	67.4	88.2	111.1	129.1	148.4	156.4	150.3	159.3	-	168.9	175.8	180.6

Table F. 2: SP1 Data

SP1																
Date		12.11.18	13.11.18	14.11.18	15.11.18	16.11.18	17.11.18	18.11.18	19.11.18	20.11.18	22.11.18	24.11.18	26.11.18	28.11.18	29.11.18	30.11.18
Time		0	22.5	46	70	94	118	142	166	190	238	286	334	382	406	430
Control Reactor Average																
Total COD	mgCOD/l	1492.0	1325.3	1313.2	1437.7	1437.7	1429.7	1510.0	1485.9	1460.0	1594.4	1638.5	1698.8	1373.5	-	1759.0
Total Soluble COD	mgCOD/l	621.0	614.0	649.6	653.6	661.6	665.7	641.6	636.5	658.0	676.7	664.6	683.7	672.7	-	699.8
Soluble Organic COD	mgCOD/l	52.6	45.6	43.2	56.2	50.2	50.2	52.2	47.2	52.0	56.2	55.2	55.2	72.3	-	90.4
Sulphide COD	mgCOD/l	568.4	568.4	606.4	597.4	611.4	615.5	589.3	589.3	606.0	620.5	609.4	628.5	600.4	-	609.4
Particulate COD	mgCOD/l	871.0	711.3	663.6	784.1	776.1	764.0	868.5	849.4	802.0	917.7	973.9	1015.0	700.8	-	1059.2
Carbonate Alk	mg/l as CaCO3	875.0	909.5	906.2	932.9	920.0	918.7	921.6	914.3	902.5	905.1	941.5	952.7	954.9	-	949.8
Sulphide Alk	mg/l as CaCO3	348.6	348.5	360.6	358.6	367.4	362.0	346.2	335.0	352.6	361.6	356.9	361.3	350.8	-	360.2
Total Alk	mg/l as CaCO3	1229.5	1264.0	1279.1	1306.2	1316.0	1319.3	1299.0	1280.9	1297.1	1311.3	1329.0	1342.9	1333.6	-	1386.6
FSA	mgN/l	15.2	17.5	17.5	17.7	18.3	18.0	18.1	17.3	19.2		18.6	18.5	18.3	-	18.7
OP	mgP/l	3.6	3.5	3.7	3.7	5.0	12.5	3.8	4.5	3.8	6.4	4.4	3.9	3.8	4.1	3.9
VSS	mgVSS/l	536.0	432.5	442.5	471.5	421.5	478.0	491.0	464.0	495.0	533.0	575.5	543.0	624.5	650.0	720.5
VFA Conc	mg/l as Acetate	0.0	0.0	7.6	10.4	25.0	26.1	30.5	30.2	43.2	42.4	28.7	27.6	26.5	-	84.7
pH	pH	7.6	7.5	7.5	7.5	7.5	7.5	7.5	7.4	7.5	7.5	7.5	7.5	7.5	7.4	7.5
Sulphate	mgSO4/l	143.0	58.6	24.5	18.2	0.0	145.8	155.0	146.8	148.6	136.8	136.8	135.9	137.4	136.0	-
CT	mgC/l	220.6	229.3	230.3	236.5	233.2	234.1	235.0	235.1	230.6	231.2	240.2	244.2	243.8	-	241.7
Test Reactor Average																
Total COD	mgCOD/l	1507.8	1404.7	1349.4	1477.9	1445.8	1441.7	1542.1	1510.0	1500.0	1538.1	1662.6	1718.8	1654.6	-	1714.8
Total Soluble COD	mgCOD/l	413.7	464.3	555.2	633.5	666.7	674.7	703.8	694.8	699.0	704.8	732.9	728.9	712.8	-	733.9
Soluble Organic COD	mgCOD/l	69.4	92.3	86.3	70.3	58.2	57.2	53.2	54.2	54.0	58.2	61.2	58.2	74.3	-	91.4
Sulphide COD	mgCOD/l	344.2	372.0	468.9	563.2	608.4	617.5	650.6	640.6	645.0	646.6	671.7	670.7	638.5	-	642.6
Particulate COD	mgCOD/l	1094.2	940.4	794.2	844.4	779.1	767.1	838.3	815.2	801.0	833.3	929.7	989.9	941.8	-	980.9
Carbonate Alk	mg/l as CaCO3	366.4	507.3	703.3	837.9	896.1	917.0	940.7	960.5	966.3	992.3	982.3	1023.1	1034.7	-	1033.6
Sulphide Alk	mg/l as CaCO3	181.9	186.0	223.5	288.1	318.8	321.4	329.6	317.7	324.8	328.0	349.1	345.7	333.0	-	339.9
Total Alk	mg/l as CaCO3	553.5	699.0	948.4	1136.1	1223.6	1243.6	1281.3	1290.9	1306.4	1333.9	1353.9	1386.2	1381.7	-	1388.1
FSA	mgN/l	10.2	15.1	14.2	13.7	14.4	14.7	14.8	15.2	15.9		16.6	16.6	16.8	-	17.5
OP	mgP/l	3.0	3.5	3.3	5.2	3.7	3.5	3.5	5.2	3.7	3.7	9.9	6.9	3.7	4.0	4.0
VSS	mgVSS/l	580.5	564.5	493.0	487.3	425.5	427.0	417.5	452.0	426.0	495.5	492.0	600.5	590.0	590.0	616.5
VFA Conc	mg/l as Acetate	1.7	1.7	21.5	4.5	4.6	0.7	7.9	7.9	12.8	10.6	17.1	10.8	11.0	-	11.1
pH	pH	7.4	7.3	7.2	7.3	7.3	7.3	7.3	7.2	7.3	7.3	7.3	7.3	7.3	7.2	7.3
Sulphate	mgSO4/l	947.6	783.9	608.2	482.2	372.8	351.5	271.5	258.5	224.5	203.0	193.0	184.8	187.8	146.0	-
CT	mgC/l	96.1	135.2	189.8	221.6	235.5	241.4	249.5	256.3	256.8	263.2	258.7	270.1	272.3	-	270.9

Table F. 3: SP2 Data

SP2																					
Date		27.01.19	28.01.19	29.01.19	30.01.19	31.01.19	01.02.19	02.02.19	03.02.19	04.02.19	05.02.19	07.02.19	10.02.19	11.02.19	12.02.19	13.02.19	14.02.19	15.02.19	16.02.19	18.02.19	19.02.19
Time		0	24	48	72	96	120	144	168	192	216	264	336	360	384	408	432	456	480	528	552
Control Reactor Average																					
Total COD	mgCOD/l	1194.4	1214.2	1224.9	1164.6	1184.7	1192.8	1160.6	1156.6	1104.0	1216.8	959.8	-	-	1409.6	1277.1	-	1289.1	-	1228.9	-
Total Soluble COD	mgCOD/l	604.1	603.1	608.4	610.4	658.6	638.5	642.6	645.6	619.0	649.6	646.6	-	-	666.7	684.7	-	689.7	-	683.7	-
Soluble Organic COD	mgCOD/l	83.3	72.4	63.3	84.3	110.4	107.4	108.4	112.4	100.0	90.4	77.3	-	-	98.4	116.5	-	114.5	-	123.5	-
Sulphide COD	mgCOD/l	520.8	530.7	545.2	526.1	548.2	531.1	534.1	533.1	519.0	559.2	569.3	-	-	568.3	568.3	-	575.3	-	560.2	-
Particulate COD	mgCOD/l	590.2	611.1	616.5	554.2	526.1	554.2	518.1	511.0	485.0	567.3	313.2	-	-	743.0	592.4	-	599.4	-	545.2	-
Carbonate Alk	mg/l as CaCO3	897.0	937.9	984.2	1002.6	971.3	975.7	987.4	972.6	985.0	962.2	944.8	979.9	938.6	-	931.3	-	919.2	-	966.6	-
Sulphide Alk	mg/l as CaCO3	320.9	311.0	320.3	302.8	314.4	307.1	306.8	315.7	302.2	330.0	341.4	333.9	339.4	-	345.3	-	350.1	-	337.3	-
Total Alk	mg/l as CaCO3	1223.1	1252.4	1309.1	1326.6	1327.6	1328.6	1349.0	1350.7	1356.9	1375.3	1376.5	1399.3	1402.8	-	1400.0	-	1430.0	-	1400.6	-
FSA	mgN/l	13.8	13.2	13.9	14.0	13.9	13.7	14.0	15.0	15.1	14.8	14.7	15.4	15.8	-	16.1	-	16.1	-	-	-
OP	mgP/l	3.0	2.1	2.9	4.6	3.0	2.9	2.8	2.9	2.9	3.1	3.2	3.2	3.1	-	3.2	-	3.4	-	-	3.4
VSS	mgVSS/l	333.0	319.0	359.0	397.0	347.0	420.5	445.5	409.0	408.0	367.0	410.5	401.5	293.0	452.5	-	-	326.5	-	351.0	-
VFA Conc	mg/l as Acetate	0.0	0.0	0.0	17.7	44.8	49.7	60.6	69.3	78.2	94.0	102.3	96.6	143.9	-	141.8	-	186.3	-	116.2	-
pH	pH	7.6	7.5	7.5	7.5	7.5	7.5	7.5	7.5	7.5	7.5	7.6	7.5	7.5	-	7.6	-	7.6	-	7.6	7.5
Sulphate	mgSO4/l	323.5	317.4	267.5	271.2	251.4	249.6	259.3	203.8	216.9	207.3	214.4	206.6	204.9	-	198.2	-	204.5	-	169.1	-
CT	mgC/l	225.9	239.2	250.9	256.9	249.1	249.7	253.1	247.3	251.6	244.9	239.5	249.8	238.2	-	235.3	-	232.2	-	244.8	-
Test Reactor Average																					
Total COD	mgCOD/l	1630.8	1698.3	1622.5	1598.4	1522.1	1642.5	1642.5	1526.1	1484.0	1590.3	1269.1	-	-	1554.2	1634.5	1662.6	1586.3	-	1582.3	-
Total Soluble COD	mgCOD/l	396.8	475.2	539.1	608.4	716.9	719.9	746.0	757.0	722.0	775.1	762.0	-	-	798.2	822.3	811.2	806.2	795.2	819.3	-
Soluble Organic COD	mgCOD/l	91.3	107.1	90.4	98.4	110.4	118.5	114.5	108.4	106.0	103.4	79.3	-	-	114.5	126.5	112.4	136.5	118.5	126.5	-
Sulphide COD	mgCOD/l	305.5	368.0	448.8	510.0	606.4	601.4	631.5	648.6	616.0	671.7	682.7	-	-	683.7	695.8	698.8	669.7	676.7	692.8	-
Particulate COD	mgCOD/l	1234.0	1223.1	1083.3	989.9	805.2	922.7	896.6	769.1	762.0	815.2	507.0	-	-	756.0	812.2	851.4	780.1	-	763.0	-
Carbonate Alk	mg/l as CaCO3	408.4	508.1	666.5	804.6	900.3	978.3	1023.2	1013.7	1077.1	1046.7	1063.6	1101.3	1040.1	-	1013.9	-	1036.2	-	1014.9	-
Sulphide Alk	mg/l as CaCO3	122.7	141.3	181.0	218.2	258.1	259.3	271.0	287.8	276.1	300.7	320.8	308.2	317.9	-	331.5	-	317.1	-	325.9	-
Total Alk	mg/l as CaCO3	533.9	651.9	855.0	1037.0	1166.7	1259.5	1313.4	1346.7	1385.6	1400.2	1461.6	1493.6	1483.8	-	1439.8	-	1492.3	-	1434.8	-
FSA	mgN/l	9.5	11.4	12.0	12.1	12.3	13.1	13.1	13.8	13.8	14.1	14.7	17.0	16.8	-	16.4	-	16.4	-	16.9	-
OP	mgP/l	3.0	2.7	3.1	4.6	2.8	3.0	2.9	3.5	3.6	3.2	3.9	6.7	3.4	-	3.9	-	4.0	-		3.7
VSS	mgVSS/l	565.0	587.0	610.5	559.0	512.0	429.0	516.5	477.5	403.5	421.5	495.0	437.0	451.0	413.5		-	394.5	-	381.0	-
VFA Conc	mg/l as Acetate	0.0	0.0	5.5	11.8	6.3	22.6	19.5	49.9	34.4	59.3	87.4	92.9	146.6	-	108.0	-	161.7	-	112.8	-
pH	pH	7.0	7.0	7.0	7.1	7.1	7.1	7.1	7.1	7.1	7.1	7.2	7.1	7.2	-	7.2	7.3	7.2	-	7.2	7.1
Sulphate	mgSO4/l	883.4	742.1	575.7	417.8	285.0	223.9	185.6	138.7	167.9	98.0	65.7	2.6	13.7	-	105.2	198.9	85.3	164.9	81.0	-
CT	mgC/l	115.8	146.9	189.5	224.5	251.5	272.2	285.1	279.5	296.1	287.8	288.3	302.1	282.8	-	273.7	-	280.2	-	274.9	-

Table F. 4: SP3 Data

SP3														
Date		04.04.19	05.04.19	06.04.19	08.04.19	09.04.19	11.04.19	12.04.19	14.04.19	15.04.19	18.04.19	19.04.19	22.04.19	23.04.19
Time		0	22.5	46	70	94	118	142	166	190	238	286	334	382
Control Reactor Average														
Total COD	mgCOD/l	916.6	873.0	847.4	971.9	1056.2	1028.1	979.9	927.7	932.0	1012.0	895.6	923.7	935.7
Total Soluble COD	mgCOD/l	411.7	409.7	395.6	429.7	422.7	424.7	415.7	396.6	394.0	425.7	380.5	395.6	395.6
Soluble Organic COD	mgCOD/l	87.3	101.2	71.3	100.4	107.4	96.4	72.3	56.2	54.0	70.3	44.2	46.2	44.2
Sulphide COD	mgCOD/l	324.4	308.5	324.3	329.3	315.3	328.3	343.4	340.4	340.0	355.4	336.3	349.4	351.4
Particulate COD	mgCOD/l	504.9	463.3	451.8	542.2	633.5	603.4	564.2	531.1	538.0	586.3	515.1	528.1	540.2
Carbonate Alk	mg/l as CaCO3	572.6	630.9	641.2	630.8	658.0	667.6	663.6	661.8	665.0	670.0	687.6	701.0	699.2
Sulphide Alk	mg/l as CaCO3	194.7	167.5	187.2	181.5	172.7	178.8	190.4	183.0	180.7	194.7	182.1	188.3	190.6
Total Alk	mg/l as CaCO3	771.2	801.8	836.2	815.6	834.5	851.4	857.2	856.9	854.9	868.4	874.4	893.6	894.7
FSA	mgN/l	7.1	8.8	7.9	8.9	8.0	7.8	8.4	8.3	8.4	9.2	10.4	9.8	9.3
OP	mgP/l	2.7	2.5	2.6	2.4	2.8	2.1	2.4	2.2	2.7	2.8	2.6	3.3	3.8
VSS	mgVSS/l	287.5	335.5	334.5	364.0	334.5	350.0	749.0	376.0	393.5	363.5	350.5	543.5	626.0
VFA Conc	mg/l as Acetate	0.0	0.0	5.1	0.0	0.0	2.6	0.0	11.0	7.0	0.0	1.5	0.0	0.0
pH	pH	7.5	7.3	7.4	7.3	7.3	7.3	7.3	7.3	7.3	7.3	7.3	7.3	7.3
Sulphate	mgSO4/l	594.7	588.8	559.3	510.7	527.8	529.1	539.3	514.2	520.3	539.6	534.9	510.4	558.6
CT	mgC/l	145.2	164.2	164.2	163.6	170.9	173.7	171.8	172.7	174.1	174.0	179.1	182.9	182.1
Test Reactor Average														
Total COD	mgCOD/l	1166.6	1091.2	1112.4	1301.2	1261.0	1273.1	1277.1	1224.9	1192.0	1353.4	1164.6	1224.9	1184.7
Total Soluble COD	mgCOD/l	267.8	283.7	323.3	492.0	529.1	536.1	533.1	547.2	539.0	573.3	541.2	556.2	557.2
Soluble Organic COD	mgCOD/l	92.3	96.2	84.3	112.4	105.4	92.4	69.3	63.3	58.0	83.3	51.2	42.2	48.2
Sulphide COD	mgCOD/l	175.6	187.5	239.0	379.5	423.7	443.8	463.8	483.9	481.0	490.0	490.0	514.0	509.0
Particulate COD	mgCOD/l	898.8	807.5	789.1	809.2	731.9	736.9	744.0	677.7	653.0	780.1	623.5	668.7	627.5
Carbonate Alk	mg/l as CaCO3	216.8	271.7	388.1	560.5	646.9	715.5	711.7	718.5	739.6	772.8	781.8	788.9	788.5
Sulphide Alk	mg/l as CaCO3	57.4	62.1	93.2	170.4	192.9	198.0	211.8	220.2	213.3	228.8	219.6	236.0	241.7
Total Alk	mg/l as CaCO3	278.4	337.6	483.8	733.2	842.4	915.9	926.2	941.8	956.6	1005.3	1004.2	1028.5	1034.3
FSA	mgN/l	5.7	6.6	6.6	6.2	6.6	6.9	6.6	6.6	6.9	7.4	7.6	8.1	8.2
OP	mgP/l	2.4	3.5	3.1	2.3	2.6	2.3	2.5	2.3	3.0	2.8	2.7	3.4	3.7
VSS	mgVSS/l	530.0	458.0	490.0	425.5	398.5	398.0	524.5	370.5	385.5	367.5	350.5	428.0	267.5
VFA Conc	mg/l as Acetate	3.1	1.6	0.0	0.0	0.0	0.0	0.2	0.8	0.8	0.8	0.0	0.0	0.0
pH	pH	6.8	6.8	6.9	7.0	7.0	7.1	7.1	7.0	7.0	7.1	7.0	7.1	7.1
Sulphate	mgSO4/l	974.1	926.2	844.1	611.5	566.7	516.1	523.0	481.0	482.2	467.5	466.7	427.6	473.7
CT	mgC/l	66.4	82.8	111.6	154.2	177.1	197.1	194.7	196.8	204.1	209.9	214.9	215.4	213.2

Appendix G: Casein Analysis

Table G. 1: Data for Casein Wet Chemistry Analysis for 1g/l

TKN									
		Date							
Dilution	Unit	14.02.2019		16.02.2019			20.02.2019		
5x	mgTKN/l	139.3	134.4	140.7	105	136.5	126.7	135.8	133
10x	mgTKN/l	161	-	141.4	144.2	145.6	-	-	-
20x	mgTKN/l	156.8	151.2	-	-	-	-	-	-

FSA								
		Date						
Dilution	Unit	14.02.2019		16.02.2019		20.02.2019		
0x	mgFSA/l	-	-	10.6	10.8	10.9	11.9	11.6
5x	mgFSA/l	14.0	11.9	16.8	14.7	-	-	-
10x	mgFSA/l	14.0	12.6	-	-	-	-	-
20x	mgFSA/l	25.2	16.8	-	-	-	-	-

COD							
		Date					
Dilution	Unit	14.02.2019		16.02.2019		20.02.2019	
5x	mgCOD/l	1280	1260	1240	1160	1260	1300
10x	mgCOD/l	1280	1280	1240	1240	-	-
20x	mgCOD/l	1200	1280	-	-	-	-

TP							
		Date					
Dilution	Unit	14.02.2019		16.02.2019		20.02.2019	
0x	mgTP/l	-	-	3.7	3.7	7.9	7.9
5x	mgTP/l	8.7	8.3	-	-	-	-
10x	mgTP/l	7.9	8.6	-	-	-	-
15x	mgTP/l	6.3	6.4	-	-	-	-

OP							
		Date					
Dilution	Unit	14.02.2019		16.02.2019		20.02.2019	
0x	mgOP/l	3.0	2.9	3.1	3.1	3.2	2.9
5x	mgOP/l	2.7	2.6	-	-	-	-
10x	mgOP/l	3.0	2.6	-	-	-	-

Alkalinity				
		Date		
Alkalinities	Unit	14.02.2019	16.02.2019	20.02.2019
Carbonate+H2O	mg/l as CaCO3	22.31	20.92	20.46
Ammonia	mg/l as CaCO3	0.50	1.15	0.29
Phosphate	mg/l as CaCO3	3.02	4.08	2.78
Sulphide	mg/l as CaCO3	0.00	0.00	0.00
VFA	mg/l as CaCO3	31.37	33.33	35.54
VFA Conc	mg/l as Acetate	37.71	40.01	42.76
Total Alk	mg/l as CaCO3	57.20	59.49	59.07

Table G. 2: Summary Casein Wet Chemistry Analysis for 1g/l

Casein Data for 1g/l											
COD	TKN	FSA	TP	OP	Carbonate+H2O	Ammonia	Phosphate	Sulphide	VFA	VFA Conc	Total
1251.67	139.40	13.99	7.74	2.89	21.23	0.65	3.30	0.00	33.41	40.16	58.59
fcv	fn	fn	fp	fp	fc						
1.252	0.139	0.014	0.008	0.003	0.005						